1 OF 3

PNL

3700

(PT.1)

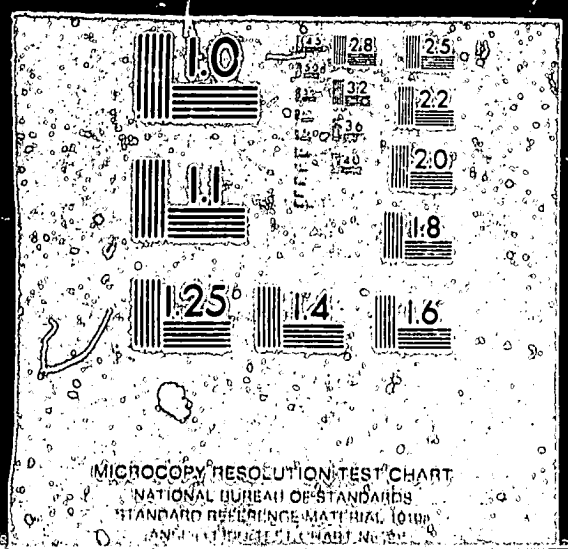

PORTIONS OF THIS DOCUMENT ARE ILLEGIBLE

PNL-3700 PT1

UC-48

Pacific Northwest Laboratory Annual Report for 1980 to the DOE Assistant Secretary for Environment

R-2563

MASTER

Part 1 Biomedical Sciences February 1981

Prepared for the U.S. Department of Energy
under Contract DE-AC06-76RLO 1830

Pacific Northwest Laboratory
Operated for the U.S. Department of Energy
by Battelle Memorial Institute

Battelle

DISTRIBUTION OF THIS DOCUMENT IS UNLIMITED

PNL-3700 PT1
UC-48

Pacific Northwest Laboratory Annual Report for 1980 to the DOE Assistant Secretary for Environment

Part 1 Biomedical Sciences

H. Drucker and Staff Members
of Pacific Northwest Laboratory

February 1981

Prepared for
the U.S. Department of Energy
under Contract DE-AC06-76RLO 1830

DISCLAIMER

Pacific Northwest Laboratory
Richland, Washington 99352

PREFACE

Pacific Northwest Laboratory's (PNL) 1980 Annual Report to the Department of Energy (DOE) Assistant Secretary for Environment describes research in environment, health, and safety conducted during fiscal year 1980. The report again consists of five parts, each in a separate volume.

The five parts of the report are oriented to particular segments of our program. Parts 1 to 4 report on research performed for the DOE Office of Health and Environmental Research. Part 5 reports progress on all other research performed for the Assistant Secretary for Environment, including the Office of Environmental Assessment and the Office of Environmental Compliance and Overview. Each part consists of project reports authored by scientists from several PNL research departments, reflecting the interdisciplinary nature of the research effort. Parts 1 to 4 are organized primarily by energy technology.

The parts of the 1980 Annual Report are:

Part 1:	Biomedical Sciences Program Manager - H. Drucker	D. L. Felton, Editor
Part 2:	Ecological Sciences Program Manager - B. E. Vaughan	B. E. Vaughan, Report Coordinator C. M. Novich, Editor
Part 3:	Atmospheric Sciences Program Manager - C. E. Elderkin	R. L. Drake, Report Coordinator M. F. Johnson, Editor
Part 4:	Physical Sciences Program Manager - J. M. Nielsen	J. M. Nielsen, Report Coordinator I. D. Hays, J. L. Baer, Editors
Part 5:	Environmental Assessment, Control, Health and Safety Program Managers - D. L. Hessel S. Marks W. A .Glass	W. J. Bair, Report Coordinator R. W. Baalman, I. D. Hays, Editors

Activities of the scientists whose work is described in this annual report are broader in scope than the articles indicate. PNL staff have responded to numerous requests from DOE during the year for planning, for service on various task groups, and for special assistance.

Credit for this annual report goes to many scientists who performed the research and wrote the individual project reports, to the program managers who directed the research and coordinated the technical progress reports, to the editors who edited the individual project reports and assembled the five parts, and to Ray Baalman and Irene D. Hays, editors in chief, who directed the total effort.

W. J. Bair, Manager
S. Marks, Associate Manager
Environment, Health, and Safety Research Program

Previous Reports in this series

Annual Report for

1951	HW-25021, HW-25709
1952	HW-27834, HW-28636
1953	HW-30437, HW-30464
1954	HW-30306, HW-33128, HW-35905, HW-35917
1955	HW-39558, HW-41515, HW-41500
1956	HW-47500
1957	HW-53500
1958	HW-59500
1959	HW-63824, HW-65500
1960	HW-69500, HW-70050
1961	HW-72500, HW-73337
1962	HW-76000, HW-77609
1963	HW-80500, HW-81746
1964	BNWL-122
1965	BNWL-280, BNWL-235, Vol. 1-4, BNWL-361
1966	BNWL-480, Vol. 1, BNWL-481, Vol. 2, Pt. 1-4
1967	BNWL-714, Vol. 1, BNWL-715, Vol. 2, Pt. 1-4
1968	BNWL-1050, Vol. 1, Pt. 1-2, BNWL-1051, Vol. 2, Pt. 1-3
1969	BNWL-1306, Vol. 1, Pt. 1-2, BNWL-1307, Vol. 2, Pt. 1-3
1970	BNWL-1550, Vol. 1, Pt. 1-2, BNWL-1551, Vol. 2, Pt. 1-2
1971	BNWL-1650, Vol. 1, Pt. 1-2, BNWL-1651, Vol. 2, Pt. 1-2
1972	BNWL-1750, Vol. 1, Pt. 1-2, BNWL-1751, Vol. 2, Pt. 1-2
1973	BNWL-1850, Pt. 1-4
1974	BNWL-1950, Pt. 1-4
1975	BNWL-2000, Pt. 1-4
1976	BNWL-2100, Pt. 1-5
1977	PNL-2500, Pt. 1-5
1978	PNL-2850, Pt. 1-5
1979	PNL-3300, Pt. 1-5

FOREWORD

This volume describes progress on biomedical and health effects research conducted at PNL in 1980. The contents of the volume are a reflection of our continuing emphasis on the evaluation of risk to man from existing and/or developing energy-related technologies. The emphasis of the PNL program is consistent with the DOE goal of increasing and diversifying national energy resources without increasing risks to human health.

Most of the studies described in this report relate to process-specific activities for four major energy technologies: *nuclear fuel cycle*, *fossil fuel cycle* (oil, gas, and coal process technologies, mining, and utilization; synfuel development), *geothermal power production*, and *fusion* (biomagnetic effects). The report is organized under these technologies. In addition, research reports are included on the application of nuclear energy to biomedical problems.

Technically, the energy-related projects presented here all center around a common research format involving multitiered toxicologic evaluation of potentially hazardous by-products, fugitive gases, and effluents from process-specific energy activities. The solvent refined coal projects, for example, are illustrative of the multitiered toxicologic concept. Products and process streams are examined by an inexpensive microbial mutagenesis assay. The results of these investigations are used to set priorities for materials to be used in the more expensive animal carcinogenicity and teratogenicity test systems. The initial acute animal studies, in turn, are used to identify the need for examining noncarcinogenic effects, such as damage to respiratory, neurologic, and immunologic systems.

The validity of applying results from animal experimentation to man is firmly based on empirical observations. However, as indicated in reports on animal lifespan studies associated with nuclear fuel cycles, some progress is being made in obtaining data which will provide a more quantitative basis for the extrapolation of animal data to man.

Major progress is being made in determining potential health effects of coal liquids relative to other fossil fuels and synfuels such as shale oil. In particular, work in progress is leading to some understanding of specific chemical entities that might be responsible for the biological effects of the complex mixtures that are coal liquids.

The biomedical and health effects program at PNL is an interdisciplinary effort requiring scientific contributions from practically all research departments at PNL. The personnel in the Biology Department are the principal contributors to the volume. Requests for reprints from the list of publications for 1980 on pages 259 to 261 will be honored while supplies last.

CONTENTS

PREFACE iii

FOREWORD v

COAL

INHALATION HAZARDS TO COAL MINERS 1

Pathologic Changes Associated with Experimental Exposure of Rats to Coal Dust and/or Diesel Exhaust - R. H. Busch, R. E. Filipy, M. T. Karagianes, and R. F. Palmer 1

Biological Effects of Chronic Inhalation of Coal Mine Dust and/or Diesel Engine Exhaust in Rodents - M. T. Karagianes, R. F. Palmer, and R. H. Busch 5

Maximal Expiratory-Flow-Volume Relationships and Lung Volumes in Normal and Elastase Impaired Rats - P. J. Minalko, R. F. Palmer, and M. T. Karagianes 8

Automatic Generation of Repeatable, Forced Vital-Capacity Maneuvers in Anesthetized Rodents - P. J. Minalko, E. G. Kuffel, and J. R. Decker 11

POLLUTANT METALS AND MALNUTRITION - H. A. Kagan 15

ALVEOLAR CLEARANCE OF INHALED METAL OXIDES 16

Metabolism of Intratracheally Instilled ^{75}Se (Selenate and Selenite) in the Presence of Cadmium - A. W. Conklin and C. L. Sanders 16

Carcinogenicity of Singly and Multipy Exposed Rats to Intratracheally Instilled Cadmium Oxide - C. L. Sanders and A. W. Conklin 19

Pulmonary Toxicity of Mount St. Helens Volcanic Ash - C. L. Sanders, P. A. Gelman, and A. W. Conklin 20

Influence of Cadmium, Selenium and Vanadium Oxides on Acute Mortality and Lung Clearance - C. L. Sanders and A. W. Conklin 22

FACTORS INFLUENCING THE CROSS-PLACENTAL TRANSFER AND TERATOGENICITY OF METALLIC POLLUTANTS 25

Cross-Placental Transfer of Vanadium Parenterally Administered to Rats - P. L. Hackett and S. A. Watson 25

SOLVENT REFINED COAL BIOSTUDIES - D. D. Mahlum 29

PERINATAL EFFECTS OF SRC - F. D. Andrew 30

MUTAGENICITY OF SRC MATERIALS - R. A. Pelroy 31

CONSERVATION

MUTAGENIC EFFECTS OF ELECTRIC FIELDS 34

Mutagenicity of Electric Fields in <u>Salmonella</u> - F. P. Hungate and S. C. Causey 34

AC E-FIELD DOSIMETRY 40

Determination of Electric Current Distributions in Man and Hanford Swine Exposed to a Uniform 60-Hz Electric Field - A. W. Guy, S. Davidow, and C. K. Chou 40

Technique for the Direct Measurement of 60-Hz Electric Fields Inside Homogeneous Models and Animals - W. T. Kaune 42

IN VIVO MUTAGENESIS - ELECTRIC FIELDS 45

Cytogenetic Effects in Rats Exposed to 60-Hz Electric Fields - B. J. McClanahan 45

Effects of Exposure to a 60-Hz Electric Field on Unscheduled DNA Synthesis in Spermatogenic Cells and on Sperm Abnormalities in Mice - B. J. McClanahan 47

IN VITRO EFFECTS OF ELECTRIC FIELDS 49

In Vitro Effects of AC Electric Fields: Mammalian Cell Assays - M. E. Frazier, W. T. Kaune, A. J. King, J. Samuel, and T. K. Andrews, Jr. 49

FISSION

AEROSOL TECHNOLOGY DEVELOPMENT 57

Progress in Aerosol Exposure Chamber Design - W. C. Cannon and E. F. Blanton 57

Progress in Dry Dust Feeder Development - O. R. Moss, D. P. Y. Chang, and E. M. Milliman 59

Dissolution Rates of $^{241}AmO_2$ - W. C. Cannon, E. J. Rossignol, and O. R. Moss 61

Mount St. Helens Ash Characterization - J. K. Briant and O. R. Moss 64

INHALED PLUTONIUM OXIDE IN DOGS 66

Dose-Effect Studies With Inhaled Plutonium Oxide in Beagles - J. F. Park, A. C. Case, D. L. Catt, S. L. Klopfer, G. E. Dagle, T. C. Kinnas, R. M. Madison, G. J. Powers, H. A. Ragan, S. E. Rowe, R. E. Schirmer, D. L. Stevens, C. R. Watson, and E. L. Wierman 66

Hematologic Changes in Plutonium-Exposed Beagles with Lung Tumors - H. A. Ragan, K. H. Debban, A. L. Slavich, and J. F. Park 74

Distribution of Plutonium Between Bone and Marrow - B. J. McClanahan 79

INHALED PLUTONIUM NITRATE IN DOGS 81

Dose-Effect Studies with Inhaled Plutonium Nitrate in Dogs - G. E. Dagle, W. C. Cannon, A. C. Case, S. L. Klopfer, T. C. Kinnas, R. M. Madison, J. F. McShane, G. J. Powers, H. A. Ragan, S. E. Rowe, R. E. Schirmer, D. L. Stevens, and E. L. Wierman 81

Interactive Plotting for the Novice - C. R. Watson, P. R. Nicholson, and G. R. Johnson 86

INHALED TRANSURANICS IN RODENTS 88

Inhalation Carcinogenesis of Repeated Exposures to High-Fired $^{239}PuO_2$ in Rats - C. L. Sanders and J. A. Mahaffey 88

Effect of Vitamin C on Pulmonary Carcinogenesis from Inhaled $^{239}PuO_2$ - C. L. Sanders 90

Pulmonary Cell Turnover Following Inhalation of $^{239}PuO_2$ - K. Rhoads and C. L. Sanders 91

Effect of Prior Neutron or Gamma Irradiation on Pulmonary Clearance of $^{239}PuO_2$ - K. Rhoads, J. P. Geraci, and C. L. Sanders 93

Effect of Lung Damage Caused by Intratracheally Instilled $^{239}PuO_2$ and Volcanic Ash on the Alveolar Clearance of ^{14}C-Benzo[a]pyrene - R. A. Gelman, C. L. Sanders, and A. W. Conklin 95

Effect of Amount of Deposited ^{239}Pu on the Alveolar Clearance of ^{237}, $^{239}PuO_2$ - C. L. Sanders and A. W. Conklin 97

Statistical Considerations for a Low-Dose $^{239}PuO_2$ Inhalation Experiment - J. A. Mahaffey and C. L. Sanders 98

Inhalation Carcinogenesis of High-Fired $^{241}AmO_2$ - C. L. Sanders and J. A. Mahaffey 100

Inhalation Toxicology of $^{241}Am(NO_3)_3$ - J. E. Ballou, R. A. Gie[illegible], H. D. Tolley, and R. A. Miller 102

Influence of Dose Protraction and Age on Lung and Bone Tumorigenesis from Inhaled $^{244}CmO_2$ - C. L. Sanders and J. A. Mahaffey 105

CIGARETTE SMOKE AND PLUTONIUM 107

The Effect of Cigarette Smoke Exposure on Clearance of $^{239}PuO_2$ from the Lungs of Beagle Dogs - R. E. Filipy, J. L. Rappin, D. [illegible] Stevens, and W. J. Bair 107

The Impairment of Pulmonary Clearance of $^{239}PuO_2$ in Rats by Prolonged Exposure to Cigarette Smoke - R. E. Filipy, J. L. Rappin, D. [illegible] Stevens, and W. J. Bair 110

TOXICOLOGY OF PLUTONIUM - SODIUM 113

Techniques for Generation of LMFBR-Fuel-Sodium Aerosols - J. K. Briant and M. C. Allen 113

Chemical Studies of LMFBR-Fuel-Sodium Aerosols - L. G. Morgan, J. [illegible] Ryan, and J. K. Briant 114

Biological Behavior of LMFBR-Fuel-Sodium Aerosols in Rodents - P. L. Hackett, D. D. Mahlum, R. L. Music, and J. K. Briant 116

Biological Behavior of Inhaled LMFBR-Fuel-Sodium Aerosols [illegible] - P. L. Hackett, A. J. Clary, D. D. Mahlum, J. K. Briant, D. [illegible] Catt, and L. R. Peters 119

Gastrointestinal Absorption of Suspensions of LMFBR-Fuel-Sodium Aerosols in Rodents - P. L. Hackett, R. L. Music, J. K. Briant, and D. D. Mahlum 122

TOXICOLOGY OF SODIUM AND LITHIUM 124

Toxicology of Sodium Metal Combustion Aerosols - R. H. Busch, K. E. McDonald, and J. K. Briant 124

Monitoring Aerosols of Sodium Metal Combustion - J. K. Briant 127

INHALATION HAZARDS TO URANIUM MINERS 130

Influence of Radon-Daughter Exposure Rate and Uranium Ore Dust Concentration on Occurrence of Lung Tumors - F. T. Cross, R. F. Palmer, R. H. Busch, and R. L. Buschbom 130

Histopathologic and Physiologic Investigation of Lungs of Dogs Exposed to Uranium Ore Dust - F. T. Cross, R. E. Filipy, S. M. Loscutoff, R. F. Palmer, and R. H. Busch 133

TOXICOLOGY OF KRYPTON-85 136

Effects of Chronic ^{85}Kr Exposure in Rats - D. H. Willard, H. D. Tolley, and J. E. Ballou 136

Effects in Newborn Rats Exposed to ^{85}Kr Atmospheres - J. E. Ballou and H. S. Deford 138

TOXICITY OF THORIUM-CYCLE NUCLIDES 140

Analysis of ^{231}Pa in Biological Samples - R. A. Gies, J. E. Ballou, and J. T. Ryan 140

Disposition and Late Effects of Inhaled $^{233}UO_2(NO_3)_2$ and $^{233}UO_2(NO_3)_2$ in Rats - J. E. Ballou, R. A. Gies, J. E. Jagle, H. D. Tolley, and R. C. Case 142

Distribution of ^{232}U Decay Products from the Lung of the Rat - J. E. Ballou, D. L. Haggard, and D. W. Murphy 146

Early Disposition of Inhaled ^{231}Pa Citrate - R. A. Gies, J. E. Ballou, and J. T. Ryan 149

FETAL AND JUVENILE RADIOTOXICITY 151

Effects of Monomeric ^{239}Pu on the Pregnant Rabbit - B. J. Kelman, M. R. Sikov, and P. L. Hackett 151

Effects of Monomeric ^{239}Pu on the Fetal Rabbit - B. J. Kelman, M. R. Sikov, and P. L. Hackett 153

Movements of Monomeric ^{239}Pu Across the Hemochorial Placenta of the Guinea Pig - B. J. Kelman 155

Artificial Insemination of Rabbits for Use in Teratological Evaluations - B. J. Kelman and L. F. Montgomery 158

Interactions of Animal Age and Particle Size with Deposition and Retention of Inhaled ^{51}Cr-Labeled Microspheres - P. L. Hackett, M. R. Sikov, W. E. Skien, W. C. Cannon, and R. L. Music 160

Effects of Prenatal Irradiation on Postnatal Brain Enzyme Ontogeny in Rats - F. D. Andrew, P. S. Lytz, and K. A. Poston 164

Sometimes Fatal Lesions - D. B. Carr and D. L. Stevens 168

MODIFYING RADIONUCLIDE EFFECTS 170

Reproduction After Administration of ^{239}Pu to Nulliparous, Pregnant or Lactating Rats - V. H. Smith, D. D. Mahlum, J. O. Hess, and M. R. Sikov . . 170

Relative Contribution of Cross-Placental Transfer and Nursing Pu Burdens in Rat Pups - V. H. Smith, D. D. Mahlum, and J. O. Hess 173

GUT-RELATED STUDIES OF RADIONUCLIDE TOXICITY 176

Effects of Fasting, Diet on "Biological Incorporation" on Absorption of Plutonium from the Gastrointestinal Tract - M. F. Sullivan 176

Absorption of Actinide Elements from the Gastrointestinal Tract of Neonatal Swine - M. F. Sullivan and L. S. Gorham 180

Long-Term Retention of Plutonium-239 Ingested by Neonatal Rats and Swine - M. F. Sullivan and L. S. Gorham 181

Influence of Oxidation State on Absorption of Inhaled Plutonium - M. F. Sullivan, J. L. Ryan, L. S. Gorham, and E. F. Blanton 183

Influence of Plutonium Mass on Absorption from the Gastrointestinal Tract of Adult and Neonatal Rodents - M. F. Sullivan 185

VIRAL AND RADIATION CARCINOGENESIS 187

In Vitro Evaluation of Cytotoxic and Mutagenic Potential of ^{244}Pu - M. E. Frazier, T. B. Andrews, Jr., and T. Samuel 187

Characterization of Porcine Radiation-Induced Viral DNA Polymerase - M. E. Frazier, L. P. Mallavia, M. J. Hooper, and M. V. Vicla 191

In Vitro Cell-Mediated Immunity in Beagle Dogs Exposed to $^{239}PuO_2$ - J. E. Morris, T. M. Graham, and J. F. Park 195

Bimodal Response of Canine Peripheral Blood Lymphocytes to Concanavalin-A - T. M. Graham and J. E. Morris 198

DEVELOPMENT OF BLOOD IRRADIATORS 201

Blood Irradiator Medical Applications - F. F. Hangate, W. D. Riemath, and L. R. Funne 201

FUSION

BIOLOGICAL EFFECTS OF MAGNETIC FIELDS 205

An Evaluation of Static Magnetic Fields on Mammalian Cell Cultures - M. E. Frazier, T. Samuel, and T. B. Andrews, Jr. 205

Environmentally Controlled Housing for Rodents for Exposure for Biomagnetic Studies - A. Nelson, E. G. Kuffel, and J. R. Decker 208

Effects of Combined Magnetic Field Exposure and Chemical Insult on Trout Development - W. A. Strand, C. S. Abernethy, R. G. Genoway, and J. R. Skalski 211

Molecular Biomagnetic Effects: Magnetophoresis of Solutes - D. R. Kalkwarf 213

OIL SHALE

HEALTH EFFECTS OF SYNTHETIC FUELS 217

Epidermal Carcinogenesis Studies in Mice of Materials from Several Fossil Fuel Technologies - R. A. Renne, L. O. Smith, and D. D. Mahlum 217

MULTITECHNOLOGY

TOXICOLOGY OF INHALED ACID AEROSOLS 223

Late Effects Following Exposure to Graded Doses of HNO_3, HCl or H_2SO_4 - J. F. Ballou, R. A. Gies, G. E. Dagle, and R. A. Miller 223

METAL-MEMBRANE INTERACTIONS 226

Purification of Extracellular Acid Protease from Neurospora crassa - W. G. Rhodes, R. A. Lindberg, and H. Drucker 226

Extracellular Modification of a Peptidase Precursor from Neurospora crassa - R. A. Lindberg, W. G. Rhodes, and H. Drucker 230

Characterization of External Phosphatase of VERO Cells - R. P. Schneider . . 233

[illegible] OF GEOTHERMAL EFFLUENTS 235

[illegible] of In Vitro Exposure to Hydrogen Sulfide on Rabbit Alveolar [illegible] Cultured on Gas-Permeable Membranes - A. V. Robinson 235

[illegible] Inhalation Toxicology of Hydrogen Sulfide and Ammonia in Rodents - [illegible] and K. E. McDonald 240

[illegible] of Mount St. Helens Ash on Cultured Rabbit Alveolar Macrophages - [illegible] Robinson 241

[illegible] STUDIES WITH INHALED PLUTONIUM IN BEAGLES 243

[illegible] 259

[illegible] 262

[illegible] . . . . . 25[illegible]

[illegible] AND DISTRIBUTION . . . . . 2[illegible]

1 Coal

COAL

Studies in the area of coal energy technology are relevant to potential occupational and environmental health concerns of coal combustion and coal liquefaction.

In the area of coal liquefaction a tiered testing approach is used, going from cellular systems to mammalian acute and chronic toxicity assays and examining systemic/mutagenic potential of materials that may be of occupational and/or environmental health concern.

Toxicologic studies deal with the potential hazard to miners of elements found in mine atmospheres, and with effects of inhaled heavy metals that may be present in fly ash. More basic studies consider the effect of the anemic state upon the translocation of heavy metals that may be released by coal combustion/processing, pharmacologic analyses of effects of aerosolized sulfuric acid and potential blockers of such effects. In addition, analysis of a basic lung process (phagocytosis of inhaled particulates) is being pursued.

• Inhalation Hazard to Coal Miners

Acceleration in coal mining activities to satisfy present and future energy needs may be constrained by potentially severe health hazards. Coal workers' pneumoconiosis (CWP), a chronic debilitating disease associated with coal mine dust, is one known entity; additional inhalation hazards may occur with the proposed extensive use of diesel engines in coal mines.

The objectives of this project are to evaluate the biological effects of specific mine air contaminants in experimental animals, and to study the progression of chronic respiratory pathologic changes that occur with coal dust and/or diesel exhaust inhalation.

PATHOLOGIC CHANGES ASSOCIATED WITH EXPERIMENTAL EXPOSURE OF RATS TO COAL DUST AND/OR DIESEL EXHAUST

Investigators: R. H. Busch, E. Filipy, M. T. Karagianes, and R. F. Palmer

Male Wistar rats exposed to bituminous coal dust [considered to have high potential for induction of coal workers' pneumoconiosis (CWP)] and/or diesel exhaust developed lesions similar to those of simple CWP, as described in human subjects. Focal bronchiolization of alveolar epithelium, though not observed in human CWP, was found, to some extent, in all groups except controls.

Pneumoconiosis resulting from exposure to coal dust and other types of carbon is a significant occupational hazard to individuals working in areas with high concentrations of aerosolized dust composed of such materials. The pathologic changes occurring in affected individuals have been characterized in detail, and several stages of the disease have been described. Like many occupation-related diseases, the condition is seldom uncomplicated. Following necropsy of rats exposed to coal dust and/or diesel exhaust (experimental protocol described in another article), lung sections were prepared for examination by both dissecting and light microscopy, the latter aided by polarized light to facilitate identification of collagen and silicon particles.

Examination of lung slices by dissecting microscopy revealed that focalization of black coal dust and/or soot had occurred after 4 mo of aerosol exposure. Histologic examination of H&E-stained sections confirmed that the deposited particulate material was contained almost entirely within the cytoplasm of alveolar macrophages. Macrophages were so burdened with the material that cellular detail was obscured (Figure 1).

By using polarized light, it was demonstrated that silica particles (much fewer in number than coal particles) were also contained within the macrophages (Figure 2). Particulate material tended to accumulate at the level of the terminal bronchiole, following the airway to the respiratory bronchiole and alveolar duct. The deposited dust/soot extended along the adjacent alveolar septa and accumulated within adjacent alveolar sacs. Adjacent lymphatics and small blood vessels were usually cuffed by macrophages laden with particulate material (Figure 3). Adjacent to the bronchiole, within the focus of macrophage accumulation (macule), alveoli appeared distended and disrupted (centrilobular emphysema).

In animals exposed for long periods, deposits of dust and/or soot were similarly located, but were larger in size and shape. Generally, early (4-mo) macules were less than 1 mm in diameter; in animals exposed for 20 mo, the lesions were 1-3 mm in size and quite often appeared to coalesce.

Increased reticulin content was evident in macules of animals exposed for 4 mo; in animals exposed longer, both interstitial reticulin and collagen were increased. These increases, as well as hypertrophy and hyperplasia of alveolar epithelial cells, contributed to focal thickening of alveolar septa. Alveolar macrophages were

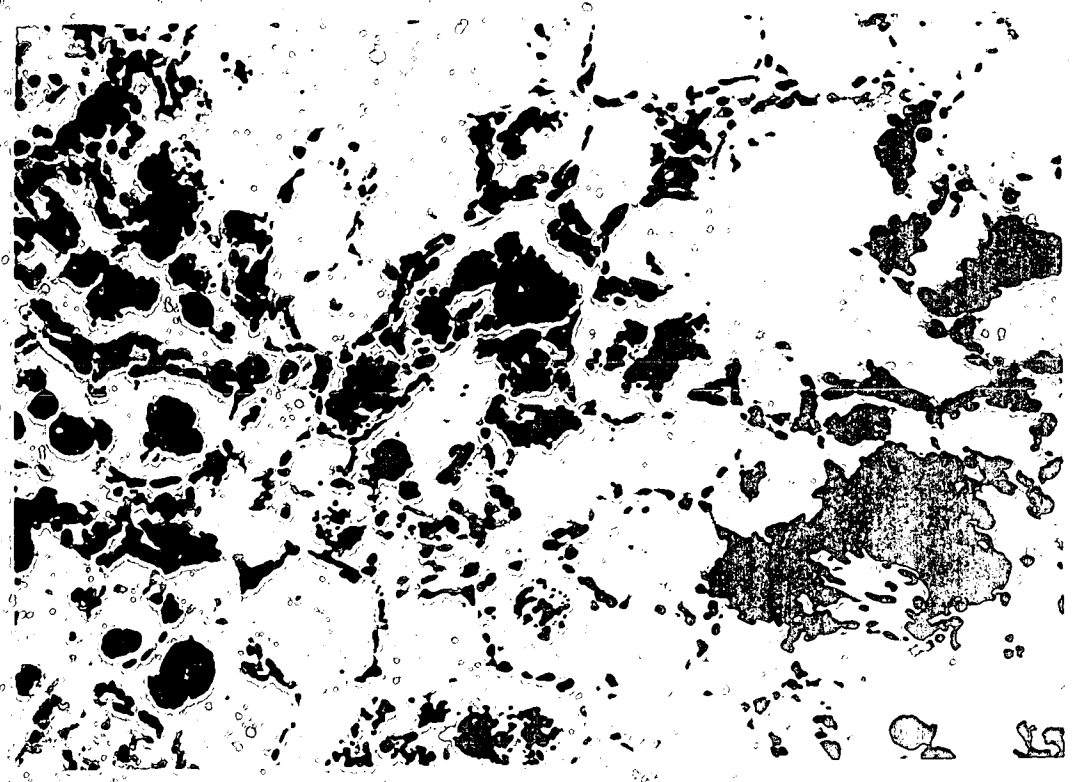

FIGURE 1. Lung of Rat Exposed to Coal Dust Aerosol for 20 Months. Coal particle accumulations within macrophages totally obscure cellular detail. (H&E, 80X)

closely associated with the alveolar walls, as well as being free within the alveoli. The overall effect of the cellular proliferation and accumulation was to produce macules which appeared to be denser and larger in the animals exposed over longer periods. Additionally, the dust-laden macrophages appeared in alveoli progressively further from the bronchioles. Emphysema associated with the larger macules of longer-exposed animals involved nearly all alveoli which contained particulates, becoming panacinar in these animals.

In animals exposed for 20 mo, several focal lesions of different character had developed adjacent to or even within the macules. These lesions consisted of focal epithelial changes commonly referred to as bronchiolization, in which the simple squamous epithelial lining of alveoli had transformed to a cuboidal type that resembled the nonciliated portion of the terminal and respiratory bronchiolar epithelium. Often, alveoli which had undergone this change contained macrophages with very dense accumulations of dust and/or soot.

The components of the focal lesions included macrophages laden with dust or soot, alveolar septa thickened by increased reticulin and collagen, and emphysema. These lesions resemble those of simple CWP as described in humans. Also similar to the disease in man are the progression (increase) of size, change of shape (becoming stellate) and increase in density of lesions as exposure time lengthened. The macule in the rat, as in man, commences formation at the level of the division of terminal bronchioles into respiratory bronchioles, then proceeds peripherally into the alveoli.

Emphysema appeared to develop and expand in concert with the progress of macule development, being centrilobular in shorter-duration macules and panacinar in longer-exposed animals.

It was observed that in the experimentally exposed rats, lesions had not progressed beyond the macule stage to the other types described in human CWP (e.g., micronodule, macronodule, silicotic nodule, progressive massive fibrosis, Caplan's lesion and infective granuloma). These larger, more-severe lesions may be the result of longer exposure periods and/or the combined effect of longer

exposure periods and additional etiologic agents. Furthermore, the difference may be partly due to a difference in the response of rat vs. human lungs to such materials.

The possibility that one or more of the advanced lesion types might develop with longer exposure periods (or that they may be the result of additional agents) can only be tested by appropriate experiments. Although silica was demonstrated within the experimentally produced lesions in our experiments, its role in their genesis was not determined.

The experimental disease resulting from exposure to coal dust and/or diesel exhaust, as observed in rats in this study, differs from descriptions of human CWP in at least one aspect: the association of focal bronchiolization of alveolar epithelium with macules found in the longer-exposed animals. Focal bronchiolization has been described as part of the proliferative tissue response of rats to other aerosols, including certain inhaled radionuclides. The lesion has also been observed in hamsters. We have not been able to identify any morphologic difference between the focal bronchiolization occurring in coal-dust- and/or diesel-exhaust-exposed rats and that occurring in rats exposed to certain other aerosols, i.e., uranium ore dust, $^{238}PuO_2$, nickel oxide, ^{210}PO, and DTPA.

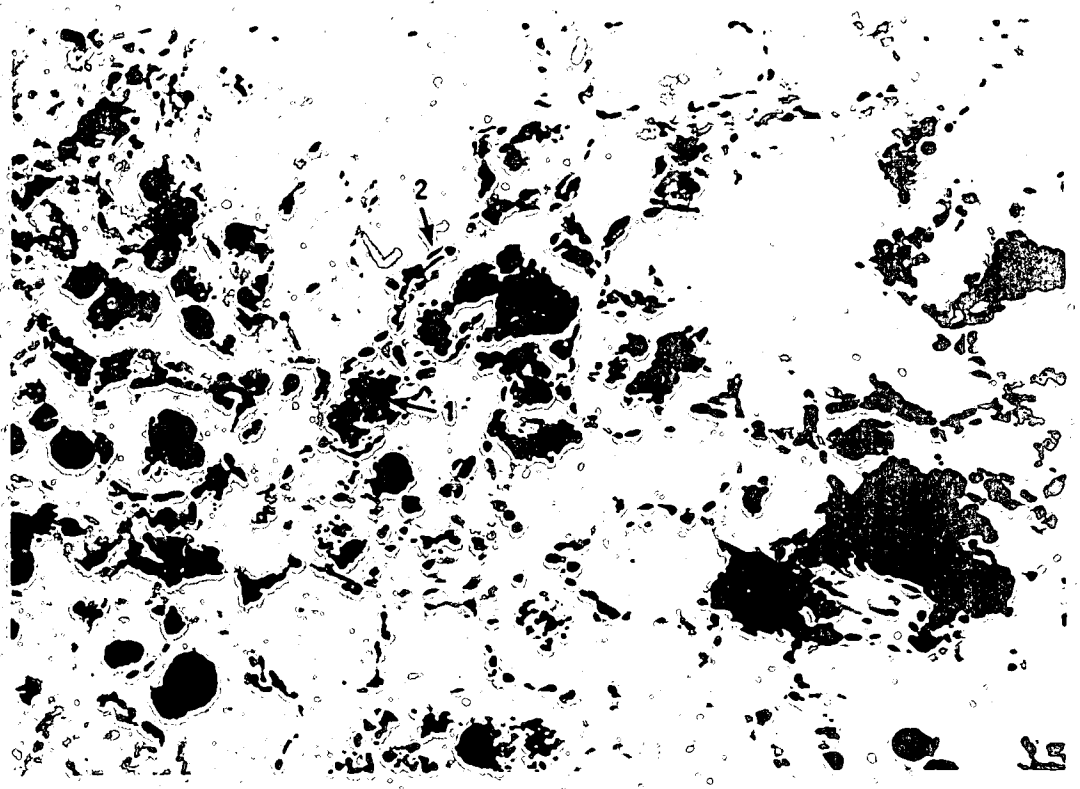

FIGURE 2. Same Field as Figure 1, Under Polarized Light. The bright points (1) are silica particles. Refractile structures within alveolar septa (2) are collagen. (H&E, 80X)

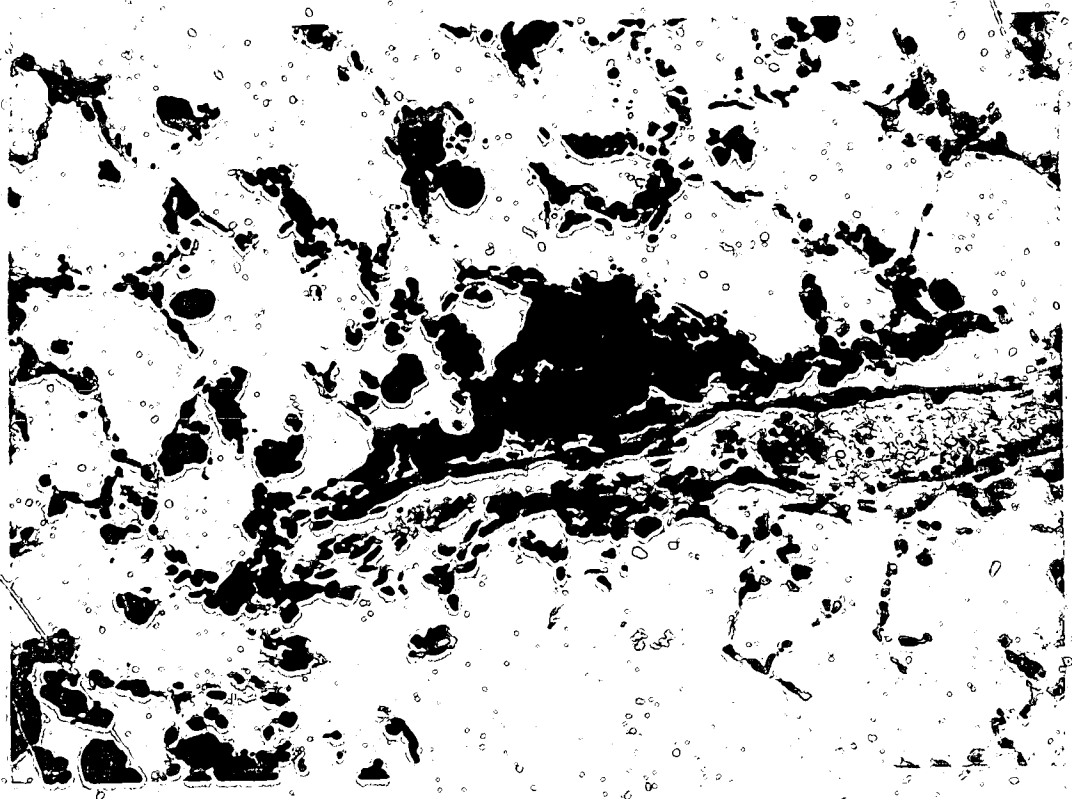

FIGURE 3. Lung of Rat Exposed to Coal Dust Aerosol for 20 Months. Particles tend to accumulate adjacent to vessels (shown), bronchioles and lymphatics. (H&E, 650X)

BIOLOGICAL EFFECTS OF CHRONIC INHALATION OF COAL MINE DUST AND/OR DIESEL ENGINE EXHAUST IN RODENTS

Investigators: M. T. Karagianes, R. C. Palmer, and R. H. Busch

Rats were exposed to coal dust and diesel exhaust emissions, separately and in combination, for 20 mo to evaluate the potential health effects of these mine air materials. The diesel exhaust was produced by an engine operated in a load/no-load mode and acceleration/deceleration cycle. It was also modified to simulate an inefficiently tuned engine. Exposure to coal dust was performed in a whole-body, cooled inhalation system. Mortality, body weight and hematologic parameters examined were normal compared with those of control rats. Lesions observed were primarily restricted to the lungs and were similar to those described for simple coal workers' pneumoconiosis (CWP). Lesion progression and severity were related to exposure duration and exposure material. Alveolar bronchiolization, though not reported in human CWP, was present in the lungs of some rats in all exposure groups except the control.

We described the development and operation of an automated diesel-engine exhaust exposure system, and of a whole-body rodent coal dust inhalation exposure system in a previous Annual Report (1977). These integrated systems have allowed us to study the biological effects of inhaled coal dust, diesel exhaust, and a combination of these aerosols (Table 1).

In addition to monitoring the chamber parameters described in Table 1, the experimental animals were weighed every 2 wk. Hematologic analysis was used to determine general health and specific blood cell response. Six animals per group were periodically killed to observe progression of possible pulmonary disease. Aerosol particle size distribution and concentrations were monitored in all exposure chambers.

Rats (six per exposure group; 30 per time interval) were killed at 4, 8, 16 and 20 mo after initiation of exposure. Additional animals were killed at 24 and 28 mo (4 and 8 mo recovery time after 20 mo of exposure) to examine the possibility of further progression of lung lesions or, possibly, of tissue repair.

Exposure to coal dust or to diesel engine exhaust, either singly or in combination, caused no significant effect on body weight or on mortality patterns of exposed animals when compared to control rats. The control and exposure groups had nearly identical weight records up to 20 mo postexposure.

Examination of blood samples taken from all rats killed at 4, 8, and 16 mo of exposure revealed no significant changes in hematocrit, erythrocyte or differential leukocyte counts, or proteins (as determined by serum electrophoresis) when compared to samples from control animals. Carboxyhemoglobin (COHb) levels were measured at the same exposure intervals, but only on the control animals and animals exposed to diesel exhaust plus coal dust or diesel exhaust alone. In general, COHb levels in the two groups exposed to diesel exhaust were approximately 2½ times greater than those in the control group.

TABLE 1. Experimental Protocol for Exposing Rats to Coal Dust and/or Diesel Exhaust.

Group	Exposure Regimen	Concentration, mg/m³
1	Diesel Engine Exhaust	8.3 - 20 Soot
2	Diesel-Engine Exhaust Plus	8.3 - 20 Soot
	Low-Concentration Coal Dust	5.8 - 15
	Total Particulate	13.5 - 4.0
3	Low-Concentration Coal Dust	6.6 - 1.9
4	High-Concentration Coal Dust	14.9 - 6.2
5	Control	Room Air

(a) 6 hr/day, 5 day/week, 40 rats/group
(b) Mean ± standard deviation over 20 mo

Chamber parameters measured:

1. CO (continuous monitoring)
2. Respirable and total coal or soot mass concentrations
3. Aerosol particle size distributions
4. NO, NO_2 and SO_2 in diesel exhaust fume chambers
5. Temperature and humidity in all chambers

Significant lesions found at gross examination were restricted, for the most part to the lungs of animals from all exposure groups except the controls, which appeared normal in most cases. Lungs of coal-dust-exposed rats had a black mottled or speckled appearance as a result of dust particle aggregation interspersed throughout the normal (pink) lung tissues. Lungs of animals exposed to high coal-dust concentrations had more pronounced lesions than those in the low-concentration coal group and, in general, the degree of severity in both groups was related to the length of exposure, i.e., mild at 4 mo, moderate at 20 mo of exposure.

Lungs from rats exposed to diesel exhaust, or diesel exhaust plus coal dust, were similar to each other in appearance and showed a more diffuse, blacker coloration than those of animals exposed to coal dust only. Again, lesion severity was related to exposure length: 20-mo exposures resulted in almost entirely black lungs, while 4-mo exposures produced much less discoloration.

In general, histopathologic examination of the rat lungs of all groups except controls showed exposure-related lesions (Figure 1) indicative of simple CWP, including: accumulation of black aggregates of inhaled particles in alveolar macrophages, alveolar histiocytosis, interstitial fibrosis, and alveolar emphysema.

The severity of these lung lesions was graded on a 0 to 4 basis: 1, trace; 4, severe. The lesions found in all exposure groups at all sacrifice times ranged from 0 to 3+, with one exception: grade 4 alveolar cell hypertrophy in one rat. Lesions in animals exposed for 20 mo were more pronounced than those in rats exposed for shorter periods; those in animals exposed for 4 mo were the least noticeable. The most extensive lesions, which were similar to each other in grade of severity, occurred in rats exposed to diesel exhaust plus coal dust, diesel exhaust only, and high-concentration coal dust. Rats in the low-concentration coal dust group showed similar but less extensive lesions, regardless of the length of exposure.

FIGURE 1. Micrograph of Lung Section of Rat Exposed to Diesel Exhaust for 20 Months. Particulate material is aggregated adjacent to a terminal bronchiole (T) at the junction with the short respiratory bronchiole (R). Alveolar histiocytosis is seen within alveoli with thickened septa (H&E, 165X).

Statistical analysis of the scoring data indicated no significant lesion severity difference at the 0.05 level of significance among the diesel exhaust, diesel exhaust plus coal dust, and high-concentration coal dust exposure groups.

Although alveolar bronchiolization is not present in simple CWP in humans, it was a significant finding in all exposed groups, but not in controls. Progression of this lesion was definitely related to length of exposure time and exposure group: it was observed in only two animals after 4 mo exposure, but was more frequent and extensive at 8 and 16 mo, and was most pronounced after 20 mo exposure. It was observed in six of six rats exposed to diesel exhaust plus coal dust, four of six exposed to diesel exhaust only, five of six exposed to high concentrations of coal dust, and in three of six exposed to the low level of coal dust. Severity grades ranged from 0-3 in all groups. Pathological descriptions of the CWP-type lesions and alveolar bronchiolization seen in the lungs of these rats is discussed in another article in this report.

No malignant respiratory tract tumors were found in any of the exposure groups on this study. A compilation of all tumors observed was included in the 1979 Annual Report. There were no significant exposure-related lesions found in the nasal turbinates, larynx, trachea, esophagus, nasal cavity or stomach of any rats examined.

Rats killed at 4 and 8 mo (after 20-mo exposures were completed) showed lung lesions similar to those of their respective groups after 20 mo of exposure. While no tissue repair had occurred, lesions had not worsened.

MAXIMAL EXPIRATORY-FLOW-VOLUME RELATIONSHIPS AND LUNG VOLUMES IN NORMAL AND ELASTASE IMPAIRED RATS

Investigators: P. J. Mihalko, R. F. Palmer, and M. T. Karagianes

Technical Assistance: S. D. Harris, B. Holloway, and L. A. McGee

To determine whether impaired pulmonary function is an additional risk factor in the occupational exposure of workers to mine-air contaminants, an elastase-induced obstructive lung lesion was produced in Sprague-Dawley rats prior to their exposure to coal dust and diesel engine exhaust. Measurements of selected lung function parameters from the impaired animal group were compared with the same measurements from a control group. Both groups are now being exposed to diesel engine exhaust and coal dust.

Mature male Sprague-Dawley rats (average body weight, 466 ± 33 g) were treated with intratracheally instilled purified porcine pancreatic elastase (Sigma Chemical Company, St. Louis, MO) dissolved in saline (250 IU/cm^3 saline). Sixty animals were treated with 50 IU/100 g body weight. Because 38% of that group died within 24 hr, an additional 22 animals were treated with 30 IU elastase/100 g body weight. Acute mortality from that treatment was reduced to 8%. These treatment-related mortality rates are higher than those in other studies recently performed at this laboratory. The differences may be due to variations in the effective enzymatic activity between different lots of the enzyme, differences in the ratio of lung size to body weight (as a function of species and/or age), or combinations of these factors.

Twelve wk after elastase treatment, an automatic system for producing repeatable, forced vital-capacity maneuvers in anesthetized rodents (described elsewhere in this Annual Report) was used to measure selected lung function parameters of the test animals. The rats were anesthetized with a metofane/ (Pitman-Moore, Washington Crossing, NJ) nitrous oxide/oxygen mixture, adjusted to maintain a spontaneous respiratory rate of ~90 breaths per minute (bpm). The anesthetized animals were transorally intubated with a large-bore, rigid-walled endotracheal tube (2.4 mm ID) to insure the production of maximal expiratory flow and demonstration of physiologic expiratory flow limitation. All animals underwent the series of respiratory testing maneuvers in the same sequence. Spirometric lung volumes were measured first, followed by a passive expiration from 100% vital capacity to functional residual capacity. Functional residual capacity was then determined by a modified Boyle's Law technique (active inspiratory effort against an occluded airway). The testing sequence was completed by three forced vital-capacity maneuvers at a negative driving pressure for expiration of -35 cm H_2O.

Table 1 is a summary of the descriptive statistics and results of t tests between the normal and elastase-treated groups. The measured increases in functional residual capacity and vital capacity of the elastase-treated rats are characteristic of an emphysema-like condition, with attendant reductions in alveolar numbers, lung elastic recoil, and increases in terminal airspace size. Although substantially increased residual volume indicates abnormal gas trapping at low lung volumes, both this measurement and total lung capacity are derived from the direct measures of functional residual capacity. Reduced lung recoil at high percentages of the vital capacity are further demonstrated by the lower maximal expiratory flows, and flows at 80% of vital capacity in elastase-treated animals. Reduced flows at lower lung volumes result from the accelerated movement of the sites of expiratory flow limitation to peripheral airways. The emphysema-like condition reduces the radial traction on peripheral airways, usually provided by a normal interstitial matrix. As a result, a greater proportion of the pressure needed to drive expiratory flow is dissipated in overcoming frictional resistance, and flow limitation occurs in more-peripheral airways having lower innate tube wave speeds. There were no significant differences in any of the measured or derived parameters between the rats surviving treatment with 50 units/100 g body weight and those treated with 30 units/100 g body

TABLE 1. Descriptive Statistics and *t* Tests Between Normal and Elastase-Treated Rats[a].

	Normal, n = 60	Elastase, n = 60	t	P
Body Weight (g)	673 ± 69.9	657 ± 67.5	-1.172	0.2443
Respiratory Rate (breaths/min)	93.7 ± 24.2	89.0 ± 25.0	-1.024	0.3082
Tidal Volume (cm^3)	2.5 ± 0.5	2.7 ± 0.7	1.676	0.1010
Vital Capacity (cm^3)	18.5 ± 2.6	20.0 ± 2.5	3.212	0.0017
Inspiratory Reserve Capacity (cm^3)	15.8 ± 2.7	16.5 ± 2.3	1.469	0.1447
Functional Residual Capacity (cm^3)	5.7 ± 1.1	7.0 ± 1.3	5.328	0.0000
Expiratory Reserve Volume (cm^3)	2.0 ± 1.0	2.1 ± 1.1	0.537	0.5925
Total Lung Capacity (cm^3)[b]	21.5 ± 3.0	23.5 ± 2.7	3.880	0.0002
Residual Volume (cm^3)[c]	3.7 ± 1.2	4.9 ± 1.6	4.772	0.0000
Time Constant of Passive Expiration (sec)	0.323 ± 0.07	0.345 ± 0.07	1.529	0.1289
Maximal Expiratory Flow Rate "$\dot{V}_{max}$" (cm^3 sec^{-1})	157.1 ± 17.3	143.6 ± 18.5	-4.135	0.0000
Expiratory Flow at 80% Vital Capacity "$\dot{V}_{80}$" (cm^3 sec^{-1})	120.2 ± 22.7	102.9 ± 18.2	-4.597	0.0000
Expiratory Flow at 60% Vital Capacity "$\dot{V}_{60}$" (cm^3 sec^{-1})	78.5 ± 16.9	61.7 ± 12.1	-6.278	0.0000
Expiratory Flow at 50% Vital Capacity "$\dot{V}_{50}$" (cm^3 sec^{-1})	58.6 ± 13.2	42.8 ± 9.9	-7.232	0.0000
Expiratory Flow at 30% Vital Capacity "$\dot{V}_{30}$" (cm^3 sec^{-1})	9.62 ± 4.5	7.7 ± 2.9	-2.769	0.0067

(a) Values are mean ± SD
(b) Derived lung volume from IRC + FRC
(c) Derived lung volume from FRC - ERV

TABLE 2. Exposure Conditions.

Chamber	Number of Rats	Conditions[a]
I	10 Normal 10 Elastase 5 Untested Normal	Unscrubbed, Diesel Exhaust 50 ppm CO, ~10 ppm NO_x ~27 mg/m³ Soot, MMAD[b] = 0.33 µm, GSD[c] = 3.67
II	10 Normal 11 Elastase 2 Untested Normal	Unscrubbed, Diesel Exhaust 50 ppm CO, 10 ppm NO_x Pittsburgh Montour #4 Coal Dust Total Particulates ~37 mg/m³ MMAD = 0.50 µm, GSD = 5.02
III	12 Normal 13 Elastase 6 Untested Normal	Pittsburgh Montour #4 Coal Dust Total Particulate ~20 mg/m³, MMAD 2.31 µm, GSD = 1.99
IV	13 Normal 11 Elastase 3 Untested Normal	Filtered Room Air

(a) 6 hr/day, 5 days/week
(b) Mass Median Aerodynamic Area, determined by Andersen cascade impactor techniques
(c) Geometric Standard Deviation
(d) Ground for 14 hr under a 100% nitrogen atmosphere

weight of elastase in saline.

Pre-exposure lung function testing caused death by asphyxiation of ~25% of the animals in each group, apparently due to laryngospasm and laryngeal edema from trauma. Histopathologic evaluation of the lungs revealed no peripheral trauma that could be attributed to the testing procedures. It is possible that the use of a volatile anesthetic agent, or variations in oropharyngeal flora among animals predisposes this percentage of animals to laryngospasm and edema. In any case, transoral intubation with the large-bore, rigid endotracheal tube (necessary to insure maximal expiratory flow rates) triggers the reactions. Further study should be directed toward reducing this disconcertingly high mortality rate.

The remaining 90 animals were randomly assigned to the exposure groups shown in Table 2. The diesel-exhaust and coal-dust-exposure system used is the same that has been described in a previous Annual Report (1977), with one exception: new Battelle-designed chambers replaced the spherical lucite chambers. Also, [illegible] tested, normal rats were added to the chambers to act as testing controls.

The animals will undergo whole-body inhalation exposure for 10 wk, 5 days per wk, 6 hr per day. After this period, the previously described testing regime will be repeated, using the same anesthetic agent, lung inflation and driving pressures, and measurement sequence.

AUTOMATIC GENERATION OF REPEATABLE, FORCED VITAL-CAPACITY MANEUVERS IN ANESTHETIZED RODENTS

Investigators: P. J. Mihalko, E. G. Kuffel, and J. R. Decker

Technical Assistance: S. D. Harris

The respiratory function of workers receiving occupational exposure to potentially toxic materials, such as coal dust, diesel exhaust and other environmental pollutants, is evaluated primarily with forced vital-capacity measurements and spirometric lung volumes. This report describes development of our automatic system for generating the respiratory maneuvers that yield these measurements in anesthetized rodents.

Forced vital-capacity maneuvers (FVCMs) quantitate characteristics of lung function that are sensitive to airway and parenchymal pathology. These maneuvers consist of full lung inflation, followed by complete exhalation with maximal effort and speed. During the FVCM, expiratory flow rate is measured and recorded with respect to the decreasing lung volume. The resulting maximal expiratory flow-volume curve (MEFV) reflects the ability of the large, intermediate, and small airways to conduct gas flow.

We have designed and fabricated an automatic system for generating these maneuvers in anesthetized laboratory rodents. The system inflates the animal's lungs to a desired transpulmonary pressure (~25 cm H_2O), briefly maintains that inflation pressure to allow for stress-relaxation, then rapidly deflates the lungs with a preselected negative airway pressure (-35 cm H_2O). It produces repeatable MEFV curves, and is also capable of generating maneuvers for measurement of standard spirometric lung volumes.

Figure 1 is a diagram of the components of this system. Of particular interest are the small-animal plethysmograph, the quick-acting, minimal-deadspace respiratory valve and valve manifold,* and the electronic comparator/controller. The plethysmograph is a Setra (Natick, MA) 239e differential pressure transducer (±0.01 psi), connected to two enclosed lucite tubes whose volumes are nearly equal when a rodent occupies one of the tubes. Each tube has a 1-in.-diameter hole covered with three layers of 400-mesh stainless steel screen. As a flow transducer, the plethysmograph offers a resistance of 0.0017 cm H_2O/ml-sec^{-1} (±0.0001 SD) between zero and ±500 ml · sec^{-1}. Preliminary calculations indicate that its amplitude and phase fidelity extend above 15 Hz using Fry's single-degree-of-freedom, distributed-gage probe approximation (D. L. Fry, Phys. Rev. 40: 753-787, 1960.)

Eupnic and maximal respiratory flows are measured directly as the output of the plethysmograph pressure transducer. This analog signal is also processed by a Grass (Quincy, MA) 7P10B integrator providing a measure of the changes in thoracic gas volume (ΔV_T). Because of the linearity and sensitivity of the plethysmograph, changes in thoracic gas volume of as little as 0.1 ml can be recorded. This allows the direct measurement of ΔV_T during the Boyle's Law maneuver (inspiratory effort against an occluded airway) used to determine Functional Residual Capacity (FRC).

The respiratory valve used to separate the animal's airway from the negative-pressure reservoir operates on the principle of a Starling Resistor (Figure 2,A). In the closed position, positive pressure (~2 psi) inside the rigid tube completely compresses the flexible inner tube. When the two-way solenoid valve is switched, the interior of the rigid tube is quickly evacuated, pulling the flexible inner tube open. This creates a short, wide channel for the passage of the animal's respiratory gas into the evacuated reservoir. The deadspace of this valve is approximately 0.44 ml. The pressure drop across the valve is equal to -0.25 + 0.0045 (ml · sec^{-1} flow) for flows between 0 and 300 ml · sec^{-1} (r^2 = 0.98). At a driving pres-

*Designed and fabricated for a Battelle, Pacific Northwest Laboratories' project.

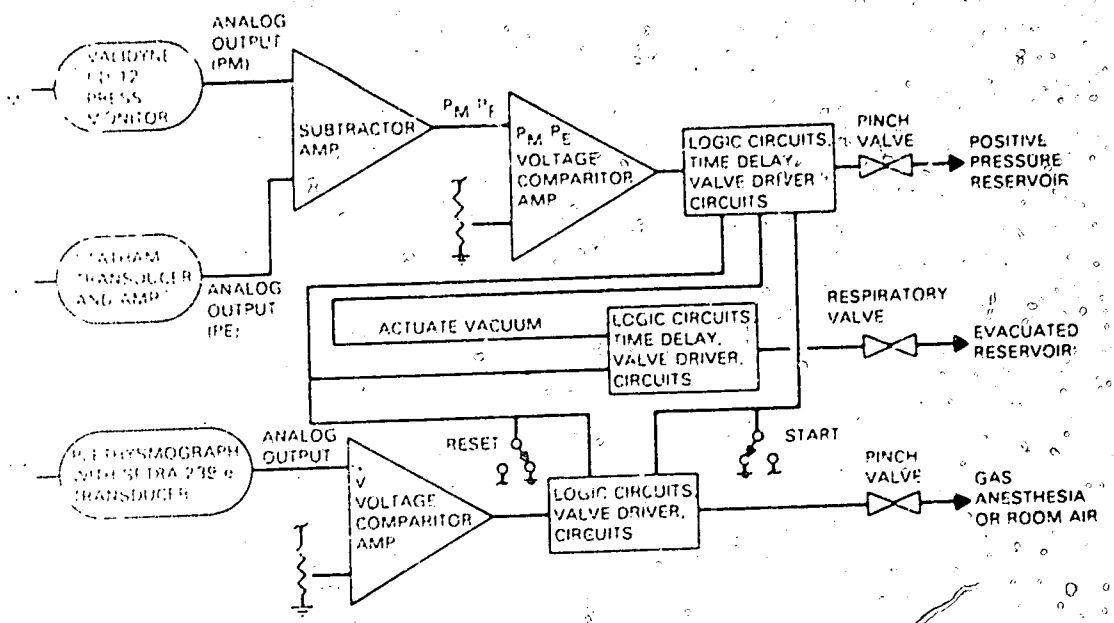

FIGURE 1. Block Diagram of Automatic EVGM System.

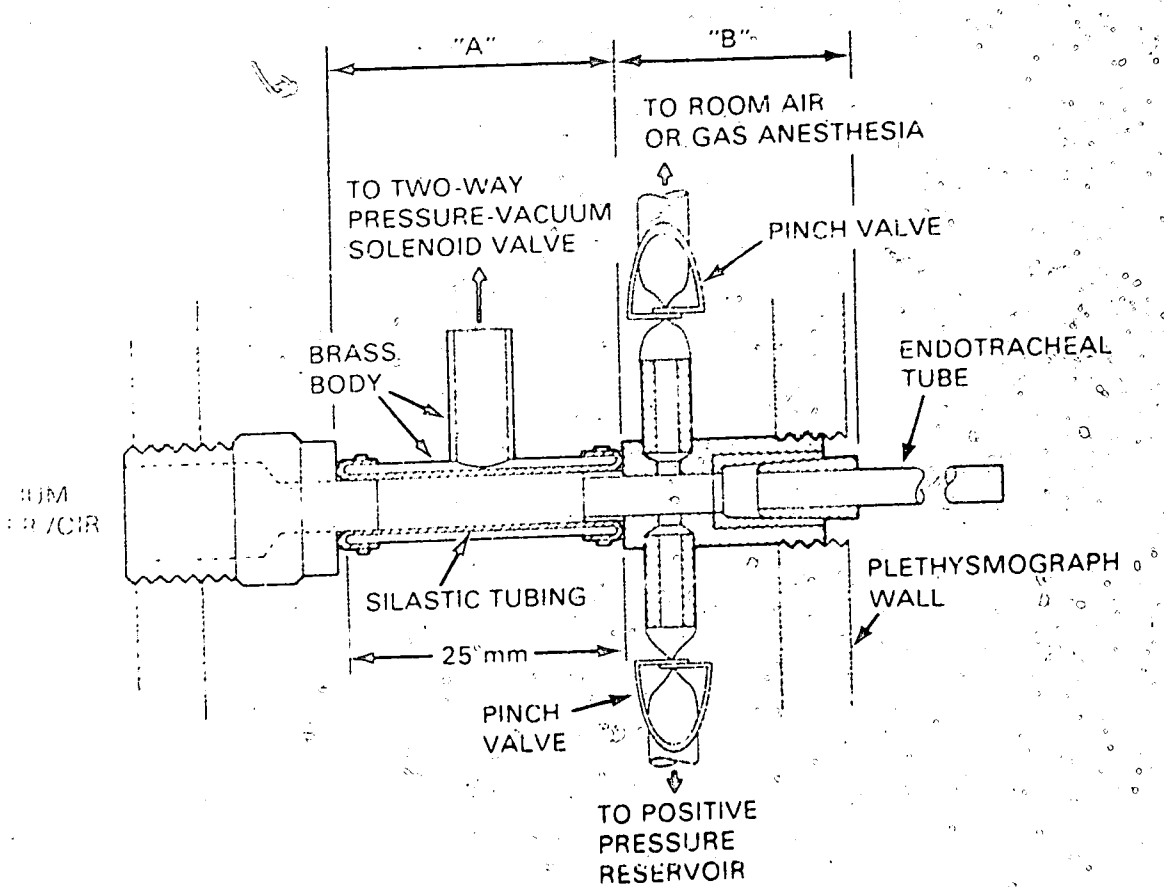

FIGURE 2. Respiratory Valve and Valve Manifold.

sure of 35 cm H_2O, peak flow rates of >200 ml · sec^{-1} through the valve are reached in less than 50 msec after valve activation.

Figure 2,B illustrates the manifold to which the respiratory valve, two commercially available pinch-type solenoid valves, and the animal's endotracheal tube are connected. The valve manifold screws into the faceplate of the plethysmograph and accepts the male luer end taper of the animal's endotracheal tube. The internal dimensions of the manifold provide for in-line communication and low resistance between the endotracheal tube and the evacuated pressure reservoir, and minimal deadspace between the endotracheal tube and the port through which room air or a gas anesthetic is introduced. A 16-ga x 1/2-in. stainless steel tube extending from the inner manifold wall is connected to a validyne (Northridge, CA) MP45 transducer to monitor airway pressure (P_m). The manifold, its connecting tubing to the pinch valves, the airway pressure port, and the endotracheal tube have a total deadspace volume of 1.20 cm^3.

The electronic comparator/controller monitors P_m, esophageal pressure (P_{es})--from a Statham (Oxnard, CA) P25db and PE90 fluid-filled catheter--and plethysmograph flow. The difference between P_m and P_{es}, transpulmonary pressure (P_{Tp}), is computed by a subtracter amplifier.

The FVCM is initiated at the end of a resting expiration by depressing the controller's "start" button. This simultaneously opens the pinch valve between the manifold and a pressurized reservoir (+30 cm H_2O) and closes the valve to the gas anesthetic (or room air). The positive pressure causes lung inflation, with a concomitant rise in P_{Tp}. The comparator monitors the rise in P_{Tp} and initiates a 1-sec "breath hold" when it reaches 25 cm H_2O. At the end of the breath hold, the positive-pressure valve is closed and, after 20 msec, the respiratory valve is opened, causing a rapid evacuation of the animal's lung volume. Expiratory flow rate rises sharply, becomes limited by physiological mechanisms, and falls in a nearly exponential manner. When the expiratory flow rate reaches zero, the comparator simultaneously closes the respiratory valve and opens the pinch valve separating the manifold from room air or anesthetic.

The repeatability of the FVCMs generated by this system is illustrated by the 10 MEFV curves in Figure 3A. Note the consistent peak flow rates and vital capacities. Figure 3B demonstrates the use of this system for standard spirometry and determination of the passive expiratory time-constant. For these maneuvers, the only change required is to lower the vacuum reservoir pressure to -20 cm H_2O. For the passive expiratory time-constant, the valve between the manifold and room air is opened after a 2-sec breath hold at P_{Tp} of 25 cm H_2O. This system rapidly produces repeatable respiratory maneuvers with consistent lung volume and time histories, and protects against overpressurization of the lungs and undue exposure of the airways to subambient pressures.

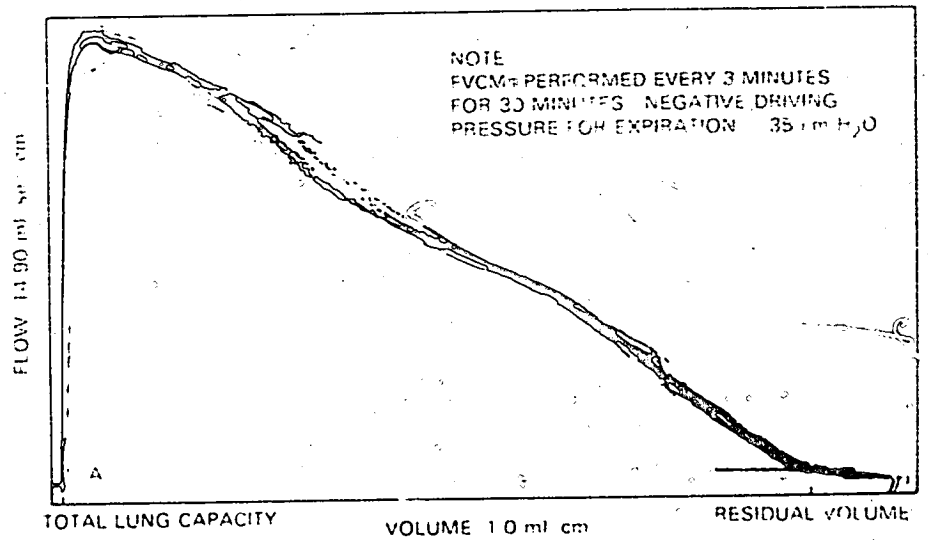

FIGURE 3A. Ten MEFV Curves From a 550-g Sprague-Dawley Rat. FVCMs performed every 3 minutes for 30 minutes. Negative driving pressure for expiration = -35 cm H_2O.

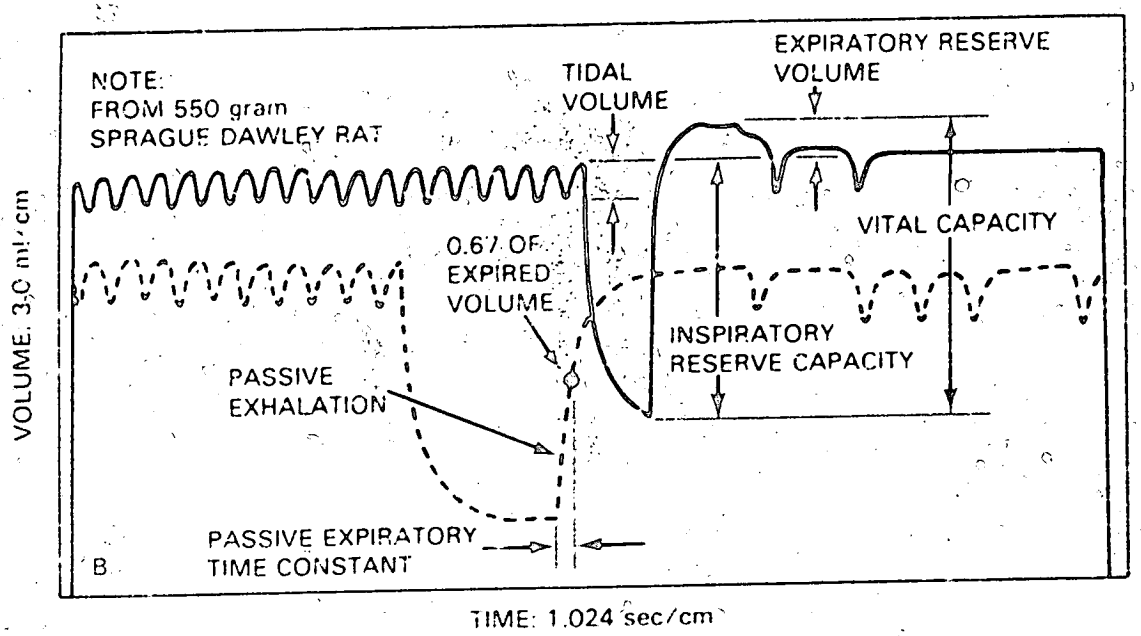

FIGURE 3B. Spirogram (top) and Passive Expiratory Time Constant Determination (bottom) from 550-g Sprague-Dawley Rat.

○ Pollutant Metals and Malnutrition

H.A. Ragan

This project was first funded in FY 1976 to study the effects of malnutrition on absorption and retention of energy-associated pollutant metals. Emphasis was placed on iron deficiency, which is common in young children and women of childbearing age, since this is one of those most prevalent in both underdeveloped and industrialized countries. For studies funded in this project, rats and mice were used as animal models to examine the influence of iron deficiency on the fate of ingested, injected, or inhaled pollutant metals.

Further research in this area would entail a more mechanistic approach which would be outside the scope of this project. Therefore, these studies are being discontinued, and future effort will be directed toward effects of products from coal liquefaction processes on hematopoiesis in vivo and in vitro.

Some of the important findings from studies funded in this project were, in brief:

1. Gastrointestinal absorption of lead, cadmium, mercury, nickel and zinc was significantly greater in iron-deficient rats than in littermate controls, whereas vanadium absorption was less in iron-deficient rats than in controls; and absorption of arsenic was equivalent in the two groups.

2. Intestinal absorption of plutonium in mice was significantly greater in the iron-deficient group, whereas absorption of plutonium in rats was the same as in the control group.

3. Chronic ingestion of 100 ppm lead or 50 ppm cadmium for 60 days had no hematologic effect on male rats in addition to those of iron deficiency alone; in the slower-growing female rats, lead tended to exacerbate the hematologic effects of the iron-deficient diet.

4. The transplacental movement of lead and cadmium was not increased in pregnant, iron-deficient rats compared to that in a similar group of control rats.

5. Chronic ingestion of 250 ppm nickel for 60 days had an apparent "sparing" effect on the hematopoietic system of iron-deficient rats; i.e., they were significantly less anemic than rats on an iron-deficient diet without nickel.

6. Iron-deficient and control rats injected intramuscularly with the carcinogenic metal, nickel (Ni), had a similar incidence of tumors at the injection site.

Alveolar Clearance of Inhaled Metal Oxides

Metal oxides produced during the combustion of fossil fuels constitute a potential hazard to man. The objectives of this project are to determine the fate of metals deposited in the lung, particularly as influenced by pulmonary cellular dynamics, and their acute and chronic toxicity. In particular, we are investigating the carcinogenicity of these metals in lung and extrapulmonary tissues that concentrate metals after exposure.

METABOLISM OF INTRATRACHEALLY INSTILLED ^{75}Se (SELENATE AND SELENITE) IN THE PRESENCE OF CADMIUM

Investigators: A. W. Conklin and C. L. Sanders

Intratracheally instilled selenite and selenate were both rapidly cleared from lung, translocated, primarily, to liver and kidneys, then excreted. In the presence of cadmium, however, clearance from the lung was significantly retarded, although uptake of ^{75}Se in other organs was not significantly affected.

Selenium is an essential trace metal that varies in toxicity, depending on its chemical form, dose, and route of exposure. Selenium occurs as an airborne pollutant mostly as a result of fossil fuel combustion, and sulfur and copper refining. Airborne Cd is also present in effluents of fossil fuel combustion. Although the toxicity of selenium administered by various routes has been studied extensively, few investigations have been made concerning the toxicology or metabolism of lung-deposited Se compounds. Selenium is known to protect against Cd toxicity when both are administered simultaneously; however, no data are available relative to the effect of Cd on Se toxicity, or the metabolism of lung-deposited Se compounds. Our study was designed to examine the translocation of intratracheally instilled selenate and selenite, the two Se compounds most prevalent as pollutants, and the effect of IT-instilled Cd on Se metabolism.

Sodium selenate-75 and selenite-75 (Amersham; 2.052 mCi and 5.1 mCi total activity, respectively) were individually diluted in 0.9% NaCl, resulting in 1 μCi per 0.75-ml dose. Each selenate dose contained 0.087 μg Se; each selenite dose, 0.16 μg Se. Thirty-seven μg Cd (1/2 LC_{50} for CdO) was added to selected doses of each Se compound. Fischer rats were anesthetized with ether and treated intratracheally with a selenium compound only (Se only), or with selenium and cadmium (Se + Cd). In the selenate study, 48 animals received Se only; 42, Se + Cd. Six rats from the Se-only group were killed immediately to determine initial deposition. Six rats each from the Se-only and Se + Cd groups were killed at 1, 4, 8, 24, and 72 hr, and at 1 and 2 wk afterward.

In the selenite study, 34 animals received Se only; six, Se + Cd. Four Se-only animals were killed immediately, and four at 1, 4, 24 hr, and 1 and 2 wk afterward. The remaining six Se-only animals, in addition to the six Se + Cd animals, were killed 48 hr after instillation to measure the difference in translocation at that time point.

Tissues and metabolism samples were collected and analyzed for ^{75}Se content by gamma spectroscopy. Selenium content is reported as percentage of recovered dose.

Both selenate and selenite were cleared rapidly from the lung: approximately 65% and 57% clearance, respectively, at 1 hr. In both studies, lung burdens after 2 wk were less than 3% of the instilled dose (Table 1). In the presence of cadmium, clearance of selenate was significantly reduced: approximately 11% retention at 2 wk. The Se retention in the selenite study was also significantly greater when Cd was introduced.

In the selenate study, liver uptake peaked at approximately 21% at 1 hr (Table 2), then cleared to 5% at 2 wk. In

the selenite study, liver content peaked at 24% at 1 hour, and cleared to approximately 6% at 2 wk. Cadmium did not significantly affect liver burdens of Se in either study.

In both studies, the kidney content of Se peaked at 4 hr, at 5.6% and 7.9%, respectively, and cleared to 1.5% and 1.9% at 2 wk (Table 3). The effect of cadmium was not significant in either study; nor was retention of Se significant in any other organ.

Urinary excretion of selenate and selenite at 2 wk was 29.5 ± 1.9% and 32.7 ± 1.7%, respectively; fecal excretion was less than 2% in both studies.

Data from these studies indicate that selenium, in the form of selenate or selenite, is rapidly absorbed from lung. Major uptake occurs in liver and kidney prior to excretion. Cadmium, when deposited simultaneously, significantly hinders the clearance of selenium from the lung.

TABLE 1. Effect of CdO on Lung Content of Selenate and Selenite After Intratracheal Instillation.

	Total Recovered ^{75}Se			
Time	Selenate	Selenate + CdO	Selenite	Selenite + CdO
0	82.3 ± 5.4	--	80.8 ± 5.9	
1 hr	34.0 ± [illegible]	29.6 ± 11.1	43.2 ± 5.8	
4 hr	20.9 ± 4.6	24.1 ± 4.8	26.8 ± [illegible]	
24 hr	10.1 ± 2.3	23.0 ± 10.8	[illegible] ± 1.7	
48 hr	[illegible]		8.9 ± [illegible]	[illegible] ± 1.9
72 hr	6.7 ± 1.9	19.8 ± 3.5		
1 wk	4.6 ± 0.7	19.2 ± 4.9	[illegible] ± [illegible]	
2 wk	2.8 ± 0.9	10.8 ± 3.5	[illegible] ± [illegible]	

TABLE 2. Effect of CdO on Liver Content of Selenate and Selenite After Intratracheal Instillation.

	Total Recovered ^{75}Se			
Time	Selenate	Selenate + CdO	Selenite	Selenite + CdO
0	1.5 ± 0.9	--	1.5 ± 0.7	
1 hr	20.9 ± 2.7	22.7 ± 6.9	23.7 ± 2.9	
4 hr	15.6 ± 0.5	13.8 ± 1.6	21.9 ± 0.8	
24 hr	12.4 ± 1.8	12.4 ± 8.4	15.1 ± 0.5	
48 hr	--	--	9.1 ± 0.5	8.8 ± 0.6
72 hr	11.5 ± 1.5	8.9 ± 0.6		
1 wk	8.6 ± 0.7	8.4 ± 0.8	11.0 ± 0.6	
2 wk	4.9 ± 0.6	3.8 ± 1.0	6.2 ± 0.2	

TABLE 3. Kidney Uptake and Clearance.

	Total Recovered ^{75}Se			
Time	Selenate	Selenate + CdO	Selenite	Selenite + CdO
0	0.6 ± 0.9	--	0.6 ± 0.3	--
1 hr	4.1 ± 0.6	4.3 ± 1.3	4.4 ± 0.4	--
4 hr	5.6 ± 0.5	4.7 ± 0.5	7.9 ± 0.7	--
24 hr	5.2 ± 0.2	6.0 ± 3.7	6.7 ± 0.2	--
48 hr	--	--	4.6 ± 0.5	5.4 ± 0.2
72 hr	3.5 ± 0.3	4.4 ± 0.4	--	--
1 wk	2.7 ± 0.1	3.6 ± 0.5	3.4 ± 0.1	--
2 wk	1.5 ± 0.2	1.5 ± 0.5	1.0 ± 0.1	--

CARCINOGENICITY OF SINGLY AND MULTIPLY EXPOSED RATS TO INTRATRACHEALLY INSTILLED CADMIUM OXIDE

Investigators: C. L. Sanders and A. W. Conklin

We are investigating the carcinogenicity of cadmium oxide in the lung and in extrapulmonary tissues following both single and multiple exposures.

Cadmium oxide is a toxic compound produced during coal combustion. It may be present in the ash and slag and thus poses an occupational and environmental health concern. Previous studies have demonstrated a high solubility of cadmium oxide in lung, and rapid translocation to liver, kidney and other tissues, along with an extended retention time in the body and limited excretion in urine and feces. Multiple exposures to cadmium compounds result in the induction of a cadmium-binding protein, metallothionein, which alters the distribution and retention patterns of cadmium in the body. There is considerable debate as to the carcinogenicity of cadmium in man, and supporting data are scarce. The purpose of this study is to examine the carcinogenicity of cadmium in rats following pulmonary deposition of cadmium oxide by intratracheal instillation. The cadmium was given as a single dose, or in multiple doses, to determine the role of induced metallothionein on the carcinogenic process.

Two hundred forty male Fischer rats were divided into four groups of 60 rats. Each group received either 0.75 ml of 0.9% saline alone, or 25 µg cadmium oxide in 0.75 ml of 0.9% saline by intratracheal instillation. Group 1 received saline only; group 2, 25 µg cadmium oxide at 70 days of age, group 3, 25 µg cadmium oxide at 70 and at 100 days of age; and group 4, 25 µg cadmium oxide at 70, 100 and 130 days of age. Animals are being held for lifespan observation. In all groups, only eight rats have died at 16 mo after instillation.

PULMONARY TOXICITY OF MOUNT ST. HELENS VOLCANIC ASH

Investigators: C. L. Sanders, R. A. Gelman, and A. W. Conklin

Early pulmonary toxicity of volcanic ash is being examined in rats. The distribution, clearance, translocation and pathobiology of intratracheally instilled (IT) Mount St. Helens volcanic ash samples are being compared with NIOSH quartz and Ritzville sandy loam samples as positive controls and saline as a negative control. Preliminary results suggest that the ash is much less toxic than quartz particles.

Respirable volcanic ash particles were separated by water sedimentation from samples obtained in Pullman and Rosalia, Washington and Missoula, Montana. In all cases, particle size distributions determined from electron micrographs of grid preparations were resolved into two log-normal-size populations for each sample. The populations consisted of a small size (CMD, 0.5-1.5 μm), which accounted for 45-84% of the particles; and a large size (CMD, 2.4-3.3 μm), which accounted for 16-55% of all particles. The particle sizes of quartz and soil samples (controls) were slightly larger than those of the ash.

Over 200 young adult female Fischer rats were used in these studies. Dust samples, suspended in 0.5 ml saline were administered to rats IT either in single 40-mg doses or in seven consecutive weekly doses averaging 11 mg each. Data given in this report are from singly exposed rats only. Routine analytical, ultrastructural and histopathological procedures were used.

Lung clearance was measured in three studies. In the first, the effect of ash on clearance of PuO_2 was measured. Lung Pu content was determined at intervals up to 30 days in rats given IT $^{239}PuO_2$ particles at 7 or 77 days after instillation of ash, soil, quartz or saline only. Compared to saline, volcanic ash, soil and NIOSH quartz decreased alveolar clearance of $^{239}PuO_2$. Translocation of Pu into thoracic lymph nodes was significantly greater in soil-, ash- and quartz-treated animals than in saline controls.

In the third study, volcanic ash lung clearance was directly measured at intervals of up to 3 mo after IT instillation. Lungs were dissolved in 5.25% sodium hypochlorite, extracted with chloroform/methanol and residual ash was gravimetrically determined. Ash was tenaciously retained in the lung: less than 10% was cleared at 3 mo after instillation of a single dose.

Lungs have been examined with the electron and light microscopes at 14, 37, 77 and 96-109 days after ash, soil or quartz deposition. Particles were rapidly phagocytized by alveolar macrophages. Cell necrosis and cytotoxicity, particularly in alveolar macrophages, were evident at 1 and 7 days in all groups; quartz particles were considerably more cytotoxic than ash or soil particles. Thickening of alveolar walls, focal bubbling of attenuated type I alveolar epithelial cytoplasm, and desquamation of type II alveolar epithelium (as well as later type II cell hyperactivity and hyperplasia) were seen in ash-exposed rats. Type II cells contained more dense lamellar bodies and exhibited prominent endoplasmic reticulum. At 14 and 37 days, in animals given ash, soil or quartz particles, alveoli near dust concentrations were partially filled with membranous debris from cell necrosis, with secreted type II lamellar bodies and a surfactant-like membranous network. These early inflammatory lesions were seen in parenchymal foci associated with high particle concentrations. Lesions in quartz-exposed rats were much more severe.

A few rats treated with ash exhibited a mild lipoproteinosis at 14 days; lipoproteinosis was much more severe in quartz-treated rats. The early, more-intense inflammatory reaction seen at 14 days had somewhat subsided in ash- and soil-treated animals by 37 days. A mild lipoproteinosis was seen in about 50% of ash treated rats at 37 days, but not in any soil-treated rats. Lipoproteinosis was severe in quartz-treated rats. Up to 37 days, pulmonary fibrosis was not seen in lungs of any saline-, soil- or ash-treated animals. Rats given quartz exhibited a pronounced nodular microgranuloma formation, characteristic of developing sili-

cosis, throughout the lung parenchyma. At 2 mo after II instillation, lung weights of rats given ash, soil or quartz particles were all significantly greater than those of saline controls.

These preliminary studies indicate that Mount St. Helens volcanic ash is nearly inert compared to quartz particles.

INFLUENCE OF CADMIUM, SELENIUM, AND VANADIUM OXIDES ON ACUTE MORTALITY AND LUNG CLEARANCE

Investigators: C. L. Sanders and A. W. Conklin

When instilled intratracheally (IT), CdO was the most toxic of a group of metal oxides tested. Selenium compounds and V_2O_5 were next highest in toxicity. In the presence of cadmium, lung clearance function was significantly reduced, and inversely related to dose.

Cadmium, selenium, and vanadium, primarily in oxide forms, are among the most common toxic metallic components of fossil fuel fly ashes. These metals also enter the atmosphere as by-products of various industrial processes. Acute mortality following various routes of exposure to these metals has been extensively studied, but few studies have been performed concerning mortality following pulmonary deposition of oxides of these metals. The purpose of this study has been to determine (1) the LC_{50} of IT-instilled CdO, SeO_2, SeO_3 and V_2O_5, common pollutant forms of these metals, and (2) the effect of CdO on lung clearance. Because of the previous use of $^{237,239}PuO_2$ in clearance modeling, it was used to determine the effect of CdO on lung clearance. Female Fischer rats, approximately 70 days of age, were used in all studies.

In determine the LC_{50} of IT-instilled CdO, 40 rats were divided into five groups of eight rats each, and instilled intratracheally with doses ranging from 0.05 to 0.820 mg/kg. In the V_2O_5 study, 64 rats were divided into seven groups of eight to ten animals each and instilled with doses ranging from 2.5 to 50.0 mg/kg. In the SeO_2 study, 40 animals were divided into five groups of eight animals each and instilled with doses ranging from 0.772 to 1.395 mg/kg. The SeO_3 study was identical to that for SeO_2. All doses were given in 0.5 ml of 0.9% NaCl.

The animals were held for 2 wk, and deaths were recorded (see Table 1 and Figure 1). The LC_{50} (concentration required to kill 50%) for the animals instilled with CdO was 0.33 mg/kg; for V_2O_5, 12.0 mg/kg; and for both SeO_2 and SeO_3, 0.87 mg/kg.

To determine cadmium oxide's effect on lung clearance, 20 µg CdO (approximately 0.15 mg/kg) was instilled either simultaneously with, 1 wk before, 24 hr before, or 24 hr after (approximately 45 nCi) of $^{237}PuO_2$ (five rats/group). At 2 and 4 wk after instillation, the animals were whole-body-counted in an Armac gamma counter for whole-body retention of ^{237}Pu. Retention of ^{237}Pu was significantly increased when CdO was given 24 hr before or 1 wk before ^{237}Pu. 84 ± 13% and 87 ± 15%, respectively, of the instilled dose was retained, compared to 59 ± 9% retention when ^{237}Pu was given alone. When Cd was instilled simultaneously with, or after, $^{237}PuO_2$, there was no significant difference in clearance from that after administration of Pu alone (Table 2). Results were similar to those found in an otherwise identical study with $^{239}PuO_2$, reported in last year's Annual Report.

Next, 24 animals were instilled with 0, 5, 10, or 20 µg CdO (five rats/group) 24 hr before instillation with $^{237}PuO_2$ (42.5 ± 3.2 nCi per dose). At 4 wk the lungs were removed and counted on a Beckman Gamma 310 System to determine lung clearance of ^{237}Pu. As the Cd dose increased to 10-20 µg, ^{237}Pu clearance from the lung was significantly reduced (Figure 2).

These results indicate that (1) CdO is the most toxic of the metal oxides given intratracheally, followed by the selenium compounds, then by V_2O_5. (2) Comparatively small amounts of CdO instilled <u>prior</u> to $^{237}PuO_2$ instillation significantly reduced lung clearance function.

TABLE 1. Metal Oxide Mortality

		At 2 Weeks	
CdO Dose mg/kg	N	No. Dead	Dead
0.05	8	0	0
0.125	8	0	0
0.250	8	2	25
0.500	8	7	88
0.820	8	8	100
SeO_2 Dose mg/kg			
0.772	8	0	0
0.800	8	1	13
0.840	8	2	25
0.885	8	6	75
1.395	8	8	100
SeO_3 Dose mg/kg			
0.772	8	0	0
0.800	8	0	0
0.840	8	3	37.5
0.885	8	5	62.5
1.395	8	8	100
V_2O_5 Dose mg/kg			
2.5	10	0	0
5.0	10	1	10
7.5	8	1	13
10.0	8	4	50
20.0	8	7	88
25.0	10	9	90
30.0	10	10	100

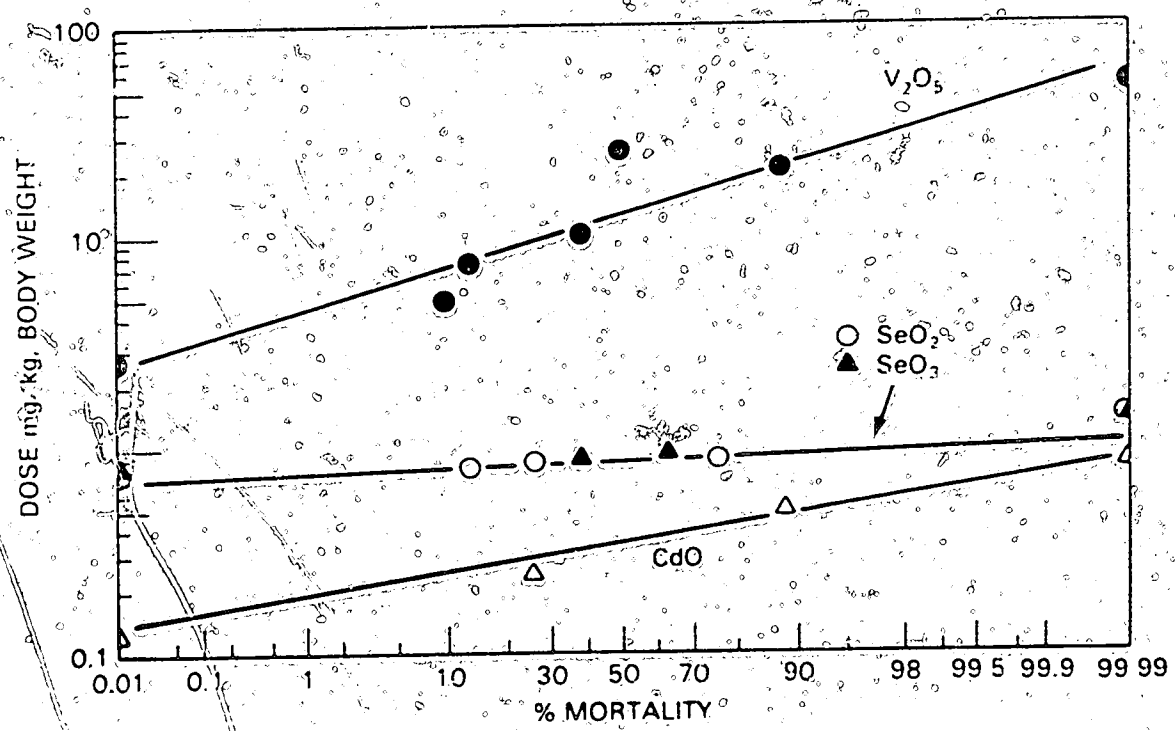

FIGURE 1. Acute Mortality of Rats Following Intratracheal Insufflation of Metal Oxide. Each point represents 8-10 rats.

TABLE 2. Influence of CdO on the Lung Clearance of $^{237,239}PuO_2$. Values are means (n,5) ± SD.

Treatment	Initial Lung Deposition nCi ^{239}Pu [b]	Percent ^{239}Pu in Body at Times Post-Instillation	
		2 Weeks	4 Weeks
Pu Only	45 ± 5.7	[illegible]	59 ± 4
Pu + Cd[a] Simultaneous	43 ± 2.3	74 ± 20	49 ± 11
Pu 24 hr Before Cd[a]	45 ± 4.5	83 ± 14	59 ± 17
Cd[a] 24 hr Before Pu	41 ± 3.4	94 ± 11	84 ± 13
Cd[a] 1 wk Before Pu	46 ± 5.3	99 ± 16	87 ± 15

[a] 20 μg CdO
[b] ^{238}Pu/^{239}Pu ratio was 1:13:1

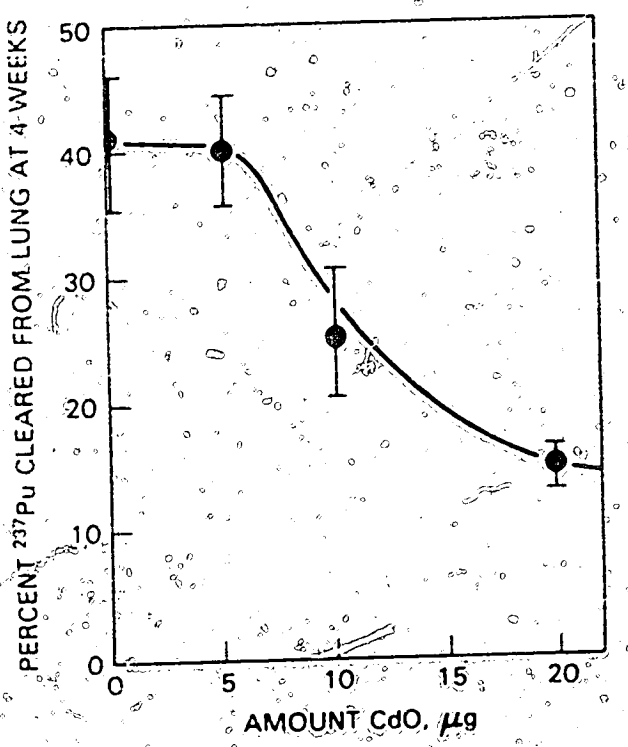

FIGURE 2. Influence of Amount of Instilled CdO on Alveolar Clearance of $^{237,239}PuO_2$. Values are mean (n,5) ± SD.

• Factors Influencing the Cross-Placental Transfer and Teratogenicity of Metallic Pollutants

This project is concerned with certain heavy metals associated with energy production, for which there is direct or inferential evidence of deleterious effects on prenatal development. Parenteral, oral and inhalation routes of administration will provide differences in the rate and, possibly, the chemical form in which the metals are presented to the fetoplacental unit during the continuum of embryonic and placental development.

Results from studies involving lead exposures at representative gestational ages (9, 15, and 19 days) have determined mass effects on metabolism using tracer ^{210}Pb administered concomitantly with various levels of stable $Pb(NO_3)_2$. A rapid uptake into the fetoplacental unit was observed following intravenous administration of the tracer or 5 and 25 mg $Pb(NO_3)_2$/kg to rats; the highest dose was embryotoxic and teratogenic. The percentages of the lead dose absorbed by the dam following inhalation or oral exposures were dose-dependent. The absorbed lead readily entered the fetoplacental unit, especially during the later stages of gestation.

Studies are in progress to determine the potentially embryotoxic effects of vanadium in rats. Preliminary results indicate that parenteral administration at 14 days gestation caused maximal embryonic resorption, but that injection at 9 days gestation produced no overt embryotoxicity. Tracer ^{48}V studies performed in rats at 9, 15, and 19 days gestation demonstrated that fetoplacental ^{48}V burdens were highest following exposure in late development. The fractions of the ^{48}V in the fetoplacental unit which were in the fetuses ranged from 4 to 29%, and were highest in fetuses whose vanadium exposure was initiated at 9 or 15 days gestation.

CROSS-PLACENTAL TRANSFER OF VANADIUM PARENTERALLY ADMINISTERED TO RATS

Investigators: P. L. Hackett and S. A. Watson

Technical Assistance: R. L. Music and A. J. Clary

Parenteral administration to pregnant rats of sodium (ortho) vanadate (5 mg V/kg) caused maximal fetal resorption following administration at 14 days gestation (dg). A 15% incidence of fetal variants was observed in rats injected at 13 dg. Results from tracer ^{48}V studies performed in rats at 9, 15, and 19 dg showed that the dams' stage of pregnancy at injection influenced vanadium distribution in blood, kidney, skeleton, lungs, and pregnant uterus. Fetoplacental vanadium burdens were highest in the 19-dg fetoplacental units (FPU). Fetal fractions of ^{48}V in the FPU ranged from 4 to 20%, depending on length of exposure. A large percentage (65%) of the ^{48}V in the FPU accumulated in the membranes.

We have initiated screening studies to determine the embryotoxic effects of soluble forms of vanadium after parenteral administration. Concurrently, we are evaluating the effects of dose level and stage of development on V distribution within the FPU.

Preliminary studies indicated that intravenous administration of V at dose levels as low as 0.9 mg V/kg body weight caused high maternal mortality. Dose levels of 5 mg V/kg caused only 14% maternal mortality when injected intraperitoneally (IP).

Embryotoxicity studies were performed using saline solutions of $NA_3VO_4 \cdot 5H_2O$ (ortho) adjusted to pH 7. The V solutions were administered IP to pregnant rats at 9, 13, 14, 15 and 16 dg. Fetal effects were evaluated at 20 dg.

Tracer ^{48}V studies were performed on groups of five to seven pregnant rats (9, 15, and 19 dg) following IP administration

^{48}V in saline at pH 7. The animals were sacrificed at 1.5, 6 and 24 hr after injection, and at 20 dg to determine ^{48}V activities in maternal and fetal tissues.

Initial results at dose levels of 0.9 to 5 mg V/Kg show that intrauterine mortality is influenced by the gestation age at injection (Table 1). Embryomortality is highest after injection at 14-15 dg at dose levels of 4-5 mg V/kg. To date, the largest incidence of morphologic malformation was observed in fetuses of rats injected with 5 mg V/kg at 13 dg. Incomplete analyses of the results from skeletal and visceral examinations indicate that skeletal defects may be the most frequent alteration. The effect of daily administration of V during early and late periods of organogenesis is being examined.

TABLE 1. Summary of Vanadium Toxicity Data.

Dose, mg V/kg	Number of Litters	Percent Embryo mortality, $\bar{X} \pm SE$	Fetal Variants, %
0.9	4	7.0 ± 2.4	0
4	5	7.0 ± 0.9	0
5[a]	4	0	4.0
5[a]	4	70 ± 14	15.0
5[a]	5	99 ± 2.8	--
2	4	30 ± 8.4	4.8
4	1	100	--
4	4	33 ± 20	5.0

[a] Maternal mortality at 5 mg V/kg.

The stage of gestation at the time of V administration significantly influenced V distribution in several maternal tissues. After injection at the more advanced stages of pregnancy (19 dg), the percentage of the ^{48}V dose was higher in blood, lungs, and pregnant uterus but lower in skeleton and kidney than in comparable tissues of the 9-dg-injected rat (Table 2). Urine levels, although variable, tended to reflect an inverse relationship to the blood levels. Deposition in liver, muscle, GI tract and skin was not influenced by the stage of pregnancy.

Blood concentrations (% dose/ml) of ^{48}V were not altered by advancing pregnancy, therefore differences in the total amount of ^{48}V in blood could be attributed to the increased blood volume at 15 and 19 dg. Vanadium-48 clearance from blood was more rapid following injection at 15 and 19 dg than at 9 dg (Figure 1). By 24 hr after injection the dose remaining in the blood was the same for all injection times.

TABLE 2. The Effect of Pregnancy on ^{48}V Distribution in Some Maternal Tissues at 90 Minutes After Administration.

Tissue	Days of Gestation at Injection Time: 9	15	19
Blood	8.37 ± 1.70[a]	15.7 ± 2.74[a,b]	18.4 ± 0.98[b]
Skeleton	13.2 ± 0.39[a]	10.1 ± 0.73[a,b]	7.69 ± 0.49[b]
Kidneys	5.14 ± 0.24[a]	4.59 ± 0.13[a,b]	3.36 ± 0.43[b]
Lungs	0.42 ± 0.05[a]	0.78 ± 0.11[a,b]	0.72 ± 0.06[b]
Uterus and Contents	0.80 ± 0.10[a]	4.65 ± 0.49[b]	13.1 ± 2.70[c]
Urine	11.9 ± 4.24	6.76 ± 3.04	5.79 ± 2.70

[a-c] Values for each tissue that do not have a common superscript are different ($P < 0.05$)

Skeletal values for rats injected at 9 and 19 dg were inversely related to blood ^{48}V values at 90 min after injection (Figure 1). The percentage of the dose in the skeleton of rats injected at 9 dg remained constant over the 11-day observation period, but values for the 15-dg injection group decreased between 16 and 20 dg. Liver retention of ^{48}V (Figure 1) was not influenced by the stage of pregnancy at injection.

The fraction of injected ^{48}V in the FPU increased with fetal development (Figure 2). However, the concentrations (percent dose/gram), indicated that, at 90 min after injection, values for the youngest FPUs were highest (0.67, 0.15, and 0.17%/g for 9, 15, and 19 dg, respectively). The percentage of the ^{48}V dose in the 15-dg FPU remained constant between 24 hr after injection and 20 dg; the 9-dg FPU accumulated additional V during this interval (Figure 2).

The placenta contained 64 or 73% of the ^{48}V FPU dose in 15- and 19-dg FPUs, respectively, at 90 min after injection (Figure 3). By 24 hr after injection, the vanadium was clearly concentrating in the fetal membranes, and remained there through 20 dg. Fetal values ranged between 4 and 10% of the FPU burden for the first 24 hr; 9- and 15-dg fetuses continued to accrete additional amounts of vanadium.

In the 20-dg fetus (Table 3), the carcass contained the largest fraction of

the ^{48}V. Carcass values tended to be higher, and kidney and GI-tract fractions lower, in fetuses which were exposed to ^{48}V for 11 days than in those exposed for only 1 or 5 days.

Tracer ^{48}V studies now in progress address the effect of embryotoxic carrier doses on V distribution in the FPU and fetus.

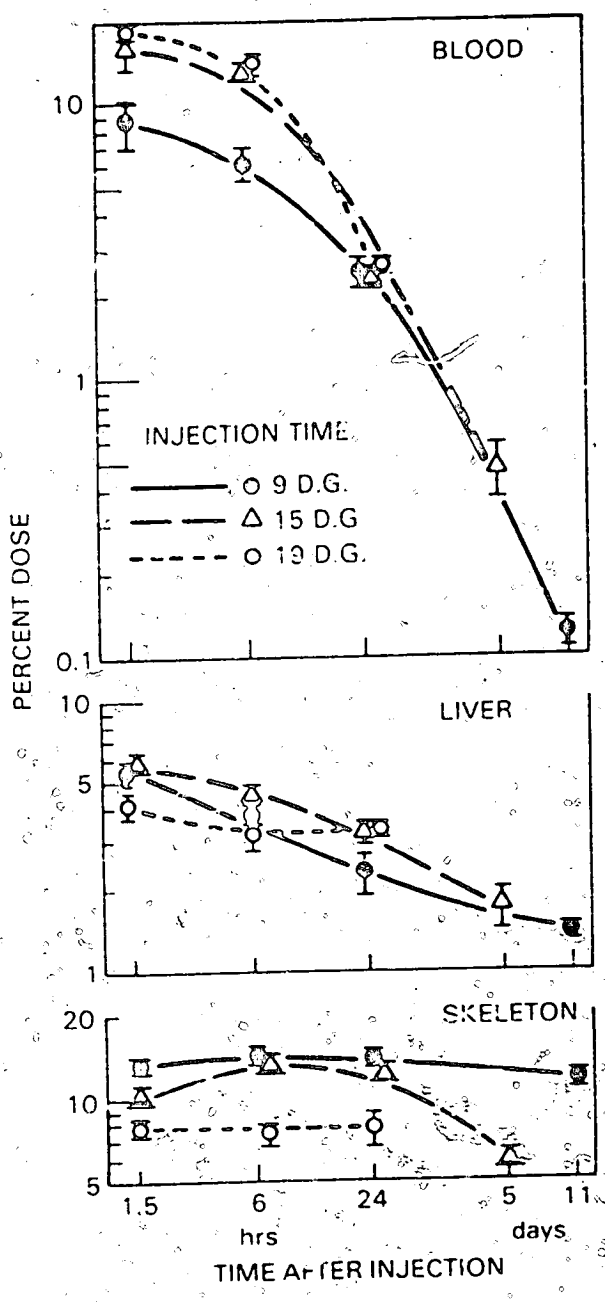

FIGURE 1. Retention Curves for the Blood, Skeleton and Liver of Pregnant Rats Injected With ^{48}V at Different Stages of Gestation.

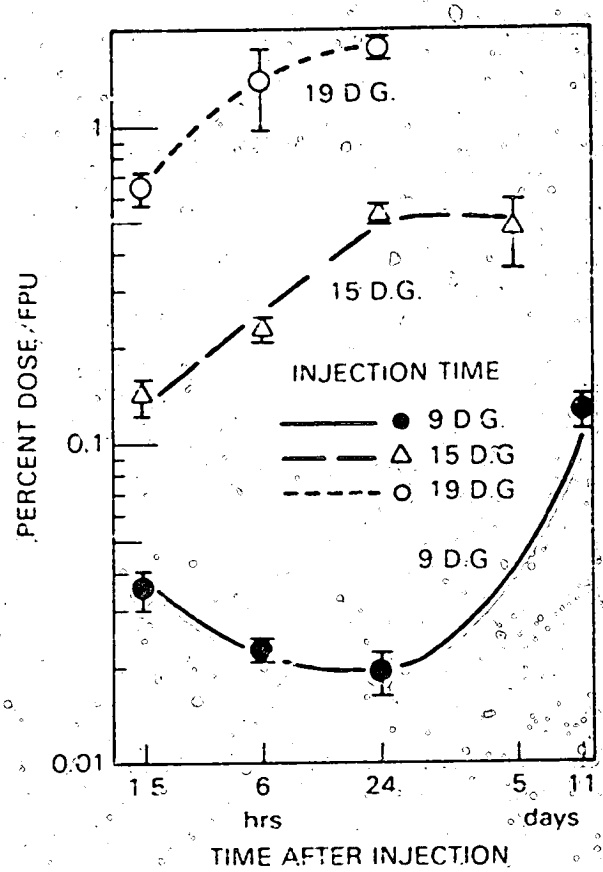

FIGURE 2. Percentage of ^{48}V in the Fetoplacental Units of Rats Injected at 9, 15 and 19 Days Gestation.

TABLE 3. Distribution of ^{48}V in Fetal Tissues at 20 Days of Gestation, Expressed as Percentages of the Fetal Burden (±SE).

Fetal Tissue	Days of Gestation at injection 9	15	19
Carcass	89.2 ± 1.5[a,b]	89.5 ± 0.37[a]	87.6 ± 0.59[b]
Liver	7.5 ± 1.1	7.3 ± 0.39	8.4 ± 0.56
Kidney	0.02 ± 0.02[a]	0.67 ± 0.06[b]	1.0 ± 0.11[b]
Brain	0.44 ± 0.18	0.97 ± 0.06	0.79 ± 0.07
G.I. Tract	1.30 ± 0.14[a]	1.84 ± 0.08[a,b]	2.14 ± 0.14[b]

[a,b] Values for each tissue that do not have a common superscript are different ($p < 0.05$).

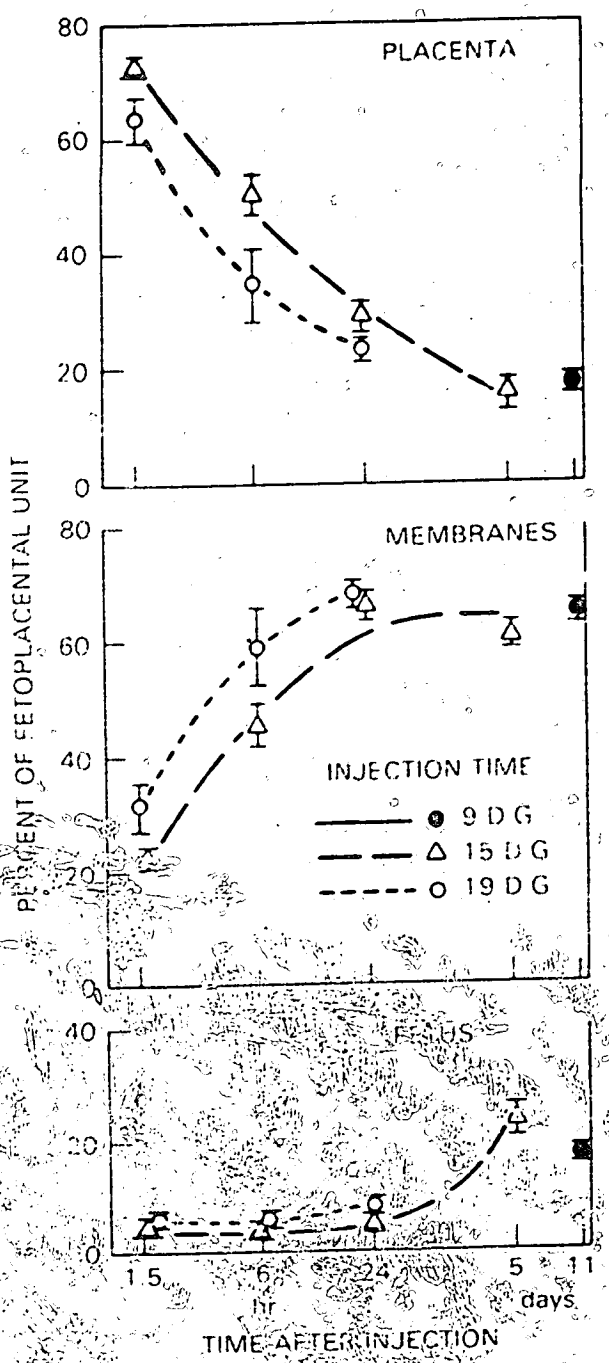

FIGURE 3. Distribution of [illegible] in the Fetoplacental Unit of Rats Injected at 9, 15 and 19 Days Gestation.

Solvent Refined Coal Biostudies

D.D. Mahlum

The objective of this program is to establish a broad biomedical data base for solvent refined coal (SRC) materials to: (1) identify possible health effects problems, (2) help identify appropriate control technologies or operating parameters to minimize potential health effects, and (3) help the SRC technology to meet present and future regulatory requirements. We are employing an approach which integrates chemical characterization, cellular and animal bioassay systems, and dosimetric studies. Thus, SRC materials are selected for toxicologic studies on the basis of plant operational data and are subjected to chemical characterization. Cellular bioassays include determination of mutagenicity in microbial systems and an evaluation of toxicity and transforming potential for cultured mammalian cells. Animal studies include determinations of: (1) acute and subchronic oral toxicity, (2) developmental toxicity, and (3) consequences of dermal and inhalation exposures. In addition, dosimetric metabolic studies are being performed to provide data to aid in the extrapolation of animal toxicologic data to man.

The results of these studies have been summarized and presented in three PNL documents:

1. PNL-3189, Biomedical Studies on Solvent Refined Coal (SRC-II) Liquefaction Materials: A Status Report, October 1979; Appendix, December 1979

2. PNL-3464, Initial Chemical and Biological Characterization of Hydrotreated Solvent Refined Coal (SRC-II) Liquids: A Status Report, July 1980.

3. Chemical, Biomedical and Ecological Studies of SRC-I Materials from the Ft. Lewis Pilot Plant: A Status Report, January 1981.

⊙ Perinatal Effects of SRC

F.D. Andrew

The objective of this project is to establish an improved set of criteria for evaluating the potential of agents to induce one or more manifestations of developmental toxicity. A general approach is being developed that is applicable for testing physical, chemical, and nutritional hazards in appropriate animal models. Our approach focuses on subtle functional impairments at various times during maturation, rather than on the more traditional emphasis on structural malformations. Four principal areas of investigation are being integrated into one test system to provide a set of maturation indices, including: 1) postnatal appearance of a standard series of anatomic landmarks, 2) sequential acquisition of metabolic homeostasis for a battery of essential tissue enzymes during the perinatal period, 3) neonatal ontogeny of neuromuscular and neurobehavioral capabilities, and 4) development of the immune system with a full complement of humoral and cellular elements. Adverse effects detected in this test system are analogous to those expressed in human neonates as stunted growth, congenital errors of metabolism, neurological or mental retardation, and immunodeficiencies. Current studies are correlating the effects of prenatal exposure on the development of the progeny with respect to the maturation indicators cited, as indicated in the Annual Report for FY 1979.

Mutagenicity of SRC Materials

R.A. Pelroy

The mutagenic components in high-boiling SRC-II liquids have been analyzed by a combination of chemical and biochemical methods. Separation of compounds from these materials was carried out by solvent-solvent extraction and thin-layer chromatography. The location of genetically active compounds in the resulting fractions was identified by testing for mutagenesis, using the Ames *Salmonella* test. Biochemical verification of primary aromatic amines (PAAs) in the same fractions was achieved by enzymatic means with a mixed-function amino oxidase (MFAO) specific for PAAs. The chemical identity of these PAAs, determined by gas chromatography/mass spectrometry, consisted of 2-, 3- and 4-ring compounds (i.e., aminonaphthalenes, anthracenes, phenanthrenes, pyrenes and chrysenes). The quantitative importance of the PAAs to the mutagenicity of the high-boiling liquids was implied by inactivation of most of the mutagenic activity in the SRC materials following treatment with nitrous acid. This treatment results in conversion of mutagenically active PAA mutagens to mutagenically inactive nitrosation products. Hydrotreatment (catalytic reduction of hydrogen) of high-boiling SRC liquids resulted in a more than 99% decrease in their mutagenic activity.

The results of these studies are presented in two reports prepared for the U.S. Department of Energy: *Biomedical Studies on Solvent Refined Coal (SRC-II) Liquefaction Materials: A Status Report*, PNL-3189; and *Characterization of Hydrotreated Solvent Refined Coal (SRC-II) Liquids: A Status Report, Initial Chemical and Biological Characterization*, PNL-3464.

CONSERVATION

This section reports on progress made on projects concerned with potential health effects of exposure to static and 60-Hz electric fields from high-voltage transmission systems. They seek to determine whether such fields can produce genetic effects in biological systems.

These projects are part of the Pacific Northwest Laboratory bioelectromagnetics program and are complemented by ongoing 60-Hz electric field studies in laboratory rodents, sponsored by the DOE Office of Electric Energy Systems, and in miniature swine, sponsored by the Electric Power Research Institute.

Mutagenic Effects of Electric Fields

Microbial and *Drosophila* test systems are being used to determine if large ac or dc electric fields may induce mutations. These organisms were chosen to enable exposure of large numbers with relatively simple apparatus, to minimize the time required for replications and dose-effect studies, and to offer the opportunity for investigating mechanisms, should effects be observed. This project complements ongoing mammalian studies with ac electric fields at PNL, sponsored by the Division of Electrical Energy Systems and the Electric Power Research Institute.

MUTAGENICITY OF ELECTRIC FIELDS IN SALMONELLA

Investigators: F. P. Hungate and S. L. Cassey

A new system for exposing cell culture to electric fields has been developed. This system uses agar bridges, having ionic constituents identical with those in the culture medium, interposed between the cell culture and the electrodes. Preliminary tests show that electrode effects are eliminated by use of the agar bridge. An earlier study using a parallel-plate exposure system was repeated. In this reevaluation, mutation frequencies of Salmonella TA-100 exposed to fields, in air, up to 750 kV/m were not significantly increased over controls.

Initial tests had shown a significant increase in mutation frequency in the Ames TA-100 strain of Salmonella following exposure to large dc fields using a parallel-plate exposure system. However, tests for mutation induction in a large number of other microbial systems failed to confirm that dc fields induce mutations. In view of this lack of confirmation we decided to repeat the initial tests with TA-100, using the same parallel-plate exposure system, with the growing cells contained in plastic petri dishes. We found no significant increase in mutation frequency as a result of exposure to the dc fields (Tables 1 and 2).

It is not apparent at this time why the initially observed mutagenic effect could not be repeated. We are not planning further tests with microorganisms in the parallel-plate exposure system because of our inability to quantitate the magnitude of the field to which the organisms were exposed. Although the field in air between the plates could be readily calculated, the field in the cell culture could neither be calculated nor measured. (Its value could be markedly affected by accumulation of atmospheric space charge on the nonconducting petri dish holding the culture medium.) Difficulties in establishing a fully defined field in the parallel-plate system led us to search for an alternative exposure system.

The simplest exposure system is one having a pair of electrodes, with a medium of known conductance between the electrodes and a known cross section through which measurable current flows. Exposure chambers were available containing platinum electrodes, which were developed for studying effects on red blood cells. These chambers have a pair of platinum-foil electrodes, 2.4 cm apart, each presenting a surface area of 5.8 cm² when 14 ml of medium is added. Although platinum is widely used as electrode material, there is evidence that soluble platinum compounds are produced by electrolysis, and that they may be mutagenic as well as toxic.

To evaluate possible effects of platinum, we exposed 14 ml of sterile, cell-free medium, overnight, in these exposure chambers. One chamber, not connected to the power supply, served as a control. Following this, the medium was withdrawn from the exposure chambers, and placed in sterile flasks having sidearms suitable for measuring turbidity in a Klett pho-

TABLE 1. Number of Mutant Salmonella (TA-100) in an Aliquot of the Control and Exposed Portions in Electric-Field Experiments

Electric Field in Air, kV/m	Exposure Time, hr	Control Culture[a] Mean ×10	Control Culture[a] S.E.	Exposed Culture[a] Mean ×10	Exposed Culture[a] S.E.	t-Statistics
500	20	74	5	85	13	-0.78
500	20	53	4	63	1	-2.15
500	20	82	2	70	2	3.55[b]
500	24	52	2	67	3	-4.54[b]
500	24	51	14	53	7	-0.10
500	24	44	1	89	1	-24.97[c]
500	24	104	1	94	1	5.48[c]
500	24	54	5	94	3	-7.29[c]
500	24	57	4	64	9	-0.78
500	24	149	9	177	2	2.91[b]
500	24	40	7	62	4	-2.62
500	24	42	1	49	1	-3.90[b]
750	16	79	10	87	6	-0.74
750	16	55	11	55	2	0.03
750	16	43	2	64	2	11.60[c]
750	20	70	5	69	6	0.09
750	20	84	2	117	8	-4.03[b]
750	20	81	2	73	3	2.20
750	20	82	5	85	10	-0.24
750	20	62	1	87	1	-12.49[c]
750	20	77	9	82	10	-0.37
750	20	70	7	81	21	-0.49
750	20	146	6	135	3	1.64
750	20	102	4	123	8	2.42
750	20	36	2	49	3	3.74[b]
750	20	79	15	71	2	0.56
750	24	80	2	81	3	-0.37
750	24	121	5	104	5	2.37
750	24	126	13	96	7	1.98
750	24	61	2	62	5	-0.45

[a] N = 3
[b] Significant at the 95% confidence level
[c] Significant at the 99% confidence level

TABLE 2. Results of t Tests on the Difference in the Number of Mutant Salmonella (TA-100) in an Aliquot of the Control Portion Versus an Aliquot of the Exposed Portion in Electric-Field Experiments

Number of Experiments Where	Confidence Level 95%	Confidence Level 99%
Control Portion Had Significantly More Mutants than the Exposed Portion	3(2)[1a]	2(1)
No Significant Difference	19(13)	5(17)
Exposed Portion Had Significantly More Mutants than the Control Portion	8(4)	3(1)

[1a] The results in parentheses are the results when the experiments that had significant differences in the total number of cells were deleted (see Table 1)

tometer. The medium was then inoculated with Salmonella TA-100, placed on a water-bath shaker, and growth rate calculated by means of turbidity measurements.

The growth rate of cells grown in medium previously exposed for 21.5 hr to an ac current density of 6.9 A/m² and a field of 6.3 V/m (medium conductivity 1.1 S/m), was significantly inhibited compared with medium in the same type of chamber not exposed in the field. During cell growth, the medium had no contact with platinum (Figure 1). There was also a suggestion of a slight effect of the platinum without field on growth rate of the bacteria. A similar test using a dc field showed essentially complete inhibition of growth (Figure 2) caused by the prior exposure of the medium to a current density of 0.18 A/m² and a field strength of 0.16 V/m (conductivity = 1.1 S/m). It is noteworthy that exposure of the medium to a low strength dc field caused greater inhibition than did the larger ac field.

No attempt was made to establish the amount of platinum in the medium, or its chemical form. It appeared that platinum and, presumably, other electrode materials in direct contact with the cell suspension might be agents for introducing toxic and/or mutagenic materials other than the fields. To eliminate this possibility, a new exposure system has been developed which uses an agar bridge to isolate the electrodes from the cell suspension.

Figure 3 is a diagram of the agar-bridge exposure system. Standard ball joints, 1.2 mm ID, 27.8 cm long, are typically used, although other sizes could serve as well. The ends of the tubes are sealed with 00 stoppers having a strip of platinum foil folded across the end to serve as the electrical contact. Graphite is currently being evaluated as an alternate electrode material. A thin layer of nutrient medium solidified with 2% agar serves to maintain the growing cells in a region of uniform current density.

The agar-plug system was tested for possible effects on the medium, in the same manner as described for the platinum-lined chambers. Medium was exposed overnight to dc or ac fields and, following exposure, placed in side-arm flasks, inoculated with Salmonella TA-100 cells, and the growth rate monitored with a Klett photometer. We compared growth rate from medium exposed to the field, medium treated similarly but not exposed to a field, and medium directly from the stock bottle. Growth rates in these three media were identical. Therefore, the agar plugs had satisfactorily isolated the growth medium from the toxic effects of the platinum electrodes. This further indicated that the inhibitory effects shown in Figures 1 and 2 were due to platinum, rather than to the presence of the dc or ac field.

The agar-bridge system is being used for further testing of Salmonella strains, and other bacterial systems, for possible mutation induction by dc or ac fields. The success of the agar bridge in isolating the growing cells from electrode effects is apparently due to its restricting movement of toxic agents from the electrode surface to the culture medium. With time, diffusion would move electrolytic products through the bridge, particularly with prolonged use of a dc field. To circumvent this problem, we are now using an automatically timed, current-reversing switch to change the polarity each hour. Thus, the movement of toxic ions would be reversed each hour, minimizing the possibility of their moving into the region of cell growth. The use of the same components in the agar bridge as in the growth medium also minimizes the extent of ionic change which can occur in the environment of the cells. If prolonged growth is required, the length of the agar bridge could be extended to further isolate the growth environment from the electrodes.

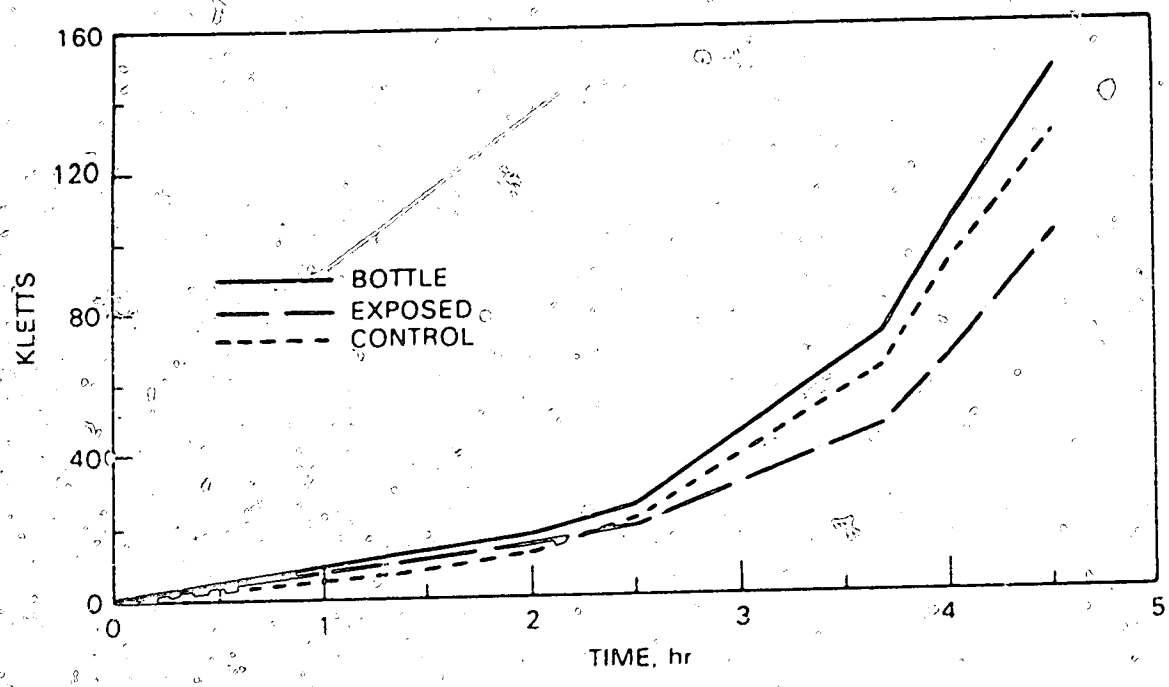

FIGURE 1. Growth of Salmonella (TA-100) in Medium Previously Exposed for 21.5 Hours to an AC Current Density of 6.9 A/m² (Field, 6.3 V/m). The surface area of the platinum to which the medium was exposed was 5.8 cm².

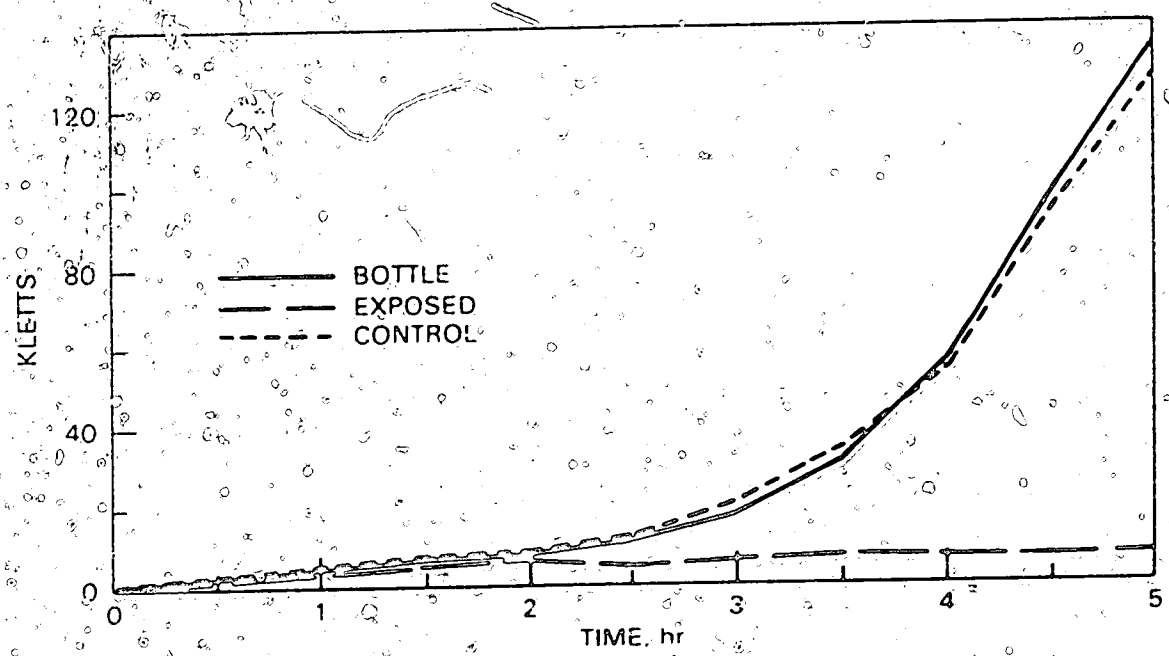

FIGURE 2. Growth of Salmonella (TA-100) Grown in Medium Previously Exposed for 22 Hours to a DC Current Density of 0.18 A/m² (Field, 0.16 V/m). The surface area of platinum to which the medium was exposed was 5.8 cm².

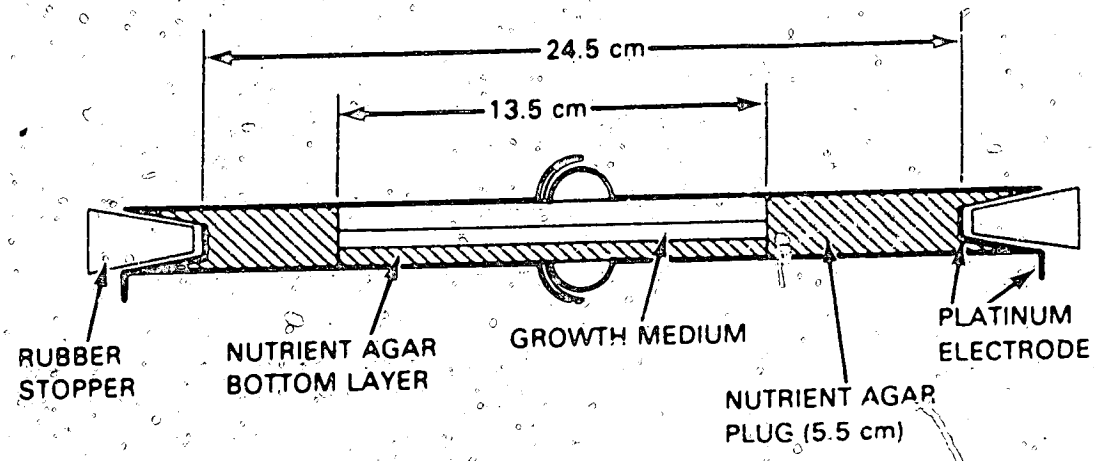

FIGURE 3. Diagram of the Agar Bridge Exposure System (ball clamp not shown).

AC E-Field Dosimetry

Living organisms may be exposed to extremely low-frequency (ELF) frequency range, 0-100 Hz) electric fields produced by electric power systems or specialized communications systems. Exposure to these fields is conventionally specified in terms of the field strength present before the organism enters the field. However, the actual electric fields to which an organism is exposed are different from the unperturbed field because of perturbations caused by the conducting body of the organism. Knowledge of these fields is crucial: data obtained in projects using animals are to be used for the assessment of possible hazards to humans exposed to ELF electric fields. The purpose of this project is to determine the actual fields experienced by electrically grounded and ungrounded human and animal models.

DETERMINATION OF ELECTRIC CURRENT DISTRIBUTIONS IN MAN AND HANFORD SWINE EXPOSED TO A UNIFORM 60-Hz ELECTRIC FIELD

Investigators: A. W. Guy,* S. Davidow,* and C. K. Chou*

Investigation of the biological effects of 60-Hz electric field exposure on animals are currently being conducted in a number of laboratories. This report concerns a project which is using a radiofrequency technique to provide dosimetric information on induced current densities in human and animal models exposed to 60-Hz electric fields.

The purpose of this project is to experimentally determine the induced current densities in human and animal models exposed to 60-Hz electric fields. Knowledge of these induced currents is essential if data from live animals exposed to 60-Hz electric fields are to be used for assessment of possible hazards to humans exposed to the same fields. The results will be compared to direct measurements made on live animals and full-scale models exposed to 60-Hz electric fields.

A large (3.66-m x 3.66-m x 2.44-m) cavity, lined with copper sheeting (0.1 mm thick), was constructed. An excitation loop with an input impedance of 50 ohms was designed and mounted at the center of the cavity's wall for exciting a TE_{101} mode. An electric-field sensor was developed to measure the field strength within the cavity. It consisted of a circular disk separated from the metal ceiling of the cavity by a thin layer of insulation. The electric field was calculated from the measured voltage between the disk and the ceiling.

A phantom tissue (Oil Center Research TX-150 16.46%, H_2O 73.54% and NaCl 10%) with a conductivity of 1 S/m was characterized using a slotted line method over a 10°C temperature range. Prolate spheroids and spheres composed of the phantom tissue were exposed in the cavity's region of maximum electric-field strength to verify that the specific absorption rate (SAR) and current distribution agreed with theoretical values obtained from the quasi-static or long-wavelength analysis. The measured SAR and induced current distribution patterns were all uniform, within 10%, along both horizontal and vertical planes.

Three scale models of man (scale factors, 3.95, 5.95 and 8.25) were individually exposed at the center of the cavity, and the SAR and induced current densities were compared in the various parts of the body. The maximum induced current densities within the body were located in the neck, knee, and ankle for each model. These values were independent of the size of the model, which supports the validity of the cavity exposures in producing results consistent with the long-wavelength analysis. Thermograms were taken using both a standard lens and a narrow-angle lens for obtaining a detailed

*Bioelectromagnetics Research Laboratory, University of Washington, Seattle, WA

description of the induced current distribution.

Prolate hemispheroids (prolate spheroids bisected perpendicular to the major axis) were individually exposed while in electrical contact with the center of the ground-plane floor of the cavity. The SAR and induced current pattern in such a hemispheroid in contact with the ground plane should be identical to that in a complete prolate spheroid exposed to a uniform electric field in free space due to the image of the model in the ground. The experiments demonstrated that the cavity exposures accurately simulated the exposure of a free-space prolate spheroid and a grounded prolate hemispheriod to a vertical, uniform, 60-Hz electric field.

The three scale models of man were also individually exposed with their feet in electrical contact with the ground plane so that the SAR and induced current densities could be compared to those obtained for exposures in the center of the cavity. It was observed that the maximum induced current densities within the body were located in the neck, knee, and ankles of each model. The relative induced current density was higher for the grounded model than for the off-ground model due to imaging in the former configuration, which increased the effective length:width ratio of the model. The experiment demonstrated that, as long as the shape of the model remained the same, the induced current density was independent of the model size, which is consistent with results expected for free-space exposure.

We continued our dosimetry experiments by simulating the exposure of scale models of swine with their hooves in contact with the ground plane. Induced current patterns were observed in the thigh, ankle, and hoof, with no observable values in the body or head. To obtain measurable heating in the body would have required the use of very strong electric fields and/or long exposure durations; this was not feasible because the temperature rise in the legs would have been large enough to invalidate the results. We are therefore developing a semiconducting plastic which can be cast in the desired forms and whose electrical conductivity is much less dependent on temperature. With this material we will characterize the induced currents and fields in grounded and ungrounded animal models exposed to 60-Hz electric fields.

TECHNIQUE FOR THE DIRECT MEASUREMENT OF 60-Hz ELECTRIC FIELDS INSIDE HOMOGENEOUS MODELS OF HUMANS AND ANIMALS

Investigator: W. T. Kaune

Technical Assistance: W. C. Forsythe, A. W. King, and M. C. Miller

We have developed a technique for the measurement of the electric fields induced inside the body of a conducting model exposed to an external 60-Hz electric field.

Numerous experiments exposing laboratory animals to 60-Hz electric fields are being conducted at this and other laboratories to provide data for the assessment of possible risks to humans exposed to such fields. An important component in any extrapolation of biological data from animals to humans is a knowledge of the internal electric fields at both the outer surface of and inside the bodies of these species. This report describes a technique which has been developed for the measurement of the electric fields induced inside conducting models of animals and humans.

The measurement technique is illustrated in Figure 1, which shows a conducting model of a man standing on the ground and exposed to a vertical, 60-Hz electric field. A small probe is inserted in the torso to measure the induced electric field. The signals from this probe are routed via a shielded cable along the outer surface of the body to the ground plane, then to a remote readout module where the electric-field strength is computed. (An alternative routing of the cable would be inside the body to the foot, then along or under the ground plane to the readout module.)

Conducting Models -- Two methods have been developed for making conducting models in complex shapes. The first uses a hollow insulating mold to hold a saline solution in a desired shape. The second uses a solid conducting material cast in the appropriate shape, with field probes permanently implanted in the body.

The feasibility of the saline approach is dependent on being able to make insulating molds which minimally perturb the electric field. We tested two materials, polyurethane foam and styrofoam. The dielectric constants were measured by noting the change in the 60-Hz electric field between two parallel metal plates, separated by 11.9 cm, when 10.1-cm-thick blocks of the materials were inserted between the plates. For both materials, we measured dielectric constants of 1.03 ± 0.01. These values are very close to the dielectric constant of air (1.00), and produce only small field perturbations (<3%).

To make hemispheroidal molds from the foam materials, a special aluminum boring tool was fabricated in the form of a hemi-ellipse. For the more complicated shapes, a three-dimensional engraving tool was used to transfer a master mold to foam.

The second approach involved using a conducting plastic material. We developed such a material by mixing small amounts of acetylene black with a polyester resin plastic. This material is prepared in liquid form, then placed in a mold, where it hardens in the desired shape. Currently, we can prepare samples with conductivities in the desired range (0.001 to 1.0 S/m). However, our ability to predict in advance the conductivity of a given sample is limited. Work is underway to provide improved control over the various steps required to make the material.

Electric-Field Probe -- The design of the electric-field probe is shown in Figure 2. The voltages at two points separated by 1 cm are sampled by the conductive tips of the probe. The remainder of its body is covered with epoxy, for electrical insulation.

For initial testing of this probe, a 19.2-cm x 37.9-cm x 13.5-cm-high hollow box of polyvinyl chloride was built, and the two opposite 19.2 x 13.5-cm-high walls were covered with 1.6-mm-thick stainless steel sheets. In operation, the box was filled to a depth of about 5 cm with saline solutions, and a 60-Hz current was passed between the two end electrodes,

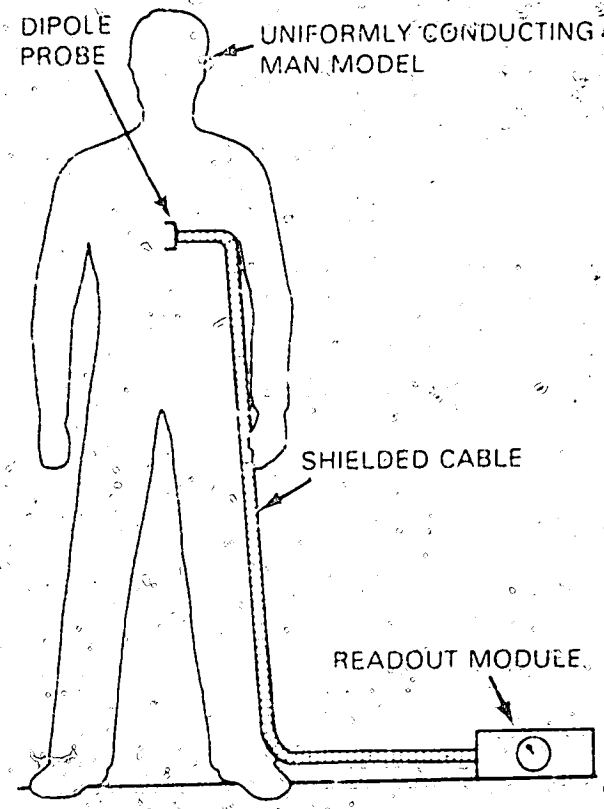

FIGURE 1. Conducting Man Model Standing on Ground and Exposed to a 60-Hz Electric Field. A probe is inserted in the torso to measure the induced electric field there.

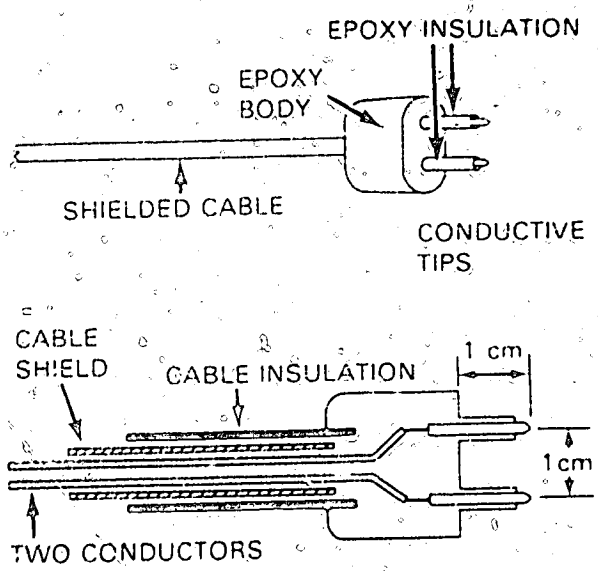

FIGURE 2. Detail Drawing of the Field Probe Design. The induced potential difference between two points separated by 1 cm are sensed and transmitted to a remote readout module through a shielded cable.

resulting in a uniform current density and electric field in the saline. Electric fields as low as 0.5×10^{-6} V/m were measured in this chamber.

An important quantity is the impedance between one of the tips of the field probe and a saline solution, because it is the basic element of the source impedance for the amplifier used to process the voltages from the probe. This impedance depends on the conductivity of the saline and on the area of the tip in conductive contact with the solution. For a typical probe design, we measured impedances (between the tip and the saline solution) ranging from 10^2 ohms (saline conductivity = 1.0 S/m) to 10^5 ohms (conductivity = 10^{-3} S/m). Estimates show that most of this impedance is from the medium surrounding the tip rather than from the tip-medium interface.

Shielded Cable -- The electric field induced inside a conducting model is greatly attenuated from the field outside the body. Therefore, the voltages detected by the probe will be small, and careful shielding of the signal leads is necessary to minimize noise pickup. We selected a 2.3-mm-diameter cable (Beldon 9640) that contained two conductors, surrounded by a foil shield to provide 100% electrostatic shielding. Experiments have shown that noise pickup with this type of cable is negligible.

Readout Module -- The readout module must measure the voltage between the two tips of the electric-field probe in the presence of a large, common-mode voltage. We selected a commercially available instrumentation amplifier module (Burr Brown 3620), used as shown in Figure 3. The differential voltage gain of this module was set to 1000, and it was followed by a second stage with switch-selectable gains of 1, 10, and 100. Capacitors were inserted in the input leads to force the small input dc bias currents of about ±25 nA to flow to ground through 1-megΩ resistors, rather than through the tips of the probe. This was necessary to avoid offset problems resulting from the large, time-dependent dc resistances between the probe tips and the saline. The measured common-mode rejection ratio of the readout module was 84 dB.

The noise level of the readout module is 1 μV referred to its input (i.e., an input of 1 μV will produce the same output-voltage as that produced by noise). The frequency spectrum of this noise is broad, therefore its contribution to the output voltage will be less than 1% for 60-Hz inputs exceeding 10 μV.

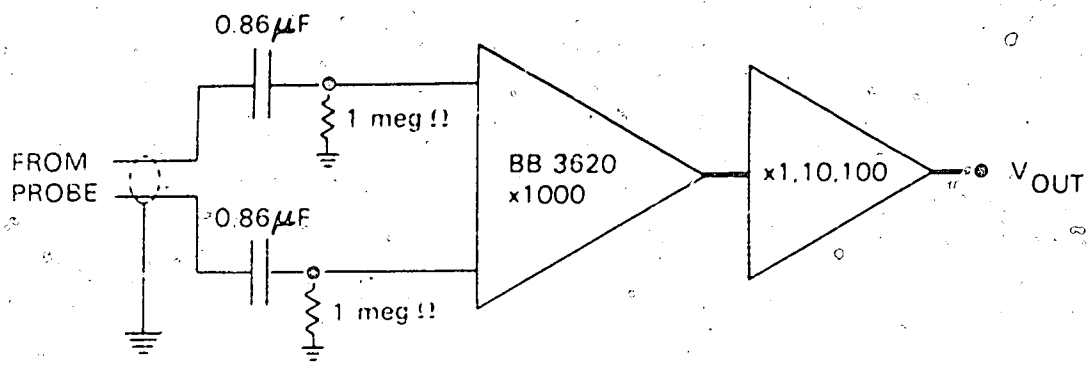

FIGURE 3. Electronics in the Readout Module. A Burr Brown 3620 instrumentation amplifier is followed by an additional gain stage. The measured common mode rejection of this unit was 84 dB.

System Tests -- Two tests of the overall measurement method were performed. In the first, a commercially available 15.2-cm-diameter hemispherical shell, made of 6.4-mm-thick plexiglass, was mounted on a stainless steel ground plane. The probe shown in Figure 2 was mounted approximately in the center of the hemisphere, on a 1.27-cm x 0.64-cm x 6.7-cm-high plexiglass stand. The hemisphere was filled with saline (conductivity = 0.090 S/m), and exposed to a 78.7-kV/m, 60-Hz electric field. The measured induced field inside was 0.00939 V/m (probe differential voltage = 99.5 μV; distance between probe tips = 1.06 cm).

The theoretical field, E, inside a hemisphere resting on ground and exposed to a uniform electric field, E_0, is $E = 3\omega\varepsilon_0 E_0/g$, where ω = angular frequency, $\varepsilon_0 = 8.85 \times 10^{-12}$ F/m, and g is the saline conductivity. We made two corrections to this formula: 1) E was multiplied by 1.06 to account for the effect of the plexiglass shell, and 2) E was multiplied by 1.02 to correct for the fact that the hemisphere spanned 40% of the gap between the parallel electrodes used to generate the exposure field. The final calculated value for the induced field inside the hemisphere was E = 0.00945 V/m, in excellent agreement with the measured value.

In a second test, a hemispheroidal model (15.2-cm-high, 5.1-cm-radius base) resting on a ground plane was exposed to a uniform field, and the induced field inside the model was measured and compared to theory. The model was made by filling with saline (conductivity = 0.021 S/m) a hemispheroidal volume which had been cut in a 13.5-cm x 14.0-cm x 16.5-cm-high block of polyurethane foam. This block was mounted on a stainless steel ground plane, a field probe was placed inside, 9.7 cm above ground level, and the block was exposed to a 11.0-kV/m electric field. The measured field in the saline was 0.0157 V/m, which compares very well with the theoretical value of 0.0160 V/m.

Conclusion -- The close agreement between calculated and measured values of the electric fields induced inside a conducting hemisphere and a conducting hemispheroid proves the feasibility and accuracy of our measurement technique. We are now using this technique to characterize the fields induced inside the bodies of human and animal models standing on a ground plane and exposed to a 60-Hz electric field.

In Vivo Mutagenesis—Electric Fields

These studies are concerned with the mutagenic potential of ac electric fields such as those which might be associated with the transmission of electric power. The project will provide indications of mutagenicity or primary DNA damage by electric field exposure in adult male, female and fetal rats. Electric-field-induced sensitization to mutagens will be evaluated by measuring the subsequent susceptibility of selected cell populations from exposed animals to chemical mutagens. This project will supplement the DOE Electrical Energy Systems (EES) Division study of the effects of electric-field exposure on rats and mice.

CYTOGENETIC EFFECTS IN RATS EXPOSED TO 60-Hz ELECTRIC FIELDS

Investigator: B. J. McClanahan

Technical Assistance: M. G. Horstman, R. L. Music, and L. I. Benton

Rats were exposed to a uniform, 60-Hz electric field at an unperturbed field strength of 100 kV/m. Examination of bone marrow cells indicated no increase in incidence of sister chromatid exchanges or micronuclei formation.

This project is concerned with mutagenic effects and damage to DNA that might result from exposure of animals to 60-Hz electric fields. Two studies were undertaken to evaluate the possible mutagenic and clastogenic potential of electric fields in bone-marrow cells of rats. In one study, the incidence of sister chromatid exchanges (SCEs) was determined in cells of animals exposed to electric fields. The SCEs, which appear to be related to both DNA repair and DNA synthesis, are increased in cells exposed either in vivo or in vitro to a wide variety of known mutagenic and carcinogenic chemicals. The other study involved measuring the frequency of micronuclei in cells of animals exposed to 60-Hz electric fields. Micronuclei are acentric chromosome and chromatid fragments resulting from chromosome breakage, which are not incorporated into daughter nuclei at mitosis. They may be detected with relative ease in maturing erythrocytes after extrusion of their nuclei. Thus, measurement of the incidence of SCEs and micronuclei can provide information on two types of DNA damage.

In the first study, female Sprague-Dawley rats were exposed to a uniform 60-Hz electric field at 100 kV/m, 20 hr/day for 5 wk. At 20 to 22 hr before sacrifice they were removed from the field and injected with 5-fluorodeoxyuridine. This was followed by a series of six injections, at hourly intervals, of 5-bromodeoxyuridine, which is incorporated into newly synthesized DNA. After injection, the animals were immediately returned to the exposure facility. At 2 to 2.5 hr before sacrifice, exposure was briefly interrupted for injection of colchicine, which arrests dividing cells in metaphase. After the end of exposure, bone-marrow cells from both femora were processed and stained with Hoechst 33258 and Giemsa to demonstrate SCEs. The frequency of SCEs did not differ in exposed and sham-exposed animals (Table 1).

Two replicate experiments were performed to measure the frequency of micronuclei in polychromatic and normochromatic erythrocytes in bone marrow of rats exposed for 5 and 30 days to a 60-Hz electric field. The marrow cells were extruded from the shaft of the femur with 70% fetal bovine serum. Air-dried smears of the cells were stained with Wright's-Giemsa and evaluated for micronuclei in erythrocytes. No differences were observed between the two treatment groups at either time period.

Under conditions employed in our facility, no statistically significant effect of electric-field exposure on the proliferation of bone-marrow cells has been demonstrated. Since the ratio of poly-

chromatic to mature erythrocytes is fairly consistent, the data can be expressed on the basis of total erythrocytes to eliminate subjective decisions on classification of cell types. When the frequency of micronuclei per total erythrocyte population were compared, no statistically significant effect due to treatment was demonstrated at either sampling. However, in both replicates, the normochromatic erythrocytes from both the sham-exposed and exposed animals killed after 5 days exposure exhibited a significantly elevated incidence of micronuclei relative to those killed after 30 days. Both control and exposed animals displayed the increase, demonstrating that the increased incidence was not related to electric-field exposure, per se. Furthermore, the fact that the increased frequency was significant only in the normochromatic erythrocytes suggests that a clastogenic event may have occurred prior to the 24- to 30-hr period preceding sacrifice of the animals. Slides from both samplings in each replicate are being re-examined to provide an independent validation of these observations and to provide a basis for design of additional experiments.

In neither study did chromosomal damage occur as a consequence of exposure to a 60-Hz electric field for up to 30 days. Experiments are now in progress to determine whether prior electric-field exposure would influence the in vitro induction of SCEs in mitogen-stimulated lymphocytes exposed to known mutagens such as methyl methanesulfonate, mitomycin-C or benzo[a]-pyrene. While exposure to a 60-Hz electric field did not significantly increase the in vivo induction of SCEs in bone-marrow cells, the susceptibility to chemical mutagens of electric-field exposed cells needs to be tested.

TABLE 1. Cytogenetic Observations in Bone Marrow Cells From Rats Exposed to a 60-Hz Electric Field.

	Duration of Exposure			
	5 Days		30 Days	
Experiment	Sham	Exposed	Sham	Exposed
1. Sister Chromatid Exchanges	--	--	2.19 ± 0.13[a]	2.24 ± 0.13
2. Micronuclei-P	0.96 ± 0.15[b]	1.62 ± 0.27	1.00 ± 0.13	0.98 ± 0.11
Micronuclei-N	3.00 ± 0.33[c]	2.55 ± 0.23	1.44 ± 0.15	1.34 ± 0.15
3. Micronuclei-P	1.62 ± 0.20	1.62 ± 0.19	0.80 ± 0.13	1.00 ± 0.11
Micronuclei-N	3.52 ± 0.36	3.14 ± 0.37	1.10 ± 0.25	1.12 ± 0.09

[a] Mean number of SCEs per cell ± SE in 20 cells from each of 10 rats per group

[b] Mean percentage ± SE micronuclei in 500 polychromatic erythrocytes scored in each of 10 rats per treatment group

[c] Mean percentage ± SE micronuclei in 500 normochromatic erythrocytes scored in each of 10 rats per treatment group

EFFECTS OF EXPOSURE TO A 60-Hz ELECTRIC FIELD ON UNSCHEDULED DNA SYNTHESIS IN SPERMATOGENIC CELLS AND ON SPERM ABNORMALITIES IN MICE

Investigator: B. J. McClanahan

Technical Assistance: S. A. Watson and R. . Music

Preliminary studies have not revealed any effect of exposure to a 60-Hz electric field (8 hr/day for 5 days) on DNA repair synthesis in spermatogenic cells or on induction of sperm abnormalities in mice.

After treatment with several chemical and physical mutagens, mouse sperm undergo DNA repair from meiotic through early to midspermatid stages. No repair occurs in late spermatids or in mature sperm. It is possible to study the effect of insult on DNA repair in meiotic and postmeiotic germ cells during spermatogenesis. After final DNA synthesis, spermatocytes continue to develop through a series of stages (lasting 28 to 30 days) until the spermatids leave the testes and enter the capita epididymides. DNA repair can be detected by sequentially measuring the incorporation of ^{3}H-thymidine (^{3}H-TdR) in spermatids found in the capita and caudae epididymides and vasa deferentia. Sperm abnormalitites can be produced as a consequence of exposure to chemicals or to certain physical agents, such as X-rays. The mechanism by which sperm abnormalities arise is not fully understood; however, the fact that an increased incidence can be correlated with exposure to certain carcinogens, mutagens and teratogens makes sperm a useful cell type for detecting possible deleterious effects of suspect agents. In addition, sperm provide information on whether exposure to such agents might be expected to alter reproductive performance.

In the study reported here, Swiss-Webster mice were exposed daily to a uniform, vertical, 60-Hz electric field at an unperturbed field strength of 100 kV/m for 8 hr (from 2300 hr to 0700 hr) for a period of 5 days. Immediately after exposure, the animals were removed from the exposure facility and were injected intratesticularly with 30 μCi ^{3}H-TdR under sodium pentothal anesthesia. Animals were killed by cervical dislocation at intervals over the next 41 days, and pooled samples of sperm from the caput epididymis, cauda epididymis and vas deferens were processed for each test interval to obtain suspensions of sperm heads free of tails, midpieces and cellular debris. The sperm heads were then dissolved in Protosol (New England Nuclear), mixed with a liquid scintillator and assayed for ^{3}H content. The intratesticular incorporation of ^{3}H-TdR by sperm sampled in the various parts of the reproductive tract are graphically represented in Figure 1. Cells that were in the last scheduled DNA synthesis stage at time of injection passed through the caput epididymis at 29-31 days after injection, then to the cauda epididymis, and into the vas by 37 to 39 days. Non-scheduled incorporation of ^{3}H-TdR by postmeiotic cells at earlier times in the sequence figure would be indicative of DNA repair synthesis. Since none occurred the DNA was apparently unaffected by exposure to the field.

The significance of the apparent differences in scheduled DNA incorporation between the sperm from the sham-exposed and exposed groups in the caput epididymis and vas deferens cannot be evaluated since the use of pooled samples precludes statistical analyses of the data. However, the inconsistency of the results in the two groups suggests that the differences are not significant. The fact that sperm from the caput and cauda epididymis and vas represent the same cell population at different points in time suggests that the relationship between treatment groups should be the same in the three sites sampled.

An experiment is in progress that employs the same exposure protocol to examine the influence of electric-field exposure on the susceptibility to subsequent insult by the mutagen ethyl methanesulfonate, which is known to induce DNA repair synthesis in mouse spermatogenic cells.

In a preliminary study, we measured the frequency of abnormal sperm in the cauda

epididymis at 1 and 37 days after exposure in Swiss-Webster mice exposed 8 hr/day for 5 days. They were then removed from the exposure facility, and smears of sperm from the cauda epididymis were stained with eosin and examined for the presence of abnormal sperm. No increase in the number of abnormal sperm was detected.

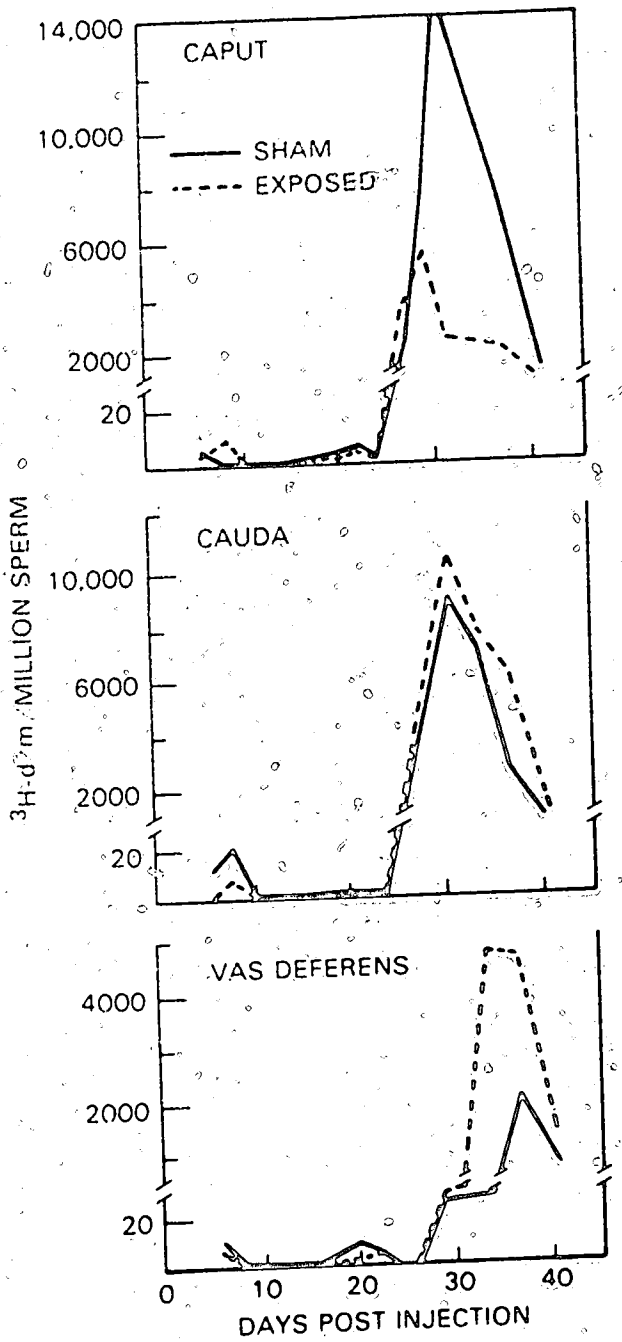

FIGURE 1. Unscheduled DNA Synthesis in Germ Cells of Mouse Measured in Sperm Moving Through the Reproductive Tract.

(Table 1) nor were differences observed in types of abnormalities between the two groups. In a future experiment, sperm from the caudae epididymides of mice that were also exposed for 5 days will be evaluated for the presence of abnormal sperm, at intervals, over a 10-week period.

TABLE 1. Incidence of Abnormal Sperm in Mice Exposed for Five Days to 60-Hz Electric Field.

	Time Postexposure	
	1 Day	37 Days
Sham	2.80 ± 0.57[a]	2.20 ± 0.81
Exposed	3.47 ± 0.27	2.13 ± 0.54

[a] Standard error of mean percentage abnormal sperm in seven mice

In Vitro Effects of Electric Fields

This project seeks to determine and quantify cytotoxicity, DNA damage and/or specific gene mutation resulting from exposure of mammalian cells in suspension to 60-Hz electric fields. In addition, these cells will be exposed to either direct-acting or indirect-acting mutagens in combination with electric fields in order to determine whether exposure to electric fields can alter (increase or decrease) the responses of mammalian cells to known mutagens. Finally, if electric field effects are detected, we will attempt to establish dose-response relationships.

IN VITRO EFFECTS OF AC ELECTRIC FIELDS: MAMMALIAN CELL ASSAYS

Investigators: M. L. Frazier, W. T. Kaune, A. J. King, J. Samuel, and T. K. Andrews, Jr.

We have developed a new method for exposing cells in vitro to 60-Hz electric fields which [illegible] the use of electrodes, either in conductive contact with, or insulated from the growth medium. During the past year, we also defined optimal conditions for cell growth in this exposure system, and attempted to solve other problems associated with its use with [illegible] cell cultures (e.g., maintaining uncontaminated cultures, obtaining representative [illegible] at real-time intervals). Using this system, we have obtained preliminary data [illegible] effect of 60-Hz electric fields (3.1 V/m) on growth rate, mutation frequency, and [illegible] viability. No effects attributable to electric-field exposure have been observed.

The objectives of this study are to ascertain whether 60-Hz electric fields can cause specific gene mutation, DNA damage, altered growth rates and/or decreased viability of in vitro suspensions of mammalian cells. We are using Chinese hamster ovary (CHO) cells. So far, we have evaluated the effect of a 3.1-V/m electric field on growth rate, viability (as determined using both trypan blue exclusion and cell-plating efficiencies), and mutation frequency (at the hypoxanthine-guanine phosphoribosyl transferase locus) of CHO cells.

Techniques used in previous research to expose cell suspensions to 60-Hz electric fields involved the use of electrodes, either in conductive contact with, or insulated from the suspending medium. Those techniques had significant limitations and uncertainties: using insulated electrodes, it is extremely difficult to generate fields in highly conducting systems (such as a mammalian-cell suspension) even approaching the size of the 0.02-0.2 V/m field induced in the human body by the 10-kV/m electric field from an ultrahigh-voltage transmission line; strong fields can be produced using conducting electrodes placed directly in the media, but compounds introduced into the media from the electrodes may affect cell growth and mutation frequencies.

In view of these considerations, we developed a new exposure system, which uses an alternating magnetic field as the source for the electric field. The use of electrodes, either insulated from or in conductive contact with the growth medium, is thereby avoided.

Essentially, the system consists of a simple transformer, in which the primary winding is connected to a 60-Hz voltage source, and the secondary winding is a cell suspension contained in a toroidal container of glass or rubber tubing (Figure 1). By selecting a material for the magnetic core that has a high saturation flux density and a high magnetic permeability, it is possible to produce sizable electric fields (3 V/m) in the medium while limiting the leakage of the magnetic field to which the cells are exposed to a very small value.

We have constructed a system using a transformer core having inside dimensions: 24 cm x 24 cm; outside dimensions, 44 cm x 44 cm; and core cross-section, 10 cm x 10 cm (Figure 1). The core material is Silectron 66 with a relative permeability

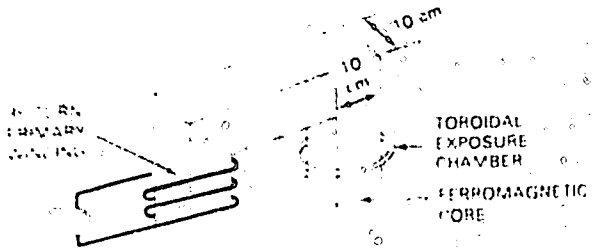

FIGURE 1. [illegible] Which Uses a 60-Hz Magnetic [illegible] Induce a 60-Hz Electric Field in a Toroidal Chamber Containing a Cell Suspension. Not shown in the figure are [illegible] and μ metal shield which enclose the [illegible] exposure chamber.

[illegible] of [illegible], and a saturation flux density of about 1 T (10 kG). The primary winding (35 turns) was wound on one leg of the core; the toroidal chamber containing the cell suspension was placed around the opposite leg. The temperature of the suspension is controlled by placing it in a water bath constructed of plexiglass covered with 0.25-mm-thick μ metal.

The system is energized by a variac connected to a filtered source of 115-V, 60-Hz power (AC Line Conditioner, California Instruments, Model 1201B, total harmonic distortion 0.5%).

A program of measurements was carried out to characterize the exposure system, with the following results:

1) For primary voltages up to 80 V, effects associated with saturation of the core were small.

2) The output impedance of the transformer into a one-turn secondary was 1.1 ohm (resistive). Therefore, the load comprised of the cell exposure chamber and its water bath is equivalent to an open circuit.

3) Measurements were made of the magnitude and harmonic content of the secondary voltage V_{sec} for primary voltages ranging from 0.05 V to 80 V (Table 1). The theoretical electric field in a conducting toroid encircling a leg of the core is V_{sec}/ℓ where ℓ is the length of the toroid. This formula was verified by direct measurement and the uniformity of the electric field around the toroid was found to be ±2%.

4) The leakage magnetic field to which cells would be exposed was found to vary around the circumference of the toroid by a factor of 3. Enclosing the exposure chamber in 0.25-mm-thick μ-metal decreased this field by a factor of 5. Maximum strengths and total harmonic distortions of the leakage magnetic field are given in Table 1 for primary voltages in the range 0.05-80 V.

5) The water bath maintained the temperature of the cell suspension at 37.1°C (±0.1°C) over a 24-hr period.

Our major concern was to develop a containment vessel for cell cultures to be exposed in the new exposure system. This exposure vessel had to: (1) allow orientation of the cells within the field so that they were in suspension (not on the surface of the exposure chamber); (2) allow easy maintenance of sterile conditions; and (3) provide conditions for optimal cell growth.

Three types of containment vessels were studied: latex, tygon, and surgical-grade silicone tubing. Initially, cells were kept suspended by either rolling or shaking the tubing. Our tests indicated that the latex tubing contained materials toxic to the cells; with the tygon tubing, the cells attached to the surface. Although the cells did not attach to the silicone tubing in the "shaking" mode, and the cells grew, the population-doubling time of the cells increased from 15 hr (controls) to about 40 hr (Figure 2), which might compromise an experiment. Furthermore, at this time we determined that in order to provide a uniform field, the exposure tubing had to be completely filled with culture medium. Therefore, a third exposure mode for keeping the cells suspended, was tested.

In this system, a layer of agar-containing medium was added and allowed to solidify prior to adding the cells. The cells were grown under a liquid medium on the surface of the agar. This system has the following advantages: it allows the cells to grow while "attached" to a surface and to remain in suspension with respect to the electric field; the cells and exposure chamber do not need to be shaken. Results indicate that this procedure yielded growth rates during the first 20-24 hr similar to those obtained under standard culturing procedures for the CHO cells (Figure 3). In the present

TABLE 1. Electric Fields and Leakage Magnetic Fields to Which Cells are Exposed in the New Induction Exposure System. Electric-field values are for exposure chamber with length of 63 cm. Measurements made inside μ-metal covered water bath, but with water removed. Total harmonic distortion (THD) values are given for both fields.

		Exposure Electric Field		Maximum Leakage Magnetic Field	
Primary Voltage, V	Secondary Voltage, V	Strength, V/m	THD[b], %	Strength, G	THD[b], %
80[a]	2.24	3.6	1.0	0.1	29
40	1.11	1.8	0.7	0.06	11
10	0.283	0.45	0.8	0.02	3.4
1.0	0.0279	0.044	1.0	0.004	6.0
0.50	0.0140	0.022	1.5	0.003	10.0
0.10	0.00266	0.0042	2.9	0.001	10.0
0.05	0.00127	0.0020	4.5	0.001	--

[a] Level at which saturation becomes significant
[b] Essentially all third harmonic

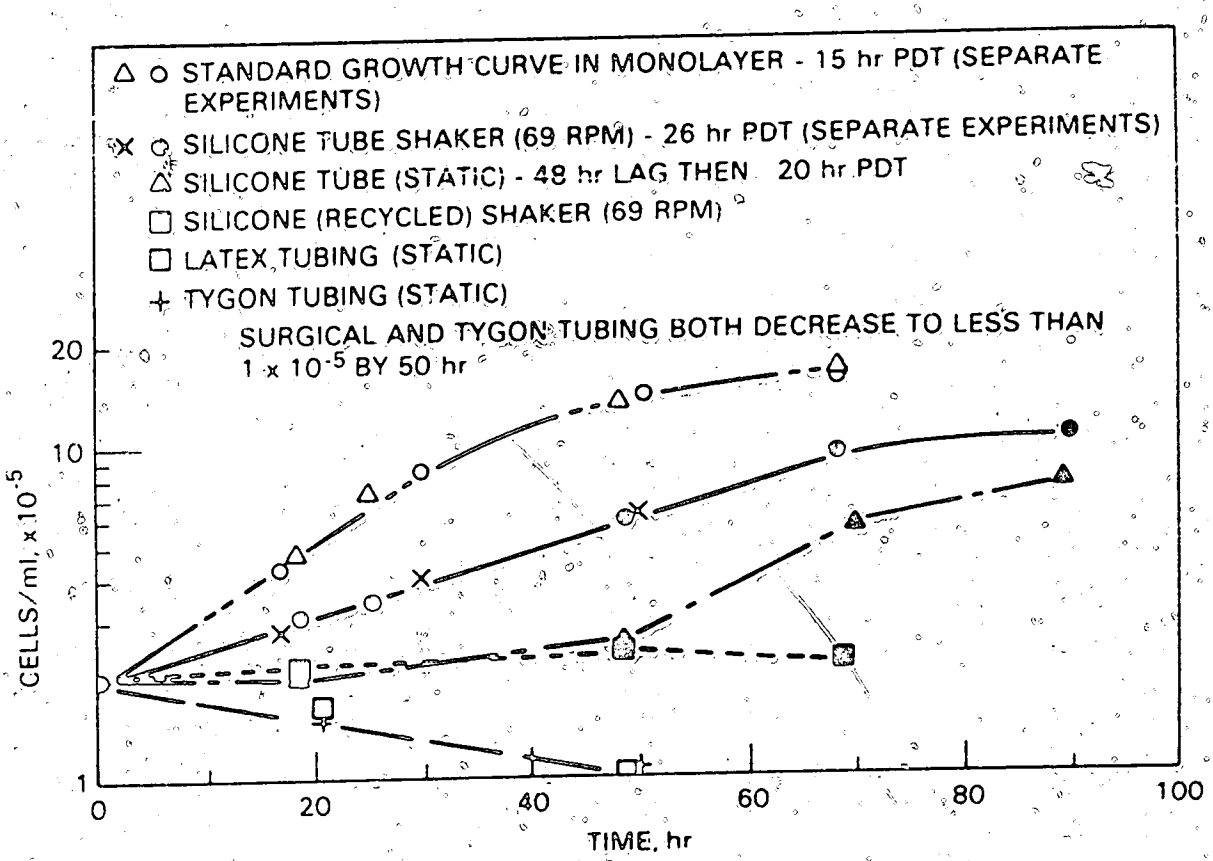

FIGURE 2. Comparison of Growth Rates of CHO Cells in Different Types of Tubing Under Standard Cell Culture Conditions.

[illegible], the population-doubling time (PDT) of CHO cells in both E-field-exposed (3.1 [illegible] m) and E-field sham-exposed chambers is approximately 20 and 24 hr, respectively. The PDT of nonexposed CHO cells under normal cell-culture conditions was 14-16 hr (Figure 4). Viability measurements on E-field-exposed cells, as determined using trypan blue, were comparable (98-99%) for exposed and control cultures. We have observed decreased plating efficiencies of E-field-exposed cells relative to E-field sham-exposed cells. Pilot growth rate studies indicated no significant difference between these two groups. Finally, mutation frequencies of cells exposed to a 60-Hz electric field of 3.1 V/m do not appear to differ significantly from those of control E-field sham-exposed cells (Table 2).

In current studies we are measuring growth rate, viability, and mutation frequency of CHO cells exposed to various E-field strengths (from [illegible] V/m to 3.1 V/m) for different time durations (8-50 hr).

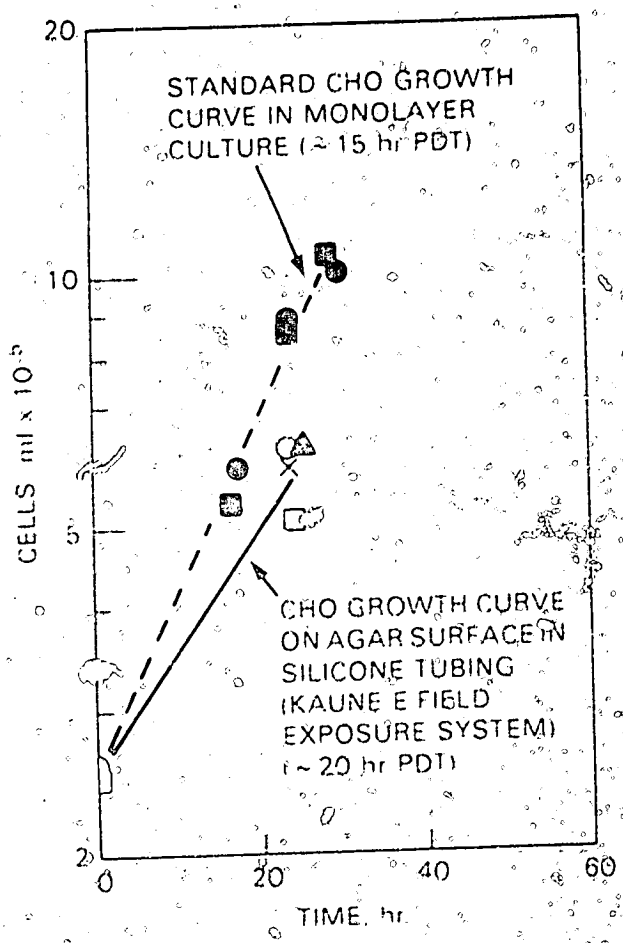

FIGURE 3. Comparison of Growth Rates of CHO Cells in the New Electric-Field Exposure System and in Standard Cell Culture Conditions

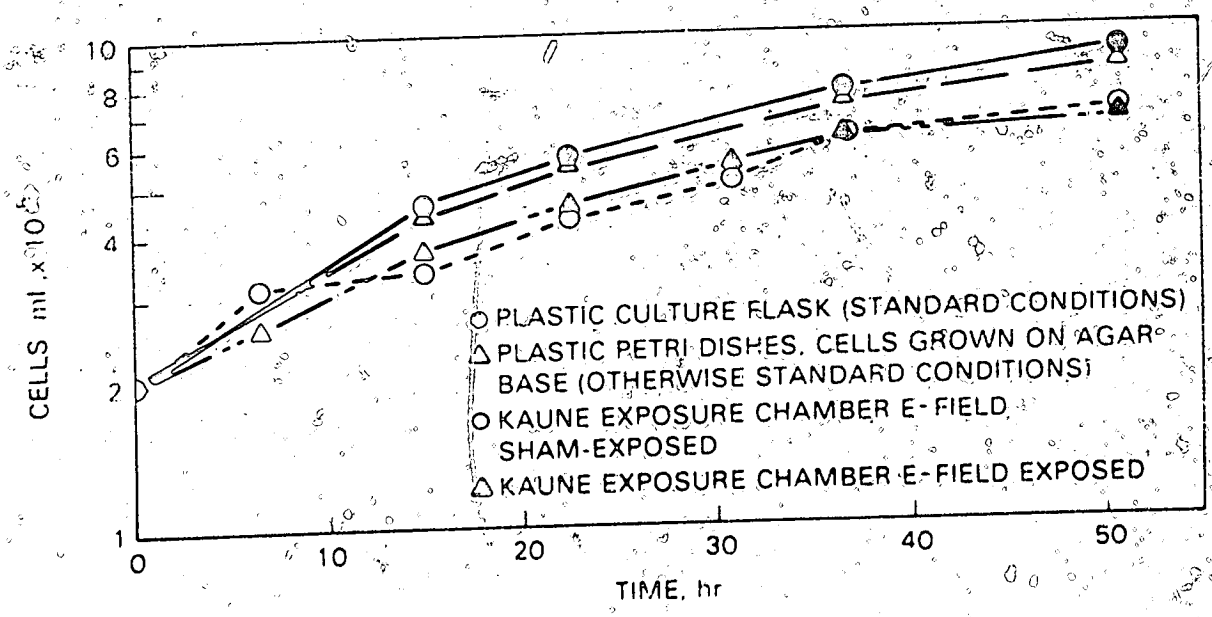

FIGURE 4. Comparison of Growth Rates of CHO Cells From Exposed, Sham-Exposed and Nontreated Cultures

TABLE 2 Effect of 60-Hz AC Electric Fields (3.1 V/m) on Cultured Mammalian CHO Cells.

Exp.	Duration of Treatment	Number of Cells (mL x10[illegible])			Cell Viability (%)			Total Survival (%)			Mutation Frequency (/10[illegible] Viable Cells)		
		EEF[a]	IEC[b]	Cont[c]	EEF	IEC	Cont	EEF	IEC	Cont	EEF	IEC	Cont
[illegible]	[illegible]	[illegible]	[illegible]	[illegible]	[illegible]	[illegible]	[illegible]	[illegible]	[illegible]	[illegible]	[illegible]	[illegible]	[illegible]
[illegible]	[illegible]	[illegible]	[illegible]	[illegible]	[illegible]	[illegible]	[illegible]	[illegible]	[illegible]	[illegible]	[illegible]	[illegible]	[illegible]
[illegible]	[illegible]	[illegible]	[illegible]	[illegible]	[illegible]	[illegible]	[illegible]	[illegible]	[illegible]	[illegible]	[illegible]	[illegible]	[illegible]
[illegible]	[illegible]	[illegible]	[illegible]	[illegible]	[illegible]	[illegible]	[illegible]	[illegible]	[illegible]	[illegible]	[illegible]	[illegible]	[illegible]
[illegible]	[illegible]	[illegible]	[illegible]	[illegible]	[illegible]	[illegible]	[illegible]	[illegible]	[illegible]	[illegible]	[illegible]	[illegible]	[illegible]
[illegible]	[illegible]	[illegible]	[illegible]	[illegible]	[illegible]	[illegible]	[illegible]	[illegible]	[illegible]	[illegible]	[illegible]	[illegible]	[illegible]
[illegible]	[illegible]	[illegible]	[illegible]	[illegible]	[illegible]	[illegible]	[illegible]	[illegible]	[illegible]	[illegible]	[illegible]	[illegible]	[illegible]
[illegible]	[illegible]	[illegible]	[illegible]	[illegible]	[illegible]	[illegible]	[illegible]	[illegible]	[illegible]	[illegible]	[illegible]	[illegible]	[illegible]
[illegible]	[illegible]	[illegible]	[illegible]	[illegible]	[illegible]	[illegible]	[illegible]	[illegible]	[illegible]	[illegible]	[illegible]	[illegible]	[illegible]
[illegible]	[illegible]	[illegible]	[illegible]	[illegible]	[illegible]	[illegible]	[illegible]	[illegible]	[illegible]	[illegible]	[illegible]	[illegible]	[illegible]
[illegible]	[illegible]	[illegible]	[illegible]	[illegible]	[illegible]	[illegible]	[illegible]	[illegible]	[illegible]	[illegible]	[illegible]	[illegible]	[illegible]
[illegible]	[illegible]	[illegible]	[illegible]	[illegible]	[illegible]	[illegible]	[illegible]	[illegible]	[illegible]	[illegible]	[illegible]	[illegible]	[illegible]

[a] [illegible]
[b] [illegible]
[illegible]
[c] [illegible] Sham-Exposed
[illegible]
[illegible] Experiments were sequentially [illegible] data from Experiments [illegible] have been [illegible] but they are not relevant to the points discussed here.

FISSION

Most of our biomedical studies in the fission energy technology area are directed toward the evaluation of long-term effects from low-level exposure to radioactive pollutants. These include studies in progress for many years in dogs that have inhaled various plutonium compounds. The inhalation toxicity of a wide variety of actinide compounds is being studied in rodents. Both dogs and rodents are employed in continuing studies of the effects of chronic exposure to simulated uranium mine atmospheres.

More recently instituted studies are concerned with the possible synergistic effects of inhaled plutonium and cigarette smoke with specific reactor technology problems, such as the toxicity of sodium or lithium that might be accidently released from a liquid metal fast breeder reactor or from a fusion reactor, or the toxicity of mixed aerosols of plutonium and sodium. A study of the toxicity of chronically inhaled krypton-85 released in small amounts from nuclear reactors is being concluded. Because of recent interest in nonproliferative fuel cycles, special hazards that might be associated with reactors employing a thorium fuel cycle are being investigated.

More basic studies are concerned with the effects of age on the toxicity of incorporated radionuclides and the effect of age and other factors on the gastrointestinal absorption of radionuclides. Viral and biochemical factors that may be involved in radiation carcinogenesis are also under study.

In the medical area, a device is being developed to irradiate the blood, which may be a useful treatment for leukemia or for the prevention of transplant rejection.

In all of these areas the development of new experimental techniques plays an important role. This has included the effort in aerosol generation and exposure technology, and increasing emphasis on the computer handling and statistical analysis of animal toxicology data.

Aerosol Technology Development

We have developed techniques for generating and characterizing aerosols of energy-source-related material. We have also improved the design of inhalation exposure chambers used in health effects studies.

[illegible] IN AEROSOL EXPOSURE CHAMBER DESIGN

[illegible] W. C. Cannon and E. F. Blanton

[illegible] Assistance: [illegible]

[illegible] exposure chambers are being studied using a dynamically [illegible] model. Data obtained predict that the [illegible] time [illegible] exposure chambers can be reduced to 34 sec by use of a new [illegible] with the present [illegible] exposure system.

[illegible]

[illegible] water [illegible] chamber, with covered [illegible] the water to simulate [illegible] are analyzed [illegible]

[illegible] chamber [illegible] model [illegible] for [illegible] exposure. The designs are [illegible] with the inlet at [illegible] at the bottom, and animal [illegible] chambers are compatible [illegible] system at [illegible] cylinder, with [illegible] at the inlet [illegible] the exhaust port [illegible] aerosol mixing, a [illegible] alternately [illegible] the outer wall or [illegible]

[illegible] concentration at an [illegible] ultimate [illegible]

[illegible] a major portion [illegible] a central [illegible] Chamber 4, [illegible] arrangement, has inlet and exhaust [illegible] that are concentric, [illegible] which the inlet system [illegible] and the exhaust [illegible] exposure port [illegible] at the [illegible] of the two [illegible]

Buildup characteristics for chambers [illegible] and 3 were compared in the 1979 Annual Report. In Figure [illegible] buildup curves [illegible] concentration are compared for all four chambers at a midlevel exposure port. From these curves it appears that chamber [illegible] not an improvement over the simple cylinder without baffles [illegible] for chamber [illegible] stream of higher dye concentration, not readily mixed, which persists for some time. Chamber 3 requires more time to reach its ultimate concentration than the other chambers. The [illegible] values of the four chambers are [illegible] min, [illegible] min, 14.25 min, and [illegible] min, respectively. The equivalent [illegible] for aerosol buildup [illegible] chambers would be [illegible] min, [illegible] min, [illegible] and 34 [illegible], respectively.

Not included in the simulation is the depletion of aerosol at lower chamber levels by animals in the levels above. This could be important in chambers 1 through 3, however, in chamber 4, this problem is avoided by supplying "fresh" aerosol to each animal. Air exhaled by one animal does not reach any other animal in the chamber.

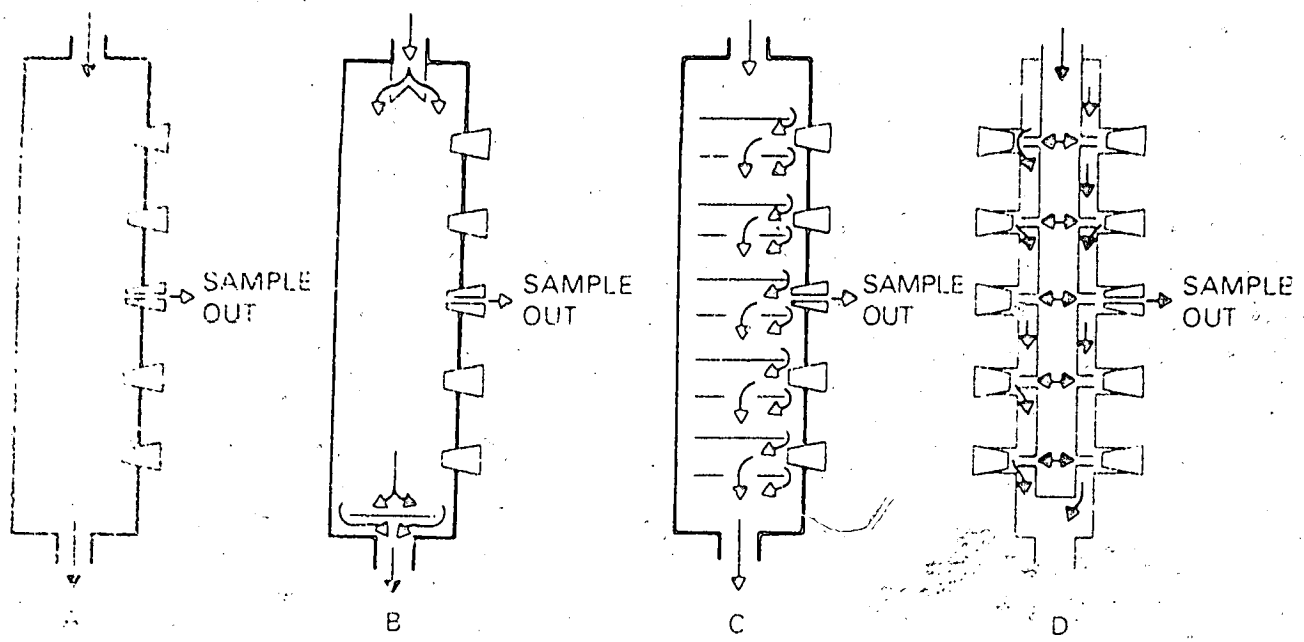

FIGURE 1. Aerosol Exposure Chamber Designs.

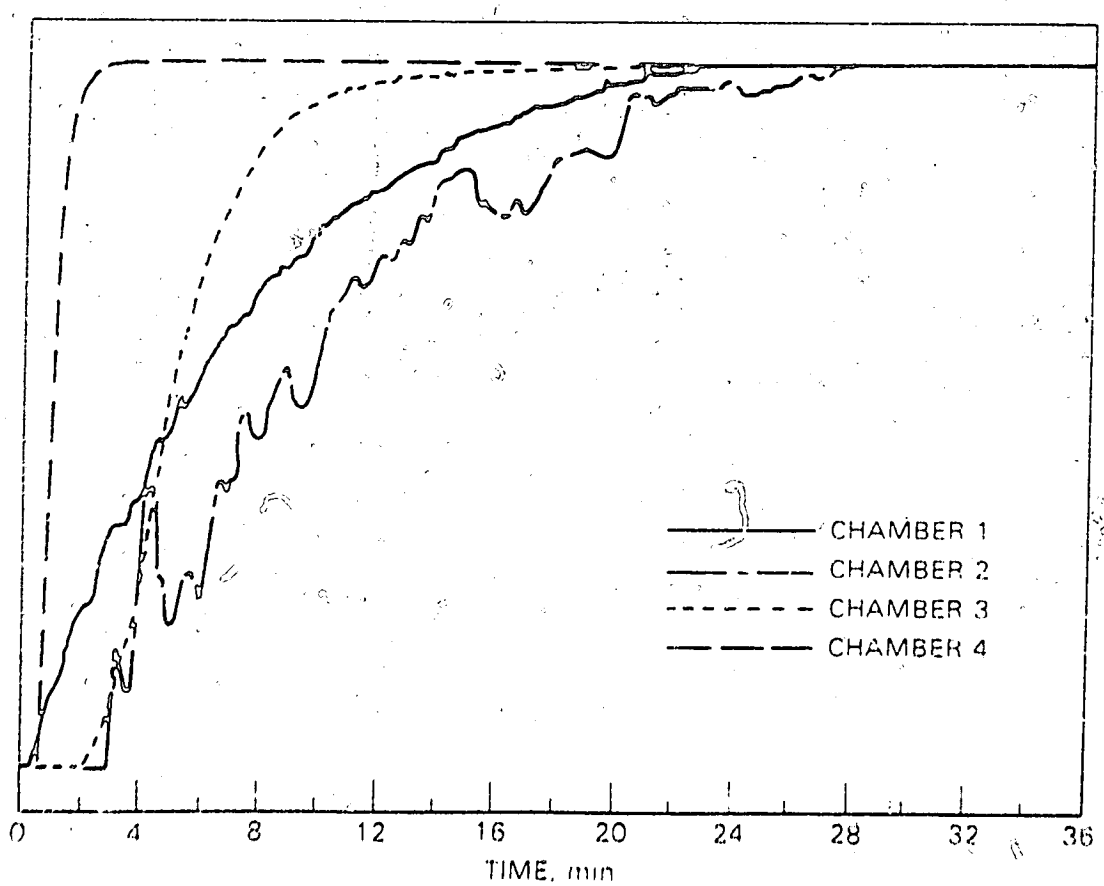

FIGURE 2. Comparison of Aerosol Exposure Chamber Concentration Buildup Curves.

PROGRESS IN DRY DUST FEEDER DEVELOPMENT

Investigators: O. R. Moss, D. P. Y. Chang, and E. M. Milliman

In further tests of a previously developed flexible-brush dust-feed mechanism, the two brushes were placed parallel instead of perpendicular and the dust output fed to a dispersion device. Feed rate of dust from the open end of the feed-brush tube increased linearly with the rotational speed of the feed brush (0.5 to 50 rpm). The coefficient of variation of the output was 2 to 7%. Tests indicate that loading and clogging of the feed-brush tube and design of the dispersion device are key problems for certain dusts in such a two-phase generator.

This year, further tests were made with the dual flexible-brush dust-feed device previously developed (Annual Report, 1972), with the feed brushes in parallel instead of perpendicular configuration (Figure 1), and with the dust output fed to a dispersion device. Dust delivery of flyash from the open end of the feed brush tube increased linearly with the rotational speed of the feed brush (mass output in mg/min = 2.3 x rpm - 0.41 for rpm between 0.5 and 50). The coefficient of variation of output was 2 to 7%. Stability of long-term output of fly ash is shown in Figure 2; decay in output was due to humidity change in the laboratory.

Four different dusts were tested in the dust-feed mechanism: fly ash, less than 45-μm sieve size; a pyrogenically formed, amorphous silica; a knife-milled mixture of red phosphorus, butyl rubber and organic binder; and a combination of the red phosphorus mixture and the amorphous silica. For the relatively noncohesive material (fly ash) a slight output decay was observed, which appeared to be a function of relative humidity. The output of the highly charged material (the silica) increased slightly with time. (The material in the hopper became more dense due to loss of entrapped air and slight agglomeration.) The red phosphorus mix-

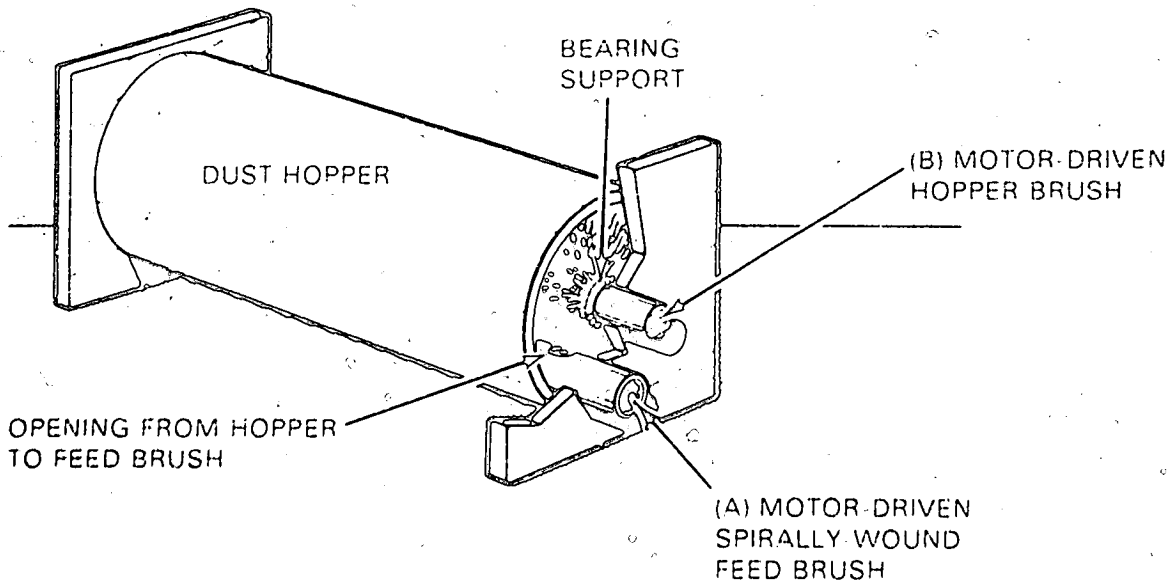

FIGURE 1. Dual Flexible-Brush Dust Feed Mechanism, Parallel Brush Geometry

ture could not be generated because it would not fall from the bristles of the feed brush. Such materials, which form adherent clumps that grow larger than the dimensions of the passages between the feed-brush bristles, cannot be successfully transported. The output of the cohesive but not agglomerated mixture (the phosphorus and silica, combined) decayed exponentially (about 10% per hour). The output feed rate changed linearly with feed-brush rotational speed regardless of the decay rate, indicating that difficult-to-deliver cohesive dusts can be metered in a reasonably constant fashion by frequent adjustment of the feed brush.

The action of the deagglomerating device was sensitive to the same dust properties as was the output of the feed-brush tube. Loading and clogging of certain dusts in the feed-brush tube in the deagglomerating device are key problems in a two-phase generator system such as ours.

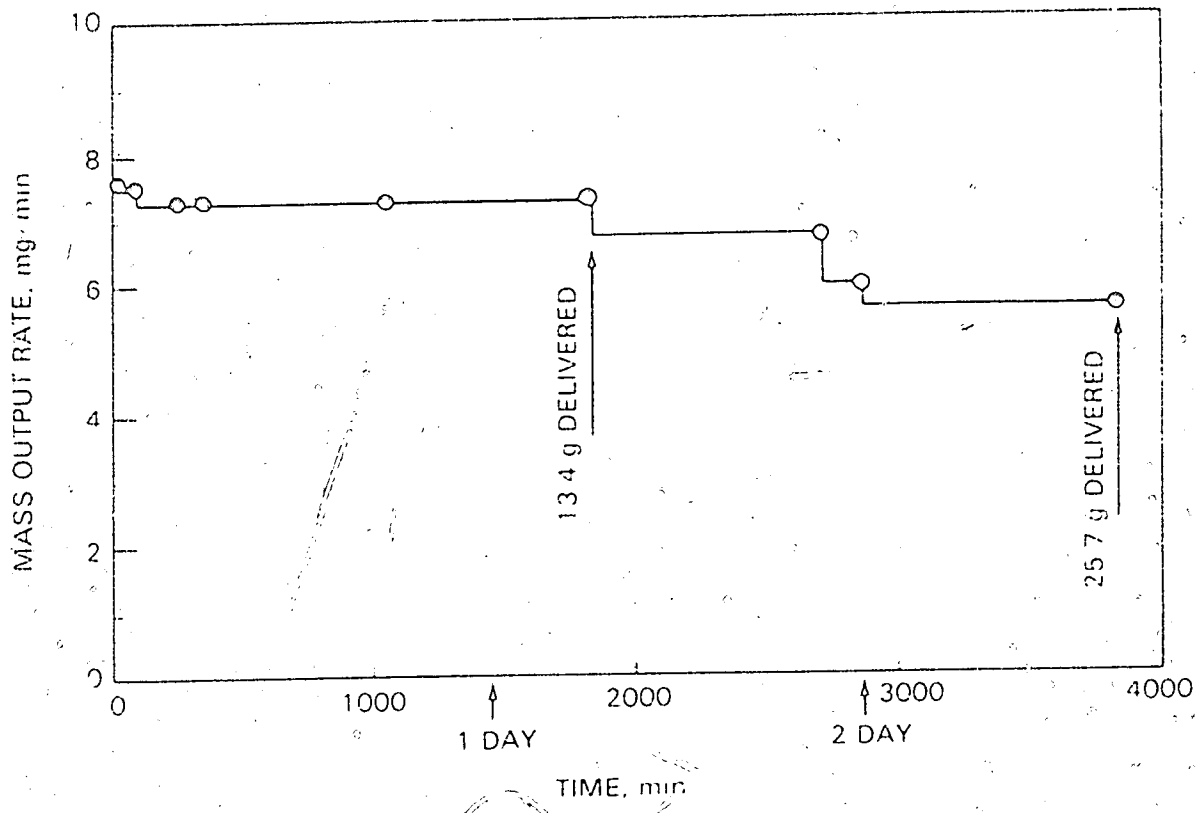

FIGURE 2. Long-Term Output of Fly Ash (Room Humidity Uncontrolled)

DISSOLUTION RATES OF $^{241}AmO_2$*

Investigators: W. C. Cannon, E. J. Rossignol, and O. R. Moss

We have measured the dissolution rates of powdered americium dioxide in water and in simulated lung interstitial fluid, with and without DTPA added. For short intervals (up to 4 hr), the dissolution rate in water was approximately 3.5×10^{-1}%/hr; in lung fluid simulant, it was less than 2×10^{-8}%/hr. Addition of DTPA increased dissolution rates by at least a factor of three.

We have been studying dissolution rates of $^{241}AmO_2$ used in the program, "Inhaled Americium Dioxide in Dogs." We have measured the short-term dissolution rate in water of $^{241}AmO_2$, as the calcined powder, as a function of time after calcination. The time between calcination of the oxide and dissolution rate measurement ranged from 6 to 90 days. The powder was stored dry until the tests were performed. Measurements were made in a stirred-cell apparatus and in a flow-past configuration (Figure 1). Percent of total activity dissolved per hour, for periods up to 4 hrs, are given in Table 1.

We have also compared dissolution rates of this chemical in water and in simulated lung fluid (SLF) (Health Phys. 36: 447-448, 1979), and have investigated the effects of adding a chelating agent (0.34 μmole/ℓ DTPA) to each solvent. Preliminary results are shown in Table 2. Water suspensions of the AmO_2 samples for dissolution studies were applied to Millipore HAWP filters and dried. A sandwich, consisting of this filter placed between 0.1-μm Nuclepore filters, was placed in a flow-past holder and solvent flowed through the system for 4 hrs. The dissolution rate in SLF was much lower than in H_2O; DTPA increased the rate by nearly a factor of three in water and by at least a factor of five in SLF. (Dissolved activity in SLF without DTPA was below our detection limit.)

We had intended to study dissolution rates over long time intervals using the flow-past apparatus. Unfortunately, up to 50% of the soluble ^{241}Am activity was deposited on flow-past cell surfaces. This material cannot be recovered or analyzed until the experiment is terminated.

*This work was jointly supported by Aerosol Technology Development, D8132-81408 and Inhaled Americium Dioxide in Dogs, D8132-80188.

TABLE 1. Effect of Dry Aging on Dissolution Rate.

Time After Calcining (days)	Percent Activity/hr Stirred Cell	Percent Activity/hr Flow Past
6	1.62×10^{-1}	1.1×10^{-1}
20	2.16×10^{-1}	5.20×10^{-1}
61	3.02×10^{-1}	6.7×10^{-1}
90	3.47×10^{-1}	3.45×10^{-1}
96	2.1×10^{-1}	

TABLE 2. Dissolution Rates in H_2O and SLF[a] Average Percent per Hour Over 4 Hours

Medium	With DTPA	Without DTPA
H_2O pH ~ 7	9.84×10^{-1}	3.45×10^{-1}
SLF pH ~ 7	1.15×10^{-1}	2×10^{-1} Detection Limit

[a] Simulated Lung Fluid (Moss, 1978).

Unless such deposition can be prevented, the flow-past cell apparatus is not useful for this experiment.

As an alternative, we are examining a serial analysis scheme in which a number of americium dioxide aerosol samples are placed in capped sample vials at time zero, then analyzed for soluble activity at the end of designated time periods. However, it is difficult to maintain a constant pH in the capped vials. In a preliminary experiment conducted for a 14-day period, the samples analyzed after 14 days had a smaller percent of dissolved activity than those analyzed after 1, 3 and 7 days (Figure 2).

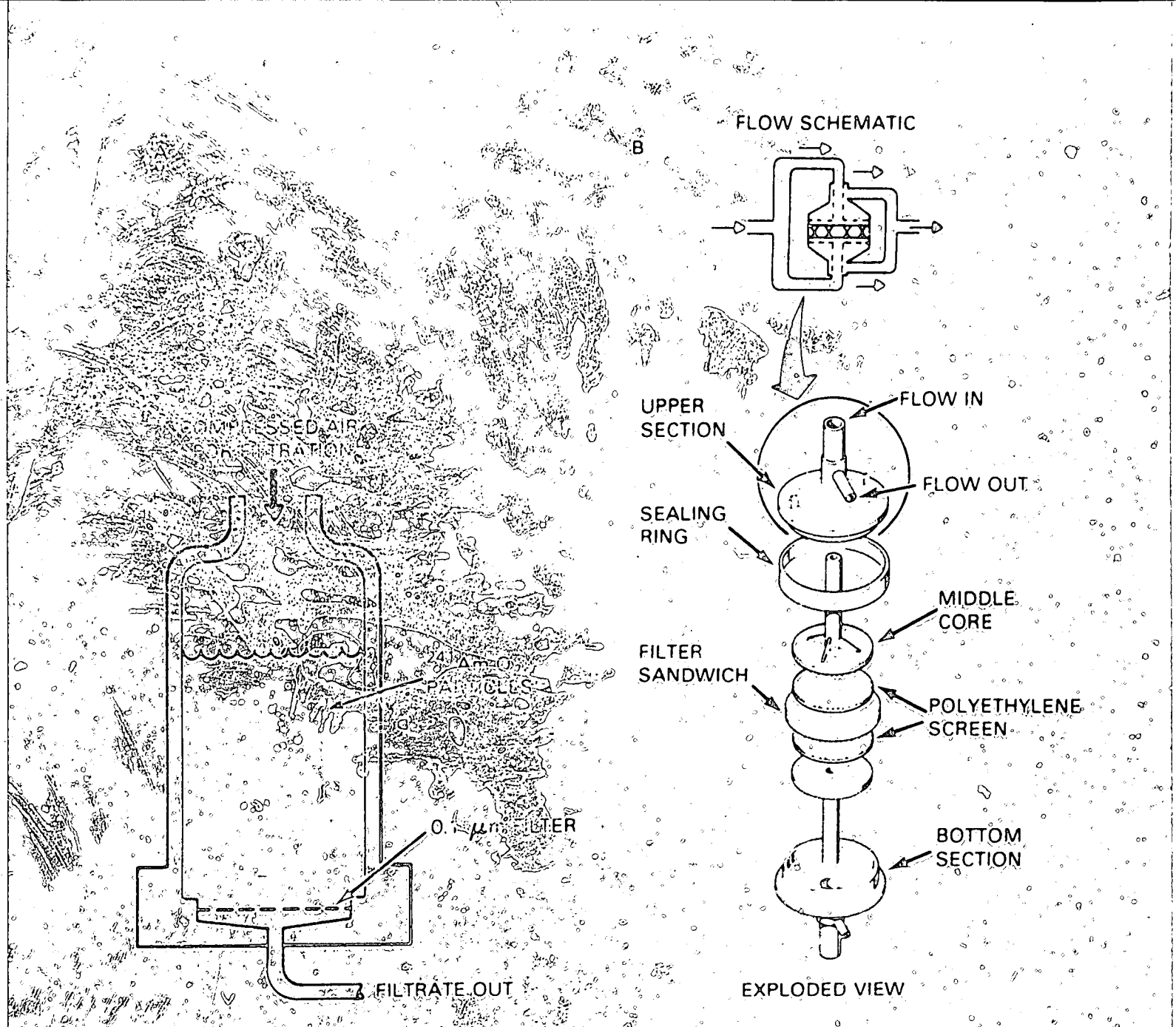

FIGURE 1. Diagram of Stirred-Cell Apparatus (A) and Flow-Past Cell (B) for Measuring Dissolution Rates of $^{241}AmO_2$ in Water or Simulated Lung Fluid.

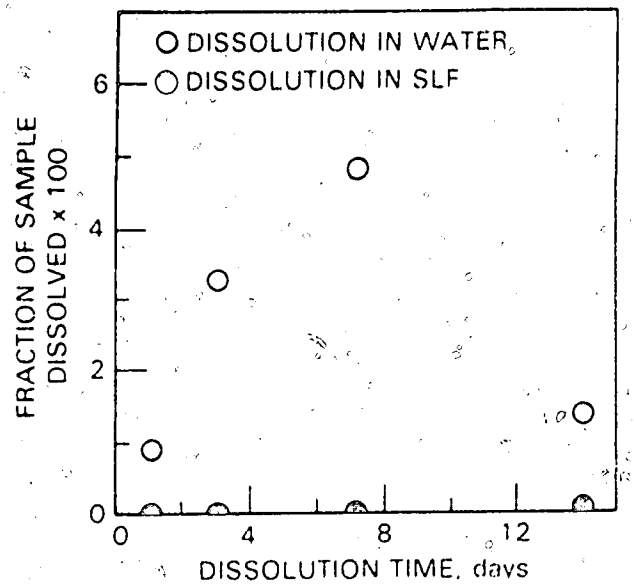

FIGURE 2. Dissolution of ^{241}Am in Capped Vials.

MOUNT ST. HELENS ASH CHARACTERIZATION

Investigators: J. K. Briant and O. R. Moss

Technical Assistance: J. R. Laidler

Samples of Mount St. Helens volcanic ash from 12 locations were separated into respirable and nonrespirable fractions.

The May 18, 1980 eruption of Mount St. Helens deposited a heavy layer of volcanic ash on parts of several Pacific Northwest states. Samples from 12 locations, noted in Table 1, were separated into three particle size ranges to be analyzed for several components of ash particles that might be inhaled. The three size ranges were: bulk powder, the less-than-20-μm fraction and the less-than-3.5-μm fraction. Table 1 lists, for each group (as a percentage of the bulk sample) the respirable fraction and the fraction of 20-μm aerodynamic equivalent diameter (AED). The results of these analyses were reported by Fruchter et al. (Science 209: 1116-1125, 1980).

TABLE 1. Fraction of the Bulk Powder Volcanic Ash Found in the Smaller Size Ranges as a Percentage of the Total Sample.

Sample	Percent Powder Respirable[a]	Percent Powder <20 μm[b]
Cougar	0.8	1.5
Woodland	1.1	2.5
Castlerock	1.8	3.1
Tietor	2.2	4.2
Ahtanum	1.2	2.3
Yakima	1.5	2.8
Richland	1.3	2.5
Moses Lake	2.6	4.7
Spokane	2.0	4.2
Rosalia	2.8	5.4
Pullman	2.8	5.2
Missoula	2.1	4.3

[a] ECD = 3.5 μm for the 10 mm nylon cyclones
[b] ECD = 20 μm for the vertical elutriator

The apparatus used to separate the powder (ash) is illustrated in Figure 1. A Wright dust feed was used to suspend the powder in an air stream. The vertical elutriator gave an aerodynamic equivalent effective cutoff diameter (ECD) of 20 μm. The aerosol was then passed through a deionizer to remove any static charge on the aerosol particles. Samples were collected from the aerosol chamber on two open-face filter and two filters with HASL 10-mm nylon cyclones. The ECD of the cyclones was 3.5 μm. All masses were determined gravimetrically.

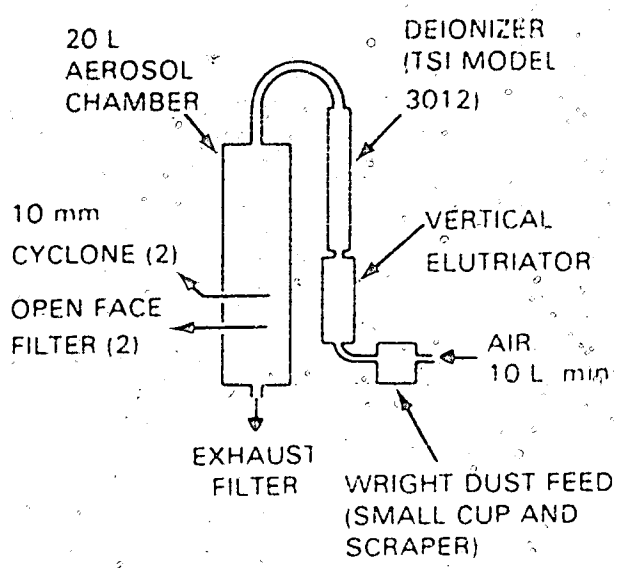

FIGURE 1. Experimental Apparatus for Size Separation of Mount St. Helens Volcanic Ash.

Figure 2 is a transmission electron micrograph of an aerosol from the chamber, sampled with an electrostatic precipitator. The powder is reported to be largely feldspar, which has a density of approximately 2.5 g/cm^3. The respirable fraction, given in Table 1, is determined by the AED of the particles in the aerosol, not by their physical dimensions.

In another setup, an Anderson 2000 cascade impactor sampled aerosol from a TSI 3400 fluidized-bed aerosol generator with an aerosol deionizer. The collected powder was periodically removed from the impactor stages until an adequate quantity was collected in the desired size range. This method allowed a separate collection of the less-than-1-μm-AED particles. Chemical composition of these samples has not yet been determined.

FIGURE 2. Transmission Electron Micrograph of Elutriated Volcanic Ash Aerosol (Missoula sample).

Inhaled Plutonium Oxide in Dogs

[illegible] concerned with long-term experiments to determine the life-span dose-effect relationships of inhaled $^{238}PuO_2$ and $^{239}PuO_2$ in beagles. The data will be used to estimate the health effects of [illegible] transuranics.

DOSE-EFFECT STUDIES WITH INHALED PLUTONIUM OXIDE IN BEAGLES

Investigators: [illegible] Park, A. C. Case, D. [illegible] Catt, S. L. Klopfer, G. E. Dagle, T. C. Kinnas, R. M. Madison, G. J. Powers, H. A. Ragan, [illegible] E. Rowe, R. E. Schirmer, [illegible] Stevens, C. R. Watson, and E. L. Wierman

Technical Assistance: J. H. Akin, L. L. Baldwin, W. J. Chandon, K. H. Deblan, E. F. Edmerson, [illegible] Faubert, R. F. Flores, F. M. Gordon, A. J. Kopriva, S. L. Krum, [illegible] Madden, B. G. Moore, M. C. Perkins, L. R. Peters, and [illegible] Fierro

Beagle dogs given a single exposure to $^{238}PuO_2$ or $^{239}PuO_2$ aerosols are being observed for life-span dose-effect relationships. The ^{238}Pu body burden of the nine dogs that died of pulmonary [illegible]-induced respiratory insufficiency during the first 3 yr after exposure was [illegible] to 12 pCi; one of these dogs had a pulmonary tumor. Twenty-two additional dogs, with body burdens ranging from 0.05 to 1.8 pCi, died due to pulmonary neoplasia 3 to 9 yr after exposure. Fifteen of the dogs exposed to ^{238}Pu have died during the first 6½ yr postexposure due to bone and/or lung tumors; their body burdens at death ranged from 1.5 to 10 pCi. Lymphopenia was the earliest observed effect after inhalation of $^{238}PuO_2$ or $^{239}PuO_2$, occurring [illegible] to [illegible] yr after deposition of 80 nCi plutonium in the lungs.

To determine the life-span dose-effect relationships of inhaled plutonium, 18-month Beagle dogs were exposed to aerosols of $^{238}PuO_2$ (mean AMAD, [illegible] μm; mean GSD, [illegible]), prepared by calcining the oxalate at [illegible] for 2 hr; or to $^{239}PuO_2$ (mean AMAD, [illegible] μm; mean GSD, 1.4), prepared by calcining the oxalate at 700°C and subjecting the product to H_2O steam in argon exposure at [illegible] for 98 hr. This material, referred to as pure plutonium oxide, is used in space-nuclear power systems.

One hundred thirty dogs exposed to [illegible] in 1970 and 1971 were selected for [illegible] studies; 22 will be sacrificed to obtain plutonium distribution and pathology data, and 108 were assigned to life-span dose-effect studies (Table 1). One hundred thirteen dogs exposed to $^{238}PuO_2$ in 1972 and 1973 were selected for life-span dose-effect studies (Table 2). Twenty-four additional dogs were exposed for periodic sacrifice. The appendix (following the entire Annual Report) shows the status of the dogs on these experiments.

TABLE 1. Life-Span Dose-Effect Studies With Inhaled $^{239}PuO_2$ in Beagles[a]

Dose-Level Group	Number of Dogs: Male	Number of Dogs: Female	Initial Alveolar Deposition[b]: nCi/dog	Initial Alveolar Deposition[b]: nCi/g lung[c]
0	10	10	0	0
1	10	10	4.2 ± 1.3	0.09 ± 0.011
2	10	10	22 ± 8	0.38 ± 0.04
3	10	10	39 ± 16	0.66 ± 0.13
4	10	10	300 ± 62	5.4 ± 0.4
5	10	10	1100 ± 170	9.3 ± 1.4
6	4	5	5800 ± 3300	50 ± 22
	64	65		

[a] Exposed in 1970 and 1971.

[b] Estimated from external thorax counts at 14 and 100 days post-exposure and estimated lung weights (0.011 × body weight).

[c] Mean ± 95% confidence intervals around the mean.

During the first 9 yr following exposure to $^{239}PuO_2$, all of the dogs in the highest-level dose group, 19 dogs in Dose

TABLE 2. Life-Span Dose-Effect Studies With Inhaled $^{238}PuO_2$ in Beagles[a]

Dose Level Group	Number of Dogs		Initial Alveolar Deposition[b]	
	Male	Female	nCi	nCi/g lung
0	10	10	0	0
1	10	10	2.3 ± 0.6	0.016 ± 0.007
2	10	10	18 ± [illegible]	0.15 ± 0.03
3	10	10	[illegible] ± 11	0.56 ± 0.07
4	10	10	[illegible] ± 81	[illegible] ± 0.5
5	10	10	1800 ± [illegible]	10 ± [illegible]
6	[illegible]	6	5200 ± 1400	43 ± 12
	[illegible]	66		

[a] Exposures in 1973 and 1974.

[b] Estimated from external thorax [illegible] at 4 and 10 days post exposure and estimated lung weight 0.01% of body weight.

[c] Mean ± [illegible] standard error of the mean.

level Group 5, five in Group 4, three in Group 3, two in Group 2 and two in Dose level Group 1 were euthanized when death was imminent. Fourteen dogs were sacrificed for comparison of plutonium tissue distribution. Table 3 and Figure 3 show the primary causes of death and the distribution of ^{238}Pu in the tissues of these animals. One 80-mo-old control dog was euthanized because of an oral tumor.

As survival time increased, the fraction of plutonium in the lung decreased to ~25% of the final body burden by 8 to 9 yr postexposure. During the first postexposure year, plutonium was translocated primarily to the thoracic lymph nodes, with little plutonium translocated to other tissues. Plutonium content of the thoracic lymph nodes was >50% of the final body burden at 8-9 yr after exposure; the abdominal lymph nodes, principally the hepatic nodes, contained ~10%. The fraction of plutonium in liver increased, accounting for >35% of the final body burden at 8 and 9 yr after exposure in the higher (0.3- to 0.6-μCi body burden) dose-level groups. The organ distribution of plutonium in the periodically sacrificed dogs was generally similar to that of the high-dose-level dogs euthanized when death was imminent during the first 2 yr after exposure. The lower-dose-level dogs (0.001- to 0.1-μCi final body burden) sacrificed or euthanized during the 4th to 9th postexposure years had a much smaller fraction of the final body burden in the liver, with a larger fraction retained in the lungs and/or thoracic lymph nodes. About 3% of the final body burden was in the skeleton at 8 to 9 yr after exposure.

The dogs euthanized because of respiratory insufficiency during the 3-yr postexposure period had increased respiration rates, and hypercapnia and hypoxemia associated with lesions in the lungs. Intermittent anorexia and body weight loss accompanied the respiratory insufficiency. Histopathologic examination of the lungs showed radiation pneumonitis characterized by focal interstitia and subpleural fibrosis, increased numbers of alveolar macrophages, alveolar epithelial hyperplasia, and foci of squamous metaplasia. Autoradiographs showed activity primarily composed of large clusters, more numerous in areas of interstitial and subpleural fibrosis. Dog 504M also had a pulmonary tumor, classified as a bronchiolar-alveolar carcinoma.

Twenty-three of the 33 dogs euthanized 3 to 9 yr after exposure had lung tumors. Radiographic evidence of pulmonary neoplasia was observed before respiratory insufficiency developed. However, respiratory insufficiency was frequently observed prior to euthanasia due to neoplasia of the lung. All of the dogs with lung tumors were in Dose-level Groups 4, 5, 6 and 6. [illegible] 503M and 839M (Dose level 6), 634M and 7[illegible]M (Dose level 5), 754M and 756M (Dose level [illegible]), and [illegible]5M and [illegible]M (Dose level [illegible]) died during the 3- to 9-yr postexposure period of causes thought, at the time of death, to be unrelated to plutonium exposure.

In [illegible] of the dogs, [illegible] were classified as [illegible] carcinoma, in four dogs as adenocarcinoma, in [illegible] as [illegible] carcinoma, in [illegible] as [illegible] carcinoma, in one dog, epidermoid and bronchiolar alveolar carcinoma, and in one dog adenocarcinoma. The epidermoid carcinoma metastasized to the [illegible], the bronchiolar-alveolar carcinomas metastasized to the [illegible] in eight dogs, and several [illegible] including the thoracic lymph nodes, mediastinum, kidney, [illegible], stomach, heart, [illegible], aorta, [illegible], prescapular, [illegible], splenic and hepatic lymph nodes in three other dogs. Two of the adenosquamous carcinomas metastasized to thoracic lymph nodes, mediastinum and thoracic pleura. The adenocarcinoma was not metastatic. Three of the dogs had lesions of secondary hypertrophic osteoarthropathy. Sclerosing lymphadenopathy was associated with the high concentration of plutonium in the thoracic and hepatic lymph nodes. There was also a generalized lymphoid atrophy that may be related to debilitation in the dogs with respiratory insufficiency, or to lymphocytopenia. Livers of the dogs euthanized during the 4- to 9-yr postexposure period showed moderate

TABLE 3. Tissue Distribution of Plutonium in Beagles After Inhalation of $^{239}PuO_2$.

Dog Number	Time After Exposure, Mo	Final Body Burden, μCi	Lungs	Thoracic Lymph Nodes[a]	Abdominal Lymph Nodes[b]	Liver	Skeleton	Cause of Death
				Percent of Final Body Burden				
[illegible]	[illegible]	[illegible]	96	0.35	[illegible]	0.24	0.08	Sarcoma
[illegible]	[illegible]	4.947	99	[illegible]	.01	[illegible]	0.94	Sarcoma
[illegible]	[illegible]	[illegible]	[illegible]	[illegible]	[illegible]	[illegible]	0.93	Sarcoma
[illegible]	[illegible]	[illegible]	[illegible]	[illegible]	[illegible]	[illegible]	0.08	Sarcoma
[illegible]	[illegible]	[illegible]	[illegible]	0.82	[illegible]	[illegible]	0.61	Sarcoma
[illegible]	[illegible]	[illegible]	[illegible]	0.47	[illegible]	0.08	0.05	Sarcoma
[illegible]	[illegible]	[illegible]	[illegible]	[illegible]	[illegible]	0.53	0.09	Sarcoma
[illegible]	[illegible]	[illegible]	[illegible]	[illegible]	[illegible]	0.01	[illegible]	Sarcoma
[illegible]	[illegible]	[illegible]	[illegible]	[illegible]	[illegible]	[illegible]	[illegible]	Sarcoma
[illegible]	[illegible]	[illegible]	[illegible]	[illegible]	[illegible]	[illegible]	[illegible]	Sarcoma
[illegible]	[illegible]	[illegible]	[illegible]	[illegible]	[illegible]	[illegible]	[illegible]	Radiation Pneumonitis
[illegible]	[illegible]	[illegible]	[illegible]	[illegible]	[illegible]	[illegible]	[illegible]	Radiation Pneumonitis
[illegible]	[illegible]	[illegible]	[illegible]	[illegible]	[illegible]	[illegible]	[illegible]	Radiation Pneumonitis
[illegible]	[illegible]	[illegible]	[illegible]	[illegible]	[illegible]	[illegible]	[illegible]	Sarcoma
[illegible]	[illegible]	[illegible]	[illegible]	[illegible]	[illegible]	[illegible]	[illegible]	Radiation Pneumonitis
[illegible]	[illegible]	[illegible]	[illegible]	[illegible]	[illegible]	[illegible]	[illegible]	Radiation Pneumonitis
[illegible]	[illegible]	[illegible]	[illegible]	[illegible]	[illegible]	[illegible]	[illegible]	Sarcoma
[illegible]	[illegible]	[illegible]	[illegible]	[illegible]	[illegible]	[illegible]	[illegible]	Radiation Pneumonitis
[illegible]	[illegible]	[illegible]	[illegible]	[illegible]	[illegible]	[illegible]	[illegible]	Radiation Pneumonitis
[illegible]	[illegible]	[illegible]	[illegible]	[illegible]	[illegible]	[illegible]	[illegible]	Radiation Pneumonitis
[illegible]	[illegible]	[illegible]	[illegible]	[illegible]	[illegible]	[illegible]	[illegible]	Radiation Pneumonitis/Lung Tumor
[illegible]	[illegible]	[illegible]	[illegible]	[illegible]	[illegible]	[illegible]	[illegible]	[illegible]
[illegible]	[illegible]	[illegible]	[illegible]	[illegible]	[illegible]	[illegible]	[illegible]	[illegible]
[illegible]	[illegible]	[illegible]	[illegible]	[illegible]	[illegible]	[illegible]	[illegible]	Lung Tumor
[illegible]	[illegible]	[illegible]	[illegible]	[illegible]	[illegible]	[illegible]	[illegible]	Lung Tumor
[illegible]	[illegible]	[illegible]	[illegible]	[illegible]	[illegible]	[illegible]	[illegible]	Lung Tumor
[illegible]	[illegible]	[illegible]	[illegible]	[illegible]	[illegible]	[illegible]	[illegible]	Lung Tumor
[illegible]	[illegible]	[illegible]	[illegible]	[illegible]	[illegible]	[illegible]	[illegible]	Lung Tumor
[illegible]	[illegible]	[illegible]	[illegible]	[illegible]	[illegible]	[illegible]	[illegible]	Lung Tumor
[illegible]	[illegible]	[illegible]	[illegible]	[illegible]	[illegible]	[illegible]	[illegible]	[illegible]
[illegible]	[illegible]	[illegible]	[illegible]	[illegible]	[illegible]	[illegible]	[illegible]	[illegible]
[illegible]	[illegible]	[illegible]	[illegible]	[illegible]	[illegible]	[illegible]	[illegible]	Lung Tumor
[illegible]	[illegible]	[illegible]	[illegible]	[illegible]	[illegible]	[illegible]	[illegible]	Lung Tumor
[illegible]	[illegible]	[illegible]	[illegible]	[illegible]	[illegible]	[illegible]	[illegible]	Lung Tumor
[illegible]	[illegible]	[illegible]	[illegible]	[illegible]	[illegible]	[illegible]	[illegible]	[illegible]
[illegible]	[illegible]	[illegible]	[illegible]	[illegible]	[illegible]	[illegible]	[illegible]	[illegible]
[illegible]	[illegible]	[illegible]	[illegible]	[illegible]	[illegible]	[illegible]	[illegible]	[illegible]
[illegible]	[illegible]	[illegible]	[illegible]	[illegible]	[illegible]	[illegible]	[illegible]	[illegible]
[illegible]	[illegible]	[illegible]	[illegible]	[illegible]	[illegible]	[illegible]	[illegible]	Lung Tumor
[illegible]	[illegible]	[illegible]	[illegible]	[illegible]	[illegible]	[illegible]	[illegible]	Lung Tumor
[illegible]	[illegible]	[illegible]	[illegible]	[illegible]	[illegible]	[illegible]	[illegible]	Lung Tumor
[illegible]	[illegible]	[illegible]	[illegible]	[illegible]	[illegible]	[illegible]	[illegible]	Lung Tumor
[illegible]	[illegible]	[illegible]	[illegible]	[illegible]	[illegible]	[illegible]	[illegible]	Lung Tumor
[illegible]	[illegible]	[illegible]	[illegible]	[illegible]	[illegible]	4.5	0.94	Pneumonia
6341	97	[illegible]	60	46	[illegible]	[illegible]	0.08	Lung Tumor
[illegible]	98	.055	24	62	[illegible]	[illegible]	2.4	Lung Tumor
8641	100	0.616	78	[illegible]	[illegible]	[illegible]	0.93	Unknown
8081	[illegible]	[illegible]	34	[illegible]	[illegible]	[illegible]	0.52	Pulmonary Thromboembolism
[illegible]	[illegible]	[illegible]	[illegible]	85	[illegible]	[illegible]	2.2	Lung Tumor
[illegible]	[illegible]	[illegible]	[illegible]	36	20	[illegible]	1.6	Lung Tumor
[illegible]	[illegible]	0.054	49	33	[illegible]	[illegible]	2.0	Lung Tumor
8141	[illegible]	[illegible]	17	15	5.8	[illegible]	[illegible]	[illegible]
8403	[illegible]	[illegible]	[illegible]	[illegible]	[illegible]	[illegible]	[illegible]	[illegible]

a. Includes tracheobronchial, mediastinal and sternal lymph nodes.
b. Includes hepatic, splenic and mesenteric lymph nodes.

diffuse centrilobular congestion. Liver cells in these areas contained fine granular yellow pigment resembling lipofuscin, and were frequently vacuolated. Focal aggregation of vacuolated lipofuscin-containing cells in the sinusoids was associated with alpha stars on autoradiographs.

Lymphopenia developed after inhalation of $^{239}PuO_2$ in the dose level groups with mean initial alveolar depositions of 79 nCi and greater (Figure 2). Through 105 mo postexposure, mean lymphocyte values were significantly lower ($P < 0.02-0.0001$) than for the control group. The reduction in lymphocytes was dose-related, both in time of appearance and magnitude. At mean alveolar depositions of 3.5 and 22 nCi, lymphocyte values were within ranges observed in control dogs. A reduction in total leukocytes was evident in the higher

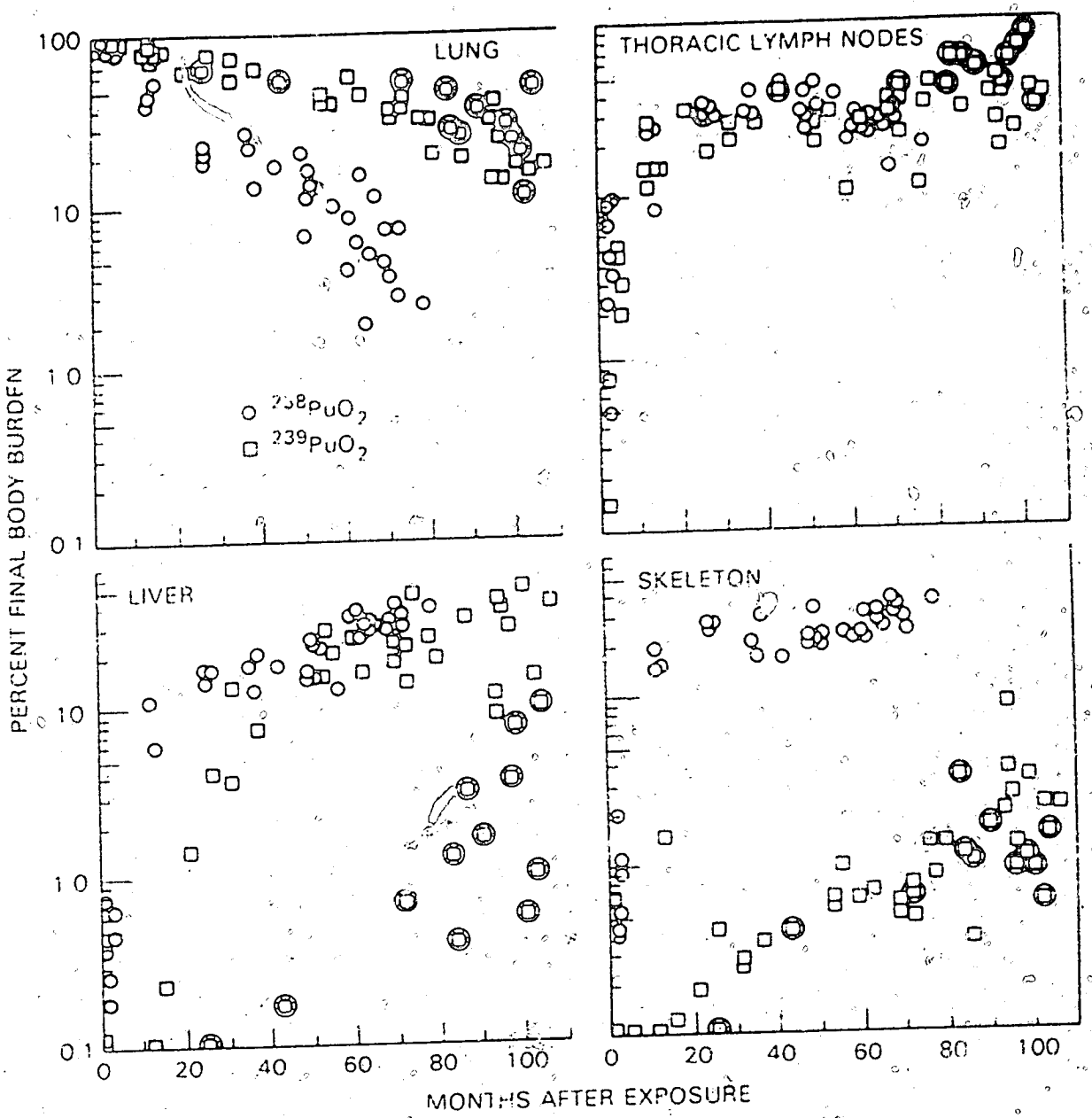

FIGURE 1. Tissue Distribution of Plutonium in Beagles After Inhalation of PuO_2 [illegible]

dose groups, which were also lymphopenic. No effects have been observed on red cell parameters following $^{239}PuO_2$ inhalation.

Serum chemistry assays have been performed to detect organ-specific damage from plutonium that translocated from lung to extrapulmonary sites. There have been no consistent, dose-related alterations in serum constituents of dogs exposed to $^{239}PuO_2$. These include glutamic pyruvic transaminase, glutamic oxaloacetic transaminase, alkaline phosphatase, urea nitrogen, and serum protein fractions.

During the first 6½ yr following exposure to $^{239}PuO_2$, 12 dogs in the highest-level dose group, seven dogs in Dose Level Group 5 and one dog in Dose level Group 4 were euthanized when death was imminent. Twenty-one were sacrificed for comparison of plutonium tissue distribution. Table 4 and Figure 1 show the causes of death and the distribution of ^{239}Pu in the tissues of these animals. One 97-mo-old control dog died due to pyometritis.

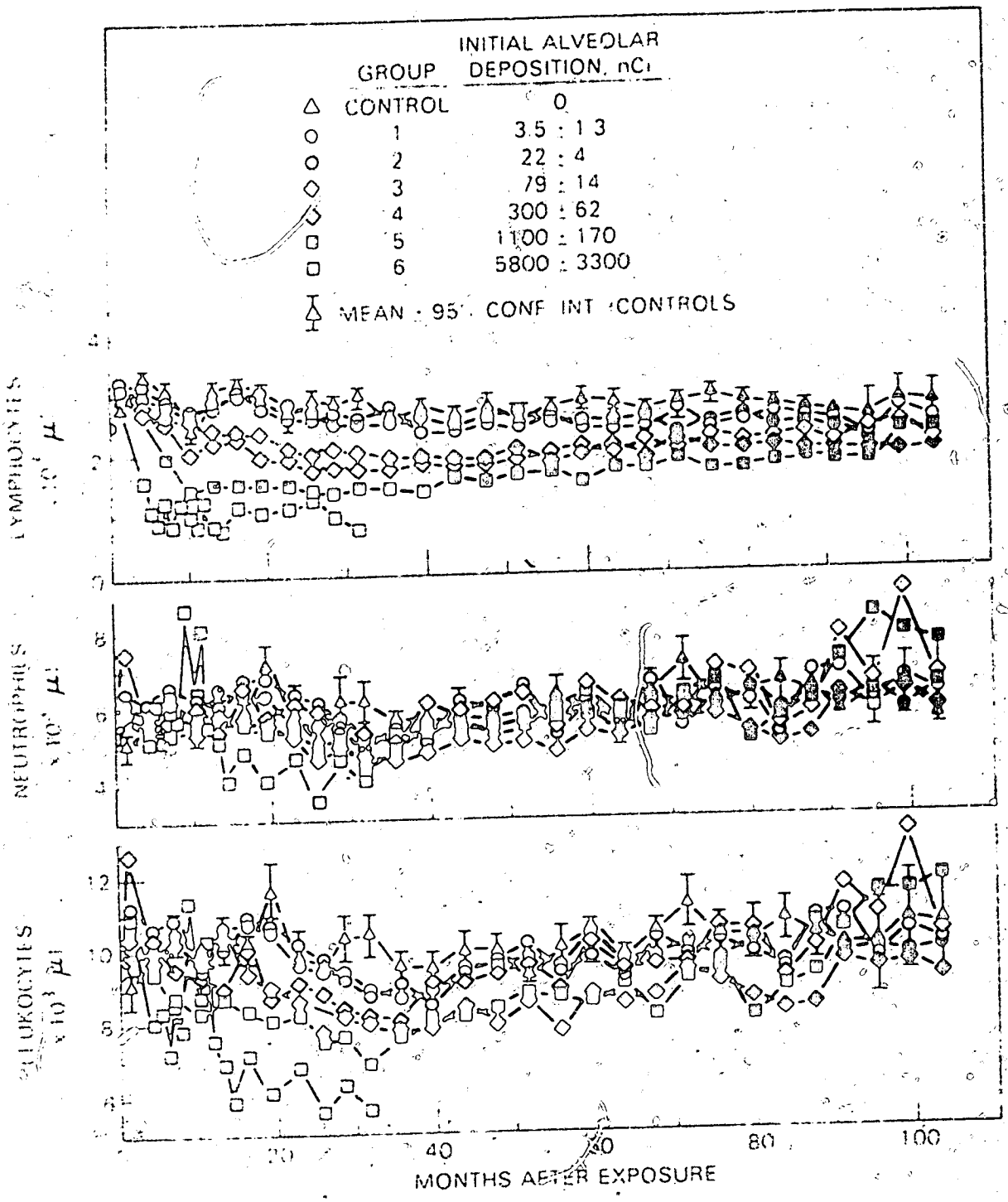

FIGURE 2. Mean Leukocyte, Neutrophil and Lymphocyte Values in Dogs After Inhalation of $^{239}PuO_2$

Of the [illegible] euthanized dogs, 12 were euthanized due to bone tumors (osteosarcoma), three due to lung tumors, three due to Addison's disease, one due to pneumonia and one due to paralysis. Six of the dogs euthanized due to bone tumors also had lung tumors. One of the dogs euthanized due to a bone tumor also had Addison's disease.

The lung tumors were classified as bronchiolar-alveolar carcinomas in three dogs, bronchiolar-alveolar adenoma in one dog, and adenosquamous carcinoma in one dog. In one dog, three lung tumor types were observed: bronchiolar-alveolar adenocarcinoma and fibrosarcoma. Lung tumor metastases were not observed. Bone tumor metastases were found in the lungs

TABLE 4. Tissue Distribution of Plutonium in Beagles After Inhalation of $^{238}PuO_2$

Dog Number	Time After Exposure, Mo	Final Body Burden, µCi	Percent of Final Body Burden: Lungs	Thoracic Lymph Nodes[a]	Abdominal Lymph Nodes[b]	Liver	Skeleton	Cause of Death
[illegible]	0.25	0.150	97	0.34	0.20	[illegible]	0.16	Sacrifice
[illegible]		0.0044	93	0.65	0.04	0.38	2.1	Sacrifice
[illegible]		0.052	99	0.63	0.01	0.07	[illegible]	Sacrifice
[illegible]	[illegible]	0.347	96	1.9	0.01	<0.05	0.36	Sacrifice
[illegible]	2	[illegible]	91	[illegible]	0.002	0.26	0.58	Sacrifice
[illegible]	2	[illegible]	96	2.9	0.01	0.18	0.39	Sacrifice
[illegible]	2	[illegible]	88	9.4	0.03	0.09	0.44	Sacrifice
[illegible]	[illegible]	[illegible]	91	4.1	0.04	0.04	1.2	Sacrifice
[illegible]	[illegible]	[illegible]	[illegible]	11	0.23	0.65	1.1	Sacrifice
[illegible]	[illegible]	[illegible]	92	4.8	1.7	0.45	0.95	Sacrifice
[illegible]	[illegible]	[illegible]	45	27	0.08	10	[illegible]	Sacrifice
[illegible]	[illegible]	[illegible]	4	[illegible]	[illegible]	15	[illegible]	Sacrifice
[illegible]	13	[illegible]	[illegible]	[illegible]	[illegible]	6.2	36	Sacrifice
[illegible]	[illegible]	[illegible]	[illegible]	36	0.09	13	28	Sacrifice
[illegible]	25	[illegible]	[illegible]	31	0.16	17	[illegible]	Sacrifice
[illegible]	[illegible]	[illegible]	[illegible]	33	0.04	[illegible]	28	Sacrifice
[illegible]	35	[illegible]	[illegible]	[illegible]	[illegible]	18	[illegible]	[illegible]
[illegible]	[illegible]	[illegible]	[illegible]	[illegible]	[illegible]	[illegible]	[illegible]	[illegible]
[illegible]	37	[illegible]	[illegible]	[illegible]	[illegible]	[illegible]	[illegible]	[illegible]
[illegible]	42	[illegible]	[illegible]	[illegible]	[illegible]	[illegible]	[illegible]	[illegible]
[illegible]	[illegible]	[illegible]	[illegible]	[illegible]	[illegible]	[illegible]	[illegible]	[illegible]
[illegible]	44	[illegible]	[illegible]	[illegible]	0.26	[illegible]	[illegible]	[illegible]
[illegible]	[illegible]	[illegible]	[illegible]	[illegible]	[illegible]	[illegible]	[illegible]	[illegible]
[illegible]	[illegible]	[illegible]	[illegible]	[illegible]	[illegible]	[illegible]	[illegible]	[illegible]
[illegible]	[illegible]	5.427	53	48	1.9	[illegible]	[illegible]	[illegible]
[illegible]	52	[illegible]	[illegible]	31	[illegible]	[illegible]	[illegible]	[illegible]
[illegible]	56	[illegible]	[illegible]	[illegible]	4.3	[illegible]	[illegible]	[illegible]
[illegible]	[illegible]	1.204	[illegible]	[illegible]	[illegible]	[illegible]	[illegible]	[illegible]
[illegible]	[illegible]	[illegible]	[illegible]	[illegible]	0.76	[illegible]	[illegible]	[illegible]
[illegible]	[illegible]	[illegible]	[illegible]	[illegible]	[illegible]	[illegible]	[illegible]	[illegible]
[illegible]	[illegible]	[illegible]	[illegible]	[illegible]	[illegible]	[illegible]	[illegible]	[illegible]
[illegible]	[illegible]	[illegible]	[illegible]	[illegible]	[illegible]	[illegible]	[illegible]	[illegible]
[illegible]	64	[illegible]	[illegible]	[illegible]	[illegible]	[illegible]	[illegible]	[illegible]
[illegible]	[illegible]	[illegible]	[illegible]	[illegible]	[illegible]	[illegible]	[illegible]	[illegible]
[illegible]	[illegible]	[illegible]	[illegible]	[illegible]	[illegible]	[illegible]	25	[illegible]
[illegible]	[illegible]	1.492	[illegible]	[illegible]	[illegible]	[illegible]	[illegible]	[illegible]
[illegible]	[illegible]	[illegible]	[illegible]	[illegible]	[illegible]	[illegible]	[illegible]	[illegible]
[illegible]	[illegible]	2.546	3.8	15	[illegible]	[illegible]	[illegible]	[illegible]
[illegible]	[illegible]	[illegible]	[illegible]	[illegible]	1.4	[illegible]	[illegible]	[illegible]
[illegible]	[illegible]	[illegible]	[illegible]	35	2.2	13	[illegible]	[illegible]
[illegible]	75	0.0083	2.4	20	[illegible]	[illegible]	34	Paralysis

(a) Includes tracheobronchial, mediastinal, and sternal lymph nodes.
(b) Includes hepatic, splenic and mesenteric lymph nodes.

of three dogs; and in one dog, the bone tumor metastasized to liver, lung, and tracheobronchial lymph nodes. The four dogs with Addison's disease had adrenal cortical atrophy.

In addition to the lesions associated with the cause of death, lesions in the lungs of the high-dose-level dogs included focal alveolar histocytosis, alveolitis, alveolar epithelial cell hyperplasia, alveolar emphysema, pleural fibrosis, and interstitial fibrosis. Numerous alpha stars were observed, mainly in foci of fibrosis, and single alpha tracks were scattered throughout sections in foci of alveolar histocytosis and in alveolar septa. The tracheobronchial and mediastinal lymph nodes were completely obliterated by necrosis and scarring, associated with high concentrations of plutonium observed as alpha stars. Similar but less severe lesions were seen in the hepatic lymph nodes. There were extensive alterations in bone, including multiple areas of focal atrophy of bone; endosteal, trabecular and peritrabecular bone fibrosis; and osteolysis of cortical, endosteal, and trabecular bone. One dog had lesions of secondary hypertrophic osteoarthropathy. Radioactivity in the bone was present as single tracks, generally scattered throughout the bone, cartilage, and bone marrow. The liver contained foci of hepatocellular fatty change, where small clusters of single tracks were seen. There was also mild focal nodular hyperplasia of hepatocytes. Elevated serum glutamic pyruvic transaminase levels, suggestive of liver damage, were observed

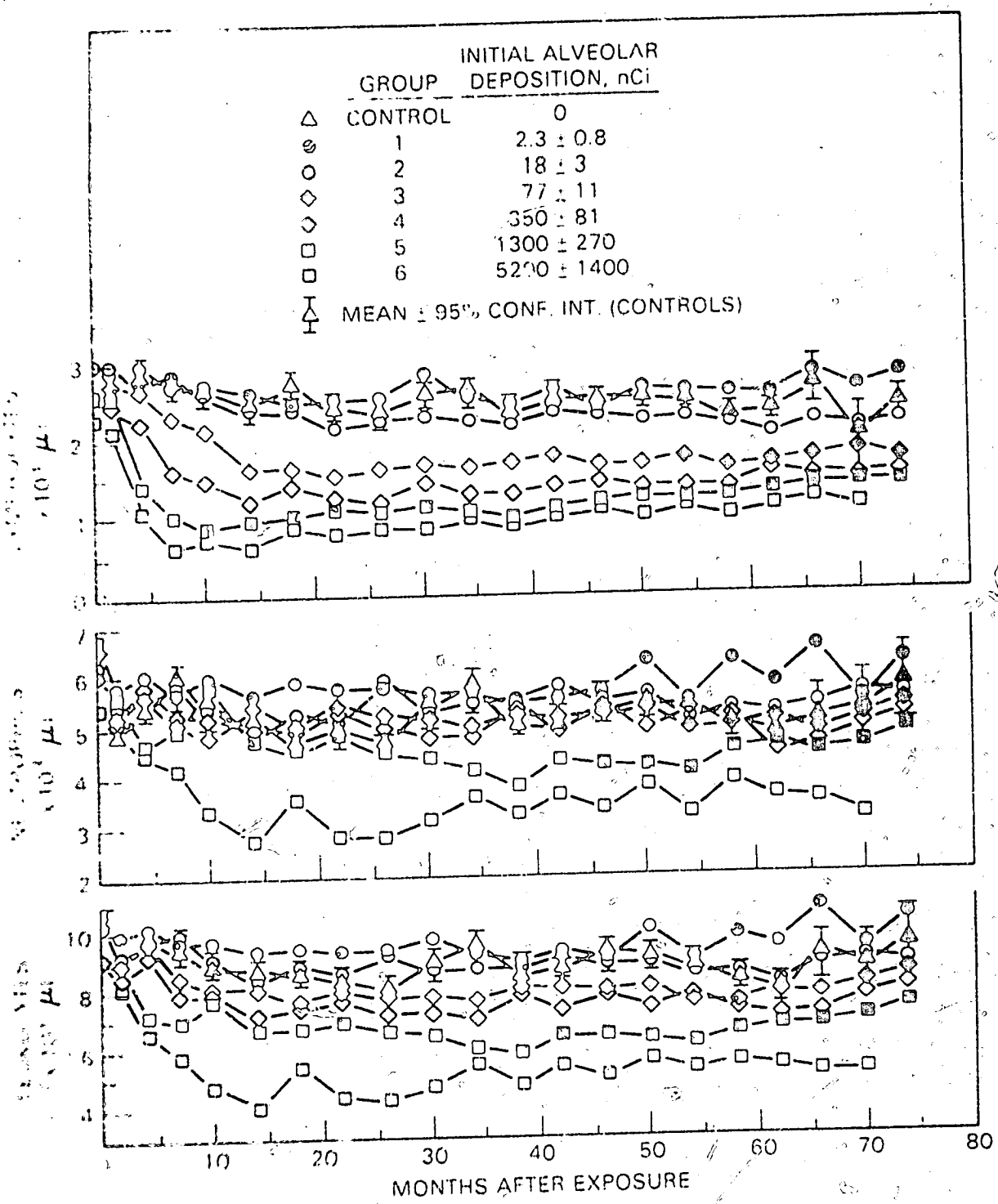

FIGURE 3. Mean Leukocyte, Neutrophil and Lymphocyte Values in Dogs After Inhalation of $^{238}PuO_2$.

[illegible] level dogs.

[illegible] was observed [illegible] deposition of [illegible] the dogs exposed to [illegible] the lymphopenia [illegible] pronounced, both [illegible] appearance, [illegible] found

with ^{239}Pu, lymphocyte values in the two lowest exposure groups, i.e., 2.3 and 18 nCi, were not different from control values. A dose-related reduction in total leukocytes was evident, primarily due to the lymphopenia, except in Groups 5 and 6, in which neutropenia was observed. No difference in monocyte values was seen in relation to dose levels. A significant and progressive reduction in eosinophils

was evident only in Group 6 dogs following ^{238}Pu inhalation. No chronic effects have been observed in the red cell parameters.

With $^{238}PuO_2$, serum chemistry assays showed only glutamic pyruvic transaminase values elevated above those of the control group, and only in Group 6 dogs (5200 nCi), after about 46 mo following exposure. Elevations in this "liver-specific" enzyme are consistent with histopathologic findings and radiochemical analyses of ^{238}Pu translocation to the liver. Alkaline phosphatase was elevated in some of the dogs with bone tumors.

At 6½ yr postexposure, the fraction of the final body burden in the lungs of the ^{238}Pu-exposed dogs was about 5%, compared to 38% in the ^{239}Pu-exposed dogs (Figure 1). At that time, 25 to 30% of the plutonium was found in the thoracic lymph nodes and 25 to 30% in the liver, for both ^{239}Pu and ^{238}Pu. About 28% of the final body burden was found in the skeleton of the ^{238}Pu-exposed dogs, at 6½ yr postexposure, compared to less than 1% in the ^{239}Pu-exposed dogs. During the same period, there were no obvious differences in the ^{238}Pu tissue distribution in low-dose-level dogs compared to that in high-dose-level dogs.

After inhalation of $^{239}PuO_2$ or $^{238}PuO_2$, lymphopenia was the earliest observed effect, occurring after deposition of ≳80 nCi plutonium in the lung. On a concentration basis, the 80-nCi dose level is about 40 times the 16-nCi maximum permissible human lung deposition, based on 0.3 rem/wk to the lung.

HEMATOLOGIC CHANGES IN PLUTONIUM-EXPOSED BEAGLES WITH LUNG TUMORS

Investigator: H. A. Ragan, K. H. Debban, A. L. Slavich, and J. F. Park

Technical Assistance: S. L. Klopfer, M. C. Perkins, and E. I. Edmerson

Beagle dogs with lung tumors after inhalation of plutonium manifested hematologic changes consistent with those expected from chronic inflammatory and/or neoplastic conditions, i.e., mild anemia and leukocytosis.

Beagle dogs exposed to plutonium oxides by inhalation subsequently developed pulmonary fibrosis and/or neoplasia (Park et al., this Annual Report). Several hematologic and serum chemistry parameters were evaluated before and after radiographic evidence of lung tumors to identify changes in the tumor-bearing dogs.

Blood samples were obtained at 3- to 4-mo intervals throughout the life of these dogs for complete blood counts and serum chemistry tests, including urea nitrogen, glucose, alkaline phosphatase, the transaminases, protein and protein electrophoretic fractions. Thoracic radiographs were taken at intervals ranging from 1-3 yr prior to a tentative lung tumor diagnosis, and at 6-mo intervals after a suspected lung tumor was diagnosed radiographically. These diagnoses were confirmed histologically.

Lung tumors were detected radiographically in 56 dogs: 41 dogs were still alive at 4 mo; 33 at 7 mo, 22 at 12 mo, 21 at 16 mo, 13 at 20 mo and 8 at 24 mo after radiographic diagnosis. Hematologic and serum chemistry values from age-related, non-plutonium-exposed control dogs were used to compare with those of dogs with lung tumors. Previous results in beagles at this laboratory have shown that following inhalation of plutonium oxides, the only consistently significant effect has been a reduction in lymphocytes (Park et al., this Annual Report). Therefore, other effects seen in lung-tumor-bearing dogs resulted from the tumor, not directly from plutonium exposure.

Erythrocyte concentrations in dogs with lung tumors and in control dogs are shown in Figure 1. For ~12 mo prior to the radiographic detection of lung tumors, erythrocyte values tended to be lower than in the control group. Then, for ~12 mo after the diagnosis, there was a highly significant decrease ($P < 0.01$) in erythrocyte levels as compared to those in control dogs. The mild anemia is likely representative of the anemia of chronic disorders.

The comparisons of total leukocytes, neutrophils, lymphocytes, and monocytes in tumor-bearing and control dogs are shown in Figures 2-5. The initial lung burdens of plutonium were at levels resulting in lymphopenia, causing the reduction in the total leukocyte count that was apparent from 25 to 4 mo before tumor diagnosis. However, beginning between 7 and 4 mo before radiographic diagnosis, a rather marked and progressive increase in leukocytes, neutrophils, and monocytes occurred, which was sustained until death of the animals. Lymphocyte values in tumor-bearing dogs increased slightly during this same time period. We have previously shown that dogs with marked plutonium-induced lymphopenia could mobilize lymphocytes in response to intravenously injected polysaccharides.

Glucose and serum albumin concentrations of tumor-bearing dogs manifested the most marked change in any of the serum chemistry parameters evaluated. Beginning at about 4 mo after radiographic tumor diagnosis, serum albumin levels were significantly lower ($P < 0.05$) than in the age-related control dogs (Figure 6), whereas glucose levels were not significantly lower ($P > 0.05$) until about 11 mo after diagnosis (Figure 7).

The hematologic findings in dogs with lung tumors, i.e., anemia and leukocytosis, are consistent with the histopathologic observations of increased inflammatory cell response in the lungs of dogs with pulmonary neoplasia and fibrosis.

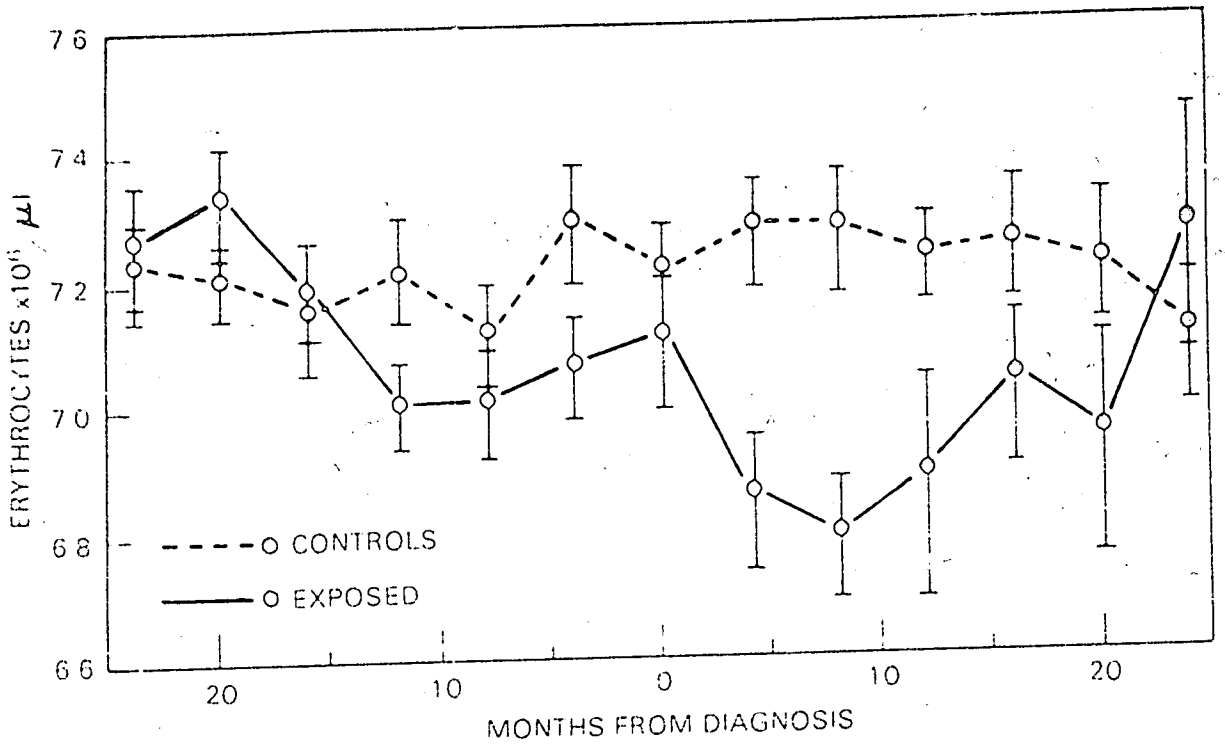

FIGURE 1. Erythrocyte Concentrations in Plutonium-Exposed Dogs With Lung Tumors and in Age-Related Control Dogs (Mean ± 1 SE)

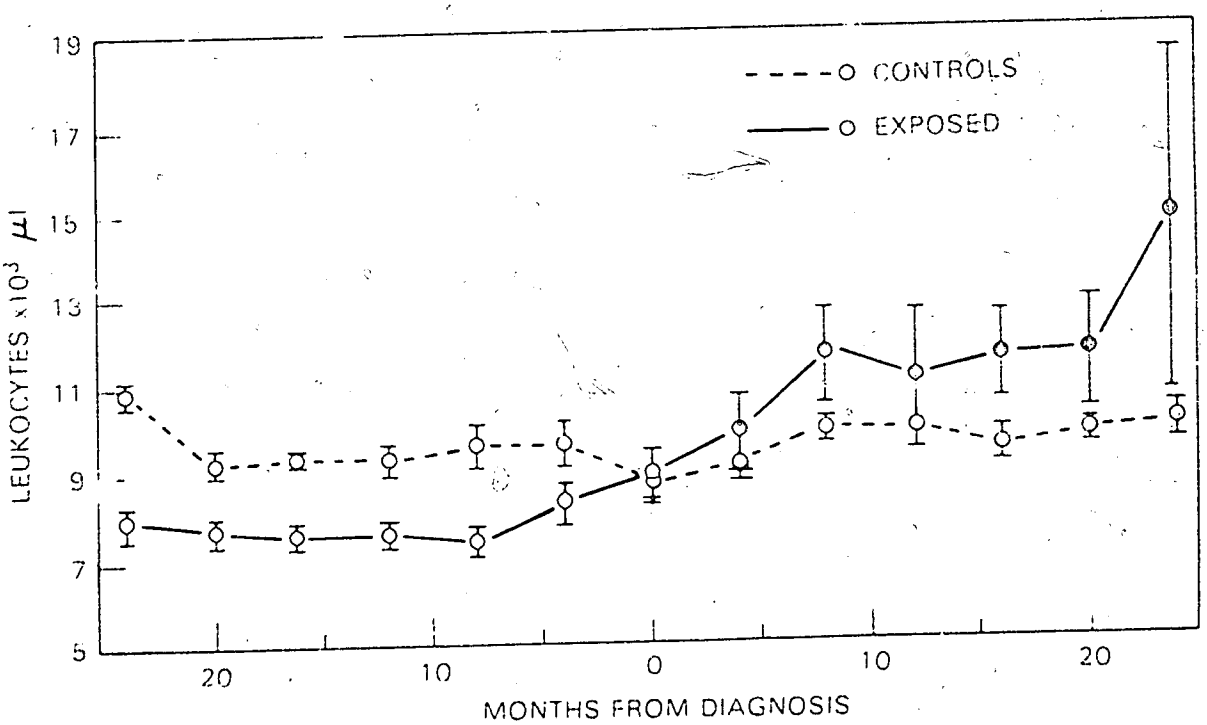

FIGURE 2. Leukocyte Concentrations in Plutonium-Exposed Dogs With Lung Tumors and in Age-Related Control Dogs (Mean ± 1 SE)

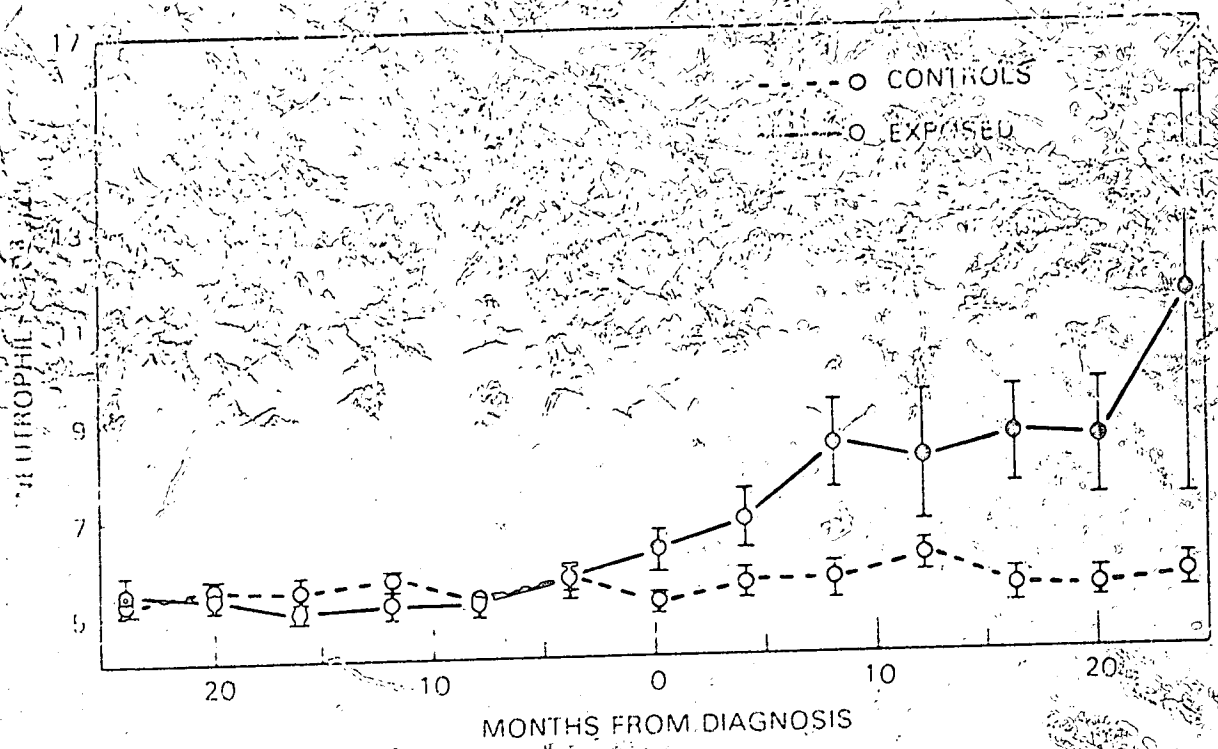

FIGURE 3. Neutrophil Concentrations in Plutonium-Exposed Dogs With Lung Tumors and in Age-Related Control Dogs (Mean ± 1 SE).

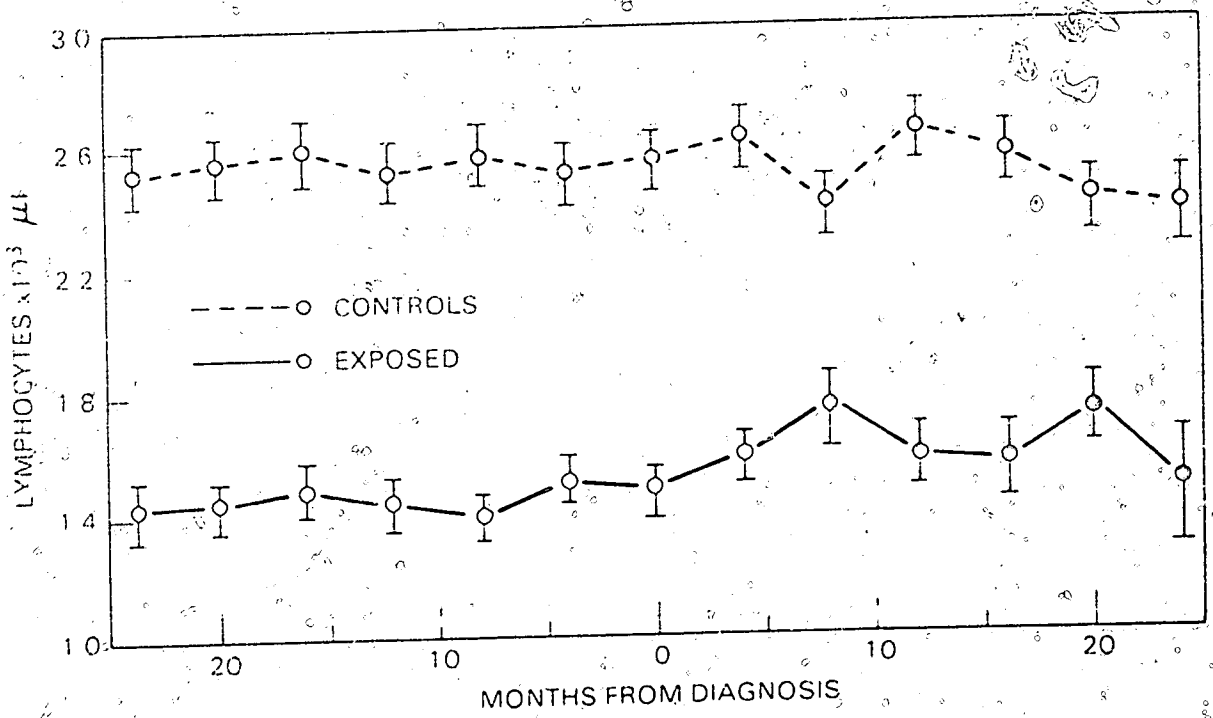

FIGURE 4. Lymphocyte Concentrations in Plutonium-Exposed Dogs With Lung Tumors and in Age-Related Control Dogs (Mean ± 1 SE).

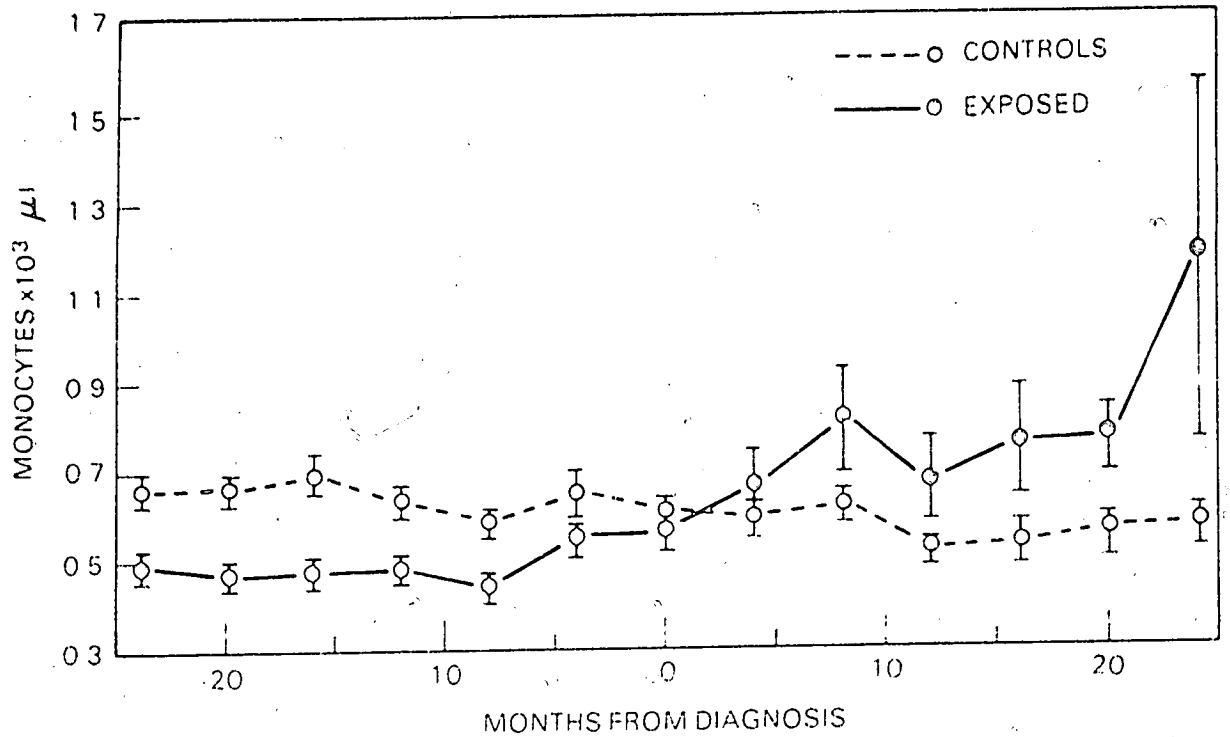

FIGURE 5. Monocyte Concentrations in Plutonium-Exposed Dogs With Lung Tumors and in Age-Related Control Dogs (Mean ± 1 SE).

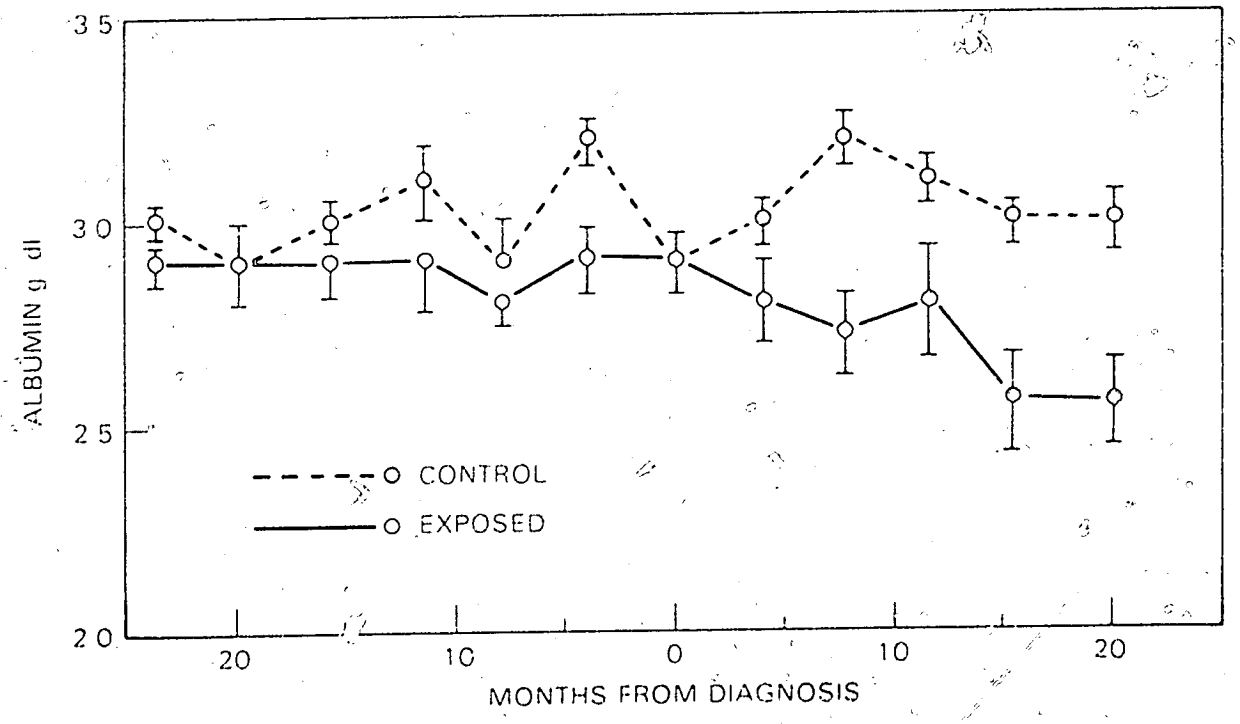

FIGURE 6. Serum Albumin Concentrations in Plutonium-Exposed Dogs With Lung Tumors and in Age-Related Control Dogs (Mean ± 1 SE).

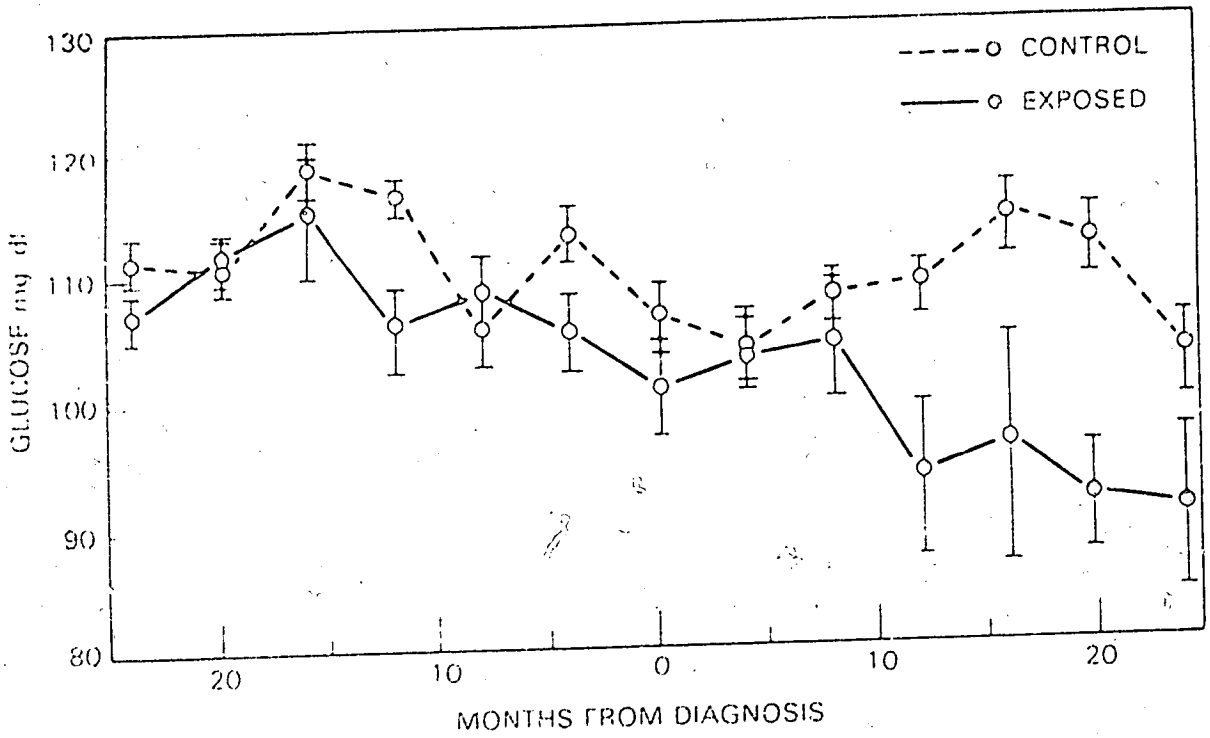

FIGURE 7. Serum Glucose Concentrations in Plutonium-Exposed Dogs With Lung Tumors and in Age-Related Control Dogs (Mean ± 1 SE)

DISTRIBUTION OF PLUTONIUM BETWEEN BONE AND MARROW

Investigator: B. J. McClanahan

Technical Assistance: M. G. Horstman

To determine the plutonium content of each component, bones from two dogs that inhaled $^{239}Pu(NO_3)_4$ and $^{238}PuO_2$ were treated ultrasonically to remove the marrow elements. Plutonium concentrations in marrow ranged from 0.05 to 0.85 that in calcified bone. The highest plutonium concentrations were found in marrow from the proximal humerus, proximal femur, and cervical and thoracic vertebrae; lowest concentrations were noted in marrow from distal humerus, distal femur, radius, ulna and scapula. Although plutonium concentrations tended to be higher in marrow from bones with higher plutonium concentrations, this relationship was not consistent, as evidenced by the range in the marrow-to-bone concentration ratios.

Selected bones from two dogs euthanized 43 and 84 mo after inhalation of $^{239}Pu(NO_3)_4$ and $^{238}PuO_2$, respectively, were treated ultrasonically to remove marrow cells. Bones, split to expose the marrow, were placed in cold 2.8% NaCl and sonicated to disrupt the cells in the marrow. The plutonium content of bone and NaCl solution containing the marrow were measured and are presented in Table 1. For comparison, previously reported data (Annual Report, 1973) from a dog killed 51 mo after inhalation of $^{238}PuO_2$ are also presented. In general, the highest marrow concentrations of Pu for each animal were noted in proximal humerus, proximal femur, and cervical and thoracic vertebrae. The lowest concentrations were seen in marrow from distal humerus, distal femur, radius, ulna and scapula. In the dog sacrificed 51 mo after inhalation of $^{238}PuO_2$, both bone and marrow from rib, sternebra and lumbar vertebra contained higher concentrations of plutonium than other bones. These findings were in contrast to those in the other two dogs.

When the marrow concentrations relative to bone concentrations are examined, it is evident that the plutonium content of marrow reflects the bone content of plutonium. For example, compared to proximal humerus, the marrow-to-bone ratios for proximal radius are not as low (proportionally) as are the concentrations in marrow from these two bones. This is not true for all bones studied. Several factors may influence the ratios. Higher marrow-to-bone ratios were obtained (1) in bones that were remodeling; or (2) resorbing bone surfaces that contained plutonium; or (3) bones that had small volumes of marrow relative to bone surfaces. The older dog which was sacrificed 84 mo after exposure tended to have proportionally higher marrow concentrations relative to bone concentrations than the other two dogs. This suggests that relatively more plutonium was being removed from its bone surfaces.

TABLE 1. Distribution of Plutonium Between Bone and Marrow

	Plutonium, nCi/gr								
	Bone and Marrow			Marrow			Marrow/Bone		
	$^{239}Pu(NO_3)_4$	$^{238}PuO_2$	$^{238}PuO_2$	$^{239}Pu(NO_3)_4$	$^{238}PuO_2$	$^{238}PuO_2$	$^{239}Pu(NO_3)_4$	$^{238}PuO_2$	$^{238}PuO_2$
Time Postexposure	43 mos	51 mos	84 mos	43 mos	51 mos	84 mos	43 mos	51 mos	84 mos
Proximal Humerus	1.74	4.06	0.62	0.44	0.35	0.58	0.24	0.069	0.85
Shaft Humerus	0.58	1.31	0.26	0.34	0.23	0.17	0.24	0.15	0.63
Distal Humerus	0.56	1.51	0.27	0.027	0.12		0.056	0.066	
Proximal Femur	1.16	3.87	0.46	0.61	0.50	0.18	0.52	0.12	0.38
Shaft Femur	0.31[a]	1.27	0.14		0.27	0.13		0.18	0.86
Distal Femur	0.99	1.93	0.36	0.042	0.09	0.0067	0.042	0.038	0.002
Proximal Radius	0.34[a]	1.37	0.20		0.15			0.093	
Shaft Radius	0.26	0.63	0.11	0.081	0.16	0.093	0.31	0.23	0.84
Distal Radius	0.49[a]	1.10	0.23		0.14	0.11		0.12	0.45
Proximal Ulna	0.34	1.65	0.18	0.054	0.10	0.006	0.13	0.091	0.030
Shaft Ulna	0.32[a]	0.35	0.16		0.16	0.061		0.11	0.36
Distal Ulna	0.44[a]	2.62	0.23		0.17	0.014		0.19	0.055
Rib 4	0.57	3.68	0.47	0.11	0.65	0.11	0.17	0.15	0.20
Rib 7	0.80	3.98	0.44	0.12	0.62	0.19	0.13	0.13	0.39
Sternebra 2	0.65	6.14	0.52	0.069	2.0	0.15	0.092	0.28	[illegible]
Sternebra 6	0.62	4.18	0.41	0.039	0.96	0.096	0.055	0.24	0.20
Cervical Vertebra 3	0.73	1.71	0.39	0.13	0.067	0.15	[illegible]	[illegible]	0.46
Cervical Vertebra 6	1.02	2.28	0.50	0.40	0.42	0.38	0.41	[illegible]	0.26
Thoracic Vertebra 4	0.92	3.98	0.63	0.22	0.37	0.42	0.22	0.078	0.64
Thoracic Vertebra 7	1.23	3.92	0.69	0.19	0.40	0.24	0.14	0.085	0.32
Lumbar Vertebra 3	1.10	3.53	0.45	0.051	0.88	0.093	0.038	[illegible]	0.19
Lumbar Vertebra 7	0.69	3.63	0.54	0.068	0.51	0.19	0.088	0.12	0.33
Sacrum	1.64	2.60	0.53	0.063	0.28	0.14	0.083	0.080	0.24
Scapula A	0.63	2.36	0.42	0.053	0.35	0.027	0.081	0.15	0.060
Scapula B	0.72	1.82	0.38	0.0087	0.38	0.042	0.011	0.15	0.11
Iliac Crest	0.81	3.33	1.34	0.089	0.54	0.076	0.032	0.15	0.049
Pelvis	0.53	4.25	0.99	0.10	0.34		0.17	0.069	

[a] Bone only, marrow not included

o Inhaled Plutonium Nitrate in Dogs

The major objective of this project is to determine dose-effect relationships of inhaled plutonium nitrate in dogs to aid in the prediction of health effects of accidental exposure in man. The critical tissue after inhalation of "soluble" plutonium (such as plutonium nitrate) is generally considered to be the skeleton or liver, on the assumption that such plutonium will be rapidly translocated from the lung to skeleton and liver. In several rodent studies, however, inhalation of "soluble" plutonium has resulted in lung tumors as well as skeletal tumors. Life-span studies are necessary to evaluate the complex interactions between tissues and organ systems directly or indirectly injured by low levels of exposure. Beagle dogs were chosen to correlate relative risks, determined in other studies, with different forms and routes of exposures to plutonium. Complete programs were developed for the interactive storage, retrieval, and evaluation of data.

DOSE-EFFECT STUDIES WITH INHALED PLUTONIUM NITRATE IN DOGS

Investigators: G. E. Dagle, W. C. Cannon, A. [illegible], [illegible], [illegible] Kinnas, R. M. Madison, J. F. McShane, G. [illegible] Power, H. A. Kagan, S. E. Rowe, R. F. Schirmer, D. L. Stevens, and E. L. Wierman

Technical Assistance: D. H. Akin, C. L. Baldwin, [illegible], [illegible], [illegible] Foubert, R. E. Flores, F. M. Gordon, S. [illegible], [illegible] Madden, R. G. Moore, M. C. Perkins, and [illegible] R. Peters

Beagle dogs were given a single inhalation exposure to [illegible] for lifespan dose-effect studies. All five dogs at the highest dose level, and [illegible] of 20 dogs at the medium-high dose level, died from radiation pneumonitis 14 to 42 mo after exposure. A dog from the highest dose level, which lived for 42 mo, also had [illegible], multiple bronchiolo-alveolar carcinomas. In addition, three dogs were euthanized because of osteosarcoma, 42 to [illegible] mo after exposure. As described in previous Annual Reports, lymphopenia, neutropenia and decreased numbers of circulating monocytes and eosinophils occurred at the two highest dose levels.

Six dose groups (105 dogs) were exposed, in 1976 and 1977, to aerosols of $^{239}Pu(NO_3)_4$ for lifespan observations (Table 1). In addition, 20 dogs were exposed to nitric acid aerosols as vehicle controls, 25 dogs were exposed to aerosols of $^{239}Pu(NO_3)_4$ for periodic sacrifice to study plutonium metabolism and the pathogenesis of developing lesions, seven dogs were selected as controls for periodic sacrifice, and 20 dogs were selected as untreated controls for lifespan observations. The dogs were exposed in aerosol chambers, using techniques described in previous reports. The appendix (following the entire Annual Report) shows the current status of each dog on these experiments.

The initial deposition and early clearance of inhaled $^{239}Pu(NO_3)_4$ aerosols were discussed in previous Annual Reports. The fraction of plutonium in the lung decreased to approximately 5% of the final body burden in dogs surviving 3 yr or more (Table 2). There was early translocation to the liver and skeleton, with an average of 36% and 56%, respectively, of final body burden present in dogs surviving 3 yr or more. Only minimal amounts were translocated to thoracic or abdominal lymph nodes. This was in contrast to dogs that inhaled $^{239}PuO_2$, in which a considerable amount translocated to the thoracic lymph nodes, and only minimal amounts translocated to liver or skeleton at these time periods. In a pilot study reported in last year's Annual Report, $^{239}Pu(NO_3)_4$ translocated more rapidly to liver and skeleton than did $^{239}Pu(NO_3)_4$ but reached a similar plateau at 1 yr after exposure.

The earliest observed biological effect was on the hematopoietic system, with lymphopenia occurring at the two highest dose levels at 4 wk after exposure to

TABLE 1. [illegible]

[illegible]	[illegible]	[illegible]	[illegible]
[illegible]	[illegible]	[illegible]	[illegible]
[illegible]	[illegible]	[illegible]	[illegible]
[illegible]	[illegible]	[illegible]	[illegible]
[illegible]	[illegible]	[illegible]	[illegible]
[illegible]	[illegible]	[illegible]	[illegible]
[illegible]	[illegible]	[illegible]	[illegible]

[illegible]

[illegible] these con- [illegible] Figure 1. [illegible] concentrations were re- [illegible] to the two highest dose [illegible] Group 5 (mean initial al- [illegible] nCi), and Group 6 [illegible] nCi). Numbers of leukocytes in Group 4 dogs [illegible] nCi) tended to be consistently (but not significantly) lower than those from control dogs. The reduction in white cells in Groups 5 and 6 is due to an effect on most leukocyte types (neutrophils, lymphocytes, monocytes and eosinophils). Lymphocyte reductions differed significantly from value for controls only in Groups 5 and 6. This is in contrast to the effects of both $^{239}PuO_2$ and $^{239}PuO_2$, which significantly depressed lymphocyte concentrations by 21 mo after exposure to initial lung burdens of ~80 nCi or more. The lymphocytopenia at lower dose levels of plutonium oxides may be related to the more-extensive translocation of plutonium oxide to the tracheobronchial lymph nodes.

Small multiple bronchioloalveolar carcinomas occurred in one dog 42 mo after exposure to the highest dose level [illegible]

[illegible] Radiographs of the lungs, and [illegible] 36 mo after exposure. There were no indications of radiation [illegible] these dogs and [illegible] radiation [illegible] osteosis was qualitative [illegible] similar to that seen after inhalation of $^{239}PuO_2$ (but not after $^{239}PuO_2$), and was generally characterized by peritrabecular fibrosis, composed of relatively hypocellular collagen fibers, partially surrounding trabeculae in vertebrae, femora and ribs.

Serum enzyme assays have been performed throughout the postexposure period in an attempt to diagnose specific damage to liver and/or bone by plutonium translocated from the lung. Although periodic elevations occurred in mean values for glutamic pyruvic transaminase, glutamic oxaloacetic transaminase, and alkaline phosphatase, there were no dose-related or dose-consistent elevations in these values. The periodic excursions in mean values were usually because of high values in one or two dogs at a particular sampling period, and occurred in all treatment groups, including controls.

TABLE 2. Tissue Distribution of Plutonium in Beagles After Inhalation of $^{239}Pu(NO_3)_4$

Dog Number	Time After Exposure, mo	Final Body Burden μCi	Percent of Final Body Burden: Lungs	Thoracic Lymph Nodes(a)	Abdominal Lymph Nodes(b)	Liver	Skeleton	Cause of Death
1359 M	0.1	0.080	90.50	0.15	0.06	2.46	3.20	Sacrifice
1375 F	0.1	0.073	89.61	0.14	0.01	0.97	4.68	Sacrifice
1407 F	0.1	0.092	51.87	0.41	0.13	10.99	18.70	Sacrifice
1389 M	0.5	0.053	24.07	0.38	0.08	41.28	26.21	Sacrifice
1390 M	0.5	0.051	24.62	0.32	0.11	20.05	44.45	Sacrifice
1445 F	0.5	0.057	26.42	0.32	0.11	21.28	44.73	Sacrifice
1329 F	1	0.485	70.05	0.16	0.04	8.28	18.19	Sacrifice
1346 M	1	0.902	76.81	0.32	0.03	10.45	10.30	Sacrifice
1347 F	1	0.699	71.71	0.36	0.08	9.33	14.09	Sacrifice
1336 M	1	0.032	71.38	0.22	0.05	5.72	19.71	Sacrifice
1341 F	1	0.022	64.43	0.29	0.10	12.92	16.63	Sacrifice
1344 F	1	0.052	58.62	0.25	0.04	21.87	16.09	Sacrifice
1335 M	1	0.003	19.52	0.07	0.06	6.68	25.04	Sacrifice
1339 F	1	0.001	19.08	0.13	0.08	20.96	45.47	Sacrifice
1351 M	1	0.002	40.68	1.22	0.09	17.09	28.89	Sacrifice
1522 F	3	0.059	54.68	0.57	0.10	21.52	28.74	Sacrifice
1529 F	3	0.049	51.68	0.40	0.07	18.48	23.74	Sacrifice
1539 M	3	0.072	52.45	0.31	0.05	18.58	25.03	Sacrifice
1564 F	12	0.037	38.00	1.27	0.11	33.53	42.63	Sacrifice
1571 F	12	0.053	22.17	1.47	0.11	28.76	42.91	Sacrifice
1588 M	12	0.053	13.14	0.40	0.12	35.85	46.18	Sacrifice
1424 M	14	4.625	33.10	1.43	0.16	26.49	36.88	Radiation Pneumonitis
1517 F	16	4.025	38.99	0.94	0.18	29.53	47.88	Radiation Pneumonitis
1510 F	17	4.048	22.00	1.15	0.05	20.71	52.00	Radiation Pneumonitis
1420 M	25	1.616	36.51	0.86	0.20	7.77	70.04	Radiation Pneumonitis
1471 F	34	1.375	9.25	0.73	0.12	26.93	[illegible]	Radiation Pneumonitis
1518 M	42	1.933	6.68	0.23	0.06	20.36	68.40	Radiation Pneumonitis + Lung Tumor
1512 M	42	2.247	4.10	0.57	0.07	47.46	45.56	Bone Tumor
1508 M	43	1.794	3.13	0.60	0.07	4.05	54.48	Bone Tumor
1387 F	55	--	--	--	--	--		Bone Tumor

(a) Includes tracheobronchial, mediastinal and sternal lymph nodes
(b) Includes hepatic, splenic and mesenteric lymph nodes

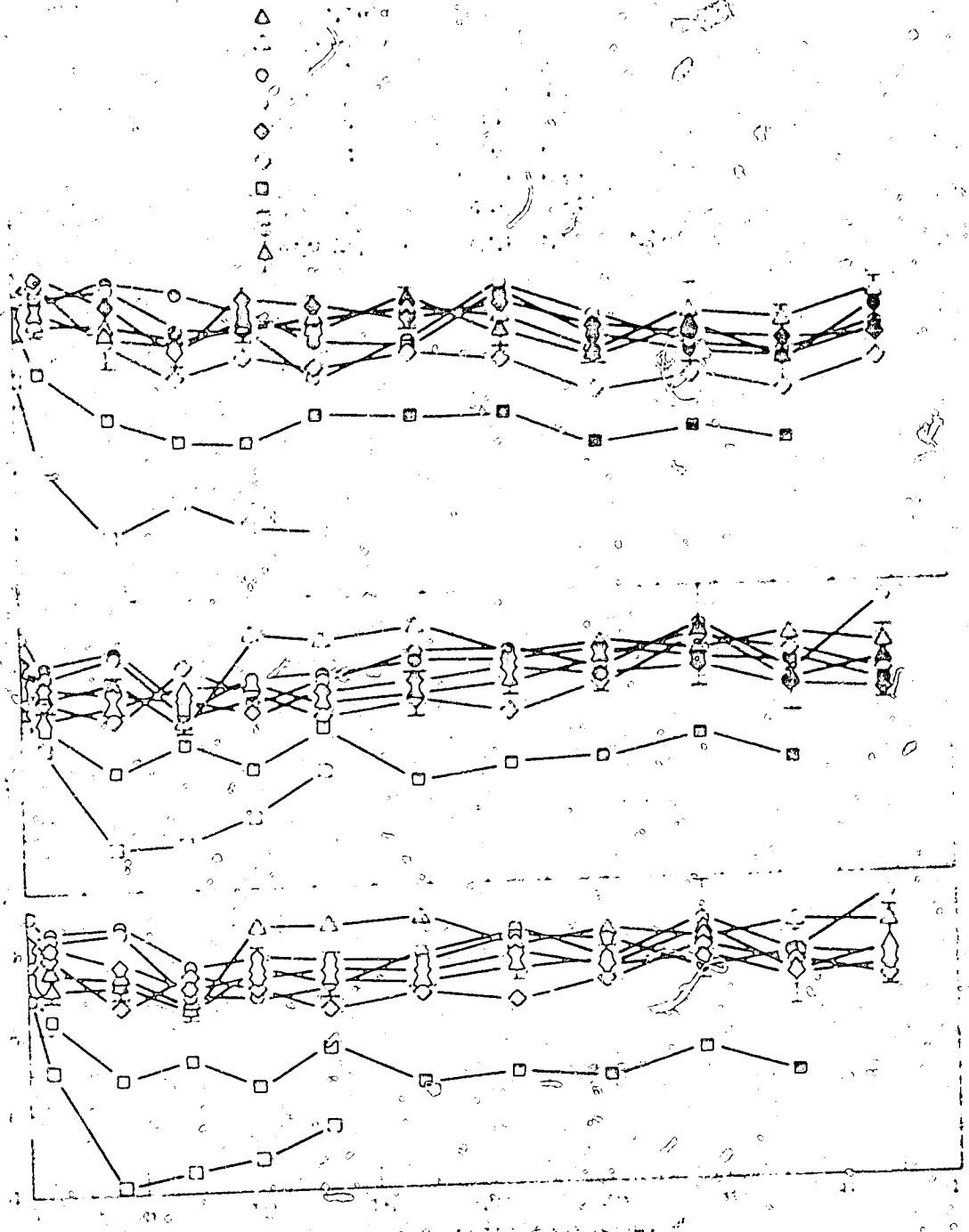

FIGURE 1.

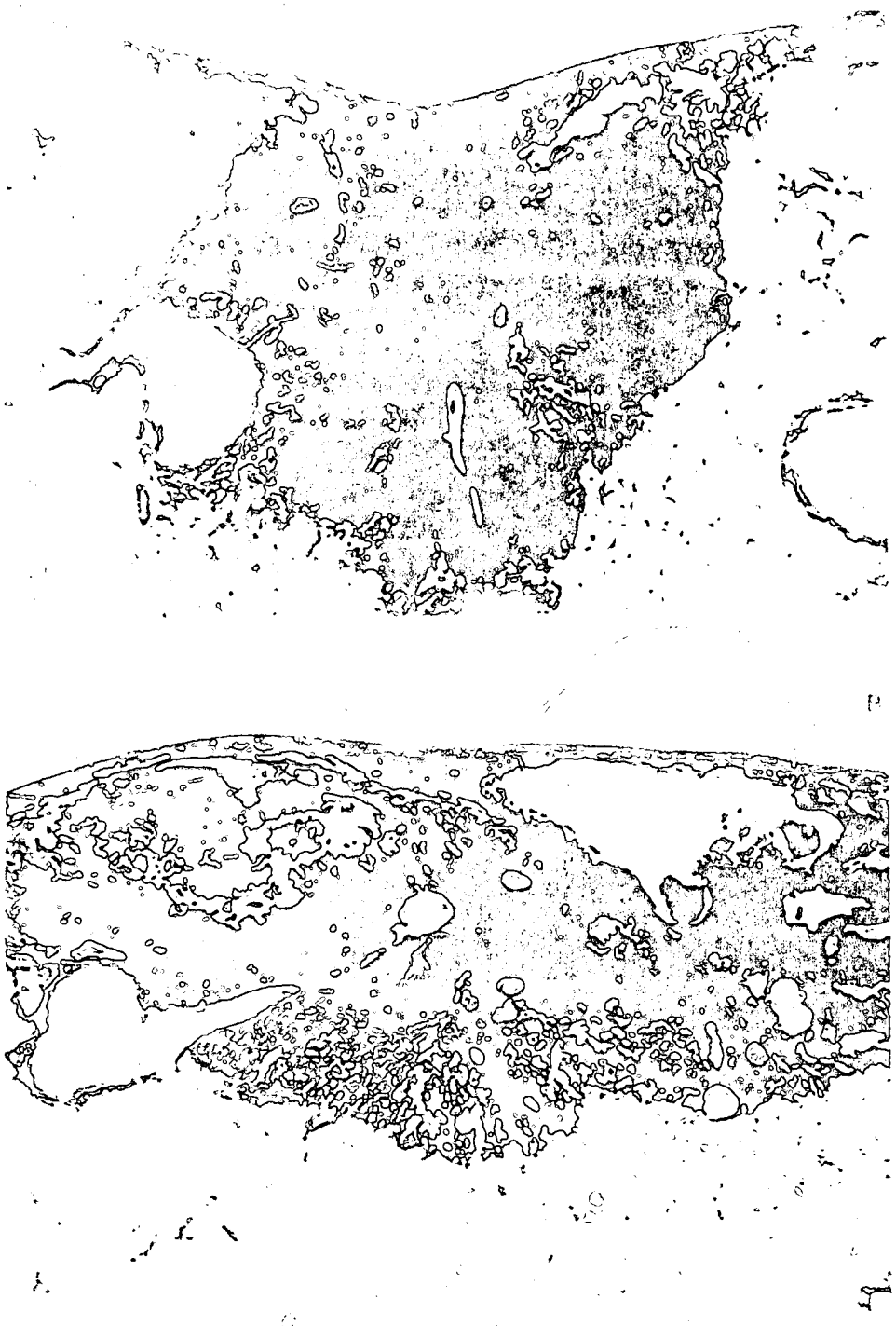

FIGURE 2 [illegible] A and B Having [illegible]

2 OF 3

PNL

3700

(PT. I)

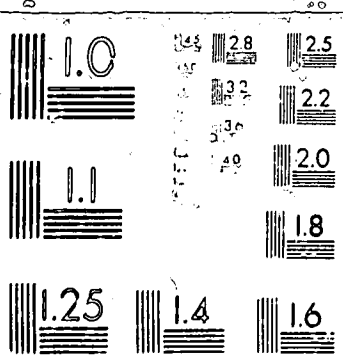

MICROCOPY RESOLUTION TEST CHART
NATIONAL BUREAU OF STANDARDS

INTERACTIVE PLOTTING FOR THE NOVICE

Investigators: C. R. Watson, P. R. Nicholson, and G. R. Johnson

An interactive plotting package, PLT, allows individuals with minimal computer skills to easily prepare X-Y plots of data and functions on linear and/or logarithmic scales. It is installed on the Biometrics Center PDP-11/70 minicomputer and uses various graphic devices through a locally developed Device-Independent Graphics software library.

Computers have been used for many years to generate graphic output. The Biometrics PDP-11/70 minicomputer has had a Tektronix 4014 graphic display terminal since 1976; in 1980, a Hewlett-Packard multiple flat-bed plotter was added. In addition, files may be transferred via magnetic tape to other computers with graphics output devices. Existing support software, including a Device-Independent Graphics (DIG) library, allows a FORTRAN programmer to produce displays such as contour plots, three-dimensional plots, pie charts, and bar charts. The PLT program was developed for the inexperienced user who wishes to produce a two-dimensional X-Y graph. The program has been used very frequently for the three years it has been available, even though its scope is narrow.

The interactive plotting package, as described in the 1977 PLT User's Manual, BNWL-MA-508, allows automatic display of data, or the development of a DIG output file. The user prepares a 4-line file to control titles, axis annotations, and scale factors, followed by lines containing X-Y pairs and, optionally, special command lines which modify subsequent processing. This was usually done by use of EDITOR. The program allowed interactive selection of input and output file names, input formats (if not standard) and global parameters (such as plot symbol size or log scales). This was satisfactory for those who understood the use of EDITOR; PLT greatly facilitated the generation of simple computer graphics, since it assumed the burden of scaling the display to the physical dimensions of the output device.

This year, the program was rewritten to eliminate the need for EDITOR. At the user's request, PLT will conduct a dialogue about various available options. In addition, we added the ability to plot data with error bars, and to superimpose a function on the data. The user may now approach PLT as a complete X-Y graphics package, using the keyboard to enter the data; or PLT may be viewed as a file processor, which transforms a particular type of file into a plot. Any approach between these extremes may also be used.

The option of superimposing a function, illustrated in Figure 1, is accomplished by menu selection. In the menu, thirty functional forms are available, from six categories: polynomial, uptake, decay or clearance, growth, modeling, and probability distributions. (It is assumed that curve fitting has been previously performed, and that the user has parameter estimates available).

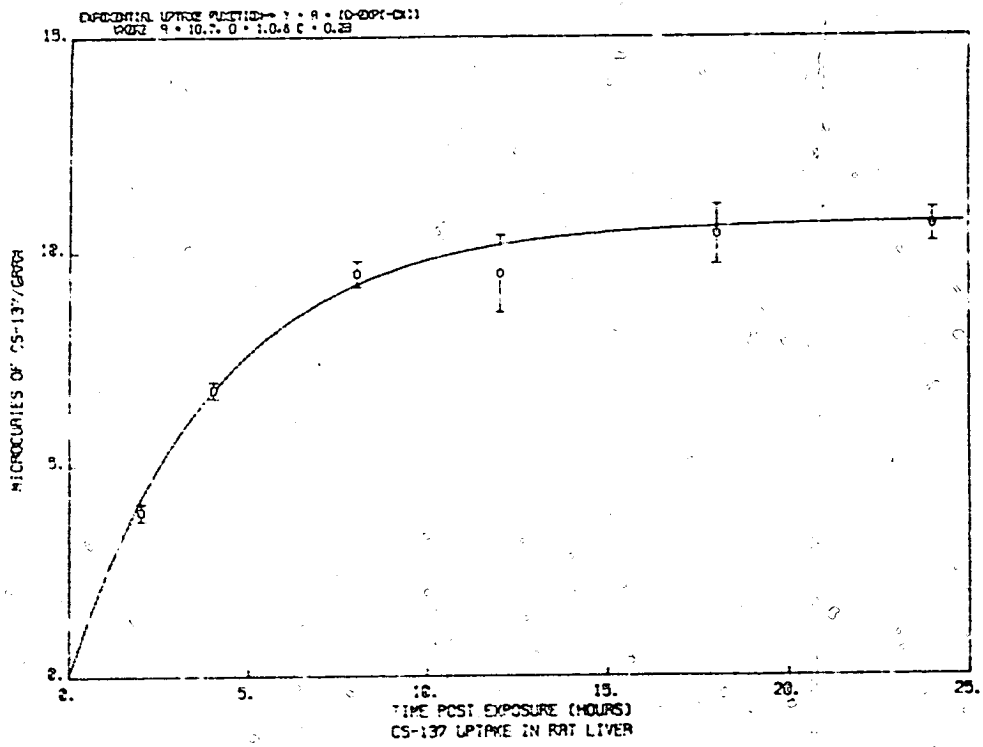

FIGURE 1. An Example of the Use of the Function Option on PLT.

○ INHALED TRANSURANICS IN RODENTS

The purpose of this project is to examine, in small animals, the fate and effects of inhaled transuranic compounds. This project should provide data for hazard evaluation and establishment of permissible exposure limits to man for inhaled transuranics, particularly with respect to the effects of radiation dose and dose distribution.

INHALATION CARCINOGENESIS OF REPEATED EXPOSURES TO HIGH-FIRED $^{239}PuO_2$ IN RATS

Investigators: C. L. Sanders and J. A. Mahaffey

Fractionation of ^{239}Pu exposure did not significantly affect its pulmonary carcinogenicity in rats when compared with that of a single exposure.

Current information on tumor incidence following plutonium exposure is based almost exclusively upon data from animals subjected to a single exposure. Repeated inhalation exposures to plutonium dioxide produce a temporal dose-distribution pattern (and, therefore, dose rate) in the lung which are different from that following a single exposure. This study compares the carcinogenicity of a single exposure to high-fired $^{239}PuO_2$ in rats to that of the same aerosol given at monthly or weekly intervals.

Plutonium dioxide was prepared by calcination of plutonium oxalate at 750°C for 2 hr. The mean ± standard deviation for the count median diameter of PuO_2 aerosols was 1.82 μm for singly exposed rats, 1.49 ± 0.19 μm for monthly exposed rats, and 1.28 ± 0.17 μm for weekly exposed rats.

Six groups of rats were treated as follows: (1) 140 unexposed control animals; (2) 67 animals given a single exposure to PuO_2 (single A); (3) 63 rats given nine exposures to PuO_2 at consecutive 7-day intervals (9-weekly); (4) 65 rats given three exposures to PuO_2 at consecutive monthly intervals (3-monthly); (5) 66 rats given 22 exposures to PuO_2 at consecutive 7-day intervals (22-weekly); and (6) 28 unexposed rats, bottle-stressed to correspond to group 5 (sham controls). In addition, a group of rats (single B) given a single exposure to $^{239}PuO_2$ as part of a separate experiment was used for comparison.

Estimated, cumulative, mean initial alveolar depositions were: 290 nCi ^{239}Pu for single A rats, 140 nCi for 9-weekly rats, 30 nCi for 3-monthly rats, 45 nCi for 22-weekly rats and 45 nCi for single B rats. Examination of autoradiograms of lungs failed to demonstrate any obvious difference due to exposure regime in distribution of $^{239}PuO_2$ particles within the lung. The dosimetry is described in another article in this Annual Report.

The mean radiation doses to lung for lifespan animals at death were 7500 rad for single A rats, 2200 rad for 9-weekly rats, 280 rad for single B rats, 260 rad for 3-monthly rats and 430 rad for 22-weekly rats. A wide range in lung doses was found in each exposure group. The dose range for single A rats, for example, was 400 rad to 30,000 rad. Because of this variability, a common (truncated) dose range was used to compare groups.

Median survival times were: 636 days for unexposed controls, 758 days for sham controls, 538 days for single A rats, 557 days for 9-weekly rats, 603 days for 22-weekly rats, 676 days for 3-monthly rats and 598 days for single B rats. No single-versus-multiple comparison of survival in animals with similar rad doses to the lung at death was significant.

A total of 44 lung tumors were found in 59 lifespan single A rats (75% incidence), 39 lung tumors in 56 9-weekly rats (70%), 15 lung tumors in 59 3-monthly rats (25%), 11 lung tumors in 58 22-weekly rats (21%), and 34 lung tumors in 91 single B rats (37%). No lung tumors were seen in regular or sham controls. Data, corrected for multiple lung tumors, are presented in Table 1.

TABLE 1. Comparison of Percent of Lung Lesions From $^{239}PuO_2$ Protraction by 2 x 2 Contingency Table.

	9-Weekly Vs Single A				22-Weekly or 3-Monthly Vs Single B						
	All Data		Truncated Data		All Data			Truncated Data		Truncated Data	
	9-Weekly	Single A	9-Weekly	Single A	3-Monthly	22-Weekly	Single B	3-Monthly	Single B[d]	22-Weekly	Single B[d]
Dose Range, rad	200-8000	400-30,000	400-6000	400-8000	20-2000	40-3000	20-2000	20-2000	20-2000	40-2000	40-2000
Mean Dose ± S.D., rad	2,200 ± 1800	7600 ± 6400	2400 ± 1800	3400 ± 1900	280 ± 270	430 ± 460	260 ± 310	180 ± 270	290 ± 320	420 ± 420	310 ± 300
Mean Survival ± S.D., days	570 ± 160	520 ± 160	570 ± 160	490 ± 180	650 ± 150	670 ± 130	600 ± 110	650 ± 150	610 ± 140	620 ± 140	620 ± 140
Number of Life Span Animals	56	59	53	36	59	58	51	59	63	53	27
Total Premalignant Lesion[c]	18	27	11[b]	42	12	[illegible]	15	[illegible]	16, 17	[illegible]	17, 18
Adenomatosis	14	12	9	17	12	[illegible]	[illegible]	[illegible]	16, 3	[illegible]	17, 18
Squamous Metaplasia	5	15	6[b]	25	0	0	0	0	0	0	0
Total Carcinoma or Sarcoma[d]	55	59	57	36	25	19	31	25	17, 16	19	17 (38)
Adenocarcinoma	36	29	38	22	17[a]	2[b]	10	[illegible]	14, 16	5	16 (35)[b]
Squamous Carcinoma	10	27	10[b]	6	9	14	5	[illegible]	[illegible]	14	5 (6)
Hemangiosarcoma	2[a]	15	2	11[b]	0	[illegible]	[illegible]	0	2	0	1
Undifferentiated Sarcoma	0	0	0	0	0	2	0	0	0	2	2[b]
Mesothelioma	2	1	2	3	0	2	0	[illegible]	[illegible]	2	[illegible]

(a) Significantly different from single-exposed group incidence based on chi-square contingency table, P < 0.05.
(b) Significantly different from single-exposed group incidence based on chi-square contingency table, P < 0.01.
(c) Animals with multiple lesions included only once in total.
(d) Lesion incidences in sacrificed animals reported as withdrawals or as failures in parentheses. Reportedly [illegible] is based on withdrawing sacrificed animals.

The Mantel-Haenszel chi-square statistic was calculated to compare incidences of pulmonary lesions between singly and multiply exposed rats, assuming that lesions were fatal. In addition, the unadjusted incidences were compared by 2 x 2 contingency tables. These comparisons were made both for entire exposure groups, and for these groups truncated to similar dose ranges. The latter comparison should more closely resemble the Mantel-Haenszel analysis. The results of these analyses are presented in Table 1. A complication in comparing the single B group to others was the early sacrifice of eight animals at 622 days and 13 animals at 808 days after exposure. These animals had a total of 15 adenocarcinomas, 1 squamous carcinoma and 1 adenomatosis. The 2 x 2 contingency table analyses were performed both with and without these animals, and they were treated both as failures and withdrawals in the Mantel-Haenszel calculations. Thus, for comparisons to the single B group in Table 1, both sets of results are reported. For the comparisons involving the single B group, the true probability associated with group differences is intermediate between the two values reported (all or truncated data).

For the 9-weekly versus single A comparison, the single A group consistently exhibited a borderline or significantly higher incidence of hemangiosarcoma and squamous metaplasia (and, consequently, of total premalignant lesions). In the truncated 2 x 2 contingency table comparison, there was a higher incidence of squamous carcinoma (thus, total tumors) in the 9-weekly group; however, the squamous carcinoma comparison was not significant, based on the Mantel-Haenszel statistic. There was no difference in the combined incidence of metaplasia and carcinoma.

In comparison with the 3-monthly group, the single B group had a higher incidence of adenocarcinoma. With adjustments for dose and survival, this difference overwhelmed the small incidences of other tumor types and resulted in a higher incidence of total tumors in the single B group. However, because of the problem of early sacrifices, these results were not conclusive.

The comparison of the 22-weekly versus single B was clearer. The incidences of adenomatosis and adenocarcinoma were borderline or significantly higher in the single B group, regardless of whether sacrificed animals were included. It was unclear whether or not total tumor incidence differed. This was due to the possibly higher incidence of squamous carcinoma in the 22-weekly group in the 2 x 2 contingency table analysis. However, when survival was used as a covariate, the differences in squamous carcinoma were no longer evident, and the total tumor comparison was inconclusive.

The data indicate that prolongation of $^{239}PuO_2$ exposure by repeated inhalation depositions over 3-monthly exposures, or 9- or 22-weekly exposures did not significantly change the incidence of lung tumors in the rats. For exposure conditions studied, the carcinogenic risk in the lung was not a function of dose rate but of total dose for inhaled, insoluble, alpha-emitting radionuclides.

EFFECT OF VITAMIN C ON PULMONARY CARCINOGENESIS FROM INHALED $^{239}PuO_2$

Investigator: C. L. Sanders

Preliminary data indicate that vitamin C in drinking water may reduce the expected incidence of lung tumors following inhalation of $^{239}PuO_2$.

Vitamin C has been implicated as a preventative factor in cancer development and has been utilized with limited success as a therapeutic agent in control of cancer growth. Many of the previous studies in humans are more anecdotal than scientific. The objective of this study was to examine the effects of administering vitamin C in drinking water on the development of lung tumors in rats that had inhaled $^{239}PuO_2$ particles.

Four groups of Fischer 344 female rats were studied: (1) rats given only $^{239}PuO_2$; (2) rats given $^{239}PuO_2$ + 30 mg/day of vitamin C in drinking water for 1 yr; (3) rats given $^{239}PuO_2$ + 300 mg/day of vitamin C in drinking water for 1 yr; and (4) rats given only 300 mg/day of vitamin C in drinking water for 1 yr. Vitamin C (Bronson Pharmaceuticals, as 50% sodium ascorbate and 50% ascorbic acid) was dissolved in drinking water at 1 mg/ml and 10 mg/ml doses. Initial mean water uptake by rats was 30 ml/day, increasing to about 45 ml per day in adult animals. No significant differences in water uptake were observed among the study groups.

Although the experiment has not been completed, preliminary data on the amount of ^{239}Pu in the lungs at death, and the histopathology of the lungs, are available for groups 1, 2 and 4 (Table 1). In rats given only $^{239}PuO_2$, 52% of autopsied rats had developed lung tumors (about what would be expected at an initital alveolar deposition of from 50-100 nCi $^{239}PuO_2$); in contrast, in rats given 30 mg vitamin C + $^{239}PuO_2$, the lung tumor incidence was only 29%. The amount of ^{239}Pu present in the lungs at death was similar in these two groups. No lung tumors were found in rats given only vitamin C (Table 1).

TABLE 1. Effect of Vitamin C on Lung Tumor Formation Following Inhalation of $^{239}PuO_2$.

Treatment	No. Rats Dead	Median Life Span[a], days	Mean ^{239}Pu Contents in Lung at Death	Incidences of Lung Lesions	
				Metaplasia	Tumors
PuO_2 Only	23	511	9.2 (13)[b]	20 (15)[c]	47 (15)[c]
PuO_2 + Vitamin C	21	540	12.1 (13)	24 (17)	18 (17)
Vitamin C Only	19	580	--	9 (11)	0

[a] After exposure at 70 days of age.
[b] Number of animals with Pu analysis.
[c] Number of animals with histopathology; about 90% of lesions are squamous type.

PULMONARY CELL TURNOVER FOLLOWING INHALATION OF $^{239}PuO_2$

Investigators: K. Rhoads and C. L. Sanders

The labeling indices of cells in pulmonary lesions following inhalation of $^{239}PuO_2$ were greater than those in normal alveolar wall or bronchiolar epithelium. Metaplasia and neoplasia of similar morphologic types had similar labeling indices.

The turnover of pulmonary tissues in rodents has been known to change in response to a number of external influences, such as respiratory infection, inhalation of oxidizing gases, and exposure to carcinogens. These changes reflect either ongoing repair processes in damaged tissue or loss of proliferative control. We have investigated the response of pulmonary tissue to inhaled $^{239}PuO_2$ particles during the [illegible] of tumorigenesis in rats.

Female Wistar rats were exposed to aerosol [illegible] $^{239}PuO_2$ at 55 days of age, achieving a mean lung burden of 185 nCi (standard deviation, 174 nCi). The animals were necropsied in groups of 5-6 at 30- to 60-day intervals, beginning 257 days after exposure and ending at 530 days. One group of animals given multiple exposures was examined about 900 days after the initial PuO_2 exposure. About 1.5 hr prior to necropsy, the animals were given 1.5 mCi ^{3}H-thymidine (approximately 3 μCi/g body weight). Lungs were fixed by instillation of glutaraldehyde-formaldehyde fixative at 25 cm H_2O pressure. One cross-section from each right lobe and two sections of the left lobe were embedded in glycol-methacrylate and cut into 0.5- to 1-μm-thick sections. Autoradiograms were prepared with K-5 emulsion, exposed for 2 wk, and stained with H&E.

Labeling indices (LI) were determined for normal alveolar wall and bronchiolar epithelium by counting labeled and unlabeled cells at 1000X on a light microscope. These were compared to the labeling indices of pulmonary lesions: fibrosis, adenomatosis, squamous cell metaplasia, adeno- or squamous-cell carcinoma, and hemangiosarcoma. Labeling indices were obtained for each tissue type by counting a total of 2000 cells per animal, using all six lung sections. When fewer than 2000 cells were available, all cells present were counted.

The number of lesions of each type examined are shown in Table I. Three animals, in the first two necropsy groups, had no lesions. Fibrosis and adenomatosis, the most common lesions, frequently occurred together. Each tumor type was found in fewer than 10% of the animals, with two animals having two morphologically different tumors.

TABLE I. Incidence of Pulmonary Lesions in Rats 257-800 Days Following Inhalation of $^{239}PuO_2$

Lesion	No. of Animals	Percentage of Animals
None	3	8.1
Fibrosis	27	73.0
Pneumonitis		0
Adenomatosis	31	83.8
Adenocarcinoma	4	10.8
Squamous Cell Metaplasia	11	29.7
Squamous Cell Carcinoma	3	8.1
Hemangiosarcoma	2	5.4
Mesothelial Hyperplasia	1	2.7
Total number of animals	37	

The LI for normal alveolar wall and bronchiolar epithelium were less than 0.5%, both for unexposed lungs and for morphologically normal regions in lungs exposed to PuO_2 (Figure 1). Labeling indices for all lesions were significantly greater than those in normal tissues (all $P < 0.001$). The range for LI in fibrotic lesions was 0.8-1.5%; in adenomatosis,

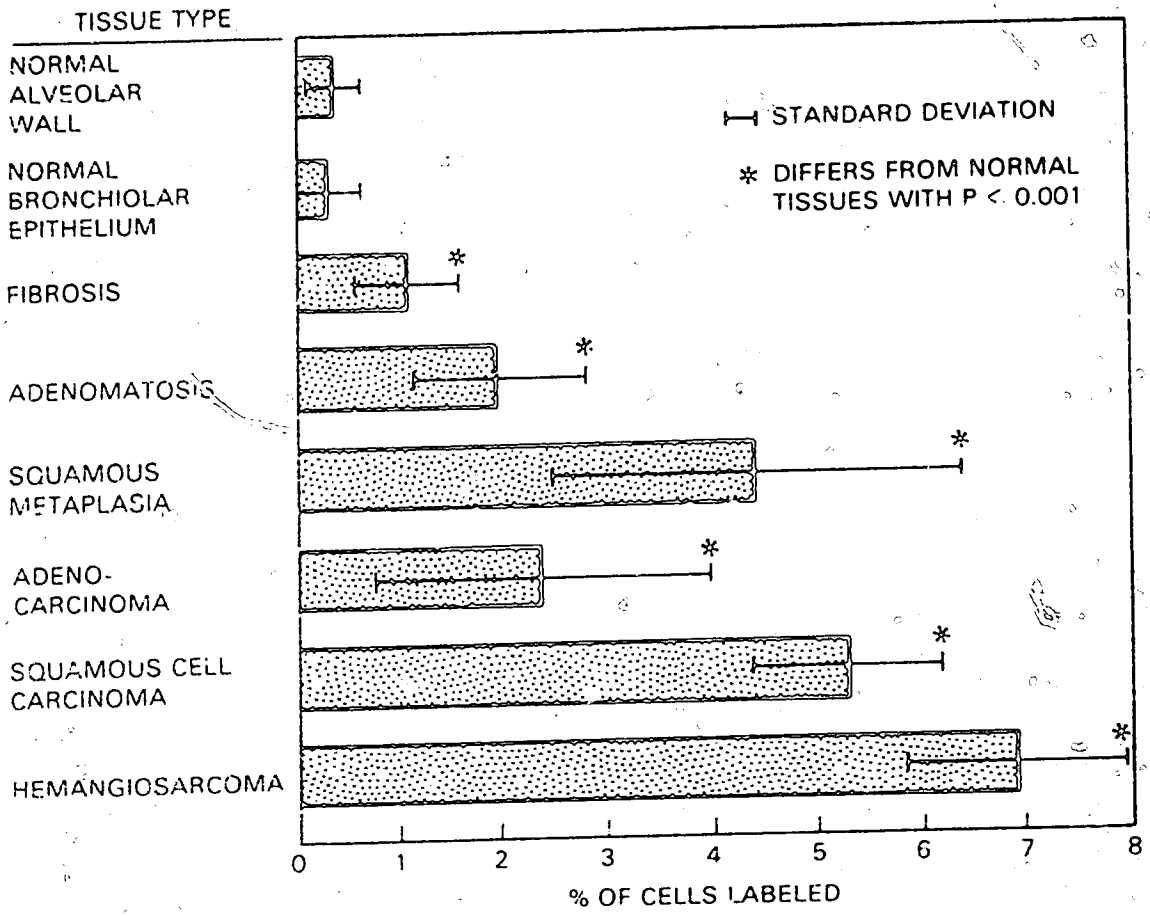

FIGURE 1. Labeling Indices of Normal Tissue and PuO_2-Induced Lesions in Rat Lung 1.5 Hours Following Administration of ^{3}H-Thymidine.

from 1.6-2.7%, adenocarcinoma, 2.3-3.9%; squamous-cell metaplasia, 2.1-6.9%; squamous cell carcinoma, 4.2-5.9%; and hemangiosarcoma, 6.1-7.7%. Labeling indices for pulmonary lesions did not show temporal changes; however, the LI for normal alveolar wall increased with time ($P < 0.01$), and that for normal bronchiolar wall decreased ($P < 0.01$).

Fibrotic lesions, especially in the subpleural and peribronchial regions, were frequently the site of origin of lung tumors. Increased cell turnover was seen in fibrotic lesions, even in the absence of well-developed epithelial pathology. Adenomatous lesions grew more slowly than corresponding squamous cell types, with metaplastic and neoplastic lesions of the same morphologic type having similar LI. Cell turnover time is not the only factor contributing to rapid tumor growth; metaplastic and neoplastic cells may differ qualitatively in other ways that affect the ability of the tumor to expand and invade surrounding tissues.

EFFECT OF PRIOR NEUTRON OR GAMMA IRRADIATION ON PULMONARY CLEARANCE OF $^{239}PuO_2$

Investigators: K. Rhoads, J. P. Geraci,* and C. L. Sanders

Technical Assistance: C. White, A. Conklin, and A. Gelman

Prior thoracic exposure to gamma or neutron irradiation depressed the alveolar clearance of inhaled or intratracheally instilled $^{239}PuO_2$ particles. This study examined the effect of external thoracic irradiation on lung clearance of $^{239}PuO_2$ particles administered 2 to 5 mo later. It was designed to assess damage to clearance mechanisms from acute external exposures during radiotherapy or accidents, and the potential for increased risk from toxic insoluble particles subsequently entering the lung. The relative biological effectiveness (RBE) for fast neutrons was also examined in comparison to a gamma standard.

In a preliminary study, seven female Fischer rats were given a thoracic dose of 1800 R gamma irradiation from ^{137}Cs. Seventy days later, these animals and 10 sham-exposed controls were given a 30-min, nose-only exposure to an aerosol of $^{239}PuO_2$. Two exposed and five sham-exposed animals were necropsied 1 day later. The remaining animals were placed in metabolism cages, and excreta were collected twice weekly for 30 days. Radioanalyses were performed on the lungs and thoracic lymph nodes of all animals, and on carcasses and excreta of animals necropsied at 30 days.

In a follow-up study, female Fischer rats were given graded doses of external thoracic irradiation from cyclotron fast neutrons (550, 750, or 950 rad), ^{137}Cs gamma (600, 900, 1200, or 1500 R), or sham-exposed.** At 150 days after external exposure, these animals were given $^{239}PuO_2$, in suspension, by intratracheal instillation (IT). Three to 11 animals per group were placed in metabolism cages, and excreta were collected twice weekly for 60 days. Lungs, thoracic lymph nodes, carcasses, and excreta of all animals were analyzed for $^{239}PuO_2$ content.

At necropsy, the lungs were instilled with fixative and the trachea was tied. After overnight immersion in fixative, part of each lobe was selected for histopathology, and the remainder was analyzed for ^{239}Pu content. Autoradiograms were made from 5-μm paraffin sections dipped in Ilford K-5 emulsion and exposed for 2 wk.

Lungs of control and exposed animals in both studies were, for the most part, normal in appearance, except for focal areas of inflammation and fibrosis associated with PuO_2 particles. Additional findings in the lungs of gamma- and neutron-exposed animals were bronchiolar and bronchial epithelial hyperplasia, late inflammatory lesions, proliferation of lymphatic regions adjacent to bronchi, pneumonitis, epithelial metaplasia, and one lung abscess. A squamous carcinoma was found on the left foreleg of a 900-R gamma-exposed rat.

The initial alveolar deposition (IAD) of inhaled $^{239}PuO_2$ in the preliminary study was 180 ± 18 nCi in controls, and 134 ± 69 nCi in the 1800-R gamma-exposed group. The IAD for the intratracheally instilled groups ranged from 74 to 123 nCi, with standard deviations from 10-25% of means. Inhalation exposure to PuO_2 resulted in a relatively uniform distribution of particles throughout the lung, whereas intratracheally instilled particles concentrated in one or two lobes. This may explain why clearance of PuO_2 was more rapid in the preliminary study, despite the fact that clearance rate is inversely related to the deposition level. Concentration of a smaller total amount of PuO_2 in a small fraction of lung volume after IT administration produced higher

*Department of Environmental Health, Division of Radiological Sciences, University of Washington, Seattle, WA.

**^{137}Cs and neutron exposures performed at University of Washington, Seattle, WA.

deposition in the affected lobes. The clearance kinetics were therefore typical of a higher dose than one would expect from the lung average.

The fraction of IAD retained in the body was significantly greater than in controls for 1800-R gamma-exposed rats in the preliminary study at 30 days after PuO_2 exposure, and for 1500-R gamma-exposed rats at 21 and 49 days after IT (two-tailed t-test, all $P < 0.05$). Clearance curves for all groups (Figure 1) indicate a dose-response for this function. Statistical characterization and comparison of the data are incomplete, but there appears to be a marked depression of clearance at doses greater than 1200 R for gamma exposures and 950 rad for neutrons. Clearance curves for the 1500-R gamma-exposed and 950-rad neutron-exposed groups were nearly identical, resulting in an RBE for neutrons of about 1.6.

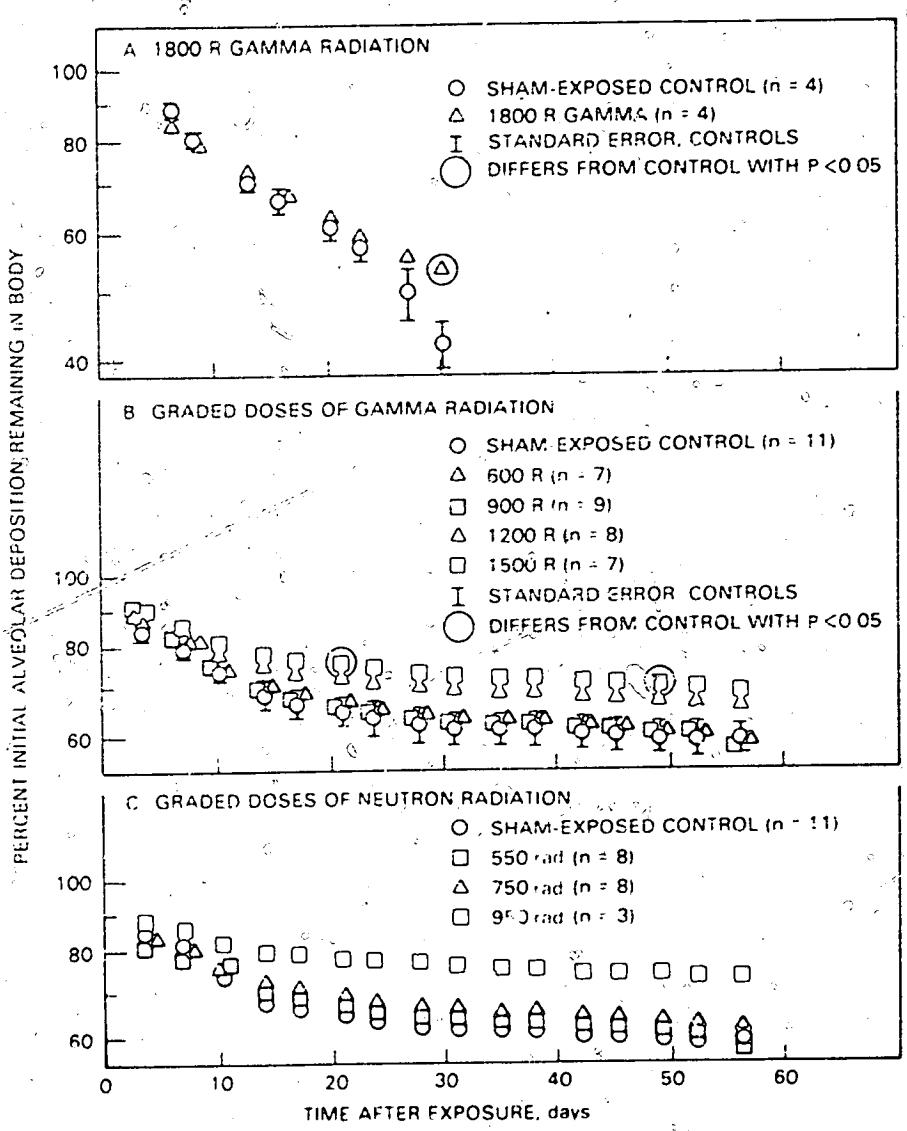

FIGURE 1. Clearance of PuO_2 Particles from Lung: A. Following 1800 R Gamma Radiation (Preliminary Study); B. Following Graded Doses of Gamma Radiation; C. Following Graded Doses of Neutron Radiation.

EFFECT OF LUNG DAMAGE CAUSED BY INTRATRACHEALLY INSTILLED $^{239}PuO_2$ AND VOLCANIC ASH ON THE ALVEOLAR CLEARANCE OF ^{14}C-BENZO[A]PYRENE

Investigators: R. A. Gelman, C. L. Sanders, and A. W. Conklin

Plutonium-induced fibrosis and volcanic-ash-induced inflammation did not significantly change the alveolar clearance of instilled ^{14}C-benzo[a]pyrene.

Polycyclic aromatic hydrocarbons (PAH) are widely distributed in the environment, largely as the result of incomplete combustion of fossil fuels. Benzo[a]pyrene (BaP), a PAH, has been shown to act synergistically with $^{239}PuO_2$ in producing lung tumors. The purpose of this study was to determine if lung damage induced by the presence of $^{239}PuO_2$ or volcanic ash alters the alveolar clearance of BaP, thereby increasing the hazards of BaP to the compromised lung.

Two groups of adult female Fischer rats were given intratracheal instillations of 0.64 μCi $^{239}PuO_2$ or 40 mg volcanic ash suspended in 0.5 ml physiological saline. At 2, 7, 14 and 30 wk following treatment, six $^{239}PuO_2$-treated animals, along with six untreated controls, received instillations of 7-30 μg of isotopically labeled ^{14}C-BaP (specific activity, 4.64 μCi/μmole BaP) suspended in 0.5 ml physiological saline. Initially, and at 2, 5 and 11 wk, a second group (ash-treated animals) and their corresponding controls were also given ^{14}C-BaP.

Following BaP instillation, the animals were placed in glass metabolism cages, and excreta were collected for 24 hr, after which the animals were killed and small amounts of lung tissue were taken for histological examination to determine the degree of lung damage. Tissue samples and excreta were heated with 10% ethanolic NaOH for 1 hr, then extracted with chloroform:methanol (1/1;v/v), and the extract was radioassayed by scintillation counting. The total ^{14}C in the excreta and in the whole body at the termination of the study period was defined as the instilled ^{14}C dose.

To establish a clearance curve, untreated rats were given an intratracheal instillation of 11 μg ^{14}C-BaP in 0.5 ml of physiological saline. Animals were killed at 1, 3 and 24 hr following instillation, and tissues radioassayed for ^{14}C content. Figure 1 illustrates the alveolar clearance curve derived from these data. Benzo[a]pyrene was rapidly cleared from the lung and excreted, principally in feces, after probable enzymatic alteration and conjugation in the liver and excretion in bile. At 3 hr following intratracheal instillation about 53% of the radioactivity was found in the gut, gut contents and feces; at 24 hr, less than 5% of the ^{14}C remained in the lung (Figure 1).

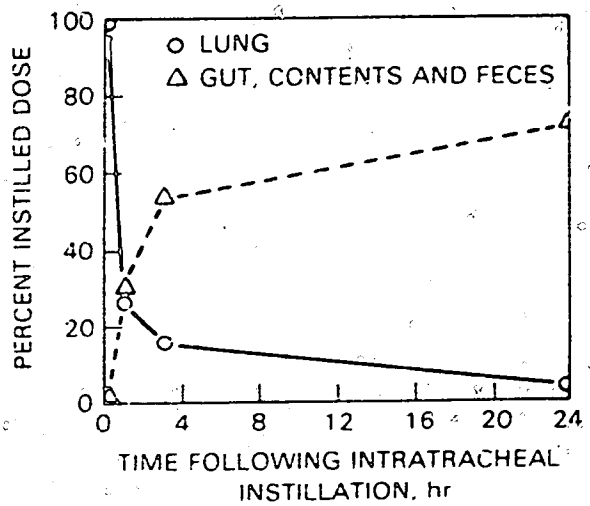

FIGURE 1. Clearance of ^{14}C-Benzo[a]pyrene and Its Metabolites From the Lung and Their Appearance in the Gut and Feces.

Table 1 shows ^{14}C remaining in the lung 24 hr after ^{14}C-BaP was given by intratracheal instillation to the treated animals and their corresponding controls. Untreated controls were instilled with BaP, as well as treated animals, to allow for differences in alveolar clearance due to the variable particle size of the BaP suspensions. As pulmonary lesions and fibrosis developed, there was no significant difference in lung clearance between the $^{239}PuO_2$-treated animals and their corresponding controls.

Alveolar clearance of ^{14}C-BaP from ash-treated animals followed a similar pattern. No change was observed in ^{14}C clearance in animals given BaP simultaneously with ash or several weeks after the ash was instilled.

In summary, pulmonary inflammation from intratracheally instilled volcanic ash or pulmonary pneumonitis and fibrosis from inhaled $^{239}PuO_2$ did not measurably alter BaP retention in the lung. Increased retention of BaP (or its metabolites) in the lung cannot account for the increased lung tumor incidences seen with inhaled $^{239}PuO_2$ and BaP.

TABLE 1. ^{14}C Remaining in the Lungs 24 Hours Following Intracheal Instillation of a Saline Suspension of ^{14}C-Benzo[a]-pyrene (Values are Means ± Standard Deviation).

Time Since Exposure to PuO_2, wk	Control	$^{239}PuO_2$ Treated	Time Since Exposure to Volcanic Ash, wk	Control	Volcanic Ash Treated
	% Dose			% Dose	
2	--[a]	3.85 ± 0.39 (6)[b]	0[c]	--[a]	0.61 ± 0.04 [c]
7	5.11 ± 1.21 (6)	4.85 ± 1.05 (6)	2	0.67 ± 0.11 (5)	0.79 ± 0.35 (5)
14	0.33 ± 0.11 (6)	0.33 ± 0.09 (6)	5	0.85 ± 0.39 (4)	0.75 ± 0.38 (6)
30	1.03 ± 0.23 (6)	1.02 ± 0.18 (6)	11	1.16 ± 0.15 (6)	0.92 ± 0.13 (6)

[a] No data
[b] Number of animals per group given in parentheses
[c] Benzo[a]pyrene was mixed with the volcanic ash prior to instillation

EFFECT OF AMOUNT OF DEPOSITED ^{239}Pu ON THE ALVEOLAR CLEARANCE OF $^{237,\ 239}PuO_2$

Investigators: C. L. Sanders and A. W. Conklin

The rate of alveolar clearance of $^{237,\ 239}PuO_2$ particles is inversely proportional to the amount of Pu deposited in the lung, over a mass range of 1×10^{-9} to 34×10^{-9} grams.

Clearance of inhaled particles from the deep lung is modified by several factors, including the total mass of material deposited in the lung. Increasing the mass deposited in the lung usually decreases alveolar macrophage-related lung clearance rates. High-level alveolar depositions of $^{239}PuO_2$ result in a decreased alveolar clearance rate, compared to lower alveolar depositions. Because of increased retention, proportionately greater radiation doses are delivered to lung following deposition of greater amounts of $^{239}PuO_2$. The externally countable gamma-emitting ^{237}Pu was employed in the present study to provide a more accurate assessment of the role of PuO_2 mass on its alveolar clearance.

Plutonium-237 has a physical half-life of 45 days, emitting gamma rays detectable, by whole-body counting, with 43% efficiency. Plutonium-237 was mixed with ^{239}Pu and calcined at 750°C for 2 hr to form a high-fired dioxide mixture (activity ratio of ^{237}Pu:^{239}Pu, 1:13.1). The mean size of individual particles was 0.05 μm; aggregates of these small particles were common in material given to rats. The plutonium mixture was suspended in distilled water and given to young adult Wistar rats in 1.0 ml volume by intratracheal instillation (IT). Tissues and excreta were analyzed for ^{237}Pu and ^{239}Pu content by gamma and alpha scintillation counting.

In an initial study, rats were given (IT) 37×10^{-12} g Pu as $^{237,\ 239}PuO_2$. The lungs contained 89 ± 14% of instilled ^{237}Pu at 1 wk, and 71 ± 8.8% at 4 wk. Thoracic lymph nodes increased from 0.8 ± 14% of instilled ^{237}Pu at 1 wk to 2.9 ± 1.2% at 4 wk. The distribution of ^{239}Pu in tissues and excreta was similar to that of ^{237}Pu. The lung clearance and tissue distribution for both ^{237}Pu and ^{239}Pu compared very well with previously published data for inhaled $^{239}PuO_2$.

The main study involved IT administration of $^{237,\ 239}Pu$ at five dose levels over a mass range of 1×10^{-9} to 34×10^{-9} grams (Table 1). Early alveolar clearance of ^{237}Pu was inversely proportional to the mass of deposited plutonium. This approach provides a simple, fast and accurate method of estimating lung dosimetry for inhaled PuO_2. The ^{237}Pu delivered less than 1% of the early lung dose from $^{237,\ 239}PuO_2$ particles in the present experiment and therefore does not constitute a significant additional carcinogenic risk.

TABLE 1. Influence of Amount of Deposited $^{237,\ 239}Pu$ on the Whole Body Retention of ^{237}Pu. Values are means (n, 5) ± standard deviation.

Initial Lung Deposition, g		Percent of Instilled ^{237}Pu in Body at Times Post-Instillation			
^{239}Pu	^{237}Pu	1 Day	1 Week	4 Weeks	8 Weeks
1.13×10^{-9}	1.69×10^{-12}	61 ± 14	29 ± 21	21 ± 14	16 ± 21
3.44×10^{-9}	5.07×10^{-12}	83 ± 21	69 ± 10	50 ± 19	29 ± 17
6.88×10^{-9}	10.0×10^{-12}	88 ± 17	67 ± 11	58 ± 6	37 ± 8
15.0×10^{-9}	21.8×10^{-12}	98 ± 10	86 ± 9	67 ± 7	44 ± 8
33.8×10^{-9}	49.6×10^{-12}	98 ± 7	91 ± 7	64 ± 7	63 ± 5

STATISTICAL CONSIDERATIONS FOR A LOW-DOSE $^{239}PuO_2$ INHALATION EXPERIMENT

Investigators: J. A. Mahaffey and C. L. Sanders

The feasibility of a low-dose experiment is supported both by statistical considerations and the analysis of data from previous inhalation experiments.

The objective of a low-dose (1.5 rad/yr) experiment in female Fischer 344 rats is to better define the shape of the dose-response curve relating lung dose to lung tumor incidence. The experimental goal is to detect a significant increase of 0.01 (1%) over spontaneous lung tumor incidence, based on 1000 each of control and exposed lifespan animals. The data from 1000 control rats will be pooled with data from other Fischer 344 female control rats from Goodman et al. (Toxicol. Appl. Pharmacol. 48: 237, 1979), who reported nine carcinomas in 1754 controls sacrificed at 110 wk of age, and from the NLM Laboratory Animal Data Bank, which found six lung tumors in 1292 controls from nine experiments. The pooled spontaneous lung tumor incidence, based on the 4036 animals, will be denoted as θ_1. For various acceptable levels of α and β, Table 1 gives the number of exposed animals required to detect a significant increase in lung tumor incidence from θ_1 to $\theta_2 = \theta_1 + 0.01$. A polygon encloses the required numbers of exposed animals of about 1000 or less. Thus, from Table 1, if $\theta_1 \leq 0.005$ (0.5%) and $\theta_2 \geq 0.015$ (1.5%), a signficant increase in lung tumor incidence can be detected with $\alpha = 0.05$ and $\beta = 0.10$, or vice versa. Based on calculations pooling all controls, observing $\theta_1 \leq 0.005$ requires ≤ 5 spontaneous lung tumors in our 1000 controls. To observe $\theta_2 \geq 0.015$ requires observing ≥ 15 lung tumors in 985 exposed lifespan rats.

It is reasonable to expect incidences similar to these based on predictions from a linear regression using dose-response data from a previous $^{239}PuO_2$ inhalation experiment in female Wistar rats (Sanders et al., Radiat. Res. 68: 349, 1976). This analysis predicted that a lifetime lung dose of 3 rad in a 2.8-g lung would produce 0.016 (1.6%) lung tumors and a spontaneous lung tumor incidence of 0.0023 (0.23%). In this experiment, median survival for the control and the 5.5-nCi exposed group was 660 and 686 days postexposure, respectively. Thus, to estimate the target IAD in the low-dose experiment, we used 675 days (~2 yr) as the postexposure survival time to have delivered about 3 rad to a 2.8-g lung.

Elsewhere in this Annual Report, whole-body counts of ^{237}Pu indicate the lung clearance of ^{239}Pu in Fischer 344 female rats. For the various levels of IAD reported, clearance appears to be related to IAD. Data from the lowest exposure group were fit by a two-compartment, nonlinear model to estimate a lung clearance curve. This curve (based on five animals measured at each time interval: 1 hr, 24 hr, 1 wk, 4 wk and 8 wk postexposure) is

$$Y(t) = 1.16\, e^{-0.72t} + 0.29\, e^{-0.0062t},$$

where Y(t) is the predicted lung content in nCi at t days postexposure. The estimated average IAD was 1.5 nCi, and the half-times were estimated as 0.97 and 113 days. Based on this curve, at 675 days postexposure, the rad dose (D) to a 2.8-g lung is related to IAD by the equation, D = 3.1 (IAD). Therefore, to deliver an average dose of 3 rad would require an IAD slightly less than 1 nCi. Based on the 8-wk time limit of the data, it was not possible to statistically test for the existence of a third, longer-term compartment, which could change the estimate of the relationship of dose and IAD described above.

TABLE 1. Number of Exposed Fischer 344 Female Rats Needed to Detect a 1% Increase Over Spontaneous Lung Tumor Incidence Based on 4036 Controls[a].

θ_1	$\theta_2 = \theta_1 + 0.01$	$\alpha = 0.01$, $\beta = 0.01$	$\alpha = 0.01$, $\beta = 0.05$ or $\alpha = 0.05$, $\beta = 0.01$	$\alpha = 0.05$, $\beta = 0.10$ or $\alpha = 0.10$, $\beta = 0.05$	$\alpha = 0.10$, $\beta = 0.10$
0	0.01	623	436	226	171
0.001	0.011	1,335	893	441	330
0.002	0.012	1,873	1,213	580	431
0.003	0.013	2,464	1,541	713	526
0.004	0.014	3,147	1,893	847	620
0.005	0.015	3,963	2,281	985	716
0.006	0.016	4,965	2,713	1,128	813
0.007	0.017	6,232	3,201	1,277	913
0.008	0.018	7,892	3,758	1,433	1,016
0.009	0.019	10,167	4,401	1,597	1,122
0.010	0.020	13,484	5,154	1,770	1,233

[a] This pool includes controls of Goodman et al. (1979), NLM LADB shelf control animals and the controls proposed in the low-dose lifespan study

INHALATION CARCINOGENESIS OF HIGH-FIRED $^{241}AmO_2$

Investigators: C. L. Sanders and J. A. Mahaffey

The incidence of lung tumors increases with increasing terminal body burden of ^{241}Am. No bone tumors were found at body burdens of less than 10 nCi ^{241}Am.

Previous studies have considered the metabolism and carcinogenicity of inhaled, high-fired $^{238}PuO_2$, $^{239}PuO_2$ and $^{244}CmO_2$. Americium, like curium, is more soluble in the lung, irrespective of chemical form, than either ^{238}Pu or ^{239}Pu. This report examines preliminary histopathology and dosimetry data for female Wistar rats given inhaled, high-fired $^{241}AmO_2$ at estimated initial alveolar depositions of 0, 0.1, 1.0, 10, 100 and 1000 nCi.

A preliminary summary of lung lesions in rats exposed to inhaled $^{241}AmO_2$ permits some observations about the probable eventual findings of this study. The rats were divided into five groups with final body burdens of: 0, 0 to 1, 1 to 10, 10 to 100, and >100 nCi. A second grouping to separate gross survival differences with respect to lesion incidences placed the results in 6-mo intervals following exposure. In the first year (0-12 mo), there were no lesions in 14 animals that died. Twelve of these rats had residual body burdens of ^{241}Am in excess of 100 nCi, suggesting that radiation pneumonitis was the cause of death. This observation was confirmed by histopathological examination. In rats surviving longer than 1 yr, none had body burdens greater than 100 nCi; therefore, this dose level is not reported in the tables.

The distribution of premalignant and malignant lung lesions, and total lesions, by body burden of ^{241}Am at death, is shown in Table 1. The incidence of premalignant lung lesions (adenomatous and squamous metaplasias) increased (0, 2.7, 5.3, 12.5%) as residual ^{241}Am increased. Lung tumor incidences (2.3, 6.3, 7.9, 50%) and total lung lesions (12.5, 15.3, 15.8, 75.0%) likewise increased with increasing ^{241}Am body burden. The category "Total Lesions" consists of two liver tumors, one bone tumor (10- to 100-nCi group) and 15 tumors at other sites, in addition to the lung lesions.

A summary of incidences for the lesions given in Table 1, but based on animals at risk at the beginning of the three reported survival intervals, is given in Table 2. The incidence of premalignant lung lesions, as a function of animals at risk, peaks in the 18- to 24-mo interval. Animals "at risk" are those that survive a specified length of time and are "at risk" to develop a lesion. For lung tumors, the percent incidence increased with increasing survival interval (0.8, 1.4, 8.5%). Similarly, percentage of animals with total lesions increased with survival (1.2, 6.8, 17.1%).

A preliminary examination of the data indicates that inhaled $^{241}AmO_2$ is not more carcinogenic in lung than inhaled $^{238}PuO_2$, or $^{244}CmO_2$, and is less carcinogenic in skeleton than inhaled $^{244}CmO_2$.

TABLE 1. (Number of Lesions)/(Number of Animals) by Americium Body Burden at Death.

nCi	Months 12-18	18-24	24-30	Total, %
	Premalignant Lung Lesions			
0	0/8	0/34	0/46	0/88 (0)
> 0-1	1/10	1/38	1/63	3/111 (2.7)
> 1-10	0/4	2/16	0/18	2/38 (5.3)
>10-100	0/2	1/4	0/2	1/8 (12.5)
	Lung Carcinoma or Sarcoma			
0	0/8	0/34	2/46	2/88 (2.3)
> 0-1	0/10	1/38	6/63	7/111 (6.3)
> 1-10	0/4	1/16	2/18	3/38 (7.9)
>10-100	2/2	1/4	1/2	4/8 (50.0)
	Total Lesions			
0	0/8	4/34	7/46	11/88 (12.5)
> 0-1	1/10	4/38	12/63	17/111 (15.3)
> 1-10	0/4	4/16	2/18	6/38 (15.8)
>10-100	2/2	3/4	1/2	6/8 (75.0)

TABLE 2. (Number of Lesions)/(Number of Animals at Risk at Beginning of Survival Interval) by Months of Survival

nCi	Months 12-18	18-24	24-30	Total
	Premalignant Lung Lesions			
0	0/8	0/34	0/46	0/88 (0)
0-1	1/10	1/38	1/63	3/111 (2.7)
1-10	0/4	2/16	0/18	2/38 (5.3)
10-100	0/2	1/4	0/2	1/8 (12.5)
	Lung Carcinoma or Sarcoma			
0	0/8	0/34	2/46	2/88 (2.3)
0-1	0/10	1/38	6/63	7/111 (6.3)
1-10	0/4	1/16	2/18	3/38 (7.9)
10-100	2/2	1/4	1/2	4/8 (50.0)
	Total Lesions			
0	0/8	4/34	7/46	11/88 (12.5)
0-1	1/10	4/38	12/63	17/111 (15.3)
1-10	0/4	4/16	2/18	6/38 (15.8)
10-100	2/2	3/4	1/2	6/8 (75.0)

INHALATION TOXICOLOGY OF $^{241}Am(NO_3)_3$

Investigators: J. E. Ballou, R. A. Gies, H. D. Toiley, and R. A. Miller

Technical Assistance: A. W. Endres

Rats exposed to inhaled $^{241}Am(NO_3)_3$ aerosols developed lung and bone tumors as the major treatment-related effects. These lesions appeared to be dose-related at cumulative radiation doses >10 rad.

This report presents progress in a study of ^{241}Am metabolism and biological effects in rats exposed nose-only for 30 min to $^{241}Am(NO_3)_3$ aerosols generated from 0.27N HNO_3 solutions. The study is complete except for statistical evaluation and analysis of the results. Details of the experimental protocol and major results up to 700 days after exposure were presented in earlier Annual Reports (1977, 1978).

Two groups of Wistar male rats (51.7 and 95.2 nCi initial lung burden, ILB) were sacrificed at intervals to determine the early retention kinetics of inhaled $^{241}Am(NO_3)_3$ during the first 200 days after exposure. Additional groups of animals (8.2 and 95.3 nCi ILB) were held for life span study of long-term effects and for determination of retention parameters at later time intervals.

Early retention and distribution of ^{241}Am in the sacrificed rats is shown in Figure 1. Approximately 90% of the inhaled $^{241}Am(NO_3)_3$ had cleared the lung by 30 days after exposure; only about 1% remained at 200 days. The amount of ^{241}Am retained in liver was about one-half that in the lung.

Inhaled $^{241}Am(NO_3)_3$ was translocated mainly to the skeleton, which retained an amount equivalent to about 20% of the ILB during the 200-day retention period. Results for the two groups of animals (51.7 and 95.3 nCi ILB) were in reasonable agreement.

In Figure 2, the early retention data for the group exposed to 95.3 nCi ILB are combined with results from rats analyzed at the time of death in the late effects study. The fitted curves give an estimate of ^{241}Am retention kinetics during the life span of the rat. Retention in lung was best described as the sum of two exponential functions with half-lives of 9 days and 210 days, accounting for 96% and 4%, respectively, of the ILB. The results for liver were similarly fitted with two exponentials (half-lives, 13 days and >200 days), accounting for ^{241}Am equivalent to approximately 24% and 5%, respectively, of the ILB. Since there was no indication of ^{241}Am turnover from the skeleton, it was assumed that the amount determined at death was retained throughout the animal's life time. This is indicated in Figure 2 by a horizontal line accounting for a skeletal burden equivalent to approximately 25% of the ILB.

The cumulative radiation dose to major target organs (lung and skeleton) was calculated based on retention parameters derived from the generalized retention curves shown in Figure 2, and the individual values for ^{241}Am content determined at the time of death. Table 1 shows the dose to lung and the corresponding tumor incidence. The cumulative radiation dose (first column, Table 1) was arbitrarily divided into the various dose ranges in order to facilitate summarizing the results. Results for rats from both late effects groups (8.2 and 95.3 nCi ILB) are listed in Table 1 along with those for nontreated control animals. Survival time did not appear to be affected by ^{241}Am exposure except in the lowest dose category (1-10 rad). There is no ready explanation for this observation, since all but one of the rats in this dose range were from the group receiving 8.2 nCi ILB, a dose expected to have little life-shortening effect. The results in Table 1 show an apparent relationship between lung tumor incidence and ^{241}Am inhalation for cumulative lung doses >10 rad. No lung tumors were observed in nontreated control rats or in rats receiving <10 rad to the lung.

Tumors of the skeleton (osteosarcomas) were less clearly related to ^{241}Am deposition (Table 2) due to the 3% incidence of

this lesion in control animals. The progressive increase in tumor incidence at a cumulative bone dose >16 rad, however, strongly suggests a causal relationship between ^{241}Am incorporation and bone-tumor induction. Radiochemical analyses of control animals with bone tumors confirmed the absence of ^{241}Am in the controls.

The tumorigenic response following ^{241}Am inhalation is compared with the results of similar studies with other transuranic nitrates in Table 3. Americium-241 appears to be no more effective in inducing lung and bone tumors than Pu or Es, with the possible exception of increased induction of bone tumors in the group accumulating 100-1000 rad. Lung tumors, on the other hand, seem to be less prevalent in rats accumulating higher radiation doses from ^{241}Am. The statistical significance of these observations has not yet been established.

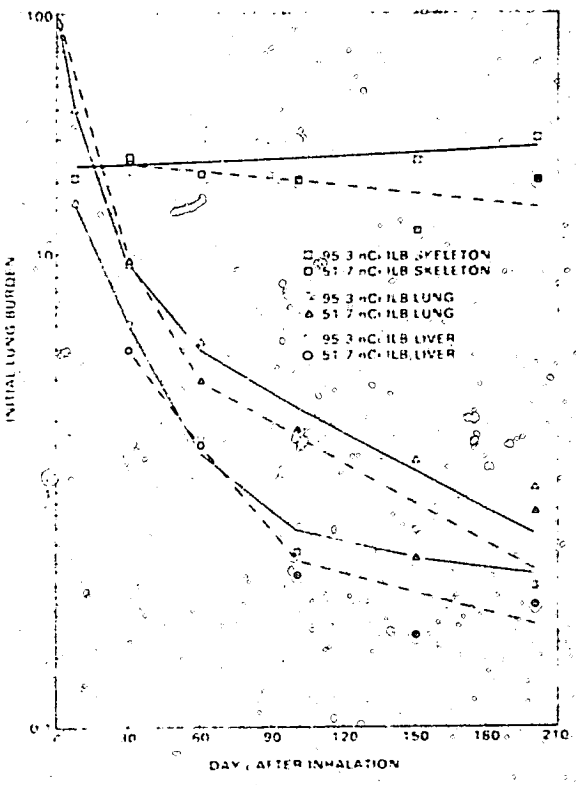

FIGURE 1. Early Distribution of Inhaled $^{241}AmNO_3$.

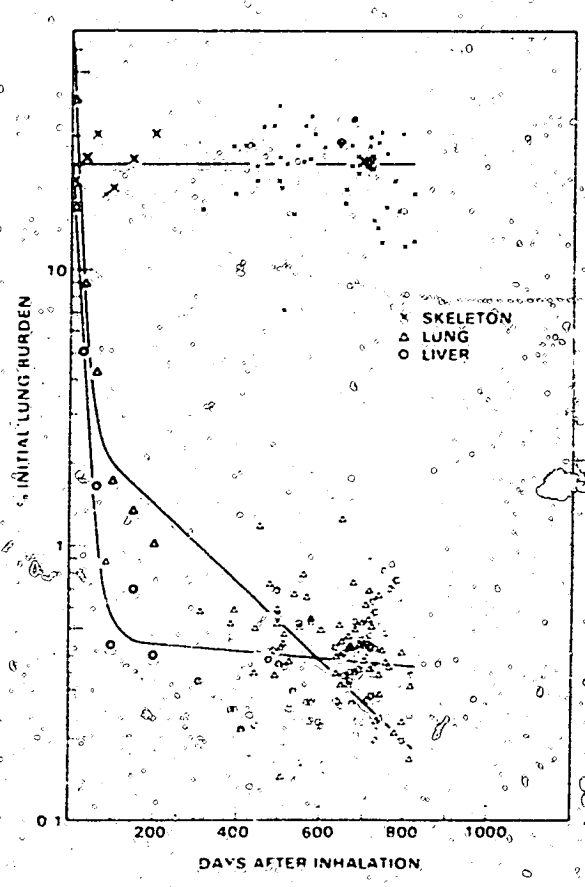

FIGURE 2. Early and Late Distribution of Inhaled $^{241}AmNO_3$.

TABLE 1. Cumulative Radiation Dose and Lung Tumor Incidence Following $^{241}Am(NO_3)_3$ Inhalation.

Cumulative Lung Dose, rad	Number of Rats	Average Survival, days	Number of Lung Tumors	Tumor Incidence, %
1-10	24	549	0	0
11-100	55	665	5	9
101-369	37	666	5	14
Controls	100	667	0	0

TABLE 2. Cumulative Radiation Dose and Bone Tumor (Osteosarcoma) Incidence Following $^{241}Am(NO_3)_3$ Inhalation.

Cumulative Bone Dose, rad	Number of Rats	Average Survival, days	Number of Bone Tumors	Tumor Incidence, %
1-10	45	638	1	2
11-100	36	620	2	6
101-200	34	669	9	26
Controls	100	667	3	3

TABLE 3. Lung and Bone Tumor Incidence in Rats Exposed to Inhaled Transuranic Nitrates. Values are expressed as percent tumor incidence by dose categories.

	Dose Range, rad							
	Lung				Bone			
	0-10	10-100	100-1000	Control	0-10	10-100	100-1000	Control
$^{239}Pu(NO_3)_4$	0	6	41	0	0.6	7	10	0 (5)(a)
$^{238}Pu(NO_3)_4$	2	6	36	0	1	1.5	3.5	0 (5)(a)
$^{252}Es(NO_3)_3$	9	19	28	0	6	10	--	
$^{241}Am(NO_3)_3$	0	9	14	0	2	6	26	3

(a) Values in parenthesis are % incidence in treated controls exposed to the vector aerosol (0.27 N HNO_3)

INFLUENCE OF DOSE PROTRACTION AND AGE ON LUNG AND BONE TUMORIGENESIS FROM INHALED $^{244}CmO_2$

Investigators: C. L. Sanders and J. A. Mahaffey

Partial data from an experiment still in progress suggests that protraction of $^{244}CmO_2$ inhalation exposure may increase the incidence of lung and bone tumors.

Earlier studies with inhaled, high-fired $^{244}CmO_2$ in Wistar rats have demonstrated its carcinogenicity in lung, liver and bone. The short retention time in lung and rapid, significant translocation to bone resulted in a temporal dose-distribution pattern quite different from that of either high-fired $^{238}PuO_2$ or $^{239}PuO_2$. Repeated or fractionated exposure to inhaled $^{244}CmO_2$ might be expected to increase the incidences of lung and, particularly, bone tumors over those observed following a single exposure. Bone tumors may be increased because ^{244}Cm, though a bone-surface seeker, is rapidly buried in the bone matrix after exposure. Protracted exposure should expose the target cells for tumor formation, located near bone surfaces, for a much longer period of time than would occur following a single exposure. The animals' age at time of exposure will also influence the rate of burial of surface deposits. This study was designed to test the role of temporal dose-distribution patterns from inhaled $^{244}CmO_2$, and the effect of animals' age at exposure on carcinogenesis from $^{244}CmO_2$.

Six groups of young adult, female Wistar rats were included in this study: (1) unexposed controls; (2) sham-exposed controls; (3) animals exposed to a single $^{244}CmO_2$ dose at 70 days of age, resulting in about 350 nCi ^{244}Cm initial alveolar deposition (IAD); (4) animals exposed at 70 days of age and at 3-wk intervals thereafter for 10 consecutive exposures, each exposure resulting in IAD of about 35 nCi ^{244}Cm; (5) animals exposed at 280 days of age, about 350 nCi IAD; and, for an early metabolism study, (6) animals exposed at 70 days of age, IAD of about 1000 nCi ^{244}Cm. All the animals in this study have died. Histopathology is nearly complete, and radioanalysis of tissues for ^{244}Cm content is approximately 50% complete. These preliminary data are summarized in Table 1. Rats given a single exposure or 10 multiple exposures to $^{244}CmO_2$ had survival times significantly less than all other groups.

Because of an unexpectedly high incidence of lung tumors in sham-exposed controls (2/30), the incidences of lung tumors in singly and multiply exposed groups was not statistically significant. There were, however, twice as many lung tumors in multiply exposed rats as in singly exposed rats. The incidence of bone tumors was greater in multiply exposed animals than in animals given a single exposure at 70 days of age. No bone tumors were observed following a single exposure at 280 days of age.

TABLE 1. Effect of Single and Fractionated Inhalation Exposures to $^{244}CmO_2$ on Cancer Induction in Liver, Lung and Bone[a].

Treatment	No. of Animals	Median Life-Span, days	Mean Amount ^{244}Cm at Death, nCi		Incidence of Tumors, %	
			Lung	Skeleton	Lung	Skeleton
Single Exposure at 70 days	38	437 [b]	1.1	8.3	9.1	12.1
10 Fractionated Exposures at 3 Week Intervals Starting at 70 days	64	493 [b]	1.9	8.0	18.2	27.3
Single Exposure at 280 Days	29	625	6.3	10.6	7.7	0
Bottle-Stressed Controls	30	779	0	0	6.7	0
Controls	17	830	0	0	0	0

[a] Data based on analyses of about 85% of animals for histopathology and 50% of animals for radioanalysis

[b] Significantly different from all other groups at $P = 0.05$ level

○ CIGARETTE SMOKE AND PLUTONIUM

A large segment of the population smokes cigarettes; therefore, a synergistic effect between inhaled plutonium and cigarette smoke might influence estimates of the health risk of plutonium and other transuranic elements relevant to the environment. Cigarette-smoke-induced changes in pulmonary airways of humans and laboratory animals include epithelial squamous metaplasia, with loss of cilia. These changes may impair the mucociliary-clearance mechanism, thereby influencing the pulmonary distribution and retention of inhaled particulate material. The overall objective of this study is to determine whether cigarette smoking increases the probability of plutonium-induced lung cancer. Initial experiments, designed to characterize the effect of chronic cigarette smoke exposure on pulmonary clearance of plutonium aerosols, are described.

THE EFFECT OF CIGARETTE SMOKE EXPOSURE ON CLEARANCE OF $^{239}PuO_2$ FROM THE LUNGS OF BEAGLE DOGS

Investigators: R. E. Filipy, J. L. Pappin, D. L. Stevens, and W. J. Bair

Technical Assistance: J. S. Cunningham, J. C. Chapman, W. Skinner, and C. R. Petty

The previously reported inhibitory effect of cigarette smoke on pulmonary clearance of $^{239}PuO_2$ in rats has now been demonstrated in beagle dogs.

To determine whether the inhibitory effect of cigarette smoke exposure on clearance of inhaled plutonium that was observed in rats (Annual Reports, 1979 and 1980) could be demonstrated in a larger animal species, a pilot experiment with groups of beagle dogs (Table 1) was begun. Since the primary objective of this pilot experiment was to test cigarette smoke delivery and plutonium detection methods on dogs, a relatively small number of animals was used.

TABLE 1. Exposure of Beagle Dogs to Cigarette Smoke and Plutonium to Determine Effects on Lung Clearance Rates.

Group	No. Old Dogs	No. Young Dogs	Exposure
1	4	2	Cigarette Smoke, Only
2	4	2	Cigarette Smoke + $^{239}PuO_2$
3	4	2	Sham Smoke + $^{239}PuO_2$

The majority of experimental animals used in this experiment were previously a part of the project, "Inhalation Hazards to Uranium Miners." They had been exposed to cigarette smoke using a mask exposure system or had served as controls for nearly 10 yr before they were reassigned. For convenience, these dogs will be referred to as "old" dogs; the "young" dogs listed in Table 1 were slightly over 2 yr of age when assigned to this experiment. Also, dogs exposed to cigarette smoke will hereafter be called "smoking" dogs as opposed to control ("nonsmoking") dogs, even though exposure of dogs to cigarette smoke does not require active participation (other than normal breathing), as the terms imply.

The mask exposure system previously used on the old smoking dogs employed a solenoid valve mounted on the front of the mask. This valve was pressure-activated by the dogs' breathing, and controlled the source of inhaled air. Dogs were allowed to breathe room air for nine breaths; on the tenth breath, the air was directed through a lighted cigarette. Smoke was directed into the mouths of the dogs by a plastic tube inserted in the mouth, and exhaled through a separate flap valve. Dogs were exposed to smoke from 10 cigarettes per day.

There was considerable dog-to-dog variation in the amount of smoke inhaled with this method, depending on respiratory rate, tidal volumes, and learned avoidance. Observations indicated that some dogs learned to use the audible click of

the solenoid valve as a cue to draw only a quick, shallow breath, thereby switching the valve back to the fresh-air source. Blood carboxyhemoglobin (COHb) concentrations, a measure of smoke inhalation, in the smoking dogs ranged between 2.0 and 4.7% after smoke from three cigarettes; corresponding control values ranged between 1.1 and 2.3%

The exposure system currently in use also utilizes a mask over the nose and mouth of each dog; however, the solenoid apparatus has been eliminated. A motorized pump, consisting of a piston within a cylinder, draws a 35-ml puff of smoke from the cigarette. This pump is attached to the mask by a short piece of flexible tubing. All air inhaled by the dog must be drawn through the pump cylinder, which is filled with smoke at 1-min intervals. The dogs are exposed to smoke from nine cigarettes per day, 7 days per week. Blood COHb concentrations in dogs exposed using the system range from 6.1% after three cigarettes to 8.5% after nine cigarettes, daily pre-exposure values are between 2 and 4%. Dog-to-dog variation is small, primarily because learned avoidance is minimal. The COHb concentrations in the blood of human smokers are generally in the range of 5 to 8%. It is concluded that the new exposure system is more effective in delivering smoke to beagle dogs than was the old system.

After approximately 7 mo exposure on the new system, dogs were exposed to an aerosol of $^{239}PuO_2$ sufficient to produce initial lung burdens of 0.3 to 1.4 μCi. In vivo whole-body counts (17 keV X-rays) were made on each dog, beginning on day 6 after exposure; smoke exposures were resumed 20 days after inhalation of [illegible]tonium

Whole-body counts were e[illegible] percent of the estimated ini[illegible] burdens of each dog. Curves representing the mean values for groups of the dogs are plotted in Figure 1. When both young and old dogs are considered, the mean pulmonary clearance rate of smoking dogs was significantly slower than the mean rate of nonsmoking dogs ($P < 0.05$). Young dogs cleared $^{239}PuO_2$ from their lungs significantly faster ($P < 0.05$) than did old dogs, whether exposed to smoke or not. Furthermore, the cigarette smoke effect is significantly greater ($P < 0.02$) on young dogs than on old dogs. The difference between old smoking dogs and old nonsmoking dogs was not statistically significant.

The regression lines in Figure 1 are straight lines, all plotted with a

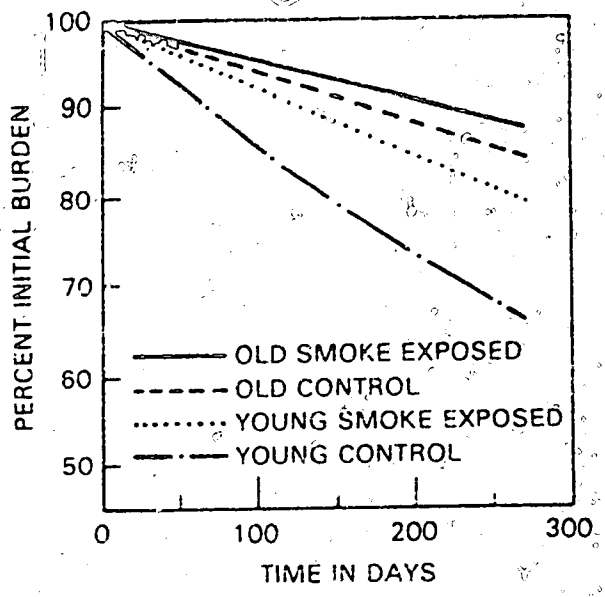

FIGURE 1. Clearance of $^{239}PuO_2$ From the Lungs of Dogs Chronically Exposed to Cigarette Smoke.

y-intercept of 100%; therefore the lines begin to separate immediately. Plots of actual means do not indicate a clear separation between smoking and nonsmoking dogs until approximately 85 days after plutonium exposure. At least three explanations for this are possible. First, the component of variation associated with differences in initial lung burden has been removed for the plots, making differences i[illegible]ance rates easier to detect. Seco[illegible]tural lung clearance rate in d[illegible]; therefore, a perturba[illegible]e would be harder to [illegible]s, which have a faster [illegible]e. Third, to minimize [illegible]ersonnel contamina[illegible] not resumed unti[illegible]on of plutonium. [illegible] instrumental in[illegible]e smoke on the [illegible]

These data do not indicate whether the reduced pulmonary clearance of plutonium results from ciliotoxicity of the cigarette smoke or from interference with the functioning of pulmonary macrophages. Urine and feces samples from each day have been retained and are being analyzed to provide additional information. The respiratory tract and associated lymph nodes will be analyzed in detail when the dogs die or are killed.

It is concluded that in this pilot experiment, chronic exposure to cigarette smoke reduced clearance of inhaled $^{239}PuO_2$ from the lungs of beagle dogs. These results agree with those obtained in two

experiments with rats. The pulmonary clearance rate in young dogs was significantly higher than in old dogs, with or without smoke exposure. Cigarette smoke was more effective in reducing the clearance rate in young dogs than in old dogs. However, these conclusions are based on small numbers of animals.

THE IMPAIRMENT OF PULMONARY CLEARANCE OF $^{239}PuO_2$ IN RATS BY PROLONGED EXPOSURE TO CIGARETTE SMOKE

Investigators: R. E. Filipy, J. L. Pappin, D. L. Stevens, and W. J. Bair

Results of an experiment that showed inhibition of the clearance of plutonium from the lungs of rats by cigarette smoke exposure were previously reported (Annual Report, 1979). These results have been reproduced in a second experiment.

In a previous experiment to determine whether pulmonary clearance of inhaled plutonium might be affected by exposure to cigarette smoke, Fischer rats were exposed to cigarette smoke (or sham exposed) for 7 mo before inhalation exposure to a $^{239}PuO_2$ aerosol (Table 1). Smoke was generated from 10 University of Kentucky research cigarettes (1R3) 16 hr/day, 7 days/week. Seven days after inhalation of the plutonium aerosol, cigarette-smoke and sham exposures were resumed, for 5 more wk.

Two additional groups of smoke-exposed and sham-exposed rats were sacrificed for determination of blood carboxyhemoglobin (COHb) concentrations, indicative of the amount of smoke inhaled. Exposure of 10 rats to smoke from 1 cigarette (7 puffs) resulted in COHb concentrations of 7.5 ± 1.3% (mean ± SD) and five sham-exposed rats had mean COHb concentrations of 3.8 ± 0.2%; the difference was statistically significant ($P < 0.01$). The results of this experiment were reported in last year's Annual Report, and are summarized in Figure 1. The rates of plutonium clearance in rats exposed to cigarette smoke were significantly less than in the sham-exposed rats.

To confirm these results, a second experiment was completed. Rats of the second experiment were sham-exposed or exposed to smoke and plutonium as shown in Table 2. Smoke and sham exposures differed from those of the original experiment in that they were conducted in 12-hr rather than 16-hr days. Also, two control groups (cigarette smoke only and sham-exposed) in the original experiment (Table 1) were replaced with Groups B and C in the second experiment (Table 2), to determine the relative influence of smoke exposure before or after plutonium inhalation. Blood COHb concentrations in smoke-exposed and sham-exposed rats of the second experiment after exposure to smoke from 1 cigarette were 12.4 ± 4.2 (mean ± SD) and 1.5 ± 1.3 percent, respectively, an even greater difference than that in the first experiment.

TABLE 1. Exposure Histories of Rats in the First Experiment to Determine the Effect of Cigarette Smoke on Pulmonary Clearance of Inhaled $^{239}PuO_2$.

Group	Number of Rats	Exposure Regimen
1	35	Cigarette Smoke, Only
2	35	Cigarette Smoke + $^{239}PuO_2$ (~80 nCi)
3	35	Sham-Smoke + $^{239}PuO_2$ (~80 nCi)
4	35	Sham-Smoke, Only

TABLE 2. Exposure Histories of Rats in the Second Experiment to Determine the Effect of Cigarette Smoke on Pulmonary Clearance of inhaled $^{239}PuO_2$.

Group	Number of Rats	Exposure Regimen
A	30	Cigarette Smoke + $^{239}PuO_2$[a]
B	30	Cigarette Smoke Before $^{239}PuO_2$ Inhalation, Not After
C	30	Cigarette Smoke After $^{239}PuO_2$ Inhalation, Not Before
D	30	Sham-Smoke + $^{239}PuO_2$

(a) Initial Lung Burden Estimated to be ~175 nCi.

Body burdens in plutonium-exposed rats were determined by in vivo whole-body counts (17 keV X-rays) made periodically from the fourth day after exposure until all rats had been killed (day 42). The day 4 count was taken as the initial lung burden for each rat, and subsequent counts were expressed as a percent of that value (Figure 1).

In both experiments, the whole-body counts indicate significantly lower lung clearance rates in rats exposed to cigarette smoke before and after inhalation of plutonium than in the sham-exposed rats. Differences between mean values were significant on day 20 ($P < 0.05$) in the first experiment and on day 13 ($P < 0.05$) in the second experiment. Smoke-exposed rats of the second experiment cleared plutonium from their lungs slightly faster over the first 15 days after exposure than rats of the original experiment; however, clearance rates in the sham-exposed rats of the original and the second experiments were nearly identical. Because of logistical problems, resumption of smoke exposure after plutonium inhalation in the second experiment was delayed by 1 day, starting on the 8th day rather than the 7th day after exposure to plutonium as in the first experiment. That delay might partly account for the slightly faster clearance of plutonium in the smoke-exposed rats of the second experiment.

Analysis of in vivo whole-body counts obtained from rats in groups B and C of the second experiment indicates that, for the decreased clearance rate to occur, cigarette smoke exposures are necessary both before and after inhalation of plutonium. Preliminary analysis of data from these groups indicated that the rates of plutonium clearance were about the same as in the sham-exposed controls.

The conclusions reached in the above report are based only on in vivo whole-body counts. Groups of rats were killed at various times after exposure to plutonium for analysis of plutonium lung content by three different methods. The first is an in vitro count of the excised lungs with the same instrument used for whole-body counts. The second is radiochemical analysis of samples of the ashed lungs. These results will be correlated with the in vitro lung counts and, coupled with lung clearance curves, will be used to obtain an estimate of the initial lung burdens. We also use an analytical method described previously (Annual Report, 1978), which consists of autoradiography of the inner surfaces of the tracheas and major bronchi of rats. This is expected to yield more detailed information about the distribution and quantity of plutonium particles in the lungs of smoke-exposed and sham-exposed rats.

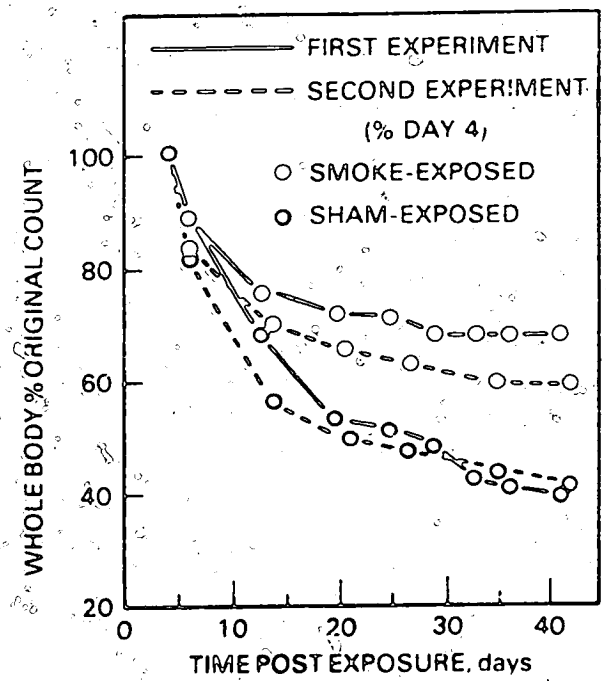

FIGURE 1. Pulmonary Clearance of $^{239}PuO_2$ From the Lungs of Rats Previously Exposed to Cigarette Smoke.

Toxicology of Plutonium- Sodium

Scenarios for liquid-metal fast breeder reactor (LMFBR) accidents predict the loss of sodium coolant, with subsequent core melt-down and release of mixed sodium-fuel aerosols [Na-$(PuU)O_2$] into the environment. Studies in other laboratories demonstrated that mixed aerosols of Na_2O-PuO_2 were more readily transported from the lung than PuO_2 aerosols. We therefore devised a continuous aerosol-generating system for animal exposures in which laser-generated fuel aerosols were swept through sodium vapor to form sodium-fuel aerosols.

Physicochemical characterization of these aerosols revealed that fuel aerosols were enriched in uranium and oxygen relative to the fuel. They consisted of branched-chain aggregates of very small particles with an activity median aerodynamic diameter (AMAD) of 1 μm. Sodium-fuel aerosols were spherical, with AMADs proportional to the sodium-fuel ratio and larger than those of the fuel aerosols. In vitro solubility of the mixed aerosols was greater than that of fuel aerosols.

Chemical studies to explore mechanisms for the enhanced solubility of the fuel-sodium aerosols revealed that uranium was rapidly converted to a soluble uranyl carbonate complex-ion species in the presence of air and moisture. Some atomically dispersed plutonium results from destruction of the fluorite-type lattice when uranium dissolves. Results from investigations of plutonium oxidation states in sodium-PuO_2 aerosols are consistent with the chemical reaction $Na + 3\,PuO_2 \rightarrow Pu_2O_3 + NaPuO_3$.

Inhalation studies in rats and dogs indicated that initial pulmonary deposition was greater for fuel aerosols, but that the rate of pulmonary clearance of sodium-fuel aerosols was higher. The appearance of larger fractions of the initial lung burden in blood, liver, and skeleton suggested an enhanced in vivo solubility of the mixed aerosols.

TECHNIQUES FOR GENERATION OF LMFBR-FUEL-SODIUM AEROSOLS

Investigators: J. K. Briant and M. D. Allen

A significant reduction in aerosol particle size was accomplished by lowering the concentration of condensation nuclei in the aerosol generator and by decreasing the fuel aerosol particle size prior to its exposure to the sodium vapor. We have designed a new generator, with an altered sodium-fuel aerosol formation sequence, to obtain concentrated aerosols of high sodium-fuel mass ratios and small particle sizes.

The generation sequence we have used to produce LMFBR-fuel-sodium aerosols consists of laser vaporization of reactor fuel to form branched, chain-like aggregates, which are then carried by argon into a sodium vapor atmosphere. Both the aerodynamic behavior and in vitro solubility of these aerosols were significantly influenced by the sodium-to-fuel mass ratio. Aerosols with larger activity median aerodynamic diameters (AMADs) and greater solubility were obtained when sodium-to-fuel mass ratios were increased (Annual Reports, 1977-1979). Results from biological studies revealed that ^{239}Pu pulmonary deposition was reduced and in vivo solubility of ^{239}Pu was enhanced at higher sodium-to-fuel mass ratios (Annual Reports, 1977-1979). For further study of the biological behavior of the inhaled aerosol, the aerosol generation technique was modified to minimize the AMAD and maximize the sodium-to-fuel mass ratio.

Reduction of sodium-fuel aerosol AMADs was accomplished by: 1) lowering the concentration of condensation nuclei in the argon carrier gas supplied to the aerosol generator; and 2) decreasing the size of the fuel particles entering the sodium furnace. Previous studies had shown that when argon was passed over hot copper turnings to remove any trace of oxygen, large numbers of nanometer-size condensation nuclei (probably CuO) were introduced into the system. When an

absolute filter was inserted between the hot copper turnings and the aerosol generator, the number of condensation nuclei decreased, and their concentration was stabilized. Subsequent condensation and coagulation in the sodium furnace yielded sodium-fuel aerosols with AMADs of 2-3 μm, rather than 3-4 μm.

In the second procedure, we increased the operating power of the laser to 220 W (rather than 110 W) during vaporization of the fuel. When the excess fuel particles generated by the laser at 220 W were tapped off, the remaining particles were about 20% smaller than those generated at 110 W. This procedure yielded sodium-fuel aerosols with AMADs of ~2 μm for sodium-to-fuel mass ratios of 30:1-60:1. We also attempted to reduce the fuel particle size by decreasing the coagulation coefficient during the fuel particle formation. Although the pressure in the vaporization chamber was increased from 1 to 3 atmospheres, no measurable decrease in fuel particle size occurred.

For the generation sequence currently in use, the fuel particle size is the limiting factor for both sodium-fuel aerosol AMADs and concentrations at high sodium-to-fuel mass ratios. To further reduce the fuel particle size, a new generator was designed to vaporize the fuel directly into a sodium vapor atmosphere rather than into the inert-argon atmosphere. Laser-vaporization of the fuel within the sodium furnace would simulate a hypothetical core-disruptive LMFBR accident with maximum sodium entrainment in the fuel vapor bubble. Reduced coagulation of the fuel particles is expected in the presence of sodium vapor, thus permitting aerosol generation of high sodium-fuel mass ratios with small AMADs.

CHEMICAL STUDIES OF LMFBR-FUEL-SODIUM AEROSOLS

Investigators: L. G. Morgan,* J. L. Ryan,* and J. K. Briant

Plutonium oxidation states in sodium-PuO_2 aerosols collected on filters in a dry argon atmosphere were determined by spectrophotometric investigations. These studies indicate that, for the aerosol generation method employed, PuO_2 reacts with sodium even in the absence of oxygen. The results, although indirect, are consistent with the chemical reaction: $Na + 3\ PuO_2 \rightarrow PuO_3 + NaPuO_3$.

Sodium-PuO_2 aerosols were generated by laser vaporization of PuO_2 and passing the PuO_2 aerosol through a sodium vapor furnace held at 500°C (Annual Report, 1977). The aerosols were collected in dry, oxygen-free argon on fiberglass filters. The complete filter housing was isolated by stainless steel inlet and exit valves, allowing the filter-collected sodium-PuO_2 aerosol to be sealed and removed from the aerosol generation system without exposure to either moisture or air. Previous studies have shown that spectrophometric results are not indicative of the actinide oxidation states present in the original aerosol if metallic sodium is not removed prior to exposure of the aerosol to moisture (Annual Report, 1979). For the present studies, a cryogenic filtering apparatus was constructed to remove metallic sodium by dissolution with liquid ammonia in an inert atmosphere.

Dissolution and removal of metallic sodium from the sodium-PuO_2 aerosol is presumed to leave only solids consisting of PuO_2 and any compounds formed by the reaction of sodium and PuO_2 in the aerosol. Although solutions of sodium in liquid ammonia are strong reductants, reaction of these solutions with the actinide solids was considered unlikely. This was because of the low solvating tendency (low coordinating power) of nitrogen donor ligands toward actinides, the relatively low dielectric constant of liquid ammonia, and the low temperatures involved.

The sealed filter housing containing the sodium-PuO_2 aerosol was attached to the filtering apparatus, and the complete system flushed with dry, oxygen-free helium. Liquid ammonia was condensed at -64°C, and flushed through the aerosol in batches, by the helium gas flow. After sodium removal was complete, the aerosol was dried by the helium gas flow, and the filter housing was removed to a low-humidity glove box. The aerosol solids on the filter were quickly added to deoxygenated 6 M perchloric acid; the acid was continually stirred during addition of the solids. The acid solution was capped and centrifuged, and the supernate removed for spectrophotometric analysis within a 10-min period.

Spectrophotometric analyses of the perchloric acid solution of the aerosols revealed the presence of Pu(III), Pu(IV) and Pu(VI) in the perchloric acid. Concentrations of both Pu(III) and Pu(VI) decreased with time, while that of Pu(IV) increased; eventually, Pu(III) completely disappeared. This behavior is consistent with the presence of substantial amounts of Pu(III) and Pu(VI) at the time the aerosol compounds were first dissolved; PuO_2 is not soluble in 6 M perchloric acid.

Although there was some variablity in the percentages of the Pu valence states observed in the first spectrum, the most reliable figures to date are: 27.6% Pu(III), 49.8% Pu(IV), and 22.7% Pu(VI). Therefore, in the aerosol phase, sodium and PuO_2 may react as follows:

$$Na + 3\ PuO_2 \rightarrow Pu_2O_3 + NaPuO_3. \qquad (1)$$

The Pu_2O_3 is expected to be readily soluble in perchloric acid as Pu(III); $NaPuO_3$ would also be readily soluble in perchloric acid but would rapidly undergo auto-oxidation-reduction to form equimolar Pu(IV) and Pu(VI). The Pu(VI) is then reduced to Pu(IV) by Pu(III) in an acid solution; the concentration of both Pu(III) and Pu(VI) decreased with time.

Using the spectral data, we obtained an average plutonium oxidation state of 4.18,

*Chemical Technology Department

which does not change with the reduction of Pu(VI) by Pu(III). The theoretical sodium-PuO_2 reaction, equation (1), requires the least amount of oxygen and yields an average plutonium oxidation state of 3.67. Any reaction of PuO_2 with Na in a totally inert atmosphere to produce a ternary oxide must yield an average oxidation state of less than 4.00. It is probable that the higher average oxidation state of 4.18, which we obtained, may have resulted from small amounts of residual oxygen in the purified argon or, more likely, from an excess of oxygen being removed from the PuO_2 surface by laser evaporation. The enriched oxygen content of laser-generated $(U,Pu)O_2$ aerosols (Annual Report, 1976) allows additional Pu(V) or even Pu(VI) compounds to be formed. The result would be a higher average plutonium oxidation state than that predicted by Equation (1).

Absorption spectra of solid (mull) samples of the sodium-PuO_2 aerosols have also been obtained. Exposure of these samples to ambient air resulted in a rapid loss of the dark color of the solids; conclusive spectra were not obtained. Color fading of mull samples prepared in a low-humidity glove box was less extensive. The spectra of these materials showed weak but distinct plutonium absorption peaks. Some of these spectral features match those of aqueous Pu(III) reasonably well, but other distinct peaks do not match known absorption spectra of aqueous solutions of any of the plutonium oxidation states. A marked change in environment around the Pu atom, such as a conversion from a ternary oxide to the aqueous species, would not alter the spectrum of Pu(III) markedly, but would change the spectra of the higher oxidation states. Therefore, it is probable that the unidentified peaks are those of either Pu(V) or Pu(VI).

Although the results from spectral analyses of the solid Na-PuO_2 aerosols or perchloric acid solutions of the aerosols are indirect, they generally support the reaction shown in Equation (1). The formation of these chemical species during the aerosol generation sequence (laser evaporation of PuO_2 followed by exposure to sodium vapor) is the explanation for the greatly enhanced solubility of the Na-PuO_2 aerosol in comparison with plutonium dioxide.

BIOLOGICAL BEHAVIOR OF LMFBR-FUEL-SODIUM AEROSOLS IN RODENTS

Investigators: P. L. Hackett, D. D. Mahlum, R. L. Music, and J. K. Briant

Technical Assistance: A. J. Clary, C. J. Powers, J. R. Rossignol, and J. P. Herring

We compared deposition and retention data for inhaled LMFBR-fuel-sodium aerosols of comparable sodium-fuel ratios but with different AMADs (2.4 and 3.2 μm). In rats, lung deposition of the 2.4-μm aerosol exceeded that of the larger-sized aerosol, with significant lung clearance within 5 days. Translocation of ^{239}Pu to the liver and skeleton was greater following inhalation of the 2.4-μm aerosol.

A significant reduction in the activity median aerodynamic diameter (AMAD) of mixed LMFBR-fuel-sodium aerosols has been achieved by refinements in our generation system (see accompanying article, this Annual Report). The availability of these smaller particles allowed us to compare their deposition, distribution, and retention following inhalation with data from previous rodent inhalation studies (Annual Report, 1978), which were performed with aerosols that had comparable sodium-fuel ratios but larger AMADs.

Female Wistar rats were exposed, nose-only, for 30 min (Exposure A) or 60 min (Exposure B) to aerosols with the properties shown in Table 1. The results from Exposure A are those from the previous experiment (Annual Report, 1978) and those from Exposure B are from the more recent experiment. In both experiments, groups of 6 to 12 rats were killed immediately after exposure, or at 1, 2, 5, or 7 days, and all tissues were analyzed for ^{239}Pu.

TABLE 1. Characteristics of LMFBR Fuel and Sodium-Fuel Aerosols.

Exposure	Sodium: Fuel	^{239}Pu Conc., nCi/ℓ	Na Conc., μg/ℓ	AMAD/GSD[a]
A	0:1	64	--	0.79/1.60
(30 min)[b]	39:1	99	127	3.21/1.30
B	0:1	210	--	0.66/1.50
(60 min)	40:1	40	154	2.40/1.41

(a) Activity Median Aerodynamic Diameter/Geometric Standard Deviation

(b) Exposure time shown in parentheses

In order to compensate for differences in exposure time and aerosol concentration among exposures, all radioanalytical values were standardized to a 60-min exposure with an aerosol concentration of 40 nCi/ℓ.

Deposition in the nasal bones and in the head (which excludes nasal bones, but includes the mouth and nasopharnyx) were highest following inhalation of a sodium-fuel aerosol with an AMAD of 2.4 μm (Figure 1). Lung deposition of the 2.4-μm sodium-fuel aerosol was markedly greater than that of the 3.2-μm aerosol and was equal to that of the fuel aerosols. Gastrointestinal deposition of both sodium-fuel aerosols was higher than that of the fuel aerosols. Parenthetically, it is of interest that initial deposition for fuel and sodium-fuel aerosols (Figure 1) were similar to patterns previously established for adult rats that inhaled ^{51}Cr-labeled microspheres of comparable AMADs (Annual Report, 1979).

Short-term lung retention values maintained the relationships established in the initial deposition. Some clearance was observed after 5 or 7 days; this was significant only in the sodium-fuel-exposed animals of Exposure B (Table 2).

Translocation of ^{239}Pu to the liver and skeleton during the first postexposure week was two to four times greater in animals exposed to the 2.4-μm sodium-fuel aerosol (B, Table 3) than to the 3.2-μm particle (A, Table 3). Since the corresponding lung deposition differed by a factor of 12, even greater differences in ^{239}Pu translocation were expected over an extended period of observation.

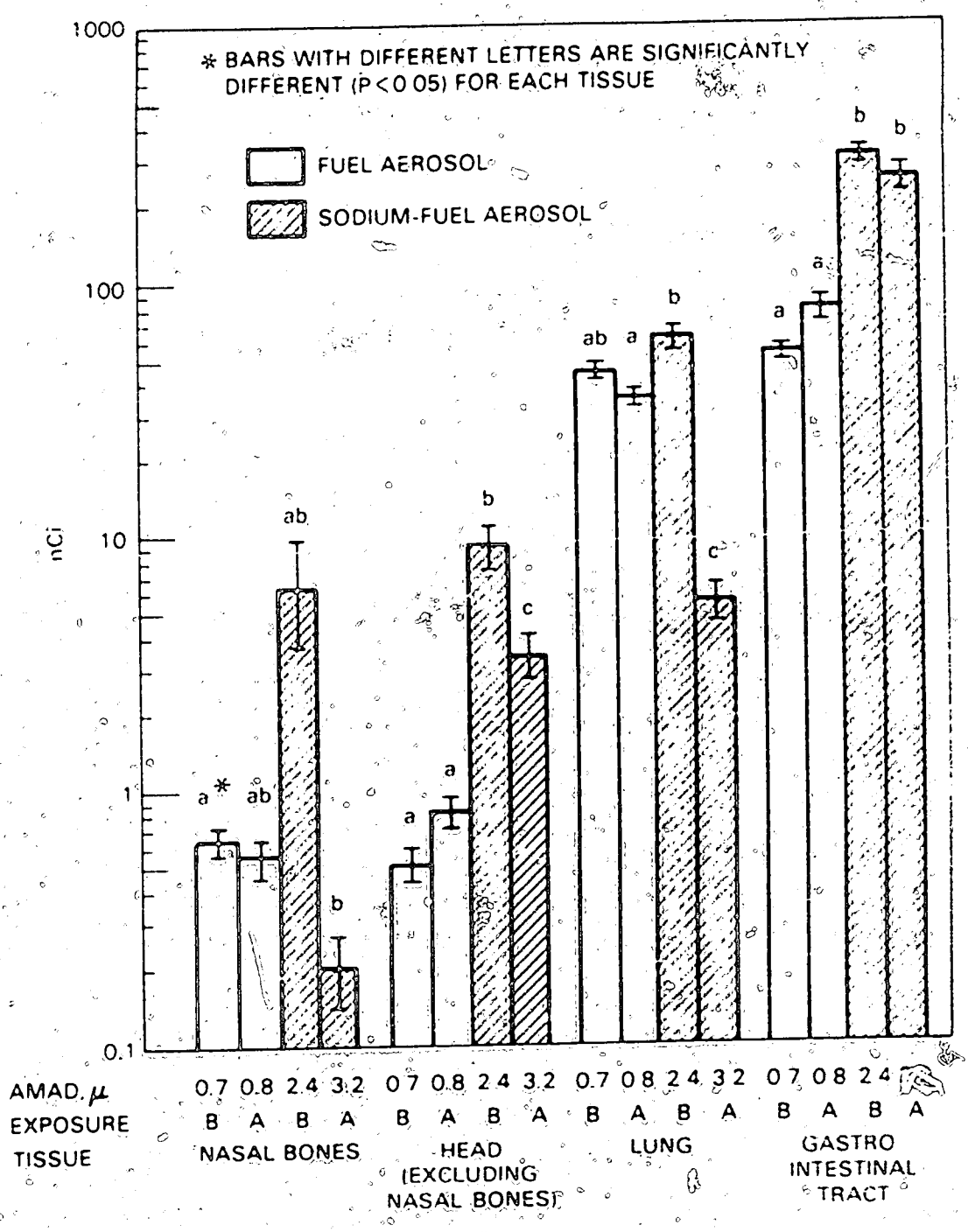

FIGURE 1. Deposition of LMFBR-Fuel and Sodium-Fuel Aerosols

TABLE 2. Lung Burden (nCi) of ^{239}Pu in Rats Following Exposure to Fuel or Sodium-Fuel Aerosols. (Mean ± SE)

Aerosol	Day of Sacrifice	Exposure A	Exposure B
Fuel	0	35 ± 2.4[b]	45 ± 2.5[a,b]
	1	37 ± 3.4[a,b]	47 ± 3.6[a,b]
	2	37 ± 1.6[b]	--
	5	--	38 ± 2.8[a,b]
	7	44 ± 3.5[a,b]	--
Sodium-Fuel	0	5.4 ± 0.9[c]	62 ± 7.6[a]
	1	5.2 ± 1.4[c]	57 ± 6.0[a]
	2	5.1 ± 1.3[c]	--
	5	--	29 ± 2.5[b]
	7	3.1 ± 0.5[c]	--

[a-c] Values with different letters are significantly different ($P < 0.05$)

TABLE 3. Liver and Skeletal ^{239}Pu Burdens (pCi) in Rats Following Exposure to Sodium-Fuel Aerosols (Mean ± SE).

Day of Sacrifice	Liver		Skeleton	
	Exp. A	Exp. B	Exp. A	Exp. B
0	48 ± 9[a]	104 ± 32[a,b]		214 ± 4[c]
1	71 ± 20[a,b]	193 ± 22[b]	637 ± 364[a,b,c]	537 ± 61[b]
2	93 ± 15[a,b]	--	592 ± 76[b]	--
5		483 ± 73[c]		1400 ± 145[c]
7	118 ± 14[b,c]		806 ± 159[a,b,c]	

[a-c] Values with different letters are significantly different ($P < 0.05$) for each tissue

BIOLOGICAL BEHAVIOR OF INHALED LMFBR-FUEL-SODIUM AEROSOLS IN BEAGLE DOGS

Investigators: P. L. Hackett, A. J. Clary, D. D. Mahlum, J. K. Briant, D. L. Catt, and L. R. Peters

Technical Assistance: R. L. Music, G. J. Powers, D. H. Akins, J. R. Rossignol, J. P. Herring, C. L. Baldwin, and T. C. Kinnas

Lungs of beagle dogs that inhaled LMFBR fuel-sodium aerosols (sodium-fuel ratios, 26 and 29; AMADs, 2.1 and 2.2μm) contained 20% of the initial body burden (IBB) on the first day after exposure. In contrast, that value for lungs of dogs exposed to fuel aerosols (AMAD, 0.8 μm) was 88% of the IBB. Percentages of the initial lung burden (ILB) appearing in the blood, liver and skeleton of animals that inhaled the sodium-fuel aerosol increased during early postexposure sampling periods and exceeded values of fuel-exposed dogs. Increases in liver and skeletal fractions of the ILB in fuel-exposed dogs observed 9 mo after exposure were accompanied by thoracic lymph node acquisition of ^{239}Pu. Values for thoracic lymph nodes of dogs that inhaled sodium-fuel aerosols were one-tenth those of fuel-exposed dogs at that time.

Many differences observed in particle deposition and partition following inhalation exposure of rodents to LMFBR-fuel or sodium-fuel aerosols have been attributed to differences in the particle size of the two aerosols. To further investigate this assumption, comparative studies of the biological behavior of inhaled fuel and sodium-fuel aerosols were initiated in the beagle dog, an animal with a much larger major-airway volume, cross-sectional area, and pulmonary vasculature.

Experimental details for the 30-min exposure of mature female beagles to fuel or sodium-fuel aerosols by the single-dog, nose-only technique, and preliminary results from a pilot study (Exposure A), were described in a previous Annual Report (1979). Aerosol characteristics are summarized in Table 1. Physical characteristics of the sodium-fuel aerosols of the later exposures, B and C, and the radioanalysis results from exposed animals differed from those of Exposure A. For this report, we have combined results from the 13 dogs in Exposures B and C (sodium-fuel aerosol) and compared them with results from the 17 dogs of the three fuel-aerosol exposures.

Percentages of inhaled ^{239}Pu activity (calculated from aerosol activity and respiratory measurements) deposited in the dogs during each exposure ranged from 31 to 45%, but did not differ significantly among exposures or between fuel and sodium-fuel aerosol exposures (Table 1). Lung burdens of animals that inhaled fuel aerosols comprised more than 80% of the IBB; ^{239}Pu activity diminished by only 16% over a period of 9 mo (Figure 1). By

TABLE 1. LMFBR Fuel and Sodium-Fuel Characteristics and Deposition in Beagle Dogs.

Aerosol	Exposure	Na:Fuel Ratio	Activity, nCi ^{239}Pu/ℓ	Sodium Conc., μg Na/ℓ	Inhaled Aerosol AMAD, μm	Inhaled Aerosol GSD	Deposited[a]
Na-Fuel	A	54:1	15 ± 2.6	79	2.8	1.5	39 ± 9
	B	29:1	18 ± 1.2	66	2.1	1.6	45 ± 3
	C	26:1	53 ± 7.0	170	2.2	1.5	39 ± 3
Fuel	A	0:1	22 ± 1.4	0	0.85	1.5	44 ± 3
	B	0:1	41 ± 5.5	0	0.75	1.5	40 ± 2
	C	0:1	77 ± 4.4	0	0.78	1.5	31 ± 3

(a) Initial body burden (excluding skin)/total inhaled activity × 100

comparison, the percentage of the IBB in lungs of sodium-fuel-exposed dogs was significantly lower, and decreased rapidly during the first 28 days after exposure. An appreciable fraction of the estimated ILB was present in the thoracic lymph nodes of the fuel-aerosol-exposed dogs at 270 days (Figure 2). At that time, a smaller percentage of the ILB was observed in the lymph nodes of the sodium-fuel-exposed animals.

A major portion of the activity deposited in the GI tract was excreted during the first week after exposure (Figure 3). Except for the fourth postexposure day, fecal fractions of the IBB of dogs inhaling sodium-fuel aerosols exceeded values for fuel-exposed animals at all time periods.

Immediately after the 30-min exposure, ^{239}Pu concentrations (expressed as percentage of IBB) in the blood of sodium-fuel-exposed dogs exceeded those of fuel-exposed dogs by a factor of 100 (Figure 4). Blood concentrations in sodium-fuel-exposed dogs reached an apparent maximum at 2 days postexposure, then declined until the second month after exposure. Blood values for the fuel-exposed group were constant for the first 2 days after exposure, then increased during the following 2 mo. After that, blood concentrations in the two experimental groups were not significantly different.

Percentages of the ILB appearing in skeletons and livers of sodium-fuel-exposed dogs increased during the first month after exposure and remained relatively constant until the 270-day sacrifice (Figure 5). Corresponding values for fuel-exposed animals remained at a lower level than values for the sodium-fuel-exposed group for the first month, but subsequently accumulated additional ^{239}Pu.

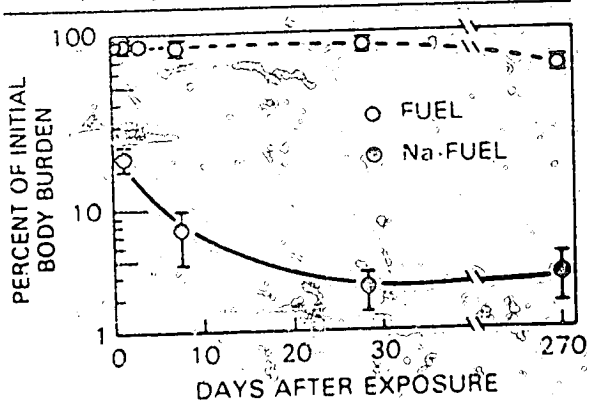

FIGURE 1. Lung Burdens of Dogs Inhaling LMFBR Fuel or Sodium-Fuel Aerosols.

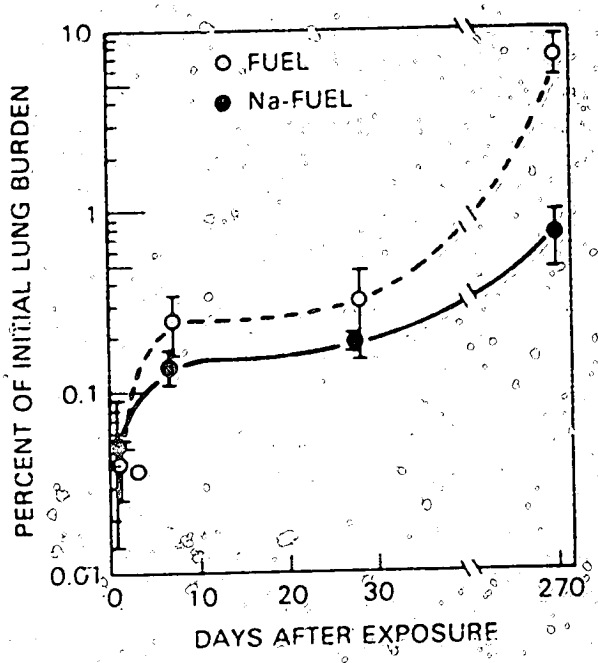

FIGURE 2. Thoracic Lymph Node Burdens Following Inhalation of LMFBR Fuel or Sodium-Fuel Aerosols.

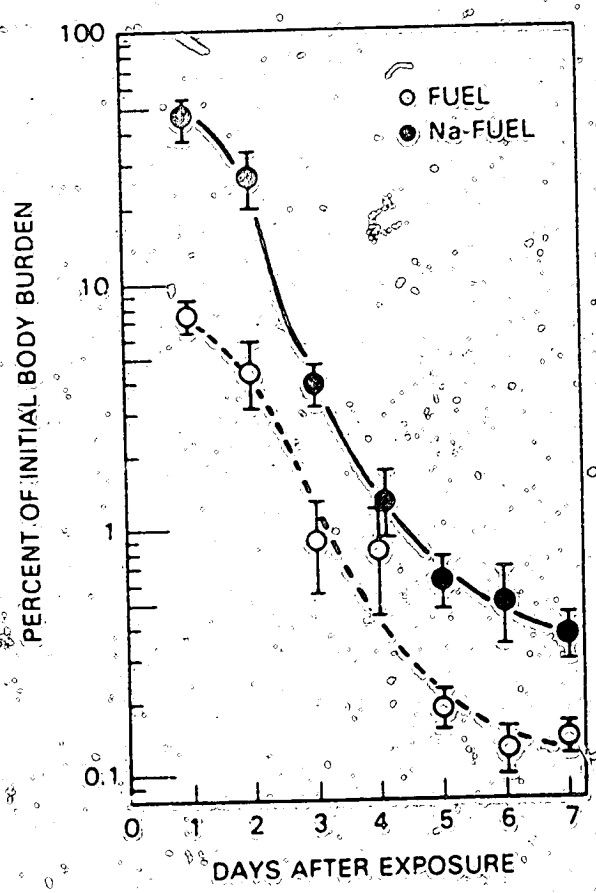

FIGURE 3. Daily Fecal Excretion of Inhaled LMFBR Fuel and Sodium-Fuel Aerosols.

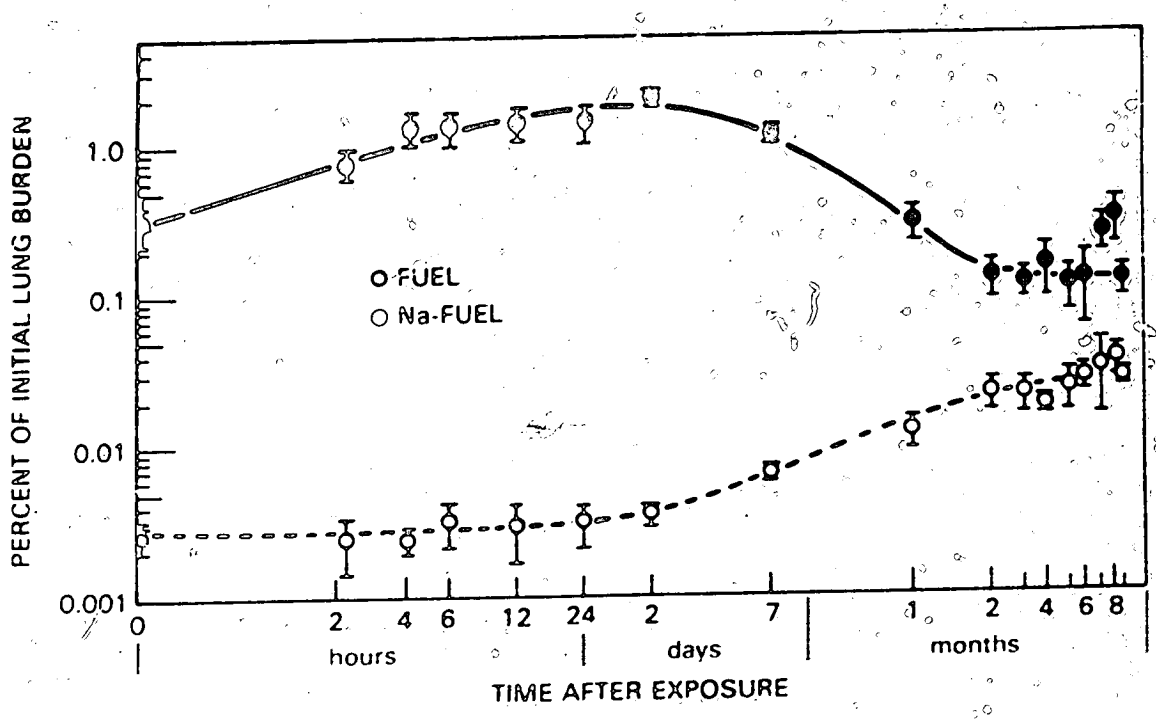

FIGURE 4. Plutonium-239 Concentrations in Blood Following Inhalation of LMFBR Fuel and Sodium-Fuel Aerosols.

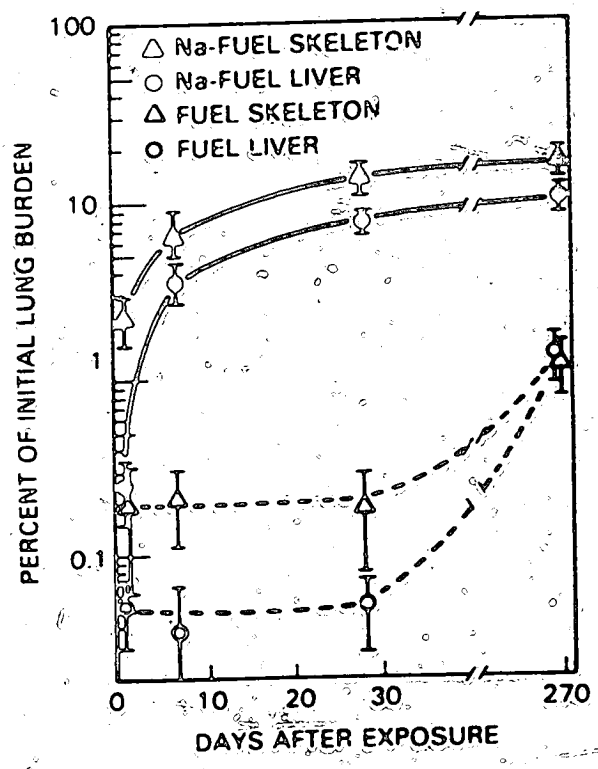

FIGURE 5. Skeletal and Hepatic ^{239}Pu Values Following Inhalation of LMFBR Fuel and Sodium-Fuel Aerosols.

GASTROINTESTINAL ABSORPTION OF SUSPENSIONS OF LMFBR-FUEL-SODIUM AEROSOLS IN RODENTS

Investigators: P. L. Hackett, R. L. Music, J. K. Briant, and D. D. Mahlum

Technical Assistance: J. P. Herring, J. O. Hess, B. L. Egbert, G. J. Powers, D. H. Akins, and J. R. Rosignol

Plutonium-239 distribution was studied in adult rats following gastric intubation of aqueous suspensions of LMFBR-fuel-sodium aerosols with sodium to fuel mass ratios of 0:1, 39:1 or 64:1. Gastrointestinal (GI) passage time for sodium-fuel aerosols tended to be shorter than that of the fuel aerosol. Initial estimates indicate that 0.006% of the dose of the 64:1 sodium-fuel aerosol was absorbed compared to 0.001% for the fuel aerosol suspension.

Significant fractions of inhaled LMFBR-fuel and sodium-fuel aerosols are deposited in the GI tract of rats and dogs (Annual Reports, 1977-1979). The sodium-fuel aerosols exhibit enhanced in vitro solubility (Annual Report, 1978), which would be expected to have a major influence on absorption and translocation of ^{239}Pu. We therefore initiated studies to determine the distribution of ^{239}Pu in the rat following gastric intubation of aqueous suspension of the aerosols.

Laser-generated fuel and sodium-fuel aerosols were collected on filters (Annual Report, 1976) and subsequently suspended in distilled water. Sodium-fuel ratios, particle sizes, and solubilities (Annual Report, 1978) were determined for the dry aerosols, and ^{239}Pu activities of the aqueous suspensions of the aerosols were measured (Table 1). Groups of 18 adult female rats were dosed by gavage with 1 ml of the fuel only (0:1), sodium-fuel (39:1), or sodium-fuel (64:1) suspension, and killed at 6, 24, or 48 hr after dosing. Animals were held in metabolism cages so that urine and feces could be collected.

At 6 hr after administration, gastric retention of ^{239}Pu in fuel-aerosol-dosed animals was 40% but was only about 25% in sodium-fuel-dosed rats (Figure 1). At that time, only 34% of the ^{239}Pu had reached the large intestine of the animals administered fuel aerosol, while 44 to 50% of the activity was in the large intestine of the rats dosed with sodium-fuel. Although these differences were not statistically significant, results suggest that GI passage may be more rapid for sodium-fuel aerosols than for fuel aerosol.

The fraction of the dose in carcass and

TABLE 1. Characteristics of Aerosols and Aqueous Suspensions for Gastric Intubation Studies.

Aerosol	Na/Fuel[a]	AMAD/GSD[b]	Solubility, %	Activity, μCi ^{239}Pu/ml
1 Fuel	0:1	0.7/1.5[c]	0.1	2.1
2 Sodium-Fuel	39:1	2.1/1.9	28	0.6
3 Sodium-Fuel	64:1	2.5/1.6	55	1.1

(a) Mass ratio
(b) Activity Median Aerodynamic Diameter/Geometric Standard Deviation
(c) Average value for fuel aerosols estimated from generator parameters

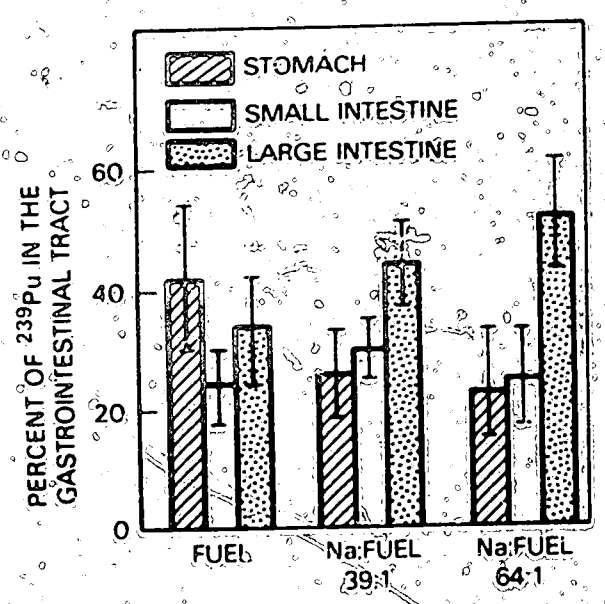

FIGURE 1. Partition of Gavaged Suspensions of Fuel and Sodium-Fuel Aerosols in Gastrointestinal Tract at 6 Hours After Dosing.

liver did not change significantly within treatment groups over the 48-hr period (Figure 2). The amount of ^{239}Pu in the carcasses of rats dosed with sodium-fuel suspensions tended to be higher than in those dosed with suspensions of the fuel. Liver burdens were significantly greater in rats intubated with sodium-fuel suspensions than in fuel-dosed animals. In fuel-aerosol-dosed rats, the liver contained 8% of the body burden (exclusive of skin and GI tract). Corresponding values for sodium-fuel-aerosol-dosed rats were higher: 13 and 22% for the 39:1 and 64:1 sodium-fuel ratios, respectively.

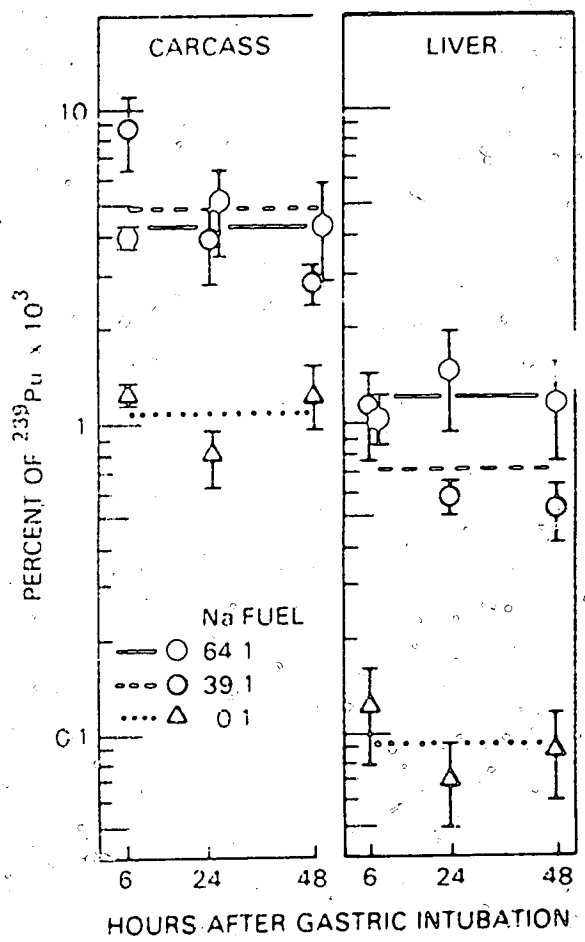

FIGURE 2. Amount of ^{239}Pu in Carcass and Liver Following Gastric Intubation of Suspensions of Fuel and Sodium-Fuel Aerosols.

Urinary excretion of ^{239}Pu was measured over the 48-hr observation period, but only the 6-hr values, obtained before the appearance of ^{239}Pu in the feces, were considered reliable. During this 6-hr time interval, ^{239}Pu urinary excretion tended to be higher in the sodium-fuel-dosed groups than in the fuel-aerosol group (Table 2).

TABLE 2. Urinary and Absorption Values for Rats 6 Hours After Gastric Intubation of Aqueous Suspensions of Fuel or Sodium-Fuel Aerosols.

Aerosol Na:Pu	Urine, % Dose × 10^3	Absorption, % Dose × 10^3
0:1	0.03 ± 0.007	1.4 ± 0.02
39:1	0.65 ± 0.32	10.3 ± 2.4
64:1	0.91 ± 0.26	5.9 ± 0.11

Summations of ^{239}Pu values for urine, carcass and liver were used to estimate ^{239}Pu absorption (or "transport") in the three treatment groups (Table 2). Percentages of the sodium-fuel aerosol dose absorbed were higher (P [illegible] for 64:1 and P [illegible] 0.1 for 39:1) than for the fuel aerosol group. The 6-hr plutonium "transport" value, 5 × 10^{-3} of the dose of 64:1 sodium-fuel aerosol (mass-ratio), is similar to the 1-day value of Brightwell and Carter (Health Phys. 28: 156-158, 1975), which was 1 × 10^{-2} for an 87:1 sodium-plutonium aerosol (atomic ratio). The proportion of the administered ^{239}Pu absorbed from the laser-generated fuel aerosol, which contains both plutonium and uranium, was 1 × 10^{-3}, in agreement with the ICRP value.

Additional GI absorption studies should be performed to confirm these results, since it is very difficult to obtain reliable sampling and analyses of such low levels of ^{239}Pu. Nevertheless, these initial results demonstrate enhanced GI absorption of ^{239}Pu from sodium-fuel aerosols.

○ Toxicology of Sodium and Lithium

This project will obtain data for establishing emergency standards for sodium and lithium release accidents involving heat transfer systems such as those designed for use in LMFBRs or, in the case of lithium, magnetic fusion reactors. It will utilize an existing aerosol generation and exposure system in exposing young adult and adult rats to different concentrations of sodium and lithium combustion products. The ID_{50} and LD_{50} will be determined for the predominant combustion products. Target organs, location of lesions and pathogenesis of lesions will be studied. Additional experiments will be designed on the basis of the data obtained from these studies.

TOXICOLOGY OF SODIUM METAL COMBUSTION AEROSOLS

Investigator: R. H. Busch, K. E. McDonald, and J. K. Briant

The respiratory tract of rodents, exposed to aerosols of sodium carbonate, exhibited respiratory distress, including dyspnea and wheezing. At higher doses, animals died during or shortly after 2-hr exposures. Lesions primarily involved the pharynx and larynx, and included accumulation of mucus, vesiculation, and edematous mucosa. Other lesions included edema and vesiculation of the anterior trachea, hemorrhage in the lungs and severe gastric tympany. Efforts were made to establish lethal concentrations (LC_{50}) for male and female rats, mice and guinea pigs. However, because of considerable variation in lethal effect among strains, sexes and species, no conclusions were possible.

Alkali metals, particularly sodium, are being studied and tested as heat transfer agent in energy-related programs such as the Fast Flux Test Facility (FFTF), an early prototypical test component of liquid metal fast breeder (LMFBR) reactor development. Solar heat collection systems might also use this metal.

Sodium, a highly active metal, combines with oxygen under a wide range of conditions to form four distinct compounds: monoxide, Na_2O; peroxide, Na_2O_2; superoxide, NaO_2; and ozonide, NaO_3. These combustion products are subject to further rapid chemical reactions with atmospheric O_2, CO_2 and H_2O, the reaction rates of which are dependent upon the partial pressures of these components. Given an unlimited supply of reactants, the reaction proceeds rapidly (within minutes) from the oxide forms to NaOH + H_2, then to Na_2CO_3.

Combustion products of sodium differ in alkalinity: oxides, peroxides and superoxides are the most alkaline; further combinants with CO_2 and H_2O are less alkaline. The acute toxicity of the various sodium compounds may be related to their caustic properties.

Determinations of toxic levels of sodium combustion products are needed for evaluation of hazards to which humans might be exposed in occupational situations. Furthermore, oxides, peroxides and superoxides might persist in the immediate vicinity of a reactor during critical phases of fire containment. Combustion product clouds might drift offsite and expose large populations to reaction products, which would eventually form Na_2CO_3.

We are continuing studies begun by Zwicker et al. (Annual Report, 1978), attempting to define more precisely the hazards accompanying exposure to Na_2CO_3 or to mixtures of Na_2CO_3, NaOH and sodium oxides.

To establish an LC_{50} for Na_2CO_3, we performed a series of whole-body exposures of rats, mice, and guinea pigs to varying concentrations of the aerosol. The animals were exposed in a chamber described in the previous report. Relative humidity, temperature and oxygen concentration were constantly monitored and controlled during each exposure. In addition, the following parameters were established for each exposure:

1) Average concentration in μg/ℓ
2) % Na_2CO_3
3) % NaOH
4) % $NaHCO_3$
5) Activity Median Aerodynamic Diameter/Geometric Standard Deviation (AMAD/GSD).

Adult male Wistar rats, Swiss-Webster mice and Hartley albino guinea pigs, obtained from commercial suppliers, were housed on arrival in clean plastic cages with sterilized corncob bedding, and given food and water ad libitum.

Exposures, each 2 hr in duration, consisted of 17 levels of concentration for rats, 11 for guinea pigs and eight for mice. Upon completion of each exposure, animals were removed from the chamber. Live animals were returned to their respective cages for observation. During the complete necropsy performed on each dead animal, the entire respiratory tree was removed and examined under a dissecting microscope; photographs were taken of all visible lesions. Tissues were then placed in 10% buffered formalin and subsequently processed for histopathologic examination.

In all dose ranges tested, live rats, examined immediately upon removal from the exposure chamber, exhibited signs of respiratory distress, including dyspnea and audible wheezing. Nearly all animals, both live and dead, had noticeably distended abdomens. Excessive salivation and repeated swallowing was noted during the first hour following exposure.

Animals which died during exposure were necropsied as soon as possible after removal from the chamber, usually within 15 minutes. Gross lesions, observed in all animals, varied in severity.

The posterior pharynx was covered with viscous mucus in nearly all animals examined. Severe edema of the pharynx, ventrolateral to the epiglottis, was consistently found, producing pillow-shaped bulges that partially closed the epiglottis and larynx (Figure 1). In most cases, the mucosa surrounding the laryngeal os was edematous and extensively vesiculated (Figure 2). Compared to controls, the larynx in most exposed animals appeared to be contracted. The lumen appeared diminished, not only by edema and vesiculation, but also by reduction of tubular diameter; this finding was interpreted as evidence of laryngospasm. In the few animals in which the trachea was involved, edema was restricted to the anteriormost 1 cm.

In most cases, lungs appeared normal. However, in approximately 3% of the dead animals the lungs exhibited widespread hemorrhage; in a few, the lungs appeared totally hemorrhagic.

Abdominal lesions were confined to the stomach which, in all cases, was severely tympanic. Estimates of gastric fluid pH varied from acidic to alkaline, suggesting that, in some rats, sufficient sodium carbonate was ingested to alter gastric pH.

Histologic examination of affected tissues was unremarkable in terms of further characterization of lesions, but confirmed the edematous and vesicular nature of mucosal lesions and congestive-hemorrhagic basis of lung changes.

Results obtained from exposures designed to determine LC_{50} varied, depending on sex and strain (rats) and among species. For example, in three trials using young adult male Wistar rats, the LC_{50} was approximately 2500 μg/ℓ of Na_2CO_3 aerosol over a 2-hr exposure period. Females of the same strain and age were simultaneously exposed with males. Mortality was too low among females to permit LC_{50} calculations.

In later exposures, young adult male Sprague-Dawley rats of approximately the same weight and age survived exposure to twice the LC_{50} for the Wistar strains, thereby preventing LC_{50} calculations. Exposure of the Sprague-Dawley strains to aerosols of 50% NAOH and 50% Na_2CO_3 also failed to produce mortality at sufficiently high levels for LC_{50} calculations.

Trials with guinea pigs and mice did not reveal differences due to sex; however, LC_{50} levels were lower than for Wistar rats. For Hartley-strain guinea pigs, LC_{50} was approximately 1900 μg/ℓ of Na_2CO_3; for Swiss-Webster mice, it was approximately 700 μg/ℓ.

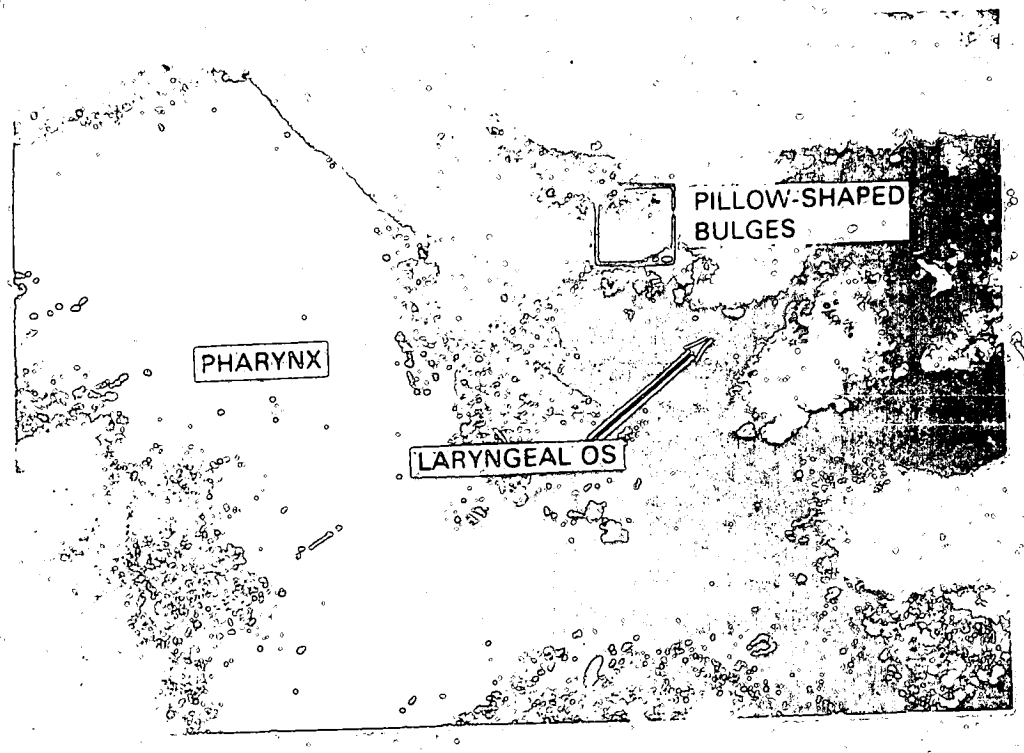

FIGURE 1. Area of Posterior Pharynx and Laryngeal Region Demonstrating the Severe Edema Producing the Pillow-Shaped Bulges Which are Partially Occluding the Larynx.

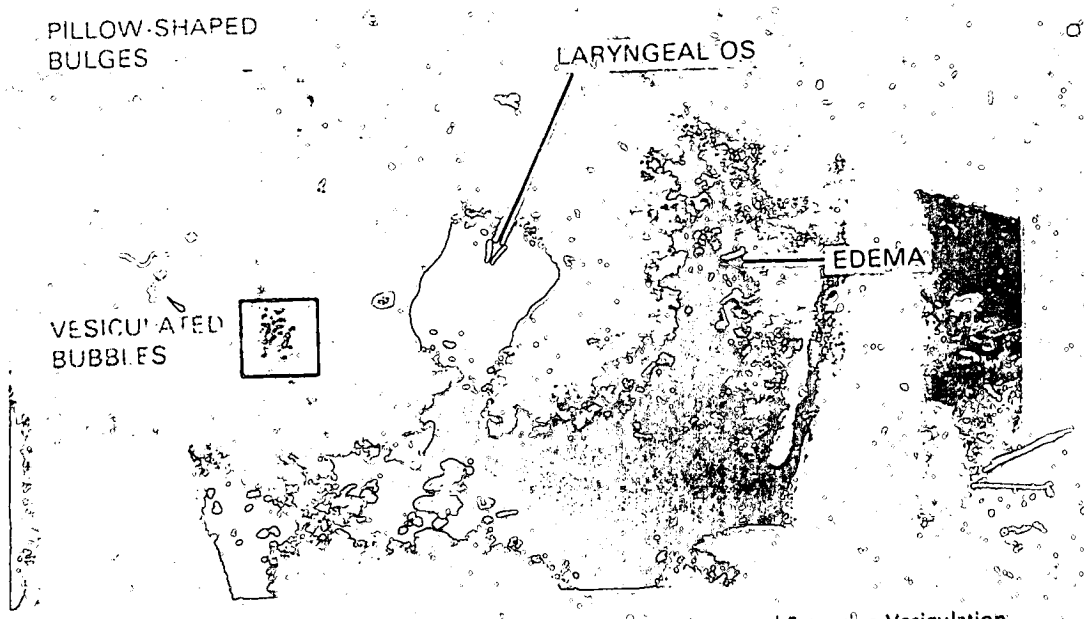

FIGURE 2. Mucosa Surrounding the Laryngeal Os Showing Edema and Extensive Vesiculation.

MONITORING AEROSOLS OF SODIUM METAL COMBUSTION

Investigator: J. K. Briant

A sodium metal fire produces an extremely dense aerosol of caustic oxides, hydroxides, and carbonates. We monitor such aerosols during inhalation exposure of animals by using an optical aerosol mass monitor for on-line, continuous measurement of the aerosol mass concentration. Gas concentrations in the exposure chamber were also monitored so that the chemical composition of the aerosol could be controlled. A model was developed to relate the various factors influencing chemical composition of aerosols in the exposure chamber.

The system for exposing small animals to an aerosol resulting from a simulated sodium metal fire was described by Allen and Zwicker in the Annual Report for 1978. Briefly, sodium metal was vaporized into argon and was subsequently burned by mixing it with air. This system allowed accurate control of the aerosol generation rate over a period of hours.

Aerosols with mass concentrations on the order of g/m^3 were sampled and measured gravimetrically after equilibrating with room air (typically at 21-23°C and 40-50% relative humidity). The aerosol was characterized aerodynamically with Mercer cascade impactors. The sodium deposited on each stage of the impactor was dissolved and measured with a flame photometer. For chemical characterization, impinger samples were titrated with dilute HCl. All samples were drawn from the Hinners exposure chamber at a level approximately 10 cm above the animals.

The high aerosol mass concentrations required for the animal exposures created sampling problems because they overloaded the sampling instruments in a very short period of time. To allow longer (and therefore more representative) sampling, an aerosol dilution probe, similar to that described by Cannon and Moss (Annual Report, 1978), was used for sampling. The 10:1 dilution of the aerosol allowed sampling times on the order of minutes for cascade impactors, and seconds for the electrostatic precipitator. In most cases, filter samples for gravimetric analysis, as well as impinger samples, could be run for minutes without dilution.

Environmental Systems Corporation Model P-5A optics and electronics package was used for on-line, continuous monitoring of the high aerosol mass concentrations in the exposure chamber. It is a nonextractive, single-ended system requiring little maintenance or alignment. The P-5A measures light (900 nm) backscattered by the aerosol from an optically defined volume of 12 cm^3. The sampling volume is external to the instrument (Figure 1), allowing a "view" of the aerosol through a window in the chamber. The window (1.6-mm-thick lucite) causes minimal attenuation of the light beam. Even at very high mass concentrations, the instrument's response during the course of an exposure was not significantly altered by aerosol deposition on the window.

The response of the P-5A to aerosol mass concentration was linear for a given aerosol chemical composition, however, any change in aerosol composition (and therefore in its optical properties) produced a change in the instrument's response. Figure 2 shows the relative response of the P-5A over a wide range of compositions for a given aerosol mass concentration. The peak response of the instrument occurred at or near the deliquescence point of the aerosol, decreasing rapidly below that point and more slowly above it. Our primary use of the P-5A was to detect any deviation from a constant aerosol mass concentration or chemical composition.

The chemical composition of the aerosol was controlled by monitoring the amount of CO_2 available to the aerosol for reaction. Chemical reactions primarily involved in the formation of the aerosol are:

$$4\,Na + O_2 \rightarrow 2\,Na_2O$$
$$2\,Na + H_2O \rightarrow Na_2O + H_2$$
$$Na_2O + H_2O \rightarrow 2\,NaOH$$
$$Na_2O + CO_2 \rightarrow Na_2CO_3$$
$$2\,NaOH + CO_2 \rightarrow Na_2CO_3 + H_2O.$$

Since a large excess of O_2 and H_2O is normally present in the dilution air, CO_2 is the only limiting factor in the conversion of the hydroxide to the carbonate. When the CO_2 in the aerosol chamber is

depleted part of the aerosol remains as the hydroxide. A 100% sodium hydroxide aerosol could be produced by removing all CO_2 from the dilution air with Ascarite. Thus, by adding or removing CO_2 from the dilution air, the chemical composition of the aerosol could be varied from 100% Na_2CO_3 and 0% NaOH, to 0% Na_2CO_3 and 100% NaOH.

To monitor gases which influence chemical composition in the aerosol chamber, a diffusion gas exchanger (Figure 3) was installed in the exposure chamber. This diffusion exchanger allows instruments to measure the gaseous components of the exposure chamber atmosphere without exposing their sensors to the aerosol. The Millipore Fluorogard filter cartridge, used as the diffusion barrier, was a hydrophobic (PTFE) rather than a hydrophilic filter medium. Hydrophilic filter media, such as those of glass fibers, were found to slow diffusion of H_2O to a rate unacceptably low for monitoring relative humidity in the exposure chamber. The instrument air system has a half-time of approximately 2 min for changes in CO_2 or H_2O concentration. The CO_2 measurements were made with a Miran-101 infrared CO_2 analyzer, and the H_2O measurements with a Humitemp relative humidity and temperature indicator.

We developed an exposure model which predicted the parameters required to expose animals to an aerosol of predetermined mass concentration and chemical composition. The mass concentration of the aerosol was set by the generation rate (controlled by varying the sodium metal temperature) and the total air flow through the system (typically, 300 ℓ/min). Although chemical composition is influenced by a number of variables, for the purposes of this model, we assumed that only those factors affecting the availability of CO_2 to the aerosol influenced chemical composition.

Two sources of CO_2 were considered: content of dilution air (CI; 320 ppm for unmodified room air), and air exhaled by the animals in the exposure chamber (15N ppm). In the aerosol particles, absorption and reaction with the NaOH (and possibly with the Na_2O, as described in the equations shown) is considered the CO_2 sink. These parameters were combined into a chemical composition parameter, $(CI + 15N)/X^2$, which could be related to the percentage of NaOH (and Na_2O) in the aerosol by the following equations:

$$(CI + 15N)/X^2 = 3.11 \times 10^{-4}\, e^{[-0.04(\%)]} \quad \text{for } >30\% \text{ NaOH}$$

$$= 2.06 \times 10^{-3}\, e^{[-0.91 \ln(\%)]} \quad \text{for } <30\% \text{ NaOH},$$

where

CI = CO_2 concentration in the dilution air (ppm)

N = number of rats in the exposure chamber

X = aerosol concentration (mg/m^3)

% = percent of aerosol present as NaOH.

A distinct break in the data (Figure 2) at 30% NaOH (70% Na_2CO_3) seems to correspond to the deliquescence point of the aerosol. A value of 15 ppm/rat in the chemical composition parameter was empirically determined for Wistar rats.

The model worked very well for a series of exposures of rats to a 50% NaOH and 50% Na_2CO_3 aerosol at various mass concentrations. The model predicted the CI required in dilution air, and in cases where CI was zero, it predicted the maximum number of rats (because of exhaled CO_2) that could be allowed in the exposure chamber. Factors other than those used in the model seemed to have no obvious effect on the chemical composition of the aerosol. For example, relative humidity and temperature might influence this system at some extremes; however, under typical exposure conditions (40-50%, 27-29°C), variations do not seem to significantly affect the chemical composition.

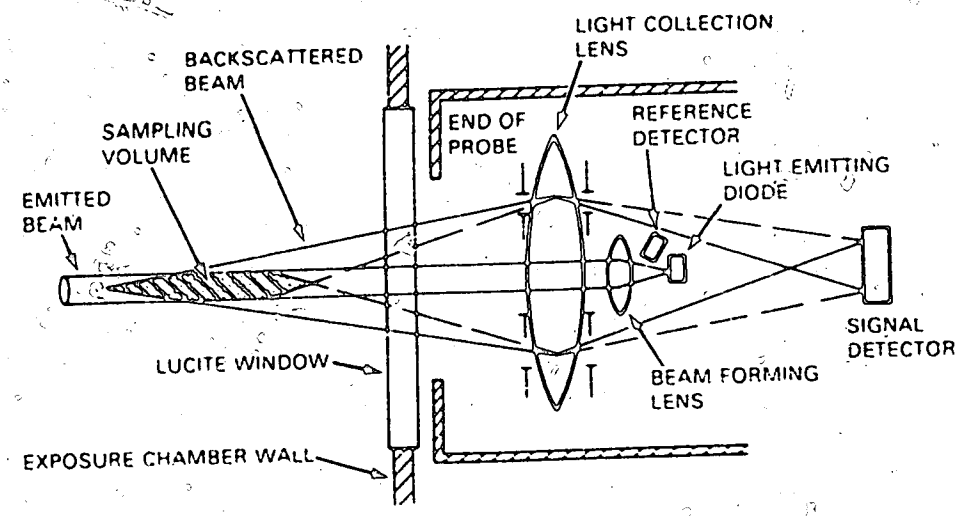

FIGURE 1. Instrument for Optically Monitoring Aerosol Mass Concentration in an Inhalation Exposure Chamber. Optically defined sampling volume of the P-5A is shown.

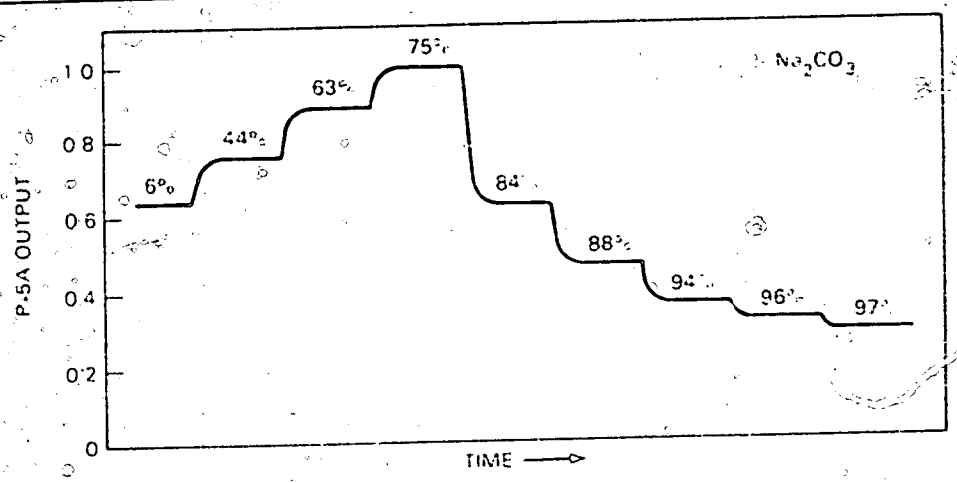

FIGURE 2. Relative Output of the P-5A Monitoring Instrument for Different Chemical Compositions of the Aerosol, Changed by Increasing CO_2 in the Dilution Air at Equal Intervals. NaOH is converted to Na_2CO_3 by the CO_2.

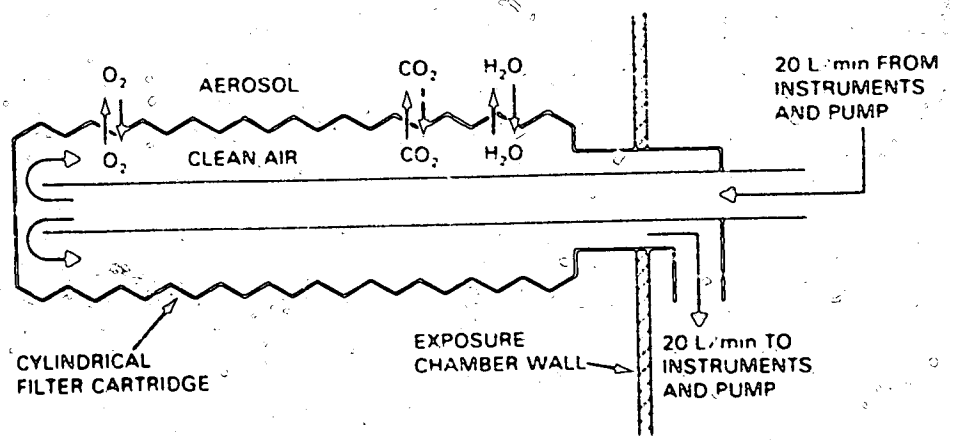

FIGURE 3. Diffusion Exchanger for Measuring Gases in an Inhalation Exposure Chamber by Means of an Instrument Air System.

Inhalation Hazards to Uranium Miners

This project determines the specific biological effects of exposure to known levels of uranium mine air contaminants, using both large and small experimental animals to model human respiratory disease. Lung cancer and deaths by degenerative lung disease were greatly enhanced among early uranium miners, but the cause-effect relationships for these diseases are based on inadequate epidemiological data. This project identifies agents or combinations of agents (both chemical and radiological), and their exposure levels, that produce respiratory tract lesions, including respiratory epithelial carcinoma, pneumoconiosis, and emphysema.

INFLUENCE OF RADON-DAUGHTER EXPOSURE RATE AND URANIUM ORE DUST CONCENTRATION ON OCCURRENCE OF LUNG TUMORS

Investigators: E. T. Cross, R. F. Palmer, R. H. Busch, and R. F. Buschbom

Technical Assistance: C. R. Petty, W. Skinner, J. C. Gaven, and M. J. Pipes

Groups of male specific-pathogen-free (SPF) Wistar rats were exposed to several levels of radon daughters plus uranium ore dust. Comparative data on survival, weight gain, clinical pathology, and histopathology reveal few differences significant at the 0.05 level. A nonsignificant trend toward increased lung tumor risk was observed with a decrease in radon-daughter exposure rate (maximizing @ 500 WL). No significant difference was observed in total lung tumor risk between 3 mg/m^3 and 15 mg/m^3 ore-dust concentrations. Lung tumor risk significantly increased as cumulative exposure to radon daughters increased. Survival time significantly decreased at the lowest radon daughter exposure rate. Four variants of epithelial tumors primary to the lung have been identified.

The epidemiology of human radon-daughter exposure suggests that lung cancer is produced more efficiently when radiation is delivered at a relatively lower exposure rate. A more efficient production of tumors at lower exposure rates has also been observed in laboratory animals irradiated with other high-LET particles. Corroboration of this type of exposure-response relationship in animals exposed to radon daughters would have definite implications for the establishment of exposure limits in the uranium mining industry.

It has long been suspected that other confounding factors (such as associated atmospheric pollutants) could alter the shape of the dose-response curves. If it can be demonstrated, for example, that the concentration of uranium ore dust alters the risk of death from lung cancer, then mining exposure standards should be based on the total environment, rather than on radon-daughter level alone.

This study of the roles of radon-daughter exposure rate and uranium ore dust concentration in the production and progression of lung lesions was initiated in 1977. Because of bacterial infection (Klebsiella and Corynebacterium kutscheri), some of the animals (including controls) died early in the experiment. Clinical pathological studies conducted in connection with these early deaths (about 1 yr after exposure) showed no significant differences (P = 0.05) between exposed and control animals in either chemical or hematological parameters.

The histopathologic data given in this report include all but six animals whose tissues were unsuitable for analysis. Because definitive classification of tumor types is still under study, the reported data may be revised.

Groups of 32 and 48 male SPF Wistar rats were exposed to several levels of radon daughters and uranium ore dust for 30 hr/wk according to the protocols shown in Tables 1 and 2. The radon-daughter exposure levels were chosen to simulate more closely those received by uranium miners in the U.S. epidemiological study

TABLE 1. Protocol for Study of Radon-Daughter Exposure Rate Versus Total Exposure in Rats.

Exposure Regimen	Cumulative Exposure, WLM
1000 WL Radon Daughters 15 mg/m³ Uranium Ore Dust	640, 2560
500 WL Radon Daughters 15 mg/m³ Uranium Ore Dust	640, 2560
250 WL Radon Daughters 15 mg/m³ Uranium Ore Dust	640
Controls	Background

TABLE 2. Protocol of Uranium Ore-Dust Exposures in Rats.

Exposure Regimen	Cumulative Exposure WLM
1000 WL Radon Daughters 15 mg/m³ Uranium Ore Dust	320, 640, 2560
1000 WL Radon Daughters 3 mg/m³ Uranium Ore Dust	320, 640, 2560
Controls	Background

than were the levels of our previous animal studies. However, the exposure rates were reasonably high to compensate for the shorter life span of the rat, and were varied by a factor of about four for detection of potential exposure-rate-dependent effects. Ore-dust concentrations were chosen to maintain low fractions of unattached radon daughters (thus minimizing differences in radon-daughter lung deposition sites), yet allow a five-fold range in concentration to determine the pathogenic role of the dust itself.

Exposure levels obtained during the experiments are shown in Table 3. From measurements of previous experiments (verified by spotchecks in the present experiments), the mass median aerodynamic diameter of the uranium ore dust was on the order of 1.0 μm, with a geometric standard deviation of about 2.0; average activity median aerodynamic diameters did not exceed 0.60 μm, with a geometric standard deviation of about 2.0. The unattachment of RaA averaged <3% for all dust concentrations; percentages of unattached RaB and RaC were only fractions of RaA levels.

None of the exposure treatments caused weight gains or losses significantly

TABLE 3. Exposures of Male SPF Wistar Rats to Radon Daughters and Uranium Ore Dust.

Group Number	No. of Animals	Exposure Rate, WL ± SD	Cumulative Exposure, WLM ± SD	Ore Dust Concentration, mg/m³ ± SD	Condensation Nuclei Conc., 10^3/cm³ ± SD
1100	48	882 ± 114	640 ± 85	15.0 ± 1.4	175 ± 24
1200	48	791 ± 245	644 ± 203	3.0 ± 0.8	39 ± 22
1300	32	490 ± 37	642 ± 48	15.0 ± 3.5	172 ± 19
1400	32	279 ± 114	644 ± 263	15.2 ± 3.9	188 ± 41
1500	32	Controls			
2100	48	994 ± 67	317 ± 21	17.6 ± 2.1	236 ± 26
2200	48	951 ± 107	322 ± 35	3.2 ± 0.5	29 ± 9
3100	32	962 ± 88	2550 ± 230	15.6 ± 1.8	248 ± 28
3200	32	971 ± 154	2570 ± 410	3.5 ± 0.7	36 ± 12
3300	32	498 ± 45	2580 ± 230	17.1 ± 2.7	238 ± 31
3500	32	Controls			

different (P = 0.05) from mean control values. Except for rats in the 1400 Group, which died earlier, mortality patterns did not differ significantly from those of controls (Table 4). There is no obvious explanation for the decreased survival time of Group 1400, other than a possible influence of exposure rate, which was lower in this group than in any other group.

Histopathologic data are shown in Table 5. Seventy-six rats have developed thoracic tumors; 72 are of lung epithelial origin, and four are of pleural mesothelial origin. The epithelial tumors are presently under study for definitive classification as to cell of origin; thus far, four variants have been identified: peripherally located benign tumors of clara cell or Type II alveolar cell origin, peripherally located malignant tumors of clara cell or Type II alveolar cell origin, adenomatoid tumors, and tumors with epidermoid characteristics.

TABLE 4. Mean Survival Time of SPF Wistar Rats Exposed to Radon Daughters and Uranium Ore Dust.

Group Number	Survival Time, mo		Remarks
1100	19.75	1.34[a]	Exposed
1200	19.98	1.26	Exposed
1300	21.45	1.49	Exposed
1400	17.59	1.44	Exposed
1500	20.19	1.53	Control
2100	20.60	1.2[illegible]	Exposed
2200	20.59	1.26	Exposed
3100	20.28	1.45	Exposed
3200	19.32	1.61	Exposed
3300	20.16	1.02	Exposed
3500	19.41	1.55	Control

(a) Standard error of the mean

TABLE 5. Summary of Primary Epithelial Tumors of the Lung[a]

Group Number	No. of Tumors in Group[b]	Animals with Lung Tumors					
		Adenoma[c]	Bronchioloalveolar Carcinoma[c]	Adenocarcinoma	Adenocarcinoma With Squamous Differentiation	Squamous Carcinoma	Total[b]
1100	6	1	2	1	1	0	5
1200	8	2	2	2	1	0	7
1300	8	3	1	2	2	0	8
1400	9	1	1	2	1	1	5
1500	0	0	0	0	0	0	0
2100	7	3	3	1	0	0	6
2200	8	5	0	1	0	1	7
3100	18	3	2	4	2	0	10
3200	14	2	1	4	1	2	9
3300	20	5	2	8	2	0	15
3500	0	0	0	0	0	0	0

(a) Not included in the table are four mesotheliomas, one each in Groups 1300, 2100, 3200 and 3300
(b) Some animals had multiple and/or mixed tumors
(c) Tumors of clara cell or Type II alveolar cell origin

HISTOPATHOLOGIC AND PHYSIOLOGIC INVESTIGATION OF LUNGS OF DOGS EXPOSED TO URANIUM ORE DUST

Investigators: F. T. Cross, R. E. Filipy, S. M. Loscutoff, R. F. Palmer, and R. H. Busch

Technical Assistance: C. R. Petty, P. Pottmeyer, and W. Skinner

Histopathologic and pulmonary function evaluations were conducted on dogs exposed to carnotite uranium ore dust. Significant changes in pulmonary function included an increased slope of the single-breath N_2 washout curve (suggesting an uneven distribution of ventilation) in dogs exposed for 10 and 27 mo. At 40 mo of exposure these changes had not progressed and were no longer different from controls, suggesting a "catch-up" in the control animals by normal aging processes. Pulmonary lesions observed were vesicular emphysema, peribronchiolitis and focal pneumoconiosis.

Pulmonary function evaluations were performed on dogs exposed to approximately 15 mg/m^3 carnotite uranium ore dust for 4 hr/day, 5 day/wk and age-matched cage controls. The first series of tests (reported in the 1979 Annual Report)* were conducted on dogs exposed for 10 and 27 mo. Dogs exposed for 10 mo were subsequently sacrificed after 1 yr of exposure and the lungs fixed for histopathologic evaluation. Dogs initially tested following 27 mo exposure were retested after 40 mo exposure. Lung function measurements included: arterial blood gases, all divisions of lung volumes, dynamic and quasistatic pulmonary compliance, pulmonary resistance, and single-breath N_2 washout following a vital capacity inflation with 100% O_2.

The most consistent functional change measured in these animals was an increased slope of the alveolar N_2 plateau (M3), recorded during the N_2 washout maneuver in exposed compared with control animals. As reported in the 1979 Annual Report, values of M3 were increased in dogs exposed for 10 mo and 27 mo, compared with controls. This increased slope indicates an uneven distribution of ventilation within the lung. However, following this initial change, there appeared to be no measurable progression of the response. Eventually, normal aging processes in controls led to similar N_2 washout patterns in exposed and control animals. Significant differences in pulmonary function (determined by the unpaired t-test) after 27 and 40 mo exposure are shown in Table 1.

*Erratum: The age of the animals and their exposure duration, which were wrongly reported in the 1979 Annual Report, should be increased by 2 mo.

The most notable types of pulmonary lesions present in the lungs of dogs exposed to uranium ore dust for approximately 1, 2 and 3 yr are: vesicular emphysema, peribronchiolitis and focal pneumoconiosis. The relative severity of these changes is shown in Table 2.

In dogs exposed for approximately 1 yr, macrophages containing ore-dust particles were visible microscopically as individual cells in alveoli and as accummulations of cells adjacent to small blood vessels and small bronchioles. Characteristically, the accumulations were located at the junction of respiratory bronchioles with alveolar ducts (Figure 1). These foci frequently included varying numbers of lymphocytes and, in dogs with exposure histories longer than 1 yr, a fibrous component. The term, focal pneumoconiosis, is used for the change described above (Figure 2): the foci appear to be a step in the progression toward development of the more severe pneumoconiotic changes generally associated with inhalation of silicotic dusts.

In the more severely affected dogs, the lymphocytic component of this focal pneumoconiosis had surrounded bronchioles to produce a "cuffing" effect, referred to in Table 2 as peribronchiolitis. Severity of this condition closely paralleled that of the focal pneumoconiosis. In the most severely affected dog (#1462), alveolar epithelial metaplasia was present adjacent to the inflamed bronchioles. The cells, which are normally squamous, had become slightly cuboidal in shape and were associated with alveolar septal fibrosis. Both of these changes (alveolar epithelial metaplasia and septal fibrosis) were present only to a very slight degree in

TABLE 1. Significant Pulmonary Function Differences in Dogs Exposed to Uranium Ore Dust.

		Slope Alveolar N_2 Plateau (M3).[a] % N_2/ℓ		Slope of Phase IV (M4).[b] % N_2/ℓ		Dynamic Pulmonary Compliance[c] ml/cm H_2O	
		27 mo	40 mo	27 mo	40 mo	27 mo	40 mo
Control	X	0.61	0.78	4.34	4.68	122	103
	SE	0.04	0.05	0.63	0.42	11	12
	N	9	9	9	9	9	9
Exposed	X	0.86	0.88	5.73	4.12	120	96
	SE	0.05	0.06	0.35	0.25	7	6
	N	16	14	16	14	16	14

(a) 27 mo controls significantly different from 27 mo exposed ($P = 0.004$ by the unpaired t-test)
27 mo controls significantly different from 40 mo controls ($P = 0.015$)
Combined controls (27 and 40 mo) significantly different from combined exposed (27 and 40 mo) ($P = 0.004$)
(b) 27 mo exposed significantly different from 40 mo exposed ($P = 0.001$)
(c) 27 mo exposed significantly different from 40 mo exposed ($P = 0.02$)

TABLE 2. Degree of Severity of Three Pulmonary Changes Resulting From Chronic Inhalation Exposure of Dogs to Uranium Ore Dust (Based on Microscopic Examination).

Dog Number	Exposure Time, mo	Emphysema	Focal Pneumoconiosis	Peribronchiolitis
1670	12	0	[illegible]	1
1675	12	1	2	1
1679	12	1	1	0
1467	20	1	2	0
1462	26	1	1	2-3
1469	26	2	2-3	1
1468	37	2	2-3	1
1493	37	2	2-3	1
1499	37	2	2-3	1

Code
1 = Barely Perceptable
2 = Readily Apparent
3 = Obvious Change

the other dogs, even after 3 yr exposure to uranium ore dust.

Pulmonary vesicular emphysema, characterized by disruptions of alveolar septa, was present in all but one of the exposed dogs. This disease exhibited a dose response in that it was present only to a very slight degree in dogs exposed for less than 2 yr. Dogs exposed for longer than 2 yr were more severely affected.

Pulmonary hyalinosis was also seen in these dogs. These lesions are characterized by small dense accumulations of hyaline-like material with smooth surfaces located within alveoli, both free and within macrophages. They are considered to be a result of cellular degradation (Dagle et. al., Vet. Pathol. 13: 138, 1976); differential staining revealed a calcium, lipid and mucopolysaccharide content. Hyalinosis was present in nearly all of the dogs in a previous study when they were exposed for more than 2 yr to uranium ore dust with radon daughters (with or without cigarette smoke). Seven of the nine dogs in the present study (exposed to uranium ore dust only) had pulmonary hyalinosis, which ranged in degree of severity from a few hyaline bodies scattered throughout a lung lobe to large clusters of the bodies with an associated granulomatous response, including Langhans' giant cells and fibrous encapsulation. Pulmonary hyalinosis may be specific to dogs; it has not been seen in the lungs of rats or hamsters after inhalation of uranium ore dust, nor has it been reported in humans.

Lesions of the major airways and upper respiratory tract, if present, were minimal in severity. Only two kinds of changes were seen in this region: goblet cell hyperplasia and dilatation of mucous glands in the larger bronchi and in the trachea. Although visible, both changes were very slight and were observed primarily in the dogs with 2 and 3 yr exposure histories. Another change consistently observed was a diffuse inflammatory reaction in the submucosa of the nasal turbinates. This was present to a very slight degree in eight of nine dogs examined. It was probably a result of the constant irritation of those surfaces by the relatively high concentrations of ore dust in the inhaled air.

These studies are being conducted primarily to determine the pathogenic role of uranium ore dust alone, without the complications of associated toxicants. They are a necessary adjunct to previous studies on the biological effects of exposure to mixtures of uranium ore dust with radon, radon daughters, diesel engine exhaust fumes and cigarette smoke.

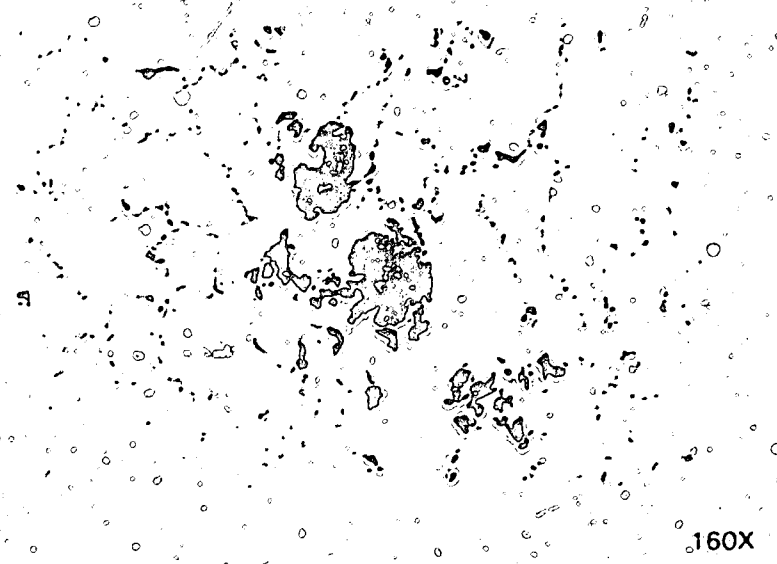

FIGURE 1. Macrophages Containing Uranium Ore Dust Accumulated Distal to Pulmonary Airways in a Dog Following 12-mo Exposure.

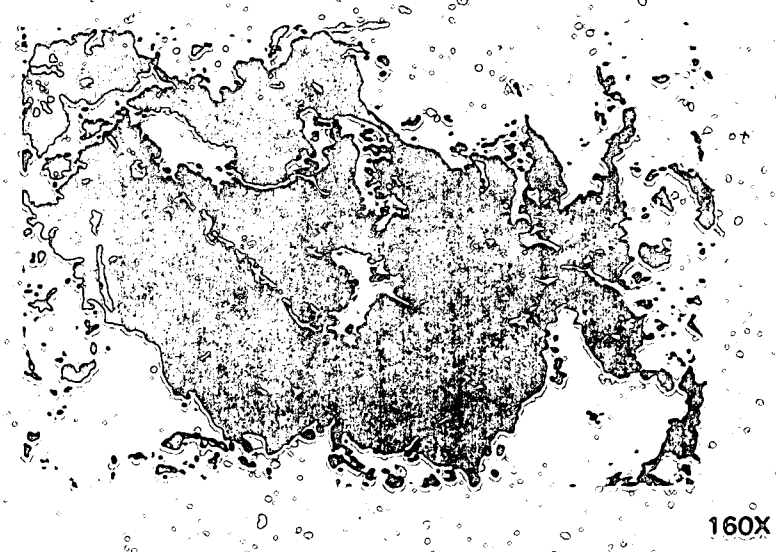

FIGURE 2. Focal Pneumoconiosis Following 37-mo Exposure to Uranium Ore Dust.

o Toxicology of Krypton-85

The purpose of this project is to obtain biological data to supplement earlier evaluations of the hazards of ^{85}Kr exposure. The studies include both short-term and chronic exposures of rats, dogs and sheep to determine tissue distribution and retention kinetics for metabolic modeling purposes. Dose-effect studies in rats exposed chronically for their life span are included to identify tissues at risk and determine tumorigenic potency. The project is scheduled for completion in FY 1981.

EFFECTS OF CHRONIC ^{85}Kr EXPOSURE IN RATS

Investigators: D. H. Willard, H. D. Tolley, and J. E. Ballou

Technical Assistance: A. W. Endres

Continuous ^{85}Kr exposures were terminated after 808 days. The few surviving animals are being held for life-span study.

Male and female Wistar rats were exposed in groups of 100 (50 males and 50 females) at concentrations of 100, 1,000 or 10,000 times the MPCa (unrestricted) of 3×10^{-7} μCi ^{85}Kr/ml. A group of controls were sham-exposed to room air, under otherwise identical conditions. Exposures were initiated at 126 days of age and were continued for 808 days. The radiation dose to the skin surface for each group was 38, 370 or 2750 rad/yr, respectively, as measured by thermoluminescent dosimeters. The dose to lung was estimated to be about 1% of the skin-surface dose. Preliminary findings and experimental details were published in the Annual Report for 1979.

When ^{85}Kr exposures were terminated, survivors (about 10% of the original number) were transferred to standard animal quarters for life-span observation. These animals are weighed at monthly intervals, and necropsied and radiographed at the time of death, following the same procedure employed during the exposure period. The study is still in progress and histopathologic examination of tissues is not complete. This report presents an update of our gross observations of ^{85}Kr toxicity.

The pattern of weight gain, peaking at about 650 days of age and declining thereafter, was quite similar for both sexes, and for both ^{85}Kr-treated and control animals (Figure 1). The fluctuations in the weight curves result from animal deaths which cause abrupt changes in weight averages.

Survival of male rats (Figure 2) was not significantly influenced by ^{85}Kr exposure ($P = 0.26$), although there was a trend suggesting lifeshortening in the ^{85}Kr-exposed groups (control mean survival time was 649 days, vs. 638, 618 and 591 days, respectively, for the ^{85}Kr-exposed groups). Female rat survival was similarly unaffected ($P = 0.23$), except for an apparent anomaly in the group exposed to 1000 times MPCa, in which survival was significantly shortened ($P = 0.004$). Analysis of the combined mortality results for both sexes showed no significant effect of ^{85}Kr exposure on animal survival ($P = 0.2$). Surviving rats will be included in the analysis when they die.

Rats exposed to the highest level of ^{85}Kr, and control rats, were screened at 6-mo intervals for evidence of radiation-induced leukemia. Peripheral-blood samples, obtained by tail vein puncture, were examined for total white count (TWC). The TWCs exceeding 14,000 cells/mm^3 were examined by differential counting for specific cell types. No evidence of early leukemia was seen, although studies in guinea pigs have suggested a correlation between ^{85}Kr exposure and this disease. A more-definitive evaluation of leukemia incidence will be obtained when the histopathologic examination of tissues from all animals in this study is completed. Completion of this project is scheduled for fiscal year 1981.

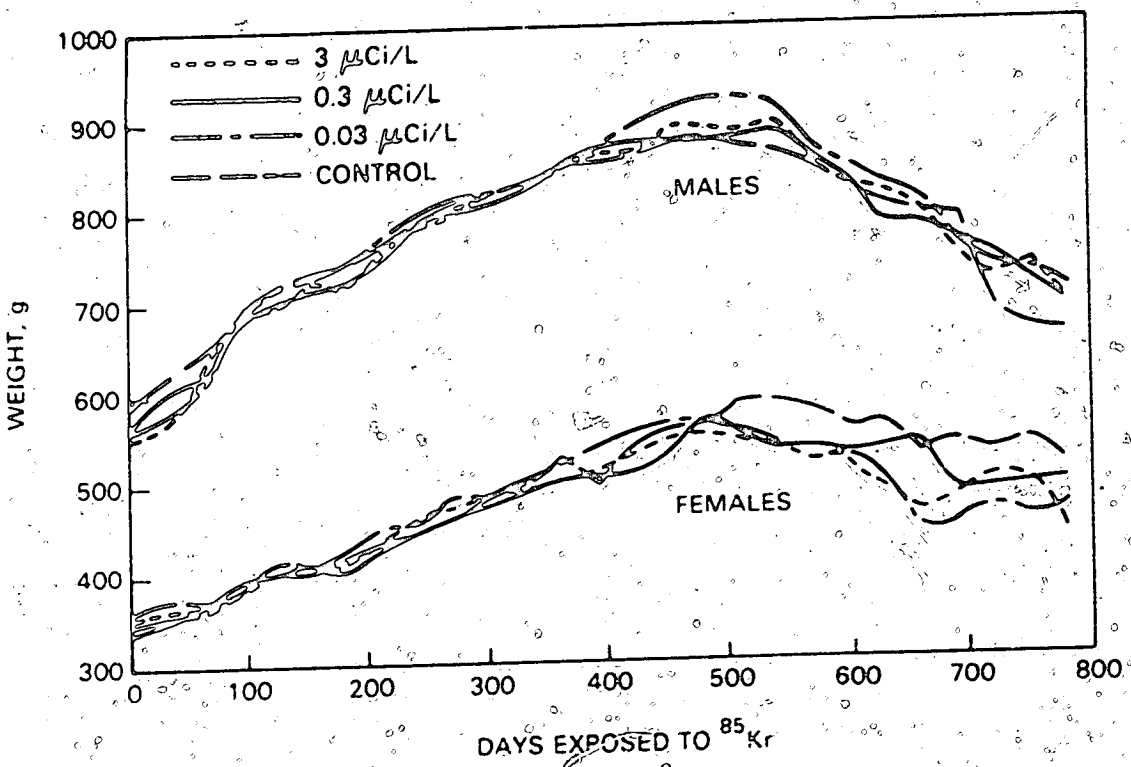

FIGURE 1. Weight Gain of Rats Exposed Chronically to ^{85}Kr.

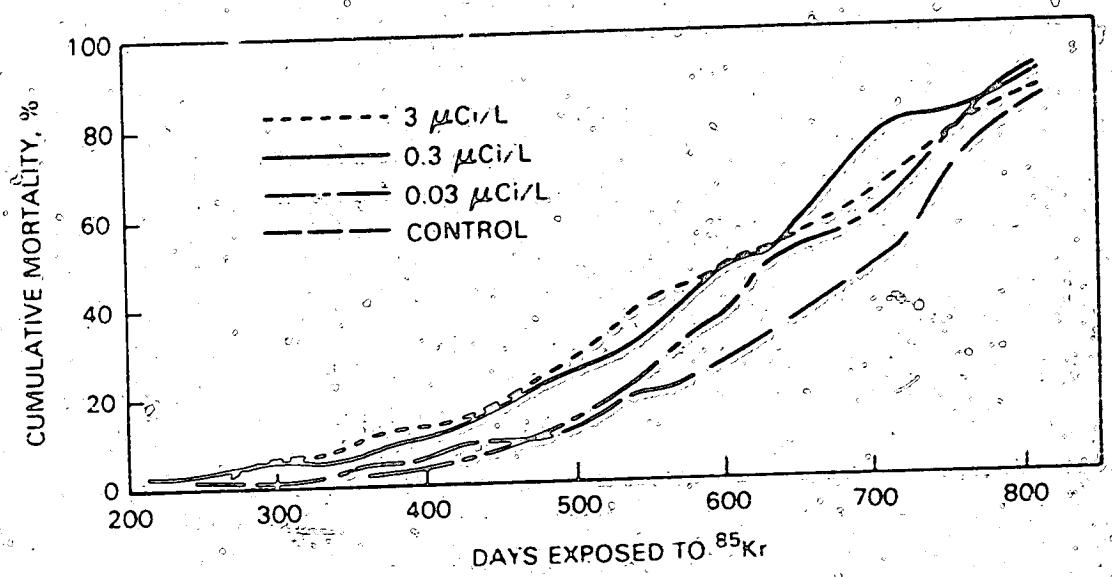

FIGURE 2. Cumulative Mortality of Rats Exposed Chronically to ^{85}Kr Atmospheres.

EFFECTS IN NEWBORN RATS EXPOSED TO ^{85}Kr ATMOSPHERES

Investigators: J. E. Ballou and H. S. DeFord

Technical Assistance: A. W. Endres

Newborn rats exposed to ^{85}Kr atmospheres showed dose-related effects on weight gain, mortality, and incidence of skin lesions over a dose range of 850 to 4700 rad to the skin surface.

Male and female Wistar rats were exposed as newborns (<48 hr after birth) to ^{85}Kr atmospheres to determine the late effects of this mode of radiation. The early effects (e.g., stunted growth, abnormal development of the extremities, impaired hair growth, and radiation dermatitis) were reported in the Annual Report for 1979, along with details of the experimental procedures. This report summarizes current results from this study, which has been in progress for approximately 600 days.

Infant rats were exposed at three skin-surface dose levels (850, 2300, or 4700 rad) accumulated during a 6-hr period. A control group was sham-exposed to room air for the same period of time. Animals were weighed at monthly intervals. Dead rats were necropsied; and tissues were taken for histopathological examination.

The effect of ^{85}Kr exposure on weight gain is shown in Figure 1. The maximum weight deficit was seen in rats exposed to

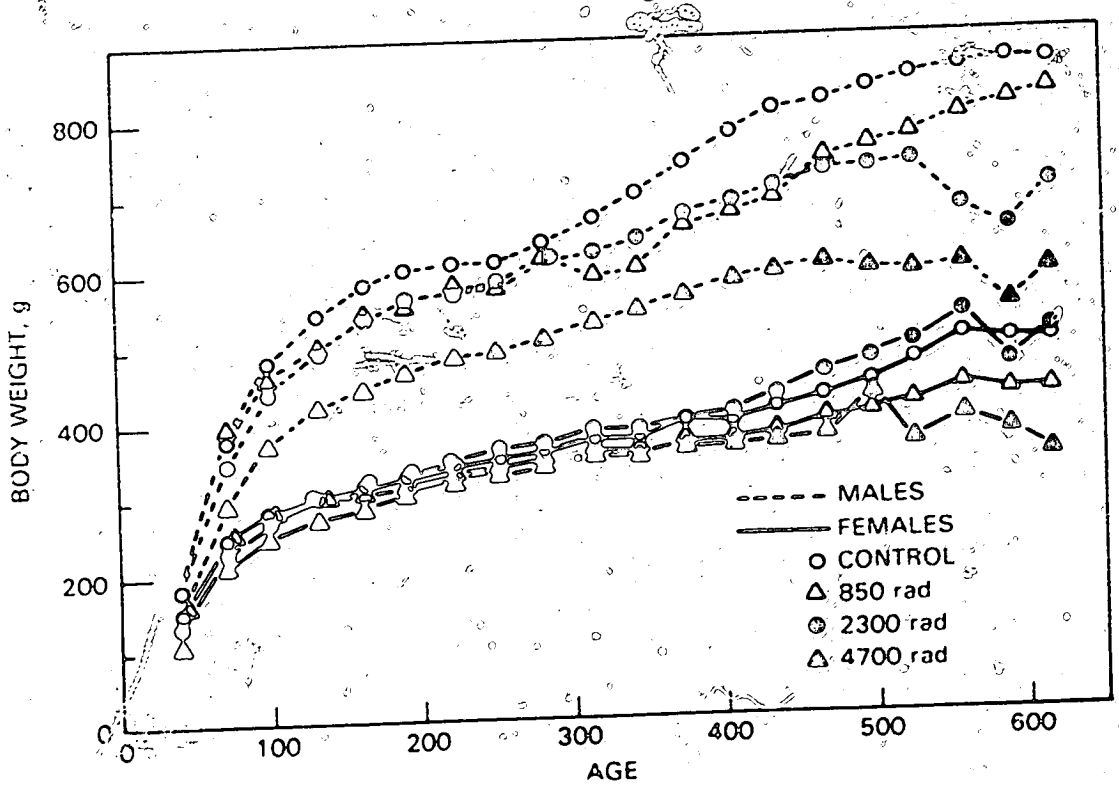

FIGURE 1. Average Weight of Rats Exposed to ^{85}Kr as Newborns.

4700 rad; it appeared earlier and was more severe in males. After 600 days, relative weight deficits were about equal in males and females. It is not known if these changes are due solely to ^{85}Kr radiation or if they are somehow influenced by physiological factors, such as sex-related differences in the rate of growth. Andrew et al. (Annual Report, 1979) reported similar effects on the growth of rats following prenatal exposure to ^{239}Pu.

The life-shortening effect of ^{85}Kr exposure is summarized in Table 1. Mortality at 600 days was significantly increased by ^{85}Kr exposure, and appears to be dose-related. Cause of death was not determined.

Nearly all animals developed some type of skin lesion by the time of death. The lesions in ^{85}Kr-exposed rats were distinctive in that they tended to be ulcerative, or formed heavy keratinous or wart-like growths of a type not usually seen in the control animals. The lesions appeared earliest in the group receiving 4700 rad, i.e., after 7-8 mo, and continued to grow at variable rates until the time of death. The histopathologic examination of sections from these lesions, which is now in progress, will complete this study.

TABLE 1. Gross Effects of ^{85}Kr Exposure of Newborn Rats.

Skin Surface Dose, rad	Number of Rats	Status After 600 Days	
		% Mortality	% Skin Lesions[a]
850	9	33	44
2300	10	50	50
4700	10	80	100
Control	10	10	20

[a] Lesions were visually observed at necropsy to involve the skin as opposed to subcutaneous lesions. Microscopic examination and classification of lesions is not complete.

○ Toxicity of Thorium Cycle Nuclides

The purpose of this project is to investigate the biological hazards associated with uranium-thorium breeder fuels and fuel recycle process solutions. Initial studies will emphasize the metabolism and long-term biological effects of inhaled ^{233}U-^{232}U nitrate and oxide fuel materials and ^{231}Pa, a major long-lived radioactive waste product.

ANALYSIS OF ^{231}Pa IN BIOLOGICAL SAMPLES

Investigators: R. A. Gies, J. E. Ballou, and J. L. Ryan

Technical Assistance: A. W. Endres

We are developing a scintillation/extraction method for the analysis of ^{231}Pa in biological samples. The method employs Aliquat-336 to extract ^{231}Pa from 9 M HCl solutions.

A method is needed for the analysis of biological samples containing ^{231}Pa (an alpha emitter) in the presence of its alpha-emitting daughter products. A search of the literature revealed no suitable method. However, Pol'shin et al. (Analytical Chemistry of Protactinium, 1970) described the separation of ^{231}Pa from its daughters by extraction; and Gerontopulos (Radiochim. Acta 4:224-225, 1965) reported a combined scintillator/extractant solution. We are modifying these procedures for use with biological samples.

The scintillation/extractant solution consists of 5% tricaprylmethylammonium chloride (Aliquat-336, General Mills, Inc.) with 22.7 g terphenyl and 2.3 g POPOP added to 3800 ml of toluene. Five ml of the scintillator/extractant was added to 10 ml of an HCl solution of the sample for counting.

Tissue samples were prepared by adding a known amount of ^{231}Pa, ashing at ~500°C in a muffle furnace, and dissolving the ash in HCl + HF. The ^{231}Pa was added before ashing to assure the validity of comparing test sample results with the results from routinely ashed laboratory samples. Hydrofluoric acid was added along with HCl to promote dissolution of the ashed ^{231}Pa. An excess of Al^{+3} was added to destroy the ^{231}Pa-fluoride complex before column separation or scintillation counting, since this compound is not bound to anion exchange resins or extracted into Aliquat-336.

Hydrochloric acid solutions of ^{231}Pa, which contained no tissue digest, were extracted quantitatively with Aliquat-336, providing the molarity of the HCl was about 5 (Figure 1). Hydrochloric acid solutions of tissue digests (lungs, liver, pelt, residual carcass) containing ^{231}Pa

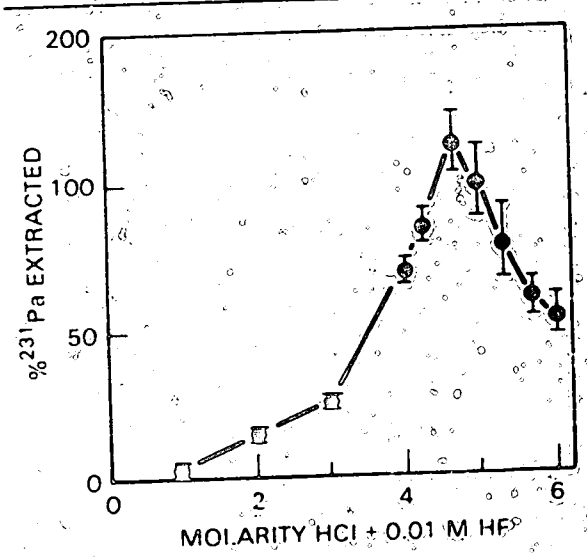

FIGURE 1. Effect of HCl Concentration on Extractability of ^{231}Pa in Aliquat-336. Values are the average of 3 determinations with standard deviation.

gave low recovery values. We suspected that the interference might be due to iron quenching, or might be related to the amount of dissolved salts in the tissue

digest. Samples were passed through an anion exchange column (Bio-Rad AG1-X4, 50-100 mesh) to remove iron, and the effect of salt concentration on counting efficiency was determined in a separate study.

The anion exchange column was prepared with 9 M HCl, and the tissue digest was loaded (10 ml in 9 M HCl + 0.01 M HF + 2 ml saturated $AlCl_3$ in 4 M HCl). The results (Table 1) show nearly complete recovery of the added ^{231}Pa, except in the case of the carcass. The poor recovery with carcass is possibly due to the relatively large amount of salts in the tissue digest. Anion exchange treatment of the samples before counting markedly improved the counting efficiency; however, the fraction of the total activity actually loaded on the column (24 to 78%, from Table 1) was somewhat less than anticipated.

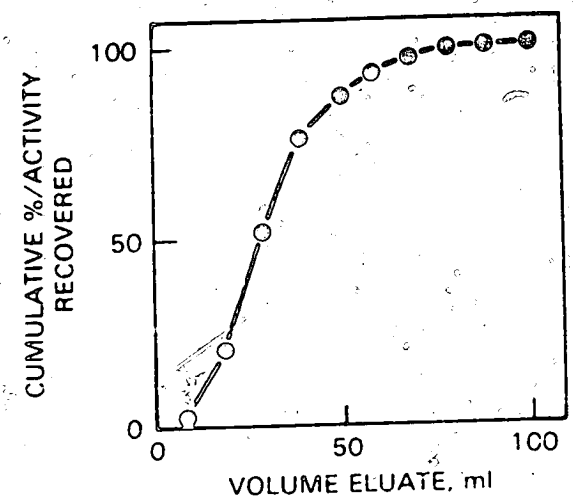

FIGURE 2. Elution of ^{231}Pa From AG1-X4 Anion Exchange Resin Using 9 M HCl + 0.01 M HF (sample added as rat carcass digest, ~70 mg salts/sample).

TABLE 1. Recovery of ^{231}Pa in Rat Tissue Digests Following Separation on Anion Exchange Resin (AG1-4X). Values are the average of 4 or 5 determinations ± standard deviation.

Tissue	Salt Concentration, mg/ml	Percent ^{231}Pa Recovered		
		^{231}Pa Eluate	Rinse	Total
Lung	37 ± 6	78 ± 3	19 ± 5	97 ± 6
Liver	47 ± 11	55 ± 5	46 ± 5	101 ± 7
Pelt	77 ± 8	77 ± 11	18 ± 12	95 ± 16
Carcass	230 ± 10	24 ± 1	47 ± 13	71 ± 13

TABLE 2. Effect of Salt Concentration on Recovery of ^{231}Pa in Rat Carcass. Samples were diluted with 9 M HCl + 0.01 M HF to obtain desired concentration.

% Original Salt Concentration	mg Salts/ml in 10 ml Sample	% of ^{231}Pa Recovered
100	230	24 ± 1
90	207	25 ± 1
80	184	28 ± 2
70	161	36 ± 1
60	138	34 ± 4
50	115	47 ± 10
40	92	74 ± 6
30	69	80 ± 4
20	46	86 ± 5
10	23	95 ± 15

The effect of salt concentration on the analysis of ^{231}Pa in rat carcass is shown in Table 2. The kinetics of column elution are shown in Figure 2. The recovery of ^{231}Pa was clearly influenced by the concentration of salts in the test solution (Table 2). In other studies, similar concentrations of $CaCO_3$ or NaCl did not affect the scintillator/extractant process, so we assume the salt concentration in some manner affects the column separation. It is not known at this time if the effect is related to salt concentration *per se*, or if the critical factor is the total salt load. Studies are now in progress to investigate further modifications of the anion exchange procedure in an attempt to obtain quantitative recovery of ^{231}Pa.

DISPOSITION AND LATE EFFECTS OF INHALED $^{232}UO_2(NO_3)_2$ AND $^{233}UO_2(NO_3)_2$ IN RATS

Investigators: J. E. Ballou, R. A. Gies, G. E. Dagle, H. D. Tolley, and A. C. Case

Technical Assistance: A. W. Endres

Lung tumors were the major treatment-related malignant lesion of rats exposed to $^{232}UO_2(NO_3)_2$ or $^{233}UO_2(NO_3)_2$ by inhalation. Bone tumors were not a significant finding, although the skeleton was the main reservoir of translocated uranium.

Male Wistar rats were given a single, nose-only, 30-min exposure to $^{232}UO_2(NO_3)_2$ or $^{233}UO_2(NO_3)_2$ aerosols to determine the distribution and biological effects of inhaled uranyl nitrate. This study has been the subject of previous reports (Annual Reports, 1976 to 1979). Recent progress is summarized in this report.

Analyses of rat skeletons for ^{232}U content have been completed for the highest dose group exposed to ^{232}U (53 nCi, initial lung burden, ILB). These data are compared in Figure 1 with similar results for the high-level ^{233}U group (36 nCi ILB). The single exponential curves which best fit the data suggest a 4000-day half-life for ^{232}U retention in skeleton, and a 400-day half-life for ^{233}U. Differences between the two uranium isotopes were highly significant ($P = 0.005$). Differences in skeletal retention of ^{232}U and ^{233}U may be related to the differing mass amounts of uranium deposited in the two cases. Although approximately equal microcurie amounts of the two isotopes were initially translocated to bone, there was about a 2000-fold difference in mass due to the greater specific activity of ^{232}U. The greater mass of ^{233}U may have influenced the site of deposition in bone (for example, enhanced deposition in bone marrow rather than in the bone matrix). Analytical results did not distinguish between marrow and hard bone. Autoradiography may provide additional information on the microscopic distribution of the two isotopes, but the alpha-emitting daughter products of ^{232}U are expected to be a complicating factor.

Osteosarcoma induction (Table 1), was not noticeably influenced by the different rates of uranium retention. This is not unexpected, since the low cumulative radiation dose to skeleton for both isotopes (35 rad with ^{232}U, compared to 12 rad in 500 days with ^{233}U) is in the range of questionable carcinogenic effect.

A detailed listing of the malignant tumors found in these animals is shown in Table 1. Osteosarcomas of the skeleton were found only in rats exposed to uranyl nitrate aerosols. In other studies (Annual Report, 1976) we have observed bone tumors in treated control rats exposed to the 0.27N HNO_3 carrier aerosol. For this reason, the few bone tumors in the present study are of doubtful significance.

Malignant tumors of the lung and pleura appear to be directly related to uranium inhalation despite two lung tumors in the nontreated control group. One of these, an osteosarcoma of the lung, had extensively metastasized to other tissues in the pleural cavity. There was no radiographic evidence of bone involvement to suggest that this tumor originated in the skeleton, therefore it was considered to be primary to the lung. A variety of other malignant tumors were found, without apparent relationship to treatment or dose level.

Table 2 lists the benign tumors observed. Pulmonary adenomas and pulmonary adenomatosis (interpreted as a preneoplastic lesion) were observed mainly in rats exposed to the two higher dose levels of ^{232}U and ^{233}U. These lesions were most prevalent in the groups with the highest incidence of malignant lung tumors. The major benign lesions (lipomas and fibromas) were more uniformly distributed throughout both control and experimental groups.

The malignant tumor incidence in bone and lung is further evaluated in Table 3. The incidence of lung tumors is reasonably well correlated with initial lung deposition and with estimated cumulative radiation dose to lung for both ^{232}U- and

^{233}U-exposed rats. The lung tumorigenicity of these high-specific-activity uranium isotopes is in reasonable agreement with that reported for other actinide nitrates studied in our laboratory (Annual Report, 1979). The bone tumor incidence in uranium-exposed rats is less clearly associated with radiation dose for the reasons discussed earlier in this report.

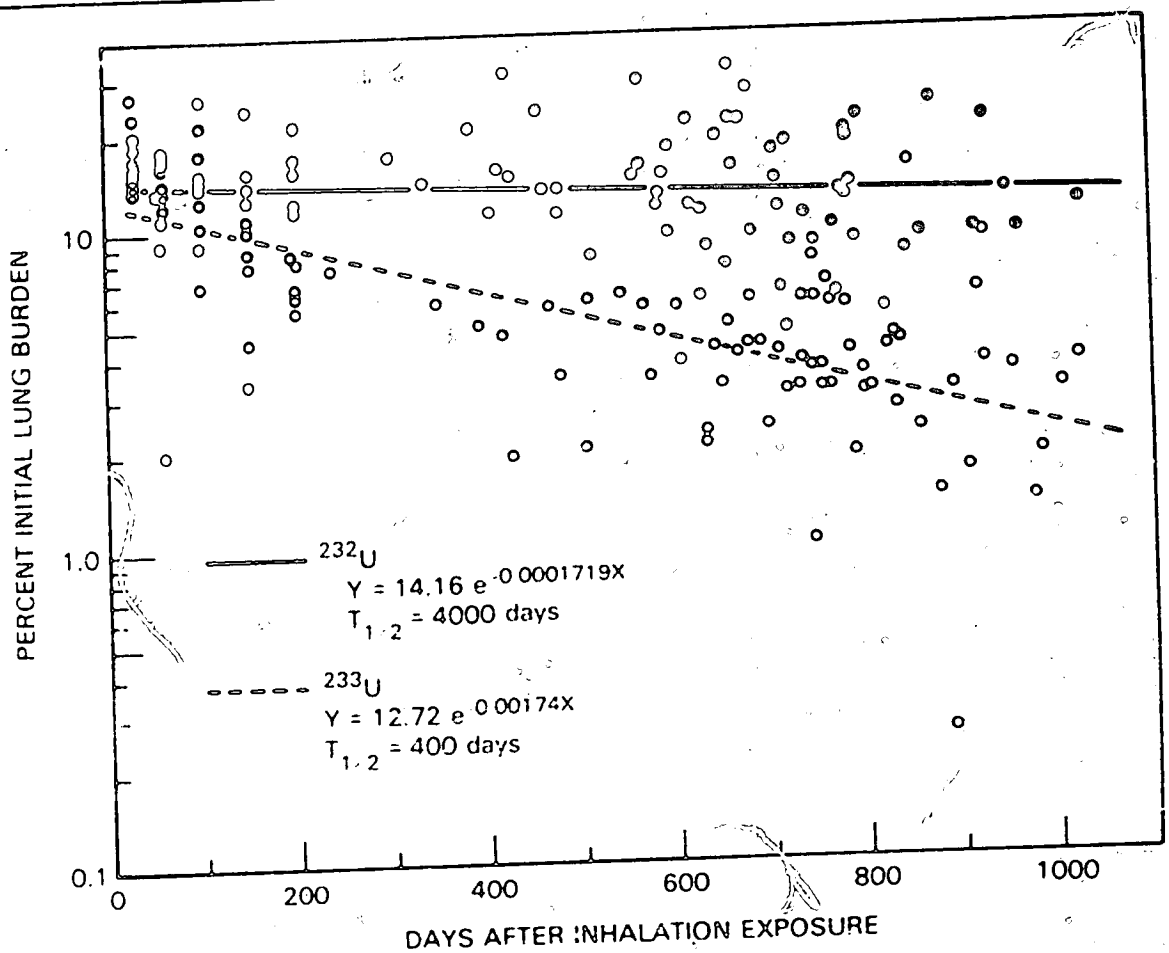

FIGURE 1. Retention of ^{232}U and ^{233}U in Skeleton After Inhalation of $UO_2(NO_3)_2$ Aerosols.

TABLE 1. Malignant Tumors in Rats Exposed to $^{232}UO_2(NO_3)_2$ or $^{233}UO_2(NO_3)_2$ Aerosols.

	Control		^{232}U ILB, nCi			^{233}U ILB, nCi		
	Nontreated	Treated[a]	0.74	5.85	53	0.63	10	36
Osteosarcoma - Skeleton				1	2		1	1
Pulmonary Adenocarcinoma				4	27	1	1	9
Pulmonary Small Cell Carcinoma				1				
Pulmonary Adenosquamous Carcinoma				1	7			
Lung Squamous Cell Carcinoma	1				4			4
Lung Fibrosarcoma			1					
Lung Osteosarcoma	1							
Malignant Mesothelioma-Pleura, Lung				1	2		3	1
Hepatoma				1	2		2	1
Hepatoblastoma								1
Kidney Carcinoma		1	1		1			1
Nephroblastoma					1			
Adrenal Cortical Carcinoma			1		1	1		
Adrenal Neuroblastoma				1				
Malignant Pheochromocytoma							2	2
Pancreatic Islet Cell Carcinoma							1	
Thyroid Adenocarcinoma		1		1			1	
Thymoma								1
Mammary Adenocarcinoma						1	1	
Salivary Gland Mixed Tumor								1
Brain Astrocytoma			1			1		
Leukemia			4	1			4	4
Myelosarcoma		1						
Leiomyosarcoma						1		
Squamous Cell Carcinoma - Skin					1			1
Sebaceous Adenocarcinoma		1						
Liposarcoma		1		1		1	1	
Fibrosarcoma	3	4	4	3	6	1	4	3
Hemangiosarcoma		1		1				
Squamous Cell Sarcoma		1	2					
Malignant Fibrous Histiocytoma	2	1	2	2	1	4	3	2
Neurofibrosarcoma				2				
Adenocarcinoma - Seminal Vesicle				1			1	
Reticulum Cell Sarcoma	1			2		1	2	1
Malignant Lymphoma	2	3	5	8	4	2	4	4
Abdominal Viscera Neoplasm			1					
Osteosarcoma - Subcutaneous Tissue				1				
Number of Tumors/Number of Rats	10/39	15/63	22/59	33/65	59/60	14/61	31/62	37/64
Number of Rats with Tumors	10	12	20	32	42	14	30	33

[a] Treated controls exposed to 0.27N HNO_3 aerosols according to experimental protocol

TABLE 2. Benign Tumors in Rats Exposed to $^{232}UO_2(NO_3)_2$ or $^{233}UO_2(NO_3)_2$ Aerosols.

	Control		^{232}U ILB, nCi			^{233}U ILB, nCi		
	Nontreated	Treated[a]	0.74	5.85	53	0.63	10	36
Lipoma	2	4	3	3	5	4	4	6
Fibroma	12	13	15	11	11	18	8	16
Pheochromocytoma		2		1	2	2	2	
Hemangioma		2	1	1		1		
Fibroadenoma		1	2	1	1	2	2	
Adrenal Cortical Adenoma		1			1		2	2
Skin Papilloma		1						
Hemartoma	1							
Adrenal Ganglioneuroma	1		1					
Pancreatic Islet Cell Adenoma			2	1				1
Thyroid Adenoma			1	1		2	2	
Pulmonary Adenomatosis[b]				9	34	4	6	8
Pulmonary Adenoma				2	6		3	2
Adnexal Adenoma				1	1			
Skin Adenoma				1		1		
Epithelioma					1	1		
Kidney Adenoma					1			
Mammary Adenoma						1	1	5
Mast Cell Tumor							1	
Leiomyoma								1
Number Tumors/Number of Rats	16/39	24/63	27/59	32/65	63/60	36/61	31/62	41/64
Number of Rats with Tumors	14	18	23	26	46	27	21	33

(a) Treated controls were exposed to 0.27 N HNO_3 aerosols according to experimental protocol

(b) Not a frank tumor but interpreted to be a pre-neoplastic lesion

TABLE 3. Malignant Lung Tumor and Bone Tumor Incidence in Rats Exposed to $^{232}UO_2(NO_3)_2$ or $^{233}UO_2(NO_3)_2$ Aerosols.

Initial Lung Burden nCi ± SD	Number of Rats	Tumor Incidence: No. Lung Tumors[a]	%	No. Bone Tumors[b]	%
$^{232}UO_2(NO_3)_2$					
0.74 ± 0.2	59	1	1.7	0	0
5.85 ± 0.29	65	7	11	1	1.5
53 ± 14	60	35	58	2	3.3
$^{233}UO_2(NO_3)_2$					
0.63 ± 0.2	61	1	1.6	0	0
10 ± 2	62	4	6.5	1	1.6
36 ± 14	64	14	22	1	1.6
Controls					
Treated[c]	63	0	0	0	0
Nontreated	39	2[d]	5	0	0

(a) Lung tumors include 6 mesotheliomas of lung or pleura
(b) Bone tumors are osteosarcomas of the skeleton.
(c) Treated controls were exposed to 0.27 N HNO_3 aerosols
(d) Control lung tumors include an osteosarcoma of the lung and a pulmonary squamous cell carcinoma

DISTRIBUTION OF ^{232}U DECAY PRODUCTS FROM THE LUNG OF THE RAT

Investigators: J. E. Ballou, D. L. Haggard, and D. W. Murphy

Preliminary results of studies with intratracheally instilled ^{232}U nitrate in equilibrium with its daughter products show rapid clearance of ^{232}U from the lung and high deposition in kidney 1 day after administration. Thorium-228 was retained principally in the lung at that time.

Determination of the in vivo distribution of ^{232}U decay products requires the availability of duplicate sets of analytical equipment to analyze several tissues simultaneously. Recently, personnel in the Occupational and Environmental Protection Department have freed three germanium detectors for use in this research. This report presents preliminary results of an investigation now in progress in which adult female Wistar rats were injected intratracheally with a nitric acid solution of ^{232}U in equilibrium with its daughter products. The injection solution was prepared by adding the calculated equilibrium amount of ^{228}Th to a solution of ^{232}U. The ^{232}U-^{228}Th solution was administered under Nembutal® anesthesia, following surgery, to expose the trachea. An 18-ga hypodermic needle was inserted into the trachea between adjacent tracheal rings and positioned in the trachea. A polyethylene catheter, attached to a 1-ml syringe, was passed through the lumen of the needle into the trachea to approximately the level of the bifurcation. A volume of 0.2 ml of the ^{232}U-^{228}Th solution was injected into the lung via the catheter, and the rat was suspended vertically, head up, for several minutes after injection. The needle and catheter were then removed, and the wound was closed with metal clips.

Animals were sacrificed 1, 7, 15 and 30 days after injection; the femur, liver, lung and kidneys were removed for analysis. The rats were kept alive under Nembutal® anesthesia during the process of removing the femur and liver, and death occurred only when the lung and kidneys were excised. Tissues were sealed in 50 x 9-mm plastic petri dishes and were counted immediately after removal from the animal. Tissues were counted initially for 1 hr, followed by seven consecutive 3-hr counts. The initial count provides data on the short-lived daughters before extensive re-equilibration; the more delayed counts provide buildup information needed to quantitate the longer-lived decay products. The lung, femur and liver were counted first; i.e., they were assumed to be the critical tissues. The kidneys were counted later, when the intrinsic germanium detector became available.

Data analyzed and presented in this report were obtained using three detectors: two right, circular-cylinder, coaxially drifted Ge(Li) detectors having efficiencies of 5.2% and 13% at the 1332 keV energy of ^{60}Co; and one intrinsic germanium detector of high resolution (470 eV at 122 keV), with a thin beryllium window. The analyzer system associated with the detectors allowed counting of the various organs simultaneously. Data analysis was accomplished by a computer-based software package which processed the spectral data, determined energies and photopeak areas for ^{232}U and its daughters, and determined the statistical errors and peak parameters needed for quantitation. The energies and branching ratios for ^{232}U and daughters were taken from a compilation by D. C. Kocher (ORNL/NUREG/TM-102, 1977). Energy and efficiency calibrations were made using standards of known activity, prepared in the same container configuration as that used for the organs. The radioisotopes used for calibration were ^{241}Am, ^{137}Cs, ^{210}Pb and ^{57}Co. The energies and branching ratios for these radionuclides are well known and widely used as calibrating standards.

Analysis of an aliquot of the injection solution (Table 1) indicated that approximately 4.8 μCi of ^{232}U were administered to the rats, along with somewhat greater amounts of ^{228}Th and subsequent decay products. A gamma spectrum of this sample is shown in Figure 1. The errors associated with the individual radionuclide analyses depend mainly on the abundance of decay events in the energy range of interest and the length of time the sample is counted. The error factors for the

TABLE 1. Analysis of Injection Solution Using Intrinsic Germanium Detector (Sample is 1/200 of Amount Administered).

Radionuclide	Amount Detected, μCi ± S.D.
^{232}U	0.024 ± 0.02
^{228}Th	0.029 ± 0.003
^{224}Ra	0.033 ± 0.005
^{212}Pb	0.031 ± 0.001
^{212}Bi	0.036 ± 0.004
^{208}Tl	0.026 ± 0.02

^{232}U and ^{228}Th values can be reduced significantly by increasing the sample-counting time. Considering these factors, the analytical values for the various daughters in Table 1 are consistent with an equilibrium solution of ^{232}U-^{228}Th.

Table 2 shows values for the ^{232}U decay series in the lung at 1, 7, 15 and 30 days after instillation. It is noteworthy that no detectable amount of ^{232}U was found in the lung as early as 1 day after administration. This was unexpected, since studies with inhaled $^{232}UO_2(NO_3)_2$ showed a more prolonged early clearance (40% cleared in 7 days). The preferential retention of ^{228}Th in lung is, however, in agreement with other results reported for ^{232}U and uranium ores. The discrepancies in clearance kinetics may be artifacts of the method of administration and the volume or physical/chemical nature of the instilled material. It seems clear, however, that the daughter products (with the possible exception of ^{212}Pb and ^{212}Bi) are not in equilibrium in the lung at any time between 1 and 30 days after intratracheal instillation of an equilibrium mixture of ^{232}U-^{228}Th nitrate.

The parent/daughter relationships in other tissues, on the first day after administration, are shown in Table 3. Approximately one-half of the instilled ^{232}U was retained in the kidney at this time. This may reflect an early rapid phase of ^{232}U excretion as has been suggested in inhalation studies with uranyl nitrate (Annual Report, 1979). Only trace amounts of ^{232}U were found in kidney at later time intervals. Before conclusions are drawn, these preliminary studies will be replicated with additional animals. However, the results appear to confirm earlier reports from our laboratory describing the predominantly nonequilibrium state of major decay products in critical tissues following incorporation of the ^{232}U decay series.

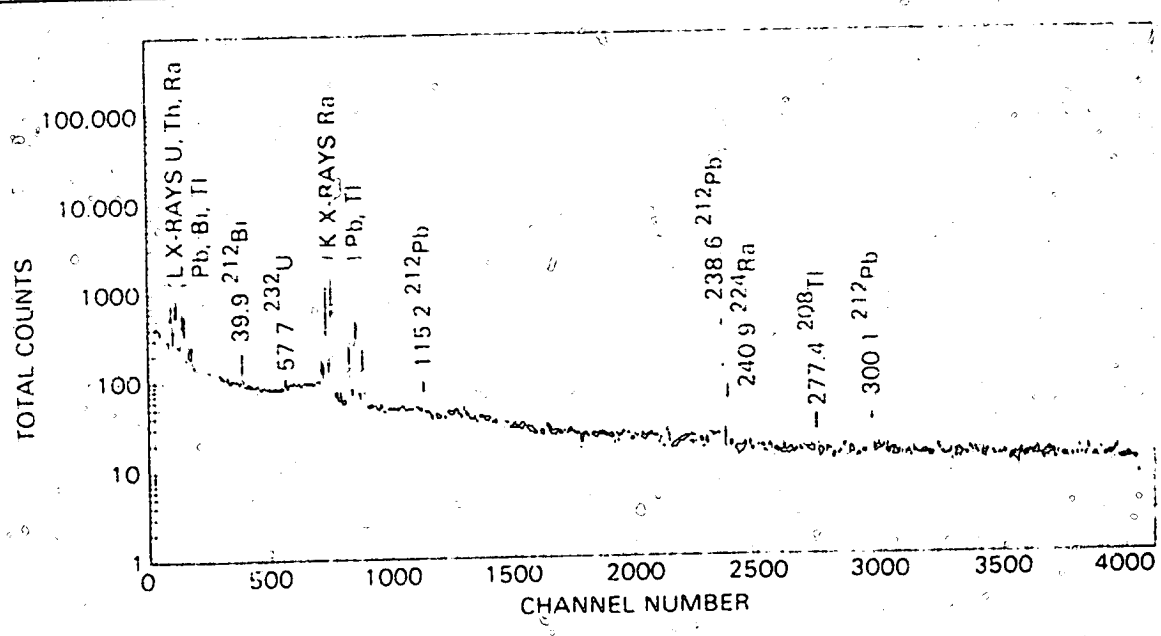

FIGURE 1. Gamma Spectrum of ^{232}U + Daughter Solution Used for Intratracheal Injection into Rat Lung. Spectrum was obtained using intrinsic germanium detector. Activity of this sample was 1/200 of the amount administered to the animals.

TABLE 2. Analysis of ^{232}U and Daughter Products in Lung (Values are Expressed in μCi).

Radionuclide	Days After Injection			
	1	7	15	30
^{232}U	ND[a]	ND[a]	ND[a]	ND[a]
^{228}Th	2.16	1.67	1.78	1.03
^{224}Ra	0.11	0.37	0.73	0.38
^{212}Pb	0.14	0.08	0.17	0.22
^{212}Bi	0.17	0.07	0.15	0.28
^{208}Tl	0.05	0.02	0.15	0.08

(a) ND = none detected

TABLE 3. Analysis of ^{232}U and Daughters in Lung, Liver, Femur and Kidney 1 Day After Intratracheal Injection.

Radionuclide	Activity in μCi			
	Lung	Liver	Femur	Kidney
^{232}U	ND[a]	ND[a]	ND[a]	1.94
^{228}Th	2.16	ND[a]	ND[a]	0.52
^{224}Ra	0.11	0.92	0.42	0.12
^{212}Pb	0.14	0.28	0.07	0.05
^{212}Bi	0.17	0.18	0.04	0.14
^{208}Tl	0.05	0.12	0.03	0.03

(a) ND = none detected

EARLY DISPOSITION OF INHALED ^{231}Pa CITRATE

Investigators: R. A. Gies, J. E. Ballou, and J. L. Ryan

Technical Assistance: A. W. Endres

Three groups of rats were exposed via inhalation to ^{231}Pa citrate aerosols. Initial lung burdens were 1, 17 and 56.4 nCi. These animals will be observed for long-term retention and biological effects of ^{231}Pa.

Protactinium-231 is an alpha-emitting radionuclide with a physical half-life of 32,500 yr and alpha energy of 5 MeV. It is formed in both conventional and breeder reactor processes, and is present in significant amounts in the nuclear waste stream. This study is designed to provide biological information relative to the potential hazard following ^{231}Pa incorporation.

Approximately 50 mg of $^{231}Pa_2O_5$ was received from Oak Ridge National Laboratory for use in this study. The material was dissolved in concentrated HCl and HF, aluminum nitrate was added, and the solution was passed through a column of Dowex 1-X4, 200-400 mesh resin to separate the ^{231}Pa from its daughters. The column was eluted with 9 M HCl + HF, and this solution was converted to a hydrated protactinium oxide with H_2O, NaOH, and Na_2SO_4. The precipitated material was dissolved in sulfuric acid, and sodium citrate was added (2%) to produce the final ^{231}Pa citrate solution.

Three groups of 60-day-old, male Wistar rats were exposed using a Lovelace nebulizer. Ten rats from each group were sacrificed immediately after the 30-min exposure to determine the initial lung burden (ILB), and five rats per time period were sacrificed after 7, 30, 60, 100, 150, and 200 days to determine distribution and retention kinetics for dosimetric purposes. Other rats were held for lifespan study of long-term biological effects. Tissues from the long-term rats will be analyzed for ^{231}Pa content at death, and these data, together with the serial sacrifice results, will be used to describe tissue retention throughout the total time course of the study. Long-term animals will be necropsied and tissues examined for histopathological changes at death.

The experimental protocol is summarized in Table 1. Animals are weighed at monthly intervals. No significant treatment-related weight changes have been observed after approximately 200 days.

Aerosol characteristics and initial disposition of the inhaled ^{231}Pa citrate are shown in Table 2. The results are similar to those seen with other actinide nitrates except for a greater early translocation to nonpulmonary tissues and a corresponding lower "initial" deposition in lung. This is probably due to the greater mobility of ^{231}Pa citrate compared to nitrate species.

Tissue samples were ashed and analyzed for ^{231}Pa content using an alpha scintillation counting method (TI21). Studies to improve ^{231}Pa counting techniques are described elsewhere in this Annual Report.

Five rats from each of the ^{231}Pa citrate-exposed groups were placed in metabolism cages immediately after exposure. Urine and feces were collected for 7 days to determine the rate and magnitude of radionuclide excretion. Analytical results are not yet available.

All ^{231}Pa-exposed rats were whole-body-counted in a gamma well counter on the seventh day after exposure. In order to estimate the lung burden, the ^{231}Pa content in the lungs of the five rats sacrificed on the seventh day after exposure (immediately after total body counting) was expressed as a fraction of the whole-body gamma activity at that time. This factor (lung count ÷ total body count) was multiplied by the individual total body counts to estimate individual lung burdens at 7 days after exposure. To obtain the estimated ILB, the 7-day lung burden was further adjusted for ^{231}Pa clearance during the initial week after

exposure. This was accomplished by multiplying the 7-day lung burden by a factor (lung activity immediately after exposure ÷ lung activity after 7 days) determined from the serially sacrificed rats. Estimated ILB values agreed reasonably well with those determined by sacrificing rats immediately after exposure, e.g., 1.4 ± 0.8 nCi compared to 1 ± 0.5 nCi, respectively, for the low-level exposure group. The estimated ILB values will be used in calculating the cumulative radiation dose in long-term rats.

TABLE 1. Experimental Protocol.

Initial Lung Burden, nCi	Number of Rats: Serially Sacrificed	Number of Rats: Life Span Study
1 ± 0.5	40	59
17 ± 9	40	59
56 ± 25	40	60
Control		
Non-treated	0	100
Treated	0	99

TABLE 2. Initial Deposition and Distribution of Inhaled ^{231}Pa Citrate Aerosols.

	Low Dose	Med Dose	High Dose
Total Deposition, nCi	6.71	119	881
Initial Lung Burden, nCi	1	17	56.4
Aerosol Characteristics			
AMAD, μm	1.44	1.76	2.88
GSD	2.01	2.1	2.38
Initial Deposition (% Total Deposition)			
Upper Respiratory Tract	48.4	36.6	41
Liver	0.11	0.05	0.04
Residual Carcass	10.4	27	14.1
Lung	14.9	14.3	6.4
Pelt	26.1	22.4	38.5

Fetal and Juvenile Radiotoxicity

A number of studies conducted under this project have demonstrated that many of the biological parameters used to calculate permissible levels of exposure of adults to radioactive materials are inappropriate for the rapidly growing infant or child or for the pregnant female. These include age-related differences in radionuclide deposition, distribution, and retention and associated differences in microdosimetry, as well as the greater intrinsic radiosensitivity of the immature organism. These findings emphasize the need for more detailed information on the metabolism and toxicity of radionuclides in the prenatal and juvenile mammal. The continuing objective of this project is to obtain such information, which is needed to establish appropriate exposure limits for radionuclides of greatest potential hazard to these age groups.

EFFECTS OF MONOMERIC ^{239}Pu ON THE PREGNANT RABBIT

Investigators: B. J. Kelman, M. R. Sikov, and P. L. Hackett

Technical Assistance: A. J. Clary, D. L. Alford, J. A. Cushing, C. J. Gerdes, P. S. Lytz, R. L. Music, K. A. Poston, and S. A. Watson

Exposure of pregnant New Zealand White does to 10-40 μCi/kg of monomeric ^{239}Pu by intravenous injection lead to increased clotting times, which were detectable as early as 24 hr after dosing. Decreased platelet counts and hematocrits were found at later times postexposure.

Severe hemorrhage of uterine origin was observed in two does which delivered prematurely (on the 28th day of gestation, 28 dg) during a study of the distribution and teratogenic effects of monomeric ^{239}Pu in the rabbit. This unusual finding prompted us to determine whether blood clotting capability was deficient, or what remaining mechanisms might explain the observed hemorrhage.

For this analysis, we have considered data from 39 New Zealand White does which were injected, via an ear vein, with either 0 (control), 10, or 40 μCi/kg of ^{239}Pu at 9, 15, or 29 dg (Figure 1). Monomeric ^{239}Pu was prepared by adding sufficient sodium citrate to a solution of ^{239}Pu nitrate (pH < 1) to provide at least a hundredfold molar excess of citrate, followed by adjustment of the pH to 4.5 and filtration through a 0.22-μm filter. At the times indicated in Figure 1, animals were killed with overdoses of ether, and blood samples were obtained by cardiac puncture. Groups of three and four control animals received solutions which were identical to those administered to animals receiving 10 μCi/kg and 40 μCi/kg of ^{239}Pu, respectively, except for the exclusion of ^{239}Pu. Platelet counts and hematocrits were obtained from four control does, and clotting times from all seven. No differences were detected between the two subgroups of control litters, therefore data were pooled in subsequent statistical analyses.

Clotting times, platelet counts, and hematocrits were obtained from all animals except when rapid clotting precluded sampling of blood. Clotting times were significantly increased above control levels in all groups of treated does (all $P < 0.005$). Furthermore, clotting time in rabbits injected with 10 μCi/kg increased linearly as a function of time between dosing and sample collection. Platelet counts decreased in all does evaluated at 14 days or more after exposure ($P < 0.05$, $P < 0.01$, $P < 0.005$ for Groups II, III, and IV, respectively). Hematocrit values were depressed in Group III ($P < 0.025$) and in Group IV ($P < 0.06$).

The basis of the observed clotting disorder is not readily apparent, but there are striking parallels between effects we observed on platelet count in rabbits and effects reported for large doses of penetrating radiation in rats and rabbits. The reported pattern included an

apparent initial increase in platelet count at 1 day postirradiation (which was not statistically significant), followed by a precipitous decline to a minimum concentration of platelets at approximately 12 days postirradiation. By 20 days postirradiation, platelet numbers had recovered to approximately 30% of control values. Marked similarities were also observed between changes in blood clotting times observed in our study and those reported in the literature after external irradiation. In both cases, clotting times appeared to be poorly correlated with thrombocytopenia. We have been unable to find previous reports of blood clotting deficiencies observed soon after administration of ^{239}Pu.

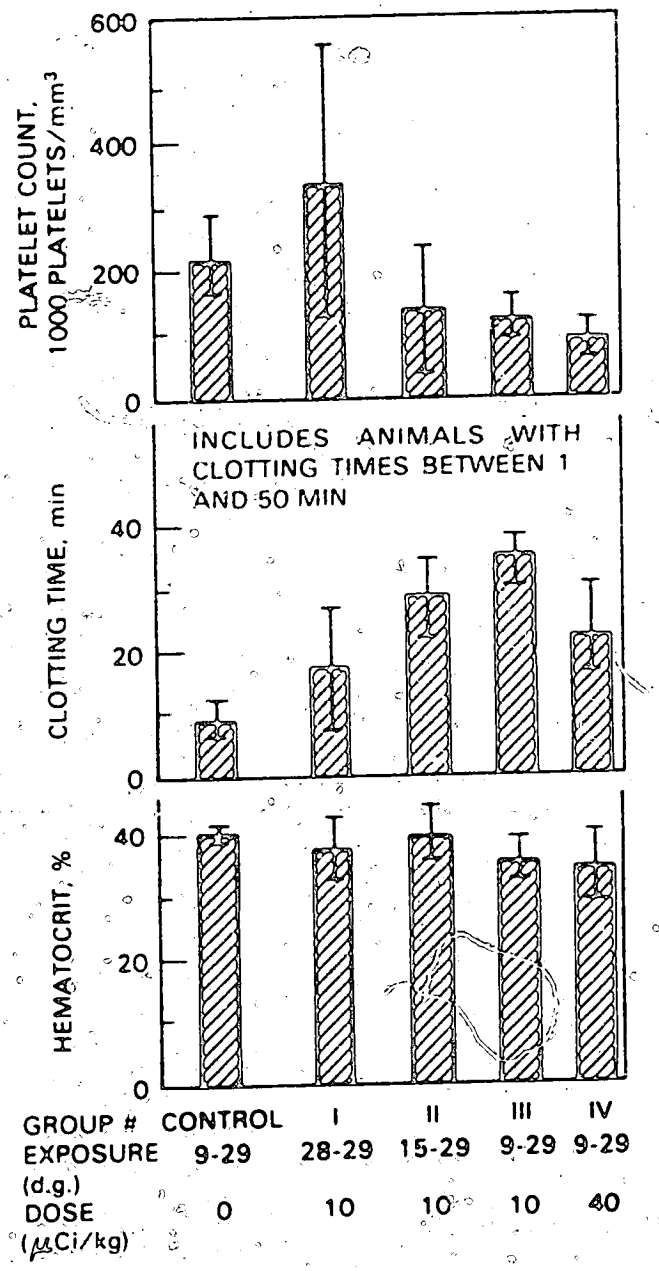

FIGURE 1. Effect of ^{239}Pu on Hematological Parameters in Pregnant Rabbits (Mean ± SD).

EFFECTS OF MONOMERIC ^{239}Pu ON THE FETAL RABBIT

Investigators: B. J. Kelman, M. R. Sikov, and P. L. Hackett

Technical Assistance: A. J. Clary, D. L. Alford, J. A. Cushing, C. J. Gerdes, J. O. Hess, P. S. Lytz, R. L. Music, K. A. Poston, and S. A. Watson

Exposure of pregnant New Zealand White does to 10-40 μCi/kg of monomeric ^{239}Pu by intravenous injection was not teratogenic. The incidence of embryolethality was similar to that in Wistar-derived rats, but the rabbit fetus (postorganogenesis) appeared to be more sensitive to the lethal effects of Pu.

Previous studies in this laboratory (Annual Report, 1978) demonstrated strain-specific differences in the embryotoxic effects of Pu in the rat. To obtain comparative data in a nonrodent species, 57 timed-pregnant New Zealand White rabbits were dosed intravenously (ear vein) with either 0 (control), 10, or 40 μCi/kg of ^{239}Pu and killed at the times shown in Figure 1. Monomeric ^{239}Pu was prepared by adding sufficient sodium citrate to a solution of ^{239}Pu nitrate to provide at least a hundredfold excess of citrate, followed by adjustment of pH to 4.5 and passage through a 0.22-μm filter. Groups of three and four control animals were administered solutions identical to those used for animals receiving 10 μCi/kg and 40 μCi/kg of ^{239}Pu, respectively, except for the exclusion of ^{239}Pu. No differences were detected between the two groups of control litters, therefore control data were pooled in subsequent statistical analyses.

Females were killed and conceptuses were examined for viability at 10, 16, and 29 days of gestation (dg). Fetuses from litters dosed at 9 and 15 dg and killed at 29 dg were weighed, measured, and examined for external abnormalities, including cleft palate. Approximately two-thirds of the fetuses from each litter were dissected under magnification immediately after removal from the uterus and examined for soft-tissue abnormalities. The heads of two fetuses from each litter were sectioned and examined for hydrocephaly and other anomalies. Carcasses rom fetuses examined for soft-tissue abnormalities were preserved in ethanol, macerated in KOH, stained with alizarin red-S, and examined for skeletal alterations.

No pattern of teratisms was evident as a result of ^{239}Pu exposure. Of the 377 fetuses examined in this study, only five showed evidence of teratogenic events. A single case of umbilical hernia was observed among control fetuses. One litter in Group V (see Figure 1 for dosing regimes in each group) contained one fetus with cleft palate, one fetus with umbilical hernia, and one fetus with hydrocephalus. A single fetus in another litter of Group V showed extensive malformations including anencephaly, holorachischisis, and gastroschisis. The very small number of teratisms, and their lack of pattern, make it unlikely that they were associated with ^{239}Pu exposure.

Exposure to monomeric ^{239}Pu did not affect the weight of viable fetuses, but led to significant increases in prenatal mortality (Figure 1). Mortality was increased above control levels in Groups III, IV, V, and VI ($P < 0.01$, $P < 0.001$, $P < 0.002$, and $P < 0.001$, respectively). Mortality did not change significantly in Groups I and II. The number of litters containing dead fetuses was increased significantly only in Group IV ($P < 0.005$).

The incidence of embryolethality in New Zealand White rabbits (11%) was similar to that reported previously (Annual Report, 1978) for Wistar-derived rats (17%). However, Pu injected later in gestation (fetal period) also produced lethality (Figure 1), which was not observed in any rat strain in previous studies.

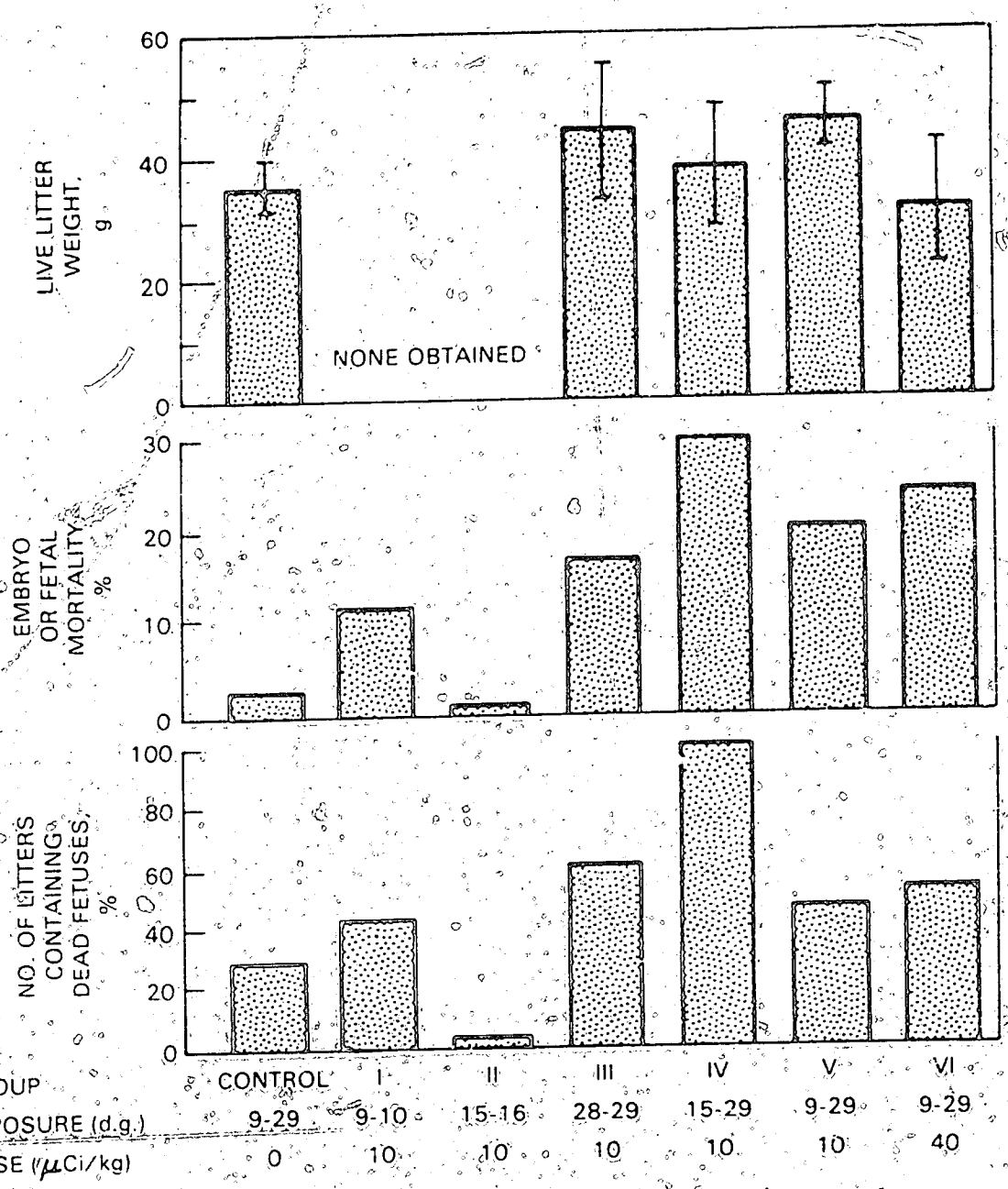

FIGURE 1. Effects of ^{239}Pu on Live Litter Weight, Embryo/Fetal Mortality and Litter Mortality in the Rabbit.

MOVEMENTS OF MONOMERIC ^{239}Pu ACROSS THE HEMOCHORIAL PLACENTA OF THE GUINEA PIG

Investigator: B. J. Kelman

Technical Assistance: J. A. Cushing, D. L. Alford, and K. A. Poston

The clearance of monomeric ^{239}Pu from mother to fetus was 2.3 ± 0.6 μl/min (mean ± SE), the lowest measured, to date, for any substance, using the placental perfusion technique. Indirect measurements of maternal blood flow to the placenta indicated that placental blood flow was greatly disrupted in dams dosed with Pu which may, in part, account for the low clearance of Pu.

Previous studies in this laboratory indicate that only small amounts of Pu accumulate in the fetus following maternal exposure (Annual Report, 1978). We have used a placental perfusion technique, previously employed for other metals, to measure the clearance of Pu from dam to fetus. Figure 1 is a schematic diagram of the perfusion system.

Monomeric ^{239}Pu was prepared by adding sufficient sodium citrate to a solution of ^{239}Pu nitrate to provide at least a hundred-fold excess of citrate, followed by adjustment of the pH to 4.5 and filtration through a 0.22-μm filter. Tritiated water and the Pu solution were injected into a cannulated jugular vein of pregnant guinea pigs at 60 days of gestation. Perfusing fluid was pumped from a series of reservoirs through a peristaltic pump into a cannulated umbilical artery. The fluid then passed through the fetal circulation of the placenta, and outflow was collected in a series of tubes. Tritium and ^{239}Pu concentrations in the perfusate were determined by liquid scintillation counting, and clearances were calculated. Clearance was defined as the amount (μl) of maternal plasma which contained the same amount of test substance (nCi) as that which entered the perfusate per minute. The clearance of tritated water from dam to fetal circulation of the placenta (T_{MF}) was measured and used to detect changes in maternal blood flow to the placenta.

The clearance of ^{239}Pu from maternal to fetal circulation of the placenta (Pu_{MF}) calculated from individual perfusions are listed in Table 1. The mean (± SE) was 2.3 ± 0.6 for 11 placentas from seven dams. The Pu_{MF} was independent of perfusion rate through the umbilical vessels and was only 20% of the clearance of inorganic mercury (the metal with the lowest clearance previously measured). The T_{MF} was low in all perfusions, indicating that placental blood flow was greatly altered in dams dosed with Pu. We have previously shown that T_{MF} is a function of blood flow on both the maternal and fetal sides of the placenta. The T_{MF} was significantly correlated with umbilical flow rate in only five of 11 perfusions. A significant correlation would be expected in not less than 10 of 11 perfusions under unperturbed conditions, which further indicates that maternal blood flow to the placenta was greatly altered. When the regression of T_{MF} on umbilical flow rate is used to calculate T_{MF} at a constant perfusion rate for each perfusion, T_{MF} becomes a function of rate at which

TABLE 1. Clearance of ^{239}Pu From Dam to Fetus (Pu_{MF}).

Dam	Placenta	Pu_{MF} μl/min
1	1	6.6 ± 0.1[a]
2	1	1.3 ± 0.1
3	1	0.9 ± 0.2
	2	1.1 ± <0.1
4	1	2.9 ± 1.2
5	1	2.0 ± 0.6
	2	0.4 ± <0.1
6	1	1.1 ± 0.8
	2	0.6 ± 1.2
7	1	2.2 ± 1.5
	2	2.5 ± 0.6
Mean		2.3 ± 0.5

[a] Mean ± SE

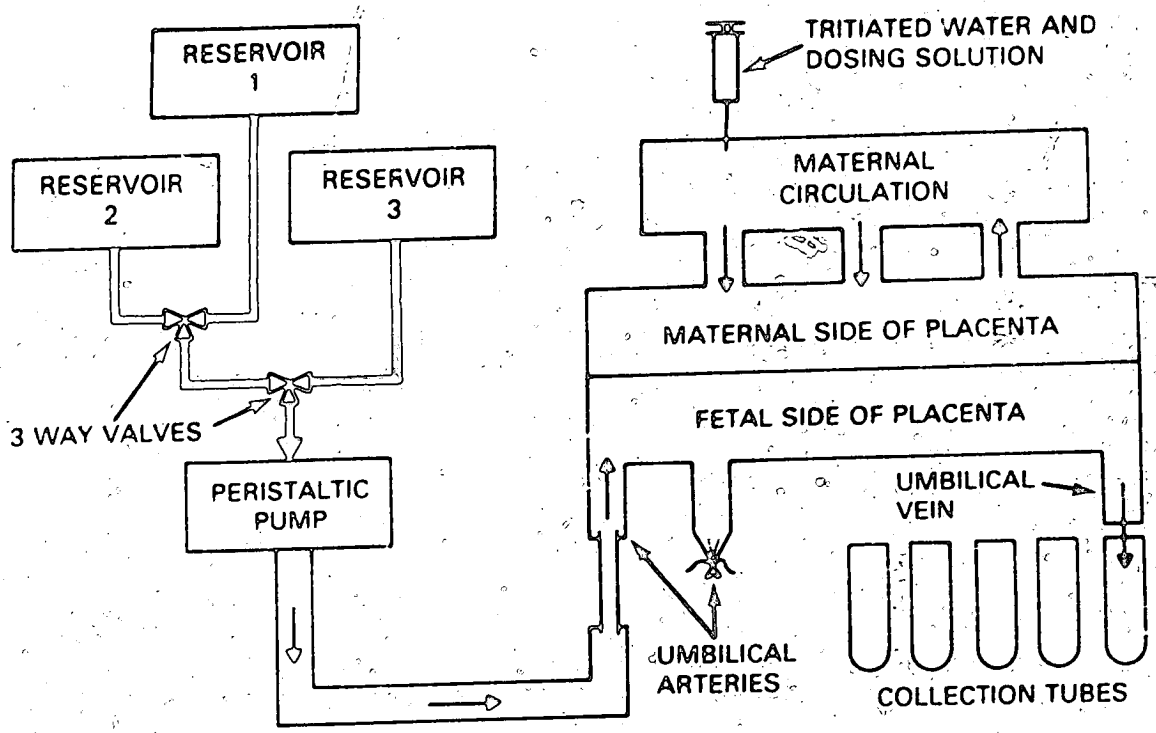

FIGURE 1. Schematic Diagram of Perfusion System.

radiolabel is supplied by the maternal circulation only. In our experiments, Pu_{MF} was related to T_{MF} in all 11 perfusions, which further suggests that the clearance of the material under study was mainly limited by maternal blood flow to the placenta. Using a T_{MF} representative of normal umbilical and maternal blood flows (1.8 ml/min), based on previous experiments we calculated that Pu_{MF} would be 16 ± 4 µl/min if blood flow were normal. This approximates the value found for clearance of inorganic mercury from dam to fetus.

Clearance measurements (µl/min) are used in this report rather than transfer (pCi/hr) since it is not possible to precisely determine the concentration of Pu in the maternal circulation of the placenta. However, such calculations can be made if the plasma concentration of Pu in the maternal carotid artery is accepted as a reasonable estimation of that in the maternal circulation of the placenta. Figure 2 is a scatter diagram of maternal plasma ^{239}Pu concentrations determined from blood sampled through a cannulated carotid artery, as a function of time after injection, together with a graph of the best-fit polynomial equation. Using a maternal plasma ^{239}Pu concentration of 6.5 nCi/ml (as determined from Figure 2 at 70 min), and the mean value for Pu_{MF} of 2.3 µl/min, we estimate the transfer of Pu from dam to fetus to be approximately 900 pCi/hr under the conditions of our experiments.

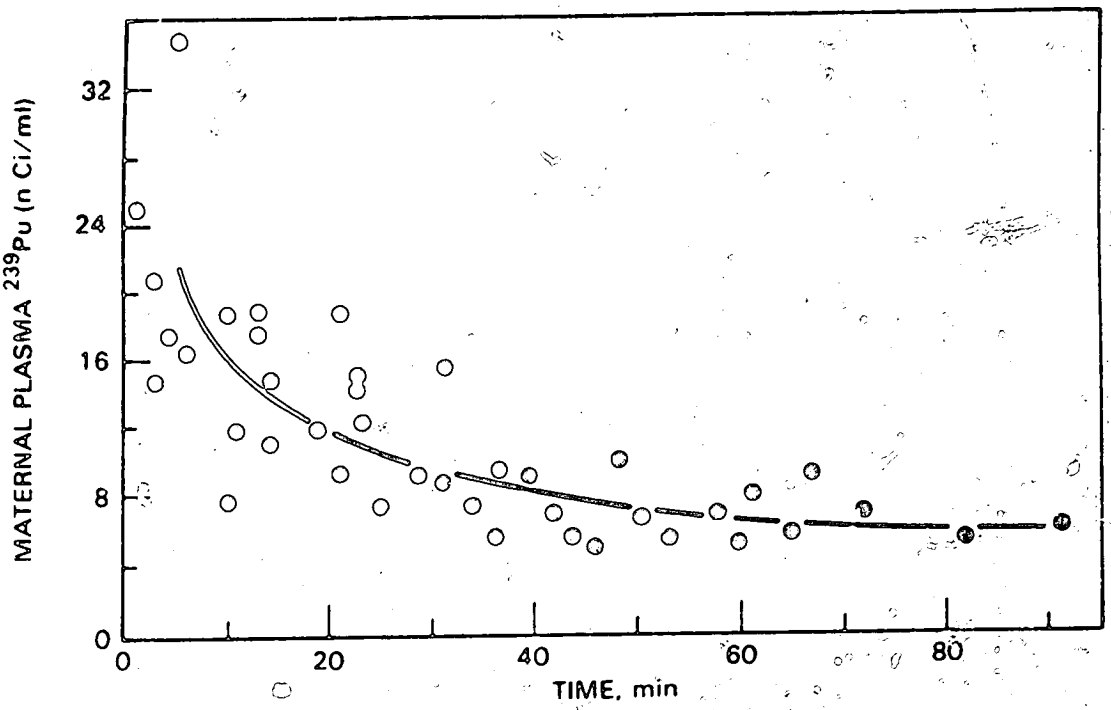

FIGURE 2. Maternal Plasma ^{239}Pu Concentration as a Function of Time Postinjection.

ARTIFICIAL INSEMINATION OF RABBITS FOR USE IN TERATOLOGICAL EVALUATIONS

Investigators: B. J. Kelman and L. F. Montgomery

Technical Assistance: S. C. Johnson and D. L. Alford

Artificial insemination (AI) procedures in rabbits were refined until a conception rate of 95% was consistently reached. Retrospective analysis of pregnancy rates after AI by procedures followed in our laboratory showed that minimal acceptable weight (age) of New Zealand White females was 3.5 kg. Collected sperm tended to adhere to glass surfaces; in addition, when glass was used, we observed a greater than 50% reduction in sperm counts in freshly extended semen samples, compared to counts of sperm collected in plastic containers.

Natural mating of rabbits is impractical in most teratology studies because of the large number of males (ideally, two per doe) and the labor necessary to obtain large numbers of timed-pregnant rabbits within a 2- to 3-day span. Because AI allows large numbers of animals to be reliably impregnated in a single day, it appears well-suited for most teratology studies.

Unfortunately, our experience, and that of other laboratories, indicated that AI often resulted in low (approximately 60%) conception rates. Therefore, we considered it important to optimize AI procedures prior to performing planned teratology studies and measurements of the transplacental movement of radionuclides and chemicals. We conducted a study using sufficiently large numbers of animals to allow comparison and statistical interpretation of several AI procedures.

A total of 80 female and 20 male New Zealand White rabbits were purchased from three separate vendors. Semen was collected from male rabbits by means of artificial vaginas. In general, the AI procedures used were similar to those recommended in the literature. Semen extender consisted of a solution containing tris (hydroxymethyl) amino methane, citric acid, glucose, and egg yolk in distilled water.

We examined the following variables for their effect on conception rates: 1) sperm morphology, 2) sperm count, 3) sample container composition, 4) storage of sperm, 5) levels of ovulation-stimulating materials, and 6) female age and weight.

Over a 3-wk period, only five of 20 bucks could be trained to the artificial vagina to the extent that they would give one semen sample per day at least 50% of the time. We found that these animals were highly sensitive to some undefined characteristic of the individual technician collecting the sample, as well as to the number of technicians in the room. Samples were collected more reliably when a single technician made the collection, with no other individuals present in the room. Approximately 50% of the sperm in the samples were normal in terms of morphology and motility. Optimal conception rates were obtained with 2×10^7 motile sperm per insemination.

We found that the composition of containers holding sperm samples was of great importance. Sperm tended to adhere to glass. When glass test tubes and insemination pipettes were used, the number of sperm introduced into females dropped by 50%, even when semen samples were extended and used immediately. The use of plastic test tubes and insemination pipettes eliminated this decrease in sperm numbers. Sperm counts obtained using glass and plastic containers are compared in Figure 1. Storage of sperm in extender for up to 22 hr at 24°C led to no detectable loss in motility.

Pituitary luteinizing hormone (PLH, Burns-Biotic Laboratories) was used to induce ovulation in female rabbits. Previous results in our laboratory had suggested that not all does ovulated when doses of 2.5 mg PLH/rabbit were used. However, in the present study, evaluation of corpora lutea at sacrifice demonstrated that doses of 5 or 2.5 mg/rabbit induced ovulation equally well. (Ovulation occurred in more than 97% of the does used in this study.)

Retrospective analysis of pregnancies

resulting from AI procedures followed in our laboratory showed a relationship between female weight at breeding (regardless of the age recorded by the vendor) and conception rate. A bimodal distribution of animals was evident: New Zealand White females weighing less than 3.5 kg had significantly lower conception rates than females that weighed more than 3.5 kg.

As a final test for conception rates, 60 female rabbits were inseminated using semen samples optimized on the basis of the factors described above. All females that weighed more than 3.5 kg were inseminated once, using plastic insemination pipettes and semen samples containing no less than 2 x 10^7 motile sperm. Fifty-seven females conceived (95% of those inseminated). Of the three that did not conceive, one had cystic ovaries; the other two had no lesions evident at gross necropsy which might account for their failure to conceive.

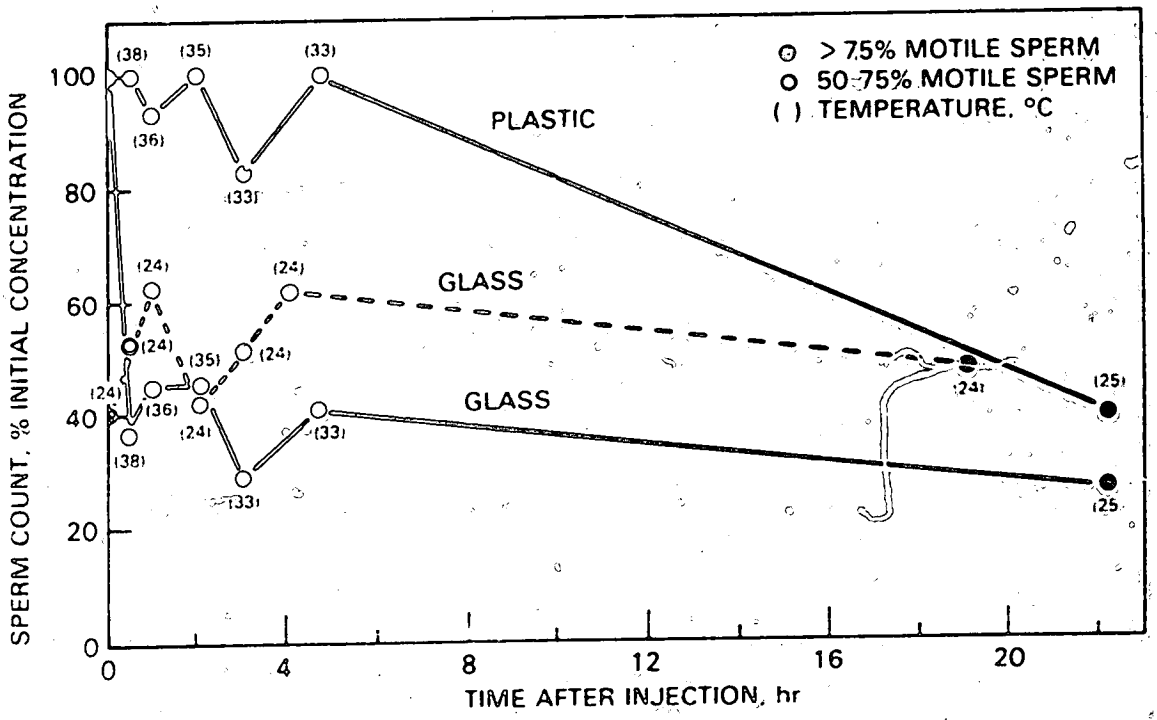

FIGURE 1. Effect of Glass and Plastic Containers on Sperm Numbers and Motility.

INTERACTIONS OF ANIMAL AGE AND PARTICLE SIZE WITH DEPOSITION AND RETENTION OF INHALED ^{51}Cr-LABELED MICROSPHERES

Investigators: P. L. Hackett, M. R. Sikov, W. E. Skiens, W. C. Cannon, and R. L. Music

Technical Assistance: E. F. Blanton, A. J. Clary, K. A. Poston, J. P. Herring, and B. L. Egbert

Newborn, juvenile, weanling and adult rats were exposed to aerosols of ^{51}Cr-labeled microspheres with activity median aerodynamic diameters (AMADs) ranging from 0.5 to 4.4 μm. Respirable particle-size ranges were inversely related to age, and there was selective deposition of the larger particles in the upper respiratory tract of younger animals. Lung retention and clearance were independent of particle size and animal age over an 8-wk observation period. Clearance from the gastrointestinal (GI) tract of microspheres administered by inhalation was slower in juvenile rats and faster in adult animals than clearance of microspheres deposited directly in the GI tract by intragastric intubation.

We previously described (Annual Report, 1979) studies to examine the relationships between the progressive development of the respiratory tree and aerosol deposition characteristics. Newborn, juvenile (13-day-old), weanling (21-day-old), and adult rats were exposed by nose-only inhalation to ^{51}Cr-labeled microspheres with AMADs ranging from 0.9 to 4.4 μm (Annual Report, 1979). We have now extended these studies to include smaller microspheres (AMADs of 0.55 and 0.69 μm).

Because a large fraction of particles inhaled is excreted through the GI tract, we also compared the patterns of GI clearance following administration of particles by gastric intubation with those found in the inhalation experiments. The influence of particle size and animal age on GI clearance was also investigated.

Microspheres were labeled with ^{51}Cr by emulsion polymerization of chromium acetylacetone dissolved in a styrene monomer (composition and characteristics given in Table 1). Aqueous suspensions of the microspheres were nebulized and used to expose rats for 60 min. Groups of 50 rats of each age were exposed to the 0.11-, 0.20-, 0.48-, 1.09-, and 2.02-μm-diameter microspheres; only adult rats were exposed to 2.77- and 4.33-μm particles. Six rats from each age group were killed immediately after exposure, at 2 and 6 hr, and at 1, 3, 7, 21 and 56 days after exposure.

Tissue samples were analyzed for the 0.325-MeV gamma emission of ^{51}Cr. Filter paper and cascade impactor samples were taken during exposure to determine aerosol concentrations and particle size distributions. To compensate for aerosol concentration differences among exposures (Table 1), all radioanalytical values were normalized to an aerosol concentration of 40 nCi/ℓ.

TABLE 1. Aerosol Properties of ^{51}Cr Microspheres

Microsphere Size, μm	Composition[a]	Aerosol Properties: nCi/ℓ, $\bar{X} \pm$ S.E.	AMAD, μm	GSD
0.11	PS	3.7 ± 0.7	0.55	2.22
0.20	PS	42.7 ± 7.7	0.69	2.01
0.48	PS	47.8 ± 10.1	0.91	1.78
1.09	PS	32.3 ± 6.3	1.42	1.49
2.02	PVT	18.7 ± 6.4	2.34	1.77
2.77	PS/PVT	16.1	3.40	2.14
4.33	PVT	39.9	4.36	2.11

[a] Polystyrene (PS); polyvinyltoluene (PVT).

The respirable particle-size range for each age group may be estimated from the calculated percent alveolar depositions (Table 2). Alveolar deposition was negligible in the newborns for all sizes of microspheres. In the adult and weanling groups, there was a clear discontinuity between alveolar deposition at smaller and larger particle sizes. These results are based on minute volumes estimated from body weight measurements. The consistently low values in the juvenile group suggest that this estimate may not be completely valid at this age. We are presently exploring methods to measure

TABLE 2. Alveolar Deposition[a] (Percentage) of Inhaled ^{51}Cr Microspheres in Adult, Weanling, Juvenile, and Newborn Rats (Mean ± SE).

Aerosol AMAD, μm	Adult	Weanling	Juvenile	Newborn
0.55	13.2 ± 1.7[b]	16.6 ± 2.8[b]	10.7 ± 5.5	0.4 ± 0.03
0.69	17.7 ± 2.7[b]	16.5 ± 3.4[b]	9.9 ± 2.1	1.6 ± 1.5
0.93	19.0 ± 2.9[b]	12.5 ± 4.6[b]	8.7 ± 3.3	0.1 ± 0.07
1.42	11.[illegible] ± 1.5[b]	19.4 ± 2.7[b]	8.4 ± 2.7	0.7 ± 0.7
2.34	11.9 ± 3.3[b,c]	0.4 ± 0.1[c]	2.8 ± 1.5	0.7 ± 0.6
3.40	4.5 ± 1.0[c]			
4.36	2.8 ± 0.3[c]			

[a] Percent alveolar deposition = $\frac{\text{Lung activity}}{\text{Total inhaled activity}}$

[b,c] Values with different superscripts are significantly different ($P < 0.05$) within each age group.

respiratory values of the animals during aerosol exposure.

Initial body burdens (IBB; total deposited activity, exclusive of activity on the skin) were significantly different for all ages at each particle size, except for juvenile and weanling rats exposed to aerosols with AMADs of 2.34 μm (Figure 1). Adult IBBs increased with increasing particle sizes; weanling values displayed a significant peak at an AMAD of 1.42; juvenile IBBs were lower for the smallest particle size; and values for newborn rats did not differ significantly from one another. The change in the IBB percentages in lung, GI tract, and head (which includes mouth and nasopharnyx), as a function of AMAD, is shown in Figure 2. Lung deposition decreased with increasing particle size in all age groups. The ^{51}Cr activity in the lung exceeded that in the GI tract following inhalation of only the smaller particle sizes (AMADs of 0.69 μm in adults and 0.55 μm in weanling and juvenile rats). Chromium-51 activity levels were high in the heads of juvenile animals exposed to larger particles and in newborn heads for all particle sizes. An example of lung retention curves for the various ages for the 0.69-μm aerosol is shown in (Figure 3).

The gastric intubation studies were performed with aqueous suspensions of 0.48-, 1.09-, and 2.77-μm-diameter-^{51}Cr microspheres. Dosage volumes for the different age groups were adjusted in a ratio proportional to calculated minute volumes, i.e., 0.1, 0.3, 0.4, and 1.5 ml for newborn, juvenile, weanling, and adult rats, respectively. Five animals from each age group were killed at 3, 7, or 24 hr after dosing. The GI tract was removed and divided into seven sections: stomach, small intestine (four equal segments), cecum and colon. The length and ^{51}Cr activity of each section was measured.

For initial comparisons of data for GI tract clearance of inhaled and intragastrically administered particles, we examined ^{51}Cr activity in the stomach, small intestine, and large intestine. Postexposure intervals were counted from the initiation of the 60-min inhalation exposure. The total amount of ^{51}Cr activity in the GI tract of newborn rats following inhalation exposure was too low to reliably compare ^{51}Cr activity in individual

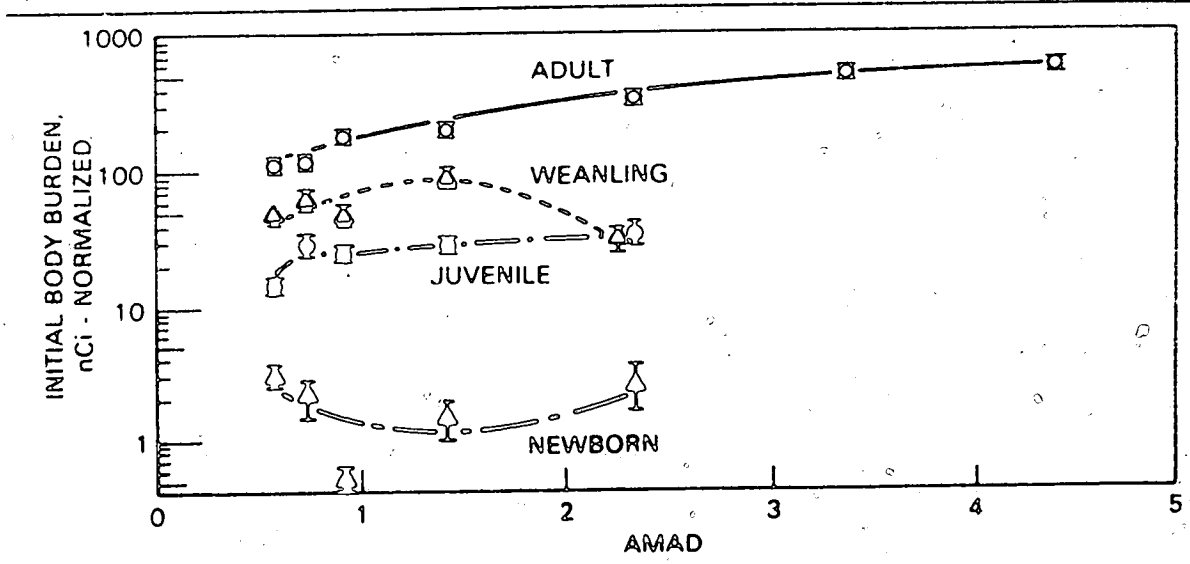

FIGURE 1. Initial Body Burden of Inhaled ^{51}Cr Microspheres in Adult, Weanling, Juvenile, and Newborn Rats.

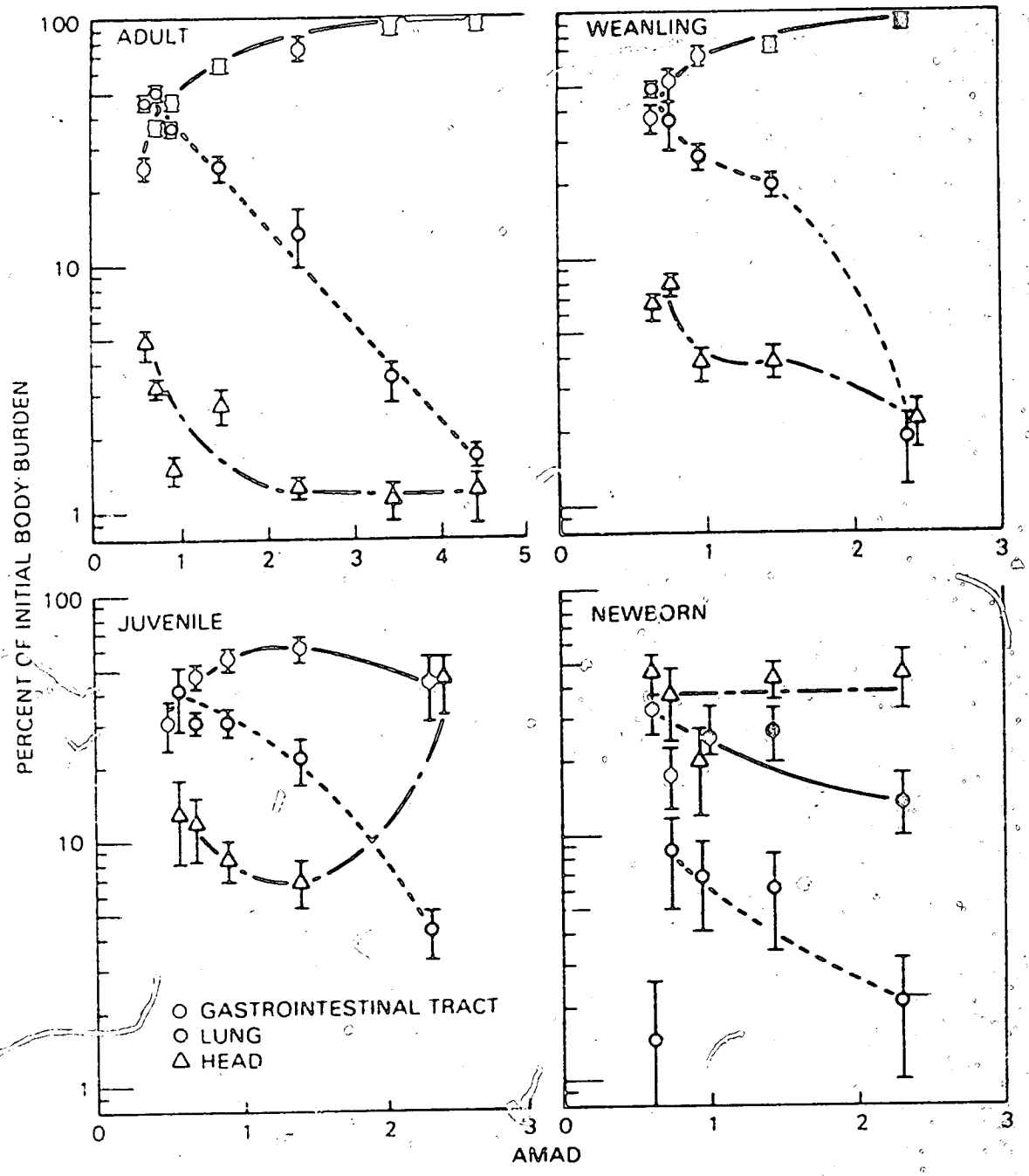

FIGURE 2. Initial Distribution of Inhaled ^{51}Cr Microspheres in Adult, Weanling, Juvenile, and Newborn Rats

segments. At all sampling periods, GI tract values in weanlings were similar for inhalation and gavage exposure to either 0.48- or 1.09-μm-diameter (0.91 or 1.42 μm AMAD) microspheres. Gastric clearance of inhaled microspheres tended to be slower in juvenile rats and faster in adults than clearance of intragastrically administered particles. Typical data (1.09-μm-diameter microspheres at 3 hr after exposure) are shown in Figure 4). By 7 hr postexposure, values were equal for the two routes of administration in juveniles, but gastric retention of intragastrically administered particles in adult rats still exceeded that of the inhaled particles.

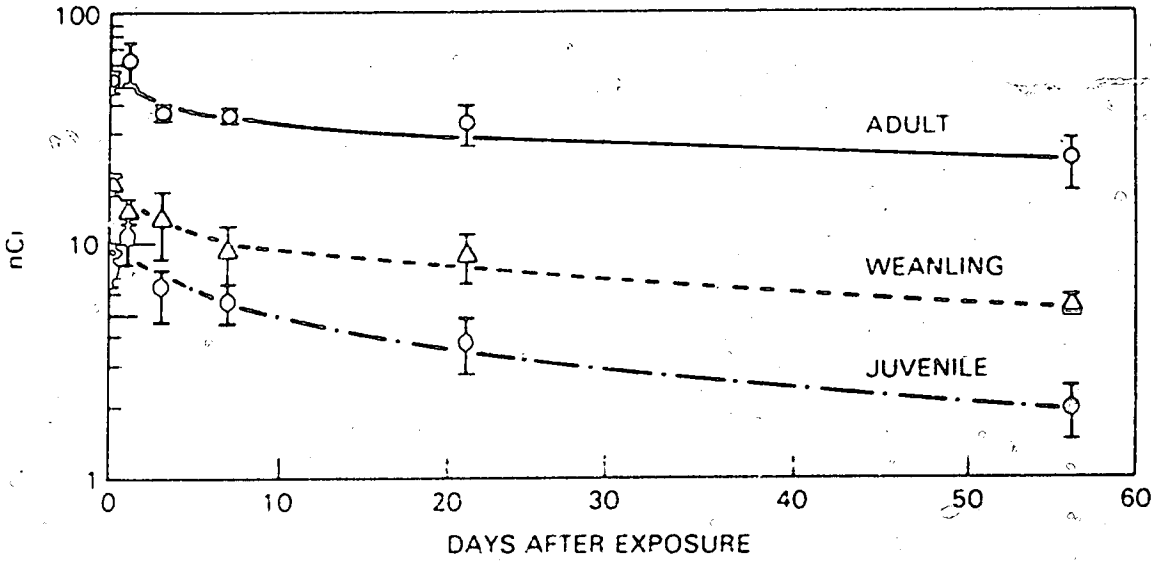

FIGURE 3. Lung Retention of 0.7 μm ^{51}Cr Microspheres in Adult, Weanling, Juvenile, and Newborn Rats.

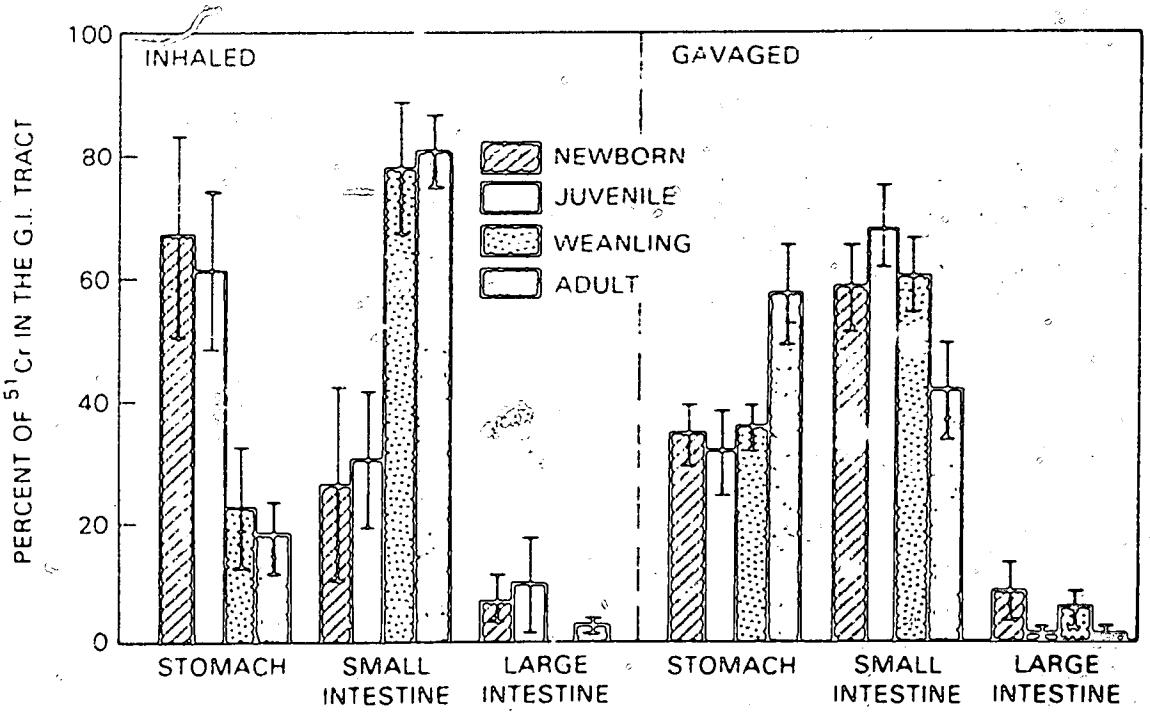

FIGURE 4. Distribution of 0.11 μm-Diameter (0.55 μm AMAD) ^{51}Cr Microspheres in the GI Tract of Adult, Weanling, Juvenile, and Newborn Rats at 3 Hr After Inhalation or Intragastric Intubation.

EFFECTS OF PRENATAL IRRADIATION ON POSTNATAL BRAIN ENZYME ONTOGENY IN RATS

Investigators: F. D. Andrew, P. S. Lytz, and K. A. Poston

Studies were initiated to compare the sensitivity of various procedures for measuring deficits in the development of the brain and its functions in the postnatal period following prenatal irradiation. To date, the data indicate that mortality and body and brain weight depression correlate more closely with dose levels than do changes in reflex ontogeny or brain enzyme activity.

We are attempting to develop more sensitive measures for detecting deleterious effects produced by prenatal exposure to radionuclides, as well as other agents. We have proposed (Andrew, Environ. Health Persp. 18: 111-116, 1976) that changes in the development of "enzyme clusters" in the perinatal period might provide such a measure, and have developed procedures for the requisite assays. To examine the applicability of this approach to radionuclide toxicology studies, experiments have been performed using X-irradiation.

It is well documented that X-irradiation of rats in utero induces a variety of effects observable at birth, including major malformations, intrauterine growth retardation, and prenatal mortality. Prenatal irradiation also has deleterious effects on postnatal growth, survival and functional development. The purpose of the preliminary study reported here was to determine whether physical measurements (e.g., body and organ weights) or functional measurements (e.g., reflex ontogeny and tissue enzyme levels) were the most sensitive and reliable indicators of postnatal disturbances resulting from prenatal insults. Because the central nervous system is the "target tissue" most readily and consistently affected by radiation in utero, studies were conducted to evaluate effects on its development.

Pregnant Sprague-Dawley-derived rats were exposed to approximately 125, 225, or 325 R whole-body X-irradiation at 15 days of gestation (dg). Additional rats were sham-exposed as controls. Dams were permitted to deliver and nurse their pups. Pups were weighed at 1 day of age; litter size was determined, and the litter culled to eight pups (generally four of each sex). Offspring were again weighed at 7, 14, and 21 days of age, and various measures of physical development and reflex ontogeny (indicated in Table 1) were obtained.

Similarly exposed litters were sacrificed at 20-22 dg, 4-6 days, or 20-22 days of age (ages corresponding to the late fetal, early neonatal, and weanling periods, respectively). Brains were removed, pooled, weighed, homogenized, and centrifuged; the supernatants were assayed for enzyme activities with a centrifugal fast analyzer using standard methods and reagents. The four enzymes measured were isocitrate dehydrogenase (ICD), alkaline phosphatase (AKP), aspartate aminotransferase (AST) and alanine aminotransferase (ALT). Results were expressed as international units of activity per gram of brain weight. These enzymes are essential for homeostatic metabolic activity, but are not involved in neurochemical (neurotransmitter substance) biosynthesis or degradation.

Several classical effects of radiation on mammalian conceptuses were induced (Table 2). Litter size was significantly reduced at 325 R, indicative of prenatal mortality. Birth weights were significantly reduced at 225 and 325 R, consistent with intrauterine growth retardation. Postnatal growth and survival were also significantly affected by 325 R and, although not statistically significant, growth of the 225 R group was less than that of the sham-exposed. Microcephaly was also induced by X-irradiation, as indicated by the dose-related depressions of brain weights between birth and weaning. Microcephaly, which is indicative of cellular hypoplasia and probably reflects neuronal depletion, is consistent with radiation-induced neurotoxicity.

Because of the anticipated neurotoxicity, a battery of neuroreflexive and behavioral tests were performed on the offspring (Table 1). Measures for which

TABLE 1. Postnatal Maturation Evaluation Battery

Physical Landmarks	Scoring Criteria	Observation Days 1	7	14	21
Body Weight	grams	X	X	X	X
Incisors Erupted	±[a]		X		
Eyes Opened	0-1-2			X	
Hair Present	±			X	
Organ Weights	grams	X	X		X
Test Measures					
Forward Locomotion	30 sec		X		
Surface Righting	60 sec		X		
Air Righting Reflex	± 3 Trials		X	X	X
Swimming Development	0-4[b]		X	X	X
Visual Cliffrissal Placing	±			X	
Forelimb Strength	[illegible]				X
Startle Reflex	±			X	

[a] Rating of [illegible] no response [illegible] response
[b] Rating per modification of Shapiro et al. Science 168 147 (1970)

[illegible] erences from controls were [illegible] indicated in Table 3. Swimming development at 7 days appeared to be affected at 125 R, but not at higher exposure levels. In the absence of a dose-dependent response, the observation is not considered biologically meaningful. The air-righting reflex at 14 days was significantly affected at 325 R, but because only one litter survived, the interpretation is equivocal. At 21 days, forelimb strength was significantly decreased in the 225 and 325 R groups, which may reflect a neurological lesion. Such variable results in reflex ontogeny are consistent with reports from other laboratories.

A few reports in the literature have demonstrated only a limited correlation between behavioral effects and neuropathology. Our approach was to determine whether brain enzyme levels correlated with altered animal behavior and with the implied neuropathology (microcephaly). The four enzymes selected had different ontogenic profiles, as seen from the values for the sham-exposed group (Table 4): ICD activity declined steadily from the fetal to the weaning periods, AKP activity increased between the fetal and weaning periods, and between the fetal and early neonatal periods, then declined. The ALT activity was undetectable until weaning, and AST activity slowly increased to a maximum at weaning. Except for AST, the activity of these enzymes in brains of

TABLE 2. Intrauterine and Postnatal Growth and Survival

Postnatal Observation[a]	Day	Weeks Post-Exposure[b]	Prenatal Irradiation Dose, R[c] 0	125	225	325
Litter Size	1	1	12 ± 4.3[illegible]	12 ± 1.5	12 ± [illegible]	8 ± 5.18[e]
Birth Weight (g)	1	1	7.0 ± 0.9	6.9 [illegible]	[illegible]	4.1 ± 0.8 (8)[e]
Body Weight (g)	7	2	17 ± 2.7		14 ± [illegible]	6 ± 3.3[e]
	14	[illegible]	[illegible]	41 [illegible]	[illegible]	22 [illegible]
	21	4	55 ± [illegible]	[illegible]	46 ± [illegible]	29 [illegible]
Percent Survival[d]	21	4	100	[illegible]	100	18[e]
Brain Weight (g)	2	1	0.20 ± 0.03 (5)	0.15 ± 0.02	0.10 ± 0.01 (6)[e]	0.07 ± 0.01 (4)[e]
	7	2	0.5[illegible] ± 0.12 (9)		[illegible] ± 0.04 (6)[e]	0.23 (2)[e]
	21	4	1.4[illegible] ± 0.07 (6)	1.08 (2)	0.84 ± 0.12 (10)[e]	0.72 (2)[e]

[a] Mean of litter means ± SD [illegible] number of litters examined except percent survival
[b] Weeks 1-4 correspond to late fetal or birth, early neonatal, late neonatal or weaning period, respectively
[c] X-irradiation to whole body of dam at 15 days of gestation; sham-exposed controls [illegible] dose
[d] Percent of all culled litters alive at weaning; does not include litters sacrificed for enzyme analysis
[e] $P \leq 0.02$ by t test, Bonferroni adjustment

adult rats was markedly lower than that detected in developing offspring.

X-irradiation in utero significantly increased activity of AKP in brains of fetuses, but no effects were seen in postnatal rats. It is possible that ALT activity was depressed in brains of weanlings, but the 325 R group was too small for valid statistical analysis. Brain ALS values appeared unaffected at all ages examined. Other laboratories have reported altered activity of similar homeostatic enzymes in brains following prenatal irradiation. However, for the enzymes measured, neither our results nor those from other laboratories appear to be more reliable, more quantitative or technically simpler than body and brain-weight measurements.

In subsequent studies we plan to consider additional brain enzymes, as well as neurotransmitters, to determine if there are irradiation-induced alterations in these materials which correlate with the microcephaly and growth retardation observed.

TABLE 3. Effects of Irradiation on Neuroreflex and Behavior Ontogeny[a]

Postnatal Observations	Age, days	Weeks Post Exposure[b]	Prenatal Irradiation Dose (R)[c] 0	125	225	325
No. of Litters Tested	1	1	18	2	12	3
	7	2	11	2	9	2
	14	3	11	2	9	1
	21	4	11	2	9	1
Swimming Development (Direction)	7	-	2.4 ± 0.4	1.6	2.1 ± 0.3	2.1 ± 0.10
Air Righting	14	3	1.1 ± 0.8	2.3	1.0 ± 0.9	0[d]
Forelimb Strength	21	4	19.7 ± 6.0	14.2	9.9 ± 3.3[d]	6.7[d]

(a) Mean ± SD
(b) Same as footnote b Table 2
(c) Same as footnote c Table 2
(d) $P \leq 0.02$ by t-test. Bonferroni, all other tests listed in Table 1 were performed but no other results were statistically significant

TABLE 4. Brain Enzyme Activity During Postnatal Development[a].

Enzyme Name	Age, days	Weeks Post Exposure[b]	Prenatal Irradiation Dose (R)[c] 0	125	225	325
Isocitrate Dehydrogenase	-2	1	3.6 ± 0.9 (5)	3.3 ± 0.6 (3)	3.3 ± 0.5 (6)	2.8 ± 0.5 (4)
	5	2	2.4 ± 0.5 (8)	--	2.2 ± 0.4 (6)	2.0 (2)
	21	4	2.0 ± 0.0 (6)	2.0 (2)	1.9 ± 0.3 (10)	2.0 (2)
	A[e]	--	1.1 ± 0.3 (14)	--	--	--
Alkaline Phosphatase	-2	1	5.8 ± 0.5 (5)	6.3 ± 0.6 (3)	7.3 ± 1.4 (6)	7.5 ± 1.0 (4)[d]
	5	2	8.3 ± 1.6 (8)	--	8.5 ± 1.1 (6)	9.0 (2)
	21	4	4.6 ± 0.6 (6)	5.0 (2)	5.0 ± 1.2 (10)	5.8 (2)
	A[e]	--	3.7 ± 1.0 (14)	--	--	--
Alanine Aminotransferase	21	4	1.6 ± 0.5 (6)	1.5 (2)	1.4 ± 0.4 (10)	1.0 (2)
	A[e]	--	2.1 ± 0.3 (14)	--	--	--
Aspartate Aminotransferase	-2	1	6.0 ± 2.2 (5)	5.0 ± 0.0 (3)	6.0 ± 0.6 (6)	6.8 ± 0.5 (4)
	5	2	7.3 ± 1.6 (8)	--	7.0 ± 0.9 (6)	8.0 (2)
	21	4	21.8 ± 2.7 (6)	24.8 (2)	22.5 ± 3.5 (10)	21.8 (2)
	A[e]	--	52.0 ± 4.5 (14)	--	--	--

(a) Mean activity of litter pools ± SD as units per gram of tissue; number of litters pooled and assayed
(b) Same as footnote b Table 2
(c) Same as footnote c Table 2
(d) $P \leq 0.02$ by t-test, Bonferroni
(e) Non-exposed, not pregnant adults

SOMETIMES FATAL LESIONS

Investigators: D. B. Carr and D. L. Stevens

Differences in group survival rates can confound the comparison of lesion occurrence rates. This report describes a method which provides a wide class of assumptions about lesion lethality, and compares lesion rates in the absence of sacrifice data.

A typical goal of animal carcinogenesis studies is to determine whether exposure conditions affect the occurrence rates of various lesions. This determination is complicated, because: (1) exposure conditions frequently affect survival, and (2) lesion occurrence is often measurable only at death. This is a recurrent problem in toxicity experiments involving exposure of animals at different ages. Without data from periodic sacrifices, analysis methods require an assumption about the lethality of the lesion of interest. Two extreme alternatives that can be dealt with by current statistical methods are: (1) the death of any animal with a lesion was caused by the lesion, or (2) lesion occurrence is unrelated to death. Intermediate situations can be investigated utilizing the concept of lesion prevalence (age-specific lesion rates). We have developed a method for estimating and comparing prevalences for situations in which animal sacrifice data, and thus direct estimates of prevalence, are not available (D. B. Carr and D. L. Stevens. PNL Technical Report, Sometimes Fatal Lesions, Pacific Northwest Laboratory, 1980).

The usual definition of lesion prevalence at age t is the conditional probability of having the lesion at age t, given survival to age t. Thus, it is the proportion of the population of age t with the lesion. The corresponding definition of prevalence in an interval $[t_1, t_2)$ is the proportion of the population surviving to age t_1 which has the lesion present in the interval. Somewhat arbitrarily, we will say that an animal dying during the interval has the lesion if it is present at death, and that an animal surviving the interval has the lesion if the lesion is present at time t_2.

Suppose the study is to compare G treatment groups over L time intervals $[t_0, t_1)$, $[t_1, t_2)$ ..., (t_{L-1}, ∞). The prevalence, p_{ij}, for treatment group i in time interval j is the conditional probability of having the lesion, given entry into the time interval. This is denoted by $p_{ij} = Pr(L_{ij} \mid E_{ij})$. Expanding this conditional probability yields:

$$p_{ij} = Pr(L_{ij} \mid E_{ij}, D_{ij})\ Pr(D_{ij} \mid E_{ij}) + Pr(L_{ij} \mid E_{ij}, S_{ij})\ Pr(S_{ij} \mid E_{ij}), \quad (1)$$

where L_{ij} is the event of having the lesion in the interval, E_{ij} is the event of entry into the interval, D_{ij} is the event of death during the interval, and S_{ij} is the event of survival through the interval. All of the conditional probabilities of (1) can be estimated from the following counts:

d_{ij} = number of deaths for treatment i, interval j

a_{ij} = number of deaths with lesion

s_{ij} = number of survivors

u_{ij} = number of survivors with lesions.

However, u_{ij} is usually unavailable since most lesions can be observed only at death of the animal. Thus, some assumption must be made about $Pr(L_{ij} \mid E_{ij}, S_{ij})$.

In the "nonlethal" model, the assumption is that lesion rates are independent of mortality, so that

$$p_{ij} = Pr(L_{ij} \mid E_{ij}, D_{ij}) = Pr(L_{ij} \mid E_{ij}, S_{ij}). \quad (2)$$

The estimate of p_{ij} is then

$$\hat{p}_{ij} = \frac{a_{ij}}{d_{ij}}. \quad (3)$$

The "lethal" model is based on analyzing rates of death with lesion. However, this analysis can also be viewed as based on prevalence, under the assumption that the

lesion rate in the surviving population is zero. That is, $Pr(L_{ij} \mid E_{ij}, S_{ij}) = 0$, and the estimate of p_{ij} becomes

$$\hat{p}_{ij} = \frac{a_{ij}}{d_{ij} + s_{ij}} \quad (4)$$

A comparison of (3) and (4) shows that a continuum between the lethal and nonlethal models can be obtained by using

$$\hat{p}_{ij} = \frac{a_{ij}}{d_{ij} + \theta_{ij} s_{ij}} \quad , \quad 0 \leq \theta_{ij} \leq 1 \quad . \quad (5)$$

The parameter θ_{ij} is the ratio of the number of excess lesions among animals which die to the total number of lesions. In the present method, we treat θ_{ij} as being fixed *a priori*. When it is known that neither the lethal nor the nonlethal model is suitable, selecting an intermediate value for θ_{ij} is no more arbitrary than selecting θ_{ij} as 0 or 1.

A modified Mantel-Haenszel statistic can be used to make prevalence comparisons and has a component for each group. The ith component has the form

$$m_i = \sum_{j=1}^{L} w_{ij}(\hat{p}_{ij} - \hat{p}_{.j}) \quad (6)$$

where the weighting factor is

$$w_{ij} = n_{ij} = d_{ij} + \theta_{ij} s_{ij} \quad . \quad (7)$$

the prevalence estimates are

$$\hat{p}_{ij} = a_{ij}/n_{ij} \quad (8)$$

and

$$\hat{p}_{.j} = \frac{a_{.j}}{n_{.j}} = \sum_{i=1}^{G} a_{ij} \Big/ \sum_{i=1}^{G} n_{ij} \quad . \quad (9)$$

The heart of this statistic is the difference, in (6), between the estimated prevalence $\hat{p}_{ij}$ for the ith group and the estimated prevalence $\hat{p}_{.j}$, which presumes no group differences and pools information. The weighting factor, w_{ij}, indicates how heavily this difference is weighted as a function of time (and survival). The weighted difference is summed across the time intervals. Large absolute values of the components m_i suggest group differences. Let $\underset{\sim}{m}' = (m_1, \ldots, m_G)$. The modified Mantel-Haenszel statistic in matrix notation is

$$M = \underset{\sim}{m}' \; \mathrm{cov}[\underset{\sim}{m}, \underset{\sim}{m}']^{-} \underset{\sim}{m} \quad (10)$$

where "-" indicates a generalized inverse. We have shown that M has a chi-square distribution with G-1 degrees of freedom, and have discussed its use in some detail in the report referenced above.

This modified Mantel-Haenszel statistic provides a way of comparing lesion prevalence rates when the lesions are sometimes, but not invariably, fatal. A prevalence analysis does not completely solve the problem of confounding between survival and lesion incidence rates. However, we have shown that this concept of lesion prevalence is helpful in relating two types of analyses that were previously viewed as distinct, and is useful in providing a whole class of assumptions from which to choose.

Modifying Radionuclide Effects

The metabolism and effects of radionuclides may be influenced by a number of dietary, physiological, and environmental factors. Since persons who might be exposed to radionuclides do not live under carefully controlled and isolated conditions, we are studying some factors which have been identified as potentially important determinants of radionuclide behavior: the reproductive performance of female rats exposed to ^{239}Pu during pregnancy or lactation, and the relative contribution of cross-placental and milk transfer to offspring.

REPRODUCTION AFTER ADMINISTRATION OF ^{239}Pu TO NULLIPAROUS, PREGNANT OR LACTATING RATS

Investigators: V. H. Smith, D. D. Mahlum, J. O. Hess, and M. R. Sikov

Rats were injected with 0, 0.5 or 2.0 μCi/kg of ^{239}Pu when nulliparous, at 19 days of gestation or at 3 days postpartum; and after 30 days, were bred and allowed to deliver. Seven days later they were rebred; this cycle was repeated until each rat experienced five pregnancies. The reproductive performance of the nulliparous group was the most affected by Pu, as indicated by decreased litter size, decreased neonatal survival, increased breeding failure and increased time to produce a fifth litter. Animals injected while pregnant or lactating showed such effects, to a lesser degree, after the third or fourth pregnancy following Pu injection.

We have shown that the biological disposition of monomeric Pu and its effects on mammary tumor incidence in the rat were influenced by pregnancy and lactation (Annual Reports, 1976 and 1979). In this report we present data on the influence of physiological state (pregnancy or lactation) at time of injection on the effects of ^{239}Pu relative to the reproductive capacity of the dam and early viability of the progeny.

Nulliparous, pregnant or lactating Wistar rats were injected intravenously with 0 (controls), 0.5 or 2.0 μCi/kg of ^{239}Pu citrate. Thirty days after injection, rats were mated and allowed to deliver. Litter size, birth weight, and sex and weight of 7-day-old pups were recorded, after which offspring were killed. At 7 days postpartum, dams were again mated. This cycle was repeated until each had experienced five pregnancies.

Figure 1 shows that litter size was decreased in a dose-related manner in all pregnancies of rats injected while nulliparous. By the fourth and fifth litters (150 days or longer after Pu injection), litter size was also smaller for rats injected while pregnant or lactating than in corresponding unexposed groups (controls). The incidence of reproductive failure (inability to complete five pregnancies) was highest in animals exposed to Pu while nulliparous (Table 1). The incidences in exposed rats of the pregnant or lactating groups were essentially the same as in the corresponding controls. In animals injected while pregnant or lactating, Pu had no effect on the median time required to achieve any of the four subsequent pregnancies. Only for the fifth pregnancy of the nulliparous group was there a notable difference: 9 days for controls, compared to 20 and 39 days for the 0.5- and 2-μCi ^{239}Pu doses, respectively.

The greatest effect of Pu on viability of progeny was also in the nulliparous group (Figure 2); the incidence of neonatal deaths (% mortality in 7 days) increased in a dose-related fashion. In the other two groups the incidence tended to increase after the third pregnancy. Generally, this neonatal mortality was a reflection of stillbirths and offspring killed shortly after birth by the dam; pups surviving the first 24 hr were alive at 7 days. No weight differences or differences in sex ratio among groups were observed.

There were almost no differences in the life spans of corresponding dose groups (Table 1). This suggests that, at the Pu

levels employed. differences in Pu distribution caused by the physiological state at the time of injection have little effect on factors responsible for death of the animal.

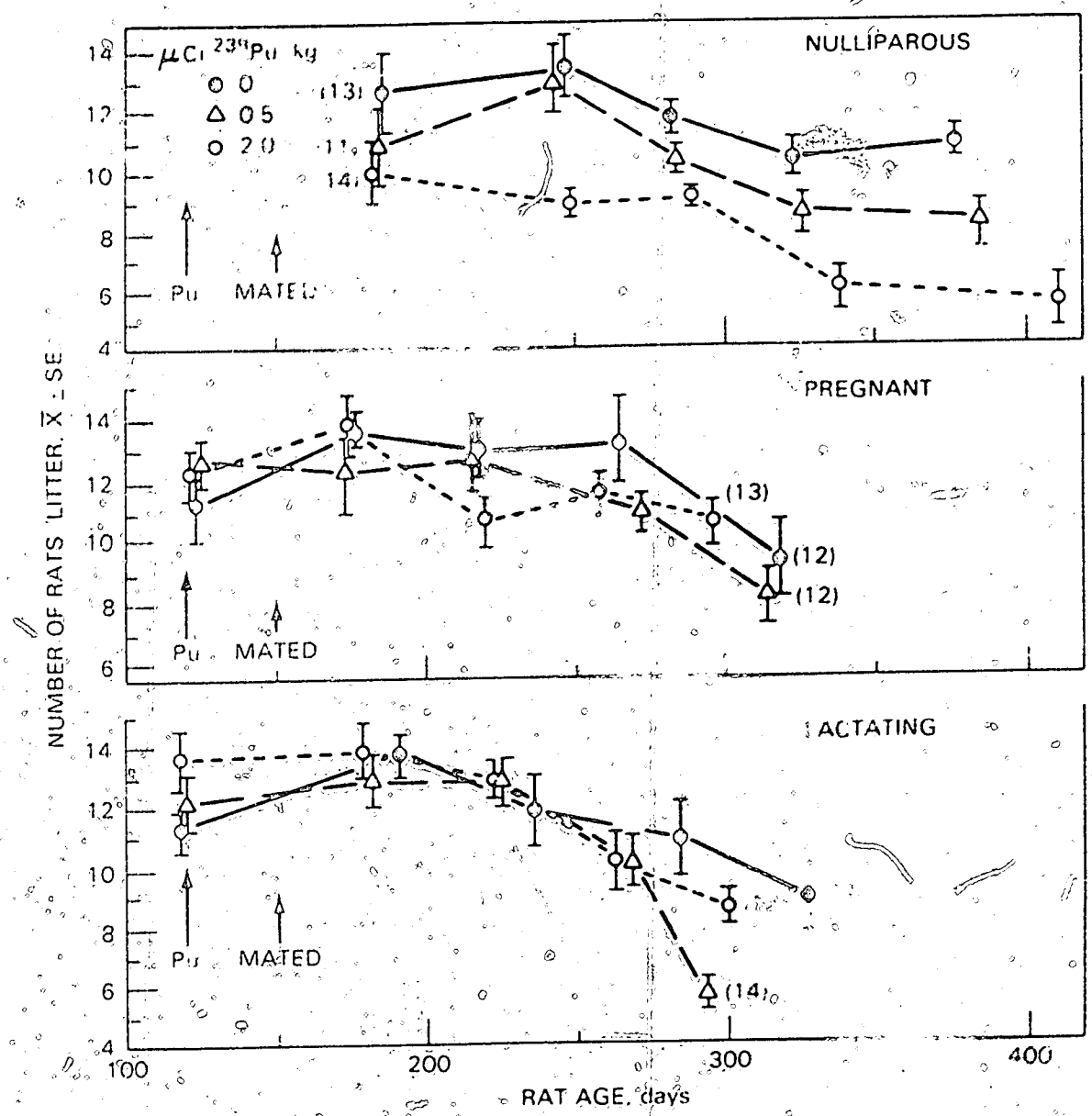

FIGURE 1. Litter Size and Age at Parturition for Rats Injected With 0 (o——o), 0.5 [illegible] ^{239}Pu Citrate When Nulliparous, Pregnant (19 Days of Gestation) or Lactating (1 Day Postpartum). The [illegible] the time of Pu injection and subsequent attempts to mate (arrows). Number of dams/group are [illegible]

TABLE 1. Effect of ^{239}Pu on Reproductive Failure and Longevity in Rats After Injection While Nulliparous, Pregnant, or Lactating.

	State at Time of Pu Injection								
	Nulliparous			Pregnant			Lactating		
μCi Pu/kg	0	0.5	2.0	0	0.5	2.0	0	0.5	2.0
No./Group	13	11	14	12	12	13	14	14	12
Pregnancy									
1 & 2	0	0	0	0	0	0	0	0	0
3	0	0	1	0	1	0	0	0	0
4	0	1	2	1	1	0	0	0	0
5	0	2	4	1	2	1	0	1	0
Median	783	588	489	759	614	533	788	523	534
Life Span in Days and Interquartile Range[a]	588-894	487-622	443-605	512-811	548-767	459-585	686-834	444-710	423-575

[a] The range between the 25th and 75th percentile

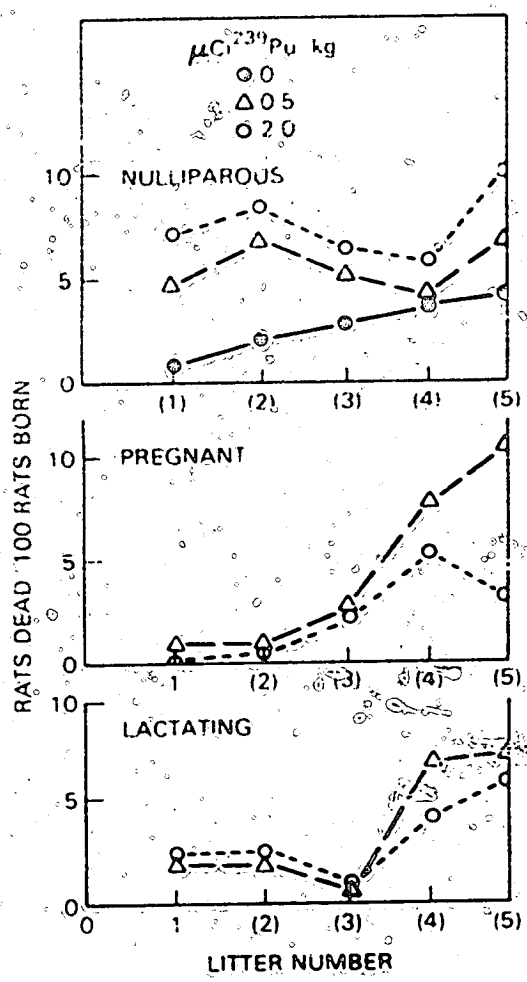

FIGURE 2. Number of Rats That Died Up to 7 Days After Birth From Dams Injected With 0 (○—— ○), 0.5 (△——△) or 2.0 (○----○) μCi ^{239}Pu/kg When Nulliparous, Pregnant or Lactating. Litters born >4 days after Pu injection are shown in parentheses. Zero-dose results from all groups were similar and have been combined; for clarity they are shown only on the "nulliparous" section of the figure.

RELATIVE CONTRIBUTION OF CROSS-PLACENTAL TRANSFER AND NURSING Pu BURDENS IN RAT PUPS

Investigators: V. H. Smith, D. D. Mahlum, and J. O. Hess

The amount of Pu available in the milk of rats injected intravenously with ^{239}Pu citrate at 3 days prepartum or 1 day postpartum was about 1.3% and 16%, respectively, of the dose. The progeny of the rats injected while pregnant received three times more Pu via the placenta than from milk. At a second pregnancy, >70 days later, milk provided at least three times more Pu than the placental route. The amount of Pu retained by the progeny was 3-5% of that available in milk.

Plutonium concentration in mammary tissues following administration to lactating rats is considerably greater than that in animals with mammary glands that are inactive at the time of Pu administration (Annual Report, 1976). The amount of Pu in milk, and subsequent transfer to progeny, may be related to mammary storage which, in turn, is influenced by the physiological state of the dam at Pu acquisition. We have therefore determined the transfer of ^{239}Pu to offspring of dams with varying concentrations of Pu in the mammary gland, and compared the relative contributions of placental and milk Pu to the neonatal body burden.

Groups of 40 female Wistar rats, ~350 g body weight, were injected intraveneously with 15.4 μCi ^{239}Pu-citrate/kg when nulliparous, pregnant (19 days of gestation, dg), or lactating (1 day postpartum). Five rats from each group were killed at 1, 7, 21, and 45 days after injection. The remaining animals were then caged with males until about half showed sperm in vaginal smears. Five of the pregnant (sperm-positive) rats were killed at 20 dg, along with nongravid rats from the same group. Sixteen days later (14 days postpartum), the remaining dams, their progeny and nongravid animals were killed. Milk samples were taken from anesthetized rats just prior to sacrifice by injecting 1-2 units of oxytocin intraperitoneally and manually expressing the milk. Mammary tissue, milk samples, and progeny, and their gastrointestinal tracts, were ashed and analyzed for Pu by liquid scintillation counting.

Near the end of lactation (21 days after injection; Table 1), the Pu concentrations in milk and mammary tissue from rats of the lactating group were 10- and 4-fold greater, respectively, than in corresponding tissues from rats of the pregnant group. Following the second pregnancy, Pu concentration in milk was still about three times higher in rats from the lactating group than in those injected while pregnant (Table 1).

Forty-five days after Pu injection to their dams, progeny of the pregnant and lactating groups retained 0.20 and 0.06%, respectively, of the dose. The placental route contributed about three times more Pu to the progeny than did milk. These roles were reversed after the second pregnancy, when Pu was well-fixed in the tissues. The neonates, after 14 days of nursing, had body burdens two to five times greater than the 20-day fetuses.

That Pu sequestered by mammary tissue is available for transfer via milk to sucklings was shown by the approximately five times greater Pu burden in progeny of lactating rats than in those of the other groups (t-test, $P < 0.05$).

The amount of Pu in rats' milk available to progeny was estimated from the concentration values calculated from our data (Figure 1) and from milk production data for rats (T. D. Luckey et al., J. Nutr. 54: 345-359, 1954). We estimate that, for the lactating group, at least 16% of the Pu dose was available in the milk during the first nursing period. Based on an average concentration of 0.005% Pu dose/g, litters from dams that received Pu while pregnant were exposed to ~1.3% of the Pu dose via milk. After the second pregnancy, litters were exposed during the 14-day nursing period to <0.02% and ~0.14%, respectively, of the Pu dose in milk from dams of the pregnant or lactating groups.

In a litter of 10 pups, each pup of the first litter born to dams injected while lactating ingested 1.6% of the Pu dose during the 20-day nursing period. These pups retained about 0.05% of the Pu dose,

thus absorbing 0.03 of that available in milk. A somewhat similar calculation for the pregnant group's second pregnancy gives an absorption of 0.05.

The amount of Pu transferred via milk depends on Pu concentration (a function of time after Pu administration and the physiological activity of the mammary tissue at the time of injection), as well as the ability of the suckling's gut to discriminate against Pu (in turn, a function of gut maturation).

In attempting to extrapolate these data to humans, one must consider that, at birth, the human infant's gut is more mature than the rat's, and likely to discriminate against Pu to a greater degree than the newborn rat. Moreover, the concentration of Pu in human milk may be considerably less. This seems likely because of the known association of Pu with transferrin, produced in large quantities by active rat mammary gland, and the exclusive carrier of large quantities of Fe in rat milk. In contrast, lactoferrins are the carriers for the comparatively small amount of Fe transported in human milk. Only a small amount of Pu, if any, would be associated with this transport mechanism.

TABLE 1. Pu in Milk and Progeny After the Intravenous Administration of Pu Citrate to Rats When Nulliparous, Pregnant (19th Day of Gestation), or Lactating (1 Day Postpartum). Values are $\bar{X} + s\ \bar{X}$ (n).

Group	Time After Pu Injection to Dam, day	Concentration of Pu in Mammary Tissue, 10^{-6} Pu dose/g	Concentration of Pu in Milk, 10^{-6} Pu dose/g	Exposure to Pu in Utero, day	Exposure to Pu Via Milk, day	Age of Progeny When Killed, days	Fraction of Injected Pu in Each Progeny, 10^{-6} Pu dose
Pregnant	1	4.4 ± 0.7(5)[a]		1	0	2	75 ± 1.10(1)[b]
	7	9.8 ± 2.1(5)	0.52 ± 0.07(5)	3	4	4	29 ± 4.4[c]
	21	8.5 ± 1.9(5)	0.56 ± 0.17(5)	5	18	18	19 ± 1.21[c]
	45	16 ± 0.6		7	21	42	20 ± 1.12[c]
Lactating	1	48 ± 2.5	2.5 ± 6.4[c]	0	1	2	0.89 ± 0.08(15)[c]
	7	31 ± 3.5	1.7 ± 0.2.4	0	7	8	3.9 ± 0.6.9[c]
	21	32 ± 6.5	5.3 ± 0.8.4	0	20	22	4.3 ± 0.6.15[c]
	45	52 ± 7.5(5)		0	20	46	6.4 ± 0.6.14[c]
Nulliparous	~84	2.2 ± 0.2(4)		20	0	2	0.050 ± 0.004(10)[b]
Pregnant	~84	3.0 ± 1.0(2)		20	0	2	0.058 ± 0.006(8)[b]
Lactating	~84	23 ± 3.0(6)		20	0	0	0.062 ± 0.002(3)[b]
Nulliparous	~107	2.5 ± 7.3(5)		22	14	14	0.15 ± 0.02(8)[c]
Pregnant	~107	2.6 ± 0.4(6)	0.087 ± 0.001(5)	22	14	14	0.17 ± 0.02(20)[c]
Lactating	~107	3.4 ± 6.3(2)	0.26(1)	22	14	14	0.84 ± 0.25(3)[c]

(a) Number of samples (n).
(b) Fetus at 20 d g.
(c) This represents 1.02 Pu in all analyzed tissues. Pu dose in gastrointestinal tract including contents. The 1.02 adds back ~2 of progeny's Pu that is in gastrointestinal tract tissues. This correction factor is based on the observed fraction of gastrointestinal tract Pu so that in the total rat of 1.2 1.7 for non-nursing progeny.

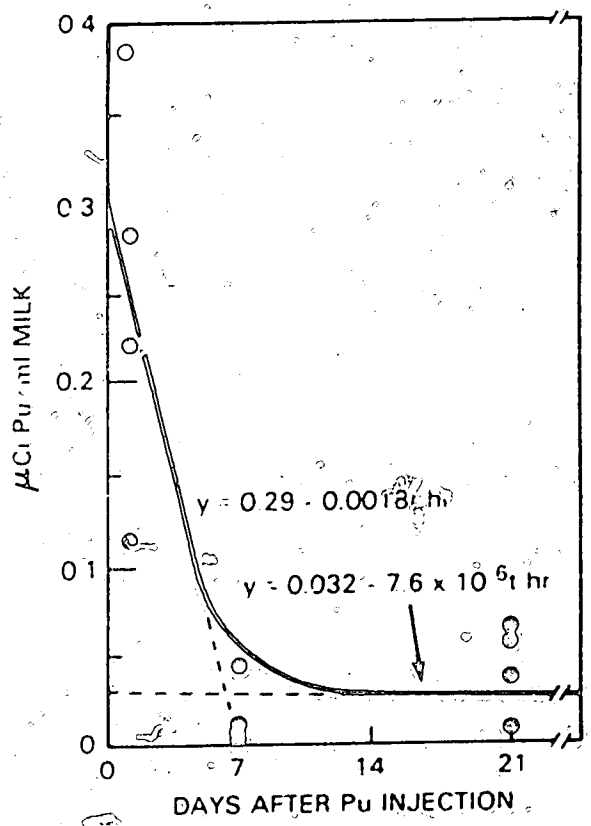

FIGURE 1. Concentration of ^{239}Pu in Milk From Rats Injected With Pu Citrate 1 Day Postpartum.

○ Gut-Related Studies of Radionuclide Toxicity

This project is concerned with the behavior of radioactive materials of importance in the nuclear industry that may be ingested as a consequence of a reactor accident, of unavoidable occupational exposure, or after release to the environment and incorporation into the food chain. Current emphasis is directed toward evaluating hazards from ingested actinides as a function of animal age, animal species, animal nutritional state, diet or chemicophysical state of the radionuclide. It is also concerned with nuclides that may be inhaled and passed through the gastrointestinal tract after clearance from the lungs.

EFFECTS OF FASTING, DIET OR "BIOLOGICAL INCORPORATION" ON ABSORPTION OF PLUTONIUM FROM THE GASTROINTESTINAL TRACT

Investigator: M. F. Sullivan

Technical Assistance: L. S. Gorham and K. D. Fisk

Solutions of ^{238}Pu nitrate (pH 2) and ^{238}Pu citrate were administered intragastrically to mice that were fasted for intervals of from 1 to 4 days. Absorption was increased 10 to 20 times over that measured in nonfasted mice. This observation was supported in a second study with rats, which were maintained on a milk and/or rat chow diet, then fasted 16 hr before gavage with ^{238}Pu nitrate. Absorption by fasted animals was twice that of unfasted animals. Absorption by milk-fed rats was about twice that of those fed milk and rat chow or water and rat chow. A third study measured absorption of organically bound (liver) Pu. The amount of organically bound ^{238}Pu retained was twice that of ^{239}Pu nitrate, but slightly less than that of ^{238}Pu citrate.

We demonstrated earlier (Annual Reports, 1975, 1976) that plutonium organically bound to either animal or plant tissue was more effectively absorbed from the gastrointestinal tract than inorganic forms. Our experiments (Annual Report, 1979) and those of Stather et al., Health Phys. 34, 1980) showed that fasting caused increased absorption of ^{239}Pu. Further, absorption of heavy metals increased in animals maintained on a milk diet (Kello and Kostial, Environ. Res. 6: 355, 1973). The purpose of the present studies was to determine: 1) if the duration of fasting directly affected absorption, 2) the effect of a milk diet on ^{238}Pu absorption, and 3) to provide further information on the effect of organic binding on gut transport of ^{238}Pu.

Mice were fasted for various intervals, then gavaged with ^{238}Pu nitrate (pH 2), as were controls that were fed ad lib. Thereafter, all animals were maintained on mouse food until they were killed 7 days later.

Rats on the milk diet received 2% (low-fat) milk as their sole source of food and drink for 2 wk prior to gavage with ^{238}Pu nitrate (pH 2). Controls received rat chow plus either milk or water. Half the animals continued on their diet until gavage; the other half were fasted for 16 hr before gavage with ^{238}Pu nitrate. All rats were maintained on their respective diets until killed 7 days after gavage.

Liver for the studies on the effect of "biological incorporation" of ^{238}Pu was obtained from dogs that received intravenous injections of 850 μCi of either ^{238}Pu nitrate or ^{238}Pu citrate, and were killed 4 hr later. A control preparation was made by injecting the liver with solutions of ^{238}Pu citrate (in 5% sodium citrate) or homogenizing it with a solution of ^{238}Pu nitrate (in 0.01 N nitric acid). Nonradioactive liver was administered to controls that were gavaged with a solution of ^{238}Pu nitrate or citrate. Excreta were collected for 7 days before the rats were killed.

Results from the fasting studies with mice (Figures 1 and 2) showed increased absorption and retention with increased

period of fasting; the major effect, however, occurred with one-day's fast. There was little difference between absorption of ^{238}Pu citrate and ^{238}Pu nitrate by the nonfasted controls, but absorption of the citrate by fasted mice was greater than that of the nitrate, as previously reported. As shown in Figure 3, fasting increased plutonium absorption in the chow-fed control rats, but had little effect on the animals that received milk. The milk diet resulted in increased retention in both skeleton and liver, and a markedly increased excretion in urine. The guts of groups fed chow with either milk or water contained 0.002% of the plutonium administered, those fed only milk contained 0.2%. This 100-fold difference deserves further investigation to determine if milk causes functional changes for plutonium absorption that resemble those of the neonatal gut.

Data from the administration of organically bound ^{238}Pu are shown in Figure 4. Solutions of ^{238}Pu nitrate or citrate fed to controls were identical to those injected intravenously into the dogs from which the liver was taken. The dose of "incorporated plutonium" was determined by the amount of liver homogenate that could be gavaged and by the radioactivity of the homogenate. Biological incorporation of the nitrate resulted in increased absorption and retention, especially in the nonskeletal carcass; urinary excretion of absorbed ^{238}Pu was also greatly increased as compared to controls. On the other hand, absorption of the citrate was higher in both control groups than in the group fed incorporated ^{238}Pu (Figure 4B). Stather et al. made similar observations with hamsters fed rat-liver-incorporated ^{239}Pu citrate (Phys. Med. Biol. 24: 396, 1979).

These studies show that fasting and diet have substantial, and complexly interacting, effects on plutonium absorption from the GI tract.

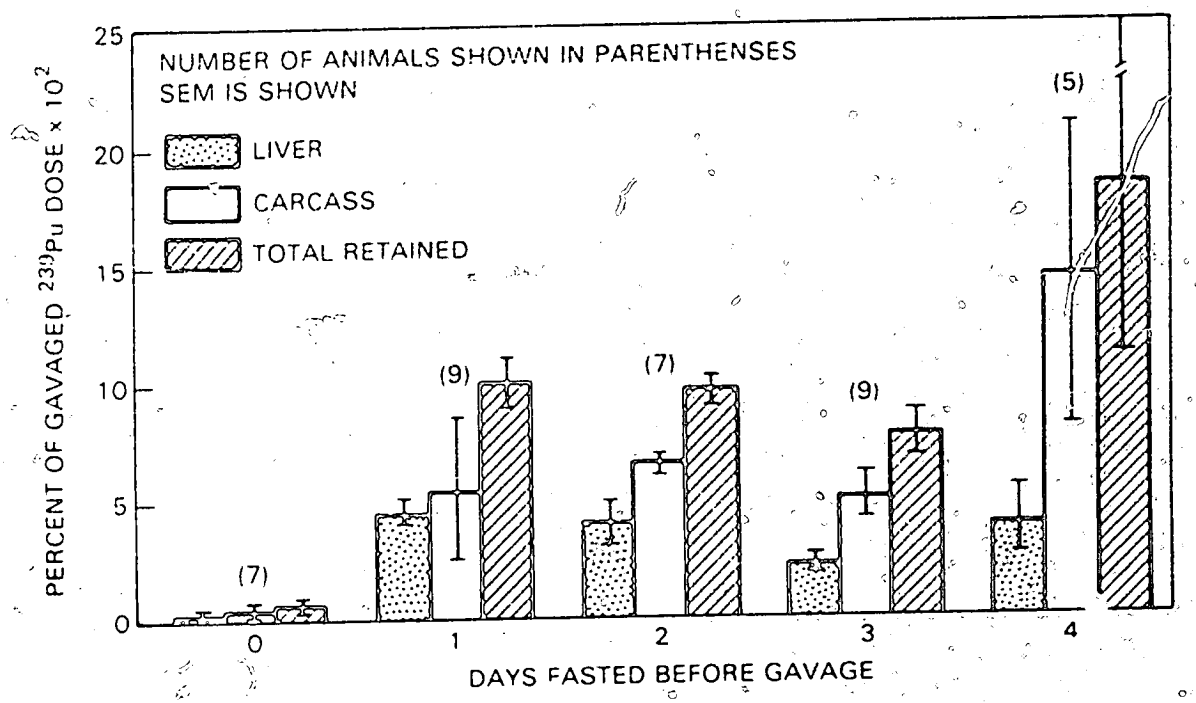

FIGURE 1. Retention of ^{238}Pu by Fasted or Nonfasted Mice Gavaged With ^{238}Pu Nitrate. "Carcass" includes all tissues except liver and GI tract. (Number of animals shown in parentheses; bar represents standard error of the mean.)

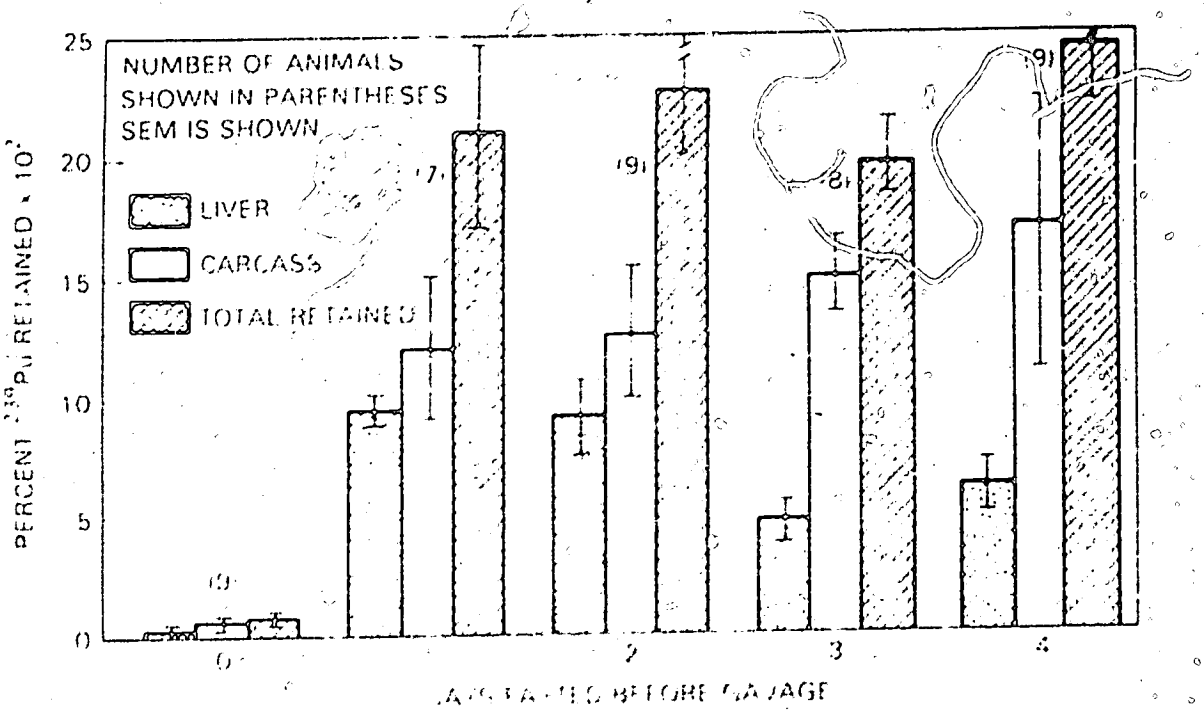

FIGURE 2. [illegible]

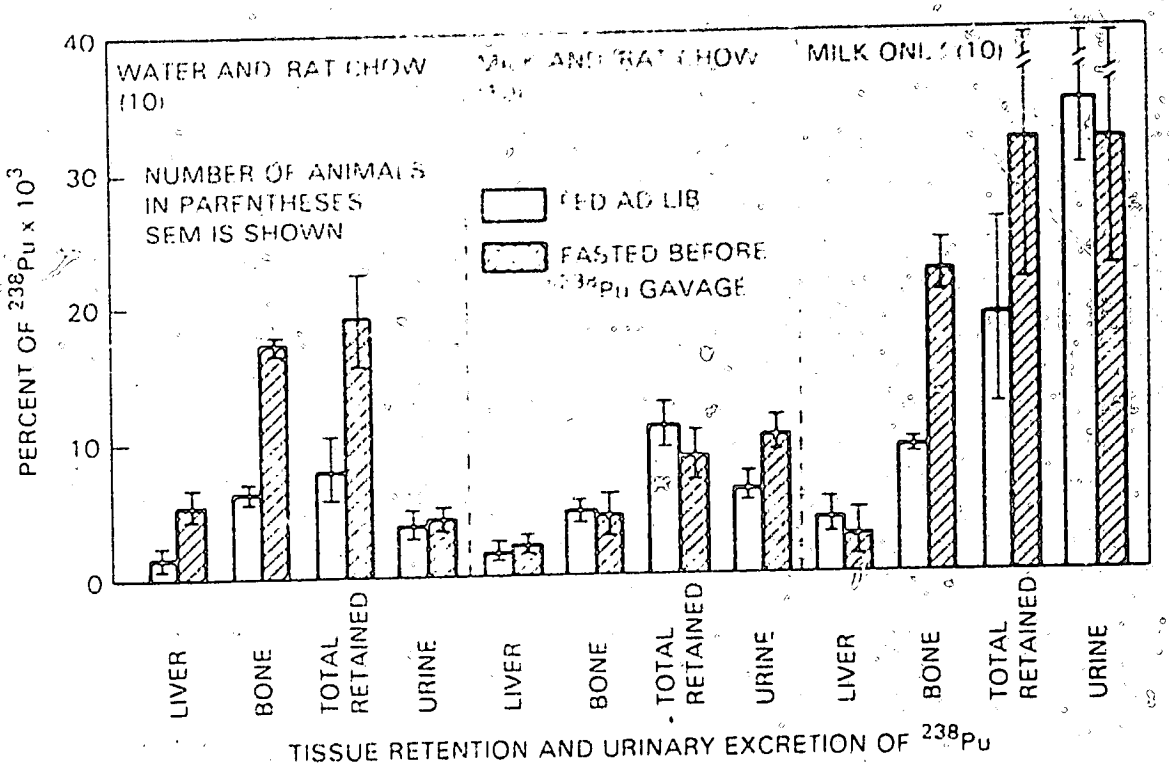

FIGURE 3. Absorption of ^{238}Pu by Fasted or Nonfasted Mice Gavaged With ^{238}Pu Citrate. "Carcass" includes all tissues except liver and GI tract. Skeletons were removed from seven rats in each group. Carcasses, excluding liver and GI tract, were measured for ^{238}Pu in the remainder.

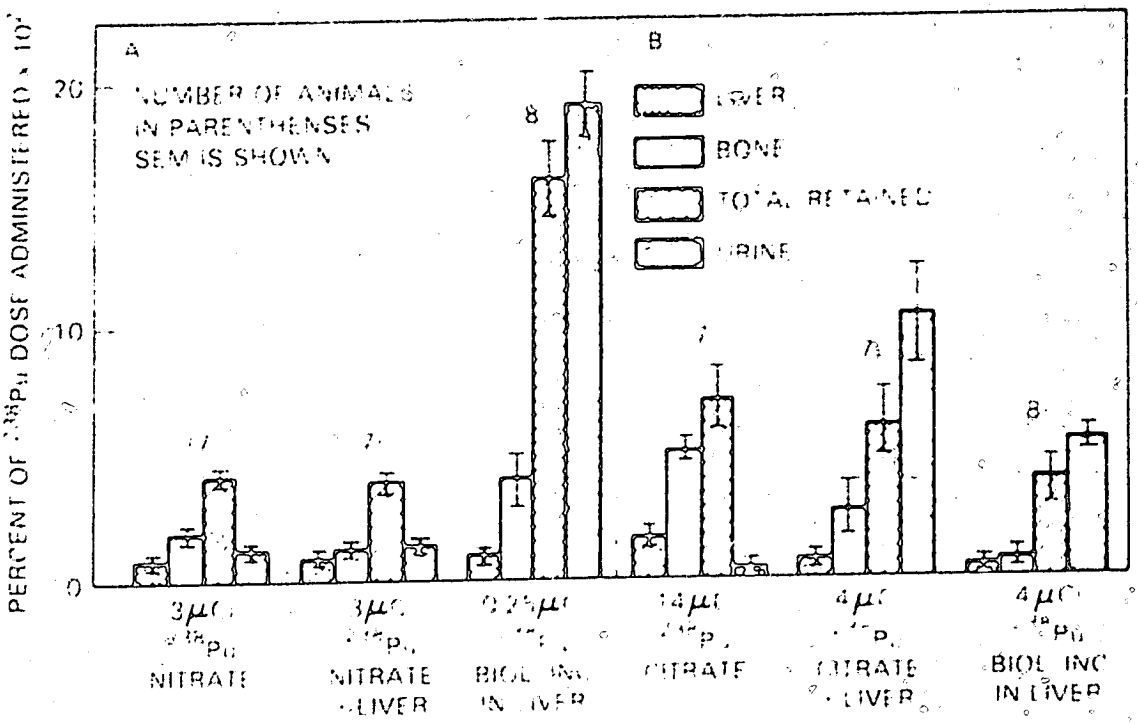

FIGURE 4A. [illegible]

FIGURE 4B. [illegible]

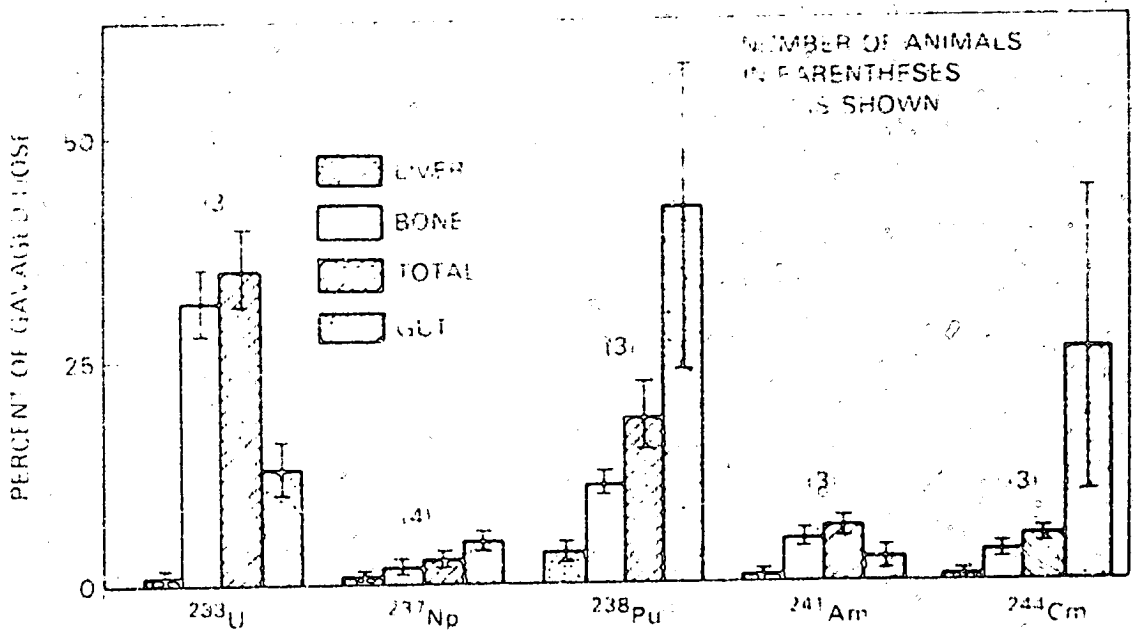

FIGURE 1. Distribution of Uranium-233, Neptunium-237, Plutonium-238, Americium-241 and Curium-244 in Neonatal Swine Gavaged at 3 Days After Birth With Nitric Acid Solutions, pH 2. Ages at necropsy were: ^{233}U, 12 days; ^{237}Np, 8 days; ^{238}Pu and ^{241}Am, 7 days; ^{244}Cm, 5 days.

LONG-TERM RETENTION OF PLUTONIUM-239 INGESTED BY NEONATAL RATS AND SWINE

Investigator: M. F. Sullivan and [illegible]

Technical Assistance: [illegible]

Litters of rats and swine gavaged with nitric acid solutions (pH 2) of ^{239}Pu were killed at intervals between a few days and a year after treatment. The ^{239}Pu content of most of the rat tissues decreased about tenfold within 4 mo; total carcass ^{239}Pu decreased from 1.4% of dose at 1 wk to 0.05% at 1 yr. Swine had absorbed about 16% at 1 wk, which increased to 26% by 1 wk. 11% was retained at 1 yr. No effect attributed to the retained plutonium were noted.

The earlier data (Annual Report, [illegible]) showed that retention of ^{239}Pu by rats gavaged as neonates decreased rapidly, by 40 days from retention by a factor of 1%, and skeletal retention by a factor of approximately 3. Rat data (Table 1) from the present experiment showed similar decreases, although the major release from the skeleton occurred after 40 days. In the animals killed at 1 yr, only [illegible] of the initial deposit remained, mostly in tissues. Littermate controls, weighed biweekly, exhibited weight gains that did not differ significantly from the treated animals.

TABLE 1. Retention of ^{239}Pu in Rats Gavaged with ^{239}Pu Nitrate at 1 Day After Birth. [illegible]

[illegible]

[illegible]

The data in Table 2 show that ^{239}Pu absorption by the neonatal swine was about [illegible] higher than for the rat. In both species, much of the nonabsorbed plutonium was retained in the mucosa of the gastrointestinal tract for a few weeks after ingestion. Much of that retained in the mucosa was eventually absorbed, but most is passed with the feces. Littermates of the pigs that were killed at preweaning intervals were killed after 3 mo [illegible]. They retained [illegible] and 4%, respectively, of the amount present at 1 wk.

Most of the ^{239}Pu in the gut of the neonatal swine had then moved [illegible]. The [illegible] was excreted by 1 wk [illegible]. In most tissues, retention was higher at 1 wk than at earlier periods. At 1 mo, most ^{239}Pu had been lost from both liver and skeleton, but the rate of loss was much lower than in rats. Although substantial quantities remained in both liver and skeleton at 1 yr after exposure, there were no grossly apparent effects. Fixed bones of both were sent to Dr. Wes[illegible], Department of Utah, for preparation of autoradiographs to determine retention [illegible] after deposition during the neonatal stage of development.

These studies demonstrate that although substantial quantities of plutonium were absorbed by neonatal rats and swine (~3 and 25%, respectively), no grossly evident effects were exhibited during their first year of life, despite the relatively high administered doses of 15 μCi/kg (swine) and 300 μCi/kg (rats). The differences in the amounts of plutonium retained by these two species may be due to differences in life span and to skeletal maturation rates. The rate at which the human will eliminate plutonium is apt to more closely resembles the rate in swine than that in rats.

TABLE 2. Plutonium Retained by Swine Gavaged at 1 Day of Age With ^{238}Pu Nitrate. (Number of animals is shown in parentheses.)

	Days After Gavage				
	2-4 (3)	15 (2)	21 (2)	90 (3)	365 (5)
	Percent of Gavaged Dose[a] ± SEM				
Lung	0.5 ± 0.12[b]	0.4 ± 0.05	0.6 ± 0.002	0.2 ± 0.07	0.02 ± 0.01
Liver	2.4 ± 0.6	3.1 ± 0.4	6 ± 1.5	3.0 ± 1.5	3.7 ± 0.3
Femur	0.5 ± 0.17	0.4	0.9 ± 0.2	0.8 ± 0.3	0.3 ± 0.5
Skeleton	9.5 ± 0.6	12.2 ± 3.7	18.0 ± 4.1	14.1 ± 4.1	7.5 ± 1.4
Kidneys	0.4 ± 0.08	0.1 ± 0.002	0.2 ± 0.03	0.2 ± 0.04	0.04 ± 0.01
Spleen	0.3 ± 0.1	0.07 ± 0.007	0.1 ± 0.03	0.05 ± 0.01	0.01 ± 0.001
Heart	0.07 ± 0.01	0.03 ± 0.001	0.07 ± 0.004	0.03 ± 0.01	
Small Gut Contents	34.9 ± 32.9 3.3 ± 0.001	14.9 ± 0.9			
Large Gut Contents	1.0 ± 0.6 24.8 ± 21.6	9.7 ± 6.1			
Total Gut	64 ± 3	24.6	6.2 ± 1	0.3 ± 0.2	
Muscle	3.1 ± 1.1	3.1 ± 1	1 ± 0.4	1.7 ± 0.9	
Skin	2.4 ± 0.7	1 ± 0.1	3.5 ± 1.2	0.2 ± 0.1	
Testes	0.02		0.02	0.02	
Total Absorbed	16.3	19	26	19.3	11.3
Total Retained	82.7	44.6	35.7	19.8	

(a) The ^{238}Pu nitrate dose was 5 μCi/kg, 95% filterable through a 0.01-μm Millipore filter and 67% TTA extractable (Pu(IV))

(b) Standard error of the mean

INFLUENCE OF OXIDATION STATE ON ABSORPTION OF INHALED PLUTONIUM

Investigators: M. F. Sullivan, J. L. Ryan, L. S. Gorham, and E. F. Blanton

Technical Assistance: B. L. Southward

Rats that were either fed ad lib., fasted for 18 hr before exposure, or fasted for 18 hr before and 72 hr after exposure, were administered either ^{239}Pu(IV) or ^{239}Pu(VI) nitrate by inhalation. Rats were killed at 5 days or 6 wk after treatment. Retention of Pu(VI) in the liver was 3- to 7-fold, and carcass retention 1- to 3-fold higher than that of Pu(IV). Fasting appeared to have no effect on absorption, suggesting that the increased absorption of Pu(VI) was due entirely to increased transport from the lung.

Considerable recent interest has centered on the fact that plutonium may be present in the environment in hexavalent form and the absorption of this Pu(VI) from the gastrointestinal tract may, under certain circumstances, be increased over that of Pu(IV). We have extended these observations to include a comparison of inhaled Pu(IV) and Pu(VI).

Groups of rats were exposed, nose-only, to aerosols of ^{239}Pu(IV) or ^{239}Pu(VI) nitrate. The Pu(VI) was prepared by passing an ozone stream through a nitric acid solution of ^{239}Pu(IV) for several hours. Some of the groups were fed ad lib. before and after exposure; some were fasted 18 hr prior to exposure; and others were fasted an additional 72 hr after exposure. One hour after exposure, five rats from each group were killed and analyzed for their ^{239}Pu content. This quantity, averaging 5.3 μCi/rat, was considered to be the inhaled dose for all groups. The remaining animals were killed at either 5 or 42 days postexposure. Data from their analysis are shown in Figure 1.

At 5 days, about 10% of the dose remained in the lungs regardless of the oxidation state inhaled. About 0.05% was retained in the livers of rats that inhaled Pu(IV); about five times that much was retained in the livers of those that inhaled Pu(VI). Retention in the skeleton was 0.1% for Pu(IV) and 0.8% for Pu(VI). Carcass values were three times higher after Pu(VI) inhalation than after Pu(IV) inhalation. Fasting had no observed effect on the retention of either Pu(IV) or Pu(VI).

Six weeks after exposure the quantity retained in the lung had decreased to 5% and was again not influenced by the oxidation state of the plutonium. The quantity in the liver increased at 5 days from 0.05% to 0.25% at 42 days in the rats that inhaled Pu(IV). There was no increase in those that inhaled Pu(VI). Carcass values increased to about four times the values found at 5 days for all groups, primarily due to plutonium movement into the skeleton. The Pu(VI) group fed ad lib. retained about one-third more plutonium than either of the fasted groups killed 6 wk after exposure.

It may be concluded from these data that two to three times as much Pu(VI) as Pu(IV) is absorbed. The effect occurs during the early period after exposure and is not influenced by the contents of the gastrointestinal tract. This suggests that none of the increase is due to enhanced gastrointestinal absorption of Pu(VI) cleared from the lungs.

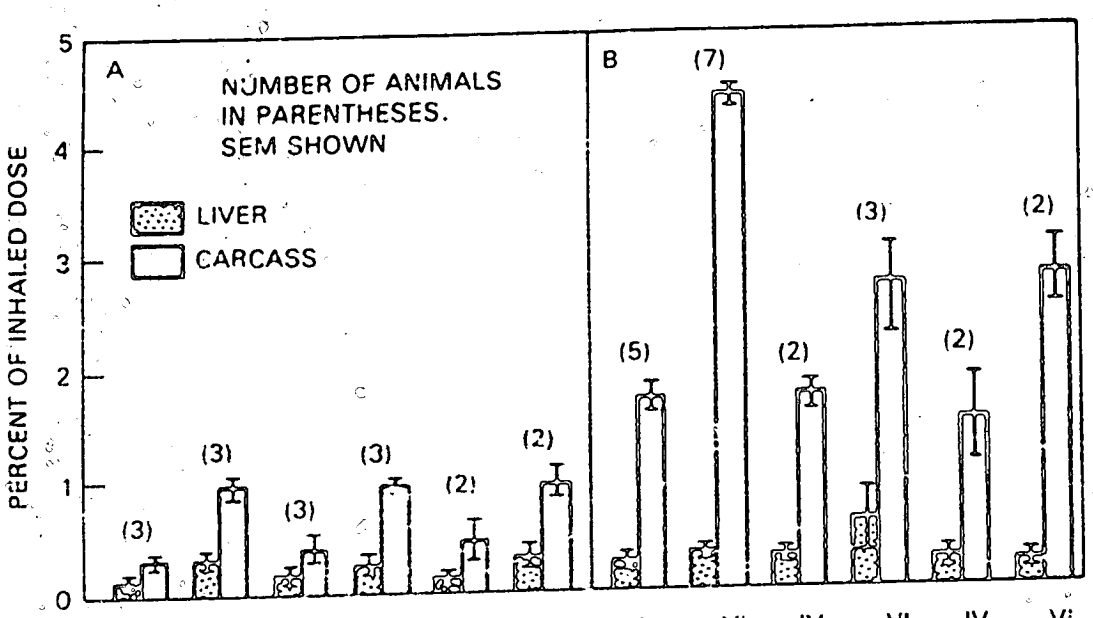

^{239}VALANCE	IV	VI	IV	VI	IV	VI	IV	VI	IV	VI	IV	VI
FASTED, hr	0	0	18	18	90	90	0	0	18	18	90	90
CMD, μm	0.199	0.225	0.199	0.225	0.199	0.225	0.199	0.225	0.199	0.225	0.199	0.225
GSD	2.187	1.045	2.187	2.045	2.187	2.045	2.187	2.045	2.187	2.045	2.187	2.045

FIGURE 1. Retention of Plutonium by Fasted and Non-Fasted Rats Administered ^{239}Pu(IV) or ^{239}Pu(VI) Nitrate by Inhalation and Killed Either 5 Days or 6 Weeks Later

INFLUENCE OF PLUTONIUM MASS ON ABSORPTION FROM THE GASTROINTESTINAL TRACT OF ADULT AND NEONATAL RODENTS

Investigators: M. F. Sullivan

Technical Assistance: L. S. Gorham

A group of adult mice gavaged with 0.15 ml of ^{237}Pu nitrate, pH 2, at a mass concentration of 1.3 x 10^{-4} g/kg of body weight, absorbed 10 times more plutonium than a group administered ^{239}Pu at a concentration about 10^{6} times higher. Neonatal rats absorbed about five times more ^{237}Pu than ^{239}Pu when the ^{237}Pu was fed at a mass level 10^{-7} times that of the ^{239}Pu. Thus, in both adult and neonatal animals, plutonium is more effectively absorbed at levels such as one might encounter in the environment than at the higher levels commonly used in experiments to measure absorption.

These experiments repeat, in a single experiment, previous observations made in different experiments on the effect of mass on absorption of plutonium by neonatal rats. The observations are also extended to adult mice.

Ten Swiss-Webster mice received 0.15 ml of ^{237}Pu or ^{239}Pu nitrate, pH 2, through a polyethylene catheter. The plutonium concentrations were 2.7 x 10^{-5} µg/ml (^{237}Pu), or 340 µg/ml(^{239}Pu). Whole-body measurements of ^{237}Pu retentions were made by measuring photon emission. Measurements were also made of tissues and total skeletons, which were separated at necropsy. Measurements of ^{239}Pu content were made by scintillation spectrometry.

Retention of the ^{239}Pu in the carcass of the adult mice after 6 days (Figure 1) was 0.01%, about three times larger than the values we have usually measured in adult rats, and equal to the absorption fraction currently employed for humans by the ICRP. Absorption of ^{237}Pu, fed at the much lower mass levels, was about 10-fold higher than that of ^{239}Pu.

Absorption by the neonate was measured using ^{237}Pu and ^{239}Pu at the same concentrations as in our previous studies. (The number of animals killed 1 week after treatment was greater because, in the previous study, we were measuring ^{237}Pu elimination by a serial, whole-body-counting procedure). Results from the experiment with neonatal rats are shown in Figure 2: about 0.26% of the ^{239}Pu was absorbed and retained, compared to five times that percentage of ^{237}Pu absorbed.

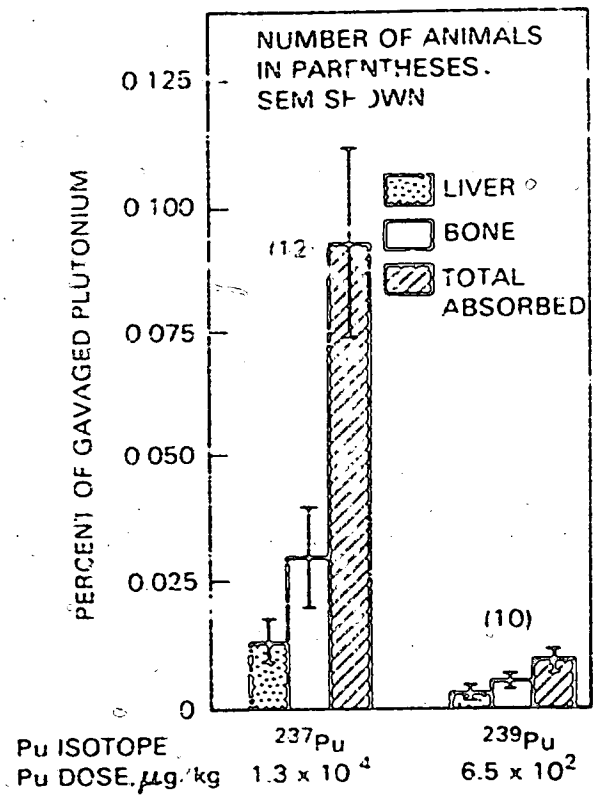

FIGURE 1. Retention of Plutonium in Adult Mice Gavaged With Either ^{237}Pu or ^{239}Pu Nitrate, pH 2 and Killed 6 Days Later.

At 1 wk after gavage, about 9% of the ^{239}Pu was found in the gut and its content, compared to 65% after ^{237}Pu administration. Based on results from prevous

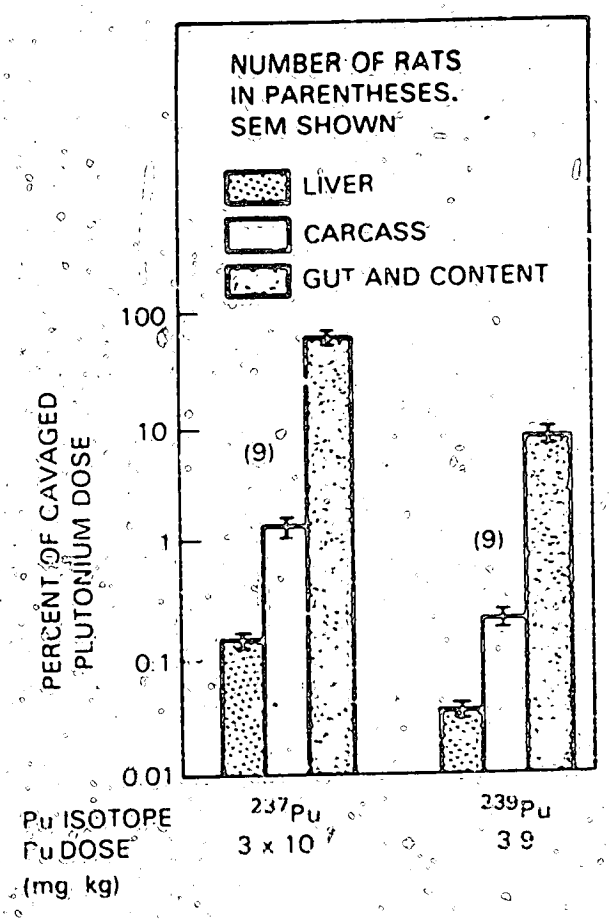

FIGURE 2. Retention of Plutonium by Neonatal Rats Gavaged at 2 Days After Birth with Either ^{237}Pu or ^{239}Pu Nitrate, pH 1.5, and Killed a Week Later.

studies, one would predict that most of the plutonium retained in the gut would eventually be excreted with the feces rather than absorbed.

These studies, and earlier reported results from this laboratory with ^{237}Pu in rats, suggest that absorption from very dilute solutions of plutonium may be substantially higher than the absorption measured at higher concentrations and employed in the derivation of intake limits by the ICRP.

Viral and Radiation Carcinogenesis

The studies included under this project are concerned with basic biological and biochemical indices that may aid in the detection and understanding of the primary effects of radiation insult and the initiation of the observed malignancies. A primary objective is to determine the role of virus in "radiation-induced" malignancies and in the process to identify those changes (biochemical, virological, immunological, etc.) which might serve to monitor the oncogenic process. Specific efforts include studies of leukemia-induced by the β-emitter ^{90}Sr, and lung and bone tumors induced by inhalation of the α-emitters, ^{238}Pu and ^{239}Pu.

IN VITRO EVALUATION OF CYTOTOXIC AND MUTAGENIC POTENTIAL OF ^{244}Pu

Investigators: M. E. Frazier, T. K. Andrews, Jr., and J. Samuel

In order to study the chemical toxicity and mutagenicity of plutonium, we evaluated the in vitro toxicity and mutagenicity of a low-specific-activity istotope (^{244}Pu; half life, 7.6×10^7 years) to mammalian cells. The cytotoxicity of ^{244}Pu, evaluated using clonal growth assay, revealed that this isotope was more toxic (on a μg/ml basis) than Cd, Hg, or Ni; less toxic than Cr, Ag, Au, or V and only slightly mutagenic.

The radiation emitted by ^{238}Pu and ^{239}Pu confounds evaluation of the chemical toxicity of the element. An estimate of the toxicity of Pu can be obtained by measuring effects of ^{244}Pu, an isotope of relatively low specific activity (1.9×10^{-6} Ci/g; half life, 7.6×10^7 yr).

In previous annual reports (1978, 1979) we described an in vitro method of evaluating the toxicity of metals in the clonal growth assay using VERO, a monkey kidney cell line. In this assay $^{244}Pu(NO_3)_4$, at varying concentrations, was added to microtiter wells containing 100 VERO cells and the number of clones (colonies) formed were counted. The proportion of cells that formed colonies (plating efficiency) was expressed as relative plating efficiency (RPE), i.e., the plating efficiency of the exposed sample divided by that of controls'. The Pu concentrations in the culture medium were measured by radioanalysis. A series of duplicate studies indicated that the ^{244}Pu did not complex with the plastic culture dishes, but remained suspended in the medium, and was therefore available to the VERO cells.

The toxicity of ^{244}Pu was compared with that of other metals by means of a value we call RPE_{50}, which is that concentration of test material that results in an RPE which is 50% that of control cells. By interpolation of concentration-response plots (Figure 1), we found an RPE_{50} for ^{244}Pu of ~0.12 μg/ml in replicate experiments. Our radioanalysis data indicated that the 0.12-μg/ml dilution represented

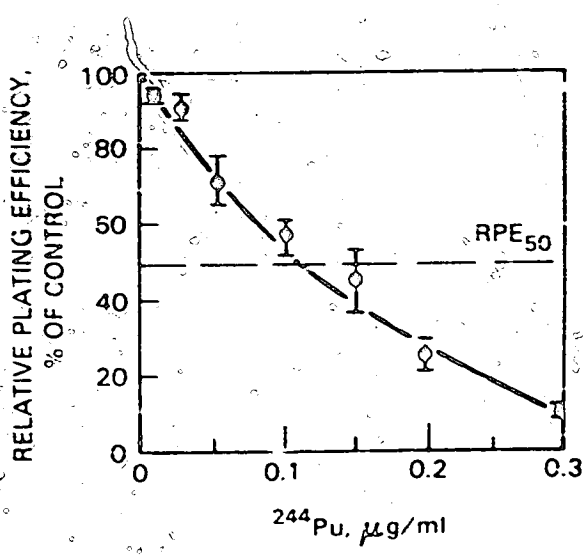

FIGURE 1. Effects of ^{244}Pu on the Plating Efficiency of VERO Cells. The means and ranges of replicates from two separate experiments are plotted.

only ~4 dpm/microtiter well. The RPE_{50} value reported here for ^{244}Pu is, therefore, a measure of the chemical toxicity of plutonium as a metal, since radiation controls using ^{238}Pu at levels of 100 dpm/microtiter well did not significantly alter the RPE from those of control cultures.

Using data from past studies (Annual Report, 1979) we have compared the RPE_{50} of several metals to that of ^{244}Pu (Table 1). These results show that although plutonium-244 is a highly toxic metal, at least five other metals tested in the VERO clonal growth assay are equally or more toxic.

Chinese hamster ovary (CHO) cells and the purine analog, 6-thioguanine (TG), were used to quantify mutation induction at the hypoxanthine guanine phosphoribosyl transferase (HGPRT) locus. The CHO/HGPRT assay is based on the fact that TG is converted to the nucleotide by HGPRT activity of wild-type cells. The nucleotide thus produced (or its metabolites) is lethal to all cells retaining the HGPRT enzyme system. Only the mutants lacking the HGPRT enzyme are able to survive and grow in the presence of TG. The CHO/HGPRT assay has shown a linear dose-response with metallic mutagens.

TABLE 1. Comparison of In Vitro Cytotoxicity of ^{244}Pu With Several Other Metallic Ions.

Test Agent[a]	RPE_{50}[b] Dose µg Metal/ml[c]
V	0.03
Au	0.05[g]
Ag[d]	0.05[g]
Cr[e]	0.06
Ru	0.1
^{244}Pu[f]	0.12
Cd[e]	0.3
Hg	0.5
Ni	1.1
Pt	3.3
Co	3.5
Pd	4.8
Zn[d]	[illegible]
Cu[d]	8.6
Mn[d]	15
Pb	37
Fe	59
Mg	>2000
Ca	>3000

(a) All metals tested as chloride salts except where noted
(b) RPE_{50} = the concentration at which the plating efficiency to the exposed cultures is 50% that of control cultures
(c) Metal concentrations were determined using X-ray fluorescence
(d) Also tested as a sulfate salt
(e) Tested as chromate
(f) Tested as a nitrate, analysis determined using radiation detection techniques
(g) Metal analyses not complete using value of dilution

In these studies, approximately 10^6 cells were exposed to varying concentrations of ^{244}Pu and placed in normal culture medium for an additional 4 hr. The cells were then trypsinized, and a portion was used to evaluate the cytotoxic effects of the exposure regime on the CHO cells. The remaining cells were subcultured for 7 days to allow phenotypic expression of the mutation. The absolute plating efficiency (APE) of the CHO cells was determined, and the number of mutants scored, by counting the numbers of colonies present in petri dishes seeded with 10^6 cells/dish in medium containing TG. Finally, the APE was divided into the number of mutants/10^6 cells to give the mutation frequency/10^6 viable cells (Figure 2). Our initial experiments (data not shown) indicated no significant increase in mutation frequency, relative to controls, for up to 5 µg/ml of ^{244}Pu. However, above that concentration, considerable toxicity resulted from either the pH of the medium or the increased osmolarity resulting from the NaOH required to neutralize the ^{244}Pu solutions originally prepared with nitric acid.

In an attempt to overcome the problem of acidity, we added HEPES buffer (25 mM) to the cell culture medium. As a result, we were able to reach levels up to 18 µg/ml of ^{244}Pu without significantly increasing toxicity or mutation in equivalent acid-containing controls. The preliminary results shown in Table 2 indicate that plutonium (as a metal) may be slightly mutagenic. At levels of 6.3 µg/ml of ^{244}Pu, or above, we observed a 4- to 5-fold increase in mutation frequency (significant at $P < 0.05$) relative to controls. However, a linear dose-response relationship was not observed in these experiments. The form of the ^{244}Pu in the culture medium is unknown and a high proportion of it may have been colloidal polymer or hydroxide and not available to the cells. Thus, the toxicity of the monomeric (soluble) form may be higher than that of our estimates.

Increased mutation frequency with ^{244}Pu appears to be the result of chemical

mutagenesis since similar levels of nitric acid or radiation (using ^{238}Pu as a control) did not affect the mutation frequency of CHO cells. Additional experiments are underway to complete in vitro comparisons of the cytotoxicity and mutagenicity of ^{244}Pu as a metal using ^{238}Pu and ^{239}Pu as radiation controls.

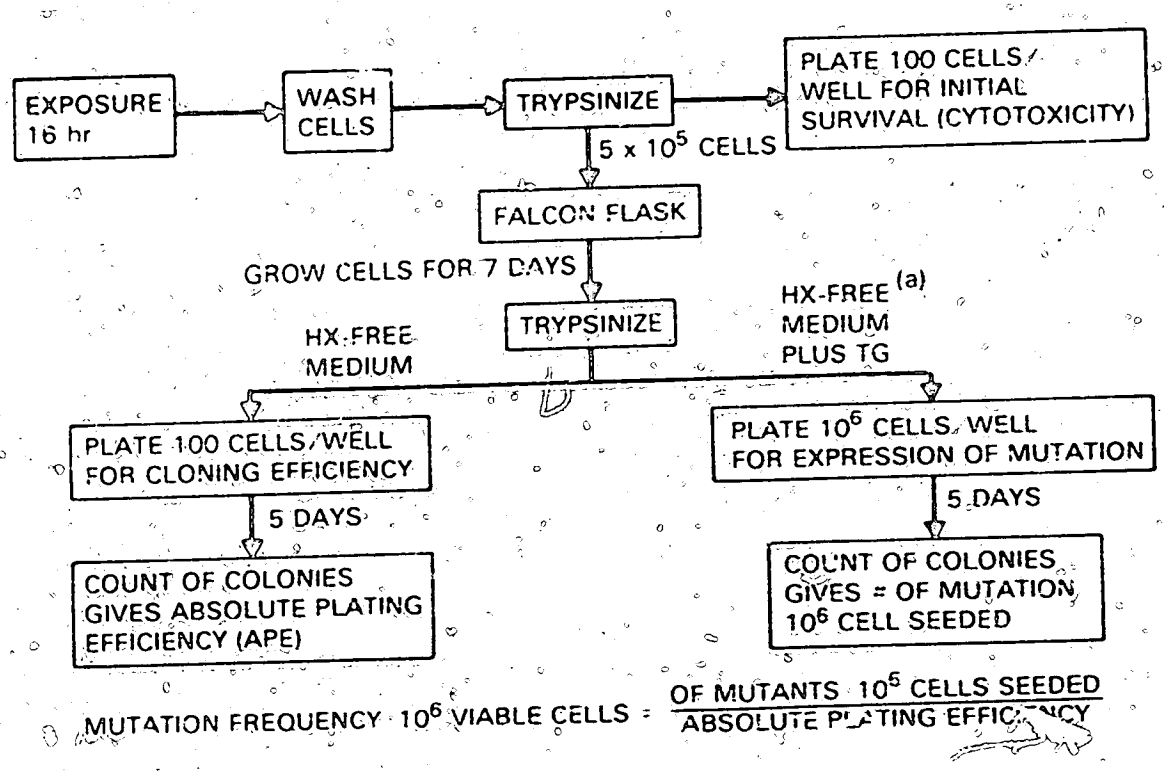

FIGURE 2. Flow Chart for the Mutation Assay Using the CHO HGPRT Assay System.

TABLE 2. Mutation Frequencies of CHO Cells Exposed to ^{238}Pu or ^{244}Pu

Treatment[a]	dpm/Plate[b]	Mutation Frequency/ 10^6 Viable Cells[c]
^{244}Pu µg/ml		
18.8	4016	30.5
12.5	2677	34.5
6.3	1399	26.5
5	1071	7
1.3	268	4.8
0.5		3
0.05	10.7	4.8
0	0	6.5
EMS[d], %		
0.03	0	216.5
^{238}Pu µg/ml		
1.97×10^{-5}	3750	4.4
1.31×10^{-5}	2500	4.2
6.55×10^{-6}	1250	2.4
2.62×10^{-6}	500	5
1.31×10^{-6}	250	4.4
2.62×10^{-7}	50	4.6
2.62×10^{-8}	5	4.8
0		5.4
EMS, %		
0.03		230

(a) Cells exposed for 16 hours. The medium used in these studies contained 25 mM HEPES buffer in addition to the normal bicarbonate buffering system. Neutralization of the initial stock solution required considerably less NaOH than was required in the previous studies.

(b) Disintegrations per minute based on 5 ml volume per plate. 3 replicate 2 ml samples were assayed for ^{244}Pu

(c) Mutation frequency based on average of 12 petri dishes corrected for viable cells based on cloning efficiency determinations.

(d) EMS = Ethyl Methane Sulfonate

CHARACTERIZATION OF PORCINE RADIATION-INDUCED VIRAL DNA POLYMERASE

Investigators: M. E. Frazier, L. P. Mallavia, M. J. Hooper, and M. V. Viola

An RNA-dependent DNA polymerase (RDDP), purified by column chromatography from porcine radiation-induced retrovirus (PoRRV), was found to have a molecular weight of ~70,000. The RDDP from PoRRV is antigenically related to similar enzymes from two other known mammalian type C viruses, and antigenically distinct from normal cellular enzymes.

In a previous Annual Report (1979) we described the purification of an RNA-dependent DNA polymerase from a virus (PoRRV) found in swine with leukemia induced by ^{90}Sr. This enzyme (PoRRV-RDDP) catalyzes the synthesis of DNA from an RNA template and was differentiated from cellular DNA polymerases by its template specificity, chromatographic characterization, and the optimal reaction conditions required for DNA synthesis. This year we have completed the final characterization, and have verified that the enzyme is a reverse transcriptase of viral origin.

The enzyme, purified by column chromatography oligo dT_{12-18} cellulose, was centrifuged on preformed gradients of 10-30% glycerol for 16 hr at 44,000 rpm (SW 50.1 rotor). Fractions were collected, dropwise, from the tubes containing the gradients and analyzed for DNA polymerase activity with poly(rA) · $(dT)_{12-18}$ and poly(dA) · $(dT)_{12-18}$ templates, protein and refractive index. Lactoperoxidase (77,500 MW) and bovine serum albumin (68,000 MW) were processed in similar fashion as sedimentation markers. Sedimentation of the poly(rA) · $(dT)_{12-18}$ synthetase activity indicates a single component with a molecular weight between 68,000 and 77,500, as determined by its relationship to the marker proteins (Figure 1). These molecular-weight determinations help to differentiate the PoRRV DNA polymerase from cellular DNA polymerases such as α (110-220,000 MW), β (45,000 MW), or γ (110-330,000 MW) polymerases. Similar results have been obtained using enzyme from three separate purification experiments. The results further indicate that the molecular weight of the PoRRV DNA polymerase is near the 70,000 value observed with most mammalian viral reverse transcriptases.

We also evaluated the immunological cross-reactivity among PoRRV DNA polymerase, viral reverse transcriptases, and cellular DNA polymerases. Antisera, prepared and standardized by contractors for the National Cancer Institute, were supplied to us by Dr. Jack Gruber. Standard neutralization assay mixtures were prepared, containing 10 μl of PoRRV-DNA polymerase and a specific concentration of an anti-DNA polymerase IgG preparation. After 30 min, the reactions were terminated and the amount of newly synthesized DNA was measured to determine the extent of neutralization by antibodies in the IgG preparation (Figure 2).

The PoRRV DNA polymerase was inhibited by anti-IgG prepared against Rauscher leukemia (RLV) and simian sarcoma virus (SSV) reverse transcriptases (both type C viruses; Figure 3). These antisera (60 μg IgG) inhibited ~40% of the PoRRV polymerase activity, indicating significant cross-reactivity. The inhibition of homologous virus reverse transcriptase was 90-95% at 60 μg/ml of IgG (data not shown). However, cross-reactivity was not observed with IgG antisera prepared against DNA polymerases from either type B retrovirus (Mason Pfizer monkey virus or murine mammary tumor virus) or from an unrelated type C virus such as the avian myeloblastosis virus (AMV) of chickens (Figure 3). Likewise, antisera against cellular DNA polymerases did not affect DNA synthesis by the PoRRV DNA polymerase (Figure 4). This lack of cross-reactivity with the α, β, and γ DNA polymerases from normal cells, and the cross-reactivity with type C virus DNA polymerases (of RLV and SSV), provide the final evidence necessary to prove that the DNA polymerase from PoRRV is a viral reverse transcriptase.

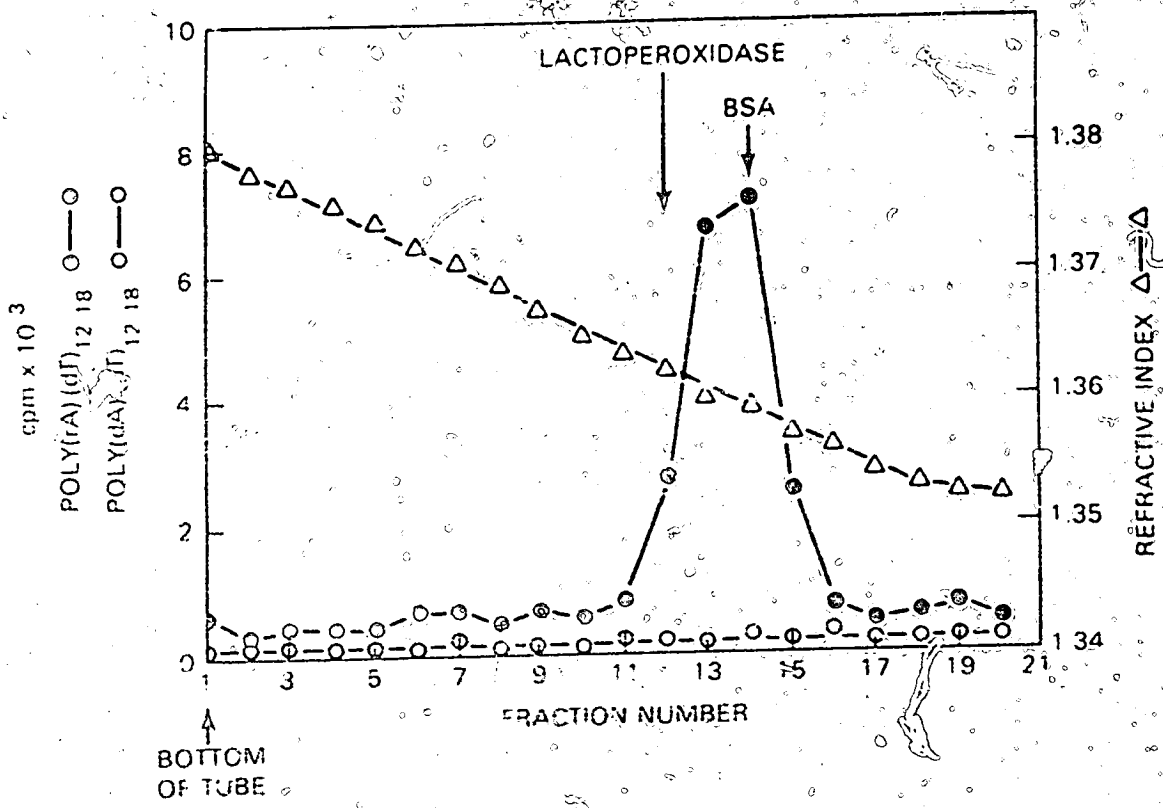

FIGURE 1. Velocity Sedimentation Analysis of DNA Polymerase Isolated From PORRV [illegible] refraction index, [illegible] poly(rA)(dT)12-18 assay [illegible] poly(dA)(dT) assay. The lactoperoxidase marker has a molecular weight of [illegible] 77,500 and a sedimentation coefficient of 5.45, bovine serum albumin, 68,000 MW and 4.35 marker.

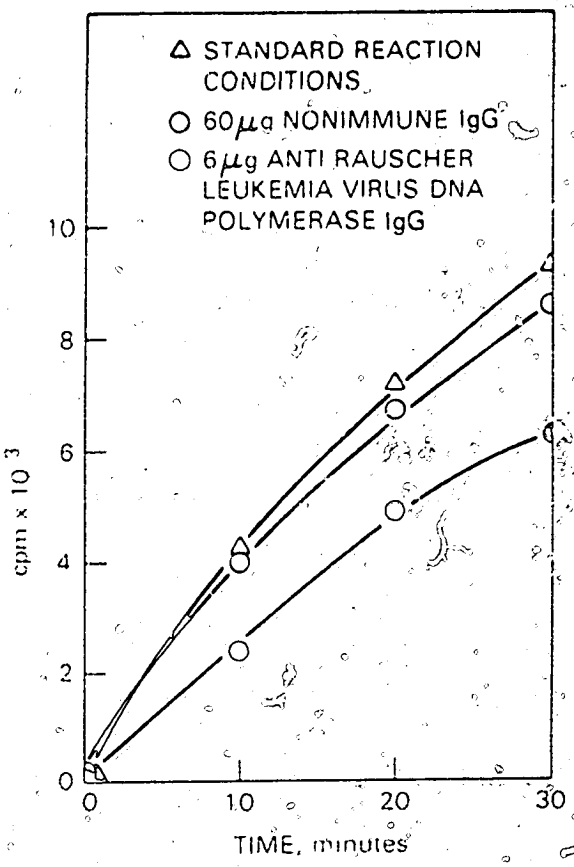

FIGURE 2. Effect of Antireverse Transcriptase and Nonimmune IgG on Kinetics of Incorporation of Synthesis of DNA by PoRRV-DNA Polymerase. The reactivity of antibodies was determined by measuring DNA synthesis by the PoRRV-RDDP in the presence of IgG containing antibodies to Rauscher leukemia virus (RLV) DNA polymerase (○-○) or nonimmune IgG (△-△).

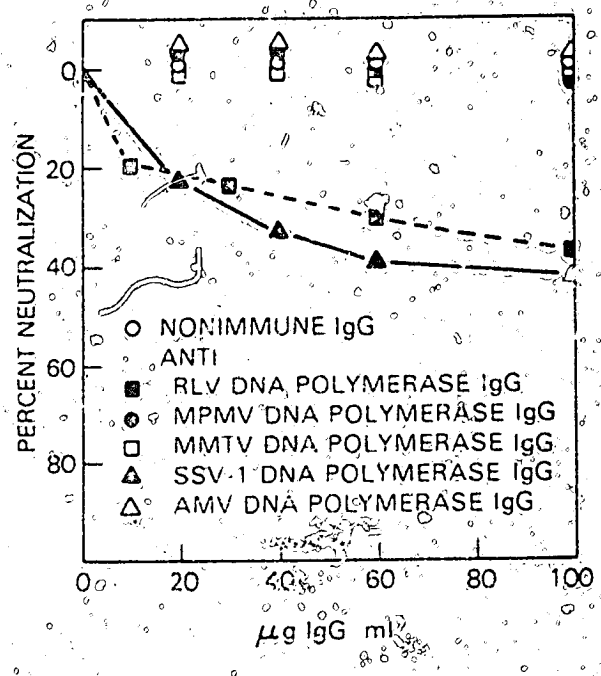

FIGURE 3. Effects of Antiviral DNA Polymerase IgG on Activity of Purified PoRRV-DNA Polymerase. Nonimmune rabbit IgG was tested at comparable concentrations for determination of percent neutralization. (○-○), nonimmune IgG; (■-■), anti-Rauscher leukemia virus (RLV) DNA polymerase IgG; (●-●), anti-Mason Pfizer monkey virus (MPMV) DNA polymerase IgG; (□-□), antimouse mammary tumor virus (MMTV) DNA polymerase IgG; (▲-▲), antisimian sarcoma virus (SSV-1) DNA polymerase IgG; and (△-△), antiavian myeloblastosis virus (AMV) DNA polymerase IgG.

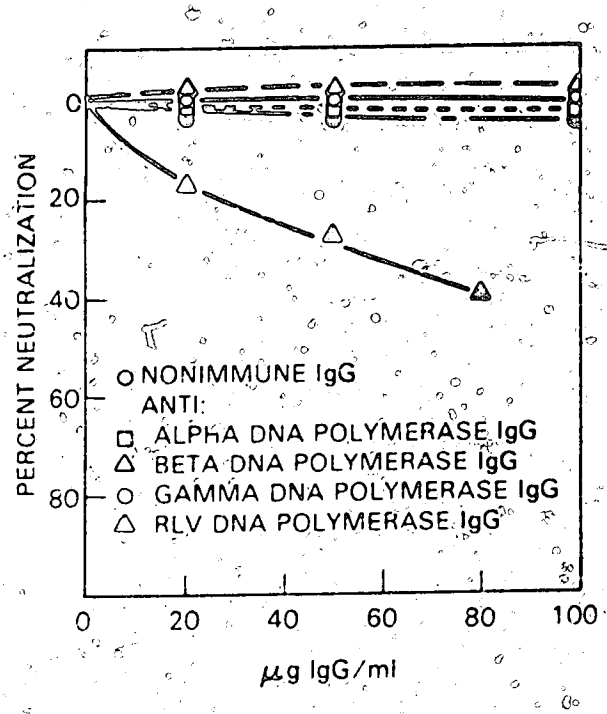

FIGURE 4. Effect of Anticellular DNA Polymerase IgG on Activity of Purified PoRRV-DNA Polymerase: (o-o), nonimmune rabbit IgG; (□-□), anti-α DNA polymerase IgG; (△-△), anti-β DNA polymerase IgG; (o-o), anti-γ DNA polymerase IgG; (△-△), anti RLV DNA polymerase IgG.

IN VITRO CELL-MEDIATED IMMUNITY IN BEAGLE DOGS EXPOSED TO $^{238}PuO_2$

Investigators: J. E. Morris, T. M. Graham, and J. F. Park

Technical Assistance: P. D. Mayes and M. J. Steele

Mitogen-induced stimulation of DNA synthesis in canine peripheral-blood lymphocytes (PBL) from $^{238}PuO_2$-exposed and control dogs was assayed in whole-blood, and density-gradient-isolated lymphocyte cultures. Mitogenic response to phytohemagglutinin (PHA) and pokeweed mitogen (PWM), but not to concanavalin-A (Con-A), was reduced in whole-blood cultures from $^{238}PuO_2$-exposed dogs. However, maximal mitogenic responses of isolated PBL cultures containing the same numbers of cells from exposed dogs were not statistically different from those of controls, indicating that the lymphopenia alone could account for the observed differences in whole-blood cultures. Lower concentrations of PHA were required for maximal stimulation of isolated lymphocytes from exposed dogs when compared to controls.

Dogs that have inhaled plutonium oxide (^{238}Pu or ^{239}Pu) develop a dose- and time-dependent lymphocytopenia as the first observed biological effect of exposure. In dogs with initial $^{238}PuO_2$ lung burdens of 0.1-2 μCi, a correlation was observed between initial deep-lung deposition and levels of B-lymphocytes in the peripheral blood. In addition, the response (DNA synthesis) to T- and B-cell-specific mitogens in both whole-blood and density-gradient-isolated lymphocytes was reduced in exposed animals as compared to controls (Annual Report, 1979).

The present studies investigated the mitogenic response of peripheral-blood lymphocytes (PBL) obtained from $^{238}PuO_2$-exposed dogs. The dogs used in this study were divided into three age-matched groups (Table 1): an unexposed control group and two exposed groups, with mean initial deep-lung depositions of 106.0 ± 9.3 and 1182.5 ± 310.7 nCi, respectively. Both exposed groups showed an average lymphocyte level approximately 65% of control values.

In the mitogen stimulation assays (employed as an in vitro correlate of cell-mediated immunity), lymphocytes were stimulated with Con-A, PHA and PWM. The Con-A and PHA are plant lectins which stimulate cell division of T-lymphocytes; PWM is a plant lectin that preferentially stimulates B-lymphocytes and a small population of T-cells. Lymphocyte activation was measured by the incorporation of ^{125}I-iododeoxyuridine (^{125}I-IUdR) into newly synthesized DNA.

In whole-blood cultures (Table 2), we observed statistically significant reductions ($P = 0.05$) in the response of PBL to PHA (Group III) and PWM (Groups II and III) when compared to controls. The reduced response of PBL to Con-A was not statistically significant, and the concentration-dependent bimodal response of canine lymphocytes to Con-A (Annual Report, 1979) was present in all three Groups.

Stimulation of a constant cell number of isolated peripheral blood lymphocytes (obtained by a density-gradient technique) resulted in no statistically significant reduction in peak mitogenic response of lymphocytes from exposed dogs when compared to controls (Figures 1 and 2). However, the concentrations of PHA required to induce maximum incorporation of ^{125}I-IUdR by PBL from exposed dogs was only 50% (Figure 2) of that required for maximal stimulation of control dogs (45 mg/ml vs ~90 mg/ml). This may indicate that ^{238}Pu exposure does, indeed, have some effect on the responsiveness of PBL to PHA stimulation.

The reduced mitogenic response in whole-blood culture of PBL from $^{238}PuO_2$-exposed dogs thus appears to result from the fewer lympocytes present; the response lymphocyte was unchanged. It should noted that this response of PBL from $^{238}PuO_2$-exposed dogs is different from that previously reported for lymphocytes from $^{239}PuO_2$ dogs (Annual Report, 1979). In the $^{239}PuO_2$ studies, mitogenic response per lymphocyte was reduced in exposed dogs.

The observation that isolated PBL from $^{238}PuO_2$-exposed dogs requires less PHA for maximal stimulation may be related to

TABLE 1. Initial Deep Lung Deposition and Peripheral Blood Lymphocyte Values in $^{238}PuO_2$-Exposed and Control Dogs.

Group	Dog No.	Sex	Age, Year	Year After Exposure	Initial Deep Lung Deposition	Lymphocyte Cells x 10^6/ml
I	1024	M	9.1	7.5	Control	2.09
	1045	M	8.9	7.4	Control	2.49
	1061	F	8.9	7.4	Control	1.56
	1097	F	8.5	7.1	Control	2.53
	1112	M	8.5	7.1	Control	2.82
II	1004	M	9.1	7.5	116	1.49
	1026	M	9.1	7.5	116	1.25
	1043	F	8.9	7.4	98	1.61
	1056	M	8.9	7.4	97	1.97
	1072	M	8.6	7.1	98	1.24
	1212	F	7.9	6.4	111	1.10
III	1047	M	8.9	7.4	900	1.25
	1071	M	8.6	7.1	1269	1.72
	1140	M	8.2	6.7	1014	1.14
	1173	M	8.1	6.7	1023	1.89
	1178	M	8.1	6.7	1125	1.30
	1211	M	7.9	6.4	1764	1.56

TABLE 2. Mitogen Stimulation of Whole-Blood Lymphocytes From $^{238}PuO_2$-Exposed and Control Dogs.

Group	N	Lymphocytes Cells x 10^6/ml ± SD	^{125}I IUdR Incorporated, cpm x 10^{-3} ± S.D.					
			Control	CON-A[b]		PHA[b]	PWM[b]	
				3.7 µg/ml	29.6 µg/ml	11.3 µg/ml	0.63 µg/ml	
I	5	2.26 ± 0.70	435 ± 177	11594 ± 4450	11430 ± 5094	5154 ± 2084	10367 ± 3276	
II	6	1.44 ± 0.33	495 ± 144	6951 ± 2203	8977 ± 3374	2841 ± 1406	5431 ± 1845[a]	
III	6	1.47 ± 0.42	393 ± 69	8807 ± 3348	7427 ± 3479	2196 ± 1423[a]	5388 ± 3069[a]	

[a] $P < 0.05$, P values determined using student's t test
[b] Defined in text

population shifts, altered cell-surface receptors, or an altered cellular regulatory mechanism. Additional studies will be required to determine the mechanism and significance of these observations.

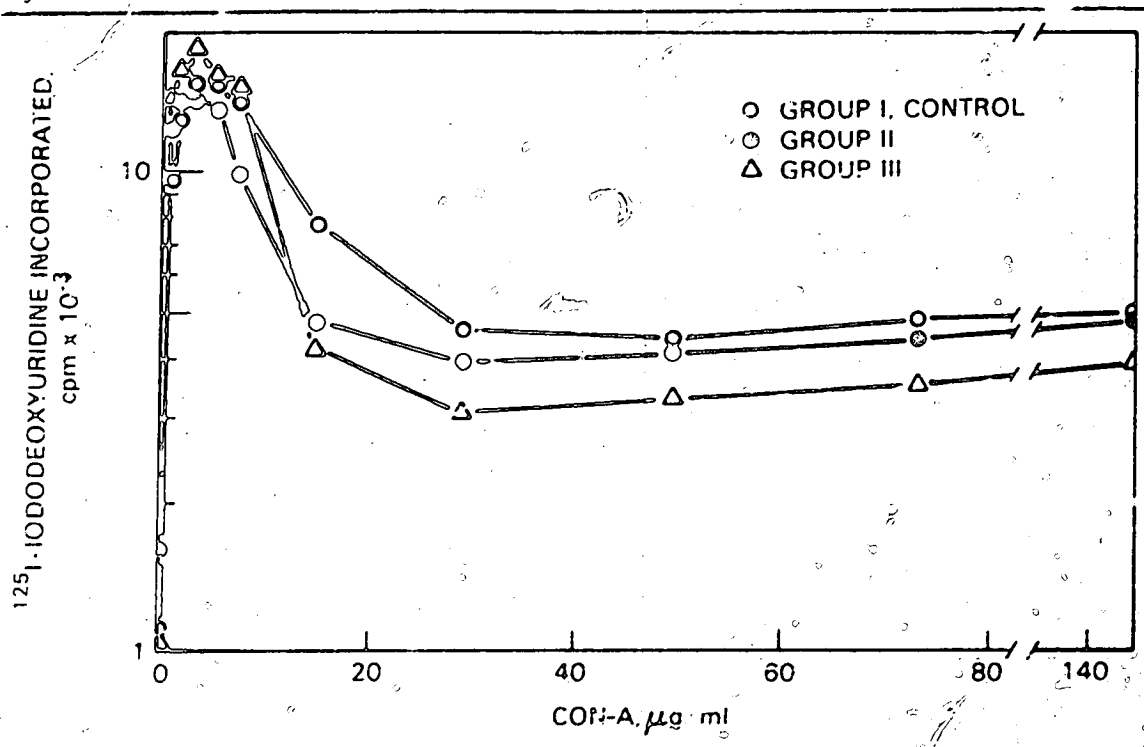

FIGURE 1. Concanavalin-A Stimulation of Canine Peripheral-Blood Lymphocytes From $^{238}PuO_2$-Exposed and Control Dogs.

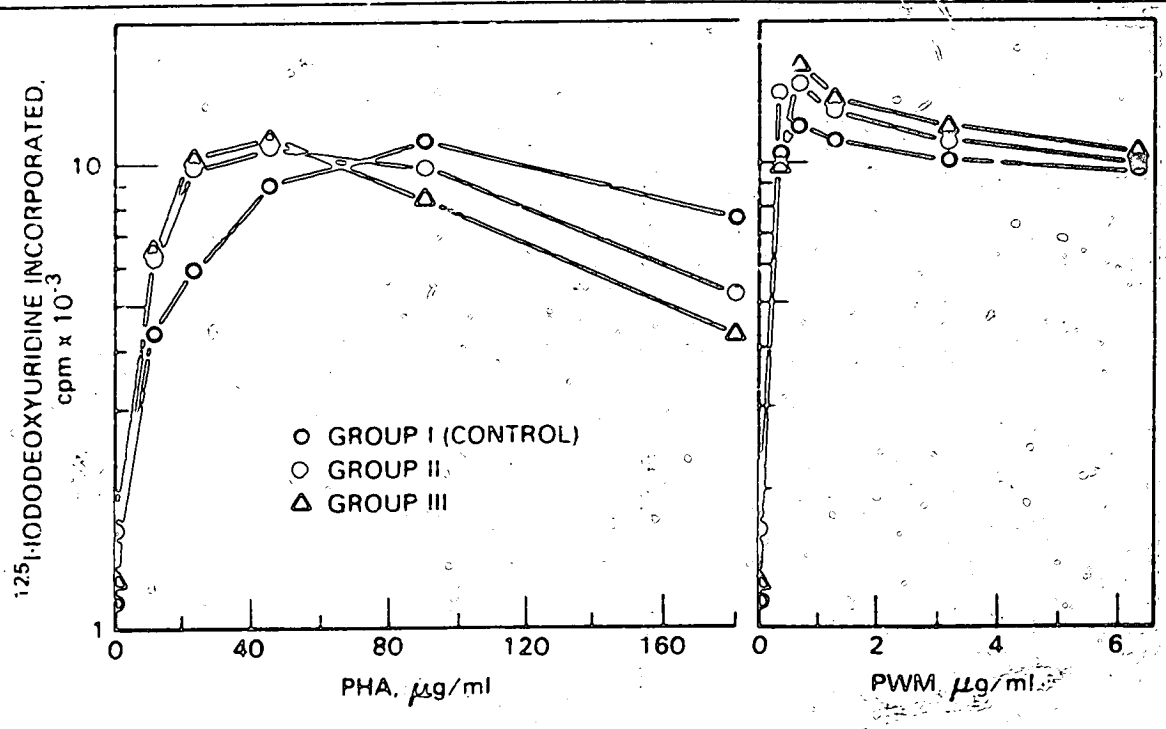

FIGURE 2. Phytohemagglutinin and Pokeweed Mitogen Stimulation of Canine Peripheral-Blood Lymphocytes From $^{238}PuO_2$-Exposed and Control Dogs.

BIMODAL RESPONSE OF CANINE PERIPHERAL BLOOD LYMPHOCYTES TO CONCANAVALIN-A

Investigators: T. M. Graham and J. E. Morris

Technical Assistance: P. D. Mayes and M. J. Steele

Mitogen-induced activation of canine peripheral-blood lymphocytes (measured by DNA synthesis) showed a concentration-dependent bimodal response to concanavalin A (Con-A) in whole-blood cultures, but not in density-gradient-isolated lymphocyte (IPBL) cultures. A bimodal response was not seen in whole-blood or IPBL cultures with swine or rat peripheral-blood lymphocytes activated by Con-A. Experiments were then designed to test red blood cell (RBC) effects on IPBL activation, including: (1) incubation of canine, swine, or rat RBC with canine IPBL cultures containing Con-A, and (2) incubation of canine RBC with swine or rat IPBL cultures with Con-A added. Bimodal responses were observed by canine and swine IPBL when cultures were reconstituted with canine RBC, but not with other combinations.

Mitogen-induced lymphocyte transformation is a widely used in vitro assay for evaluating cell-mediated immunity. In previous studies (Annual Report, 1979), this assay system was used to compare immune system responses of plutonium-exposed ($^{239}PuO_2$) and unexposed beagle dogs. At that time, a concentration-dependent bimodal response to Con-A, a mitogen, was observed in whole-blood cultures of canine peripheral-blood lymphocytes, as reported in last year's Annual Report. In contrast, the stimulation response to Con-A of canine PBL following density-gradient isolation was not bimodal.

The bimodal response might be the result of a number of factors, including the choice of anticoagulant, cooperation between lymphocytes and other cells in the peripheral blood (i.e., RBCs), or the presence of serum factors that are removed upon isolation of the lymphoctyes. It is also possible that density-gradient isolation of PBL selectively altered the lymphoid populations.

In an attempt to characterize and define the bimodal response, a series of mitogen assays were conducted with whole-blood and IPBL cultures from dogs, swine, and rats. The mitogens used in our assays included Con-A and phytohemagglutinin (PHA), which stimulate T-cell populations, and pokeweed mitogen (PWM), which is primarily specific for B-cells. Lymphocyte activation was measured by assessing the incorporation of ^{125}I-Iododeoxyuridine (^{125}I-IUdR) into newly synthesized DNA. (The culture methods are described in the Annual Report for 1979.) The response of PBL from dogs, swine or rats to PHA, PWM, or LPS was not bimodal in either the whole-blood or the density-gradient IPBL cultures. The bimodal response was not observed in rat or swine PBL activated by Con-A in either the whole-blood (Figure 1) or IPBL cultures (Figure 2).

Initial experiments enabled us to discount any obvious differences in the culture preparation of the whole-blood and IPBL methods. Preservative-free heparin was the anticoagulant used in whole-blood cultures, whereas EDTA was used to collect blood for the IPBL procedure. Our experiments showed that the bimodal response to Con-A by canine PBL was not altered by the choice of anticoagulant.

The Con-A responses of PBL in whole-blood cultures of dogs, swine and rats (Figure 1) are different for these species. Only canine PBL exhibit a bimodal response to concentrations of Con-A, with peak responses occurring at ~2-3 μg/ml and ~50 μg/ml. In swine, the peak response occurs at ~15 μg/ml. The response of rat PBL to Con-A results in a maximum response at ~30 μg/ml, remaining at this peak level throughout the higher concentrations of Con-A employed.

The response of dog, swine and rat IPBL cultures are shown in Figure 2. In this assay system, canine IPBL exhibit a peak response at ~5 μg/ml. In swine and rats, the peak responses of IPBL are observed at ~15-30 μg/ml and 8-10 μg/ml, respectively.

Since RBCs are removed upon density-gradient isolation of PBL, experiments were designed to test RBC effects on PBL activation. These included: (1) incubation of canine, swine, or rat PBCs with

canine IPBL cultures containing Con-A, and (2) incubation of canine RBCs with swine or rat IPBL cultures with Con-A added.

Only canine RBCs altered the response of IPBL populations in culture. Bimodal responses were seen in both canine and swine IPBL cultures containing canine RBCs (Figure 3). The rat IPBL response was not bimodal, and appeared to be unaffected by canine RBCs (Figure 3). Rat and swine RBCs did not appear to change the Con-A response of the IPBL cultures in any of the three species (Figure 4).

A control assay was run with cultures containing dog, swine, or rat RBCs, Con-A, and our response-marker, ^{125}I·IUdR, without lymphocytes. There was no observable direct incorporation of ^{125}I·IUdR by the RBCs (solid data points in Figure 4).

Canine RBCs appear to play a large role in the observed bimodal response to Con-A by PBL in whole-blood cultures; however, we do not understand how this interaction alters the PBL response. Possibly, RBC receptor sites for Con-A bind the mitogen in a manner that causes a change in the effective concentration of Con-A available to the lymphocytes. Alternatively, a second lymphocyte population may be involved, requiring interaction with RBCs before activation by the mitogen can occur.

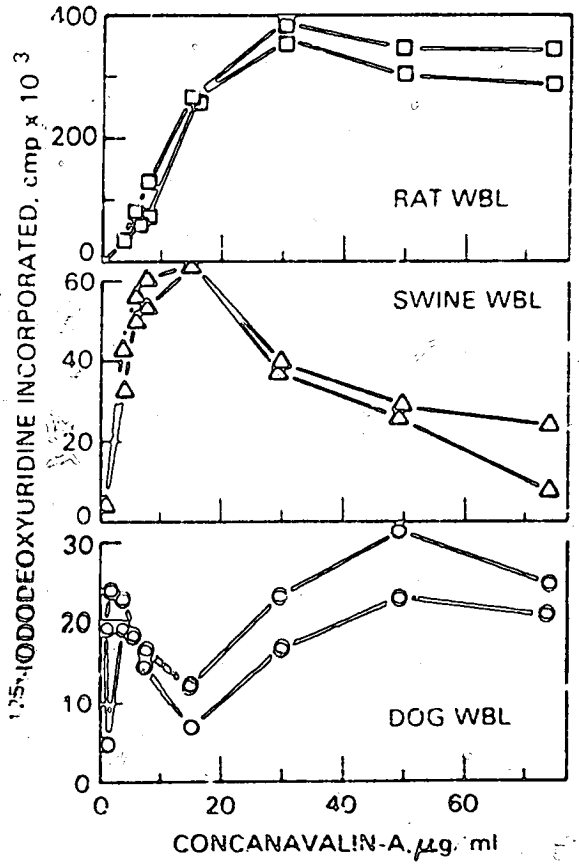

FIGURE 1. Concanavalin-A-Induced Peripheral-Blood Lymphocytes From Dogs, ○; Swine, △; or Rats, □. Results are from two representative animals of each species.

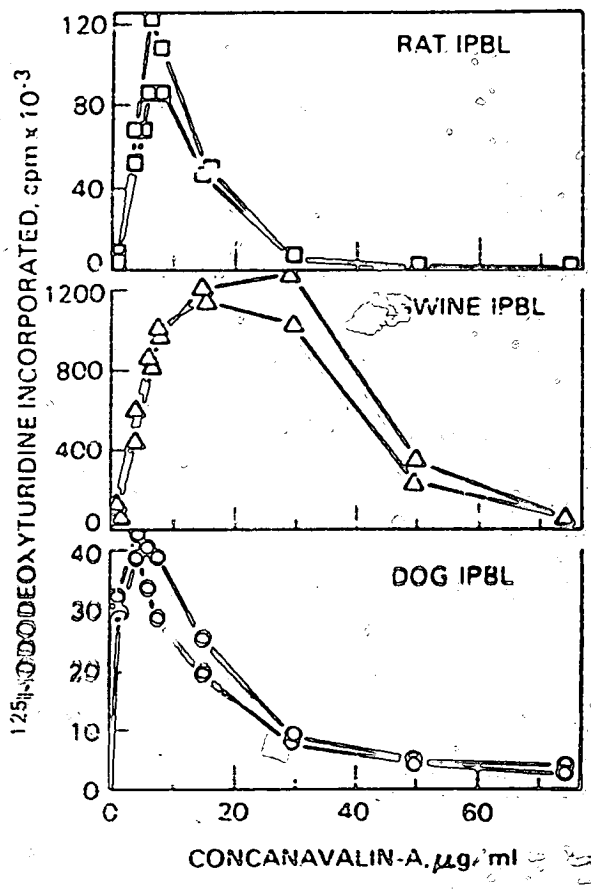

FIGURE 2. Concanavalin-A-Induced Peripheral-Blood Lymphocytes From Dogs, ○; Swine, △; or Rats, □, Following Density-Gradient Isolation. Results are from two representative animals of each species.

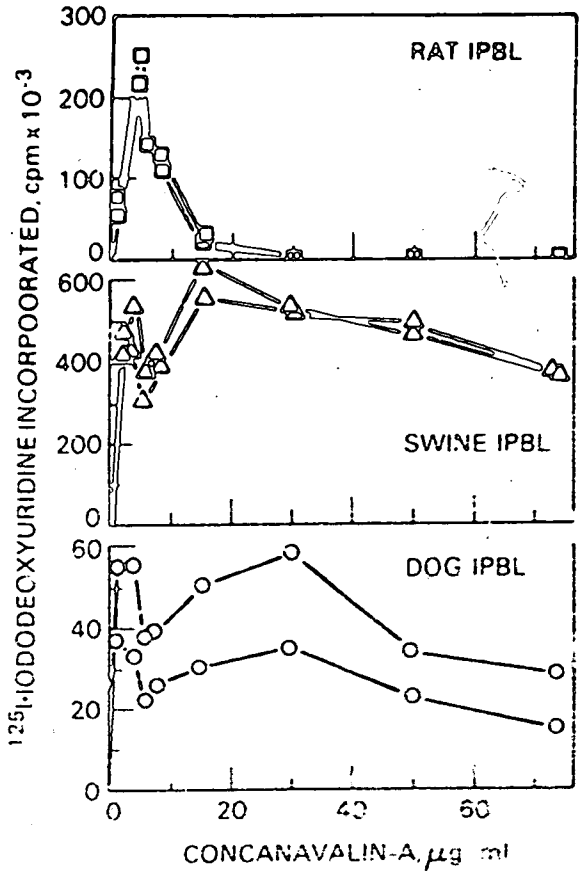

FIGURE 3. Concanavalin-A-Induced Dog, Swine, or Rat, IPBL Cultures Containing Dog RBC. Results are from two representative animals of each species.

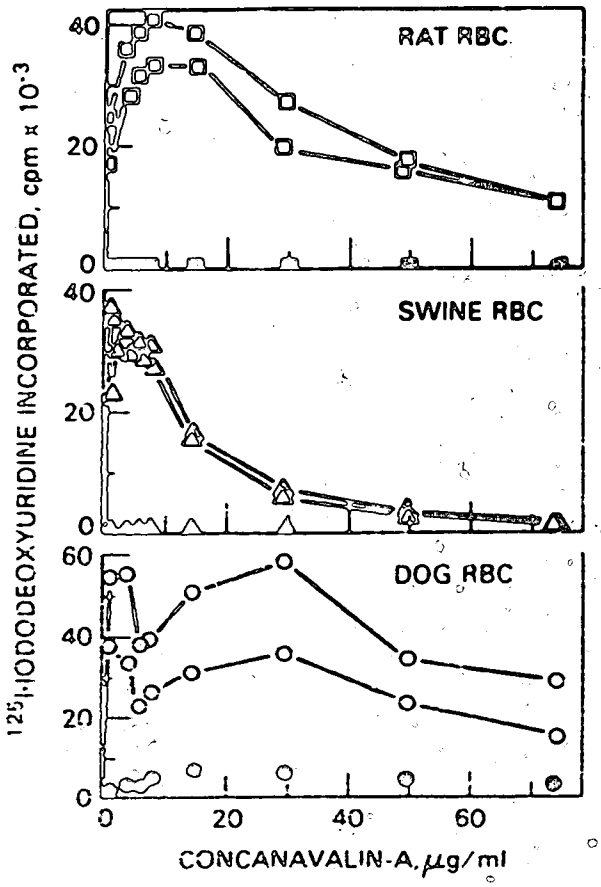

FIGURE 4. Concanavalin-A-Induced Canine IPBL Cultures Containing Dog, Swine, or Rat, RBC. Results are from two representative animals of each species. ○, △, □ represent ^{125}I-IUdR control where cultures contained mitogens, RBC and ^{125}IUdR, but no lymphocytes.

○ Development of Blood Irradiators

Extracorporeal irradiation of blood, using repeated brief exposures, has been shown to suppress rejection of tissue transplants and to inhibit progression of chronic lymphocytic leukemia. This project is designed to study the basic processes by which blood irradiation produces such effects, to establish the conditions of dose administration which optimize therapeutic effect, to improve the techniques of blood irradiation through the development of improved and portable blood irradiators, and to move this technique toward clinical applications.

BLOOD IRRADIATOR MEDICAL APPLICATIONS

Investigators: F. P. Hungate, W. D. Riemath,* and L. R. Bunnell**

A portable blood irradiator, consisting of a vitreous carbon body and thulium-170 radiation source, was attached to dogs via a carotid-jugular shunt, and its effects on the immune system measured. The device has demonstrated both significant suppression of circulating lymphocytes and prolonged retention of skin allografts. The units used on dogs have had limited success because of difficulties in protecting the shunt tubing from the animal's natural efforts to scratch and bite the device. This year's effort was devoted largely to improving the supportive hardware.

Previously, we produced a portable blood irradiator for potential clinical use in treating leukemia and in controlling immune reactions during organ or tissue transplantation. It consists of nonthrombogenic vitreous carbon containing stable thulium, which becomes the beta radiation source, thulium-170, after neutron activation.

In the present phase of the work we have established methods for maintaining long-term function and assessing the effects of the device in beagle dogs. The carotid artery and jugular vein are the most accessible and useful vessels for establishing a long-term shunt in animals. To minimize the length of tubing, we have placed the irradiator and supportive hardware either under the animal's head or on its back at the level of the shoulder. The shoulder position has the potential advantage of easier access for the investigator and reduced accessibility to the dog. To support the units securely atop the shoulder we used a nylon mesh jacket, designed for dog research by A. Chatham, 5043 Oaknoll Avenue, Los Angeles, CA. The jackets are sized for beagle dogs and can accommodate individual animals by adjusting the lacings.

To limit sideways shifting of the unit, the irradiator was attached to the mesh of the jacket by a series of linen or nylon ties through a thermoplastic strip in the shape of an inverted U. A protective cover of thermoplastic was also attached to the mesh of the jacket in such a way that it could be readily opened for access to the irradiator. The shunt tubing was tunneled beneath the skin on each side to the midlateral portion of the neck, and was protected from that point by the thermoplastic cover over the irradiator.

Despite our attempts to adjust the lacings for a snug fit on the animal, the weight of the shielded irradiator unit (approximately 500 g) gradually shifted it so that, on one side or the other, the shunt became stressed. This produced severe irritation by the Teflon vessel tips on the artery and vein, with consequent loss of shunt flow. None of our attempts to limit this lateral movement were successful. The shoulder position was therefore abandoned in favor of attempts to develop a way of mounting the irradiators under the animal's neck.

Earlier chest-mounted holders had failed to fully protect the shunt tubing

*Chemical Technology Department
**Materials Department

from damage by the dog, and had offered only limited access for shunt maintenance, i.e., restoration of blood flow and replacement of irradiator units when flow stopped. A new holder was therefore developed using thin-walled aluminum tubing, 5 cm in diameter, to hold the irradiator and protect the shunt in the area where it connects with the irradiator. This tubing was mounted to a semirigid unit which wraps around the thoracic cage with holes for the forelimbs. This unit is thermoplastic, and padded around the leg holes with lamb's wool to minimize chafing. We have two of these padded "vests," so that they can be exchanged, washed and dried each week, and ready for use by the following week.

This unit was tested on dog 1305, using an irradiator giving a 27-rad transient dose (assuming a flow of 100 ml/min). The irradiator remained functional throughout the test (30 days), but was periodically removed when flow stopped. At such times, the obstructing thrombi in the vessel tip region were removed by aspiration, the irradiator was cleaned and resterilized with a solution of benzalkonium chloride, followed with a sterile saline rinse, and reinstalled. At no time was there evidence of primary obstruction occurring in the irradiator. The test was terminated at 30 days when skin grafts failed and there was no apparent benefit from further treatment. The shunt was still operational and, after removal, examination of the artery and vein connection to the vessel tips indicated that flow could have been maintained for a substantially longer time.

Results of the test on dog 1305 showed strong suppression of circulating lymphocyte levels, as in previous tests. Allograft rejection could not be evaluated because of early subgraft bleeding, so that little (if any) vascularity was attained in the graft. The same problem prevented autograft adhesion; all skin patches came off at approximately the same time.

The new hardware provided encouragement that further testing with dogs is feasible, with the expectation that shunt patency can be maintained throughout the test period.

4 Fusion

FUSION

Environmental, health and safety problems associated with the fusion technology cannot be precisely identified because of the early stage of development of this technology. Of probable major concern are problems associated with high-strength magnetic fields, with tritium and tritium-breeding materials, with heat transfer materials, with energetic neutrons and the radioactive activation products resulting from interactions with these neutrons. Some of these problems are common to fission as well as fusion technologies and we have considered, in the Fission section, our studies involving the toxicology of sodium and lithium, which may serve as heat transfer and breeding materials in a fusion reactor. In this section, we consider only studies relating to magnetic-field effects.

PAGE 204 DOES NOT EXIST IN ORIGINAL DOCUMENT.

Biological Effects of Magnetic Fields

The development of magnetic fusion power sources, as well as other technologies such as superconducting magnetic energy storage, magnetohydrodynamic power generation and magnetically levitated vehicles, increases the probability of exposure of people to magnetic fields. The lack of a credible data base from which exposure limits can be established led to the initiation of a broadly based program to study possible effects in a number of biological systems under carefully controlled conditions. Reported here are studies using cultured mammalian cells, trout eggs, and stable, organic free radicals exposed to magnetic fields.

AN EVALUATION OF STATIC MAGNETIC FIELDS ON MAMMALIAN CELL CULTURES

Investigators: M. E. Frazier, J. Samuel, and T. K. Andrews, Jr.

We have evaluated, in mammalian cells in culture, the effects of magnetic fields on mutagenicity, toxicity (effect on cell survival), and possible interactive effects of simultaneous exposure to magnetic field and mutagens (ethylmethane sulfonate, EMS). No direct mutagenic effect of magnetic fields was observed; however, our initial studies indicated that EMS interacted in some way with the magnetic field to decrease survival of exposed cells when the two exposures (to EMS and magnetic fields) occurred simultaneously. Preliminary data indicated that the interaction between EMS and the magnetic fields may have slightly increased the mutation frequency of exposed CHO cells, but further studies have failed to substantiate these initial findings.

It has been reported that magnetic-field exposure induces mutational changes in Drosophila and other organisms. We have systematically examined the effect of magnetic fields on Chinese hamster ovary (CHO) cells using cytotoxicity and mutation at the hypoxanthine guanine phosphoribosyl transferase (HGPRT) locus. In addition, we have studied simultaneous exposure of CHO cells to a known mutagen and to magnetic fields to determine whether interactive effects occur.

The HGPRT assay is based on the ability of wild-type CHO cells to convert thioguanine to a nucleotide (or its metabolites) which is lethal. Mutation at the HGPRT locus results in loss of the enzyme, thus allowing survival of mutant cells. Linear dose-response relationships have been found for a number of chemical and physical agents using this CHO/HGPRT assay system.

Cell survival was determined using CHO cells in the clonal growth assay. This assay requires the seeding of a known number of monodispersed cells from each exposure group into suitable culture dishes containing growth medium, and counting the resultant clones to derive the proportion of cells that formed clones. Results are expressed as relative plating effiency (RPE), i.e., the plating efficiency of test cultures divided by that of controls.

Three permanent horseshoe magnets were used in these studies. Field strengths were measured at several points, using a gaussmeter, and the cells placed in appropriate positions to be exposed to the field strengths selected for each experiment (Tables 1-4). Exposures were performed in an incubator at 36 ±1°C. Control cells were maintained in the same incubator in an area remote from the magnets (background = 0.0002 T).

In the first series of experiments, CHO cells were exposed to 0.17 or 0.31 T, alone or in combination with varying concentrations of EMS (Table 1). Up to 0.3 T, no consistent effect of the magnetic field alone on cloning efficiency was observed. However, a cooperative effect between EMS and the magnetic field apparently resulted in decreased survival of cells treated with EMS plus magnetic field relative to EMS treatment alone. At 0.31 T, the combined treatment caused at least six times the cytotoxicity found in

TABLE 1. Effect of Various Treatments on Cloning Efficiency[a] of CHO Cells.

Treatment[c]	Cloning Efficiency[a] at EMS[b] Concentration of 0.06%	0.15%	0.2%	0.25%	0.33%
EMS Alone	105[d]	74	51	25	10
EMS + 0.31	12	12	3.8	4.1	--
EMS + 0.17T	--	36	--	9.5	10
0.31 Alone	99	116	89	102	101
Toxicity Ratio[e] (0.31)	9X	6.2X	13.4X	6.1X	--
Toxicity Ratio (0.17T)	--	2.1X	--	2.6X	1

(a) Percent cloning efficiency expressed relative to control cultures
(b) Ethylmethane sulfonate
(c) All exposures were for 16 hr
(d) Each data point represents the average of at least 6 plates
(e) Toxicity ratio $\frac{\text{Cloning efficiency (EMS + magnetic field)}}{\text{Cloning efficiency (EMS only)}}$

EMS controls that were not exposed to magnetic fields. Since a variety of EMS concentrations (from 0.06% to 0.25%) seemed to cause similar effects (not all data are shown), this effect appeared to be independent of EMS concentration. Exposure to the 0.31-T field appeared to decrease survival of EMS-treated cells more than did exposure to 0.17 T.

Results of early studies indicated that the magnetic field alone had no effect on mutation frequency under the conditions of these experiments. However, mutation frequency appeared to be slightly increased (Table 2) when cells were simultaneously exposed to EMS and magnetic fields (0.31 T), although results were highly variable. Additional experiments were performed to verify our initial results.

The acquisition of an additional magnet permitted us to use three replicates/treatment group and to double the number of plates (from 6 to 12) for each determination. Table 3 shows the results of two such experiments. The cooperative toxic effect of EMS and magnetic fields observed in earlier studies was not apparent. Mutation assays (Table 4) also indicated a lack of synergism between EMS and magnetic fields.

The reasons for the failure of our recent experiments to replicate our earlier findings are not clear. Improvements in performing the CHO assay and the consequent decrease in variability may be involved. We are now attempting to resolve the differences between the two sets of data.

TABLE 2. Study of Cooperative Effect of a Magnetic Field and a Direct-Acting Mutagen.

Treatment	Mutation Frequency[a] Expt A[b]	Expt B[b]	Expt C[c]	Expt D[b]
Control	18	2	1	1
EMS Alone	210	31	50	23
EMS + 0.31 Magnetic Field	694	33	63	36
Magnetic Field (0.31) Alone	21	0.6	2	1.3
Ratio of Mutation Frequency[d]	3.3	1.1	1.3	1.6

(a) Mutants 10^6 viable cells
(b) EMS conc 0.02%
(c) EMS conc 0.03
(d) Ratio of mutation frequency $\frac{\text{Mutation frequency of EMS + magnetic field}}{\text{Mutation frequency of EMS alone}}$

TABLE 3. Initial Survival of Cells Exposed to Magnetic Fields and/or EMS.

Treatment	APE[a] Expt 1	APE[a] Expt 2	RPE[b] Expt 1	RPE[b] Expt 2
Mag A + EMS	32.3[c]	12.2	41	19
Mag B + EMS	29 } 32.1	23.8 } 21	37 } 41	37.6 } 33.2
Mag C + EMS	34.8	27.2	45	43
EMS	30.6	24.2	39	38.3
EMS	24.4 } 28.2	19.4 } 20.2	31 } 36	30.7 } 32
EMS	29.7	17.1	38	27
Mag A	100.9	62.1	129	98.3
Mag B	86.5 } 92.1	59.6 } 60.7	113 } 118	94.3 } 96.1
Mag C	88.9	60.5	114	95.7
Cont	79.4	61.8	102	97.7
Cont	80.3 } 78	57.8 } 63.2	103 } 100	91 } 100
Cont	74.4	70.3	95	111.3

(a) Absolute plating efficiency
(b) Relative plating efficiency
(c) Each data point is average of 12 plates

TABLE 4. Mutation Frequencies of CHO Cells Exposed to Magnetic Fields and/or EMS.

Treatment	Mutants/Plate[a]				Cloning Efficiency[b]		Mutants/10^6 Viable Cells[a]			
	Expt 1		Expt 2		Expt 1	Expt 2	Expt 1		Expt 2	
Mag A + EMS	17.5		*				168.3		*	
Mag B + EMS	16.8	18.3	73.9	68.5	10.4	24.3	161.5	176.3	304.1	282.1
Mag C + EMS	20.7		63.2				199		260.1	
EMS	21.8		75.2				206.7		334.2	
EMS	16.9	20.1	68.5	64.8	12	22.5	140.8	167.5	304.2	287.2
EMS	18.6		50.6				155		224.9	
Mag A	3.3		4.9				4.9		7.4	
Mag B	9.4	6	3.7	4	66.9	66.5	14.1	9.1	5.6	6.1
Mag C	5.5		3.5				8.2		5.3	
Cont	6.4		3.1				11.5		4.1	
Cont	3.7	4.1	2.6	3.5	55.9	76.5	6.6	7.3	3.4	4.6
Cont	2.2		4.8				3.9		6.3	

(a) 12 plates/data point
(b) 36 plates/data point
* No data available

ENVIRONMENTALLY CONTROLLED HOUSING FOR RODENTS FOR EXPOSURE FOR BIOMAGNETIC STUDIES

Investigators: D. A. Nelson, E. G. Kuffel, and J. R. Decker

Magnetic field effect studies on mice have been performed by housing two groups of mice in special chambers between the pole faces of two beam-bending magnets, during which time one magnet is on and the other is not. We have improved control of the environment within the chambers by replacing the original air conditioner/plenum system with (1) temperature-controlling heat exchangers in the chamber roofs and (2) a temperature/humidity/flow controller in the inlet air circuit to the chambers.

We previously described a system for housing rodents for exposure to dc magnetic fields (Annual Report, 1979). Temperature in the mouse chamber was controlled by a room air conditioner which delivered chilled air to a plenum. Conditioned air from the plenum was blown into the chamber by muffin fans mounted in the manifold.

With that system, heating from the energized magnet subjected the exposed animals to environments up to 4°F warmer than that of the sham-exposed group. Moreover, large fluctuations in relative humidity occurred due to cycling of the thermostatically controlled air conditioner. A high rate of air flow (90 changes per hour) was required to maintain the animal cages near 72°F. We have therefore redesigned the environmental chambers for magnetic-field exposures to better control temperature, relative humidity, and air flow.

Improved temperature control was attained by building an aluminum-polyvinyl chloride (PVC) top to the exposure chamber. The piece incorporates an open-loop heat exchanger with water as the cooling medium (Figure 1). The 1/8-in. PVC top layer of the roof is an effective insulator between the magnet pole and the heat exchanger. The aluminum section on the bottom serves to maximize heat transfer between the animal environment and the heat exchanger. Water is siphoned through longitudinal troughs in the 1/4-in. gap between the plates. The air conditioner and buffer plenum are eliminated.

A thin, leak-proof seal was established by preparing the aluminum and the PVC with a primer. Dow Corning 1205 and 1200 primers were used to prepare the PVC and aluminum surfaces, respectively. The pieces were bonded with Dow Corning #732 Silicone RTV sealant and cured under pressure.

Tests with a population of 80 Swiss-Webster mice demonstrated the effectiveness of the heat exchanger in removing metabolic heat. With the water supply regulated by an on-off, thermostatically controlled valve, chamber temperature was regulated to 68°F ± 2°F with the thermostat set to 2°F hysteresis (see Figure 2). The valve was operating at a duty cycle of approximately 25% throughout the period. In the final configuration, a constant 55°F water flow of somewhat less than 2.0 ℓ/min per chamber will be required to relieve the heat load.

While the heat exchanger provided adequate temperature control, control of relative humidity within the chamber was accomplished with a Miller-Nelson Controls Model HCS-201 Temperature/Humidity/Flow Controller. This unit delivers conditioned air at a desired relative humidity, temperature and flow rate. Feedback to the controller is via a General Eastern Model 400CD Relative Humidity/Temperature Indicator placed in the exhaust manifold of the chamber.

Heat load can be relieved by the heat exchanger; fine temperature contol, as well as humidity control, is exerted by conditioning of ventilation air. Full tests have not been conducted on the entire system, however it is anticipated that this arrangement will allow control of chamber temperature to ±1°F and relative humidity to ±10%.

We have assumed that differences in moisture levels between the two chambers will be slight. This allows us to use a single humidity sensor and controller. The sensor is placed in an insulated duct which is fed the combined exhaust air from

the two chambers. A buffered, 0-5 VDC relative humidity analog signal is continuously recorded on a strip chart. A similar signal, corresponding to the temperature of the combined exhaust, is recorded on a second chart. A Yellow Springs Instruments thermometer provides a multiplexed 0- to 100-mV signal for recording individual chamber temperatures, as sensed by thermistor probes placed in each chamber. A fourth chart records field strengths from a 0- to 100-mV analog output at the power supply field regulator (Alpha Scientific Model 3056).

Lighting for the chambers is provided by incandescent bulbs connected in series to a Power Mate BFA-60D dc power supply. The lighting is controlled by an adjustable on-off 24-hour timer for daylength control.

All instruments, controls and recorders, with the exception of the temperature/humidity/flow controller, are mounted on a 19-in. rack to simplify operation and facilitate access. Instrumentation is summarized in Figure 3.

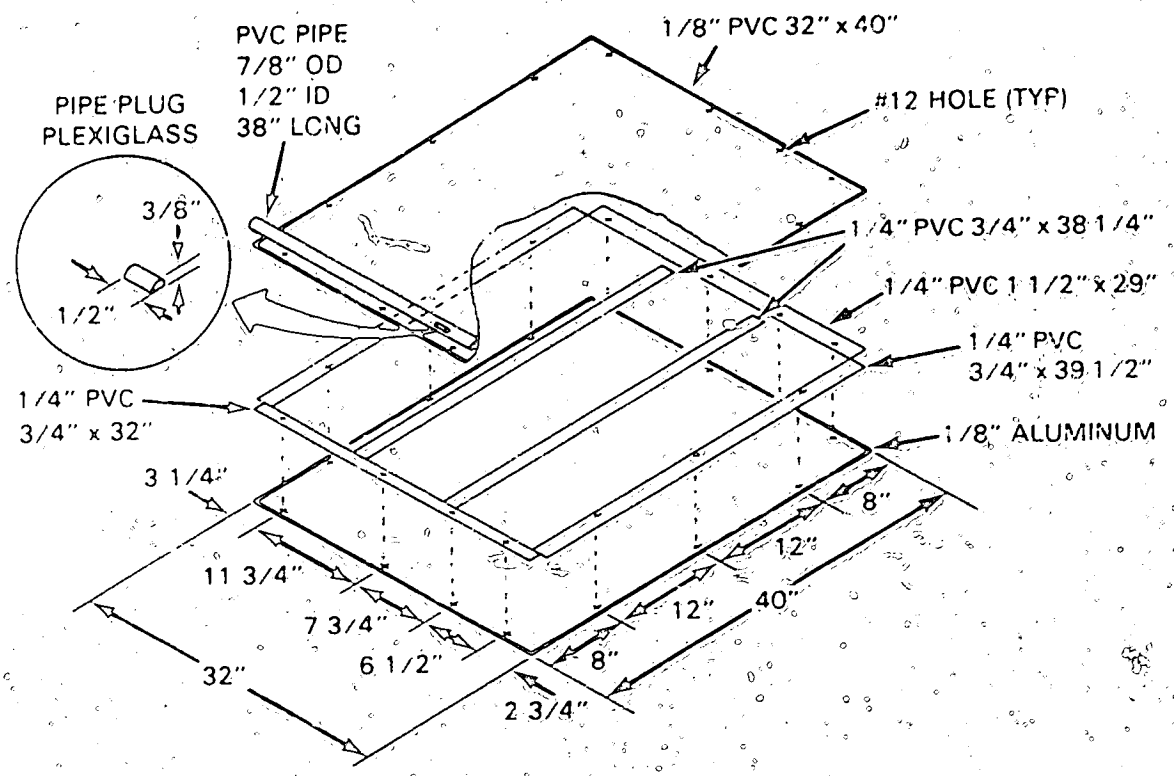

FIGURE 1. Sketch of Heat Exchanger.

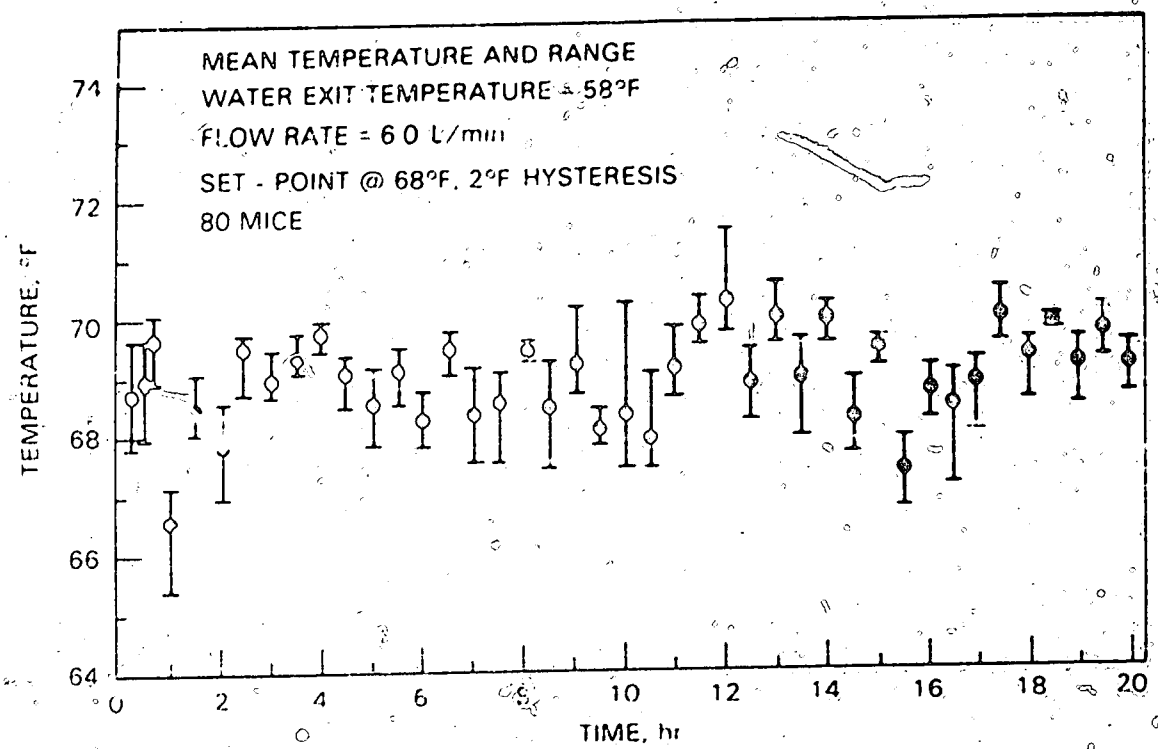

FIGURE 2. Temperature of Chamber Housing 80 Swiss-Webster Mice Over Period of 20 Hours. Range shown is for simultaneous measurements in each quadrant of the chamber, approximately 3 cm from the floor.

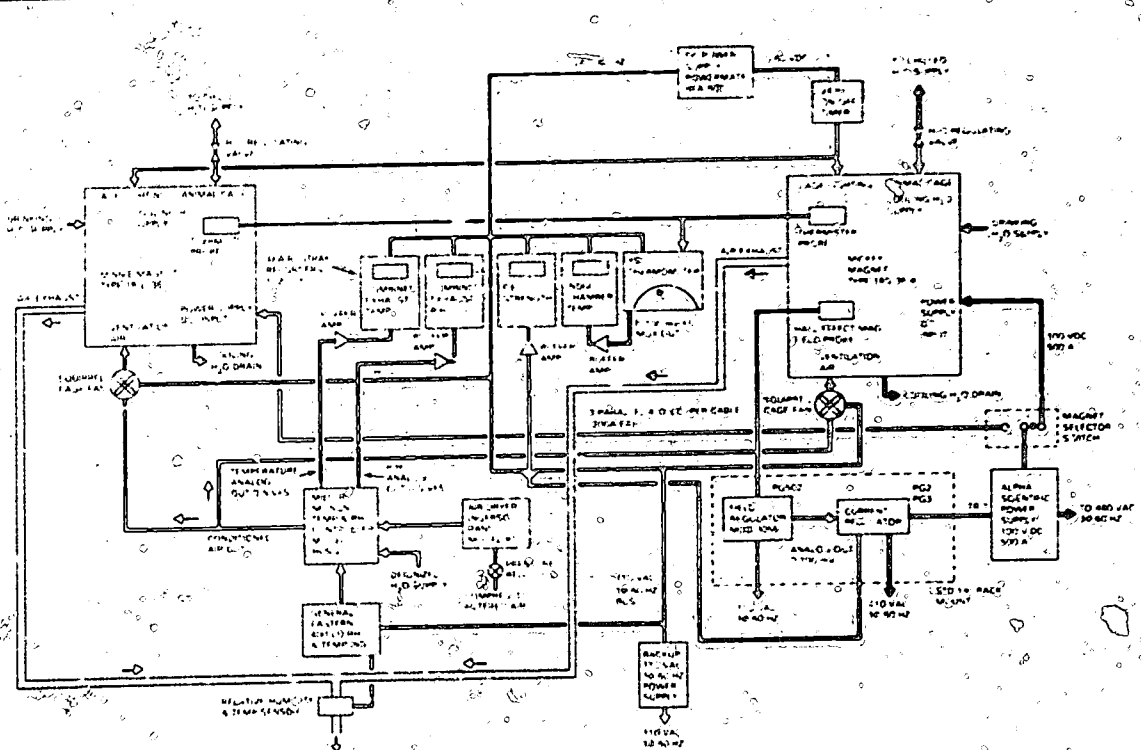

FIGURE 3. Block Diagram of Magnetic Field Exposure System.

EFFECTS OF COMBINED MAGNETIC FIELD EXPOSURE AND CHEMICAL INSULT ON TROUT DEVELOPMENT

Investigators: J. A. Strand, C. S. Abernethy, R. G. Genoway, and J. R. Skalski

Studies conducted in FY 1980 were directed toward developing potentially more sensitive techniques to detect and measure effects of magnetic fields on biological systems. Partial results of an approach using a secondary chemical stress, in addition to the primary stress of magnetic-field exposure, are presented. Indices of potential effects include fertilization, early development, hatching, growth and survival of juvenile rainbow trout, Salmo gairdneri.

Previous studies of effects of magnetic-field exposure on fertilization, development, hatchability, and juvenile survival of rainbow trout produced conflicting results. In general, most parameters, with the exception of fertilization, were unaffected by exposure to either a static (10,000-gauss) or oscillating (2,800- to 11,200-gauss) magnetic field. Accordingly, studies conducted in FY 1980 were directed toward developing potentially more sensitive approaches to determine effects of magnetic fields on representative vertebrates.

One approach has been to use a secondary stress, in addition to magnetic-field exposure. The reasoning for this approach is that although we cannot detect any effect of magnetic field exposure, if an interactive effect is observed (an effect greater than that predicted for either agent alone), then it may be reasonable to assume that the magnetic field has some degree of influence.

Equal numbers (2,500) of rainbow trout eggs were exposed, under flow-through conditions, from fertilization to 30 days of development to either: a) an oscillating, homogeneous, magnetic field (1,500-10,000 gauss), b) a continuously maintained 50 ppb (TRC) concentration of chlorine (sodium hypochlorite), c) both a magnetic field and chlorine, or d) neither agent (control). Incubation chambers for exposed and control embryos were identical.

At 20 days (eyed stage), the embryos were transferred to standard drip incubators, where hatching occurred in 28 ± 1.5 days at 10.5 ± 0.3°C. Two weeks after hatching, the fry from each exposure group were subdivided into four equal groups and placed in four fiberglass rearing troughs. Each trough consisted of four compartments; each compartment received one test group, forming a 4 x 4 Latin Square design.

Survival was monitored for 3 mo. A chi-square test of homogeneity was applied to determine the potential for differences among treatment groups. Evaluation of each index was conducted blind to eliminate any possibility of investigator bias.

Results of the influence of magnetic-field exposure, chlorine exposure, or both, on survival through 6 wk are presented in Table 1. Although a relatively low survival through hatching was observed, no significant differences ($P = 0.05$) in hatchability were found among treatments. Similarly, there was no significant difference ($P = 0.05$) among groups for survival through 6 wk. The relatively low hatching percentages are thought to be attributable to use of spawn from 2-yr-old parental fish in the absence of mature 3- or 4-yr-old fish.

TABLE 1. Effect of Magnetic/Chlorine Exposure on Early Life Stages of Rainbow Trout.

Condition	Number of Eggs	Percent Hatched	Percent Survival at 6 Weeks[a]
Control	2355	58.64	87.69
Magnet	2447	60.37	85.95
Chlorine	2542	63.92	89.78
Magnet/Chlorine	2397	59.61	87.54

[a] Percent survival of hatched fry.

Fingerlings are being assessed for growth and survival in an ongoing study according to the following protocol:

When the fingerlings were 8-12 g in weight, 25 individuals from each group (4 troughs x 4 compartments = 16 groups, a total of 400 fish) were selected for uniformity of size, marked for identification (liquid nitrogen cold-branded), and placed in each of two 1.5-m-diameter fiberglass circular rearing ponds. An additional 10 fish from each group were used for initial weight and length measurements. Fish stocks were fed twice daily 5 days per week. In one pond, excess food (3% body weight per day) was provided to allow for study of optimal growth and survival rates. In the other, a subsistence level (1.5% body weight per day) was made available to study competition among treatment groups. After completion of 4 and 8 wk of feeding, individual weights and lengths of at least 10 fish from each group (160 from each pond) were recorded. Separate analyses for growth and survival rates are being performed on the data from each pond. Analysis of variance is being used to compare the growth of treatment groups. The treatment sum of squares was partitioned using orthogonal contrasts. A chi-square test of homogeneity for a 2 (alive vs. dead) x 4 (treatments) contingency table will be used to compare survival rates among treatment groups.

Because the race of experimental fish presently reared in the Hanford hatchery breed only during winter months (December-March), studies to determine the potential for magnetic field effects on growth will carry over to FY 1981. The test fish were not of sufficient size for "cold-branding" until August 1980, so that analyses of growth must continue through October 1980.

MOLECULAR BIOMAGNETIC EFFECTS: MAGNETOPHORESIS OF SOLUTES

Investigator: D. R. Kalkwarf

Large magnetic-field gradients were found to affect the migration of organic solutes on thin-layer chromatographic plates: one paramagnetic and three supposedly diamagnetic species moved toward regions of higher field strength. The effects were qualitatively similar on thin layers of either silica gel or cellulose.

This study was undertaken to determine if large magnetic-field gradients affect the diffusional motion of organic compounds in liquid solution. Such behavior could greatly influence the rates of biochemical reactions involving the diffusion of solutes to a membrane surface or through an assembly of membrane components. In experiments performed this year, thin-layer chromatographic (TLC) plates were used to position migrating organic solutes in magnetic-field gradients of up to 6 T/m. One paramagnetic and three supposedly diamagnetic solutes were diverted toward the direction of increasing field strength. It seems appropriate to call this phenomenon "magnetophoresis," an analog of the term "electrophoresis," used for the movement of molecules in an electric field.

Glass-backed TLC plates proved to be convenient media for the migration studies. Such plates can be precisely positioned in regions of measured field gradient. As a solvent rises by capillary action through the adsorbent layers, samples adsorbed in the layer are repeatedly dissolved, readsorbed and redissolved, moving in a direction perpendicular to the surface of the solvent reservoir. In the experiments reported here, an effort was made to maximize the diffusional freedom of the samples by selecting systems in which sample adsorption was weak. Even under these conditions, slight changes in the migration paths of the solutes could be detected by utilizing small, confined samples on the plates.

The arrangement of equipment used in the experiments is shown in Figure 1. The magnet, which had 9-in. pole faces, was used to generate field strengths of up to 1 T. Field strengths in and around the magnet gap were measured with a gaussmeter. Glass containers for the TLC plates were located at positions of maximum and minimum field gradients (positions A and B, Figure 1).

We examined the migrational behavior of the following compounds: diphenylpicrylhydrazyl, a stable, organic free-radical; C.I. Acid Blue 9, an anionic triphenylmethane dye; C.I. Acid Red 14, an anionic monoazo dye; and C.I. Basic Violet 10, a cationic xanthene dye. Diphenylpicrylhydrazyl is paramagnetic in both the solid and liquid states, whereas solutions of the other compounds were thought to be diamagnetic. Samples containing 2 nmol of the test compound in 20 nℓ of solvent were applied to 5 × 20-cm TLC plates. After drying, the resultant spots had diameters of 1 mm. The plate was then placed in a glass cylinder so that the edge nearest the samples rested on a level brass disk. The plate was held perpendicular to this disk by plastic foam spacers. With the magnetic field on, methanol was slowly added to the bottom of the cylinder so that the surface of the resulting solvent reservoir rose parallel to the bottom edge of the TLC plate until it was 5 mm below the sample spots. Capillary action then carried the samples up the TLC plate from the points of origin. After a selected time interval, the plate was removed and the positions of the samples and the solvent front were noted. The plate was then dried, fresh samples were applied to the origin points used previously, and the migration process was repeated with the magnetic field off.

Typical displacements of the solutes in field gradients of 0 and 6 T/m are shown in Figure 2. The closed symbols indicate the positions of the samples after moving in a gradient of 6 T/m; the open symbols indicate their positions after moving in a zero-intensity field. All four compounds moved toward positions of higher field strengths; in each case, the displacement in that direction was proportional to the square root of the migration time. Displacements of several millimeters were attained in less than an hour. Qualitatively similar effects were observed for samples on either silica gel-coated plates

(E. Merck 5762) or cellulose-coated plates (E. Merck 5772). No lateral displacements of solutes were detected on plates placed in fields of high strength, e.g., 1 T, at low gradients (position B, Figure 1).

More information is needed to provide a clear explanation of the magnetophoretic phenomenon reported here and to assess the possibility of its occurrence in living systems. If many biochemicals are found to be displaced by high magnetic-field gradients, a new perspective on the molecular basis for biomagnetic effects may be attained. Future experiments will be directed toward that end.

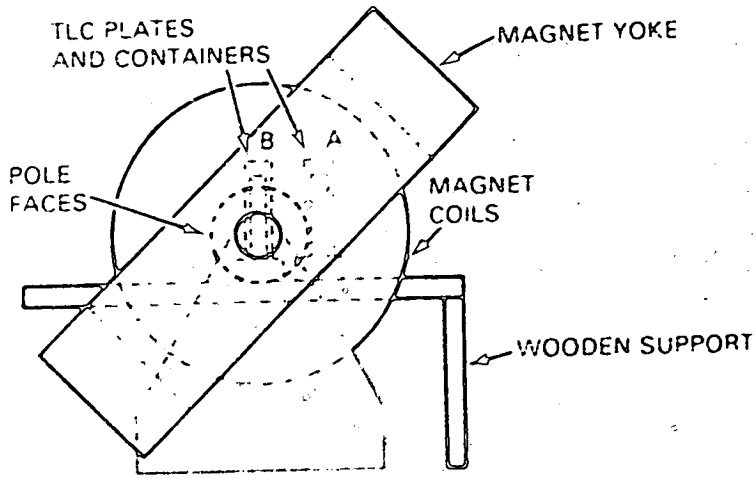

FIGURE 1. Arrangement of Magnet and Thin-Layer Chromatographic (TLC) Plates Used in the Magnetophoresis of Solutes.

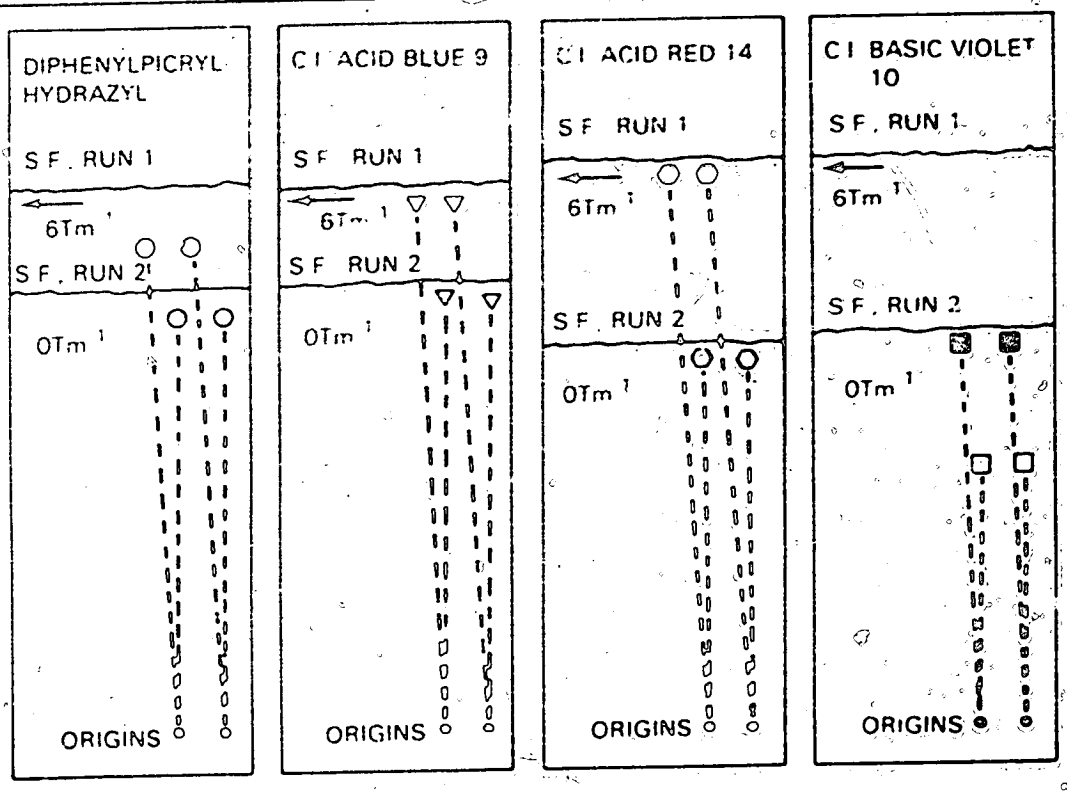

FIGURE 2. Migration Paths of Samples During Their Elution With Methanol in Thin Layers of Silica Gel Placed in the Designated Magnetic-Field Gradients. Open symbols indicate position in a 0-T/m gradient; closed symbols indicate position in a 6-T/m gradient. Heights attained by the methanol in successive runs are designated by "S.F." (solvent front).

5 Oil Shale

OIL SHALE

Potential biomedical concerns in the area of oil shale fuel technology are being investigated, in part, by a tiered testing approach utilizing the Ames assay and mammalian cell transformation, followed by more standard toxicologic procedures. Fractions of potential importance, as defined by the Ames assay, were assayed for pulmonary carcinogenesis using the lung pellet implantation technique.

Health Effects of Synthetic Fuels

The purpose of this project is to investigate the potential human health hazards associated with synthetic fossil fuel technologies. Current studies are investigating the carcinogenic potential of epidermal exposure to materials and products from solvent-refined coal and shale oil technologies on a comparative basis with natural crude petroleum and known positive carcinogens.

EPIDERMAL CARCINOGENESIS STUDIES IN MICE OF MATERIALS FROM SEVERAL FOSSIL FUEL TECHNOLOGIES

Investigators: R. A. Renne, L. G. Smith, and D. D. Mahlum

Technical Assistance: B. J. Holloway, S. M. Baze, V. L. Dedmond, J. C. Chapman, and S. R. Eldridge

A mouse skin-painting assay system was used to determine the relative carcinogenicity of several crude fossil fuel materials and two known carcinogens. Of the fossil fuel materials tested, the heavy distillate (HD) from the solvent refined coal (SRC-II) process had the highest carcinogenic potency; crude shale oil was less potent than HD and crude petroleum the least active. Light distillate (LD) from the SRC-II process was not an active carcinogen. Data from similar assays in progress on chemical fractions of HD indicate that the basic tar and neutral tar fractions are the most carcinogenically active constituents. The PNA fraction is less active; the basic fraction of HD shows very little carcinogenic activity at this point in the assay.

Epidermal carcinogenesis studies of materials from several fossil fuel technologies are in progress. Details of the sources of materials, experimental methods, and initial results were presented previously (Annual Report, 1979; Status Report PNL-3189). All synthetic fuel materials used were derived from pilot plant operations and may not be representative of commercial practice.

The initial 2-yr exposure of mice to crude materials from the solvent-refined coal (SRC-II), shale oil, and crude petroleum technologies is complete except for histopathologic evaluation of remaining tissues and statistical analysis of data. The incidence of skin tumors observed at gross examination, and tumor latency for each group, and for those groups of mice exposed to the known carcinogens, benzo[a]pyrene (BaP) or 2-aminoanthracene (2-AA) are indicated in Table 1 and Figures 1 and 2. Most tumor diagnoses are based on gross examination only; the tumor incidence rate may change slightly when histopathologic examination is complete.

These results clearly reveal differences of tumorigenic potential and tumor latency among these materials. From Figure 1 it is apparent that repeated applications of 22.8 mg of HD or 0.05 mg of BaP induce somewhat similar rates of tumorigenic response; however, the neoplastic response to HD had a somewhat shorter latency. The high dose of either shale oil, 2-AA, or crude petroleum induced tumors with longer latency periods than did the highest dose of HD or BaP.

Figure 2 graphically presents epidermal tumor incidence in the middle-dose groups. Comparison of Figures 1 and 2 demonstrates that the neoplastic response is related to dose; in all groups, tenfold dilution of the test material increased the latency period. The only low-dose group to exhibit a neoplastic response at the site of application was that of the SRC-II HD-exposed mice (data included in Figure 2), which had an incidence of 82% at the end of the 2-yr study.

All tumors included in these data were located at the application site, and appeared to be epidermal. The gross and microscopic appearance of these tumors was described previously (Annual Report, 1979).

The data in this study indicate some degree of carcinogenicity in all the fossil fuel materials studied, with the exception of SRC-II LD. Considering latency periods and tumor incidence, SRC-II HD demonstrated the most carcinogenic activity, followed by crude shale oil and crude petroleum, in that order. Furthermore the very short tumor latency period observed in response to the highest dose of HD (relative to that of other materials, including the highest dose of BaP) indicate that SRC-II HD is a potent carcinogen in mouse skin under these experimental conditions.

Further skin-painting studies are currently in progress on the basic fraction, basic tar fraction, neutral tar fraction and PNA fraction of SRC-II HD, in an attempt to determine the components of HD responsible for its carcinogenic activity, and to assess the correlation of mutagenicity data from in vitro systems with carcinogenicity in mammalian in vivo systems. Data from in vitro studies on these fractions of HD (Pelroy et al., Annual Report, 1979) were used in choosing materials and doses for carcinogenesis assays in mice. We are also repeating the assay of SRC-II at the higher (22.8 mg per application) and medium (2.28 mg per application) doses.

Incidence and latency data on skin tumors observed at gross examination in mice exposed to fractions of HD or HD itself (replicate assay) are presented in Table 2 and Figure 3. It is apparent that the basic tar and the neutral tar are the most active fractions being tested from the standard point of tumor latency and incidence. The PNA fraction shows much less tumorigenic activity than the tar fractions; basic fraction has relatively little activity at this point in the assay. Tumor latency and incidence data from the replicate assay of HD are similar to those of the original study.

The data from our studies suggest that the carcinogenic potency of SRC-II HD is due in large part to constituents present in its basic tar and neutral tar fractions. Data from other researchers (Pelroy et al., Annual Report, 1979) indicate that these tar fractions contain large amounts of highly mutagenic polycyclic aromatic amines. Our data suggest that these polycyclic aromatic amines may play a major role in the carcinogenic as well as the mutagenic potency of HD.

Future work planned for this project includes examination of the potential role of ultraviolet light in carcinogenesis induced by fossil fuel liquids, studies of the effects of nitrosation of HD on its carcinogenicity (Pelroy et al., Annual Report, 1979), assay of the carcinogenicity of various boiling-point cuts of SRC materials, and carcinogenesis assay of hydrotreated SRC products.

TABLE 1. Incidence of Grossly Observed Skin Tumors at the End of 2 Year Exposure to Crude Fossil Fuel Materials or Known Carcinogens.

Material	Dose Group	No. Mice at Risk[a]	Mice With Skin Tumors	Percent Tumor Response	Minimum Latency, days	Median Latency, days	Maximum Latency, days
Untreated	Control	14	0	0	--	--	--
Acetone	Vehicle	14	0	0	--	--	--
Livermore Shale Oil	Low	11	0	0	--	--	--
	Middle	49	49	100	148	351	590
	High	38	38	100	95	213	409
Wilmington Crude Petroleum	Low	12	0	0	--	--	--
	Middle	28	13	46	282	--	--
	High	42	42	100	260	471	680
SRC-II Heavy Distillate	Low	33	27	82	282	603	--
	Middle	46	46	100	72	294	372
	High	49	49	100	56	95	147
SRC-II Light Distillate	Low	16	0	0	--	--	--
	Middle	14	0	0	--	--	--
	High	12	0	0	-	--	--
2-Aminoanthracene	Middle	37	37	100	442	610	736
	High	30	30	100	115	386	485
Benzo(a)pyrene	Low	23	0	0	--	--	-
	Middle	46	46	100	232	358	519
	High	50	50	100	106	143	193

(a) Number of mice at risk excludes only those mice that died in less than two years without developing any skin tumors. It includes all live animals in the group plus dead animals with skin tumors.

TABLE 2. Incidence of Grossly Observed Skin Tumors in Mice After Exposure to Chemical Fractions of SRC-II Heavy Distillate.

Material	Dose Group	Days on Study	No. Mice at Risk[a]	Mice With Skin Tumors	Percent Tumor Response	Minimum Latency, days	Median Latency, days	Maximum Latency, days
30% MeOH	Vehicle	525	41	0	0	--	--	--
Replication SRC-II Heavy Distillate	Medium	463	49	49	100	163	291	354
	High	463	50	50	100	44	112	232
SRC-II Heavy Distillate Basic Fraction	Low	539	40	0	0	--	--	--
	Medium	539	42	0	0	--	--	--
	High	539	42	8	19	323	--	--
SRC-II Heavy Distillate PNA Fraction	Low	413	47	1	2	393	--	--
	Medium	413	47	18	38	239	--	--
	High	413	49	49	100	171	267	351
SRC-II Heavy Distillate Neutral Tar	Low	364	49	2	4	240	--	--
	Medium	364	49	48	98	177	281	--
	High	364	50	50	100	99	183	235
SRC-II Heavy Distillate Basic Tar	Low	295	48	3	6	239	--	--
	Medium	295	49	45	92	162	252	
	High	295	50	50	100	74	148	204

(a) Number of mice at risk excludes only those mice that have died without developing skin tumors. It includes all live animals in the group plus dead animals with skin tumors.

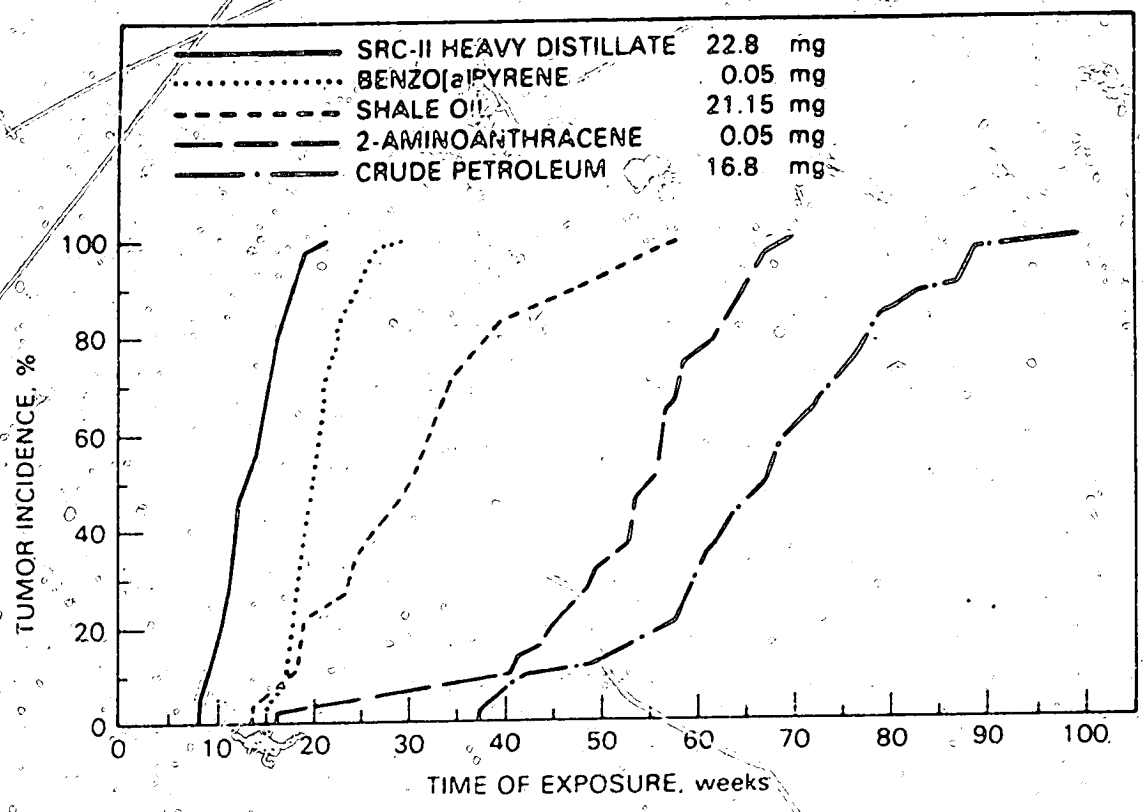

FIGURE 1. Skin Tumor Incidence Vs. Duration of Exposure of Mice to High Doses of Fossil Fuel Materials or Known Carcinogens.

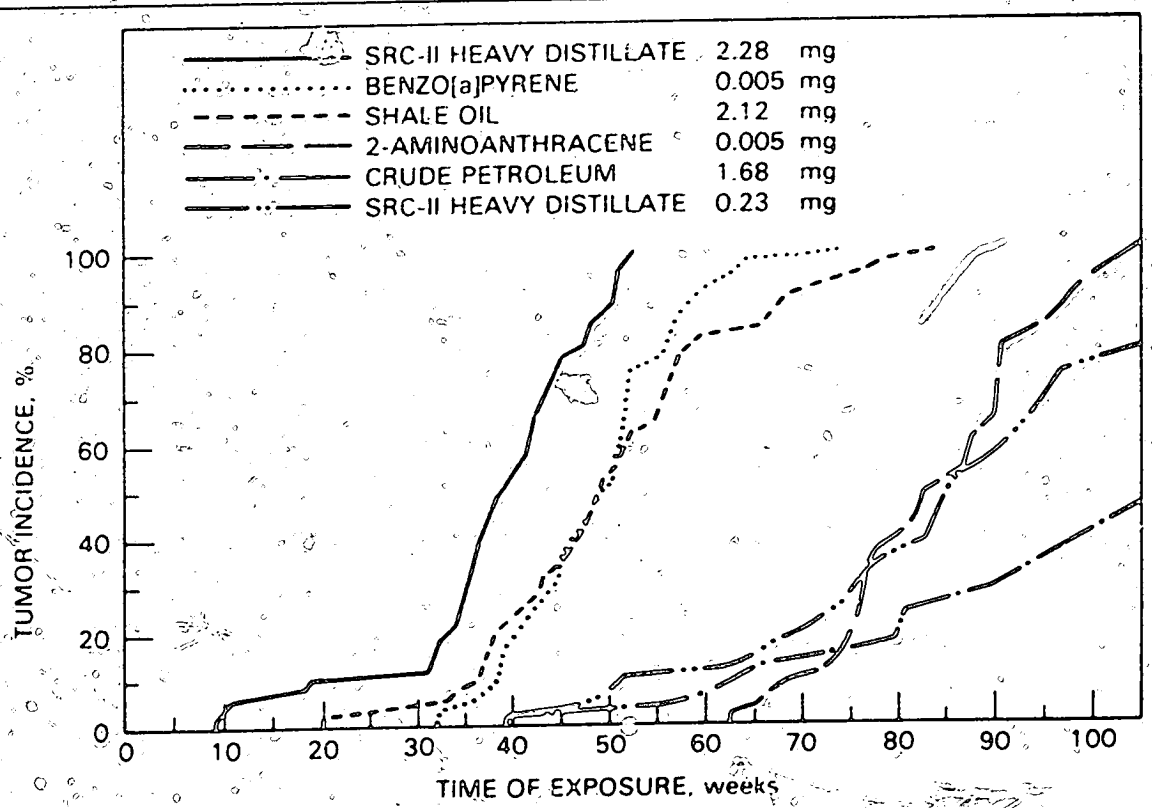

FIGURE 2. Tumor Incidence Vs. Duration of Exposure of Mice to Middle and Low Doses of Fossil Fuel Materials or Known Carcinogens.

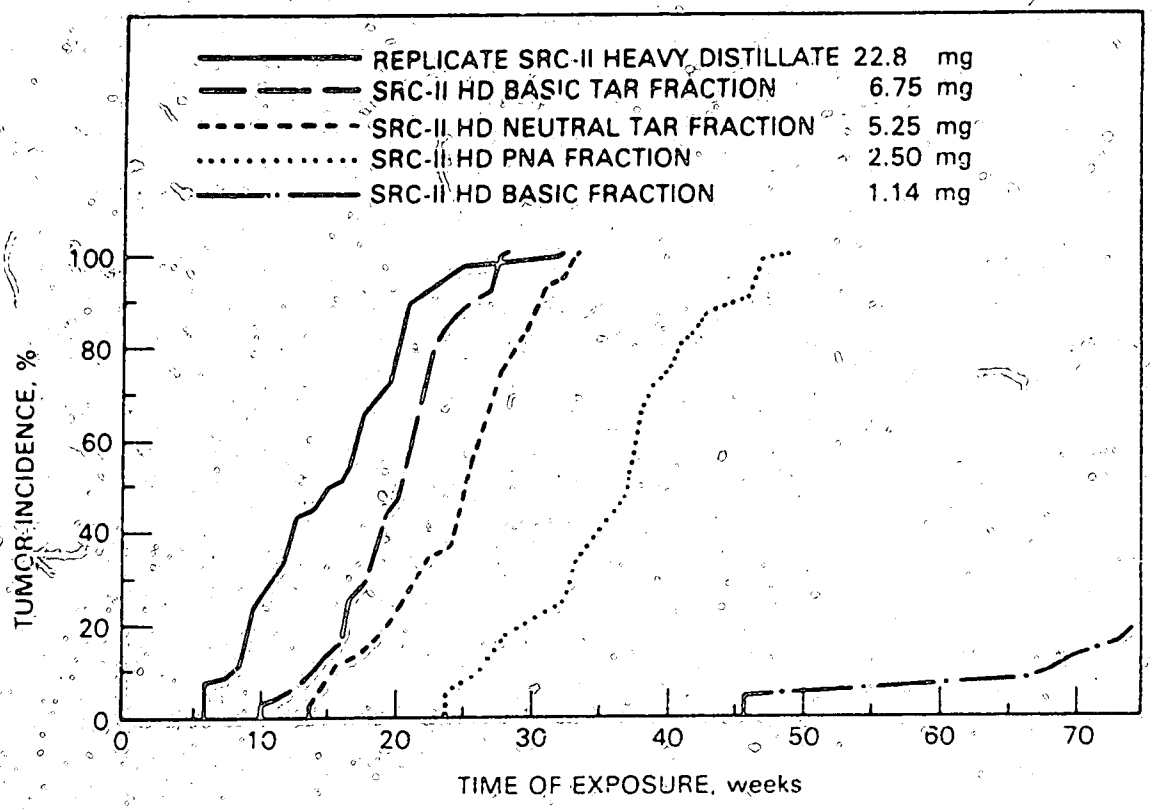

FIGURE 3. Tumor Incidence Vs. Duration of Exposure of Mice to SRC-II Heavy Distillate or Its Fractions.

6 Multitechnology

• Toxicology of Inhaled Acid Aerosols

This project is concerned with determining the long-term biological effects of exposure to inorganic acid aerosols, which are common to many industrial processes and to fossil fuel plant effluents. Rats were exposed to graded, subacutely toxic doses of HNO_3, HCl and H_2SO_4 to determine dose-related tumorigenesis. This publication completes the scheduled work on this project.

LATE EFFECTS FOLLOWING EXPOSURE TO GRADED DOSES OF HNO_3, HCl OR H_2SO_4

Investigators: J. E. Ballou, R. A. Gies, G. E. Dagle, and R. A. Miller

Rats exposed to HNO_3, HCl or H_2SO_4 aerosols developed bone tumors (6); no bone tumors were found in controls. Rats exposed to HNO_3 or HCl developed lung tumors (3); two were also found in H_2O-treated controls. The statistical evaluation of these observations is not yet complete.

Male Wistar rats were exposed to three graded dose levels of HNO_3, HCl or H_2SO_4 aerosols in a study of the causative relationship between acid exposure and bone tumor (osteosarcoma) development. The work was suggested by an earlier finding of bone tumors in rats exposed only to 0.27N HNO_3 carrier aerosols (Ballou et al., Health Phys. 32: 479, 1977). The animals were exposed repeatedly (six times, 6 hr/exposure, on alternate weekdays) to subacute levels of acid aerosols ranging from 0.7 to 160 times the threshold limit value (TLV). The treatment did not influence weight gain or average life span of rats surviving >200 days after exposure. Acute effects of acid exposure, (e.g., burns on exposed skin, transient respiratory distress, early death) were observed at the highest dose level of HCl and HNO_3 (3 and 10 times the TLV, respectively). Details of the experimental protocol were reported in the Annual Report for 1976.

The long-term effects in these animals were characterized by a variety of benign and malignant lesions, found in both experimental and control groups (Tables 1 and 2).

The benign lesions (Table 1) were rather uniformly distributed throughout all groups with fibromas, lipomas, and tumors of the adrenal gland predominating. (Mammary tumors were not a major factor since only male rats were used in this study.) We found few benign changes in the lung which might have been suggestive of progressive damage due to acid inhalation.

The malignant lesions (Table 2) included six osteosarcomas of the skeleton, associated only with those animals subjected to the repeated acid exposure regimen. The incidence of bone tumors, however, was not correlated with the amount of acid deposited, as would be expected if mineral acid exposure were the causative agent. On the other hand, there were no osteosarcomas in the H_2O-treated controls or in nontreated shelf control animals, indicating that the tumors may have been acid-treatment-related.

We found lung tumors in animals exposed to HNO_3 (2) and HCl (1); two primary lung tumors in the treated control group exposed to H_2O aerosols, but none in nontreated control rats. The small number of lung tumors, and the fact that these tumors were not dose-related and were also found in treated control animals, does not indicate that the lesions are related to acid inhalation. They may be associated with the exposure/handling procedure, as seems to be the case with the bone tumors.

This work with acid aerosol inhalation will be terminated after completion of statistical analysis of the data.

TABLE 1. Tabulation of Benign Lesions in Rats Exposed to Acid Aerosols.

	Control		Total Amount Deposited, mg[a]									
			HNO_3				HCl			H_2SO_4		
	Nontreated	Treated[b]	0.1[c]	2.02	2.3	6.8	0.7	1.3	2.5	0.7	1.2	26
Fibroma	27	12	13	6	8	13	10	15	10	9	15	10
Fibroadenoma (Mammary)	1		1	3	3			1	3	2		
Lipoma	8	2	4	3	2	6	3	4	2	3	2	5
Hemangioma	1		2	2	1	2						
Sebaceous Adenoma	1										1	
Benign Islet Cell Tumor												
Epithelioma					1							
Parathyroid Adenoma					1							
Trichoepithelioma	2				2	1		2		1		
Interstitial Cell Tumor (Testis)	1						1	1				
Hemangiopericytoma										1		
Adrenal Cortical Adenoma	6		1	1		1		2	1	1		1
Neurofibroma							1	1				
Squamous Papilloma			1				1	2				
Benign Pheochromocytoma	5		2	2	3	2	2	3	1		4	1
Mammary Adenoma	1							1				
Keratoacanthoma												1
Thyroid Adenoma										1		
Adrenal Ganglioneuroma		1										
Pulmonary Adenoma							1					
Benign Endocrine Tumor							1					
Hemartoma		1										
Number with Tumors/Number of Rats	53/90	16/39	24/63	17/49	21/50	26/50	20/49	32/49	17/50	18/50	22/50	18/50

(a) Total deposition was estimated from aerosol concentration, characteristics and assumed respiration parameters.
(b) Rats were exposed to H_2O aerosol as explained in text.
(c) Rats were exposed to 0.27% HNO_3 aerosols, nose only, for 30 minutes using a Lovelace nebulizer. Other acid-treated rats were exposed as described in the text.

TABLE 2. Tabulation of Malignant Lesions in Rats Exposed to Acid Aerosols.

	Control		Total Amount Deposition, mg[a]									
			HNO_3				HCl			H_2SO_4		
	Nontreated	Treated[b]	0.3[c]	2.02	2.3	6.8	0.7	1.3	2.5	0.7	3.2	26
Osteosarcoma					2			1	2	1		
Lung Squamous Cell Carcinoma		1										
Lung Osteosarcoma		1										
Lung Carcinosarcoma				1								
Bronchioalveolar Adenocarcinoma					1		1					
Hepatocellular Carcinoma				1				2		1	1	
Pancreatic Acinar Carcinoma							1					
Malignant Islet Cell Tumor					1					1		
Malignant Lymphoma		2	3	2	5	4	8	8	4	5	3	3
Reticulum Cell Sarcoma	3	1			1	2	2			1	6	1
Leukemia	4			1	4		1			1		1
Myelosarcoma	1		1									
Malignant Fibrous Histiocytoma	5	2	1	1	1	1	1	1	3	2		2
Synovial Sarcoma	1											
Undifferentiated Sarcoma	1					2	1					
Fibrosarcoma	3	3	4	1	5	4			2	4	1	1
Liposarcoma	1		1							1		
Hemangiosarcoma			1	1						1		
Neurofibrosarcoma										1		
Thymic Carcinoma				1								
Thyroid Adenocarcinoma/Carcinoma	1		1					1		1		
Undifferentiated Carcinoma/Adenocarcinoma								1				1
Prostatic Adenocarcinoma					1							
Malignant Mixed Salivary Tumor					1							
Malignant Hemangiopericytoma							1					
Adrenal Cortical Cell Carcinoma							1				1	
Malignant Mesothelioma			1	1								
Squamous Cell Carcinoma					1			2	1		1	
Intestinal Adenocarcinoma					1							
Rhabdomyosarcoma					1							
Malignant Pheochromocytoma				1	2			1				
Mammary Adenocarcinoma								1				
Malignant Neoplasm (Uncertain Type)				1								
Leiomyosarcoma										1	1	
Basal Cell Carcinoma											1	
Sebaceous Carcinoma			1						1			
Kidney Carcinoma			1									
Number of Tumors/Number of Rats	27/90	10/39	15/61	17/49	28/50	13/50	20/49	22/49	13/50	21/50	15/50	9/50

(a) Total deposition was estimated from aerosol concentration characteristics and assumed respiration parameters.
(b) Rats were exposed to H_2O aerosol as explained in text.
(c) Rats were exposed to 0.27 N HNO_3 aerosols, nose only, for 30 minutes using a Lovelace nebulizer. Other acid-treated rats were exposed as described in the text.

Metal-Membrane Interactions

The ionic forms of most toxic metals penetrate cell membranes slowly, and their primary effects are probably exerted on control systems and enzymes in the cell membrane. Although entry of the toxic metals into the cells is poorly understood, it is probably mediated by specific transport systems in the plasma membrane. Information on the interaction of metals with defined membrane functions should therefore aid in predicting potential effects of trace metals derived from fossil-fuel combustion.

In the present stage of the research we are attempting to define the role of membranes in regulating protein synthesis in *Neurospora crassa*, and to study membrane alterations that accompany cell transformation to the neoplastic state. During the past year, we have purified an acid protease secreted by *Neurospora*, and have discovered that it is secreted in response to deprivation of carbon, sulfur or nitrogen, and induction by protein, and that it is regulated by conversion to an alternate form by acidic medium. A highly sensitive and specific assay was developed for another (pepsin-like) acid protease secreted by *Neurospora* in response to starvation, and the enzyme was partially purified and characterized.

We previously observed an apparent correlation between the presence of an enzyme (ATPase) on the surface of some cell types and the tumorigenicity of the cells. This correlation was tested on other cell types this year, but results were inconsistent. However, we found and characterized an alkaline phosphatase activity on the external surface of a tumorigenic cell line derived from monkey kidney. We have not found this enzyme on other cell types, therefore it may be a useful marker for identifying the original type of some transformed cells.

PURIFICATION OF EXTRACELLULAR ACID PROTEASE FROM NEUROSPORA CRASSA

Investigators: W. G. Rhodes, R. A. Lindberg, and H. Drucker

We have shown that the pepstatin-sensitive acid protease (AcP) of Neurospora crassa activates trypsinogen, allowing us to develop an assay that distinguishes AcP from the other exocellular N. crassa proteases. By using its inhibitor, pepstatin, as a ligand in affinity chromatography, we have made substantial progress toward purifying this enzyme.

As described in the 1979 Annual Report, Neurospora crassa secretes three acidic proteases: two metalloenzymes (M1 & M2), and one enzyme (AcP) that is inhibited by pepstatin. Production of these proteases requires induction by exocellular protein and derepression by starvation for either carbon, nitrogen, or sulfur. The derepression conditions determine the relative quantities of these proteases that appear in medium filtrates. AcP is not detectable during inductions carried out under carbon starvation; it is present in trace amounts under nitrogen starvation, and is produced in greatest quantity under sulfur starvation. The effects of various conditions of derepression on production of M1 and M2 are described in an accompanying report. As reported earlier, N. crassa also produces large quantities of alkaline and neutral proteases under all three conditions of derepression. Our goal is to understand the differential regulation of protease production in this organism.

We have found that a trypsinogen-activation assay allows detection of AcP in the presence of the other proteases, and we are developing a purification procedure for AcP, using ion exchange and affinity chromatography. During development of this procedure, our primary criterion of purity is homogeneity of enzyme preparations on polyacrylamide gel electrophoresis in the presence of sodium dodecyl sulfate.

The AcP assay entails incubation of AcP solutions with trypsinogen at the desired pH, followed by adjustment to pH 8.0 and addition of casein, which is digested by the trypsin produced during incubation with AcP. Undigested protein is precipitated with trichloroacetic acid, the

solution is filtered, and absorbance of the filtrate is measured at 280 nm. The absorbance is converted to units of trypsin activity using a calibration curve obtained from treatment of casein with various quantities of trypsin under the assay conditions. Finally, trypsin samples used in calibration are assayed for activity toward benzoylarginine ethyl ester (BAEE). One unit of AcP activity is defined as the amount required to liberate 1 BAEE unit of trypsin per minute at 37° and specified pH. On the basis of the data shown in Figure 1, pH 4.0 is used in these assays.

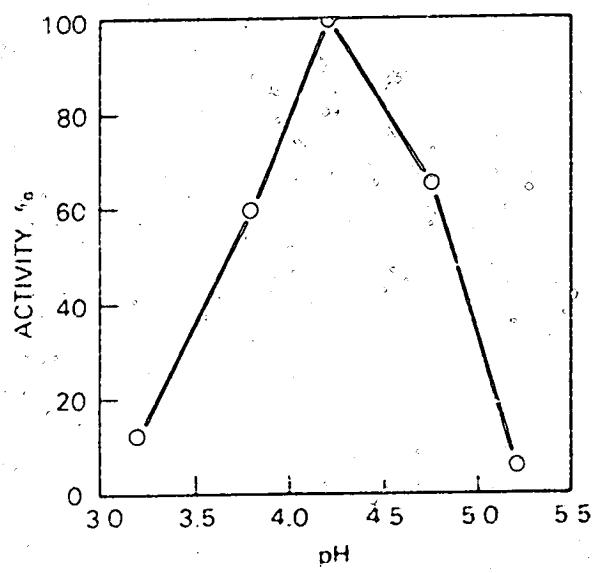

FIGURE 1. Effect of pH on Activity of N. crassa Acid Protease. Samples from CM-cellulose chromatography were assayed for trypsinogen activation at various pH values.

Sulfur derepression is used to produce medium filtrates containing enough AcP for purification. In a typical preparation, 4 ℓ of medium filtrate are obtained from an 8-hr induction using 1% bovine serum albumin (BSA) as the inducing protein. The filtrate is adjusted to pH 3.4 with 1 M citric acid, and concentrated 10-fold on a Pellicon® cassette with a 10,000 dalton cutoff. The concentrate is dialyzed against 0.01 M sodium citrate, pH 3.4. The retentate is applied to a 5.0 x 30-cm column of carboxymethyl cellulose and eluted with a gradient of KCl. The fractions containing activity are pooled and concentrated 15-fold on an Amicon® PM-10 membrane.

Samples of AcP concentrate are dialyzed against 0.1 M sodium citrate, 0.5 M NaCl, pH 3.0, and subjected to affinity chromatography on diaminodipropylamine-pepstatin-Sepharose CL-6B. Bound AcP is removed by elution with 0.1 M $NaHCO_3$, 0.5 M NaCl, pH 8.7, and the pH of AcP-containing fractions is immediately adjusted to 4.0. A typical affinity chromatogram is shown in Figure 2.

Polyacrylamide gel electrophoresis of AcP from affinity chromatography (Figure 3A) shows that the enzyme is contaminated with small amounts of several species, two of which appear at positions corresponding to the neutral and alkaline proteases of N. crassa.

Samples of affinity-purified AcP have been subjected to chromatography on Sephadex G-75 and on DEAE Sephadex A-25. Both chromatographies resulted in a single peak of protein and activity, but the same contaminants were present, although they were markedly reduced in the DEAE Sephadex effluent (Figure 3B).

To find out whether the contaminants resulted from autodigestion of AcP, an affinity-purified sample was incubated at 37°C for 30 min and examined by polyacrylamide gel electrophoresis; there was no detectable increase in contamination. The persistence of contamination by alkaline and neutral proteases, if confirmed, might imply that AcP has an affinity for these enzymes, because they should be eluted in the void volume during both the DEAE Sephadex and the pepstatin-affinity chromatographies. If these enzymes are binding to AcP, they might be eliminated by extensive washing of affinity-bound AcP with buffer, protein solutions, or mild denaturants.

The weight of the AcP molecule from sulfur-derepressed N. crassa is estimated from G-75 chromatography at 34,000 daltons and from polyacrylamide gels at 32,500 daltons. As described in the 1979 Annual Report, the weight of AcP from nitrogen-derepressed organisms is approximately 66,000 daltons. The N-derepressed enzyme may be a dimer or, more likely, it may contain a large carbohydrate moiety, as does the 62,000-dalton acid protease from Aspergillus oryzae.

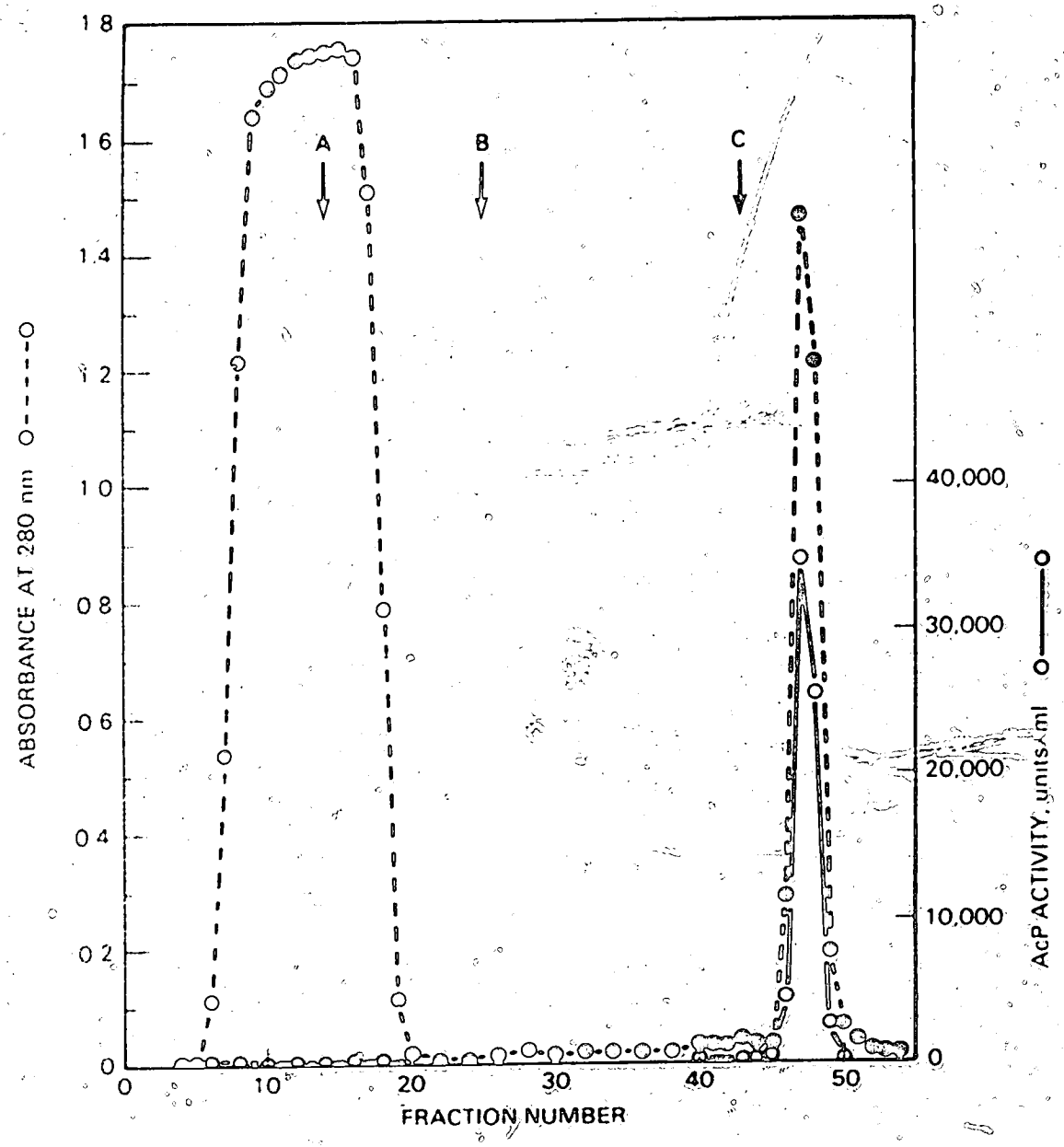

FIGURE 2. Affinity Chromatography of AcP. The sample is AcP pooled from CM-cellulose chromatography. A. End of elution of sample onto column, beginning of elution with 0.1 M sodium citrate, 0.5 NaCl, pH 3.0. B. Elution with 0.5 M NaCl. C. Elution with 0.1 M $NaHCO_3$, 0.5 M NaCl, pH 8.7, into tubes containing 0.25 ml 1 M sodium citrate, pH 3.0.

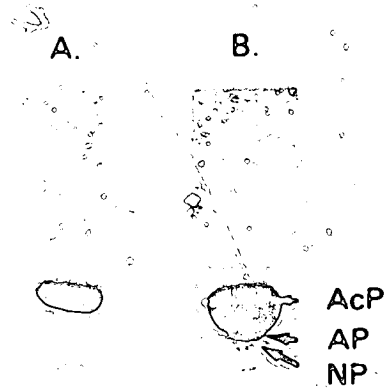

FIGURE 3. Polyacrylamide Gel Electrophoresis of AcP. A. AcP after affinity chromatography. B. AcP after chromatography on DEAE Sephadex. AP: Alkaline protease. NP: Neutral protease.

EXTRACELLULAR MODIFICATION OF A PEPTIDASE PRECURSOR FROM NEUROSPORA CRASSA

Investigators: R. A. Lindberg, W. G. Rhodes, and H. Drucker

An extracellular peptidase, M-1, was purified from culture filtrates of N. crassa grown with protein as the sole source of carbon. Characterization of this enzyme and another peptidase, M-2, obtained from nitrogen-starved cultures, indicated that: M-1 is a precursor of M-2; that the conversion of M-1 to M-2 occurs extracellularly; and that the rate of conversion is a function of nutrilite deprivation.

N. crassa secretes three electrophoretically distinct proteases of acid pH optima. All three require induction by exogenous protein, but regulation by derepression is different for all three (Figure 1). The AcP, a pepsin-like protease, is electrophoretically detectable only when sulfur (S) is limiting. The M-1 peptidase is secreted when carbon (C) is limiting, and also when cells are limited for nitrogen (N), but in the case of N, activity disappears with time. The M-2 peptidase is present when cells are derepressed for N or S. To elucidate the differential appearance of these extracellular enzymes, M-2 (previously purified from N-starved filtrates, Annual Report, 1979), was characterized, and M-1 was purified and characterized.

To obtain purified M-1, 4 ℓ of carbon-starved, gelatin-induced mycelia were grown for 5 hr and a cell-free filtrate collected. The pH of the filtrate was raised to 5.8, sodium azide (0.02%, to prevent bacterial growth) and PMSF (1 mM, to inhibit alkaline protease) were added and the filtrate was cooled to 4°C. After concentration of 200 ml by ultrafiltration, the retentate was chromatographed on DEAE cellulose at pH 6.8, CM cellulose at pH 6.15, and Sephadex G-75, also equilibrated at pH 6.15 with histidine buffer (0.01 M). The resultant enzyme preparation was rechromatographed on the G-75 column, equilibrated with imidazole (0.01 M), pH 6.7.

The purity of the M-1 and M-2 preparations is unknown, but no other proteases are detectable by electrophoretic methods in either case. The M-2 is 100% inhibitable by EDTA, implying that only one acid protease species is present in active form. The M-1 activity eluted from the G-75 column with an absorbance at 280 nm of 0.008, indicating that almost no protein was present. Activity of this small an amount of enzyme can be followed due to the extreme sensitivity of the fluorescamine protease assay.

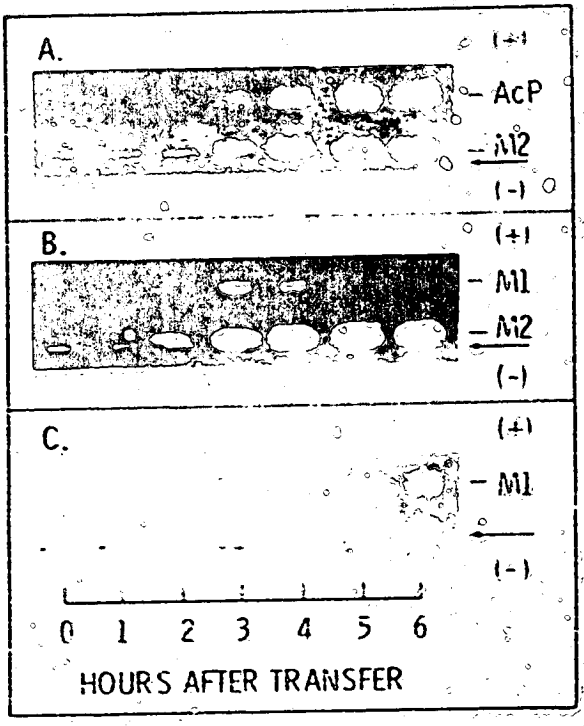

FIGURE 1. Electrophoretic Pattern of Protease Activity at pH 5.0 From Culture Filtrates of N. crassa. Hourly samples of 2.75 µl were electrophoretically separated on cellulose acetate and strips laid on milk-agar to visualize protease activity. The arrow indicates the origin, which is marked with a slash. All three cultures were induced: A, B and C were -S, -N and -C, respectively.

The measured pH optima of both enzymes were found to be nearly identical (Figure 2). These optima were obtained by standard assay proceedures, incubated at

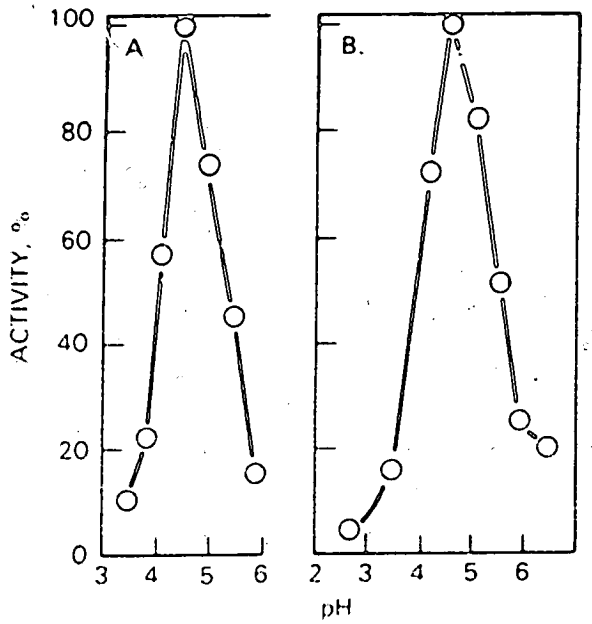

FIGURE 2. Effect of pH on Activity of M-2 Purified From Nitrogen-Limited Cells (A), and of M-1 From Carbon-Limited Cells (B)

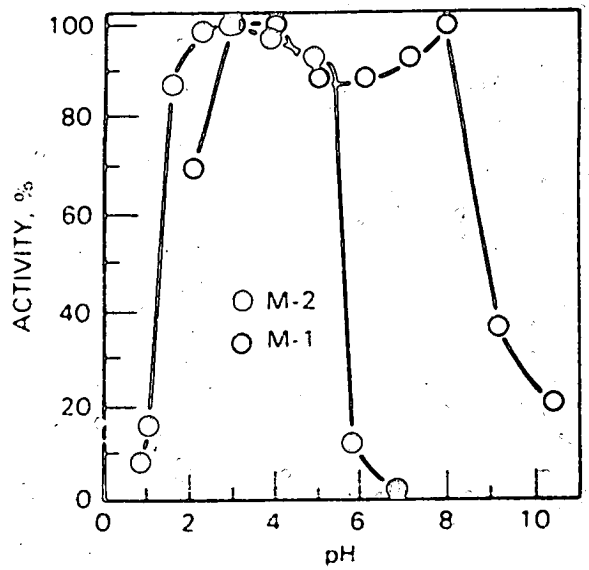

FIGURE 3. Profile of pH Stability of Peptidases M-1 and M-2. Enzyme was allowed to remain for 24 hours at room temperature at pH indicated, and assayed for remaining activity.

various pH levels, using bovine serum albumin as the substrate. The previously reported pH optimum for M-2 (Annual Report, 1979) was found to be inaccurate. The carboxyl groups on the citrate buffer used in that study are strong enough chelators to inhibit M-2. Further, the chelation ability changes with pH as the carboxyls of citrate are protonated.

Stability as a function of pH was also investigated (Figure 3): M-2 is stable at low pH and rapidly loses activity above pH 5.0. On the other hand, M-1 is stable up to at least pH 8.0. The two enzymes also differ in sensitivity to chelators. Both are cation-requiring enzymes, but incubation with 1 mM EDTA prior to the electrophoretic assay eliminates all M-2 activity, whereas 20 mM EDTA does not completely inhibit M-1.

Despite these differences, M-1 and M-2 appear to be different forms of the same enzyme. Electrophoresis of the samples from M-1 pH stability studies demonstrates that M-1 changes electrophoretic mobility to that of M-2 between pH 5.0 and 6.0 (Figure 4). These results, and the similar pH optima, suggest that M-1 is being converted, extracellularly, to M-2. A molecular weight change accompanies the electrophoretic mobility change. The M-1 activity eluted from the second G-75

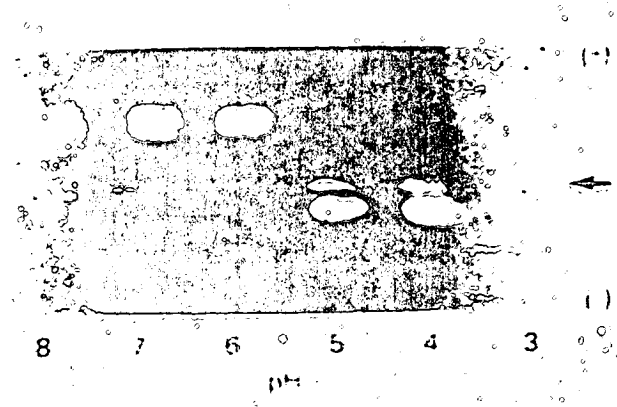

FIGURE 4. Electrophoresis of Purified M-1 Incubated 1 Hr at Various pH Levels. Activity was visualized as described in Figure 1.

column at ≈ 36,000 MW, whereas M-2 peaked at ≈ 16,000 MW (Figure 5).

It is not yet known if conversion is a function of pH or an autocatalytic change involving proteolysis, contingent upon pH. To resolve this problem, larger quantities of M-1 are needed. It is possible that M-1 may be an enzyme-inhibitor complex with inhibition relaxed by lowered pH, or a zymogen, capable of autocatalytic activation at the appropriate pH.

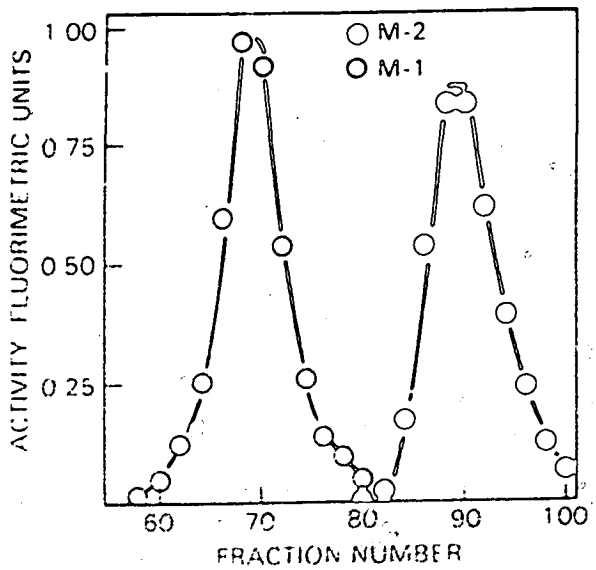

FIGURE [illegible] Elution Profiles From G-75 Filtrations. M-1 was chromatographed on a Sephadex G-75 column equilibrated with imidazole pH 6.[illegible] M-2 was chromatographed under the same conditions equilibrated with acetate pH 4.6

If, as the data suggest, M-1 and M-2 are different forms of the same enzyme, and the irreversible conversion of M-1 to M-2 is a function of pH, then the differential regulation shown in Figure 1 can be explained by the following hypothesis. During induction in media lacking C, N or S, M-1 is secreted, and its conversion to M-2 is controlled by the pH of the media and/or the pH of the localized cellular environment, i.e., the periplasmic space. Fungal growth in liquid medium lowers the pH of the medium at a rate dependent on several factors. The decrease in pH is attributed to organic acid secretion, a cellular ATPase pump that excretes H^+, and cation utilization. The lowering of pH is proportional to cell growth which, for the three states of derepression is, -S>, -N>, -C

Measurement of pH showed that during inductions in the absence of C, the pH of the media remained constant at 5.75, and conversion does not take place. The pH of a -N induction drops from 5.75 to 5.55, and conversion takes place during the induction. In a -S induction, secretion takes place 2 hr after nutrilite deprivation: the pH of the medium is already below 5.5 when secretion takes place. In this case, conversion is immediate, and M-1 is never detectable. These conclusions imply that, at the transcriptional level, the low-pH-optimum enzyme is regulated in a fashion similar to that of the alkaline and neutral proteases investigated earlier.

CHARACTERIZATION OF EXTERNAL PHOSPHATASE OF VERO CELLS

Investigator: R. P. Schneider

Technical Assistance: L. M. Butcher

In addition to an external nucleoside triphosphatase activity, VERO cells have an external alkaline phosphatase. The enzyme, which is noncompetitively inhibited by ATP, appears to be the same enzyme commonly found in mammalian liver, gut and kidney. Previously, it was considered an intracellular membrane enzyme.

We have been studying the properties and distribution of an external nucleoside triphosphatase enzyme (NTPase) found on an avian leukemia virus (AMV), in leukemia cells that produce the virus, and in cultured mammalian cell lines. Data obtained at this and other laboratories suggest that this enzyme may be a useful marker for identifying tumorigenic cells, cell type prior to transformation, or both. In an experiment that assessed the substrate specificity of the NTPase we found that intact VERO cells hydrolyzed phosphate esters (phosphatase) as well as nucleotide phosphate-phosphate bonds (NTPase).

We then conducted a series of experiments to ascertain whether the NTPase or another external enzyme was responsible for the phosphatase activity. Phosphatase activity was measured using a chromogenic substrate (o-nitrophenyl phosphate) and NTPase by measuring inorganic phosphate release from ATP. Both activities were measured in intact cells, thus assaying externally localized enzymes.

The bimodal response of phosphatase activities to variation in pH was clearly different from that of NTPase (Figure 1). Phosphatase activity decreased as pH was decreased from 6 to 7, then increased more than 10-fold as the pH was increased to 9. The NTPase activity, on the other hand, was essentially constant from pH 6 to 9. The data suggest that in addition to NTPase, both an acid phosphatase and an alkaline phosphatase are present on the surface of the cells.

The alkaline phosphatase activity was further characterized by performing the assays at pH 9. The enzyme was strongly inhibited by ATP (Figure 2) and other nucleotides (ADP, ITP, CTP and GTP) hydrolyzed by the NTPase. This inhibition may be the result of overlapping specificities

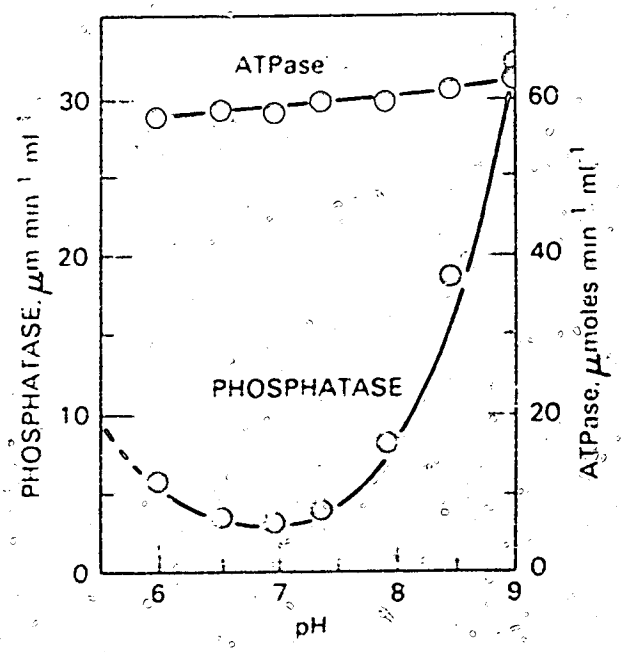

FIGURE 1. Effect of pH on External Phosphatase and NTPase Activity of VERO Cells

(competitive), or may be caused by more indirect effects of the nucleotides on the phosphatase, i.e., at a site distinct from the active site (noncompetitive). The first alternative suggests the possibility that the NTPase has phosphatase activity (or the converse) in spite of the different response of the two activities to altered pH. A kinetic analysis of the dependence of the phosphatase on substrate concentration (Figure 3) demonstrates that the inhibition of activity by ATP is noncompetitive. Together with the pH effect, this clearly demonstrates that the phosphatase and NTPase activities are catalyzed by separate enzymes.

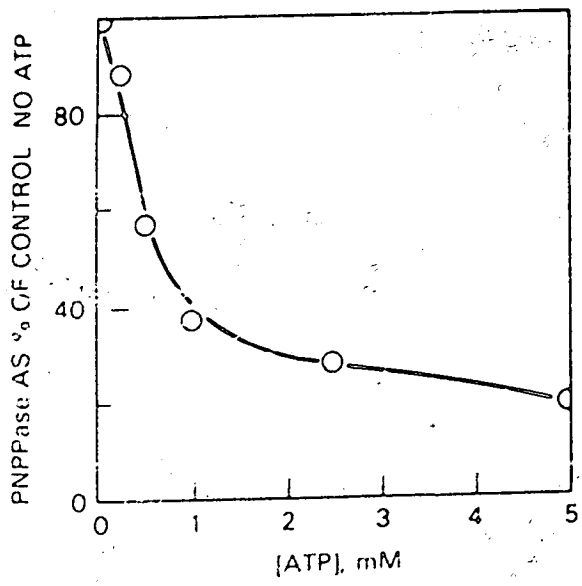

FIGURE 2. Effect of ATP Concentration on External Phosphatase Activity of VERO Cells

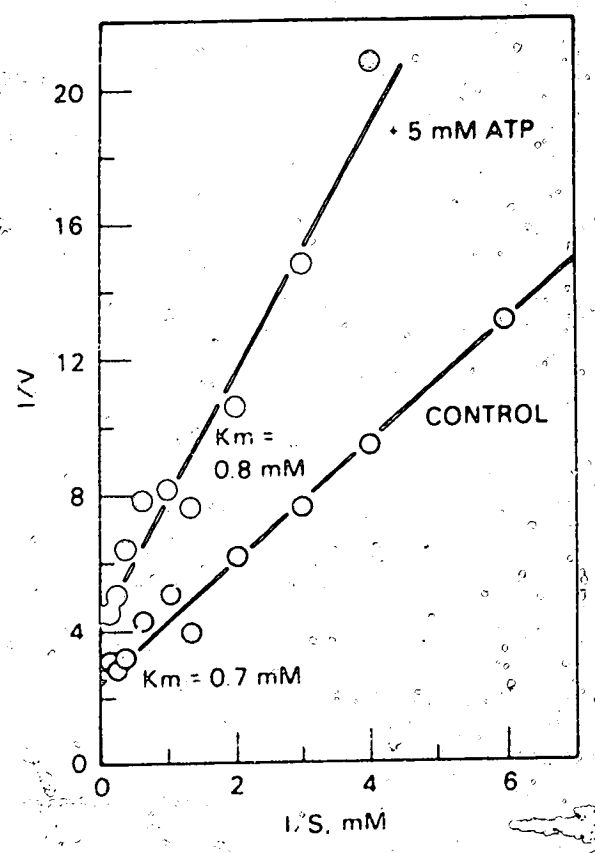

FIGURE 3. Effect of ATP on Dependence of the Alkaline Phosphatase on the Concentration of Substrate (1/v vs. 1/s plot).

The divalent metal ion requirements of the phosphatase were examined by varying the external concentrations of Ca^{2+} and Mg^{2+}. Other than an inhibition of activity at high Mg^{2+} concentrations, no effect of these ions was observed. These data are consistent with the notion that the external phosphatase is alkaline phosphatase, a ubiquitous enzyme of unknown function. Demonstration of its activity on the external surface of mammalian cells is a new observation. Previously, it was considered a membrane-bound enzyme, which was assumed to be localized on the interior surface of the plasma membrane. The enzyme is found in greatest amount in gut and kidney. VERO cells, derived from monkey kidney, apparently retain the enzyme after transformation. A normal fibroblast cell line and two virus-transformed lines derived from it do not possess the activity. Therefore, its presence appears to be specific for cell lines, and it may be a useful marker for determining the histogenesis of some transformed lines from liver, gut and kidney.

The effect of nucleotides on the alkaline phosphatase activity suggests that control of unknown functional signficance is exerted on the enzyme activity by the external nucleoside triphosphates. This might be exerted by the binding of ATP to the phosphatase at a regulatory site, or by the NTPase altering the membrane conformation via NTP hydrolysis.

○ Toxic Effects of Geothermal Effluents

The purpose of this project is to investigate the potential for toxic effects of exposure to effluents from geothermal power plants. We are currently examining the potential toxic effects of exposure to hydrogen sulfide and/or ammonia, utilizing in vivo and in vitro biological systems.

EFFECT OF IN VITRO EXPOSURE TO HYDROGEN SULFIDE ON RABBIT ALVEOLAR MACROPHAGES CULTURED ON GAS PERMEABLE MEMBRANES

Investigator: A. V. Robinson

Technical Assistance: L. Daughtry and S. Strankman

Exposure of alveolar macrophages (AM) cultured on gas-permeable membranes to approximately 60 ppm of H_2S for 24 hr resulted in a decrease in the number of AM containing one or more phagocytized beads to 5% of control values. In contrast, AM cultured on plastic tissue-culture flasks showed no decrease in phagocytic ability. Cytotoxicity was more pronounced under continuous than interrupted exposure regimens. Above a critical level of H_2S exposure, a time-dependent degradation of phagocytic ability occurred.

The growing development of geothermal resources has increased the probability of chronic, high-level exposure to H_2S gas. We therefore examined the effect of H_2S on alveolar macrophages, which are important in the maintenance of alveolar sterility, the clearance of inhaled particles and immune function. We have previously measured (Annual Report, 1979) the effect of H_2S exposure on the phagocytic ability [illegible] and exposure in vitro. The studies reported here extend the earlier results in a culture system that more closely approximates the environment of the alveolar macrophage in vivo.

The AM were obtained by saline lavage from the lungs of male New Zealand White rabbits and cultured in RPMI 1640 culture medium containing 0.4% BSA, 5 μg/ml insulin, 5 μg/ml transferrin, 2.5 μg/ml Fungizone®, 100 IU/ml penicillin, and 100 μg/ml streptomycin. They were incubated overnight in a 5% CO_2 atmosphere. Exposure to H_2S and measurement of dose levels were as previously described (Annual Report, 1979).

At 0, 24, or 48 hr following exposure, 2.02-μm polyvinyltoluene (PVT) beads were added to the cells (calculated bead:cell ratio, 250:1). At the end of 2 hr incubation, we added 0.5 ml of 50 mM adenosine triphosphate (ATP) in 0.05 M Tris buffer, pH = 7.5, and the cultures were allowed to incubate another 20-40 min. The detached cells were harvested and the numbers of beads per cell (100-200) were then counted by light microscopy of stained smears.

Table 1 compares the phagocytic ability of AM cultured on either gas-permeable membranes or a gas-impermeable surface and exposed to 60 ppm H_2S for 24 or 48 hr. [illegible] of phagocytic capability were performed 24 hr following the end of the 24-hr exposure and immediately following the end of the 48-hr exposure. A marked difference in cytotoxicity was evident between the two culture methods. Examination of the cells cultured on Falcon tissue-culture flasks (gas-impermeable surface) revealed no decrease in phagocytic ability at 24 hr and approximately 20% inhibition of phagocytosis, compared to controls, at 48 hr. In contrast, the AM cultured on Petriperm® dishes (gas-permeable membranes) revealed approximately 95% inhibition of phagocytosis, compared to controls.

The mechanism for the increased sensitivity to H_2S of AM cultured on gas-permeable membranes is not known at this time. In the lung, the AM reside on the alveolar wall, and are covered with a thin film of surfactant. Exposure of the AM to H_2S directly through a gas-permeable membrane is more similar to in vivo exposure

TABLE 1. A Comparison of the Effect of 60 ppm H_2S on Rabbit Alveolar Macrophages Cultured on Falcon Tissue Culture Flasks Versus Petriperm® Dishes.

Treatment	Percent of Cells Containing ≥1 Bead	
	Flasks[a]	Dishes[a]
Control	80 ± 7	80 ± 8
24 hr Exposure + 24 hr Delay	88 ± 6	4 ± 6
48 hr Exposure + No Delay	53 ± 13	2 ± 3

[a] 5 replicates per point

than is exposure through an intervening 5-mm layer of culture medium, and thus more accurately reflects the in vivo AM response to an irritant gas such as H_2S. However, one would expect that the H_2S would be equilibrated with the liquid phase in experiments lasting 24-48 hr in either exposure system.

We noted previously (Annual Report, 1979) that, in the 24-hr interval between the time when AM were exposed to H_2S and the time we measured phagocytic ability and viability, the level of cellular damage increased dramatically. To further investigate this phenomenon, AM cultured on Petriperm® dishes received a single exposure to H_2S. The phagocytic ability of the exposed macrophages was measured at 0, 24 and 48 hr after exposure.

The data (Table 2) show no effect of 73 ppm on the percentage of cells containing one or more beads. The percentage of cells containing more than 21 beads was inhibited by about 50% immediately (70% at 24 hr), but recovered to control levels at 48 hr after the end of exposure. In contrast, a 6-hr exposure to 170 ppm apparently caused an irreversible decrease in the percentage of cells that contained more than 21 beads, as did exposure to 60 ppm for 20-22 hr. Further, the percentage of cells containing more than one as well as those with more than 21 beads decreased during the delay between the end of exposure and measurement of phagocytizing capability. These data indicate that the full expression of the H_2S-induced inhibition of phagocytosis is dependent on the length of time after the end of exposure as well as the duration and level of exposure.

The increased cytotoxicity following cessation of exposure could be due to the presence of persistent toxic compounds, generated in the medium during exposure, which exert toxic effects after exposure ceases. To test this hypothesis, AM culture medium in Petriperm® dishes was exposed for 24 hr to 54 ppm H_2S. Cultured AM were freed of overlying medium by aspiration, and treated or untreated medium was added to the cultures. Following 24 hr further incubation, the phagocytic ability of the AM was measured as described above. The phagocytic ability of the cells which received treated medium was not impaired, indicating that toxic compounds were not generated in the medium.

TABLE 2. Time Course of Phagocytic Impariment Following a Single In Vitro Exposure of Rabbit Alveolar Macrophages to H_2S.

Duration of Exposure, hr	ppm	Hours to Sample Following Cessation of Exposure	% of Cells Relative to Controls Containing the Indicated Number of Beads	
			1-21	>21
6	73	0	100 ± 6	55 ± 18
6	73	24	88 ± 10	33 ± 6
6	73	48	94 ± 4	81 ± 22
6	170	0	100 ± 2	49 ± 35
6	170	24	94 ± 8	32 ± 16
6	170	48	74 ± 11	21 ± 20
20	60	0	82 ± 3	62 ± 7
22	60	24	35 ± 15	4 ± 5

In order to relate AM exposure more closely to occupational exposure, a series of experiments were performed in which the exposure regimen was varied to measure the effect of continuous versus intermittent exposure. The results of one such experiment, given in Table 3, clearly indicate that although intermittent exposures resulted in phagocytic impairment, they did not cause as much damage as continuous exposure at the same concentration and for the same time. Two 8-hr exposures of AM to 54 ppm H_2S with a 16-hr delay between exposures decreased the number of cells containing one or more beads to 77% that of controls. In comparison, 16 hr continuous exposure of AM to 54 ppm H_2S resulted in a reduction to 11% that of controls. In both cases, phagocytic ability was measured 24 hr after the end of exposure to H_2S. An even greater reduction was seen in the number of cells containing >21 beads.

TABLE 3. Effect of In Vitro H_2S Exposure on Phagocytic Ability of Cultured Rabbit Alveolar Macrophages.

Exposure Regimen[a]	Percent of Cells Relative to Controls Containing the Indicated Number of Beads[b]	
	>1	>21
1. 8 hr	99 ± 3	102 ± 30
2. 8 hr + 16 hr Delay + 8 hr	77 ± 9	44 ± 22
3. 8 hr + 16 hr Delay + 8 hr + 16 hr Delay + 8 hr	63 ± 5	26 ± 18
4. 16 hr	11 ± 8	0
5. 24 hr	5 ± [illegible]	0

(a) H_2S level 53.9 ± 0.8 ppm, except final 8-hr exposure, regimen 3, was 47 ppm.
(b) Five replicates per treatment. Phagocytosis measured 24 hr after cessation of last exposure.

Morphologic differences were observed, at the light microscopy level, between AM exposed to H_2S and control AM. To further investigate these observations, preliminary SEM and TEM studies were performed: SEM of representative AM from cultures exposed for 24 hr (no delay after cessation of exposure and fixation) at 54 ppm are shown in Figures 1A and B; representative control AM in Figures 1C and D. Major differences were clearly evident in the number of extended pseudopodia and the degree of ruffling. The involvment of pseudopodia in the phagocytic process has been previously reported (Hadley, Annual Reports, 1977, 1978); this suggests a possible mechanism for the decreased phagocytic ability observed following exposure to H_2S.

Transmission electron microscopy of pooled samples of the AM from the intermittent-exposure experiment (Table 3) revealed a distinct contrast between AM exposed to 54 ppm for 16 hr (24-hr delay before fixation) and 24 hr compared to controls (Figures 2A and B). The exposed AM exhibited karyolysis, pyknotic nuclei, disrupted cytoplasmic membranes, generalized disruption of interior organelles and loss of membrane ruffling. A significant decrease in surface ruffling was also seen at the lowest H_2S exposure (8 hr at 54 ppm). The other morphological changes described above were not visible in any of the intermittent-exposure groups.

The results of this study provide evidence of disruption of cellular morphology in H_2S-exposed AM when examined at the ultrastructural level, as well as a distinct loss of phagocytic ability in AM exposed to levels of H_2S as low as 54 ppm for two 8-hr periods. There appears to be a threshold level of damage above which cellular damage is irreversible. The degree of intracellular degradation seen in cultured AM exposed to H_2S for 24 hr, then examined following a 24-hr delay, indicates a possible triggering of autophagocytic processes.

A more detailed study of continuous, low-level exposure, as well as the time course of shorter-duration, high-level exposure, would yield more information on the time course of the damage, and allow a more accurate determination of the value of these results in assessing occupational and environmental exposures.

The damage to cultured pulmonary macrophages seen following 16-hr or 24-hr continuous exposures suggests that functional damage may occur from in vitro exposure near the threshold limit value for human exposure, "20 ppm per 8 hr day with one 10 minute exposure to 50 ppm if no other exposure >20 ppm occurs in an 8 hour shift."

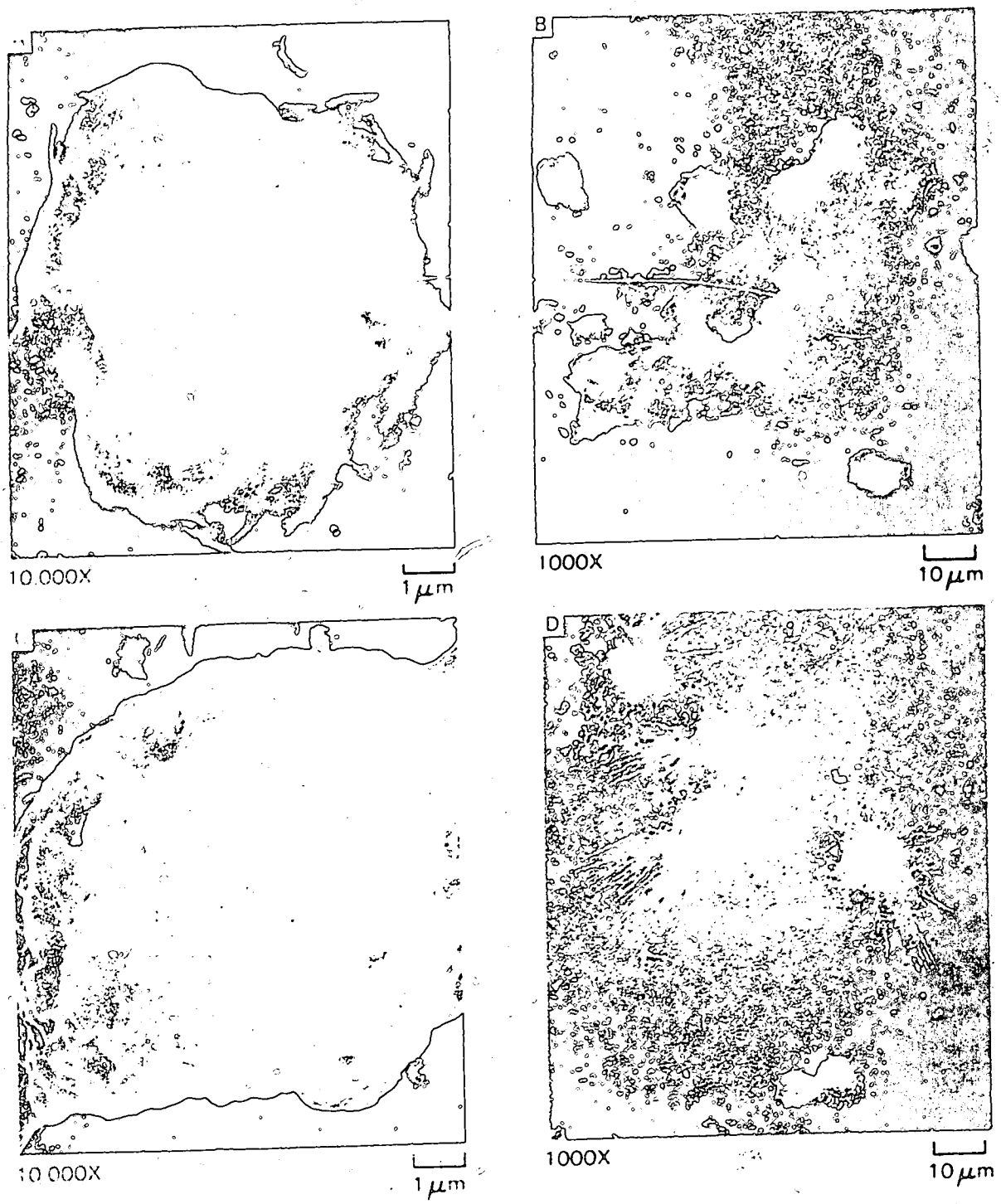

FIGURE 1. Scanning Electron Photomicrographs of Rabbit Alveolar Macrophages Exposed to 54 ppm H_2S for 24 Hours (A,B) and Control Macrophages (C,D). Cells were fixed immediately after exposure as described in text.

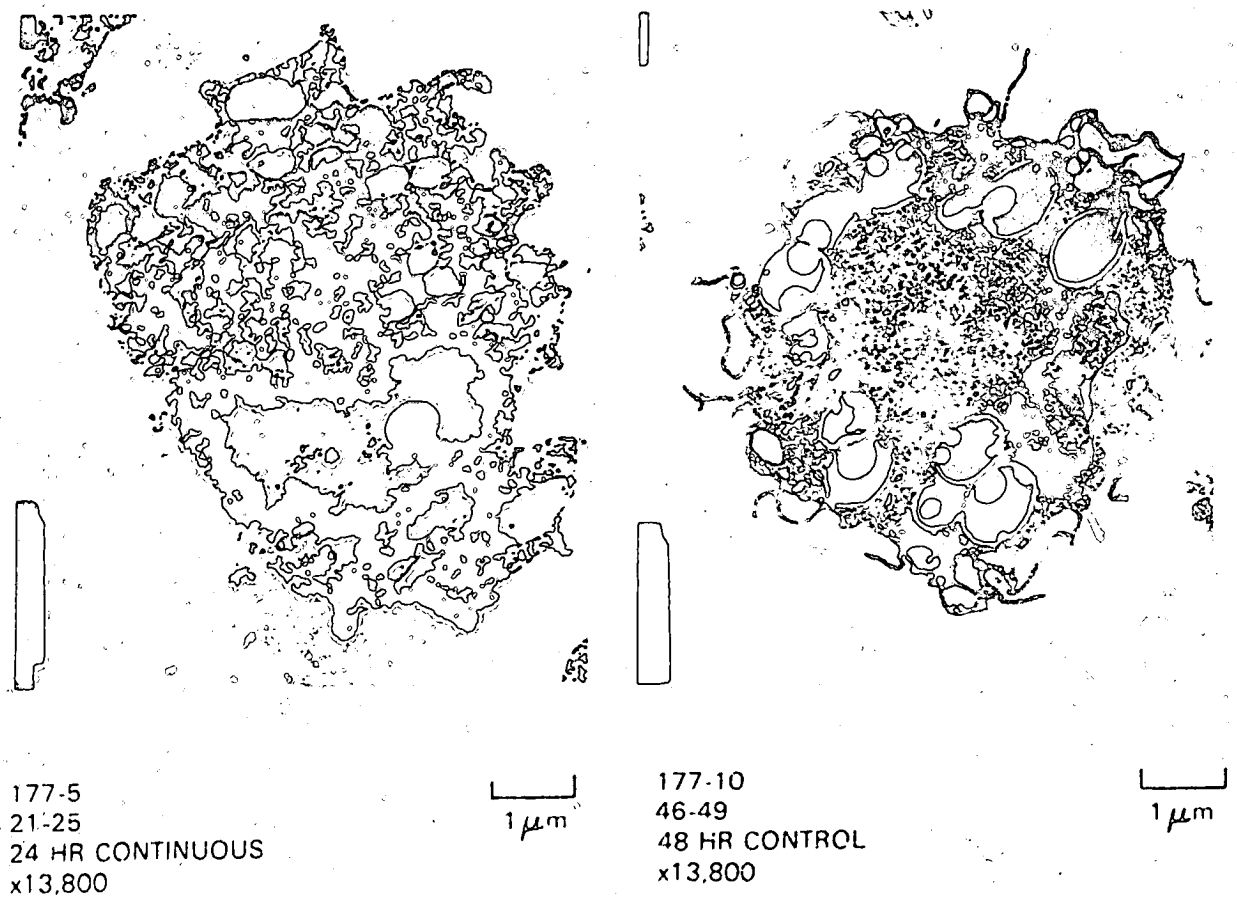

FIGURE 2. Transmission Electron Photomicrographs of Macrophages Exposed to 54 ppm H_2S for 24 Hours (A) and Control Macrophages (B). Cells depicted were incubated with 2.02-μm polyvinyl toluene particles as described in the text, and were fixed 24 hours after exposure to H_2S.

SUBACUTE INHALATION TOXICOLOGY OF HYDROGEN SULFIDE AND AMMONIA IN RODENTS

Investigators: R. A. Renne and K. E. McDonald

Technical Assistance: B. R. Garrity, W. C. Cannon, E. C. DeBattista, K. T. Brasel, L. G. Smith, J. F. McShane, J. C. Chapman, and S. R. Eldridge

Rats and guinea pigs were exposed for 22 days to hydrogen sulfide, ammonia, or a combination of the two gases. Exposure for 22 days to 220 ppm H_2S, 250 ppm NH_3, or a combination of these two gases at these concentrations induced a mild inflammation of the respiratory tract in guinea pigs. Exposure to NH_3 or H_2S + NH_3 apparently induced intraluminal calcification and chronic inflammation in the renal cortical tubules of exposed guinea pigs.

In FY 1979, we exposed rats and guinea pigs for 22 days to 220 ppm H_2S, 250 ppm NH_3 or a combination of the two gases at these concentrations. Tissues from the respiratory tract, kidney, liver, adrenal, heart, gastrointestinal tract, brain, spleen and eyes were examined microscopically.

No evidence of exposure effect was observed in rats. A mild, acute, suppurative, inflammatory infiltrate was observed in the lungs and trachea of guinea pigs exposed to either gas, or a combination of the two gases. A mild, acute, suppurative rhinitis and laryngitis was present in guinea pigs exposed to a combination of H_2S and NH_3. There was a slight increase in the incidence and severity of intraluminal calcification of renal cortical tubules in guinea pigs exposed to NH_3 or H_2S + NH_3, and a slight increase in incidence and severity of chronic inflammation in the renal cortical interstitium in guinea pigs exposed to NH_3.

The respiratory tract lesions observed in exposed guinea pigs represent a response to the irritant properties of these gases. There was evidence of an irritant effect of a combination of these two gases in the turbinates and larynx. Exposure to NH_3 apparently increased intraluminal calcification and chronic inflammation in the renal cortical tubules.

EFFECTS OF MOUNT ST. HELENS ASH ON CULTURED RABBIT ALVEOLAR MACROPHAGES

Investigator: A. V. Robinson

Technical Assistance: L. Daughtry

Samples of volcanic ash dispersed by the May 18, 1980 eruption of Mount St. Helens were collected from several locations in Eastern Washington and Montana, and their cytoxicity to alveolar macrophages was measured in vitro.

Several experimental studies have shown a correlation between the cytoxicity of mineral dusts to macrophages in vitro and their ability to induce pulmonary fibrosis when inhaled. To obtain a preliminary assessment of the pulmonary fibrogenic potential of the volcanic ash from the May 18, 1980 eruption of Mount St Helens, we examined its toxicity to rabbit alveolar macrophages in vitro and compared it to that of known cytotoxic and fibrogenic particles (quartz), a particulate soil of the area where the volcanic ash sample was obtained (Ritzville silt loam), and nontoxic particles (polyvinyltoluene beads).

The pulmonary macrophages were obtained by lung lavage of rabbits and cultured in RPMI 1640 (Gibco) supplemented with bovine serum albumin (0.4%), transferrin (5 μg/ml), insulin (5 μg/ml), penicillin (100 IU/ml), streptomycin (100 μg/ml), and amphotericin B (2.5 μg/ml). After overnight incubation, nonadherent cells were aspirated and discarded, and 5 ml of fresh culture medium was added.

Volcanic ash, soil, and quartz samples were suspended in a 7.5-cm column of RPMI 1640. After a 2-min settling period, the top 4.5 cm was aspirated, and an aliquot was weighed and dried to determine particle content. Examination of the aspirated fraction by light microscopy and electron microscopy revealed that 99% of the particles (by count) of each material were less than 5 μm in diameter. Samples of Ritzville silt-loam soil were placed in a vibrating gravity sieve containing nylon cloth (mesh sizes: 7, 20, or 140 μm). The fraction that passed through the 20-μm mesh was treated as described above. Polyvinyltoluene beads (2.02 μm; Dow Diagnostics) were diluted with RPMI 1640.

Samples of each particle suspension were then added to culture flasks to give 1.25 mg of particles per flask (0.25 mg/ml). After incubation for 20 to 24 hr, the cells remaining attached to the flask were released by addition of 0.5 ml of 50 mM adenosine triphosphate and incubated for 20 to 45 min. The viable and dead cells (identified by trypan blue stain) were counted in a hemocytometer to ascertain the percentage of the population that was viable. Selected portions of Experiment 1 were repeated (Experiment 2).

The cellular viability data, presented in Table 1, suggest that the volcanic ash samples did not differ significantly in cytotoxicity from the nontoxic polyvinyltoluene particles; nor did they differ significantly from each other in any consistent manner. In contrast, fibrogenic quartz (positive control) was much more cytotoxic than any of the volcanic ash samples. Ritzville silt loam was also more cytotoxic than the volcanic ash samples, most notably in Experiment 2. This may be due to leachable matter on the soil or to a mineral fraction in the soil.

These preliminary data indicate that the volcanic ash samples tested are not highly cytotoxic and thus, within the constraints of the model linking fibrogenicity to cytotoxicity, are not highly fibrogenic compared to quartz. These data are consistent with mineralogical data indicating that the ash consists mostly of weakly fibrogenic feldspar and nonfibrogenic glass; fibrogenic cystalline silica makes up less than 3% of the material.

TABLE 1. Viability of Cultured Rabbit Alveolar Macrophages Exposed to Particles of Volcanic Ash, Polyvinyltoluene, Soil and Fibrogenic Quartz.

Particle	Percentage of Viable Cells Relative to Controls[a]	
	Exp[b] 1	Exp 2
Polyvinyltoluene	96 ± 21	113 ± 29
Fibrogenic Quartz	42 ± 14	30 ± 8
Tieton Ash	79 ± 25	96 ± 31
Ahtanum Ash	87 ± 32	
Yakima Ash	89 ± 23	91 ± 25
Richland Ash	94 ± 23	66 ± 31
Ritzville Silt Loam Soil	70 ± 27	32 ± 9
Rosalia Ash	91 ± 39	
Pullman Ash	101 ± 26	111 ± 24
Missoula Ash	87 ± 22	

[a] $\frac{\text{No. viable recovered experimental cells}}{\text{No. viable recovered control cells}} \times 100$

[b] Means ± 1 standard deviation, five replicates per point (Exp. = experiment)

Appendix

APPENDIX

DOSE-EFFECT STUDIES WITH INHALED PLUTONIUM IN BEAGLES

On the following pages data are presented for all dogs employed in current life-span dose effect studies with inhaled $^{239}PuO_2$, $^{238}PuO_2$, and ^{239}Pu nitrate. Information is presented on the estimated initial alveolar deposition, based on external thorax counts and on estimated lung weights (0.011 x body weight) at time of exposure. Information is also provided on the current interpretation of the most prominent clinical-pathological features associated with the death of animals. These data represent information presently available, and are presented as reference material for scientists who desire to follow in detail the progress of these experiments.

DOSE-EFFECT STUDIES WITH INHALED PU-239 OXIDE IN BEAGLES

DOSE GROUP	DOG NUMBER	SEX	INITIAL ALVEOLAR DEPOSITION NCI	NCI/G LUNG	NCI/KG	INHALATION EXPOSURE WEIGHT (KG)	AGE* (MO)	DATE	DATE OF DEATH	MONTHS SINCE INHALATION 9/30/80	DEATH	COMMENTS ON DEAD DOGS
CONTROL	738	F	0	0.00	0.00					137.2*		
CONTROL	740	F	0	0.00	0.00					137.2*		
CONTROL	749	F	0	0.00	0.00					135.9*		
CONTROL	755	M	0	0.00	0.00					135.9*		
CONTROL	766	M	0	0.00	0.00					135.5*		
CONTROL	775	F	0	0.00	0.00					135.1*		
CONTROL	785	M	0	0.00	0.00					134.4*		
CONTROL	789	M	0	0.00	0.00					134.1*		
CONTROL	792	M	0	0.00	0.00				04/26/76		79.5*	Oral Tumor
CONTROL	800	F	0	0.00	0.00					131.3*		
CONTROL	801	M	0	0.00	0.00					131.3*		
CONTROL	811	F	0	0.00	0.00					130.2*		
CONTROL	846	M	0	0.00	0.00					129.4*		
CONTROL	861	M	0	0.00	0.00					129.1*		
CONTROL	868	F	0	0.00	0.00					127.7*		
CONTROL	872	F	0	0.00	0.00					127.6*		
CONTROL	876	M	0	0.00	0.00					125.7*		
CONTROL	882	M	0	0.00	0.00					125.5*		
CONTROL	885	F	0	0.00	0.00					124.9*		
CONTROL	903	F	0	0.00	0.00					122.6*		
CONTROL SACRIFICE	701	F	0	0.00	0.00				04/18/79		121.0*	Sacrificed
CONTROL SACRIFICE	703	M	0	0.00	0.00				03/24/77		96.2*	Sacrificed
CONTROL SACRIFICE	724	M	0	0.00	0.00				03/30/78		107.9*	Sacrificed
D-1 LOWEST	756	M	0	0.00	0.00	13.0	19.5	01/19/71		116.4		
D-1 LOWEST	762	M	0	0.00	0.00	11.5	19.3	01/19/71	01/24/77		72.2	Sacrificed
D-1 LOWEST	847	M	0	0.00	0.00	15.0	18.5	07/06/71		110.9		
D-1 LOWEST	856	M	0	0.00	0.00	15.5	18.2	07/06/71		110.9		
D-1 LOWEST	865	F	0	0.00	0.00	7.0	17.4	07/06/71		110.9		
D-1 LOWEST	879	M	0	0.00	0.00	14.5	17.9	10/07/71		107.8		
D-1 LOWEST	886	F	0	0.00	0.00	16.5	16.2	11/10/71		106.7		
D-1 LOWEST	907	F	0	0.00	0.00	11.5	15.9	11/10/71		106.7		
D-1 LOWEST	825	F	1	0.01	0.12	11.5	18.1	06/08/71		111.8		
D-1 LOWEST	849	F	1	0.01	0.10	10.0	21.3	10/07/71	10/26/72		12.6	Sacrificed
D-1 LOWEST	904	F	1	0.01	0.07	10.0	15.9	11/10/71		106.7		
D-1 LOWEST	832	F	2	0.02	0.24	8.5	16.5	04/26/71		113.2		
D-1 LOWEST	900	M	3	0.02	0.27	13.0	16.0	11/10/71		106.7		
D-1 LOWEST	870	F	4	0.03	0.32	12.0	16.9	07/06/71		110.9		
D-1 LOWEST	899	F	4	0.03	0.31	11.5	16.0	11/10/71		106.7		
D-1 LOWEST	867	M	5	0.04	0.41	11.5	17.4	07/06/71		110.9		
D-1 LOWEST	891	M	6	0.04	0.41	14.0	16.0	11/10/71		106.7		
D-1 LOWEST	850	F	5	0.05	0.59	8.5	21.3	10/07/71		107.8		
D-1 LOWEST	853	M	8	0.05	0.51	15.0	21.3	10/07/71		107.8		
D-1 LOWEST	875	M	8	0.05	0.54	14.0	16.8	07/06/71	05/21/78		82.5	Kidney:Malignant Lymphoma

* Indicates age in months since birth, all other ages are in months since exposure.

DOSE-EFFECT STUDIES WITH INHALED PU-239 DAIOL IN BEAGLES

DOSE GROUP	DOG NUMBER	SEX	[illegible]	[illegible] LUNG	[illegible]	WEIGHT	AGE* (MO)	DATE	DATE OF DEATH	[illegible]	[illegible]	COMMENTS ON LEAD DOGS
D-1 LOWEST	770	F	[illegible]	0.06	0.63	[illegible]	[illegible]	[illegible]		[illegible]		
D-1 LOWEST	788	M	8	0.06	0.62	[illegible]	16.7	[illegible]		115.		
D-1 LOWEST	893	M	[illegible]	0.06	[illegible]	[illegible]	14.9	[illegible]		[illegible]		
D-1 LOWEST	807	F	[illegible]	0.06	[illegible]	11.0	14.6	02/03/71		112.		
D-1 LOWEST	841	F	6	0.0	0.7	[illegible]	17.7	06/08/71		[illegible]		
D-1 LOWEST	908	M	[illegible]	[illegible]	[illegible]	[illegible]	[illegible]	[illegible]	04/01/80		[illegible]	Unknown, Put. Hyalinosis
D-2 LOW	770	M	10	0.07	0.74	[illegible]	[illegible]	03/04/71		114.9		
D-2 LOW	842	M	10	0.07	[illegible]	[illegible]	16.8	[illegible]		[illegible]		
D-2 LOW	[illegible]	M	11	0.08	[illegible]	[illegible]	[illegible]	[illegible]		[illegible]		
D-2 LOW	920	M	11	0.08	[illegible]	[illegible]	16.0	06/08/71	[illegible]		[illegible]	Sacrificed
D-2 LOW	862	M	12	0.09	1.00	[illegible]	15.7	06/08/71		[illegible]		
D-2 LOW	811	M	15	0.09	0.96	[illegible]	[illegible]	07/06/71		[illegible]		
D-2 LOW	814	M	16	0.11	1.24	[illegible]	16.6	07/06/71		[illegible]		
D-2 LOW	754	M	[illegible]	0.12	1.69	[illegible]	14.9	[illegible]	[illegible]		85.7	Status Epilepticus
D-2 LOW	849	F	16	0.15	1.83	[illegible]	[illegible]	06/08/71		111.8		
D-2 LOW	746	F	14	0.16	1.73	[illegible]	[illegible]	05/19/71		116.4		
D-2 LOW	798	F	[illegible]	0.16	1.78	[illegible]	[illegible]	[illegible]	[illegible]		42.6	Sacrificed
D-2 LOW	826	F	24	0.16	1.81	[illegible]	[illegible]	[illegible]		[illegible]		
D-2 LOW	831	F	27	0.18	2.00	16.5	[illegible]	06/08/71		111.8		
D-2 LOW	887	F	[illegible]	0.19	2.09	[illegible]	[illegible]	[illegible]		[illegible]		
D-2 LOW	760	F	24	0.22	2.40	[illegible]	16.2	05/19/71		116.4		
D-2 LOW	819	M	4[illegible]	0.22	2.41	14.7	16.7	[illegible]		[illegible]		
D-2 LOW	[illegible]	M	46	0.23	2.5	14.0	16.5	12/21/70		[illegible]		
D-2 LOW	839	F	3[illegible]	0.25	2.51	[illegible]	[illegible]	[illegible]		[illegible]		
D-2 LOW	806	F	48	0.25	2.74	[illegible]	15.5	03/04/71		114.9		
D-2 LOW	813	F	5[illegible]	0.26	3.05	10.5	17.1	03/03/71		114.9		
D-2 LOW	871	F	54	0.29	3.24	[illegible]	17.4	[illegible]		[illegible]		
D-2 LOW	769	F	[illegible]	0.34	3.50	8.[illegible]	16.2	12/21/70	06/23/78		90.1	Ovarian Tumor
D-2 LOW	802	M	4[illegible]	0.33	3.64	11.0	16.1	04/26/71		113.2		
D-3 MED-LOW	781	F	46	0.38	4.17	11.5	17.3	12/21/70		117.3		
D-3 MED-LOW	771	F	44	0.40	4.46	10.0	19.2	01/20/71		116.3		
D-3 MED-LOW	782	M	6[illegible]	0.42	4.59	13.5	19.0	02/10/71		115.6		
D-3 MED-LOW	786	M	6[illegible]	0.42	4.59	13.5	19.5	03/04/71		114.9		
D-3 MED-LOW	752	M	62	0.43	4.77	13.0	18.6	12/21/70	02/22/79		98.1	Lung Tumor, Adrenal Tumor
D-3 MED-LOW	823	M	55	0.44	4.81	13.5	16.8	04/26/71		113.2		
D-3 MED-LOW	883	M	63	0.44	4.85	13.0	17.7	10/07/71		107.8		
D-3 MED-LOW	778	M	74	0.46	5.10	14.5	20.2	03/04/71	08/26/79		101.7	Put. Thromboembolism
D-3 MED-LOW	838	M	56	0.46	5.09	11.0	17.8	06/08/71		111.8		
D-3 MED-LOW	795	F	54	0.52	5.66	9.5	15.0	01/20/71		116.3		
D-3 MED-LOW	815	M	68	0.52	5.67	12.0	16.8	04/26/71	05/22/73		24.9	Sacrificed
D-3 MED-LOW	851	F	55	0.54	5.89	9.0	21.3	10/07/71		107.8		
D-3 MED-LOW	918	M	74	0.58	6.43	11.5	16.0	06/08/72	07/06/72		0.9	Sacrificed
D-3 MED-LOW	834	F	67	0.68	7.44	9.0	17.8	06/08/71	07/05/79		96.9	Pyometra

* Indicates age in months since birth, all other ages are in months since exposure.

DOSE-EFFECT [illegible] AFTER INHALATION OF [illegible] IN BEAGLES

DOSE GROUP	DOG NUMBER	SEX	INITIAL ALVEOLAR DEPOSITION NCI	NCI/G LUNG	NCI/[illegible]	INHALATION EXPOSURE WEIGHT (KG)	AGE* (MO)	DATES	DATE OF DEATH	MONTHS SINCE INHALATION % SURVIVED	DEATH	COMMENTS ON DEAD DOGS
L-3	MED-LOW	F	85	0.70	[illegible]	[illegible]	[illegible]	[illegible]		[illegible]		
L-3	MED-LOW	F	[illegible]	0.72	[illegible]	[illegible]	[illegible]	[illegible]		[illegible]		
D-3	MED-LOW	F	84	[illegible]	[illegible]	[illegible]	[illegible]	[illegible]		[illegible]		
D-3	MED-LOW	M	140	[illegible]	[illegible]	[illegible]	[illegible]	[illegible]	[illegible]		[illegible]	Processing
D-3	MED-LOW	M	118	[illegible]	[illegible]	[illegible]	[illegible]	[illegible]		[illegible]		
D-3	MED-LOW	M	[illegible]	[illegible]	[illegible]	[illegible]	[illegible]	[illegible]		[illegible]		
D-3	MED-LOW	F	[illegible]	[illegible]	[illegible]	[illegible]	[illegible]	[illegible]		[illegible]		
D-3	MED-LOW	F	[illegible]	[illegible]	[illegible]	[illegible]	[illegible]	[illegible]		[illegible]		
L-4	MEDIUM	M	[illegible]	[illegible]	[illegible]	[illegible]	[illegible]	[illegible]		[illegible]		
D-4	MEDIUM	F	[illegible]	[illegible]	[illegible]	[illegible]	[illegible]	[illegible]		[illegible]		
D-4	MEDIUM	F	[illegible]	[illegible]	[illegible]	[illegible]	[illegible]	[illegible]		[illegible]		
L-4	MEDIUM	F	[illegible]	[illegible]	[illegible]	[illegible]	[illegible]	[illegible]	[illegible]		[illegible]	Red Cell Sarcoma
L-4	MEDIUM	F	[illegible]	[illegible]	[illegible]	[illegible]	[illegible]	[illegible]		[illegible]		
D-4	MEDIUM	F	[illegible]	[illegible]	[illegible]	[illegible]	[illegible]	[illegible]	[illegible]		[illegible]	Lung Tmr, Thyroid Adenoma
L-4	MEDIUM	M	[illegible]	[illegible]	[illegible]	[illegible]	[illegible]	[illegible]		[illegible]		
L-4	MEDIUM	F	[illegible]	[illegible]	[illegible]	[illegible]	[illegible]	[illegible]		[illegible]		
L-4	MEDIUM	M	[illegible]	[illegible]	[illegible]	[illegible]	[illegible]	[illegible]	[illegible]		[illegible]	Lung Tumor
D-4	MEDIUM	F	[illegible]	[illegible]	[illegible]	[illegible]	[illegible]	[illegible]		[illegible]		
D-4	MEDIUM	M	[illegible]	[illegible]	[illegible]	[illegible]	[illegible]	[illegible]		[illegible]		
D-4	MEDIUM	F	[illegible]	[illegible]	[illegible]	[illegible]	[illegible]	[illegible]		[illegible]		
L-4	MEDIUM	F	[illegible]	[illegible]	[illegible]	[illegible]	[illegible]	[illegible]		[illegible]		
L-4	MEDIUM	M	[illegible]	[illegible]	[illegible]	[illegible]	[illegible]	[illegible]		[illegible]		
L-4	MEDIUM	M	[illegible]	[illegible]	[illegible]	[illegible]	[illegible]	[illegible]		[illegible]		
L-4	MEDIUM	M	[illegible]	[illegible]	[illegible]	[illegible]	[illegible]	[illegible]		[illegible]		Sacrificed
D-4	MEDIUM	F	[illegible]	[illegible]	[illegible]	[illegible]	[illegible]	[illegible]		[illegible]		
L-4	MEDIUM	F	[illegible]	[illegible]	[illegible]	[illegible]	[illegible]	[illegible]		[illegible]		
L-4	MEDIUM	M	[illegible]	[illegible]	[illegible]	[illegible]	[illegible]	[illegible]		[illegible]		Lung Tumor
L-4	MEDIUM	M	[illegible]	[illegible]	[illegible]	[illegible]	[illegible]	[illegible]		[illegible]		Processing
L-4	MEDIUM	M	[illegible]	[illegible]	[illegible]	[illegible]	[illegible]	[illegible]		[illegible]		
L-4	MEDIUM	M	[illegible]	[illegible]	[illegible]	[illegible]	[illegible]	[illegible]		[illegible]		Sacrificed
L-4	MEDIUM	M	[illegible]	[illegible]	[illegible]	[illegible]	[illegible]	[illegible]	[illegible]	[illegible]		Processing
L-4	MEDIUM	M	[illegible]	[illegible]	[illegible]	[illegible]	[illegible]	[illegible]	[illegible]	[illegible]		Interstitial Pneumonitis
L-5	MED-HIGH	M	[illegible]	[illegible]	[illegible]	[illegible]	[illegible]	[illegible]	[illegible]	[illegible]		Lung Tmr, Intestinal Tmr
L-5	MED-HIGH	F	[illegible]	[illegible]	[illegible]	[illegible]	[illegible]	[illegible]	[illegible]	[illegible]		Lung Tumor
L-5	MED-HIGH	M	[illegible]	[illegible]	[illegible]	[illegible]	[illegible]	[illegible]	[illegible]	[illegible]		Lung Tumor
D-5	MED-HIGH	F	[illegible]	[illegible]	[illegible]	[illegible]	[illegible]	[illegible]		[illegible]		
D-5	MED-HIGH	F	[illegible]	[illegible]	[illegible]	[illegible]	[illegible]	[illegible]	[illegible]		[illegible]	Lung Tumor
D-5	MED-HIGH	M	[illegible]	[illegible]	[illegible]	[illegible]	[illegible]	[illegible]	[illegible]		[illegible]	Lung Tumor
D-5	MED-HIGH	F	[illegible]	[illegible]	[illegible]	[illegible]	[illegible]	[illegible]	[illegible]		[illegible]	Lung Tumor
D-5	MED-HIGH	M	[illegible]	[illegible]	[illegible]	[illegible]	[illegible]	[illegible]		[illegible]		
L-5	MED-HIGH	M	[illegible]	[illegible]	[illegible]	[illegible]	[illegible]	[illegible]	[illegible]		4.7	Sacrificed
L-5	MED-HIGH	M	1,85	[illegible]	[illegible]	[illegible]	16.8	[illegible]	[illegible]		72.5	Lung Tumor
D-5	MED-HIGH	F	980	8.48	[illegible]	[illegible]	[illegible]	[illegible]	[illegible]		75.5	Lung Tumor

* Indicates age in months [illegible], all other ages are in months since exposure.

Group	Dog Number	Sex	Values	Survival	Comments
[illegible]	[illegible]	[illegible]	[illegible]	[illegible]	[illegible] Tumor
[illegible]	[illegible]	[illegible]	[illegible]	[illegible]	Lung Tumor
[illegible]	886	[illegible]	[illegible]	[illegible]	Lung Tumor
[illegible]	[illegible]	[illegible]	[illegible]	[illegible]	Lung Inf, Osteoarthropathy
[illegible]	[illegible]	[illegible]	[illegible]	[illegible]	Lung Tumor
[illegible]	[illegible]	[illegible]	[illegible]	57.4	Lung Tumor, Rad. Pneum.
[illegible]	[illegible]	[illegible]	[illegible]	[illegible]	Lung Tumor
[illegible]	[illegible]	[illegible]	[illegible]	[illegible]	Radiation Pneumonitis
[illegible]	[illegible]	[illegible]	[illegible]	[illegible]	Lung Inf, Osteoarthropathy
[illegible]	[illegible]	[illegible]	[illegible]	[illegible]	Lung Tumor
[illegible]	[illegible]	[illegible]	[illegible]	[illegible]	Sacrificed
[illegible]	[illegible]	[illegible]	[illegible]	[illegible]	Lung Inf, Osteoarthropathy
[illegible]	[illegible]	[illegible]	[illegible]	[illegible]	Sacrificed
[illegible]	[illegible]	[illegible]	[illegible]	[illegible]	Sacrificed
[illegible]	[illegible]	[illegible]	[illegible]	[illegible]	Lung Tumor
[illegible]	[illegible]	[illegible]	[illegible]	[illegible]	Radiation Pneumonitis
[illegible]	[illegible]	[illegible]	[illegible]	[illegible]	Radiation Pneumonitis
[illegible]	[illegible]	[illegible]	[illegible]	[illegible]	Radiation Pneumonitis
[illegible]	[illegible]	[illegible]	[illegible]	[illegible]	Sacrificed
[illegible]	[illegible]	[illegible]	[illegible]	[illegible]	Sacrificed
[illegible]	[illegible]	[illegible]	[illegible]	[illegible]	Radiation Pneumonitis
[illegible]	[illegible]	[illegible]	[illegible]	[illegible]	Radiation Pneumonitis
[illegible]	[illegible]	[illegible]	[illegible]	11.8	Radiation Pneumonitis
[illegible]	[illegible]	[illegible]	[illegible]	[illegible]	Radiation Pneumonitis

* Indicates age ... months after birth, all other ages are ... months after exposure.

"DOSE-EFFECT" STUDIES WITH INHALED PLUTONIUM DIOXIDE IN BEAGLES

GROUP	DOG NUMBER	SEX	TOTAL ALVEOLAR DEPOSITION (KBQ/KG)			INHALATION EXPOSURE WEIGHT (KG)	AGE* (MO)	DATE	DATE OF DEATH	MONTHS SINCE INHALATION (AT 60 DEATH)	COMMENTS ON CLINICAL FINDINGS
CONTROL	[illegible]	M	[illegible]	.00	[illegible]					112.7*	
CONTROL	[illegible]	F	[illegible]	.00	[illegible]					112.7*	
CONTROL	[illegible]	M	[illegible]	[illegible]	[illegible]					[illegible]	
CONTROL	[illegible]	F	[illegible]	.00	.00				07/08/79	[illegible]*	Hysterectomy
CONTROL	[illegible]	F	[illegible]	.00	[illegible]					[illegible]*	
CONTROL	[illegible]	M	[illegible]	[illegible]	[illegible]					[illegible]*	
CONTROL	[illegible]	F	[illegible]	[illegible]	[illegible]					[illegible]*	
CONTROL	[illegible]	M	[illegible]	[illegible]	[illegible]					[illegible]*	
CONTROL	[illegible]	M	[illegible]	[illegible]	[illegible]					109.4*	
CONTROL	[illegible]	M	[illegible]	[illegible]	[illegible]					109.4*	
CONTROL	[illegible]	F	[illegible]	[illegible]	[illegible]					109.1*	
CONTROL	[illegible]	F	[illegible]	[illegible]	[illegible]					109.0*	
CONTROL	[illegible]	M	[illegible]	[illegible]	[illegible]					105.3*	
CONTROL	[illegible]		[illegible]	[illegible]	[illegible]					104.6*	
CONTROL	[illegible]	M	[illegible]	[illegible]	[illegible]					104.4*	
CONTROL	[illegible]	F	[illegible]	[illegible]	[illegible]					104.1*	
CONTROL	[illegible]	F	[illegible]	[illegible]	[illegible]					97.5*	
CONTROL	[illegible]	M	[illegible]	[illegible]	[illegible]					97.0*	
CONTROL	[illegible]	M	[illegible]	[illegible]	[illegible]					96.7*	
CONTROL	[illegible]	F	[illegible]	[illegible]	[illegible]					95.9*	
CONTROL SACRIFICED	[illegible]	M	[illegible]	[illegible]	[illegible]				04/30/77	71.6*	Sacrificed
CONTROL SACRIFICED	[illegible]	F	[illegible]	.00	[illegible]				[illegible]/18/78	63.9*	Sacrificed
CONTROL SACRIFICED	[illegible]	F	[illegible]	.00	0.00				05/29/79	95.6*	Sacrificed
CONTROL SACRIFICED	168	M	[illegible]	.00	[illegible]				12/14/76	66.0*	Sacrificed
CONTROL SACRIFICED	[illegible]	M	[illegible]	.00	[illegible]				01/13/76	47.5*	Sacrificed
CONTROL SACRIFICED	[illegible]	M	[illegible]	.00	[illegible]				05/15/75	31.9*	Sacrificed
CONTROL SACRIFICED	[illegible]	M	[illegible]	[illegible]	[illegible]				12/[illegible]/76	49.9*	Sacrificed
CONTROL SACRIFICED	[illegible]	M	[illegible]	[illegible]	[illegible]				[illegible]/31/78	72.9*	Sacrificed
D-1 LOWEST	[illegible]	M	[illegible]	[illegible]	[illegible]	[illegible]	[illegible]	01/16/73		92.4	
D-1 LOWEST	[illegible]	M	[illegible]	[illegible]	[illegible]	14.0	19.6	01/16/73		92.4	
D-1 LOWEST	[illegible]	F	[illegible]	0.00	.00	[illegible]	19.2	01/16/73		92.4	
D-1 LOWEST	[illegible]	M	[illegible]	0.00	[illegible]	13.0	17.0	01/16/73		92.4	
D-1 LOWEST	1044	F	[illegible]	0.00	[illegible]	13.5	17.0	01/16/73		92.4	
D-1 LOWEST	1055	M	[illegible]	0.00	0.00	13.0	16.8	01/16/73		92.4	
D-1 LOWEST	1063	M	[illegible]	0.00	0.00	14.5	16.7	01/16/73		92.4	
D-1 LOWEST	1105	F	[illegible]	0.00	.00	16.0	16.4	05/31/73		86.0	
D-1 LOWEST	1194	F	0	0.00	0.00	16.5	19.8	04/18/74		77.4	
D-1 LOWEST	1215	M	[illegible]	0.00	0.00	15.5	19.3	04/18/74	04/26/77	36.3	Sacrificed
D-1 LOWEST	1230	M	0	0.00	0.00	12.5	18.4	04/18/74		77.4	
D-1 LOWEST	951	M	2	0.01	0.14	14.0	19.3	12/19/72		93.4	
D-1 LOWEST	1008	M	2	0.01	0.15	13.5	19.6	01/18/73		92.4	
D-1 LOWEST	1193	F	2	0.01	0.16	17.5	19.8	04/18/74		77.4	
D-1 LOWEST	959	M	3	0.02	0.22	13.5	19.2	12/19/72		93.4	

* Indicates age in months since birth, all other ages are in months since exposure.

DOSE-EFFECT STUDIES WITH INHALED PU-23 XIDE IN BEAGLES

DOSE GROUP	DOG NUMBER	SEX	INITIAL ALVEOLAR DEPOSITION NCI	NCI/G LUNG	NCI/KG	INHALATION EXPOSURE WEIGHT (KG)	AGE* (MO)	DATE	DATE OF DEATH	MONTHS SINCE INHALATION 9/30/80	DEATH	COMMENTS ON DEAD DOGS
D-1 LOWEST	1069	F	2	0.02	0.24	8.5	18.1	05/31/73		88.0		
D-1 LOWEST	1095	F	2	0.02	0.19	10.5	16.6	05/31/73		88.0		
D-1 LOWEST	921	F	3	0.03	0.31	10.0	19.5	11/30/72	12/27/72		0.9	Sacrificed
D-1 LOWEST	923	F	3	0.03	0.35	8.5	19.5	11/30/72	01/26/73		1.9	Sacrificed
D-1 LOWEST	989	F	3	0.03	0.32	9.5	18.8	12/19/72		93.4		
D-1 LOWEST	925	M	5	0.04	0.40	12.5	19.5	11/30/72	02/27/73		2.9	Sacrificed
D-1 LOWEST	1204	M	6	0.04	0.43	14.0	17.7	02/26/74		79.1		
D-1 LOWEST	970	F	6	0.05	0.55	11.0	19.2	12/19/72	01/04/77		48.5	Sacrificed
D-1 LOWEST	993	F	6	0.05	0.50	12.0	18.8	12/19/72		93.4		
D-1 LOWEST	1106	F	5	0.05	0.50	10.0	16.4	05/31/73		88.0		
D-2 LOW	1065	F	6	0.05	0.60	10.0	18.3	05/31/73		88.0		
D-2 LOW	1082	M	11	0.06	0.69	16.0	18.0	05/31/73	12/04/79		78.1	Paralysis, Spinal Crd Deg
D-2 LOW	1188	M	11	0.06	0.71	15.5	18.4	02/26/74		79.1		
D-2 LOW	1084	M	13	0.07	0.74	17.5	17.5	05/31/73		88.0		
D-2 LOW	1090	F	10	0.08	0.83	12.0	17.3	05/31/73		88.0		
D-2 LOW	1222	M	15	0.10	1.11	13.5	19.0	04/18/74		77.4		
D-2 LOW	971	F	13	0.11	1.24	10.5	19.2	12/19/72		93.4		
D-2 LOW	999	F	11	0.11	1.16	9.5	18.7	12/19/72		93.4		
D-2 LOW	1229	M	16	0.11	1.23	15.0	16.8	02/26/74		79.1		
D-2 LOW	1070	M	22	0.12	1.33	16.5	18.1	05/31/73		88.0		
D-2 LOW	1214	M	17	0.12	1.36	12.5	19.3	04/18/74	05/12/75		12.8	Sacrificed
D-2 LOW	955	M	17	0.14	1.55	11.0	19.2	12/19/72		93.4		
D-2 LOW	1033	M	17	0.14	1.55	11.0	19.1	02/22/73		91.2		
D-2 LOW	1036	F	16	0.14	1.52	10.5	18.2	02/22/73		91.2		
D-2 LOW	1216	M	23	0.16	1.77	13.0	19.3	04/18/74		77.4		
D-2 LOW	1060	F	22	0.18	2.00	11.0	17.8	02/22/73		91.2		
D-2 LOW	981	M	30	0.21	2.31	13.0	19.0	12/19/72		93.4		
D-2 LOW	1046	M	27	0.22	2.45	11.0	18.1	02/22/73		91.2		
D-2 LOW	1050	F	22	0.22	2.44	9.0	18.1	02/22/73		91.2		
D-2 LOW	1078	F	29	0.22	2.42	12.0	18.0	05/31/73		88.0		
D-2 LOW	1207	F	22	0.24	2.59	8.5	17.6	02/26/74		79.1		
D-2 LOW	1196	F	28	0.25	2.80	10.0	17.9	02/26/74		79.1		
D-2 LOW	1189	M	38	0.26	2.81	13.5	20.0	04/18/74	04/25/79		60.2	Sacrificed
D-2 LOW	930	M	38	0.27	2.92	13.0	19.2	11/30/72	12/28/72		0.9	Sacrificed
D-3 MED-LOW	1066	M	54	0.31	3.38	16.0	18.3	05/31/73		88.0		
D-3 MED-LOW	1089	F	41	0.31	3.42	12.0	17.3	05/31/73		88.0		
D-3 MED-LOW	972	F	40	0.33	3.64	11.0	19.2	12/19/72		93.4		
D-3 MED-LOW	1310	M	54	0.34	3.72	14.5	18.5	03/04/75	04/01/77		24.9	Sacrificed
D-3 MED-LOW	1312	M	58	0.34	3.74	15.5	18.5	03/04/75	03/26/79		48.7	Sacrificed
D-3 MED-LOW	1311	M	54	0.36	4.00	13.5	18.5	03/04/75	04/03/78		37.0	Sacrificed
D-3 MED-LOW	1219	F	46	0.40	4.38	10.5	19.0	04/18/74		77.4		
D-3 MED-LOW	1317	M	72	0.41	4.50	16.0	18.1	03/04/75	04/01/77		24.9	Sacrificed
D-3 MED-LOW	1158	M	73	0.43	4.71	15.5	17.7	11/06/73		82.8		

* Indicates age in months since birth, all other ages are in months since exposure.

DOSE-EFFECT STUDIES WITH INHALED PU-238 OXIDE IN BEAGLES

DOSE GROUP	DOG NUMBER	SEX	INITIAL ALVEOLAR DEPOSITION NCI	NCI/G LUNG	NCI/KG	INHALATION EXPOSURE WEIGHT (KG)	AGE* (MO)	DATE	DATE OF DEATH	MONTHS SINCE INHALATION 9/30/80	DEATH	COMMENTS ON DEAD DOGS
D-3 MED-LOW	1165	M	76	0.43	4.75	16.0	17.3	11/06/73		82.8		
D-3 MED-LOW	1309	M	60	0.44	4.80	12.5	18.5	03/04/75		66.9		
D-3 MED-LOW	1318	M	67	0.45	4.96	13.5	18.1	03/04/75	03/08/76		12.2	Sacrificed
D-3 MED-LOW	929	F	41	0.50	5.47	7.5	19.2	11/30/72	01/25/73		1.8	Sacrificed
D-3 MED-LOW	1316	M	84	0.53	5.79	14.5	18.1	03/04/75		66.9		
D-3 MED-LOW	960	M	68	0.54	5.91	11.5	19.2	12/19/72		93.4		
D-3 MED-LOW	1072	M	98	0.54	5.94	16.5	18.1	05/31/73		88.0		
D-3 MED-LOW	1190	F	71	0.54	5.92	12.0	18.1	02/26/74		79.1		
D-3 MED-LOW	926	M	75	0.55	6.00	12.5	19.5	11/30/72	02/28/73		3.0	Sacrificed
D-3 MED-LOW	1315	M	90	0.55	6.00	15.0	18.1	03/04/75	03/31/77		24.9	Sacrificed
D-3 MED-LOW	982	M	76	0.58	6.33	12.0	19.0	12/19/72		93.4		
D-3 MED-LOW	1040	M	84	0.61	6.72	12.5	18.2	02/22/73		91.2		
D-3 MED-LOW	1059	F	71	0.65	7.10	10.0	17.8	02/22/73		91.2		
D-3 MED-LOW	1319	M	99	0.67	7.33	13.5	18.1	03/04/75	03/09/76		12.2	Sacrificed
D-3 MED-LOW	1108	F	84	0.69	7.64	11.0	16.4	05/31/73		88.0		
D-3 MED-LOW	1000	F	70	0.71	7.78	9.0	18.7	12/19/72		93.4		
D-3 MED-LOW	1056	M	97	0.71	7.76	12.5	17.9	02/22/73		91.2		
D-3 MED-LOW	1004	M	116	0.73	8.00	14.5	19.6	01/18/73		92.4		
D-3 MED-LOW	1026	M	116	0.78	8.59	13.5	19.2	01/18/73		92.4		
D-3 MED-LOW	1043	F	98	0.89	9.80	10.0	18.1	02/22/73		91.2		
D-3 MED-LOW	1031	F	76	0.92	10.13	7.5	19.1	02/22/73		91.2		
D-3 MED-LOW	1212	F	111	1.12	12.33	9.0	17.6	02/26/74		79.1		
D-4 MEDIUM	1176	M	129	0.87	9.56	13.5	15.5	10/06/73		83.8		
D-4 MEDIUM	1221	F	124	1.13	12.40	10.0	19.0	04/18/74		77.4		
D-4 MEDIUM	1195	M	228	1.38	15.20	15.0	18.1	02/26/74		79.1		
D-4 MEDIUM	1032	M	162	1.40	15.43	10.5	16.3	11/30/72	12/08/72		0.3	Sacrificed
D-4 MEDIUM	1053	F	148	1.42	[illegible].58	9.5	17.9	02/22/73		91.2		
D-4 MEDIUM	997	M	203	1.60	17.65	11.5	19.6	01/18/73		92.4		
D-4 MEDIUM	991	F	194	1.76	19.40	10.0	18.8	12/19/72		93.4		
D-4 MEDIUM	1177	M	262	1.76	19.41	13.5	16.6	11/06/73		82.8		
D-4 MEDIUM	932	F	216	1.79	19.64	11.0	19.1	11/30/72	01/25/73		1.8	Sacrificed
D-4 MEDIUM	1103	F	260	1.89	20.80	12.5	16.5	05/31/73		88.0		
D-4 MEDIUM	973	F	271	2.24	24.64	11.0	19.2	12/19/72		93.4		
D-4 MEDIUM	931	F	289	2.39	26.27	11.0	19.1	11/30/72	12/28/72		0.9	Sacrificed
D-4 MEDIUM	1091	F	243	2.60	28.59	8.5	17.3	05/31/73		88.0		
D-4 MEDIUM	1014	M	430	2.70	29.66	14.5	16.4	05/31/73		88.0		
D-4 MEDIUM	1062	M	435	2.93	32.22	13.5	17.8	02/22/73		91.2		
D-4 MEDIUM	934	M	454	3.06	33.63	13.5	19.1	11/30/72	03/01/73		3.0	Sacrificed
D-4 MEDIUM	1081	M	541	3.07	33.81	16.0	18.0	05/31/73	01/18/80		79.6	Hemanglosarcoma, Heart
C-4 MEDIUM	1030	F	340	3.25	35.79	9.5	19.1	02/22/73		91.2		
D-4 MEDIUM	952	F	365	3.49	38.42	9.5	19.2	12/19/72		93.4		
D-4 MEDIUM	1198	M	539	3.50	38.50	14.0	17.9	02/26/74		79.1		
D-4 MEDIUM	1166	M	673	4.08	44.87	15.0	17.3	11/06/73		82.8		

* Indicates age in months since birth, all other ages are in months since exposure.

DOSE-EFFECT STUDIES WITH INHALED PU-238 OXIDE IN BEAGLES

DOSE GROUP	DOG NUMBER	SEX	INITIAL ALVEOLAR DEPOSITION NCI	NCI/G LUNG	NCI/KG	INHALATION EXPOSURE WEIGHT (KG)	AGE* (MO)	DATE	DATE OF DEATH	MONTHS SINCE INHALATION 9/30/80	DEATH	COMMENTS ON DEAD DOGS
D-4 MEDIUM	1220	F	516	4.26	47.09	11.0	19.0	04/16/74		77.4		
D-4 MEDIUM	992	F	555	4.39	48.26	11.5	18.6	12/19/72		93.4		
D-4 MEDIUM	983	M	517	4.67	51.42	12.0	19.0	12/19/72		93.4		
D-5 MED-HIGH	1191	F	591	4.48	49.29	12.0	19.0	04/16/74	[illegible]		[illegible]	Interstitial Pneumonitis
D-5 MED-HIGH	1157	M	700	4.71	51.85	13.5	17.7	11/06/73		82.8		
D-5 MED-HIGH	1035	F	571	5.46	60.11	9.5	18.2	02/22/73		91.2		
D-5 MED-HIGH	1192	F	754	6.25	68.55	11.0	18.1	02/26/74		79.1		
D-5 MED-HIGH	1140	M	1014	6.58	72.43	14.0	18.2	11/06/73		82.8		
D-5 MED-HIGH	1071	M	1269	6.79	74.69	17.0	18.1	05/31/73		88.0		
D-5 MED-HIGH	1173	M	1023	7.75	85.25	12.0	17.3	11/06/73		82.8		
D-5 MED-HIGH	1178	M	1125	8.52	93.75	12.0	18.0	11/06/73		82.8		
D-5 MED-HIGH	1047	M	900	8.61	94.74	9.5	18.1	02/22/73		91.2		
D-5 MED-HIGH	1109	F	1114	8.85	97.30	11.5	18.4	05/31/73	[illegible]		88.2	Processing
D-5 MED-HIGH	1160	M	1344	10.18	112.00	12.0	17.5	11/06/73		82.8		
D-5 MED-HIGH	1211	M	1764	11.00	121.00	14.5	17.0	02/26/74		79.1		
D-5 MED-HIGH	1096	F	1476	12.20	134.18	11.0	18.6	05/31/73	05/08/78		59.2	Addison's Disease
D-5 MED-HIGH	1218	F	1710	12.95	142.50	12.0	17.3	02/26/74		79.1		
D-5 MED-HIGH	1092	M	1848	13.44	147.84	12.5	17.3	05/31/73	10/23/78		64.8	Bone Tumor
D-5 MED-HIGH	1027	M	2148	13.95	153.43	14.0	19.2	01/18/73	12/01/78		70.4	Bone Tumor, Lung Tumor
D-5 MED-HIGH	1115	F	1885	14.90	163.91	11.5	18.1	05/31/73	07/11/78		61.3	Bone Tumor
D-5 MED-HIGH	974	F	1718	15.62	171.80	10.0	20.2	01/18/73	05/24/76		64.1	Bone Tumor
D-5 MED-HIGH	1079	M	2620	15.88	174.67	15.0	18.0	05/31/73	02/12/78		56.4	Addison's, G.I. Tumor
D-5 MED-HIGH	1056	F	1907	16.51	181.62	10.5	17.8	02/22/73	11/01/79		80.3	Bone Tumor, Adrenal Tumor
D-6 HIGH	1002	M	2907	18.86	207.64	14.0	19.6	01/18/73	01/21/80		84.1	Processing
D-6 HIGH	1057	M	3116	20.98	230.81	13.5	17.9	02/22/73	03/07/79		72.4	Bone Tumor
D-6 HIGH	1009	M	3630	26.40	290.40	12.5	19.6	01/18/73	04/01/78		62.4	Lng Tmr, Osteoarthropathy
D-6 HIGH	1042	F	2959	28.32	311.47	9.5	18.1	02/22/73	11/10/78		66.6	Bone Tumor, Lung Tumor
D-6 HIGH	994	F	3453	31.39	345.30	10.0	19.6	01/18/73	07/04/76		41.5	Addison's Disease
D-6 HIGH	1006	F	3810	31.49	346.36	11.0	19.6	01/18/73	01/18/79		72.0	Bone Tumor, Lung Tumor
D-6 HIGH	975	F	3968	36.07	396.80	10.0	20.2	01/18/73	07/25/78		66.2	Bone Tumor, Lung Tumor
D-6 HIGH	1037	M	4854	44.13	485.40	10.0	18.2	02/22/73	11/21/78		68.9	Bone Tumor
D-6 HIGH	1143	M	7691	53.78	591.62	13.0	18.2	11/06/73	12/05/77		49.0	Bone Tumor, Lung Tumor
D-6 HIGH	1025	M	8479	57.10	628.07	13.5	19.2	01/18/73	03/17/77		49.9	Lung Tumor
D-6 HIGH	1064	M	9453	63.66	700.22	13.5	16.7	01/18/73	04/14/77		50.8	Bone Tumor, Lung Tumor
D-6 HIGH	1162	F	6959	70.29	773.22	9.0	17.3	11/06/73	12/19/78		61.4	Bone Tumor, Addison's
D-6 HIGH	1175	F	6201	75.16	826.80	7.5	16.6	11/06/73	02/24/78		51.6	Lung Tumor

* Indicates age in months since birth, all other ages are in months since exposure.

INHALED PLUTONIUM NITRATE IN DOGS

DOSE GROUP	DOG NUMBER	SEX	INITIAL ALVEOLAR DEPOSITION NCI	NCI/G LUNG	NCI/KG	INHALATION EXPOSURE WEIGHT (KG)	AGE* (MO)	DATE	DATE OF DEATH	MONTHS SINCE INHALATION 9/30/80	DEATH	COMMENTS ON DEAD DOGS
CONTROL	1356	M	0	0.00	0.00					76.7*		
CONTROL	1365	M	0	0.00	0.00					76.6*		
CONTROL	1376	F	0	0.00	0.00				05/11/80		70.8*	Pneumonia
CONTROL	1388	M	0	0.00	0.00					75.3*		
CONTROL	1393	M	0	0.00	0.00					75.3*		
CONTROL	1405	M	0	0.00	0.00					74.9*		
CONTROL	1409	M	0	0.00	0.00					74.8*		
CONTROL	1418	M	0	0.00	0.00					74.5*		
CONTROL	1425	M	0	0.00	0.00					74.5*		
	1450	F	0	0.00	0.00					74.3*		
	1455	F	0	0.00	0.00					73.9*		
CONTROL	1483	F	0	0.00	0.00					72.9*		
CONTROL	1509	M	0	0.00	0.00					72.1*		
CONTROL	1516	F	0	0.00	0.00					71.9*		
CONTROL	1525	M	0	0.00	0.00					71.6*		
CONTROL	1527	M	0	0.00	0.00					71.6*		
CONTROL	1528	F	0	0.00	0.00					71.1*		
CONTROL	1543	M	0	0.00	0.00					70.9*		
CONTROL	1563	F	0	0.00	0.00					60.8*		
CONTROL	1572	F	0	0.00	0.00					60.7*		
CONTROL	1577	M	0	0.00	0.00					60.7*		
CONTROL	1584	F	0	0.00	0.00					60.6*		
CONTROL	1594	F	0	0.00	0.00					60.6*		
CONTROL	1608	M	0	0.00	0.00					60.4*		
CONTROL	1633	F	0	0.00	0.00					53.6*		
CONTROL	1638	F	0	0.00	0.00					53.3*		
VEHICLE	1361	M	0	0.00	0.00	8.5	21.0	02/13/76		55.6		
VEHICLE	1381	F	0	0.00	0.00	9.0	19.8	02/13/76		55.6		
VEHICLE	1392	M	0	0.00	0.00	15.0	22.0	04/22/76		53.3		
VEHICLE	1406	M	0	0.00	0.00	13.5	21.6	04/22/76		53.3		
VEHICLE	1412	F	0	0.00	0.00	9.0	19.0	02/13/76		55.6		
VEHICLE	1421	M	0	0.00	0.00	13.0	23.3	06/23/76		51.3		
VEHICLE	1457	F	0	0.00	0.00	12.0	20.6	04/22/76		53.3		
VEHICLE	1491	F	0	0.00	0.00	8.5	21.6	06/23/76		51.3		
VEHICLE	1504	F	0	0.00	0.00	10.0	20.9	06/23/76		51.3		
VEHICLE	1514	M	0	0.00	0.00	14.0	20.9	06/23/76		51.3		
VEHICLE	1524	M	0	0.00	0.00	12.0	21.5	07/27/76		50.1		
VEHICLE	1531	F	0	0.00	0.00	9.0	20.9	07/27/76		50.1		
VEHICLE	1542	M	0	0.00	0.00	12.0	20.8	07/27/76		50.1		
VEHICLE	1566	M	0	0.00	0.00	14.0	18.3	03/15/77		42.5		
VEHICLE	1578	M	0	0.00	0.00	10.5	18.2	03/15/77		42.5		
VEHICLE	1593	F	0	0.00	0.00	11.0	18.0	03/15/77		42.5		
VEHICLE	1601	F	0	0.00	0.00	8.5	15.0	03/15/77		42.5		

* Indicates age in months since birth. All other ages are in months after exposure.

INHALED PLUTONIUM NITRATE IN DOGS

DOSE GROUP	DOG NUMBER	SEX	INITIAL ALVEOLAR DEPOSITION NCI	NCI/G LUNG	NCI/KG	INHALATION EXPOSURE WEIGHT (KG)	AGE* (MO)	DATE	DATE OF DEATH	MONTHS SINCE INHALATION 9/30/80	DEATH	COMMENTS ON DEAD DOGS
VEHICLE	1620	M	0	0.00	0.00	13.0	21.1	12/01/77		34.0		
VEHICLE	1634	F	0	0.00	0.00	10.5	19.6	12/01/77		34.0		
VEHICLE	1651	F	0	0.00	0.00	11.0	19.2	12/01/77		34.0		
D-1 LOWEST	1416	M	0	0.00	0.00	12.0	22.1	05/20/76		52.4		
D-1 LOWEST	1458	F	0	0.00	0.00	10.5	21.5	05/20/76		52.4		
D-1 LOWEST	1489	F	0	0.00	0.00	8.5	20.5	05/20/76		52.4		
D-1 LOWEST	1501	M	0	0.00	0.00	14.0	20.4	05/20/76		52.4		
D-1 LOWEST	1515	M	0	0.00	0.00	13.5	19.8	05/20/76		52.4		
D-1 LOWEST	1573	M	0	0.00	0.00	11.5	19.4	04/19/77		41.4		
D-1 LOWEST	1581	M	0	0.00	0.00	16.5	19.3	04/19/77		41.4		
D-1 LOWEST	1596	M	0	0.00	0.00	14.0	19.2	04/19/77		41.4		
D-1 LOWEST	1600	F	1	0.01	0.11	11.0	19.2	04/19/77		41.4		
D-1 LOWEST	1603	M	2	0.01	0.12	14.0	19.2	04/19/77		41.4		
D-1 LOWEST	1339	F	2	0.02	0.22	9.0	17.5	10/16/75	11/13/75		0.9	Sacrificed
D-1 LOWEST	1519	M	2	0.02	0.16	12.5	19.5	05/20/76		52.4		
D-1 LOWEST	1570	F	2	0.02	0.17	10.5	19.4	04/19/77		41.4		
D-1 LOWEST	1465	F	4	0.03	0.35	12.0	21.0	05/20/76		52.4		
D-1 LOWEST	1470	F	3	0.03	0.29	10.5	21.0	05/20/76		52.4		
D-1 LOWEST	1507	M	4	0.03	0.32	14.0	19.8	05/20/76		52.4		
D-1 LOWEST	1592	F	4	0.03	0.29	13.5	19.2	04/19/77		41.4		
D-1 LOWEST	1607	M	5	0.03	0.35	13.0	19.0	04/19/77		41.4		
D-1 LOWEST	1335	M	5	0.04	0.42	11.5	18.0	10/16/75	11/13/75		0.9	Sacrificed
D-1 LOWEST	1487	F	6	0.04	0.46	13.0	20.5	05/20/76		52.4		
D-1 LOWEST	1583	F	4	0.04	0.40	9.5	19.2	04/19/77		41.4		
D-1 LOWEST	1351	M	7	0.06	0.61	11.0	17.2	10/16/75	11/13/75		0.9	Sacrificed
D-1 LOWEST	1565	F	8	0.06	0.67	11.5	19.4	04/19/77		41.4		
D-2 LOW	1513	M	0	0.00	0.00	11.5	19.8	05/20/76		52.4		
D-2 LOW	1520	M	1	0.01	0.12	10.5	19.5	05/20/76		52.4		
D-2 LOW	1415	M	2	0.02	0.20	11.5	22.2	05/20/76		52.4		
D-2 LOW	1575	M	3	0.02	0.19	14.0	19.4	04/19/77		41.4		
D-2 LOW	1466	F	5	0.03	0.37	14.0	21.0	05/20/76		52.4		
D-2 LOW	1606	F	5	0.04	0.42	12.5	19.0	04/19/77		41.4		
D-2 LOW	1579	M	8	0.05	0.59	14.0	19.3	04/19/77		41.4		
D-2 LOW	1590	F	6	0.05	0.51	12.0	19.2	04/19/77		41.4		
D-2 LOW	1585	F	8	0.06	0.68	12.0	19.2	04/19/77		41.4		
D-2 LOW	1580	F	9	0.07	0.82	11.0	19.3	04/19/77		41.4		
D-2 LOW	1591	M	11	0.07	0.76	15.0	19.2	04/19/77		41.4		
D-2 LOW	1417	M	11	0.08	0.89	12.0	22.1	05/20/76		52.4		
D-2 LOW	1423	M	10	0.08	0.87	11.0	22.1	05/20/76		52.4		
D-2 LOW	1567	M	10	0.08	0.83	12.0	19.4	04/19/77		41.4		
D-2 LOW	1472	F	10	0.0[illegible]	1.01	10.0	21.0	05/20/76		52.4		
D-2 LOW	1503	F	9	0.09	0.97	9.0	19.8	05/20/76		52.4		
D-2 LOW	1602	M	15	0.09	1.03	14.5	19.2	04/19/77		41.4		

* Indicates age in months since birth, all other ages are in months since exposure.

INHALED PLUTONIUM NITRATE IN DOGS

DOSE GROUP	DOG NUMBER	SEX	INITIAL ALVEOLAR DEPOSITION NCI	NCI/G LUNG	NCI/KG	INHALATION EXPOSURE WEIGHT (KG)	AGE* (MO)	DATE	DATE OF DEATH	MONTHS SINCE INHALATION 9/30/80	DEATH	COMMENTS ON DEAD DOGS
D-2 LOW	1484	F	11	0.10	1.08	10.0	20.5	05/20/76		52.4		
D-2 LOW	1599	F	10	0.10	1.14	9.0	19.2	04/19/77		41.4		
D-2 LOW	1490	F	16	0.15	1.65	9.5	20.5	05/20/76		52.4		
D-3 MED-LOW	1336	M	21	0.14	1.52	13.5	18.0	10/16/75	11/13/75		0.9	Sacrificed
D-3 MED-LOW	1341	F	19	0.16	1.78	10.5	17.2	10/16/75	11/13/75		0.9	Sacrificed
D-3 MED-LOW	1605	F	25	0.20	2.19	11.5	17.8	03/15/77		42.5		
D-3 MED-LOW	1386	M	34	0.21	2.36	14.5	22.0	04/20/76		53.4		
D-3 MED-LOW	1389	M	27	0.23	2.54	10.5	21.9	04/20/76	05/04/76		0.5	Sacrificed
D-3 MED-LOW	1413	F	29	0.24	2.68	11.0	16.2	01/20/76		56.3		
D-3 MED-LOW	1445	F	34	0.24	2.60	13.0	21.0	04/20/76	05/05/76		0.5	Sacrificed
D-3 MED-LOW	1568	M	46	0.29	3.17	14.5	16.3	03/15/77		42.5		
D-3 MED-LOW	1390	M	43	0.30	3.29	13.0	21.9	04/20/76	05/04/76		0.5	Sacrificed
D-3 MED-LOW	1391	M	54	0.30	3.26	16.5	21.9	04/20/76		53.4		
D-3 MED-LOW	1587	M	53	0.31	3.40	15.5	18.1	03/15/77		42.5		
D-3 MED-LOW	1595	M	50	0.31	3.45	14.5	18.0	03/15/77		42.5		
D-3 MED-LOW	1359	M	50	0.32	3.57	14.0	20.2	01/20/76	01/23/76		0.1	Sacrificed
D-3 MED-LOW	1540	M	54	0.32	3.51	15.5	20.7	07/22/76		50.3		
D-3 MED-LOW	1344	F	41	0.33	3.60	11.5	17.2	10/16/75	11/14/75		1.0	Sacrificed
D-3 MED-LOW	1589	F	41	0.34	3.75	11.0	18.0	03/15/77		42.5		
D-3 MED-LOW	1588	M	50	0.36	3.98	12.5	18.1	03/15/77	03/22/78		12.2	Sacrificed
D-3 MED-LOW	1529	F	43	0.37	4.08	10.5	20.8	07/22/76	10/19/76		2.9	Sacrificed
D-3 MED-LOW	1574	M	46	0.38	4.21	11.0	18.2	03/15/77		42.5		
D-3 MED-LOW	1375	F	50	0.40	4.35	11.5	19.1	01/20/76	01/23/76		0.1	Sacrificed
D-3 MED-LOW	1564	F	40	0.40	4.44	9.0	18.5	03/15/77	03/20/78		12.2	Sacrificed
D-3 MED-LOW	1444	F	49	0.41	4.50	11.0	21.0	04/20/76		53.4		
D-3 MED-LOW	1439	F	53	0.42	4.61	11.5	21.0	04/20/76		53.4		
D-3 MED-LOW	1525	F	55	0.42	4.60	12.0	21.5	07/22/76		50.3		
D-3 MED-LOW	1534	M	65	0.45	4.99	13.0	20.7	07/22/76	10/20/76		3.0	Sacrificed
D-3 MED-LOW	1380	M	63	0.46	5.06	12.5	19.1	01/20/76		56.3		
D-3 MED-LOW	1407	F	50	0.51	5.56	9.0	18.5	01/20/76	01/23/76		0.1	Sacrificed
D-3 MED-LOW	1569	F	58	0.53	5.82	10.0	18.2	03/15/77		42.5		
D-3 MED-LOW	1576	M	70	0.53	5.86	12.0	18.2	03/15/77		42.5		
D-3 MED-LOW	1582	F	57	0.54	5.96	9.5	18.1	03/15/77		42.5		
D-3 MED-LOW	1571	F	68	0.57	6.22	11.0	18.2	03/15/77	03/21/78		12.2	Sacrificed
D-3 MED-LOW	1427	F	68	0.62	6.81	10.0	21.1	04/20/76		53.4		
D-3 MED-LOW	1522	F	78	0.71	7.78	10.0	21.5	07/22/76	10/18/76		2.9	Sacrificed
D-3 MED-LOW	1363	M	85	0.74	8.09	10.5	20.2	01/20/76		56.3		
D-3 MED-LOW	1604	M	85	0.74	8.10	10.5	18.0	03/15/77		42.5		
D-3 MED-LOW	1530	F	72	0.76	8.41	8.5	20.8	07/22/76		50.3		
D-3 MED-LOW	1456	F	61	0.77	8.68	7.0	20.5	04/20/76		53.4		
D-3 MED-LOW	1598	F	93	1.06	11.65	8.0	18.0	03/15/77		42.5		
D-3 MED-LOW	1422	F	99	1.12	12.35	8.0	18.1	01/20/76		56.3		
D-4 MEDIUM	1637	M	192	1.45	15.99	12.0	18.9	11/07/77		34.8		

* Indicates age in months since birth, all other ages are in months since exposure.

DOSE-EFFECT STUDIES WITH INHALED PU-238 OXIDE IN BEAGLES

DOSE GROUP	DOG NUMBER	SEX	INITIAL ALVEOLAR DEPOSITION NCI	NCI/G LUNG	NCI/KG	INHALATION EXPOSURE WEIGHT (KG)	AGE* (MO)	DATE	DATE OF DEATH	MONTHS SINCE INHALATION 9/30/80	DEATH	COMMENTS ON DEAD DOGS
CONTROL	939	M	0	0.00	0.00					112.9*		
CONTROL	949	F	0	0.00	0.00					112.7*		
CONTROL	978	M	0	0.00	0.00					112.6*		
CONTROL	990	F	0	0.00	0.00				[illegible]		97.4*	Pyometra
CONTROL	996	F	0	0.00	0.00					112.0*		
CONTROL	1005	M	0	0.00	0.00					112.0*		
CONTROL	1007	F	0	0.00	0.00					112.0*		
CONTROL	1024	M	0	0.00	0.00					111.5*		
CONTROL	1056	M	[illegible]	0.00	0.00					109.4*		
CONTROL	1049	M	[illegible]	[illegible]	[illegible]					109.4*		
CONTROL	1054	F	[illegible]	[illegible]	[illegible]					109.1*		
CONTROL	1061	F	[illegible]	[illegible]	[illegible]					109.0*		
CONTROL	1092	M	[illegible]	[illegible]	[illegible]					105.3*		
CONTROL	[illegible]	F	[illegible]	[illegible]	[illegible]					104.8*		
CONTROL	1114	M	[illegible]	[illegible]	[illegible]					104.4*		
CONTROL	1116	F	[illegible]	[illegible]	[illegible]					104.1*		
CONTROL	1166	F	[illegible]	[illegible]	[illegible]					97.5*		
CONTROL	1174	M	[illegible]	[illegible]	[illegible]					97.0*		
CONTROL	1209	M	[illegible]	[illegible]	[illegible]					96.7*		
CONTROL	1225	F	[illegible]	[illegible]	[illegible]					96.9*		
CONTROL SACRIFICE	966	M	[illegible]	[illegible]					[illegible]		71.0*	Sacrificed
CONTROL SACRIFICE	1011	F	[illegible]	[illegible]	[illegible]				[illegible]		85.9*	Sacrificed
CONTROL SACRIFICE	1013	F	[illegible]	[illegible]					[illegible]		95.0*	Sacrificed
CONTROL SACRIFICE	1087	M	0	[illegible]	[illegible]				[illegible]		60.0*	Sacrificed
CONTROL SACRIFICE	1118	M	0	[illegible]	[illegible]				[illegible]		47.5*	Sacrificed
CONTROL SACRIFICE	1223	M	0	0.00	[illegible]						31.9*	Sacrificed
CONTROL SACRIFICE	1227	M	0	0.00	[illegible]				[illegible]		49.9*	Sacrificed
CONTROL SACRIFICE	1228	M	0	0.00	[illegible]						72.9*	Sacrificed
D-1 LOWEST	996	M	0	0.00	[illegible]	[illegible]	[illegible]			92.4		
D-1 LOWEST	1003	M	0	0.00	0.00	[illegible]	[illegible]			92.4		
D-1 LOWEST	1023	F	0	0.00	0.00	[illegible]	[illegible]	[illegible]		92.4		
D-1 LOWEST	1039	M	0	0.00	0.00	11.0	[illegible]	01/16/73		92.4		
D-1 LOWEST	1044	F	0	0.00	0.00	11.5	17.0	01/16/73		92.4		
D-1 LOWEST	1055	M	0	0.00	0.00	13.0	16.8	01/16/73		92.4		
D-1 LOWEST	1083	M	0	0.00	0.00	14.5	16.7	01/18/73		92.4		
D-1 LOWEST	1109	F	0	0.00	0.00	10.0	16.4	05/31/73		88.0		
D-1 LOWEST	1144	F	[illegible]	[illegible]	[illegible]	10.5	19.6	04/16/74		77.4		
D-1 LOWEST	1215	M	4	[illegible]	[illegible]	[illegible]	19.3	04/18/74	04/26/77		36.3	Sacrificed
D-1 LOWEST	1230	M	0	[illegible]	[illegible]	[illegible]	16.4	04/16/74		77.4		
D-1 LOWEST	951	M	2	0.01	0.14	[illegible]	[illegible]	[illegible]		93.4		
D-1 LOWEST	1008	M	2	0.01	[illegible]	[illegible]	[illegible]	[illegible]		92.4		
D-1 LOWEST	1193	F	2	0.01	[illegible]	[illegible]	[illegible]	[illegible]		77.4		
D-1 LOWEST	959	M	3	0.02	[illegible]	[illegible]	[illegible]	[illegible]		93.4		

* Indicates age in months since birth, all other ages are in months since exposure.

INHALED PLUTONIUM NITRATE IN DOGS

DOSE GROUP	DOG NUMBER	SEX	INITIAL ALVEOLAR DEPOSITION NCI	NCI/G LUNG	NCI/KG	INHALATION EXPOSURE WEIGHT (KG)	AGE* (MO)	DATE	DATE OF DEATH	MONTHS SINCE INHALATION 9/30/80	DEATH	COMMENTS ON DEAD DOGS
D-4 MEDIUM	1404	M	260	1.48	16.25	16.0	21.5	04/20/76		53.4		
D-4 MEDIUM	1521	F	205	1.49	16.37	12.5	21.3	07/22/76		50.3		
D-4 MEDIUM	1656	M	211	1.54	16.90	12.5	18.4	11/07/77		34.8		
D-4 MEDIUM	1579	M	278	1.74	19.16	14.5	19.1	01/20/76		56.3		
D-4 MEDIUM	1562	M	267	1.87	20.54	13.0	20.2	01/20/76		56.3		
D-4 MEDIUM	1645	F	257	2.05	22.37	11.5	18.5	11/07/77		34.8		
D-4 MEDIUM	1639	F	248	2.05	22.57	11.0	18.5	11/07/77		34.8		
D-4 MEDIUM	1647	M	294	2.05	22.58	13.0	18.5	11/07/77		34.8		
D-4 MEDIUM	1640	M	307	2.06	22.71	13.5	18.5	11/07/77		34.8		
D-4 MEDIUM	1534	M	295	2.14	23.57	12.5	20.6	07/22/76		50.3		
D-4 MEDIUM	1414	F	253	2.35	25.80	9.0	16.2	01/20/76		56.3		
D-4 MEDIUM	1618	F	277	2.40	26.36	10.5	20.5	11/07/77		34.8		
D-4 MEDIUM	1585	M	375	2.42	26.63	14.0	19.0	01/20/76		56.3		
D-4 MEDIUM	1408	F	331	2.62	28.77	11.5	16.1	01/20/76		56.3		
D-4 MEDIUM	1428	F	378	3.12	34.36	11.0	21.1	04/20/76		53.4		
D-4 MEDIUM	1535	F	345	3.13	34.48	10.0	20.6	07/22/76		50.3		
D-4 MEDIUM	1446	F	354	3.22	35.40	10.0	21.0	04/20/76		53.4		
D-4 MEDIUM	1564	M	463	3.24	35.65	13.0	20.2	01/20/76		56.3		
D-4 MEDIUM	1587	F	345	4.46	49.30	7.0	14.0	01/20/76	08/13/80		54.6	Bone Tumor
D-5 MED-HIGH	1379	F	363	5.50	56.27	10.0	18.0	10/16/75	11/14/77		1.0	Sacrificed
D-5 MED-HIGH	1346	M	656	4.42	48.59	13.5	17.2	10/16/	11/14/		1.0	Sacrificed
D-5 MED-HIGH	1648	M	811	5.90	64.90	12.5	18.5	11/07/77		34.8		
D-5 MED-HIGH	1659	F	990	6.93	76.16	13.0	18.5	11/07/77		34.8		
D-5 MED-HIGH	1547	F	688	6.95	76.41	9.0	17.2	10/16/75	11/14/75		1.0	Sacrificed
D-5 MED-HIGH	1636	M	1217	8.48	93.25	13.0	18.9	11/07/77		34.8		
D-5 MED-HIGH	1621	M	1334	8.66	95.26	14.0	20.5	11/07/77		34.8		
D-5 MED-HIGH	1646	F	1001	8.77	96.45	11.0	18.5	11/07/77		34.8		
D-5 MED-HIGH	1429	M	1376	9.62	105.85	13.0	21.2	06/23/76		51.3		
D-5 MED-HIGH	1641	M	1275	9.66	106.24	12.0	18.5	11/07/77		34.8		
D-5 MED-HIGH	1660	M	1518	10.22	112.41	13.5	18.5	11/07/77		34.8		
D-5 MED-HIGH	1508	M	1516	10.76	118.37	14.5	20.9	06/23/76	03/24/80		45.0	Bone Tumor
D-5 MED-HIGH	1655	M	1394	11.05	121.56	9.0	18.4	11/07/77		34.8		
D-5 MED-HIGH	1652	F	1520	12.00	131.95	11.0	18.4	11/07/77		34.8		
D-5 MED-HIGH	1619	F	1490	12.32	135.50	11.0	20.5	11/07/77		34.8		
D-5 MED-HIGH	1512	M	2411	14.61	160.71	15.0	20.9	06/23/76	12/23/79		42.0	Bone Tumor
D-5 MED-HIGH	1419	M	1559	14.97	164.11	9.5	23.5	06/23/76		51.3		
D-5 MED-HIGH	1498	F	2018	16.68	183.49	11.0	21.5	06/23/76		51.3		
D-5 MED-HIGH	1502	F	3008	20.25	222.80	13.5	20.9	06/23/76		51.3		
D-5 MED-HIGH	1485	F	2550	21.18	233.00	10.0	21.7	06/23/76		51.3		
D-5 MED-HIGH	1471	F	2508	21.71	238.82	10.5	22.1	06/23/76	05/01/79		34.2	Radiation Pneumonitis
D-5 MED-HIGH	1492	F	2475	24.98	274.82	9.0	21.6	06/23/76		51.3		
D-5 MED-HIGH	1459	F	2645	26.72	293.89	9.0	22.6	06/23/76		51.3		
D-6 HIGH	1516	M	3562	29.46	324.09	11.0	20.6	06/23/76	02/18/79		41.8	Lung Tumor

* Indicates age in months since birth, all other ages are in months since exposure.

INHALED PLUTONIUM NITRATE IN DOGS

DOSE GROUP	DOG NUMBER	SEX	INITIAL ALVEOLAR DEPOSITION NCI	NCI/KG LUNG	NCI/KG	INHALATION EXPOSURE WEIGHT (KG)	AGE* (MO)	DATE	DATE OF DEATH	MONTHS SINCE INHALATION 9/30/80	DEATH	COMMENTS ON DEAD DOGS
D-6 HIGH	1426	M	3840	50.36	355.91	[illegible]	25.5	06/23/70	01/12/70		24.6	Radiation Pneumonitis
D-6 HIGH	1517	F	5185	49.62	545.79	9.5	[illegible]	06/23/70	11/02/71		16.3	Radiation Pneumonitis
D-6 HIGH	1516	F	6969	55.09	606.02	11.5	[illegible]	06/23/70	11/09/71		16.6	Radiation Pneumonitis
D-6 HIGH	1424	M	7081	69.83	768.12	[illegible]	[illegible]	06/23/70	08/31/72		14.3	Radiation Pneumonitis

* Indicates age if months since birth, all other ages are in months since exposure.

PUBLICATIONS

Anderson, L. E. and R. D. Phillips. 1980. Biological effects of 60-Hz electric fields on rodents. Bioelectromagnetics J. 1: 243 (#132).

Bair, W. J., M. Metivier, and J. F. Park. 1980. Comparison of acute mortality in baboons and dogs after inhalation of $^{239}PuO_2$. Radiat. Res. 82: 588-612.

Creim, J. A., R. H. Lovely, R. D. Phillips, and W. T. Kaune. 1980. Test for induction of illness/malaise in rat by exposure to a 60-Hz electric field. Bioelectromagnetics J. 1: 241 (#124).

Dunning, W. F., J. F. Park, H. A. [illegible], and J. E. Morris. 1974. Toxicity of inhaled plutonium in dogs. pp. 105-119. In: IAEA-SM-237/48. Vol. I. IAEA, Vienna, Austria.

Dagle, G.oE., C. L. Sanders, J. F. Park, and J. A. Mahaffe. 1980. Pulmonary carcinogenesis with inhaled plutonium in rats and dogs. pp. 601-615. In: Pulmonary Toxicology of Respirable Particles. CONF-791002. NTIS, Springfield, VA.

Decker, J. R., E. G. Kuffel, D. D. Mahlum, M. R. Sikov, and C. P. Harris. 1979. An environmentally controlled system for exposure of mice to large DC magnetic fields. pp. 447-461. In: Biological Effects of Extremely Low Frequency Electromagnetic Fields. CONF-781016. NTIS, Springfield, VA.

Drucker, H., T. R. Garland, and R. E. Wildung. 1979. Metabolic response of microbiota to chromium and other metals. In: Trace Metals in Health and Disease. N. Kharasch (ed.). Raven Press, NY.

Frazier, M. E. and T. K. Andrews. 1979. In vitro clonal growth assay for evaluating toxicity of metal salts. pp. 71-81. In: Trace Metals in Health and Disease. N. Kharasch (ed.). Raven Press, NY.

Frazier, M. E., T. K. Andrews, and R. C. Thompson. 1979. In vitro evaluations of biomagnetic effects. pp. 417-435. In: Biological Effects of Extremely Low Frequency Electromagnetic Fields. CONF-781016. NTIS, Springfield, VA.

Frazier, M. E., R. N. Ushijima, T. K. Andrews, and M. J. Hooper. 1979. Comparative studies on cell lines established from normal and radiation-exposed mouse [illegible]

Fr[illegible]

Ev[illegible]

[illegible]

Ha[illegible]

[illegible]

[illegible]

Hu[illegible] Mutagenic effects of [illegible] In: Biological Effects of Extremely Low Frequency Electromagnetic Fields. CONF-781016. NTIS, Springfield, VA.

Jaffe, R. A., B. Jaszewski, J. E. Carr, and R. D. Phillips. 1980. Chronic exposure to a 60-Hz electric field: Effects on synaptic transmission and peripheral nerve function in the rat. Bioelectromagnetics J. 1: 131-147.

Jaffe, R. A., R. D. Phillips, and W. T. Kaune. 1979. Effects of chronic exposure to a 60-Hz electric field on synaptic transmission and peripheral nerve function in the rat. pp. 277-296. In: Biological Effects of Extremely Low Frequency Electromagnetic Fields. CONF-781016. NTIS, Springfield, VA.

Kaune, W. T. 1979. A prototype system for exposing small laboratory animals to 60-Hz electric fields: Electrical measurements. pp. 225-240. In: Biological Effects of Extremely Low Frequency Elec-

tromagnetic Fields. CONF-781016, NTIS, Springfield, VA.

Kaune, W. T. and R. D. Phillips. 1980. Comparison of the coupling in grounded humans, swine, and rats to vertical 60-Hz electric fields. Bioelectromagnetics J. 1: 117-129.

Kaune, W. T., A. J. King, F. C. Causey, M. L. Frazier, F. P. Hungate, and R. P. Schneider. 1980. Exposure of cell suspensions to 60-Hz electric fields. Bioelectromagnetics J. 1: 234 (#14).

Kaune, W. T., M. C. Miller, and A. J. King. 1980. Technique for direct measurement of 60-Hz electric fields inside homogeneous models of human and animals. Bioelectromagnetics J. 1: 221 (#64).

[illegible] Effects of monomer [illegible] of the pregnant and fetal rat [illegible]

[illegible] and W. T. Kaune. 1980. [illegible] induced [illegible] the rat. Bioelectromagnetics [illegible]

Mahlum, D. D., M. R. Sikov, and J. R. Decker. 1979. Dominant lethal studies in mice exposed to direct current magnetic fields, pp. 474-484. In: Biological Effects of Extremely Low Frequency Electromagnetic Fields. CONF-781016, NTIS, Springfield, VA.

McShane, J. F., G. E. Dagle, and I. F. Park. 1980. Pulmonary distribution of inhaled $^{239}PuO_2$ in dogs, pp. 248-255. In: Pulmonary Toxicology of Respirable Particles. CONF-791002, NTIS, Springfield, VA.

Montgomery, L. D., D. D. Mahlum, and J. R. Decker. 1980. Effect of magnetic fields on EMS-induced dominant lethality in mice. Bioelectromagnetics J. 1: 204 (#14).

Morris, J. E. and H. A. Ragan. 1979. Immunological studies with 60-Hz electric fields, pp. 326-334. In: Biological Effects of Extremely Low Frequency Electromagnetic Fields. CONF-781016, NTIS, Springfield, VA.

Morris, J. E., H. A. Ragan, T. M. Graham, M. J. Pipes, and R. D. Phillips. 1980. In vivo and in vitro cell-mediated immunity in mice exposed to 60-Hz, 100 kV/m electric fields. Bioelectromagnetics J. 1: 237 (#112).

Phillips, R. D. 1979. Health aspects of power transmission, pp. 304-319. In: Energy and Human Health: Human Costs of Electric Power Generation. EPA-600/9-80-030. Office of Research and Development, U.S. Environmental Protection Agency, Washington, DC.

Poston, K. A. and F. D. Andrew. 1980. Effects of complex chemicals on behavioral teratology in rats. Teratology 21: 62A (abstract).

Ragan, H. A., M. J. Pipes, W. T. Kaune, and R. D. Phillips. 1979. Clinical pathologic evaluations in rats and mice chronically exposed to 60-Hz electric fields, pp. 297-325. In: Biological Effects of Extremely Low Frequency Electromagnetic Fields. CONF-781016, NTIS, Springfield, VA.

Renne, R. A., J. E. Lund, K. E. McDonald, and L. G. Smith. 1980. Morphologic effects of intratracheally administered [illegible] in rats, pp. 509-514. In: Health Implications of New Energy Technologies, William N. Rom and V. E. Archer (eds.). Ann Arbor Science Publishers, Inc., Ann Arbor, MI.

[illegible], A. V. and R. P. Schneider. 1980. Phagocytosis, toxicity, and solubility of AmO_2 in alveolar macrophages, pp. 325-337. In: Pulmonary Toxicology of Respirable Particles. CONF-791002, NTIS, Springfield, VA.

Sanders, C. L. and J. A. Mahaffey. 1979. Inhalation toxicology of transuranics in rodents, pp. 501-514. In: Biological Implications of Radionuclides Released from Nuclear Industries. IAEA Symposium, Vol. 1. IAEA, Vienna, Austria.

Sanders, C. L., F. T. Cross, G. E. Dagle, and J. A. Mahaffey. 1980. Pulmonary Toxicology of Respirable Particles. Proceedings of the Nineteenth Annual Hanford Life Sciences Symposium, Richland, WA, October 22-24, 1979. CONF-791002, NTIS, Springfield, VA.

Sikov, M. R., D. D. Mahlum, L. D. Montgomery, and J. R. Decker. 1979. Development of mice after intrauterine exposure to DC magnetic fields, pp. 462-473. In: Biological Effects of Extremely Low Frequency Electromagnetic Fields. CONF-781016, NTIS, Springfield, VA.

Sikov, M. R., L. D. Montgomery, and L. G. Smith. 1979. Developmental toxicology studies with 60-Hz electric fields, pp. 335-347. In: Biological Effects of Extremely Low Frequency Electromagnetic

Fields. CONF-781016, NTIS, Springfield, VA.

Sullivan, M. F., [illegible] R. Garland, [illegible] A. Cataldo, and R. G. Schreckhise. 1979. Absorption of plant incorporated nuclear fuel cycle elements from the gastrointestinal tract, pp. 447-458. In: Biological Implications of Radionuclides Released From Nuclear Industries, IAEA-SM-237 [illegible] IAEA, Vienna, Austria.

Sullivan, M. F. 1980. Absorption of actinide elements from the gastrointestinal tract of rats, guinea pigs and dogs. Health Phys. 38: 159-[illegible].

Sullivan, M. F. 1980. Absorption of actinide elements from the gastrointestinal tract of neonatal animals. Health Phys. 38: 173-[illegible].

Sullivan, M. F., [illegible] Cataldo, R. E. Wildung, and [illegible] 1980. Absorption of plutonium from the gastrointestinal tract of rats [illegible] pigs after ingestion of [illegible] Health Phys. 38: [illegible].

Sullivan, M. F., [illegible] Gorham, [illegible] Brantom. 1980. Absorption of [illegible] from the gastrointestinal tract [illegible] neonatal animals after inhalation, [illegible] 238-247. In: Pulmonary [illegible] Respirable Particles. CONF-[illegible] Springfield, VA.

Sullivan, M. F., [illegible] S. Gorham, and [illegible] Ryan. 1980. The effect of oxidation state on absorption of ingested [illegible] plutonium, pp. 127-129. In: Proceedings of the 5th International Congress of the International Radiation Protection Association, [illegible] March [illegible]-14, [illegible].

[illegible] Mitchell, and [illegible] Rhoads. [illegible] Effect of plutonium [illegible] 224-[illegible]. In: Pulmonary Toxicology [illegible] CONF-79[illegible], NTIS [illegible].

[illegible] A. [illegible] deration of [illegible] trends [illegible] radiation [illegible] 6-7. In: [illegible] Systems [illegible] IAEA-SR-[illegible] IAEA, Vienna, Austria.

[illegible] Committee [illegible] Proceedings [illegible] Inter[illegible] Association [illegible].

[illegible] International [illegible] Radiation [illegible].

[illegible] Springfield, VA.

[illegible]

PRESENTATIONS

Anderson, [illegible] E. and R. D. Phillips. Biological Effects of 60-Hz Electric Fields on Rodents. Bioelectromagnetics Society, San Antonio, TX. September.

Anderson, L. E., F. D. Andrew, and R. A. Pelroy. Half-Life of Hepatic Mutagen-Activating Enzymes in Rats Exposed to High and Low Boiling Coal Distillates. 20th Hanford Life Sciences Symposium: Coal Conversion and the Environment. October.

Ballou, J. E., R. A. Gies, and N. A. Wogman. The Disposition of ^{239}Pu Daughters Following Inhalation of $^{239}UO_2(NO_3)_2$ Aerosols. Health Physics Society Meeting, Seattle, WA. July.

Beamer, J. [illegible] Let's Improve Our Image - A Workshop Presentation and Demonstration of Biomedical Photography Methods and Materials. American Association of Laboratory Animal Science Meeting, Monterey, CA. March.

Briant, J. K. and O. R. Moss. Monitoring High Aerosol Mass Concentration with Back-Scattered Light. Aerosol Technology Meeting, Boston, MA. August.

Chang, D. P. Y., E. M. Milliman, O. R. Moss. Experience with a Flexible-Brush Dust Feed Mechanism. American Industrial Hygiene Conference, Houston, TX. November.

Conklin, A. W. and C. L. Sanders. Metabolism of Intratracheally Instilled Selenate and Selenite. Northwest Section, Federation of American Societies for Experimental Biology and Medicine. Vancouver, BC. October.

Creim, J. A., R. B. Lovely, R. D. Phillips, and W. T. Kaune. Test for Induction of Illness/Malaise in Rats by Exposure to a 60-Hz Electric Field. Bioelectromagnetics Society Meeting, San Antonio, TX. September.

Cross, F. T., R. F. Palmer, R. [illegible] Buschbom, and R. H. Busch. Influence of Radon Daughter Exposure Rate and Uranium Ore Dust Concentration on Occurrence of Lung Tumors. C.N.E.N., Rome, Italy. March.

Dagle, G. E., J. E. Ballou, and R. A. Gies. The Morphology of Lung Tumors Induced in Rats with Inhalation of Uranyl Nitrates. American College of Veterinary Pathologists Meeting, New Orleans, LA. December.

Dagle, G. E., J. F. McShane, W. C. Cannon, and D. L. Stevens. Deposition and Translocation of Inhaled $^{238}Pu(NO_3)_4$ in Beagle Dogs. Health Physics Society Meeting, Seattle, WA. July.

DeFord, H. A. Maintaining Constant Reservoir Concentration and Aerosol Output for Compressed Air Nebulizers. American Industrial Hygiene Conference, Houston, TX. May.

Filipy, R. E. The Effect of Chronic Exposure to Cigarette Smoke on Lung Clearance of Inhaled Plutonium in Rats. Health Physics Annual Meeting, Seattle, WA. [illegible].

Frazier, M. E. Radiation-Induced Porcine Petrovirus. Oregon State University, Corvallis, OR. April.

Gelman, R. A. Percutaneous Penetration and Tissue Distribution of ^{14}C Benzo[a]pyrene in the Mouse. FASEB Annual Meeting. April.

Gies, R. A. Inhalation Toxicology of $^{241}Am(NO_3)_3$. Health Physics Society Meeting, Seattle, WA. July.

Graham, T. M. In Vitro Stimulation of Canine Peripheral Blood Lymphocytes with Concanavalin-A. Northwest Section, Federation of America Societies for Experimental Biology and Medicine Meeting, Vancouver, BC. October.

Graham, T. M., J. F. Morris, and F. S. Andrew. Effects of Complex Chemicals on Ontogeny of Immunocompetence in Rats Exposed In Utero. 19th Annual Meeting, Society of Toxicology, Washington, DC. March.

Hackett, P. L. Comparative Deposition and Retention of Inhaled Microspheres in the Neonatal Rat. 20th Annual Teratology Society Meeting, Portsmouth, NH. June.

Holloway, B. D. Skin Painting: A Tool for Cancer Research. AAAS Conference, Monterey, CA. March.

Kaune, W. T. Biological Effects of 60-Hz Electric Fields: Dosimetry. Graduate Students Seminar in Biophysics, Minneapolis, MN. May.

[illegible]

[illegible]

[illegible]

[illegible]

[illegible]

[illegible]

[illegible] Chronic [illegible] on Rat [illegible] Northwest Section, Federation of American Societies for Experimental Biology and Medicine, Vancouver, BC. October.

[illegible]enberg, R. A. Regulation of Extracellular Acid Proteases in *Neurospora crassa*. American Society for Microbiology, Miami Beach, FL. May.

[illegible], S. M. Interaction Between [illegible]ase Induced Emphysema and Sulfuric Acid Aerosol Exposure in Guinea Pigs. Federation of American Societies for Experimental Biology and Medicine, Anaheim, CA. April.

[illegible], S. M. [illegible] Principle, [illegible] Experimental Results [illegible] Multiple Breath. Workshop on [illegible] Function Testing in Small Laboratory Animals, Baltimore, MD. May.

[illegible], S. M., B. W. Killand, and R. L. [illegible] Characteristics of Single Breath N2 and Inflation Pressure vs Volume Curves [illegible] Anesthetized Guinea Pigs. American [illegible] Society, Washington, DC. May.

[illegible], S. M., B. W. Killand, D. L. [illegible] Histamine [illegible] Pulmonary Function Evaluation [illegible] Animals Exposed to a High Boiling [illegible] 20th Hanford Life Sciences Symposium, Richland, WA. October.

[illegible] Analysis [illegible] Electric [illegible] Conditioned Taste Aversion in the Rat. Bio[illegible] Meeting, San [illegible]

[illegible] Health [illegible] WA.

[illegible] Chemical [illegible] Coal [illegible] Materials [illegible] Energy [illegible] October.

Mahlum, D. D. [illegible] Solvent Refined [illegible] Washington [illegible] Seattle, WA. March.

Mahlum, D. D., R. A. [illegible], R. W. Wilson, M. [illegible], H. [illegible]cker, and D. R. [illegible] Toxicologic Studies of SRC Materials and SRC Environmental Control [illegible], Boston, MA. March.

Mihalko, P. J., [illegible] Ruffel, and [illegible] R. Decker. An Automatic System for Generating Repeatable Forced Vital Capacity Maneuvers in Rodents. Northwest Section, Federation of American Societies for Experimental Biology and Medicine, Vancouver, BC. October.

Miller, B. M. The Effect of Age on Cadmium Absorption. Northwest Section, Federation of American Societies for

Experimental Biology and Medicine. Vancouver, BC. October.

Milliman, E. M. Experience With a Flexible-Brush Dust Feed Mechanism. American Industrial Hygiene Conference. Houston, TX. May.

Montgomery, L. D., D. D. Mahlum, and J. R. Decker. Effect of Magnetic Fields on EMS-Induced Dominant Lethality in Mice. Bioelectromagnetic Society Meeting, San Antonio, TX September.

Morris, J. E., H. A. Ragan, I. M. Graham, M. J. Pipes. In Vivo and In Vitro Cell-Mediated Immunity in Mice Exposed to 60-Hz, 100 kV/m Electric Fields. Bioelectromagnetics Society Meeting, San Antonio, TX. September.

Petroy, R. A. Overview of In Vitro Studies Applied to Complex Materials. 20th Hanford Life Sciences Symposium, Richland, WA. October.

Phillips, R. D. Analysis of Possible Synergy of 60-Hz Electric Fields and Cyclophosphamide in Inducing Conditioned Taste Aversions in the Rat. Second Annual Meeting of the Bioelectromagnetics Society, San Antonio, TX. September.

Phillips, R. D. Bioelectrical Effects of 60-Hz Electric Fields. Central Electrical Research Laboratory, Leatherhead, England. July.

Poston, K. A. and F. D. Andrew. Effects of Complex Chemicals on Behavioral Teratology in Rats. 20th Annual Teratology Society Meeting, Portsmouth, NH. June.

Renne, R. A. Carcinogenic Effects of Coal Conversion By-Products. Industrial Hygiene and Occupational Medicine in Coal Conversion Workshop. Washington, DC. November.

Renne, R. A., E. G. Smith, and D. D. Mahlum. Epidermal Carcinogenicity of Some Crude Fossil Fuels in Mice: A Preliminary Report. 20th Hanford Life Sciences Symposium, Richland, WA. October.

Rhoads, K. and C. L. Sanders. Morphology and Cell Kinetics of Lung Lesions Following Inhalation of $^{239}PuO_2$. Health Physics Society Meeting, Seattle, WA. July.

Samuel, J. E., T. K. Andrews, Jr., and M. E. Frazier. Toxicity of Metals In Vitro. Northwest Section, Federation of American Societies for Experimental Biology and Medicine, Vancouver, BC. October.

Sanders, C. L. Pulmonary Toxicity of Mount St. Helens Volcanic Ash. Northwest Section, Federation of American Societies of Experimental Biology and Medicine Meeting, Vancouver, BC. October. Seminar at Huley College of Environmental Studies, Western Washington University, Bellingham, WA. October. Biology Department Seminar, Battelle, Richland, WA. October. Seminar, University of Washington, Seattle, WA. December.

Sanders, C. L. Radiobiology of Alpha Emitters: Health Hazards from Alpha Emitters in Air. Owens-Corning Fiberglass Corp., Technical Center, Newport, OR. April.

Sikov, M. R. Developmental Toxicology of Environmental Pollutants. University of Washington Radiological Sciences Series Seminar, Seattle, Wa. February.

Sikov, M. R. Embryotoxicity of Plutonium. OSU Marine Science Center, Newport, OR. April.

Sikov, M. R., B. P. Hildebrand, H. D. Collins, K. A. Poston, and P. J. Crowley. Analysis of Temperature Changes During Ultrasound Exposure to Pregnant Rat. American Institute of Ultrasound in Medicine. New Orleans, LA. September.

Smith, V. H. and R. A. Gelman. Tissue Disposition of Pu and Am After Intramuscular Injection of Equimolar Amounts of Plutonium and Americium Nitrate in the Rat. 5th International Congress of International Radiation Protection Association, Jerusalem, Israel. March.

Springer, D. L., D. H. Willard, C. J. Gerdes, D. W. Phelps, and D. D. Mahlum. A Method for Generating a Respirable Aerosol of a High Boiling Coal Liquid. 20th Hanford Life Sciences Symposium, Richland, WA. October.

Sullivan, M. F. An Evaluation of Cf-252 as a Potential Radiation Source for Use in Treatment of Cervical Cancer. Seminar, Radiological Sciences Winter Quarter, University of Washington, Seattle, WA. February.

Sullivan, M. F. Maximum Permissible Concentrations of Plutonium in Drinking Water. 5th International Congress of International Radiation Protection Association, Jerusalem, Israel. March.

Thompson, R. C. An Approach to the Derivation of Radionuclide Intake Limits for the General Population. 5th International Congress of International Radiation Protection Association, Jerusalem, Israel. March.

Thompson, R. C. Radiation and Its Effects: Basic Biology. LASL Life Sciences Symposium, Los Alamos, NM. October.

Thompson, R. C. Recent, Past and Near Future Activities of ICRP Committee 2. 5th International Congress of International Radiation Protection Association, Jerusalem, Israel. March.

Thompson, R. C. Refresher Course on New ICRP Limits for Intakes of Radionuclides by Workers. Health Physics Society Meeting, Seattle, WA. July.

Thompson, R. C. Standards for Limiting Radiation Exposure--The ICRP Approach. Short Course on Radiation Protection Standards and Effects of Low Level Ionizating Radiation, Richland, WA. May.

Thompson, R. C. Toxicity of Plutonium. Seminar, Radiological Sciences Winter Quarter at the University of Washington, Seattle, WA. February.

Wilson, B. W., L. E. Anderson, D. I. Hilton, and R. D. Phillips. Pineal Gland Function in Rats Exposed to 60-Hz Electric Fields. First International Symposium on Melatonin. University of Bremen, Germany. September.

Wilson, B. W., S. Hewett, D. I. Hilton, and L. E. Anderson. Pineal Gland Function in Rats Exposed to 60-Hz Electric Fields. Bioelectromagnetics Society Meeting, San Antonio, TX. September.

Author Index

AUTHOR INDEX

Abernethy, C. S.: 211
Allen, M. D.: 112
Andrew, F. D.: 30, 164
Andrews, T. K.: 49, 187, 205

Bair, W. J.: 107, 110
Ballou, J. E.: 102, 136, 138, 140, 142, 146, 149, 223
Blanton, F. F.: 57, 183
Briant, J. K.: 64, 112, 114, 116, 119, 122, 124, 127
Bunnell, F. R.: 201
Busch, R. H.: 1, 5, 124, 130, 133
Buschbom, R. L.: 130

Cannon, W. C.: 57, 61, 81, 160
Carr, D. B.: 168
Catt, D. L.: 66, 119
Case, A. C.: 66, 81, 142
Causey, S. C.: 35
Chang, D. P. Y.: 59
Chou, C. K.: 40
Clary, A. J.: 119
Conklin, A. W.: 16, 19, 20, 22, 95, 97
Cross, F. T.: 130, 133

Dagle, G. E.: 66, 81, 142, 223
Debban, K. H.: 74
Decker, J. R.: 11, 208
Davidow, S.: 40
DeFord, H. S.: 138
Drucker, H.: 226, 230

Frazier, M. E.: 49, 187, 191, 205
Filipy, R. E.: 1, 107, 110, 133

Gelman, R. A.: 20, 95
Genoway, R. G.: 211
Geraci, J. P.: 93
Gies, R. A.: 102, 140, 142, 149, 223
Gorham, L. S.: 180, 181, 183
Graham, T. M.: 195, 198
Guy, A. W.: 40

Hackett, P. L.: 25, 116, 119, 122, 151, 153, 160
Haggard, D. L.: 146
Hess, J. O.: 170, 173
Hoeper, M. J.: 191
Hurgate, F. P.: 35, 201

Johnson, G. R.: 86

Kalkwarf, D. R.: 213
Karagianes, M. T.: 1, 5, 8
Kaune, W. T.: 42, 49
Kelman, B. J.: 151, 153, 155, 158
King, A. I.: 49
Kinnas, T. C.: 66, 81
Klopter, S. L.: 63, 81
Kuffel, E. G.: 11, 208

Lindberg, R. A.: 226, 230
Loscutoff, S. M.: 133
Lytz, P. S.: 164

Madison, R. M.: 66, 81
Mahaffey, J. A.: 88, 98, 100, 105
Mahlum, D. D.: 29, 116, 119, 122, 170, 173, 217
Mallavia, L. P.: 191
McClanahan, B. J.: 45, 47, 79
McDonald, K. E.: 124, 240
McShane, J. F.: 81
Mihalko, P. J.: 8, 11
Miller, R. A.: 102, 223
Milliman, E. M.: 59
Montgomery, L. F.: 158
Morgan, L. J.: 114
Morris, J. E.: 195, 198
Moss, O. R.: 59, 61, 64
Murphy, D. W.: 146
Music, P. L.: 116, 122, 160

Nelson, D. A.: 208
Nicholson, P. R.: 86

Palmer, R. F.: 1, 5, 8, 130, 133

Pappin, J. L.: 107, 110
Park, J. T.; 66, 74, 195
Pelrov, R. A.: 31
Peters, L. R.: 119
Poston, K. A.: 164
Powers, G. J.: 66, 81

Ragan, H. A.: 15, 66, 74, 81
Renne, R. A.; 217, 240
Rhoads, K.; 91, 93
Rhodes, W. G.: 226, 230
Riemath, W. D.: 201
Robinson, A. V.; 235, 241
Rossignol, E. J.: 61
Rowe, S. E.: 66, 81
Ryan, J. T.: 114, 140, 149, 183

Samuel, J.: 49, 187, 205
Sanders, C. L.; 16, 19, 20, 22, 88, 90, 91, 93, 95, 97, 98, 100, 105
Schirmer, R. E.; 66, 81
Schneider, R. P.; 233
Sikov, M. R.; 151, 153, 160, 170
Skalski, J. R.; 211
Skiens, W. E.; 160
Slavich, A. L.; 74
Smith, L. G.; 217
Smith, V. H.; 170, 173
Stevens, D. L: 66, 81, 107, 110, 168
Strand, J. A.; 211
Sullivan, M.; 176, 180, 181, 183, 185

Tolley, H. D.; 102, 136, 142

Viola., M. V.; 191

Watson, C. R.; 66, 86
Watson, S. A.: 25
Wierman, E. L.: 66, 81
Willard, D. H.: 136

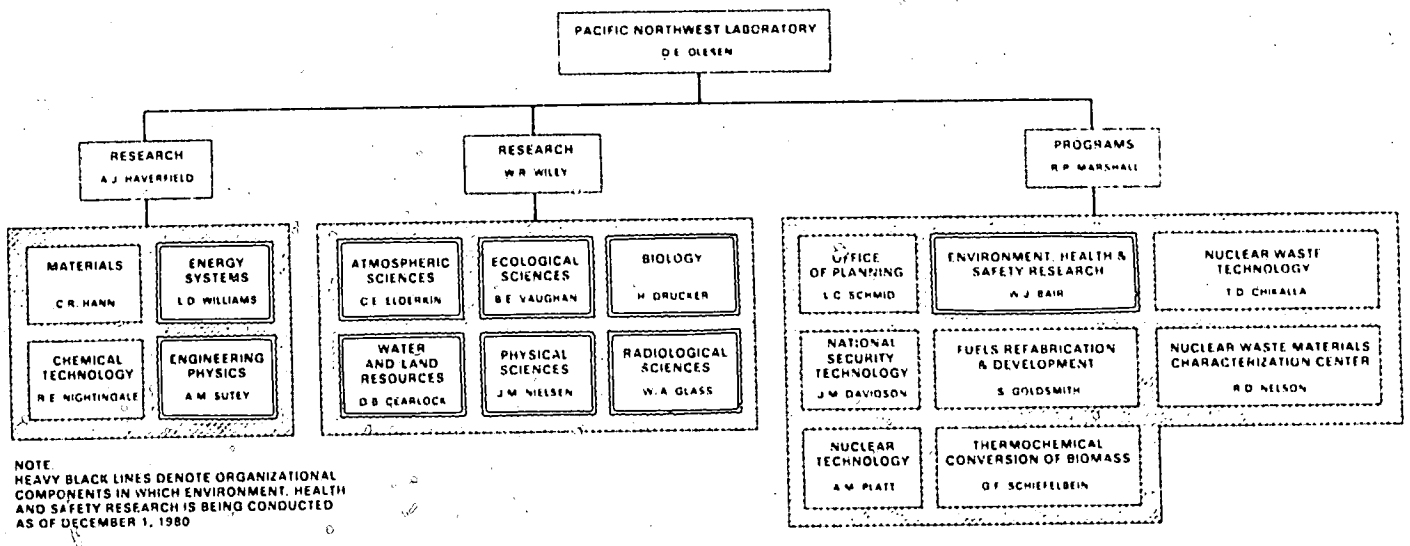

NOTE:
HEAVY BLACK LINES DENOTE ORGANIZATIONAL COMPONENTS IN WHICH ENVIRONMENT, HEALTH AND SAFETY RESEARCH IS BEING CONDUCTED AS OF DECEMBER 1, 1980

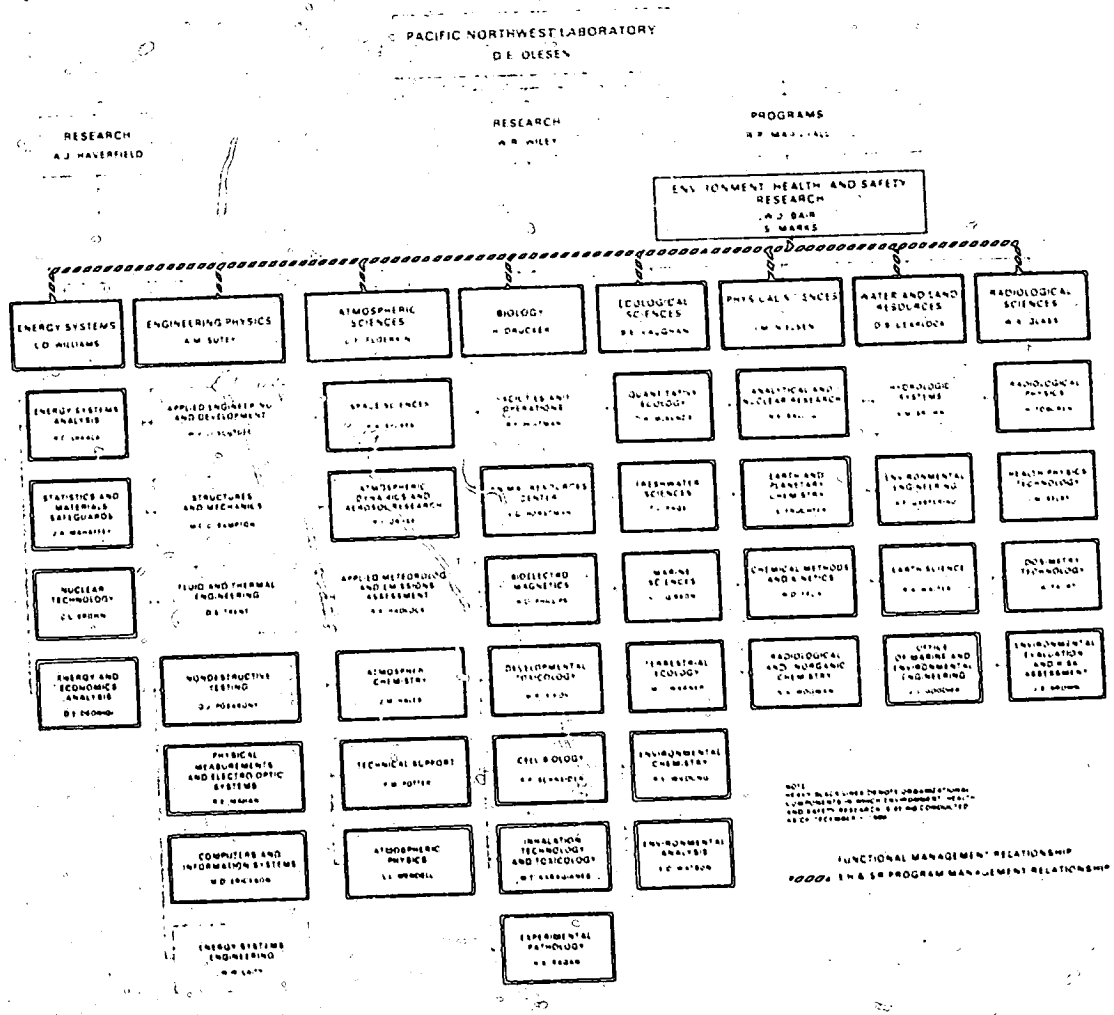
PACIFIC NORTHWEST LABORATORY
D E OLESEN
RESEARCH
A J HAVERFIELD
RESEARCH
PROGRAMS
ENVIRONMENT HEALTH AND SAFETY RESEARCH
ENERGY SYSTEMS
ENGINEERING PHYSICS
ATMOSPHERIC SCIENCES
BIOLOGY
ECOLOGICAL SCIENCES
PHYSICAL SCIENCES
WATER AND LAND RESOURCES
RADIOLOGICAL SCIENCES
ENERGY SYSTEMS ANALYSIS
STATISTICS AND MATERIALS SAFEGUARDS
NUCLEAR TECHNOLOGY
ENERGY AND ECONOMICS ANALYSIS
APPLIED ENGINEERING AND DEVELOPMENT
STRUCTURES AND MECHANICS
FLUID AND THERMAL ENGINEERING
NONDESTRUCTIVE TESTING
PHYSICAL MEASUREMENTS AND ELECTRO OPTIC SYSTEMS
COMPUTERS AND INFORMATION SYSTEMS
ENERGY SYSTEMS ENGINEERING
SPACE SCIENCES
ATMOSPHERIC DYNAMICS AND AEROSOL RESEARCH
APPLIED METEOROLOGY AND EMISSIONS ASSESSMENT
ATMOSPHERIC CHEMISTRY
TECHNICAL SUPPORT
ATMOSPHERIC PHYSICS
QUANTITATIVE ECOLOGY
FRESHWATER SCIENCES
BIOELECTRO MAGNETICS
MARINE SCIENCES
DEVELOPMENTAL TOXICOLOGY
CELL BIOLOGY
INHALATION TECHNOLOGY AND TOXICOLOGY
EXPERIMENTAL PATHOLOGY
TERRESTRIAL ECOLOGY
ENVIRONMENTAL CHEMISTRY
ENVIRONMENTAL ANALYSIS
ANALYTICAL AND NUCLEAR RESEARCH
EARTH AND PLANETARY CHEMISTRY
CHEMICAL METHODS AND SERVICES
RADIOLOGICAL AND INORGANIC CHEMISTRY
HYDROLOGIC SYSTEMS
ENVIRONMENTAL ENGINEERING
EARTH SCIENCE
OFFICE OF MARINE AND ENVIRONMENTAL ENGINEERING
RADIOLOGICAL PHYSICS
HEALTH PHYSICS TECHNOLOGY
DOSIMETRY TECHNOLOGY
ENVIRONMENTAL EVALUATION AND RISK ASSESSMENT
FUNCTIONAL MANAGEMENT RELATIONSHIP
ENVIRONMENT HEALTH AND SAFETY RESEARCH PROGRAM MANAGEMENT RELATIONSHIP

END

DATE FILMED

04/28/81